Diss. ETH No. 23213

Ir-Catalyzed Reverse Prenylation of 3-Substituted Indoles
and
Rh-Catalyzed Stereoselective Synthesis of Allenes

A thesis submitted to attain the degree of

DOCTOR OF SCIENCES of ETH ZURICH

(Dr. sc. ETH Zurich)

presented by

Jonathan Ruchti

M.Sc. ETH Zurich

born on 09.08.1984

citizen of Rapperswil (BE), Switzerland

accepted on the recommendation of

Prof. Dr. Erick. M. Carreira, examiner

Prof. Dr. Antonio Togni, co-examiner

2016

Acknowledgements

I am grateful to *Prof. Erick M. Carreira* for the opportunity to conduct my Ph.D. studies under his supervision. I am indebted to him for his support throughout my time as a master and PhD student at ETH Zurich. I would like to express my gratitude to *Prof. Antonio Togni* for being my co-examinor and for his invaluable comments and corrections to the manuscript of this thesis. I have had the privilege to share my time in the Carreira group with motivating colleagues who have been a source of inspiration and knowledge. In particular, I would like to thank my former labmates *Drs. Oliver Jeker*, *Martin McLaughlin*, *Julian Egger*, *Philippa Cranwell*, *David Sarlah*, *Keita Tanaka*, *Erik Daa Funder* as well as *Stefan Künzi*, *Adrian Bailey*, *Andrej Shemet*, *Tobias Sandmeier*, *Marco Brandstätter*, *Minh Dao,* and *Gabriele Zirpoli*. While working on Ir-catalyzed reactions, I profited tremendously from the knowledge and experience of other group members. The advice I got from *Dr. David Sarlah*, *Dr. Nicolás Armanino*, *James Hamilton,* and *Michael Schafroth* was of great value. *Dr. David Sarlah* in particular has contributed significantly to the project described in part I of this thesis. I would like to express my thanks to *Adrian Bailey*, *Robert Gillespie*, *Stefan Künzi*, *Raffael Vorberg*, *Matthias Westphal*, and *Hannes Zipfel* for proofreading parts of this thesis. Their suggestions, comments and corrections were highly appreciated. When writing this thesis, I was fortunate to be able to ask *Simon Krautwald* and *Dr. Nikolas Huwyler* for advice at any time. I am grateful to *Franziska Peyer* and *Anke Kleint* for taking care of all administrative affairs during my time in the Carreira group. I would like to thank the ETH Zurich and the SNF for providing infrastructure and funding. The work described herein would not have been possible without the excellent facilities provided by ETH Zurich and all ETH staff. In particular I would like to thank *Dr. Nils Trapp* and *Michael Solar* for X-ray diffraction analysis, *Louis Bertschi*, *Oswald Greter*, *Rolf Häfliger* and *Dr. Xiangyang Zhang* for mass spectrometrical analysis, *Dr. Marc-Olivier Ebert*, *René Arnold*, *Rainer Frankenstein*, *Philipp Zumbrunnen*, *René Arnold* and *Stephan Burkhardt* for assistance with NMR spectroscopy. Alex Lauber and Oliver Engl are acknowledged for their assistance with HPLC and SFC measurements.

Publications

Ruchti, J.; Carreira, E. M.

Rh-Catalyzed Stereospecific Synthesis of Allenes from Propargylic Benzoates and Arylboronic Acids

Org. Lett. **2016**, *18*, 2174–2176.

Ruchti, J.; Carreira, E. M.

Ir-Catalyzed Reverse Prenylation of 3-Substituted Indoles: Total Synthesis of (+)-Aszonalenin and (−)-Brevicompanine B

J. Am. Chem. Soc. **2014**, *136*, 16756–16759.

Table of Contents

Appendix

Abstract

Prenylated indole alkaloids are a class of structurally diverse natural products which display a wide array of biological activites. A subset of these compounds is characterized by the presence of a reverse prenyl group at C3 of a hexahydropyrroloindole skeleton. However, general methods for the C3 reverse prenylation of 3-substituted indoles in one step have not been reported previously. In the first part of this thesis, the development of a method to access this structural motif is described. The disclosed Ir-catalyzed reaction allows for a highly chemo- and regioselective reverse prenylation at C3 of an assortment of 3-substituted indoles. This method represents the first example of an Ir-catalyzed allylation reaction to access vicinal quaternary centers.

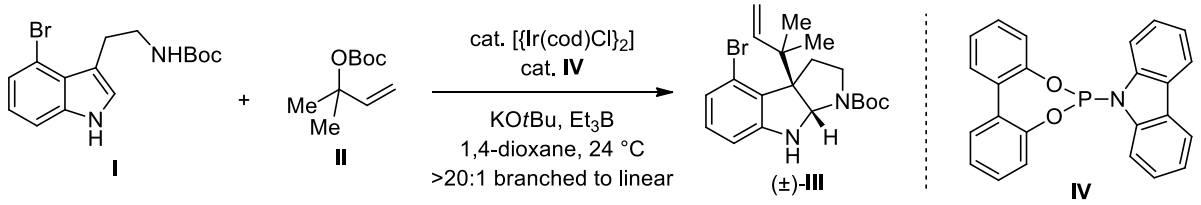

Scheme I: Example for the Ir-catalyzed reverse prenylation disclosed in part I of this thesis.

A diastereoselective variant of this reaction provided reverse prenylated hexahydropyrroloindole (–)-**VI** in one step from tryptophan methyl ester (*S*)-(**V**) with excellent *exo*-stereoselectivity. Notably, the transformation yields the product in high regioselectivity (>20:1 branched to linear). The utility of this approach was illustrated in the syntheses of (+)-aszonalenin and (–)-brevicompanine B.

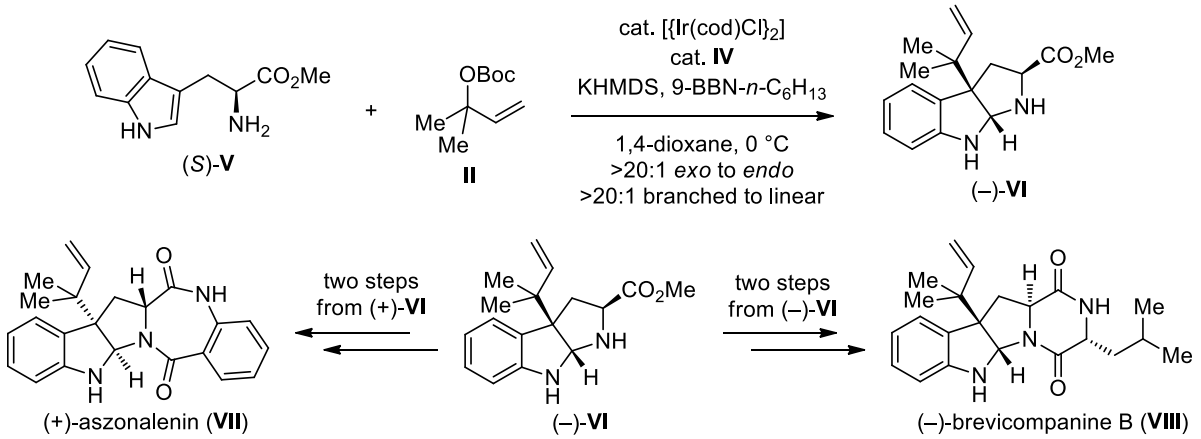

Scheme II: Diastereoselective Ir-catalyzed reverse prenylation of tryptophan methyl ester and synthesis of (+)-aszonalenin and (–)-brevicompanine B.

In the second part of this thesis, a Rh-catalyzed stereoselective synthesis of allenes is disclosed. This method allows access to trisubstituted chiral allenes from widely available arylboronic acids and chiral propargylic benzoates using a catalyst generated *in situ* from a Rh^{I} organometallic complex and phosphoramidite ligand **XII**. The reaction proceeds under mild conditions and with high degree of chirality transfer. Various arylboronic acids as well as structurally different propargylic benzoates can be employed to yield a broad range of allenes in a stereoselective manner. The transformation is thought to proceed via regioselective *cis*-addition of an arylrhodium species to the alkyne to furnish a vinylrhodium intermediate. This intermediate then undergoes *syn*-elimination to form the allene. This rational is based on the determination of the absolute stereochemistry of one product by X-ray crystallographic analysis.

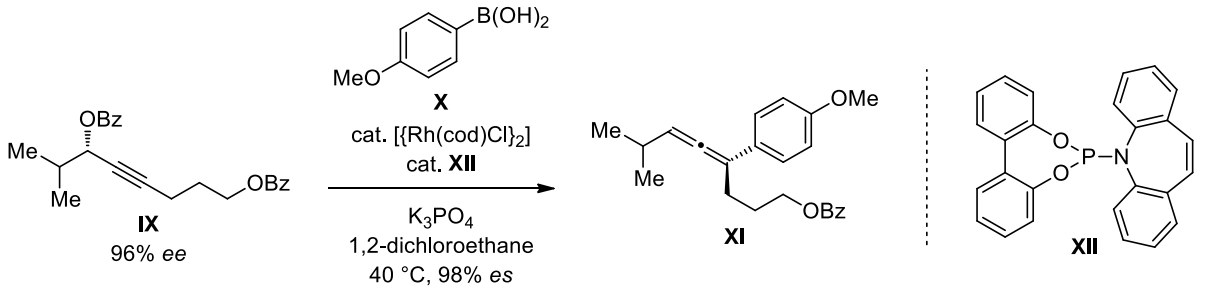

Scheme III: Example for the Rh-catalyzed stereoselective synthesis of allenes described in part II.

Different from the majority of previous approaches, this method enables the synthesis of chiral allenes without using moisture sensitive reagents. It is also the first example of a transition metal catalyzed synthesis of chiral trisubstituted allenes from readily available chiral propargylic alcohol derivatives and arylboronic acids. Moreover, no Rh-catalyzed stereoselective synthesis of allenes employing boronic acids as nucleophiles has been reported previously.

Zusammenfassung

Prenylierte Indolalkaloide bilden eine strukturell sehr heterogene Klasse von Naturstoffen mit vielfältigen biologischen Aktivitäten. Eine Untergruppe dieser Verbindungen ist durch das Vorhandensein einer inversen Prenylgruppe am C3 Kohlenstoff eines Hexahydropyrroloindolgerüstes gekennzeichnet. Jedoch sind allgemeine Methoden für die einstufige, inverse Prenylierung am C3 Kohlenstoff von 3-substituierten Indolen bisher nicht beschrieben worden. Im ersten Teil der vorliegenden Arbeit wird die Entwicklung einer Synthesemethode beschrieben, die einen Zugang zu diesem Strukturelement gewährt. Die beschriebene Ir-katalysierte Reaktion ermöglicht die inverse Prenylierung am C3 Kohlenstoff von verschiedenen 3-substituierten Indolen mit hoher Chemo- und Regioselektivität. Die Reaktion das erste Beispiel einer Ir-katalysierten allylischer Substitution, die das Motiv von benachbarten, quaternären Zentren erschliesst.

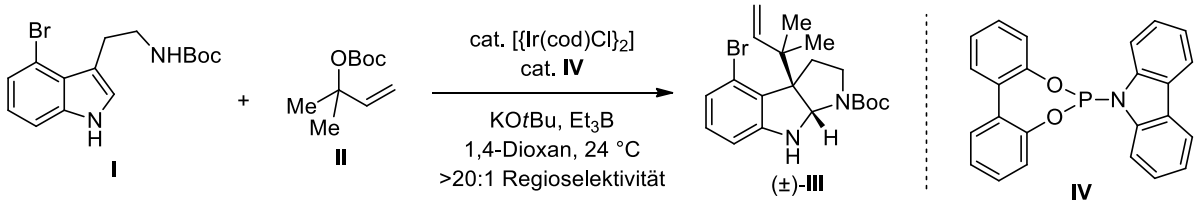

Schema I: Beispiel für die Ir-katalysierte, inverse Prenylierung wie sie im ersten Teil dieser Arbeit beschrieben wird.

Eine diastereoselektive Variante der Reaktion ermöglichte die Synthese von Hexahydropyrroloindol (–)-**VI** mit hoher *exo*-Selektivität. Die Reaktion verläuft mit hoher Regioselektivität (>20:1). Die Nützlichkeit des hier entwickelten Ansatzes wurde durch die Synthesen von (+)-Aszonalenin und (–)-Brevicompanine B illustriert.

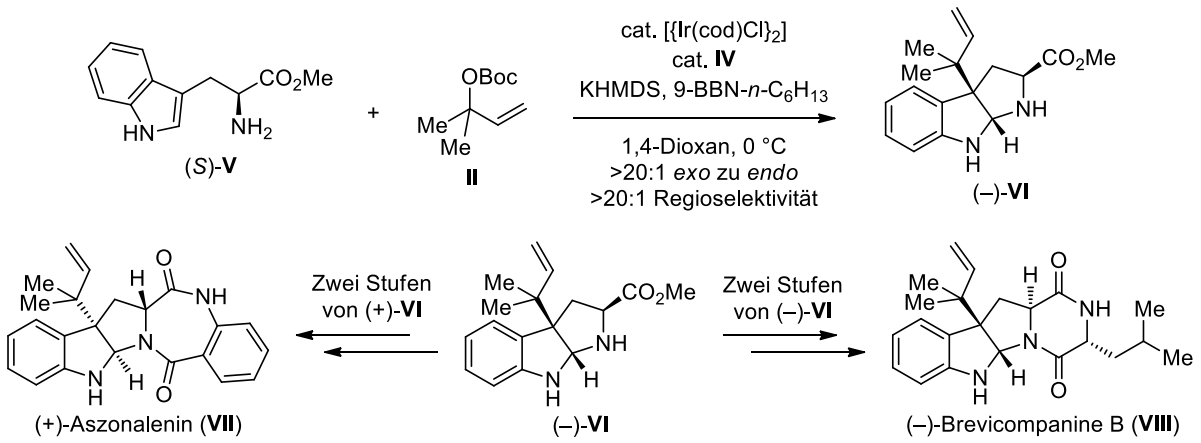

Schema II: Diastereoselektive, Ir-katalysierte, inverse Prenylierung von Tryptophan Methylester und die Synthesen von (+)-Aszonalenin sowie (–)-Brevicompanine B.

Im zweiten Teil dieser Arbeit wird eine Rh-katalysierte, stereoselektive Synthese von trisubstituierten Allenen beschrieben. Die Methode erlaubt den Zugang zu dreifach substituierten, chiralen Allenen ausgehend von gut verfügbaren Arylboronsäuren und chiralen, propargylischen Benzoaten. Als Katalysator wird ein Rh^{I} Organometall-Komplex verwendet, der *in situ* aus einem Rh^{I}-Vorläufer und dem Phosphoramiditliganden **XII** gebildet wird. Die Reaktion verläuft unter milden Bedingungen, mit hohem Chiralitätstransfer und es können eine Vielzahl von Arylboronsäuren sowie propargylischen Benzoate als Reaktionspartner eingesetzt werden. Als Produkte werden eine Reihe von Allenen in hoher Stereoselektivität erhalten. Die Reaktion verläuft vermutlich über ein Vinylrhodium-Intermediat, das durch eine regioselektive *cis*-Addition einer Arylrhodium-Verbindung an das Alkin gebildet wird. Durch anschliessende *syn*-Eliminierung wird schliesslich das Allen gebildet. Diese Annahme basiert auf der Bestimmung der absoluten Stereochemie eines Produktes durch Kristallstrukturanalyse.

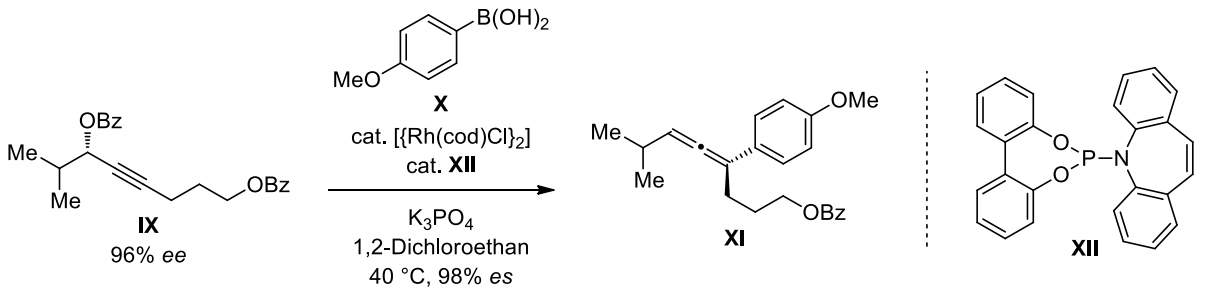

Scheme III: Beispiel für die Rh-katalysierte, stereoselektive Synthese von Allenen, wie sie im zweiten Teil der vorliegenden Arbeit beschrieben wird.

Im Unterschied zu den bereits in der Literatur beschriebenen Allensynthesen, ermöglicht die hier beschriebene Methode die Synthese von chiralen Allenen ohne die Verwendung von wasserempflindlichen Reagenzien. Es ist ebenfalls das erste Beispiel einer übergangsmetallkatalysierten Synthese von enantiomerenangereicherten, dreifach substituierten Allenen ausgehend von einfach zugänglichen enantiomerenangereicherten, propargylischen Estern und Arylboronsäuren. Ebenfalls wurde bisher keine Rh-katalysierte, stereoselektive Synthese von Allenen unter der Verwendung von Boronsäuren als Nukleophile beschrieben.

List of Abbreviations, Acronyms and Symbols

$[\alpha]_D^T$	specific rotation at temperature T at the sodium D line
Å	Ångstrom
Ac	acetyl
AcOH	acetic acid
Ala	alanine
Alloc	allyloxycarbonyl
anhydr.	anhydrous
aq.	aqueous
Ar	aryl
BINOL	1,1‘-bi-2-naphthol
Bn	benzyl
Boc	*tert*-butyloxycarbonyl
Boc_2O	di-*tert*-butyl dicarboxylate
BOM	benzyloxymethyl
BOP-Cl	bis(2-oxo-3-oxazolidinyl)phosphinic chloride
bp	boiling point
bs	broad signal
Bu	butyl
Bz	benzoyl
ºC	degree centrigrade
calcd	calculated
CAM	cerium ammonium molybdate stain
cat.	catalytic, catalyst
cod	cycloocta-1,5-diene
conc.	concentrated
convn.	conversion
COSY	correlation spectroscopy
Cy	cyclohexyl
δ	NMR chemical shift in ppm downfield from a standard
d	doublet, day
dba	dibenzylideneacetone
DBU	1,8-diazabicyclo[5.4.0]undec-7-ene
DCC	*N*,*N*′-dicyclohexylcarbodiimide
DMAP	4-*N,N’*-dimethylamino pyridine
DMF	*N*,*N*-dimethyl formamide
DMP	Dess–Martin periodinane
d.r.	diastereomeric ratio
ee	enantiomeric excess
e.g.	for example
EI	electron impact ionization

elim.	elimination
ent	opposite enantiomer
equiv.	equivalent
er	enantiomeric ratio
es	enantiospecificity
ESI	electron spray ionization
Et	ethyl
ETH	Eidgenössische Technische Hochschule
EtOAc	ethyl acetate
et al.	and others
Fmoc	fluorenylmethyloxycarbonyl
g	gram
h	hour
HATU	1-[bis(dimethylamino)methylene]-1*H*-1,2,3-triazolo[4,5-*b*]pyridinium 3-oxidhexa-fluorophosphate
HMBC	heteronuclear multiple-bond correlation
HOBt	1-hydroxybenzotriazole
HPLC	high performance liquid chromatography
HRMS	high resolution mass spectrometry
HSQC	heteronuclear single quantum coherence
Hz	Hertz
i	*iso*
i.d.	that is
in situ	on site
IR	infrared
J	coupling constant
KHMDS	potassium bis(trimethylsilyl)amide
l	liter
L	ligand
Leu	leucine
LiAlH	lithium aluminum hydride
LDA	lithium diisopropyl amide
m	multiplet
m	*meta*
µ	micro
M	Molar, molecular ion
mbar	millibar
Me	methyl
mg	milligram
MHz	Megahertz
min	minute
mL	milliliter
m.p.	melting point

mmol	millimol
Ms	methylsulfonyl
MS	molecular sieves
n	unbranched alkyl chain
n. d.	not determined
nbd	norborna-2,5-diene
NBS	*N*-bromosuccinimide
NMP	1-methylpyrrolidin-2-one
NMR	nuclear magnetic resonance
Ns	nosyl, nitrosulfonyl
ν	vibration frequency in cm^{-1}
o	ortho
ORTEP	Oak Ridge Thermal Ellipsoid Plot
p	para
PG	protecting group
pH	negative logarithm of hydrogen ion concentration
Ph	phenyl
pin	pinacolato
PMB	4-methoxybenzyl
ppm	parts per million
PPTS	pyridinium *p*-toluenesulfonate
Pr	propyl
p-TsOH	*para*-toluenesulfonic acid
py	pyridine
q	quartet
quant.	quantitative
rac	racemic
R_f	retention factor
r.t.	room temperature
s	second, singlet
sat.	saturated
SFC	supercritical fluid chromatography
t	triplet
t	*tert*
T	temperature
TADDOL	2,2-dimethyl-α,α,α′,α′-tetraphenyldioxolane-4,5-dimethanol
TBAF	tetrabutylammonium fluoride
TBAT	tetrabutylammonium difluorotriphenylsilicate
TBDPS	*tert*-butyldiphenylsilyl
TBS	*tert*-butyldimethylsilyl
TEMPO	2,2,6,6-tetramethylpiperidine 1-oxyl
TES	triethylsilyl
Tf	trifluormethanesulfonyl

TFA	trifluoroacetic acid, trifluoroacetyl
TFAA	trifluoroacetic acid anhydride
THF	tetrahydrofuran
TLC	thin layer chromatography
TMP	2,2,6,6-tetramethyl piperidine
TMS	trimethylsilyl
Trp	tryptophan
Ts	tosyl, 4-methylphenylsulfonyl
UV	ultraviolet
vide infra	see below
vide supra	see above

I

Ir-Catalyzed Reverse Prenylation of 3-Substituted Indoles

1 Background and Introduction

The prenylated indole alkaloids are a structurally diverse class of natural products isolated predominately from fungi, bryozoans, and cyanobacteria. Many compounds from this family exhibit a wide array of biological activities and have been the subject of numerous synthetic and biosynthetic studies.[1] An important subset within this group of natural products possess a 1-(1,1-dimethylallyl) substituent at the C3 junction of a hexahydropyrroloindole motif (*e.g.* **1** in Figure 1.1).[2]

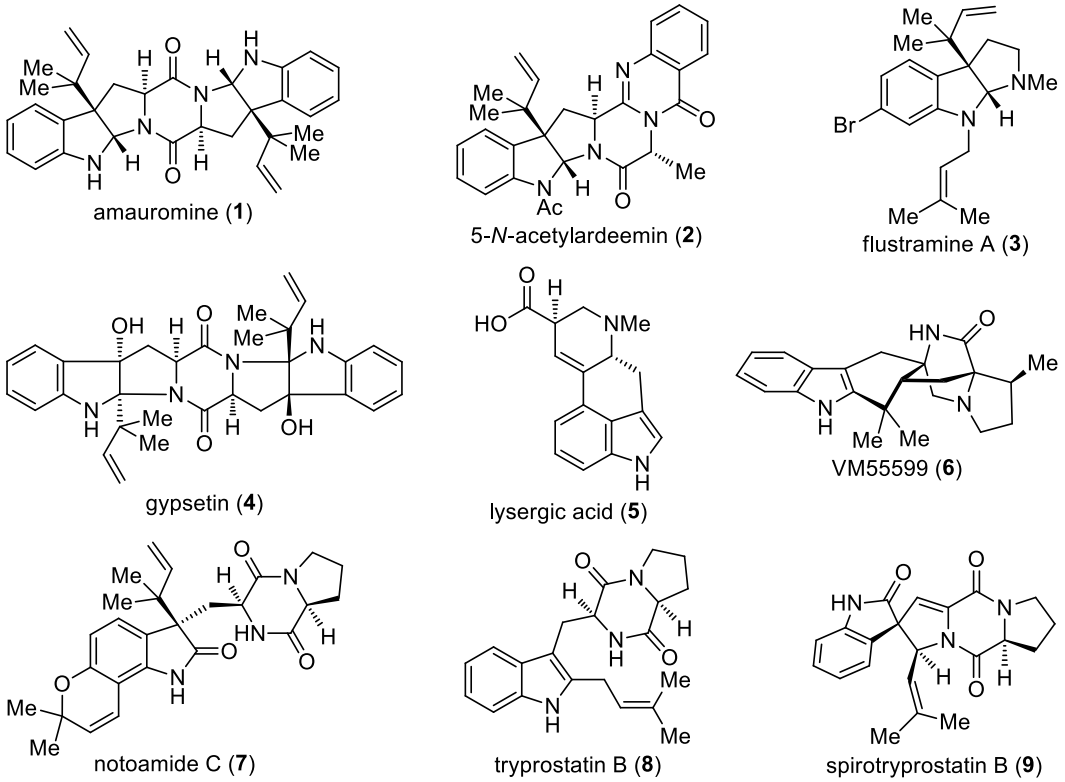

Figure 1.1 A selection of prenylated indole natural products.

The introduction of such a substituent has been referred to as "reverse prenylation", on fewer occasions as "inverse prenylation", or as the introduction of an "inverted isoprene unit".

[1] For selected reviews on the structures and biosynthesis of prenylated indoles, see: (a) Li, S.-M. *Nat. Prod. Rep.* **2010**, *27*, 57. (b) Williams, R. M.; Stocking, E. M.; Sanz-Cervera, J. F. *Top. Curr. Chem.* **2000**, *209*, 97.

[2] For the isolation of the natural products shown in Figure 1.1, see: (a) Amauromine: Takase, S.; Iwami, M.; Ando, T.; Okamoto, M.; Yoshida, K.; Horiai, H.; Kohsaka, M.; Aoki, H.; Imanaka, H. *J. Antibiot.* **1984**, *37*, 1320; Takase, S.; Kawai, Y.; Uchida, I.; Tanaka, H.; Aoki, H. *Tetrahedron* **1985**, *41*, 3037. (b) 5-*N*-Acetylardeemin: Hochlowski, J. E.; Mullally, M. M.; Spanton, S. G.; Whittern, D. N.; Hill, P.; McAlpine, J. B. *J. Antibiot.* **1993**, *46*, 380. (c) Flustramine A: Carle, J. S.; Christophersen, C. *J. Am. Chem. Soc.* **1979**, *101*, 4012. (d) Gypsetin: Shinohara, C.; Hasumi, K.; Takei, Y.; Endo, A. *J. Antibiot.* **1994**, *47*, 163; Nuber, B.; Hansske, F.; Shinohara, C.; Miura, S.; Hasumi, K.; Endo, A. *J. Antibiot.* **1994**, *47*, 16. (e) Lysergic acid (isolated by degradation of ergotinine): Jacobs, W. A.; Craig, L. C. *J. Biol. Chem.* **1934**, *104*, 547. (f) VM55599: Blanchflower, S. E.; Banks, R. M.; Everett, J. R.; Reading, C. *J. Antibiot.* **1993**, *46*, 1355. References continued on the next page.

The 1-(1,1-dimethylallyl) group is described as a reverse prenyl group in order to distinguish this substructure from the normal or linear prenyl group, which is also found in natural products. The occurrence of the reverse prenyl group in indole alkaloids has prompted the development of a variety of methods to access this motif.[3] The introduction of a reverse prenyl group at C3 of 3-substituted indoles poses numerous challenges. First, the regioselectivity of the prenylation has to be controlled as outlined schematically below for a tryptamine derivative **10** (Scheme 1.1). Secondly, when accessing the reverse prenylated product, two vicinal quaternary centers are formed. The synthesis of such a motif has long been recognized as a formidable task in natural product synthesis.[4] Moreover, the established difficulty in accessing such a sterically congested target is likely to impact the regioselectivity. In other words, the need to form vicinal quaternary centers is expected to favor formation of the undesired linear prenylated isomer. Thirdly, the chemoselectivity of the transformation could be problematic if the indole nitrogen is unprotected and thus nucleophilic. When a hexahydropyrrolo moiety is crafted, a second nucleophilic nitrogen is present which increases the need for a chemoselective reaction at C3.[5] Lastly, the stereochemistry of the process has to be addressed.

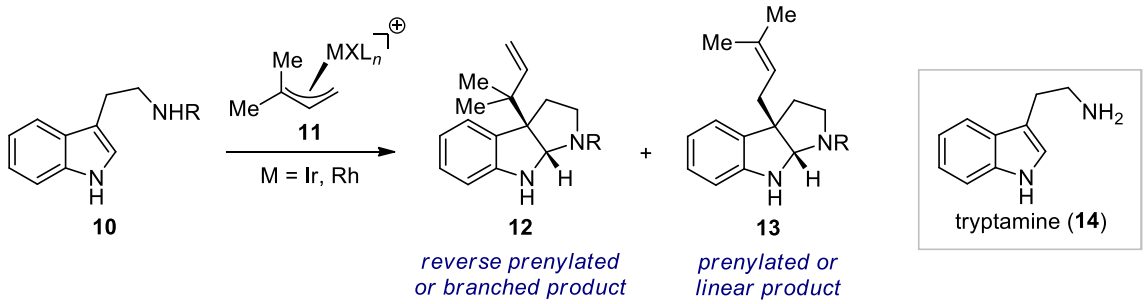

Scheme 1.1 Conceptual alkylative cyclization of a tryptamine derivative **10** with an allyl-metal complex **11** to give either a reverse (**12**) or normal (**13**) prenylated hexahydropyrroloindole. M is either Ir or Rh, R is a protecting group, L and X are ligands, all of which are unspecified.

When an achiral substrate, such as a tryptamine derivative, is employed (Scheme 1.1), the enantioselectivity needs to be controlled. If a chiral substrate is used, such as a tryptophan derivative (Scheme 1.2), two diastereomers can be formed.[6] Despite these difficulties, methods

---

[2] continued (g) Notoamide C: Kato, H.; Yoshida, T.; Tokue, T.; Nojiri, Y.; Hirota, H.; Ohta, T.; Williams, R. M.; Tsukamoto, S. *Angew. Chem., Int. Ed.* **2007**, *46*, 2254. (h) Tryprostatin B: Cui, C. B.; Kakeya, H.; Okada, G.; Onose, R.; Ubukata, M.; Takahashi, I.; Isono, K.; Osada, H. *J. Antibiot.* **1995**, *48*, 1382. (i) Spirotryprostatin B: Cui, C. B.; Kakeya, H.; Osada, H. *J. Antibiot.* **1996**, *49*, 832.

[3] For a review of methods of prenylation and reverse prenylation, see (a) Lindel, T.; Marsch, N.; Adla, S. K. *Top. Curr. Chem.* **2012**, *309*, 67.

[4] Peterson, E. A.; Overman, L. E. *Proc. Natl. Acad. Sci. U.S.A.* **2004**, *101*, 11943.

[5] For a selected, enantio- and chemoselective *N*-allylation of indoles, see: Stanley, L. M.; Hartwig, J. F. *Angew. Chem., Int. Ed.* **2009**, *48*, 7841.

[6] The two distereomers are refered to as *exo*- and *endo*-product. The relative stereochemistry for the 5,5-ring system is always assumed to be *cis*.

for the introduction of a reverse prenyl group at the C3 of an indole or related structures have been documented, namely the transition metal-catalyzed reverse prenylation of oxindoles, isatins, and C3 unsubstituted indoles.[7] However, the regioselectivity of these processes is variable, ranging from perfect regiocontrol to a 2:1 mixture (reverse/normal prenylation).

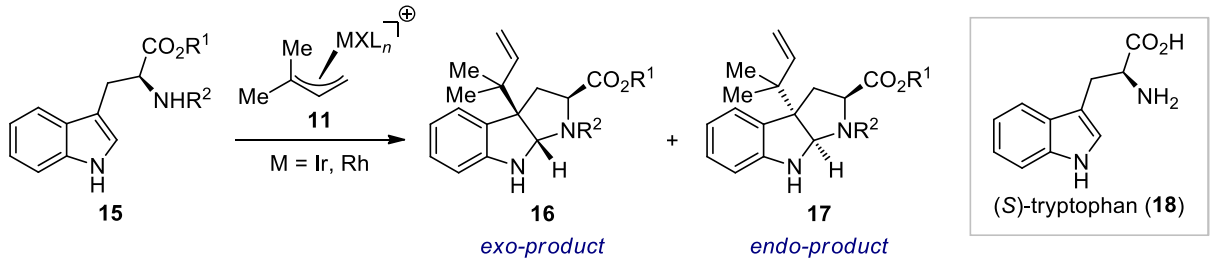

Scheme 1.2 Conceptual alkylative cyclization of a (*S*)-tryptophan derivative **15** with an allyl-metal complex **11** to furnish reverse prenylated hexahydropyrroloindoles with *exo*- (**16**) or *endo*-diastereoselectivity (**17**). Possible normal (linear) prenylated and *N*-prenylated products are not shown. M is either Ir or Rh, R^1 and R^2 are protecting groups, L and X are ligands, all of which are unspecified.

Besides chemical transformations, enzymatic processes to furnish C3 reverse prenylated indole derivatives have been described. Such chemoenzymatic reactions were employed in the synthesis of natural products as well as unnatural prenylated indole derivatives.[8] Substitution reactions at C3 of 3-substituted indole with allyl, substituted allyl and benzylelectrophiles have been reported.[9] However, to the best of our knowledge, chemical methods for the one-step reverse prenylation of 3-substituted indoles at C3 have not been reported.[10]

---

[7] For enantioselective, reverse prenylation of oxindoles, see: (a) Trost, B. M.; Malhotra, S.; Chan, W. H. *J. Am. Chem. Soc.* **2011**, *133*, 7328. For enantioselective, reverse prenylation of isatins, see: (b) Itoh, J.; Han, S. B.; Krische, M. J. *Angew. Chem., Int. Ed.* **2009**, *48*, 6313. For selected examples of one-step C3 reverse prenylation of C3 unsubstituted indoles, see: (c) Kimura, M.; Futamata, M.; Mukai, R.; Tamaru, Y. *J. Am. Chem. Soc.* **2005**, *127*, 4592. (d) Usui, L.; Schmidt, S.; Keller, M.; Breit, B. *Org. Lett.* **2008**, *10*, 1207. (e) Gruber, S.; Zaitsev, A. B.; Woerle, M.; Pregosin, P. S.; Veiros, L. F. *Organometallics* **2008**, *27*, 3796. (f) Sundararaju, B.; Achard, M.; Demerseman, B.; Toupet, L.; Sharma, G. V. M; Bruneau, C. *Angew. Chem., Int. Ed.* **2010**, *49*, 2782.

[8] For selected chemoenzymatic reactions and biosynthetic studies involving reverse prenylation of indoles, see: (a) Yin, W.-B.; Cheng, J.; Li, S.-M. *Org. Biomol. Chem.* **2009**, *7*, 2202. (b) Yin, W.-B.; Xie, X.-L.; Matuschek, M.; Li, S.-M. *Org. Biomol. Chem.* **2010**, *8*, 1133. (c) Yin, W.-B.; Yu, X.; Xie, X.-L.; Li, S.-M. *Org. Biomol. Chem.* **2010**, *8*, 2430. (d) Fan, A.; Li, S.-M. *Adv. Synth. Catal.* **2013**, *355*, 2659. (e) Luk, L. Y. P.; Qian, Q.; Tanner, M. E. *J. Am. Chem. Soc.* **2011**, *133*, 12342. (f) Rudolft, J. D.; Wang, H.; Poulter, C. D. *J. Am. Chem. Soc.* **2013**, *135*, 1895.

[9] For selected enantioselective allylations, see: (a) Trost, B. M.; Quancard, J. *J. Am. Chem. Soc.* **2006**, *128*, 6314. (b) Liu, Y.; Du, H. *Org. Lett.* **2013**, *15*, 740. (c) Zhang, X.; Han, L.; You, S.-L. *Chem. Sci.* **2014**, *5*, 1059. (d) Zhang, X.; Liu, W.-B.; Tu, H.-F.; You, S.-L. *Chemical Science* **2015**, *6*, 4525. (e) Kaiser, T. M.; Yang, J. *Eur. J. Org. Chem.* **2013**, 3983. For selected racemic benzylation and allylations, see: (f) Montgomery, T. D.; Zhu, Y.; Kagawa, N.; Rawal, V. H. *Org. Lett.* **2013**, *15*, 1140. (g) Zhang, X.; Liu, W.-B.; Wu, Q.-F.; You, S.-L. *Org. Lett.* **2013**, *15*, 3746.

[10] The exceptions being the enzyme catalyzed reactions cited in ref 8 and reactions were a two-step process takes place in one pot. For an example of the latter, see: (a) Ignatenko, V. A.; Zhang, P.; Viswanathan, R. *Tetrahedron Lett.* **2011**, *52*, 1269. Of notice, the scope of the chemoenzymatic reactions and the two-step approach is rather limited or was not determined.

So far, total syntheses of natural products bearing this structural motif have relied on multistep processes.[11] Early work by *Takase* and coworkers employed rearrangement of a previously installed prenyl moiety.[11b] This approach was low yielding and furnished the reverse prenylated product without stereocontrol. Later work by *Danishefsky* and coworkers involved an oxidative cyclization followed by a substitution reaction to install the reverse prenyl moiety.[12] The first and most influential example of the latter strategy is discussed below.

The first example of a stereoselective reverse prenylation of a 3-substituted indole within the synthesis of a complex natural product was reported by *Danishefsky* and coworkers in the syntheses of amauromine (**1**) and 5-*N*-acetylardeemine (**2**).[12] Amauromine (**1**) was found to exhibit potent vasodilating activity[13] while 5-*N*-acetylardeemine (**2**) reversed multiple-drug resistance in tumor-cells.[14] The goal of the work by *Danishefsky* and coworkers was not only to achieve the first total syntheses of the aforementioned natural products but also to provide material for biological studies. A practical route to both bioactive compounds needed to be found and the synthetic approach should allow to access analogs of **2** as well. At the outset of the work by *Danishefsky* and coworkers, no stereoselective method to access C3 reverse prenylated tryptamine or tryptophan derivatives was known. Furthermore, the reported multistep methods to access this structural motif from tryptamine derivatives occured with modest yields.[15] Therefore, the development of a new method to access a C3 reverse prenylated hexahydropyrroloindole intermediate was envisioned. A chiral pool approach was first examined, as many variable protected tryptophan derivatives are readily accessible. The existing stereocenter of the amino acid starting material should enable control of the relative stereochemistry. Starting from protected tryptophan **19**, they outlined two possible pathways to access hexahydropyrroloindole intermediate **22**, which was intended to be a precursor for both natural products (Scheme 1.3).

---

[11] For selected examples, see: (a) Bhat, B.; Harrison, D. M. *Tetrahedron Lett.* **1986**, *27*, 5873. (b) Takase, S.; Itoh, Y.; Uchida, I.; Tanaka, H.; Aoki, H. *Tetrahedron* **1986**, *42*, 5887. (c) Kawasaki, T.; Shinada, M.; Ohzono, M.; Ogawa, A.; Terashima, R.; Sakamoto, M. *J. Org. Chem.* **2008**, *73*, 5959. (d) Miller, K. A.; Tsukamoto, S.; Williams, R. M. *Nat. Chem.* **2009**, *1*, 63. (e) Takiguchi, S.; Iizuka, T.; Kumakura, Y.-s.; Murasaki, K.; Ban, N.; Higuchi, K.; Kawasaki, T. *J. Org. Chem.* **2010**, *75*, 1126. (f) Adla, S. K.; Golz, G.; Jones, P. G.; Lindel, T. *Synthesis* **2010**, 2161. See also ref 12.

[12] (a) Marsden, S. P.; Depew, K. M.; Danishefsky, S. J. *J. Am. Chem. Soc.* **1994**, *116*, 11143. (b) Depew, K. M.; Marsden, S. P.; Zatorska, D.; Zatorski, A.; Bornmann, W. G.; Danishefsky, S. J. *J. Am. Chem. Soc.* **1999**, *121*, 11953.

[13] For isolation and bioactivity, see ref 2a, for previous synthesis, see ref 11b.

[14] For isolation see ref 2b, for bioactivity, see: Karwowski, J. P.; Jackson, M.; Rasmussen, R. R.; Humphrey, P. E.; Poddig, J. B.; Kohl, W. L.; Scherr, M. H.; Kadam, S.; McAlpine, J. B. *J. Antibiot.* **1993**, *46*, 374.

[15] (a) Hino, T.; Hasumi, K.; Yamaguchi, H.; Taniguchi, M.; Nakagawa, M. *Chem. Pharm. Bull.* **1985**, *33*, 5202. (b) Nakagawa, M.; Ma, J.; Hino, T. *Heterocycles* **1990**, *30*, 451.

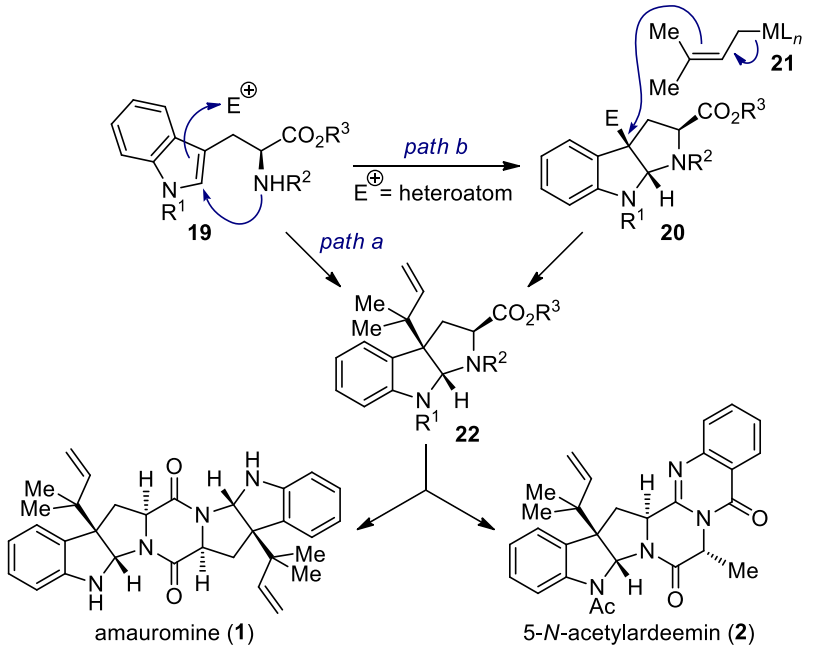

Scheme 1.3 Two possible pathways for the reverse prenylation of tryptophan derivative **19** in the total synthesis of amauromine (**1**) and 5-*N*-acetylardeemine (**2**) as described by *Danishefsky* and coworkers.[12] M is a metal such as Sn, R^1, R^2 and R^3 are protecting groups, L are ligands or alkyl groups, all of which are unspecified. This scheme is adapted from reference 12a.

In the first scenario, a direct alkylative cyclization would lead to **22** installing the reverse prenyl group with formation of the hexahydropyrroloindole (path a). An alternative two-step approach consists of an oxidative cyclization to give intermediate **20** which subsequently undergoes substitution with a prenyl metal species **21** (path b). The authors noted the following about these two options: "*We were not optimistic about the prospects for introduction of a 1,1-dimethallyl moiety at the gem-dimethyl carbon in the required series, in serviceable yield, via direct alkylative cyclization (path a).*"[12a] Therefore, their studies focused on realization of the strategy shown in Scheme 1.3 as path b. Firstly, their goal was to find conditions for a diastereoselective oxidative cyclization to access a compound such as **20**. While such cyclizations were known for tryptamine derivatives,[16] no suitable stereoselective cyclization had been described for tryptophan derivatives at that time. After extensive experimentation by *Danishefsky* and coworkers[12] it was found that a selenocyclization in the presence of anhydrous PPTS accessed selenide **25** from protected tryptophan **24** in good yield and high diastereoselectivity (Scheme 1.4).

[16] For a selected example, see: Bruncko, M.; Crich, D. *J. Org. Chem.* **1994**, *59*, 4239.

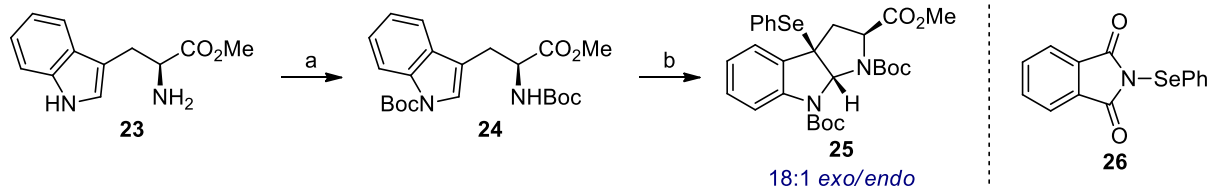

Scheme 1.4 Diastereoselective, oxidative selenocyclization of **24** to yield selenide **25** reported by *Danishefsky* and coworkers in the total synthesis of amauromine (**1**) and 5-*N*-acetylardeemine (**2**).[12] Reagents and conditions: (a) (*S*)-tryptophan methyl ester hydrochloride (**23**•HCl, 1.0 equiv.), NaOH (5.1 equiv.), $(n\text{Bu})_4\text{NHSO}_4$ (0.10 equiv.), Boc_2O (3.0 equiv.), CH_2Cl_2 (0.10 M), 20 h, r.t., **25** isolated in 91% yield. (b) **24** (1.0 equiv.), *N*-phenylselenophthalimide (**26**, 1.5 equiv.), anhyd. PPTS (1.0 equiv.), CH_2Cl_2 (0.12 M), 36 h, r.t., **25** isolated in 93% yield as a 18:1 *exo*/*endo* ratio.

One possible explanation for the predominant formation of the desired *exo*-product is illustrated in Scheme 1.5. Assuming that the initial selenation is reversible under the reaction conditions, both species **27** and **28** can be formed. Cyclization of the Boc-protected amine then leads to either *exo*-product **25** or *endo*-product **29**. The ratio of **25** to **29** was found to be constant during the course of the reaction and it was suggested that **27** is the major compound in the **27**/**28** equilibrium and that the *exo*-product is the kinetic product.[17]

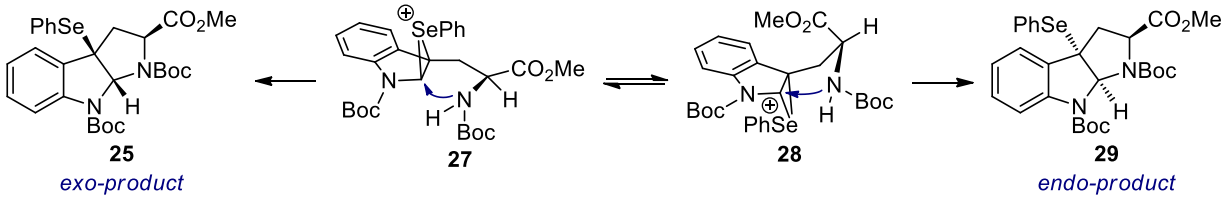

Scheme 1.5 Possible rational for the favored formation of *exo*-product **25** in the selenocyclization of bis(Boc) tryptophan methylester **24** as proposed by *Danishefsky* and coworkers.[12] This scheme is adapted from reference 12b.

Having successfully achieved the stereoselective cyclization to **25**, the second challenge was to install the reverse prenyl group. Again, significant screening of reaction parameters was needed in order to identify the right conditions for this task. The combination of methyl trifluoromethanesulfonate and prenyl tri-*n*-butylstannane as the source of the prenyl group ultimately affected the difficult substitution from **25** to **30** (Scheme 1.6). The diastereoselectivity was not affected by this reaction and after recrystallization, the C3 reverse prenylated product could be isolated as single diastereomer.

[17] The initial assumption made in ref 12a, that the *exo*-product is formed through thermodynamic control was revised in the later publication (ref 12b).

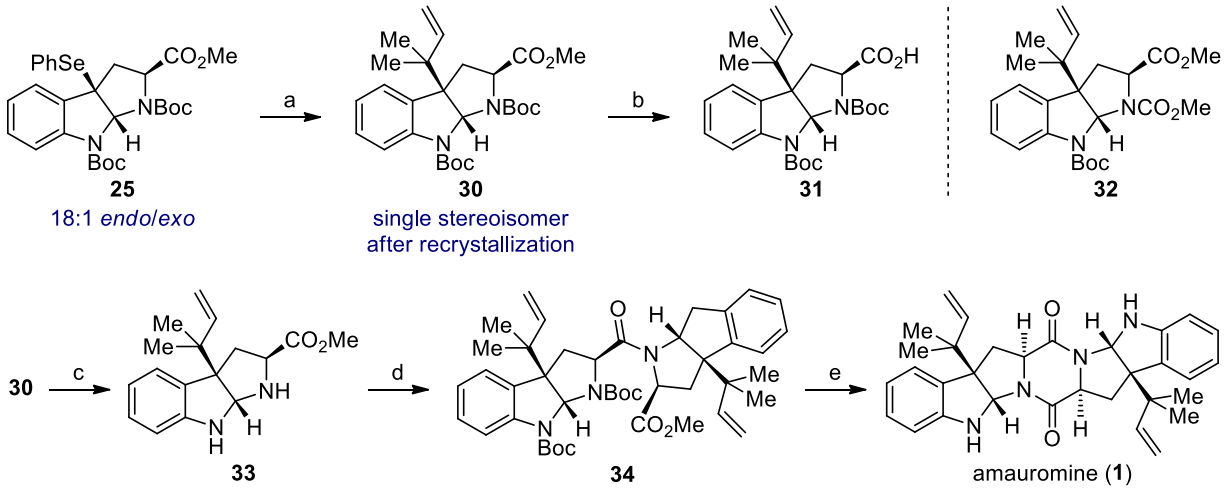

Scheme 1.6 Completion of the total synthesis of (–)-amauromine (**1**) as reported by *Danishefsky* and coworkers.[12] Reagents and conditions: (a) **25** (1.0 equiv.), 2,6-di-*t*butylpyridine (2.0 equiv.), prenyl tri-*n*-butylstannane (1.3 equiv.), methyl trifluoromethanesulfonate (3.9 equiv.), CH_2Cl_2 (0.091 M), 12 h, -10 °C to reflux, 61% yield of **30** (in 18:1 d.r.) and 15% yield of **32** (separated), 57% yield of **30** after recrystallization (single stereoisomer). (b) **30** (1.0 equiv.), aq. NaOH (1.0 M, 5.0 equiv.), THF/MeOH 1:1 (0.060 M), 3 h, reflux, 98% yield. (c) **30** (1.0 equiv.), TMSI (2.3 equiv.), MeCN (0.23 M), 15 min, 0 °C, 83% yield. (d) **33** (1.0 equiv.), **31** (1.1 equiv.), Et_3N (1.1 equiv.), BOP-Cl (1.2 equiv.), CH_2Cl_2 (0.052 M), 20 h, 0 °C to r.t., 78% yield. (e) **34** (1.0 equiv.), TMSI (4.0 equiv.), MeCN (concentration not reported), 30 min, 0 °C, (–)-amauromine (**1**) isolated in 58% yield.

Hydrolysis of the ester and deprotection of the carbamates of **30** furnished **31** and **33**, which were coupled to give amide **34**. The total synthesis of (–)-amauromine (**1**) was completed by deprotection of the carbamate in **34** and spontaneous cyclization under the same conditions. *Danishefsky* and coworkers also reported the synthesis of the related bioactive natural products (–)-ardeemin (**38**) and (–)-5-*N*-acetylardeemin (**2**) (Scheme 1.7).[12] Starting from carboxylic acid **31**, the amide bond formation was found to be troublesome under various conditions[18] and lead to partial epimerization of the α-stereocenter. Ultimately, a two-step procedure involving preparation of the acyl fluoride of **31** and subsequent coupling[19] furnished dipeptide **35** in 71% yield without any observed epimerization. Deprotection of the carbamates was again effected by TMSI, however in contrast to the previous synthesis, exposure to methanolic ammonia and DMAP was required for the cyclization to diketopiperazine **37**. Acylation of **37** and a *Staudinger* type reaction yielded (–)-ardeemin (**38**). The multiple drug resistance reversal agent (–)-5-*N*-acetylardeemin (**2**) was then readily obtained by acetylation of **38** in 71% yield. It is noteworthy that all reactions in Scheme 1.7 were conducted on a scale larger than 15 mmol yielding 6.0 g of (–)-5-*N*-acetylardeemin (**2**) in a single batch.

[18] Examined coupling reagents include DCC/DMAP, DCC/HOBt, isobutyl chloroformate and BOP-Cl
[19] Carpino, L. A.; Mansour, E-S. M. E.; Sadat-Aalaee, D. *J. Org. Chem.* **1991**, *56*, 2611.

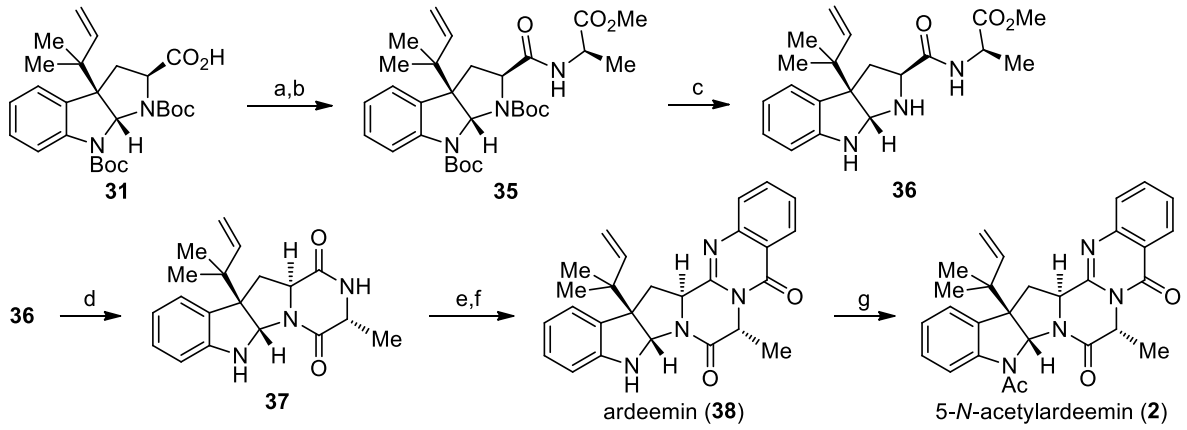

Scheme 1.7 Total synthesis of (–)-5-*N*-acetylardeemin (**2**) from hexahydropyrroloindole **31** as reported by *Danishefsky* and coworkers.[12] Reagents and conditions: (a) **31** (1.0 equiv.), pyridine (1.0 equiv.), cyanuric fluoride (4.0 equiv.), CH_2Cl_2 (0.091 M), 1 h, -15 °C. (b) D-Ala-OMe•HCl (1.0 equiv.), $NaHCO_3$ (2.0 equiv.), CH_2Cl_2/water 1:1 (0.10 M), 1.5 h, r.t., 71% yield from **31**. (c) **35** (1.0 equiv.), TMSI (3.0 equiv.), MeCN (0.10 M), 40 min, 0 °C, 86% yield. (d) **36** (1.0 equiv.), NH_3 (sat. in MeOH, 0.20 M), DMAP (0.40 equiv.), overnight, 0 °C to r.t., 86% yield. (e) **37** (1.0 equiv.), KHMDS (0.5 M in toluene, 1.0 equiv.), 2-azidobenzoyl chloride (2.0 equiv.), THF (0.11 M), 30 min, -15 °C. (f) tri(*n*-butyl)phosphine (1.1 equiv.), benzene (0.10 M), overnight, r.t., 71% yield from **37**. (g) **38** (1.0 equiv.), Ac_2O (0.25 M), *N*,*N*-diisopropylethylamine (3.1 equiv.), 36 h, 60 °C, 71% yield.

In summary, *Danishefsky* and coworkers achieved the first stereoselective total synthesis of (–)-amauromine (**1**), (–)-ardeemin (**38**), and (–)-5-*N*-acetylardeemin (**2**).[12] Furthermore, a novel method was developed for diastereoselective introduction of a reverse prenyl group at C3 of a protected tryptophan. This method was of great importance and influential for application in the synthesis of other targets with this structural feature. As a result of this, most transformations developed were modifications of the work described above.

The group of *Qin* reported a strategically related two-step method for the introduction of the reverse prenyl unit to tryptophan derivative **24** (Scheme 1.8).[20] Their method builds on an *exo*-selective bromocyclization reported by *Lera* and coworkers (step a in Scheme 1.8).[21] Compared to the previous work by *Danishefsky* and coworkers[12] the diastereoselectivity of the oxidative cyclization was slightly improved (from 18:1 to 24:1) and the selenium reagent *N*-phenylselenophthalimide could be replaced by NBS. In the second step, the yield was improved from 57% to 91% albeit with stoichiometric amounts of silver (I) perchlorate employed in this variant (step b, Scheme 1.8). This silver mediated transformation was shown to be suitable to introduce a variety of arenes via a *Friedel-Crafts* type reaction.[20]

[20] Wang, Y.; Kong, C.; Du, Y.; Song, H.; Zhang, D.; Qin, Y. *Org. Biomol. Chem.* **2012**, *10*, 2793.
[21] López, C. S.; Pérez-Balado, C.; Rodríguez-Graña, P.; de Lera, Á. R. *Org. Lett.* **2008**, *10*, 77.

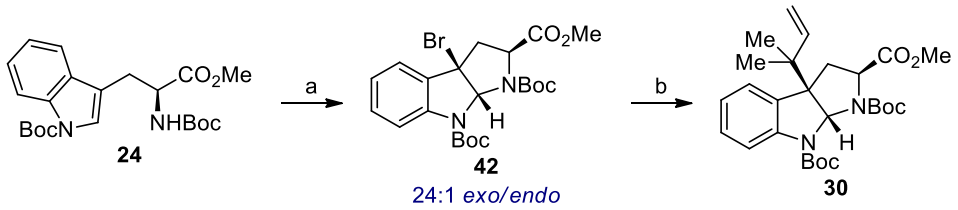

Scheme 1.8 Two-step C3 reverse prenylation of protected tryptophan **24** described by *Qin* and coworkers[20] based on work by *Lera*[21] and *Danishefsky*.[12] Reagents and conditions: (a) **24** (1.0 equiv.), pyridine (1.0 equiv.), PPTS (1.0 equiv.), NBS (1.0 equiv.), CH_2Cl_2 (0.13 M), 4 h, 0 °C, 85% yield. (b) **42** (1.0 equiv.), Cs_2CO_3 (1.5 equiv.), prenyl tri-*n*-butylstannane (1.5 equiv.), $AgClO_4$ (2.0 equiv.), CH_2Cl_2 (0.067 M), 16 h, -78 °C, **30** isolated in 91% yield and undisclosed diastereoselectivity.

Another approach to C3 reverse prenylated indoles was reported by *Ōmura*, *Sunazuka* and coworkers (Scheme 1.9).[22] In contrast from the previous examples, their work started from an achiral compound, namely tryptophol (**43**). Stoichiometric epoxidation under *Sharpless* asymmetric epoxidation conditions furnished **44** in good yield and high enantiomeric excess (72% yield, 99% *ee*).[23] The tertiary alcohol in **44** was activated as trichloroacetimidate **45** and prenyl tri-*n*-butylstannane was again used as source of the prenyl group. Introduction of the reverse prenyl moiety occurred in 91% yield to give **46** with efficiency comparable to the one obtained by *Qin* and coworkers (87% yield). One drawback of the strategy pursued by *Ōmura*, *Sunazuka* and coworkers is that they required rather tedious protecting group manipulations, shown in the steps following intermediate **46**. Nevertheless, they achieved the first total synthesis of (+)-neoxaline (**49**) utilising an enantioselective two-step method for the introduction of the reverse prenyl group present in the target molecule **49**.

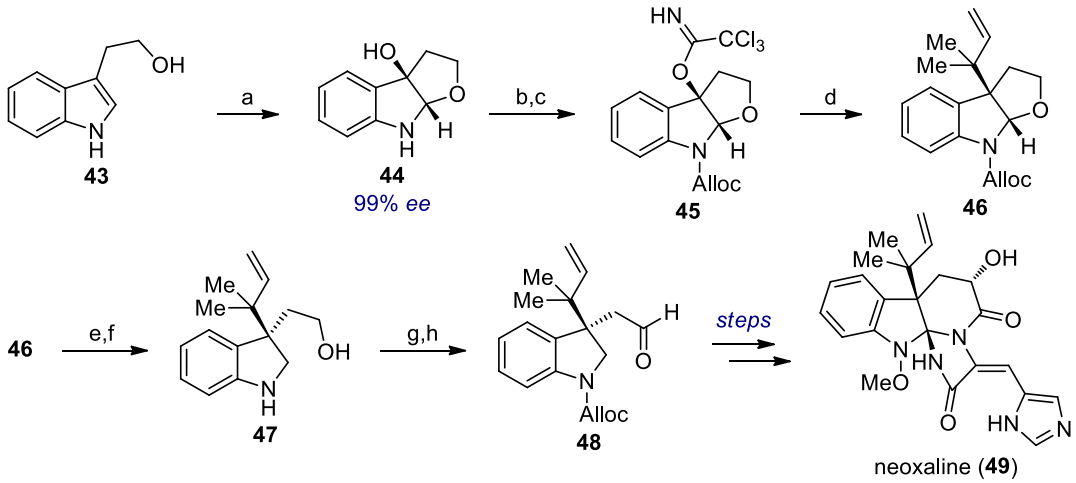

Scheme 1.9 Enantioselective synthesis of C3 reverse prenylated indole derivative **46** in the total synthesis of (+)-neoxaline (**49**) reported by *Ōmura*, *Sunazuka* and coworkers.[22] Reagents and

[22] Ideguchi, T.; Yamada, T.; Shirahata, T.; Hirose, T.; Sugawara, A.; Kobayashi, Y.; Omura, S.; Sunazuka, T. *J. Am. Chem. Soc.* **2013**, *135*, 12568.

conditions: (a) **43** (1.0 equiv.), (+)-diisopropyl tartrate (1.2 equiv.), $Ti(OiPr)_4$ (1.0 equiv.), *t*BuOOH (2.5 equiv.), 4 Å MS, CH_2Cl_2 (0.010 M), 6 h, -20 °C, 72% yield, this step has been reported previously.[23] (b) **44** (1.0 equiv.), allyl chloroformate (4.0 equiv.), water/aq. sat. $NaHCO_3$ 1:1 (0.20 M), 45 min, r.t. (c) Cl_3CCN (12 equiv.), DBU (0.10 equiv.), 2 h, r.t., 94% from **44**. (d) prenyl tri-*n*-butylstannane (1.1 equiv.), BF_3•OEt_2 (1.0 equiv.), CH_2Cl_2 (0.19 M), 5 min, -40 °C, **30** isolated in 87% yield as a single diastereomer. (e) **46** (1.0 equiv.), 5,5-dimethyl-1,3-cyclohexanedione (2.0 equiv.), $Pd(PPh_3)_4$ (0.10 equiv.), MeOH (0.10 M), 2 h, r.t. (f) $NaBH(OAc)_3$ (3.0 equiv.), AcOH (2.0 equiv.), 1,2-dichloroethane (0.20 M), 3 h, r.t, 86% yield from **46**. (g) **47** (1.0 equiv.), allyl chloroformate (4.0 equiv.), water/aq. sat. $NaHCO_3$ 1:1 (0.10 M), 1 h, r.t. (h) DMP (2.0 equiv.), CH_2Cl_2 (0.095 M), 30 min, r.t., 97% yield from **47**.

In summary, various methods for the introduction of a reverse prenyl group at C3 of a 3-substituted indole have been described. However, no general, synthetic method to achieve this goal in one step was known at the outset of the work described herein. Moreover, the synthetic transformations reported in the course of total syntheses of complex natural products relied on the use of stoichiometric prenyl tri-*n*-butylstannane. Alternative approaches were low yielding, lacked stereocontrol, or were not applicable to the synthesis of natural products. Given the interest of our group in Ir-catalyzed allylic substitution reactions and the utilization of them in complex settings,[24] we envisioned the development of an Ir-catalyzed reverse prenylation reaction of indoles. The high intrinsic selectivity for the branched product observed in Ir-catalyzed allylic substitutions[25] should facilitate this task. The goal was to disclose a direct alkylative reverse prenylation of 3-substituted indoles based on an Ir-catalyzed allylic substitution. As such, the transformation would not require the quantitative use of organometallic reagents. Such an approach would access a C3 reversed prenylated hexahydropyrroloindole in fewer steps than the previous approaches. Depending on the protecting groups employed, the step count may be further reduced.

---

[23] (a) Sunazuka, T.; Hirose, T.; Shirahata, T.; Harigaya, Y.; Hayashi, M.; Komiyama, K.; Ōmura, S.; Smith, A. B., III. *J. Am. Chem. Soc.* **2000**, *122*, 2122. (b) When using the catalytic variant the yield and enantioselectivity of the reaction was found to be considerably lower (*e.g.* 37% yield, 28% *ee*).

[24] For selected enantio- and diastereoselective Ir-catalyzed allylic substitution reactions from our group, see: (a) Schafroth, M. A.; Sarlah, D.; Krautwald, S.; Carreira, E. M. *J. Am. Chem. Soc.* **2012**, *134*, 20276. (b) Krautwald, S.; Sarlah, D.; Schafroth, M. A.; Carreira, E. M. *Science* **2013**, *340*, 1065. (c) O, F.; Kravina, A. G.; Carreira, E. M. *Angew. Chem., Int. Ed.* **2013**, *52*, 12166. (d) Krautwald, S.; Schafroth, M. A.; Sarlah, D.; Carreira, E. M. *J. Am. Chem. Soc.* **2014**, *136*, 3020. For selected enantioselective Ir-catalyzed allylic substitution reactions from our group, see: (e) Lafrance, M.; Roggen, M.; Carreira, E. M. *Angew. Chem., Int. Ed.* **2012**, *51*, 3470. (f) Hamilton, J. Y.; Sarlah, D.; Carreira, E. M. *Angew. Chem., Int. Ed.* **2015**, *54*, 7644.

[25] (a) Takeuchi, R.; Kashio, M. *Angew. Chem., Int. Ed.* **1997**, *36*, 263. (b) Takeuchi, R.; Kashio, M. *J. Am. Chem. Soc.* **1998**, *120*, 8647. (c) Janssen, J. P.; Helmchen, G. *Tetrahedron Lett.* **1997**, *38*, 8025. (c) Ohmura, T.; Hartwig, J. F. *J. Am. Chem. Soc.* **2002**, *124*, 15164. (d) Kiener, C. A.; Shu, C.; Incarvito, C.; Hartwig, J. F. *J. Am. Chem. Soc.* **2003**, *125*, 14272. (e) Leitner, A.; Shekhar, S.; Pouy, M. J.; Hartwig, J. F. *J. Am. Chem. Soc.* **2005**, *127*, 15506. (f) Yamashita, Y.; Gopalarathnam, A.; Hartwig, J. F. *J. Am. Chem. Soc.* **2007**, *129*, 7508. (f) Marković, D.; Hartwig, J. F. *J. Am. Chem. Soc.* **2007**, *129*, 11680. (g) Madrahimov, S. T.; Markovic, D.; Hartwig, J. F. *J. Am. Chem. Soc.* **2009**, *131*, 7228. (h) Hartwig, J. F.; Stanley, L. M. *Acc. Chem. Res.* **2010**, *43*, 1461. (i) Madrahimov, S. T.; Li, Q.; Sharma, A.; Hartwig, J. F. *J. Am. Chem. Soc.* **2015**, *137*, 14968.

In the following chapter, the realization of this concept is described. The scope of the method and its application in a direct and stereoselective reaction with a tryptophan derivative is outlined. The latter was employed in the total synthesis of two natural products, and (+)-aszonalenin (**130**) and (–)-brevicompanine B (**132**).

2 Results and Discussion

2.1 Initial Reaction Development

2.1.1 Development of a Reverse Prenylation Reaction of 3-Substituted Indoles

The reaction development was initiated with subjecting Boc-protected trypamine **50** to allylic substitution conditions related to the ones previously employed in our group.[26] In the presence of an acid promoter a reaction took place but no desired C3 allylated product was observed. Instead it is believed that the allylation occurred at C2 of the indole (Scheme 2.1, tentatively assigned structure **52**).

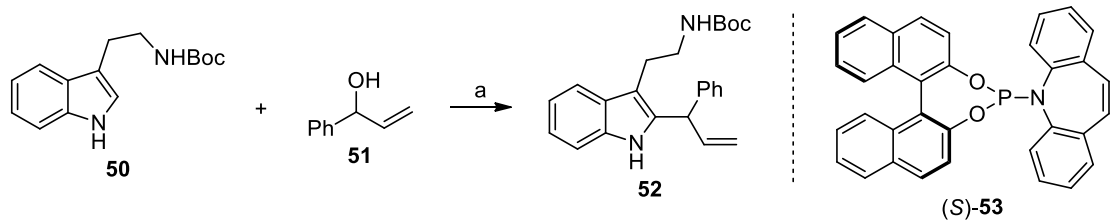

Scheme 2.1 Examination of the Ir-catalyzed allylic substitution of allylic alcohol **51** with Boc-protected tryptamine **50** as a preliminary experiment for the intended reverse prenylation. Reagents and conditions: (a) **50** (1.0 equiv.), (±)-**51** (1.1 equiv.), Cl_3CCO_2H (0.34 equiv.), [{Ir(cod)Cl}$_2$] (0.028 equiv.), (*S*)-**53** (0.13 equiv.), 1,2-dichloroethane (0.38 M), r.t., 12 h, convn. not determined, **52** is the tentatively assigned structure, the *ee* was not determined, the reaction was run on a 0.073 mmol scale.

Changing to basic conditions required the use of a leaving group on the allylic alcohol. The desired C3 allylated product was first observed when carbonate **55** was allowed to react with tryptamine **54** in the presence of KO*t*Bu and Et_3B (Scheme 2.2). The activation of indoles with these two reagents has been described previously. It was also shown, that with this activation C3 alkylation occures in high yield when using activated electrophiles (such as BnBr).[27]

---

[26] For selected examples, see: (a) C. Defieber, M.A. Ariger, P. Moriel, E.M. Carreira, *Angew. Chem., Int. Ed.* **2007**, *46*, 3139. (b) Roggen, M.; Carreira, E. M. *Angew. Chem., Int. Ed.* **2011**, *50*, 5568. (c) Roggen, M.; Carreira, E. M. *Angew. Chem., Int. Ed.* **2012**, *51*, 8652. (d) Schafroth, M. A.; Sarlah, D.; Krautwald, S.; Carreira, E. M. *J. Am. Chem. Soc.* **2012**, *134*, 20276. (e) Hamilton, J. Y.; Sarlah, D.; Carreira, E. M. *Angew. Chem., Int. Ed.* **2013**, *52*, 7532. (f) Krautwald, S.; Schafroth, M. A.; Sarlah, D.; Carreira, E. M. *J. Am. Chem. Soc.* **2014**, *136*, 3020. (g) Hamilton, J. Y.; Hauser, N.; Sarlah, D.; Carreira, E. M. *Angew. Chem., Int. Ed.* **2014**, *53*, 10759. (h) Breitler, S.; Carreira, E. M. *J. Am. Chem. Soc.* **2015**, *137*, 5296.

[27] (a) Lin, A.; Yang, J.; Hashim, M. *Org. Lett.* **2013**, *15*, 1950. (b) For related reports on the use of Et_3B, see ref 7c and references therein.

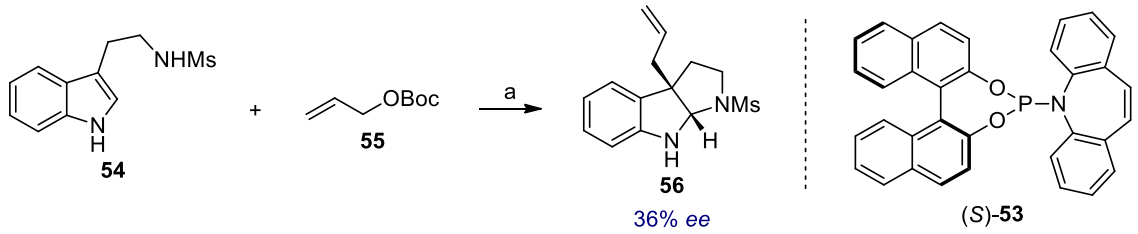

Scheme 2.2 Reagents and conditions: (a) **54** (1.0 equiv.), **55** (1.2 equiv.), KO*t*Bu (1.3 equiv.), Et_3B (1.1 equiv., 1.0 M in hexanes), [{Ir(cod)Cl}$_2$] (0.030 equiv.), (*S*)-**53** (0.13 equiv.), 1,4-dioxane (0.25 M), r.t., 16 h, 86% convn. as estimated by ^{1}H-NMR analysis of the crude product, an arbitrary enantiomer of **56** is shown, **56** isolated with 36% *ee*, the reaction was run on a 0.13 mmol scale.

With a catalyst generated in situ from [{Ir(cod)Cl}$_2$] and ligand **53**, allylated hexahydropyrroloindole **56** was isolated in low enantiomeric excess (36% *ee*). Encouraged by the reactivity observed, more hindered allylic carbonate **57** was examined under the same conditions (Scheme 2.3). Pleasingly, C3 allylated product **58** was formed, albeit with low stereocontrol.

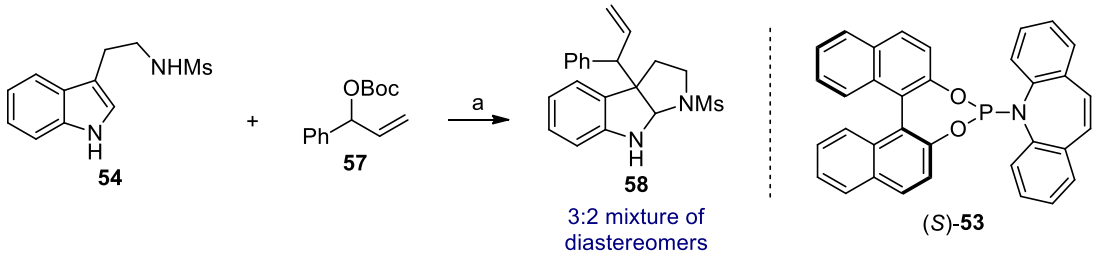

Scheme 2.3 Reagents and conditions: (a) **54** (1.0 equiv.), (±)-**57** (1.0 equiv.), KO*t*Bu (1.0 equiv.), Et_3B (1.0 equiv., 1.0 M in hexanes), [{Ir(cod)Cl}$_2$] (0.025 equiv.), (*S*)-**53** (0.12 equiv.), 1,4-dioxane (0.20 M), r.t., 21 h, 71% convn. as estimated by ^{1}H-NMR analysis of the crude product, **58** obtained in a ~3:2 mixture of diastereomers, the enantioselectivity of both diastereomers was not determined, the reaction was run on a 0.26 mmol scale.

Subsequently, the envisioned reverse prenylation was studied. When **54** was allowed to react with carbonate **59** in presence of a Rh^I catalyst, C3 reverse prenylated product **60** was isolated (Scheme 2.4). Compared to the allylation with the less hindered electrophiles **55** and **57**, this transformation required heating (50 °C). Of note, an Ir^I and Rh^I catalyst yielded the desired product, however, the Rh-catalyzed reaction showed higher conversion. At this point, no enantioinduction was observed, thus **60** was furnished as the racemate.

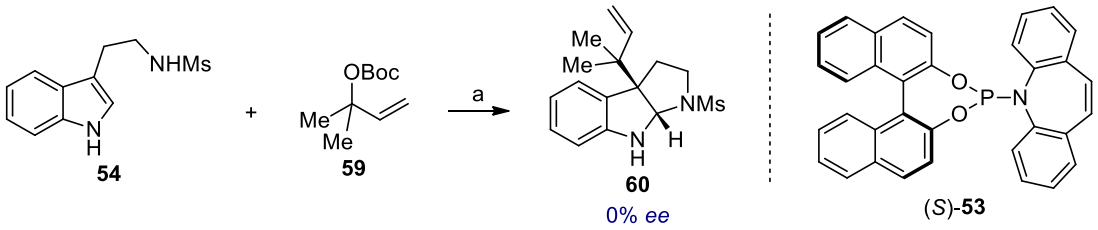

Scheme 2.4 Reagents and conditions: (a) **54** (1.0 equiv.), **59** (1.8 equiv.), KO*t*Bu (1.3 equiv.), Et_3B (1.1 equiv., 1.0 M in hexanes), $[Rh(cod)_2SbF_6]$ (0.026 equiv.), (*S*)-**53** (0.11 equiv.), 1,4-dioxane/CH_2Cl_2 6:1 (0.20 M), 50 °C, 24 h, 63% convn. as judged by ^{1}H-NMR analysis of the crude material, **60** isolated with 0% *ee*, the reaction was run on a 0.14 mmol scale.

An initial screening of chiral ligands with Ir^I and Rh^I organometallic complexes was conducted (Table 2.1). None of the combinations tested provided **60** with any measurable enantiomeric excess. The good conversion observed for catalysts generated from Ir^I and Rh^I organometallic complexes warranted further investigations with both metals.

Table 2.1 Preliminary screening of chiral ligands and metal complexes in the C3 reverse prenylation of tryptamine derivative **54**. Representative conditions (entry 2): (a) **54** (1.0 equiv.), **59** (2.2 equiv.), KO*t*Bu (1.5 equiv.), Et_3B (1.3 equiv., 1.0 M in hexanes), $[\{Ir(cod)Cl\}_2]$ (0.037 equiv.), **61** (0.13 equiv.), 1,4-dioxane (0.19 M), convn. estimated by ^{1}H-NMR analysis of the crude material, the reaction was run on a 0.077 mmol scale. Prior to the addition ligand **61** and $[\{Ir(cod)Cl\}_2]$ were stirred in THF/*n*-propylamine 1:1 (0.6 mL, 50 °C, 45 min), followed by concentration under reduced pressure. This activation was only conducted for entry 2.

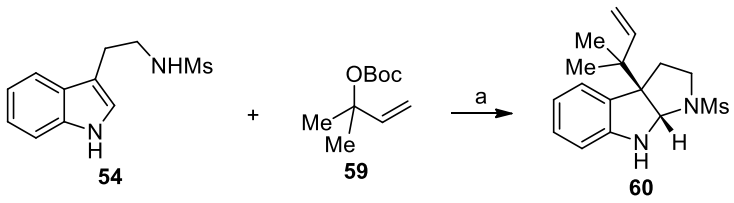

Entry	Metal Source	Ligand	Conditions	Conversion	*ee* (**60**)
1	$[\{Ir(cod)Cl\}_2]$	(*S*)-**53**	67 h, 60 °C	74%	0%
2	$[\{Ir(cod)Cl\}_2]$	**61**	21 h, 70 °C	85%	0%
3	$[Rh(cod)_2SbF_6]$	(*S*)-**53**	24 h, 50 °C	60%	0%
4	$[\{Rh(C_2H_4)_2Cl\}_2]$	**62**	21 h, 70 °C	<5%	n. d.
5	$[\{Rh(C_2H_4)_2Cl\}_2]$	**63**	21 h, 70 °C	<10%	n. d.

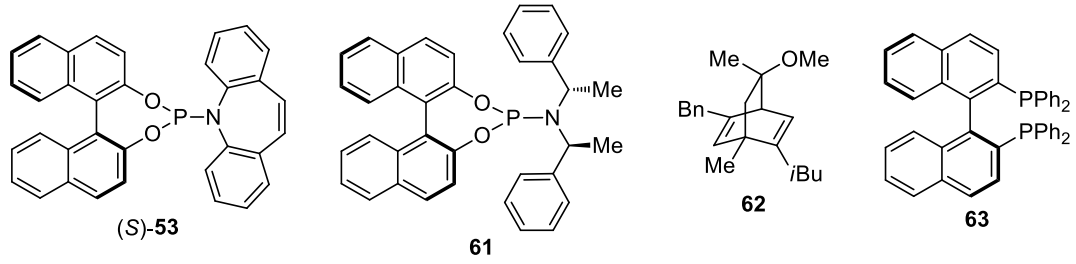

Because the Rh-catalyzed transformation showed a higher reactivity, a screening of chiral ligands was performed exclusively with Rh^I complexes (Table 2.2). Surprisingly, the linear

(normal) prenylated product **65** was generated in high selectivity (20:1) with a 1/1 ligand to Rh ratio (entry 1). Branched product **64** was formed predominantely when the ratio was changed to 2/1 (ligand to Rh). However, the regioselectivities were considerably lower than with an Ir-catalyst, ranging from 4:1 to 6:1 (entries 2-5). The enantioselectities of both regioisomers was found to be minimal throughout this survey. The three phosphine-olefin phosphoramidite ligands evaluated showed similar regio- and enantioselectivities (entries 3-5). No distinct difference between Rh^I complexes with a chloride or a weakly coordinating SbF_6 counterion was observed.

Table 2.2 Follow-up screening of chiral ligands and metal complexes in the reverse prenylation of tryptamine derivative **50**. Representative conditions (entry 4): (a) **50** (1.0 equiv.), **59** (2.0 equiv.), KO*t*Bu (1.4 equiv.), Et_3B (1.1 equiv., 1.0 M in THF), $[Rh(cod)_2SbF_6]$ (0.040 equiv.), **66** (0.13 equiv.), 1,4-dioxane (0.32 M), 45 °C, 3 d, ~75% convn. estimated by ^{1}H-NMR analysis of the crude material, the reaction was run on a 0.081 mmol scale. An arbitrary enantiomer is shown for **64** and **65**.

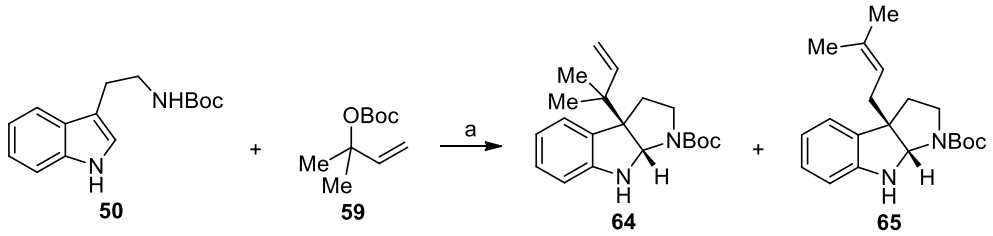

Entry	Metal Source	Ligand	Ligand/Rh	64/65	*ee* (64)	*ee* (65)
1	$[\{Rh(C_2H_4)_2Cl\}_2]$	(*S*)-**53**	1:1	1/20	–9%	23%
2	$[\{Rh(C_2H_4)_2Cl\}_2]$	(*S*)-**53**	2:1	4/1	0%	23%
3	$[Rh(cod)_2SbF_6]$	(*S*)-**53**	2:1	6/1	0%	–5%
4	$[Rh(cod)_2SbF_6]$	**66**	2:1	4/1	13%	13%
5	$[Rh(cod)_2SbF_6]$	**67**	2:1	4/1	5%	9%

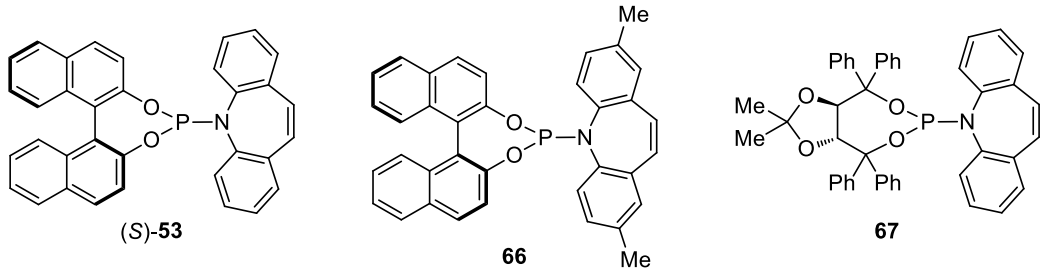

In order to gain more insight in the differences of the Rh^I and Ir^I catalytic systems, allylation of **50** was examined (Scheme 2.5). Under the same conditions a low *ee* was obtained under Ir-catalysis but racemic **50** was isolated when using a Rh catalyst.

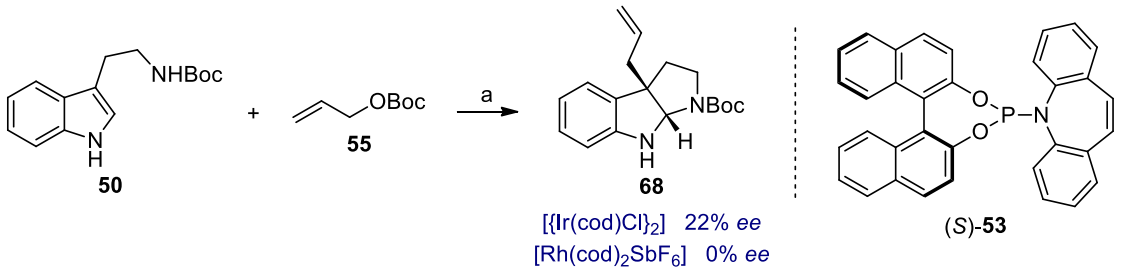

Scheme 2.5 Reagents and conditions: (a) **50** (1.0 equiv.), **55** (1.5 equiv.), KO*t*Bu (1.4 equiv.), Et_3B (1.1 equiv., 1.0 M in THF), [{Ir(cod)Cl}$_2$] (0.028 equiv.), (*S*)-**53** (0.19 equiv.), 1,4-dioxane (0.26 M), r.t., 26 h, >95% convn. estimated by ^{1}H-NMR analysis of the crude material, the reaction was run on a 0.13 mmol scale, under these conditions **68** was isolated with 22% *ee* and an arbitrary enantiomer of **68** is shown. When conducting the reaction under the same conditions but with [$Rh(cod)_2SbF_6$], the conversion was found to be lower (21%) and **68** was obtained as a racemate.

It was speculated that triethylborane may influence the catalyst and lower the enantioselectivity. Therefore, Ir-catalyzed allylic substitution of racemic **69** with benzylalcohol as nucleophile was studied (Scheme 2.6). A substantial decrease in the enantiomeric excess of **70** was observed in the presence of Et_3B (80% *ee* to 32% *ee*). Since this transformation is quite different from the reverse prenylation, this finding is not necessarily true in the latter case. However, it led to the examination of a variety of other activation modes for the indole. In this regard, most attempts were not successful, yielding no desired product. On the other hand, when the transformation occurred in the absence of Et_3B the *ee* was still found to be low (*vide infra*).

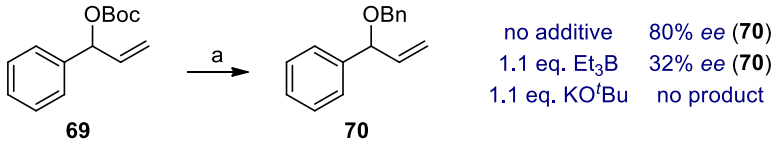

Scheme 2.6 Reagents and conditions: (a) (±)-**69** (1.0 equiv.), BnOH (5.0 equiv.), additive (none or 1.1 equiv.), [{Ir(cod)Cl}$_2$] (0.023 equiv.), (*S*)-**53** (0.10 equiv.), 1,4-dioxane (0.43 M), r.t., 24 h, the reaction was run on a 0.087 mmol scale.

A rare case where reverse prenylation of a 3-substituted indole occurred in the absence of Et_3B and added base is shown in Scheme 2.7. Decarboxylative prenylation occured with low enantioinduction when an Ir-catalyst was used. No reaction took place with a Rh-catalyst under the same conditions.

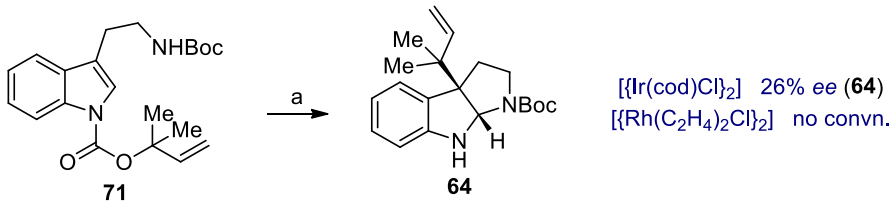

Scheme 2.7 Reagents and conditions: (a) **71** (1.0 equiv.), [{Ir(cod)Cl}$_2$] (0.042 equiv.), (*S*)-**53** (0.21 equiv.), THF (0.19 M), 65 °C, 13 h, >95% convn. estimated by ^{1}H-NMR analysis of the crude material, the reaction was run on a 0.067 mmol scale, under these conditions **64** was isolated with 26% *ee* and an arbitrary enantiomer of **64** is shown. When conducting the reaction under the same conditions but with [{Rh(C_2H_4)$_2$Cl}$_2$], no product was formed.

Trialkylboranes were employed as additives in the C3 allylation of indoles by *Tamaru* and coworkers[7c] (in contrast to the work by *Yang* and coworkers[27a] without additional base). In the corresponding enantioselective Pd-catalyzed C3 allylation of 3-substituted indoles reported by *Trost* and coworkers, the use of a sterically more demanding trialkylborane increased the enantioselectivity.[9a] For this reason the effect of replacing Et_3B with 9-BBN-(*c*Hex) was studied (Table 2.3). With KO*t*Bu as base, reverse prenylated **64** was obtained as racemate (as for Et_3B, see Table 2.2, entry 2). The combination of KHMDS and 9-BBN-(*c*Hex) provided **64** in 33% *ee*.

Table 2.3 Evaluation of 9-BBN-*n*C_6H_{13} as a sterically more hindered borane in the reverse prenylation of tryptamine derivative **50**. Representative conditions (entry 2): (a) **50** (1.0 equiv.), **59** (1.5 equiv.), KHMDS (1.1 equiv.), 9-BBN-*n*C_6H_{13} (0.90 equiv., 1.0 M in THF), [{Rh(C_2H_4)$_2$Cl}$_2$] (0.020 equiv.), (*S*)-**53** (0.10 equiv.), THF (0.23 M), 60 °C, 2 d, the reaction was run on a 0.12 mmol scale.

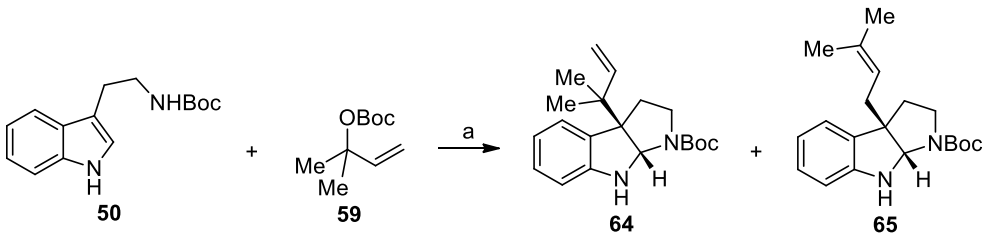

Entry	Base	64/65	*ee* (**64**)	*ee* (**65**)
1	KO*t*Bu	5/1	0%	5%
2	KHMDS	3/1	33%	9%

Given the challenges to induce enantioselectivity in the reverse prenylation with chiral Rh- or Ir-catalysts, the racemic reaction was studied instead. Because the regioselectivity was generally higher under Ir-catalysis, the corresponding Rh-catalyzed reaction was not studied further. The four possible combinations from employing either [{Ir(cod)Cl}$_2$] or [{Rh(cod)Cl}$_2$] with or without ligand **72** (in a 2:1 ratio to Ir or Rh) were studied. The highest

conversion was obtained with ligand **72** in a 2/1 ratio to Ir furnishing (±)-**64** in 71% yield (Scheme 2.8). The optimization of the racemic reverse prenylation reaction of indoles was conducted based on this result.

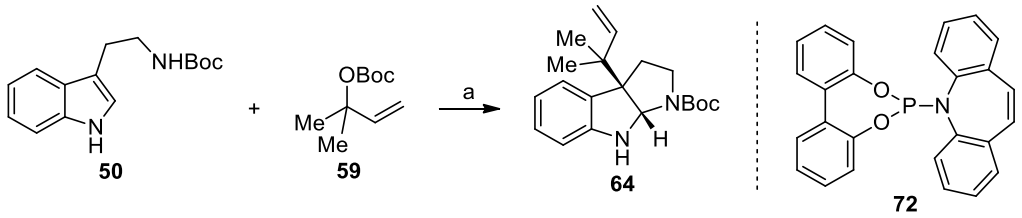

Scheme 2.8 Reagents and conditions: (a) **50** (1.0 equiv.), **59** (1.5 equiv.), KO*t*Bu (1.1 equiv.), Et_3B (1.2 equiv., 1.0 M in THF), [{Ir(cod)Cl}$_2$] (0.029 equiv.), **72** (0.14 equiv.), 1,4-dioxane (0.31 M), 60 °C, 22 h, the reaction was run on a 0.15 mmol scale, (±)-**64** isolated in 71% yield.

For the optimization studies described in the next chapter, substrate **73** was prepared. The F-substituent in vicinity to the newly formed bond greatly facilitated the screening process due to analysis of the reaction by ^{19}F-NMR. Ir-catalyzed reverse prenylation of **73** occurred smoothly to yield **74** in high branched to linear selectivity (Scheme 2.9). The linear regioisomer could be accessed through Pd-catalysis and by using the regioisomeric carbonate **84**.

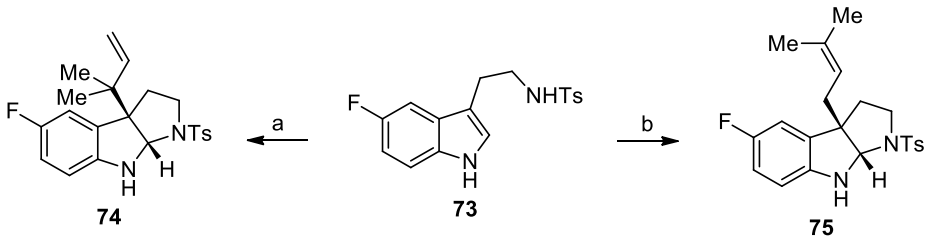

Scheme 2.9 Reagents and conditions: (a) **73** (1.0 equiv.), **59** (2.0 equiv.), KO*t*Bu (1.1 equiv.), Et_3B (1.2 equiv., 1.0 M in THF), [{Ir(cod)Cl}$_2$] (0.027 equiv.), **72** (0.052 equiv.), 1,4-dioxane (0.25 M), 50 °C, 2 h, 85% convn. to (±)-**74** and 31:1 regioselectivity (**74/75**) as estimated by ^{19}F-NMR analysis of the crude material, the reaction was run on a 0.10 mmol scale. (b) **73** (1.0 equiv.), **84** (2.0 equiv.), KO*t*Bu (1.1 equiv.), Et_3B (1.2 equiv., 1.0 M in THF), $Pd(PPh_3)_4$ (0.039 equiv.), 1,4-dioxane (0.17 M), 50 °C, 2 h, the reaction was run on a 0.10 mmol scale, 29:1 regioselectivity (**75/74**) as estimated by ^{19}F-NMR analysis of the crude material, (±)-**75** isolated in 56% yield and 33:1 regioselectivity (**75/74**, determined by ^{19}F-NMR analysis) after purification.

A selected preliminary result with a different electrophile is illustrated in Scheme 2.10. When linalool derived tertiary carbonate (±)-**77** was subjected to the reaction conditions, reverse geranylated product **78** was formed in 83% yield. Using an achiral ligand, the diastereocontrol was low (3.5:1) but this result suggested that other electrophiles may be engaged in the disclosed indole functionalization. A method for the enantioselective normal and reverse geranylation of oxindoles has been reported by *Trost* and coworkers.[7a] Only few C3

geranylated indole natural products are known to date[28] and no reverse geranylated natural product has been isolated.[29]

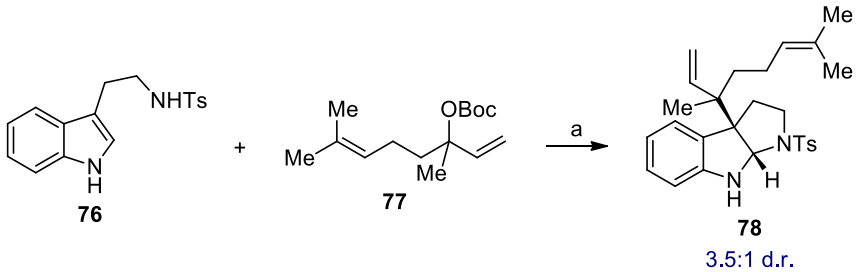

Scheme 2.10 Reagents and conditions: (a) **76** (1.0 equiv.), (±)-**77** (1.4 equiv.), KO*t*Bu (1.1 equiv.), Et_3B (1.1 equiv., 1.0 M in THF), [{Ir(cod)Cl}$_2$] (0.010 equiv.), **87** (0.020 equiv.), 1,4-dioxane (0.23 M), 24 °C, 4 h, the reaction was run on a 1.0 mmol scale, (±)-**78** isolated in 83% yield and a 3.5:1 mixture of diastereomers, an arbitrary stereoisomer of (±)-**78** is shown.

2.2 Optimization Process

2.2.1 Reverse Prenylation of 3-Substituted Indoles

Most of the optimization reactions were conducted with tosylate **73**. This is because the F-substituent in **72** facilitated the analysis of the outcome through ^{19}F-NMR. Various derivatives of 2-methyl-3-buten-2-ol and one 3-methyl-2-buten-1-ol derivative were examined as sources of the prenyl group (Table 2.4). A high regioselectivity was obtained for many derivatives (entries 1-4) and only in one case linear product **75** was predominantly generated (entry 7). The reactivity was largely different, yielding in conversions from 92% to 1%. Tertiary carbonate **59** proved to be the best choice among the allylic alcohol derivatives tested.

[28] (a) Peters, L.; König, G. M.; Terlau, H.; Wright, A. D. *J. Nat. Prod.* **2002**, *65*, 1633. (b) Rochfort, S. J.; Moore, S.; Craft, C.; Martin, N. H.; Van Wagoner, R. M.; Wright, J. L. C. *J. Nat. Prod.* **2009**, *72*, 1773.
[29] Search done with Reaxys®, December 16, 2015.

Table 2.4 Screening of 2-methyl-3-buten-2-ol derivatives and one 3-methyl-2-buten-1-ol derivative in the racemic reverse prenylation of tryptamine derivative **73**. Reagents and conditions: (a) **73** (1.0 equiv.), allylic alcohol derivative (2.0 equiv.), KO*t*Bu (1.1 equiv.), Et_3B (1.2 equiv., 1.0 M in THF), [{Ir(cod)Cl}$_2$] (0.030 equiv.), **72** (0.060 equiv.), 1,4-dioxane (0.27 M), 50 °C, 3.5 h, ratio **74/75** and convn. estimated by ^{19}F-NMR analysis of the crude material, the reactions were run on a 0.10 mmol scale.

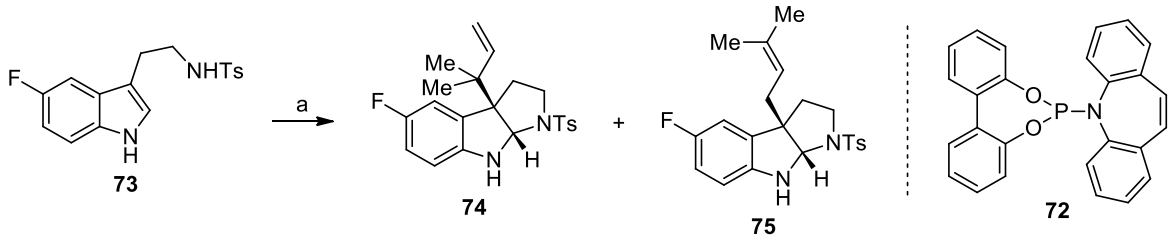

Entry	Allylic Alcohol Derivative	74/75	Conversion
1	**59**	22/1	92%
2	**79**	32/1	50%
3	**80**	22/1	21%
4	**81**	>50/1	35%
5	**82**	9/1	2%
6	**83**	2/1	30%
7	**84**	1/5	1%

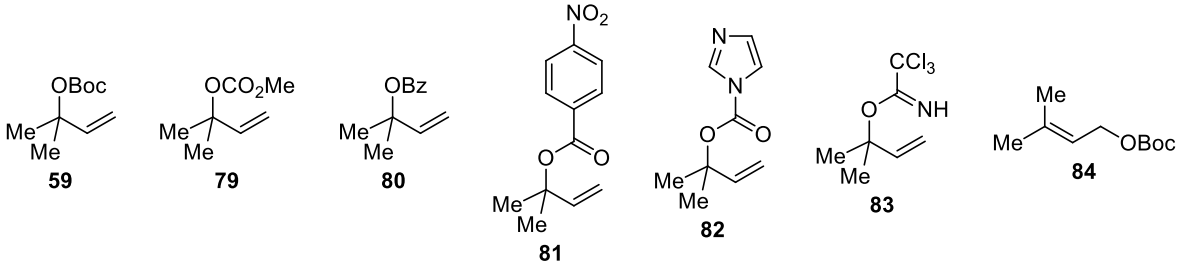

Evaluating the Ir-catalyzed reaction between **73** and **59**, an initial ligand screening was performed (Table 2.5). In general a ligand to Ir ratio of 1/1 resulted in increased reactivity while the regioselecitivity was not decreased. The use of phosphoramidite ligands resulted in better conversion compared to the phosphine and phosphite ligands tested. Phosphoramidite ligand **85** gave the best results. The difference between **72** and **85** was marginal under these conditons and therefore these ligands were re-examined in a later screnning. The reaction time was shortend in this follow-up study in order to obtain a clearer difference between these two ligands.

Table 2.5 Initial ligand screening in the racemic reverse prenylation of tryptamine derivative **73**. Reagents and conditions: (a) **73** (1.0 equiv.), **59** (2.0 equiv.), KO*t*Bu (1.1 equiv.), Et_3B (1.2 equiv., 1.0 M in THF), [{Ir(cod)Cl}$_2$] (0.030 equiv.), ligand (0.060 or 0.012 equiv.), 1,4-dioxane (0.20 M), 50 °C, 4 h, ratio **74/75** and convn. estimated by ^{19}F-NMR analysis of the crude material, the reactions were run on a 0.10 mmol scale.

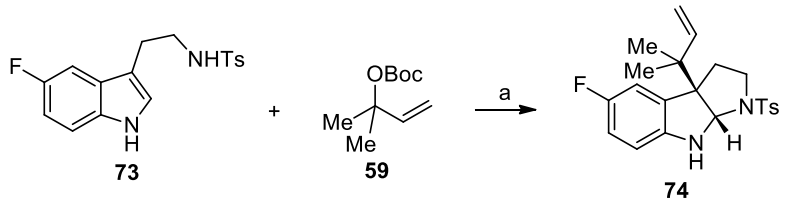

Entry	Ligand	Ligand/Ir	74/75	Conversion
1	**72**	1:1	20:1	94%
2	**72**	2:1	8:1	18%
3	**85**	1:1	>20:1	96%
4	(*R*)-**53**	1:1	5:1	80%
5	(*R*)-**53**	2:1	5:1	<5%
6	PPh_3	1:1	20:1	13%
7	$(tBu)_2MePBF_4H$	1:1	>20:1	21%
8	$P(OPh)_3$	1:1	18:1	45%

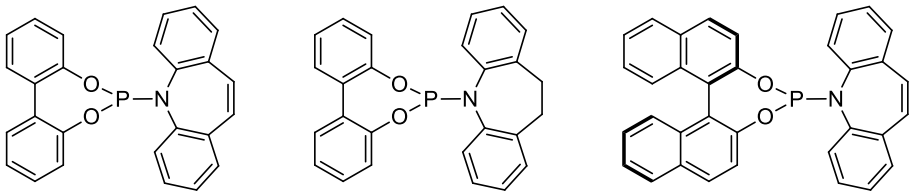

A follow-up ligand screening was conducted with the same reactants and conditions but the reaction was stopped earlier (3 h at 50 °C instead of 4 h at 50 °C, Table 2.6). Prenylated **74** was accessed with excellent regioselectivity for all but one ligand (**53**). The observation made in the previous ligand screening, namely that ligand **85** leads to a higher conversion compared to **72**, was confirmed. Again, the differences were marginal (95% versus 92% convn.). The use of ligand **86**, which has not been evaluated before, resulted in low reactivity (10% convn., entry 4).

Table 2.6 Follow-up ligand screening in the racemic reverse prenylation of tryptamine derivative **73**. Reagents and conditions: (a) **73** (1.0 equiv.), **59** (2.0 equiv.), KO*t*Bu (1.1 equiv.), Et_3B (1.2 equiv., 1.0 M in THF), [{Ir(cod)Cl}$_2$] (0.030 equiv.), ligand (none or 0.060 equiv.), 1,4-dioxane (0.20 M), 50 °C, 3 h, ratio **74/75** and convn. estimated by ^{19}F-NMR analysis of the crude material, the reactions were run on a 0.10 mmol scale.

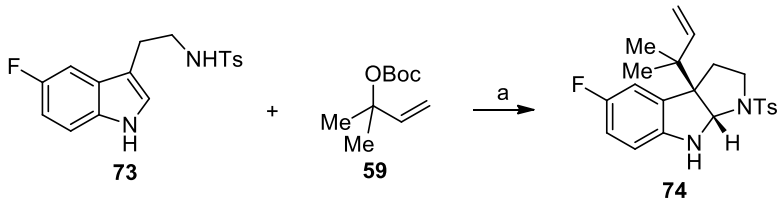

Entry	Ligand	74/75	Conversion
1	**none**	>20:1	28%
2	**72**	>20:1	92%
3	**85**	>20:1	95%
4	**86**	>20:1	10%
5	(*R*)-**53**	5:1	77%

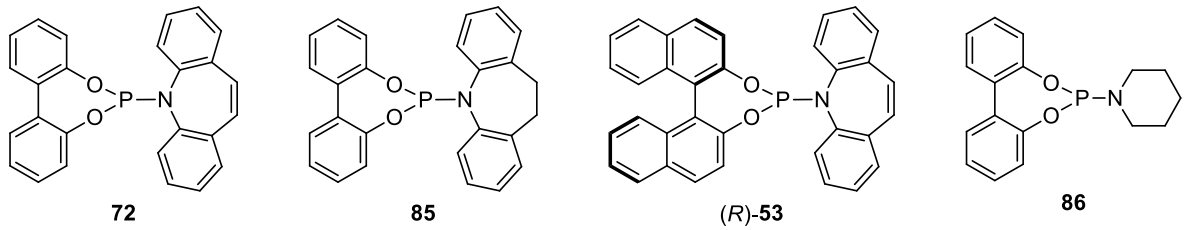

In a final ligand screening, two newly prepared ligands (**87**, **88**) were included (Table 2.7).

Table 2.7 Final screening in the racemic reverse prenylation of tryptamine derivative **73**. Reagents and conditions: (a) **73** (1.0 equiv.), **59** (2.0 equiv.), KO*t*Bu (1.1 equiv.), Et_3B (1.2 equiv., 1.0 M in THF), [{Ir(cod)Cl}$_2$] (0.030 equiv.), ligand (0.060 equiv.), 1,4-dioxane (0.20 M), 50 °C, 1 h, ratio **74/75** and convn. estimated by ^{19}F-NMR analysis of the crude material, the reactions were run on a 0.10 mmol scale.

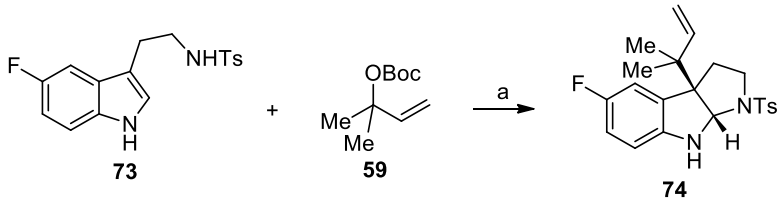

Entry	Ligand	74/75	Conversion
1	**72**	>20:1	65%
2	**85**	>20:1	93%
3	**86**	n. d.	<5%
4	**87**	>20:1	97%
5	**88**	>20:1	93%
	(*R*)-**53**	7:1	29%

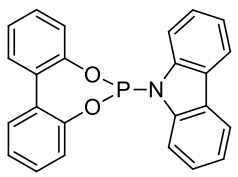

87

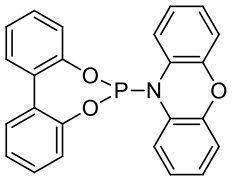

88

While the branched to linear ratio was high for both new ligands, the use of **87** led to an increased conversion compared to what was the best ligand to this point (**85**). Given the superior performance of **87**, this ligand was utilized in all subsequent reactions.

In the last set of optimization experiments, the catalyst loading was studied (Table 2.8). For the reaction between tryptamine derivative **73** and carbonate **59**, the catalyst loading could be decreased to 0.20 mol% (entry 3). When the loading was reduced to 0.020 mol%, the conversion was found to be incomplete (entry 5). In later experiments it was found that the purity of the tosylate is crucial when using such low catalyst loadings. Minor impurities present in the tosylate starting materials (**73** or **76**) would prevent the reaction to reach completion when using a catalyst loading lower than 0.20 mol%. As described in the scope of the reaction, tosyl protected tryptamines are particular good substrates for this reaction. Fot other substrates, the catalyst loading could not be lowered to this extent.

Table 2.8 Influence of the catalyst loading in the racemic reverse prenylation of tryptamine derivative **73**. Representative conditions (entry 3): (a) **73** (1.0 equiv.), **59** (2.0 equiv.), KO*t*Bu (1.1 equiv.), Et_3B (1.1 equiv., 1.0 M in THF), [{Ir(cod)Cl}$_2$] (0.0010 equiv.), **84** (0.002 equiv.), 1,4-dioxane (0.19 M), convn. estimated by ^{19}F-NMR analysis of the crude material, the reactions were run on a 0.10 mmol scale. (b) A catalyst loading of 0.020 equiv. refers to the use of 0.020 equiv. **84** and 0.010 equiv. [{Ir(cod)Cl}$_2$], stock solutions of the *in situ* formed catalyst were used.

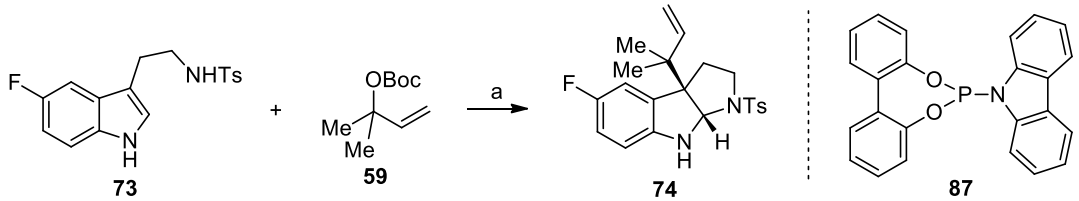

73 59 74 87

Entry	Cat. Loading[b]	Temperature	Time	Conversion
1	0.020 equiv.	50 °C	1.5 h	>95%
2	0.010 equiv.	50 °C	0.50 h	>95%
3	0.0020 equiv.	24 °C	2.0 h	>95%
4	0.00050 equiv.	24 °C	13 h	>95%
5	0.00010 equiv.	24 °C	13 h	24%

2.2.2 Diastereoselective Reverse Prenylation of Tryptophan Derivatives

In order apply the disclosed racemic reverse prenylation reaction to the synthesis of natural products, diastereoselective variants of this transformation were examined. When simple tryptophan derivatives were subjected to the reaction conditions, the desired product was obtained, albeit with low diastereocontrol. As an example, Boc-protected tryptophan methyl ester **89** provided the reverse prenylated hexahydropyrroloindoles **90** and **91** in a combined yield of 84% (Scheme 2.11). In this case no diastereoselectivity was observed and the partial separation of the two compounds by flash column chromatography on silica gel was possible but not practical.

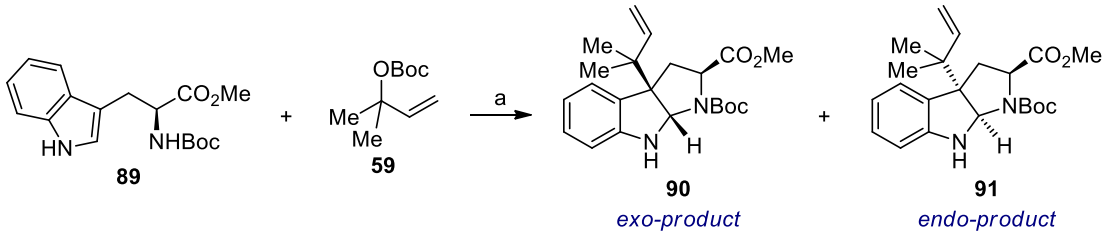

Scheme 2.11 Reagents and conditions: (a) **89** (1.0 equiv.), **59** (1.4 equiv.), KO*t*Bu (1.1 equiv.), Et_3B (1.1 equiv., 1.0 M in THF), [{Ir(cod)Cl}$_2$] (0.0025 equiv.), **72** (0.0050 equiv.), 1,4-dioxane (0.23 M), 24 °C, 4 h, the reaction was run on a 1.0 mmol scale. The *exo* to *endo* diastereoselectivity was found to be ~1:1 by ^{13}C-NMR analysis; both in the crude and purified product. The regioselectivity (branched to linear) was found to be >20:1 by ^{1}H-NMR analysis of the crude product. The combined yield of **90** and **91** was 84%.

The assigned relative stereochemistry of **90** and **91** could be confirmed by X-ray crystallographic analysis of *exo*-product **90** (Figure 2.1).

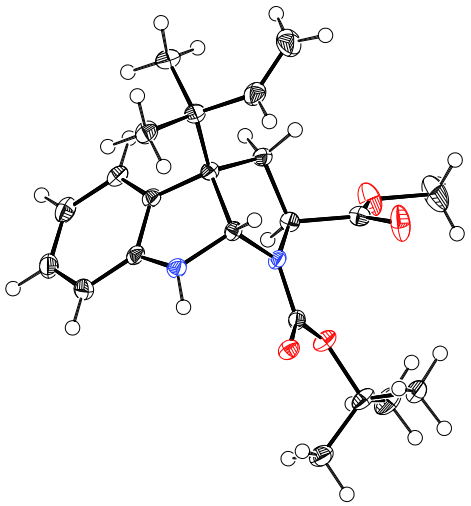

Figure 2.1 Structure of (–)-*exo*-product **90** in the solid state (ORTEP view with thermal ellipsoids set at 50% probability).

A variety of conditions were examined for the diasteroselecitve reverse prenylation of **89**, however, the observed diastereoselectivity remained low (<2:1). Various tryptophan

derivatives were prepared by changing the protecting group on the carboxylic acid and aliphatic amine (a selection is given in Figure 2.2). While some of these substrates displayed a different reactivity, the diastereoselectivity remained low for all examples studied (<2:1 d.r.).

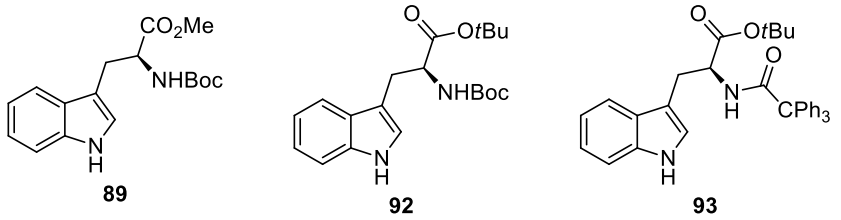

Figure 2.2 Selected substrates evaluated for the diastereoselective reverse prenylation reaction.

Another approach to a diastereoselective reaction was pursued by the preparation of precursors for a specific natural product target. In this event, amide **94** was reacted to directly provide the two natural products **95** and **96** (Scheme 2.12). This strategy is arguably biomimetic, as not only the products but also the starting material **94** has been found in nature.[30] A variety of conditions for this transformation were screened but the selectivity for either target never exceeded 2:1.

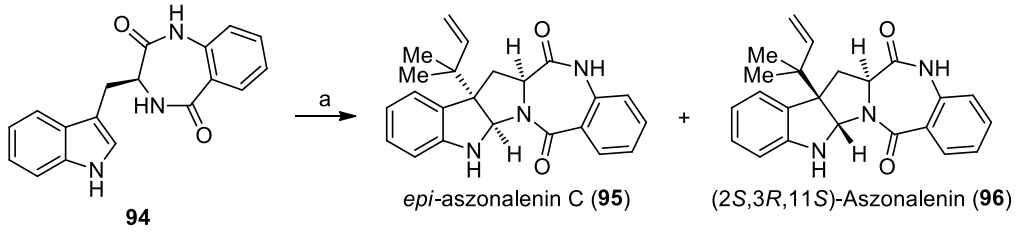

Scheme 2.12 Attempted diastereoselective synthesis of natural product **95** or **96**. Selected conditions: (a) **94** (1.0 equiv.), **59** (1.4 equiv.), KO*t*Bu (0.50 equiv.), Et_3B (1.0 equiv., 1.0 M in THF), [{Ir(cod)Cl}$_2$] (0.0089 equiv.), **87** (0.045 equiv.), 1,4-dioxane (0.20 M), 50 °C, 13 h, >95% convn. analyzed by ^{1}H-NMR analysis of the crude material, the diastereoselectivity was found to be 2:1 (**96/95**) by ^{1}H-NMR analysis of the crude material, the reaction was run on a 0.10 mmol scale.

Inspired by the Pd-catalyzed diastereoselective allylation of tryptophan methyl ester reported by *Tamaru* and coworkers,[7c] the same substrate was examined in the reverse prenylation reaction (Scheme 2.13). When excess triethylborane was used (2.0 equiv.), the reverse prenylated products were obtained in a reasonable yield (58% combined). The stereoselectivity was again found to be low. The two isomers could be readily separated by

[30] All three compounds have been isolated from different *Aspergillus* strains. For the isolation of benzodiazepinedione **94**, see: (a) Barrow, C. J.; Sun, H. H. *J. Nat. Prod.* **1994**, *57*, 471. For *epi*-aszonalenin C, see: (b) Rank, C.; Phipps, R. K.; Harris, P.; Frisvad, J. C.; Gotfredsen, C. H.; Larsen, T. O. *Tetrahedron Lett.* **2006**, *47*, 6099. For (2*S*,3*R*,11*S*)-aszonalenin, see: (c) Rukachaisirikul, V.; Rungsaiwattana, N.; Klaiklay, S.; Pakawatchai, C.; Saithong, S.; Phongpaichit, S.; Borwornwiriyapan, K.; Sakayaroj, J. *Tetrahedron* **2013**, *69*, 11116.

flash column chromatography on silica gel. However, the yield of the desired exo-isomer after sepatation was rather low (33%).

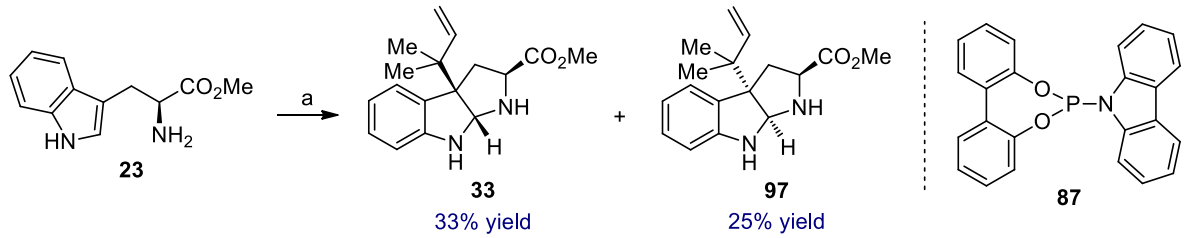

Scheme 2.13 Attempted diastereoselective synthesis of **33**. Reagents and conditions: (a) **23** (1.0 equiv.), **59** (1.2 equiv.), KO*t*Bu (1.0 equiv.), Et_3B (2.0 equiv., 1.0 M in THF), [{Ir(cod)Cl}$_2$] (0.0050 equiv.), **87** (0.010 equiv.), 1,4-dioxane (0.18 M), 0 °C to 24 °C, 26 h, the reaction was run on a 0.50 mmol scale, *exo*-diastereomer **33** isolated in 33% yield, *endo*-diastereomer **97** in 25% yield.

Considerable experimentation led to the identification of reaction conditions, which provided reverse prenylated bis-amine **33** in high *exo*-selectivity and good yield (58%, Scheme 2.14). Key to to selectivity of this transformation was the use of a sterically more demanding trialkylborane (9-BBN-*n*C_6H_{13}). Replacing KO*t*Bu with KHMDS and conducting the reaction at lower temperature (0 °C) increased the yield of the process. Analysis of **33** showed no loss of the enantiomeric purity. Having established a diastereoselecitive reverse prenylation of tryptophan methyl ester (**23**) in a serviceable yield, the goal was to access natural products with **33** as a common intermediate. The realization of this task was achieved in the synthesis of the two bioactive natural products, (+)-aszonalenin (**130**) and (−)-brevicompanine B (**132**), and is described in the following.

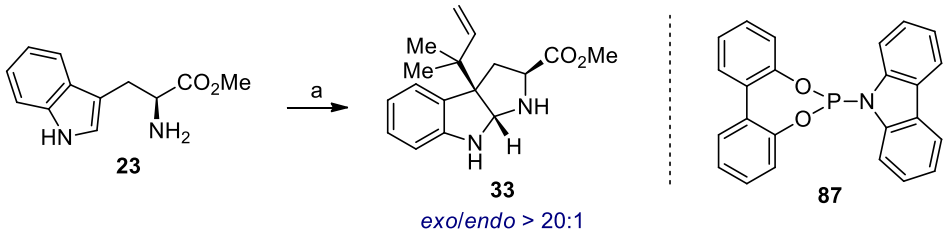

Scheme 2.14 Diastereoselective synthesis of *exo*-hexahydropyrroloindole **33**. Reagents and conditions: (a) **23** (1.0 equiv.), **59** (1.1 equiv.), KHMDS (1.0 equiv.), 9-BBN-*n*C_6H_{13} (2.5 equiv., 0.5 M in 1,4-dioxane), [{Ir(cod)Cl}$_2$] (0.0050 equiv.), **87** (0.010 equiv.), 1,4-dioxane/THF 3:1 (0.15 M), 0 °C, 3 h, the reaction was run on a 1.0 mmol scale.

2.3 Scope of the Reverse Prenylation Reaction of 3-Substituted Indoles

An assortment of 3-substituted indoles was prepared in order to study the scope of the racemic reverse prenylation reaction (Figure 2.3).[31] Because the ultimate goal was to apply the method in natural product synthesis, the focus of the reaction scope was on tryptamine derivatives. Nevertheless other substrates, most of them bearing a pendent nucleophile, were also prepared.

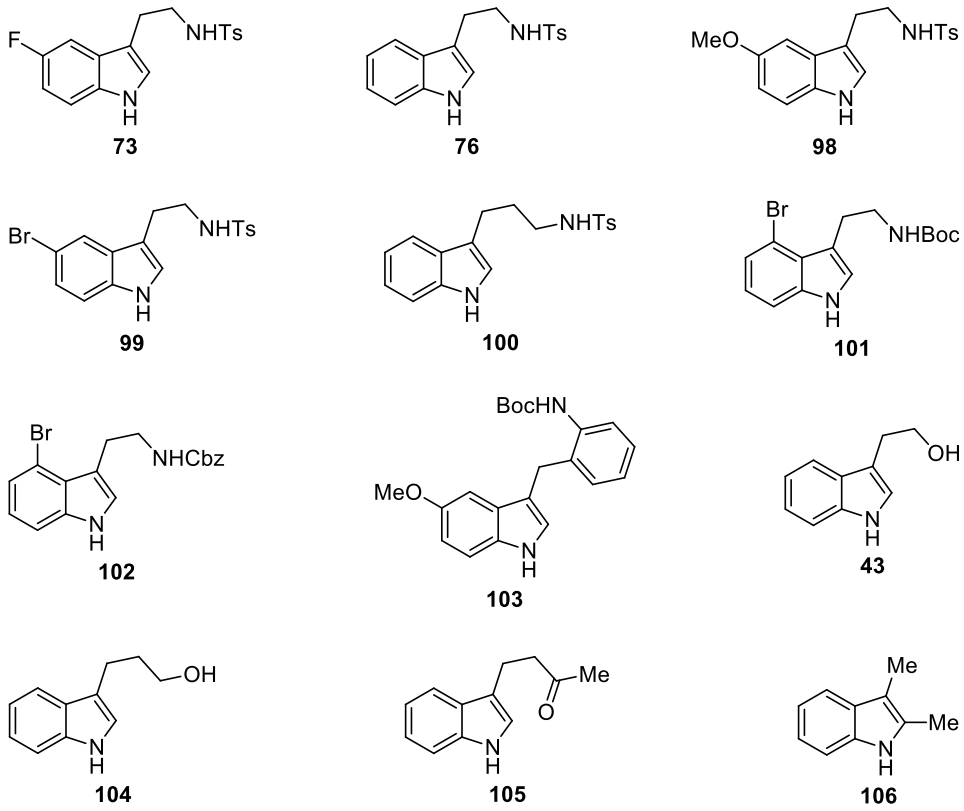

Figure 2.3 Indoles successfully used in the racemic C3 reverse prenylation reaction.

The scope of the racemic reverse prenylation reaction is shown in Table 2.9. Tosyl protected tryptamines were found to be particularly good substrates and substoichometric amounts of KO*t*Bu and Et_3B could be used (**73**, **76**, **98**, **99**). This finding is likely because most of the reaction optimization was carried out using **73** as substrate. A slight excess of KO*t*Bu and Et_3B was needed for all other substrates examined. The reactions reached completion within 1–5 h at 24 °C with the exception of **105** and **106** (50 °C). A low catalyst loading could be used (0.50 mol%) for most examples.

[31] Two commercially available substrates were also employed, namely **43** and **106**.

Table 2.9 Scope of the racemic reverse C3 prenylation of 3-substituted indoles. Reagents and conditions: (a) indole (1.0 mmol, 1.0 equiv.), **59** (1.4 equiv.), KO*t*Bu (1.1 equiv.), Et_3B (1.1 equiv., 1.0 M in THF), [{Ir(cod)Cl}$_2$] (0.0025 equiv.), **87** (0.0050 equiv.), 1,4-dioxane (0.19 M), 24 °C, 1 h. All products were isolated as single diastereomers (not applicable for **118**) with >20:1 branched to linear selectivity. All reactions were run on a 1.0 mmol scale and the yields are given for the purified products.

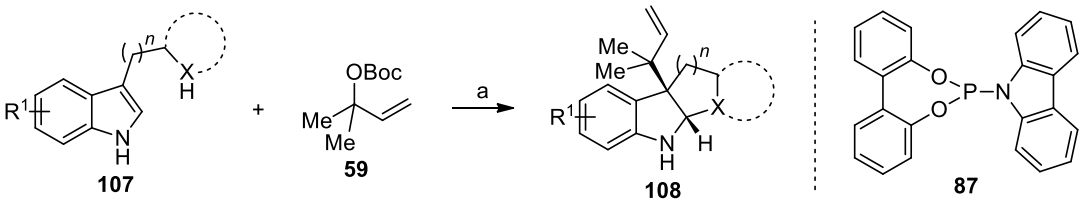

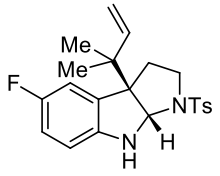
74
92% yield

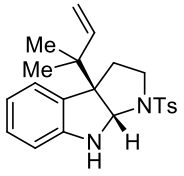
109
95% yield

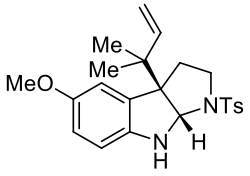
110
93% yield

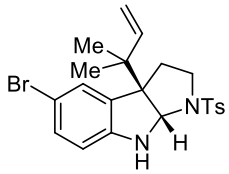
111
93% yield

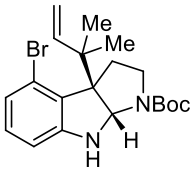
112
90% yield

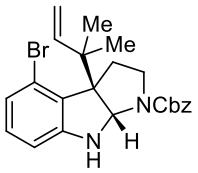
113
90% yield

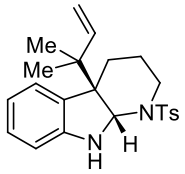
114
79% yield

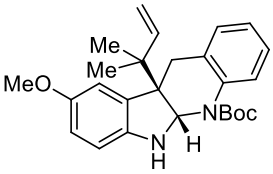
115
90% yield

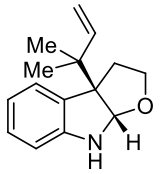
116
72% yield

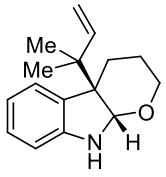
117
62% yield

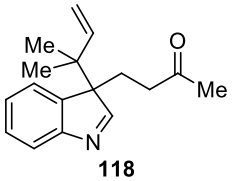
118
88% yield

Electronically different indoles could be employed as substrates (**73**, **98**). Substitution on indole was tolerated on C2, C4 and C5. Indoles with substituents at C6 were not examined, and those with C7 substitution were not suitable substrates (*vide infra*). Most substrates had a pendant nucleophile in the molecule, giving rise to a variety of structurally diverse scaffolds.

For the two examples where no such pendant nucleophile was present, the imine was isolated (**105**, **106**). A notable feature of the reaction is the high regioselectivity (>20:1) observed for all products as determined by ^{1}H-NMR analysis of the unpurified reaction mixture. Moreover, the process shows high site selecitivity and no *N*-prenylated products were observed. The structures of two products were confirmed by X-ray crystallographic analysis (**109**, **112**, Figure 2.4). Compound **116** was prepared previously by *Ōmura*, *Sunazuka* and coworkers and the analytical data obtained was in accordance with that which was published.

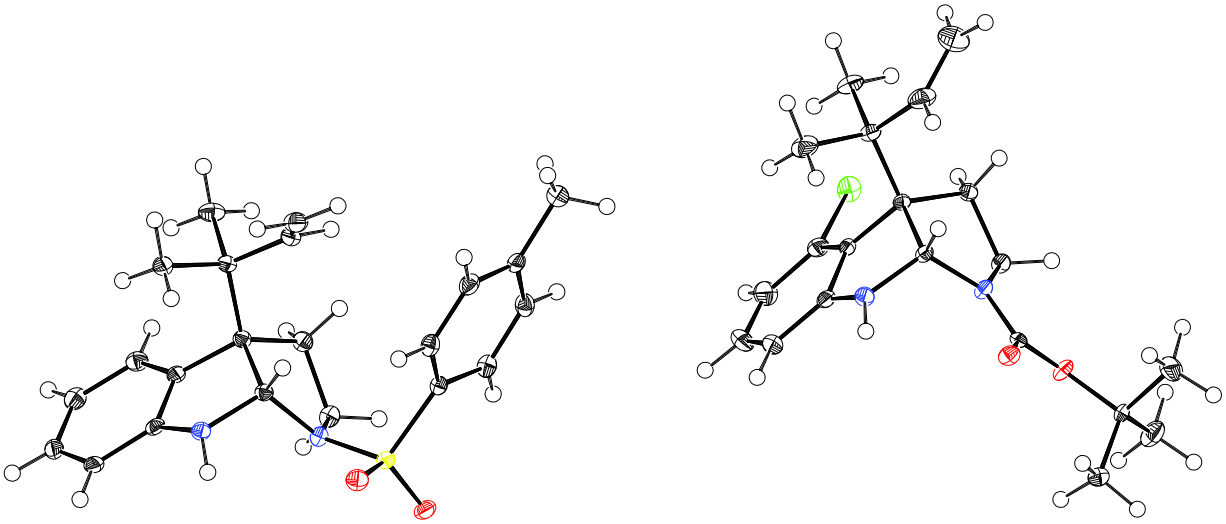

Figure 2.4 Structures of reverse prenylated products **109** (left) and **112** (right) in the solid state (ORTEP view with thermal ellipsoids set at 50% probability).

A selection of challenging substrates is given in Figure 2.5. These indole derivatives provided no desired products and the starting materials were recovered. The exceptions were **125** and **126**, which gave a complex product mixture and which showed low conversion in a preliminary experiment, respectively.

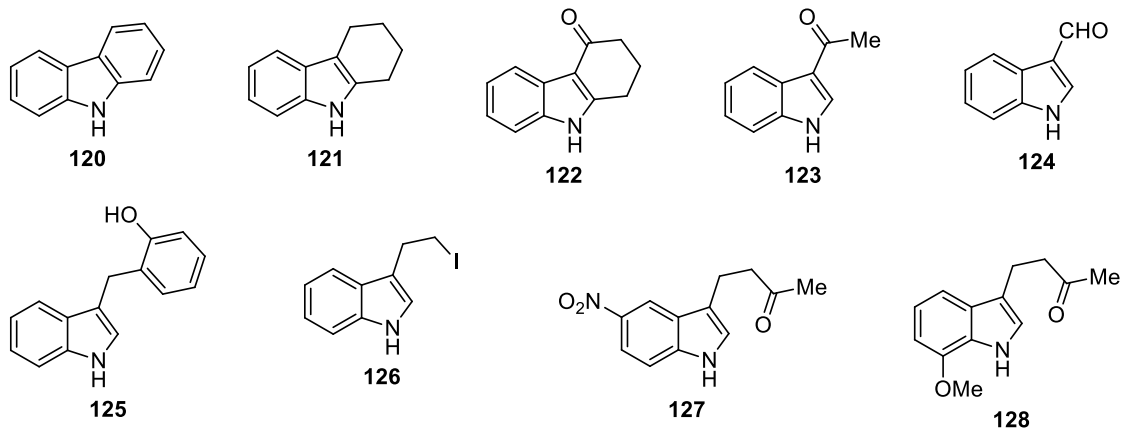

Figure 2.5 Selection of challenging indole substrates in the racemic reverse C3 prenylation of 3-substituted indoles as described in Table 2.9.

2.4 Synthesis of (+)-Aszonalenin and (−)-Brevicompanine B

Diastereoselective reverse prenylation of tryptophan methyl ester provided **33** in high *exo*- and regioselectivity (*vide supra*). This compound proved to be a versatile intermediate *en route* to prenylated indole alkaloids as described in this chapter. Both enantiomers of **33** were readily accessible from either enantiomer of tryptophan methyl ester.

The fungal metabolite (+)-aszonalenin (**130**) was isolated from *Aspergillus zonatus* by Kimura and coworkers.[32] *Barrow* and *Sun* found that the derived acyl aszonalenin (**130** mono acylated at the indoline nitrogen) is a neurokinin-1 receptor.[33] A chemoenzymatic synthesis of **130** has been reported by *Harrison* and coworkers as well as *Li* and coworkers.[34] The absolute stereochemistry was established in the synthesis of (−)-dihydroaszonalenin by *Bhat* and *Harrison*.[35] To the best of our knowledge, no chemical synthesis has been disclosed prior to the work described herein. The synthesis (+)-aszonalenin commenced by coupling *ent*-**33** with 2-aminobenzoic acid in the presence of HATU and Et_3N (Scheme 2.15). Crude amide **129** contained some of the cyclized product (**130**). Therefore, it was more convenient to directly subject the crude material to an $AlMe_3$ mediated cyclization. The natural product (+)-aszonalenin (**130**) was accessed in 85% yield from *ent*-**33** as single diastereomer. The structure of (+)-aszonalenin (**130**) could be confirmed by X-ray crystallographic analysis (Figure 2.6).

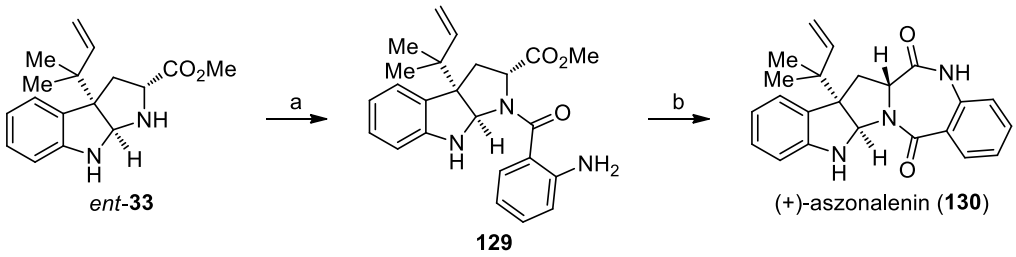

Scheme 2.15 Synthesis of (+)-aszonalenin from *ent*-**33**. Reagents and conditions: (a) **33** (1.0 equiv.), 2-aminobenzoic acid (1.4 equiv.), Et_3N (2.0 equiv.), HATU (1.4 equiv.), CH_2Cl_2 (0.10 M), 25 °C, 30 h; (b) $AlMe_3$ (4.0 equiv., 2.0 M in toluene), toluene (0.10 M), 0 °C, 1 h, 85% (over two steps), the reaction was run on a 0.17 mmol scale.

[32] Kimura, Y.; Hamasaki, T.; Nakajima, H.; Isogai, A. *Tetrahedron Lett.* **1982**, *23*, 225.
[33] Barrow, C. J.; Sun, H. H. *J. Nat. Prod.* **1994**, *57*, 471.
[34] (a) Bhat, B.; Harrison, D. M.; Lamont, H. M. *Tetrahedron* **1993**, *49*, 10663. (b) Yin, W.-B.; Cheng, J.; Li, S.-M. *Org. Biomol. Chem.* **2009**, *7*, 2202.
[35] Bhat, B.; Harrison, D. M. *Tetrahedron Lett.* **1986**, *27*, 5873.

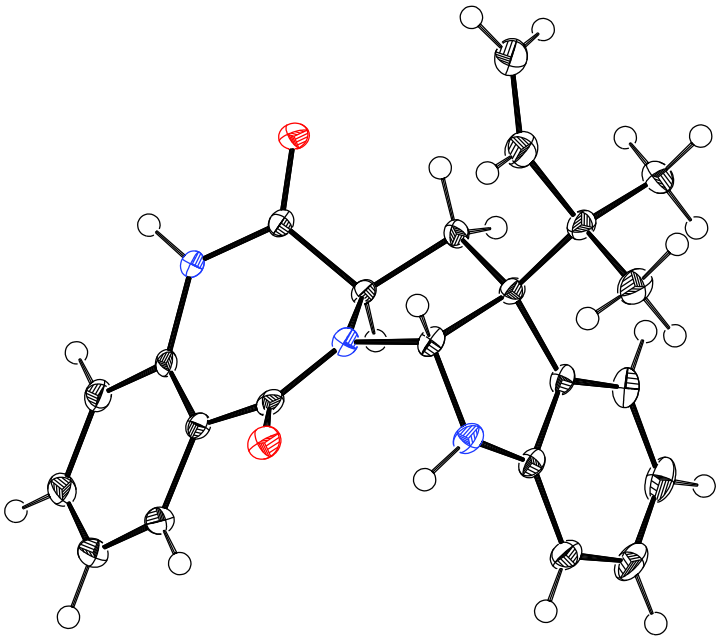

Figure 2.6 Structure of (+)-aszonalenin **130** in the solid state (ORTEP view with thermal ellipsoids set at 50% probability).

The plant growth regulator (−)-brevicompanine B (**132**) was isolated from *Penicillium brevicompactum* by *Kimuara* and coworkers.[36] The only synthesis prior to this work was reported by *Matsumura* and *Kitahara*.[37] They accessed the reverse prenylated motif using the procedure by *Danishefsky* and coworkers.[12] For the synthesis of this natural product relying on the method disclosed herein, **33** was coupled with (*R*)-Fmoc-Leu under conditions used for the previous synthesis providing amide **131** in 82% yield. Deprotection of the carbamate and spontaneous cyclization gave the target natural product **132** in 83% yield and as a single diastereomer. The diketopiperazine natural product **132** was accessed in three steps from tryptophan methyl ester. This compares favorably to the previously published synthesis (8 steps from tryptophan methyl ester).

[36] Kusano, M.; Sotoma, G.; Koshino, H.; Uzawa, J.; Chijimatsu, M.; Fujioka, S.; Kawano, T.; Kimura, Y. *J. Chem. Soc., Perkin Trans.* **1998**, *1*, 2823.
[37] Matsumura, K.; Kitahara, T. *Heterocycles* **2001**, *54*, 727.

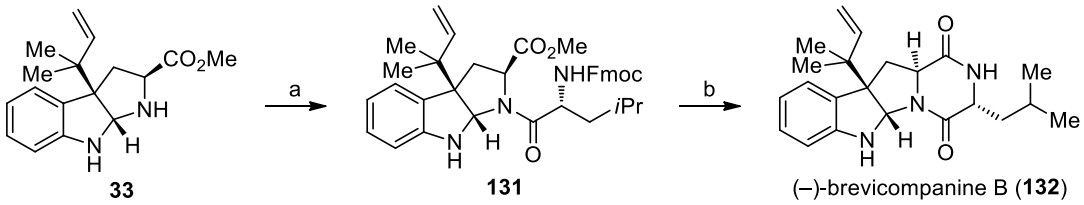

Scheme 2.16 Synthesis of (−)-brevicompanine B from **33**. Reagents and conditions: (a) **33** (1.0 equiv.), (*R*)-Fmoc-Leu (1.5 equiv.), Et_3N (2.0 equiv.), HATU (1.1 equiv.), CH_2Cl_2 (0.10 M), 0 °C to 19 °C, 19 h, 82% yield, the reaction was run on a 0.24 mmol scale.; (b) Et_2NH (35 equiv.), THF (0.020 M), 0 °C to 22 °C, 14 h, 83% yield, the reaction was run on a 0.16 mmol scale.

3 Conclusion and Outlook

In summary, the first method for direct, C3 selective, reverse prenylation of 3-substituted indoles was developed. The reaction employs a readily accessible Ir-catalyst and a simple carbonate as precursor for the prenyl group with a variety of 3-substituted indoles as substrates. All products are obtained in good regioselectivity (>20:1), involving the formation of vicinal quaternary centers. The diastereoselective reaction with tryptophan methyl ester enables access to a versatile hexahydropyrroloindole intermediate, which is employed in the stereoselective synthesis of two bioactive natural products, (+)-aszonalenin and (−)-brevicompanine B. The Ir-catalyzed cyclization reaction for tryptophan derivatives was observed to give high selectivity with the free amine and a bulky trialkylborane. The same intermediate and its derivatives are expected to be useful for the synthesis of other C3 reverse prenylated indole alkaloids. In a broader context, an additional and important feature of this method is that it represents the first use of Ir-catalysis to effect reverse prenylation of C3 substituted indoles. Moreover, this is the first example of any Ir-catalyzed allylation reaction to access vicinal quaternary centers. This expands the reaction scope of Ir-catalyzed allylations and suggests additional avenues for investigation.

II

Rh-Catalyzed Stereoselective Synthesis of Allenes

4 Background and Introduction

Allenes are an important class of compounds due to their unique reactivity.[38] The transition metal-catalyzed formal SN2´ reaction between propargyl alcohol derivatives and organometallic reagents constitute one of the most important preparations of allenes.[39] The coupling partners employed were traditionally moisture sensitive oranometallics used in stoichiometric fashion.[39,40] More recently, organoboron reagents or catalytically generated organocopper reagents have found increasing use as nucleophiles in the stereoselective, catalytic synthesis of allenes. Alkyl-, vinyl-, and arylboron reagents were employed in the preparation of chiral allenes from enantioenriched propargylic alcohol derivatives under Pd and Cu catalysis.[41] This process was found to be challenging to conduct in a stereoselective manner when using other transition metals such as Rh or Fe.[42] In order to achieve high regio- and stereoselectivity, propargyl epoxides have been used as substrates instead.[43] Since highly

[38] (a) Modern Allene Chemistry; Krause, N.; Hashmi, A. S. K., Eds.; Wiley-VCH, Weinheim, 2004; Vols. 1 and 2. For selected reviews on reactions of allenes, see: (b) Marshall, J. A. *Chem. Rev.* **2000**, *100*, 3163. (c) Zimmer, R.; Dinesh, C. U.; Nandanan, E.; Khan, F. A. *Chem. Rev.* **2000**, *100*, 3067. (d) Ma, S. *Chem. Rev.* **2005**, *105*, 2829. (e) Ma, S. *Acc. Chem. Res.* **2009**, *42*, 1679. (f) Krause, N.; Winter, C. *Chem. Rev.* **2011**, *111*, 1994. (g) Yu, S.; Ma, S. *Angew. Chem., Int. Ed.*, **2012**, *51*, 3074. (h) Neff, R. K.; Frantz, D. E. *Tetrahedron* **2015**, *71*, 7.

[39] For a review on the transition-metal catalyzed synthesis of allenes, see: (a) Ogasawara, M.; Hayashi, T. in Modern Allene Chemistry, Vol. 1 (Eds.: N. Krause, A. S. K. Hashmi), Wiley-VCH, Weinheim, **2004**, pp. 93. For selected reviews on the synthesis of allenes, see: (b) Hoffmann-Röder, A.; Krause, N. *Angew. Chem., Int. Ed.*, **2004**, *43*, 1196. (c) Krause, N.; Hoffmann-Röder, A. *Tetrahedron* **2004**, *60*, 11671. (d) Brummond, K. M.; DeForrest, J. E. *Synthesis* **2007**, 795. (e) Yu, S.; Ma, S. *Chem. Commun.* **2011**, *47*, 5384. (f) Neff, R. K.; Frantz, D. E. *ACS Catalysis* **2014**, *4*, 519. (g) Ye, J.; Ma, S. *Org. Chem. Front.* **2014**, *1*, 1210. For a recent review covering the transition-metal catalyzed, enantioselective and enantiospecific synthesis of allenes from organometallic reagents, see: (h) Cherney, A. H.; Kadunce, N. T.; Reisman, S. E. *Chem. Rev.* **2015**, *115*, 9587.

[40] For a selected review on the corresponding reaction with cuprates, see: (a) N. Krause, A. Hoffmann-Röder, in Modern Organocopper Chemistry (Ed.: N. Krause), Wiley-VCH, Weinheim, **2002**, pp. 145. For early work on reaction between propargylic alcohol derivatives and organocuprate reagents, see: (b) Rona, P.; Crabbe, P. *J. Am. Chem. Soc.* **1968**, *90*, 4733. (c) Rona, P.; Crabbe, P. *J. Am. Chem. Soc.* **1969**, *91*, 3289.

[41] For Pd-catalyzed, stereoselective synthesis of allenes from propargylic alcohol derivatives and aryl- or alkenylboron compounds, see: (a) Yoshida, M.; Gotou, T.; Ihara, M. *Tetrahedron Lett.* **2004**, *45*, 5573. (b) Molander, G. A.; Sommers, E. M.; Baker, S. R. *J. Org. Chem.* **2006**, *71*, 1563. (c) Yoshida, M.; Okada, T.; Shishido, K. *Tetrahedron* **2007**, *63*, 6996. For Cu-catalyzed, stereoselective preparation of allenes from propargylic alcohol derivatives and boron nucleophiles, see: (d) Ito, H.; Sasaki, Y.; Sawamura, M. *J. Am. Chem. Soc.* **2008**, *130*, 15774. (e) Vyas, D. J.; Hazra, C. K.; Oestreich, M. *Org. Lett.* **2011**, *13*, 4462. (f) Ohmiya, H.; Yokobori, U.; Makida, Y.; Sawamura, M. *Org. Lett.* **2011**, *13*, 6312. (g) Uehling, M. R.; Marionni, S. T.; Lalic, G. *Org. Lett.* **2012**, *14*, 362. (h) Yang, M.; Yokokawa, N.; Ohmiya, H.; Sawamura, M. *Org. Lett.* **2012**, *14*, 816. (i) Hazra, C. K.; Oestreich, M. *Org. Lett.* **2012**, *14*, 4010. (j) Yokobori, U.; Ohmiya, H.; Sawamura, M. *Organometallics* **2012**, *31*, 7909.

[42] For a selected example with a Rh-catalyst, see: (a) Murakami, M.; Igawa, H. *Helv. Chim. Acta* **2002**, *85*, 4182. For a selected example under Fe catalysis, see: (b) Fürstner, A.; Méndez, M. *Angew. Chem., Int. Ed.*, **2003**, *42*, 5355.

[43] (a) For an example with Fe catalysis, see ref 42b. For a selected example with a Pd catalyst, see: (b) Yoshida, M.; Ueda, H.; Ihara, M. *Tetrahedron Lett.* **2005**, *46*, 6705. For Rh catalysis, see: (c) Miura, T., Shimada, M., Ku, S.-Y., Tamai, T.; Murakami, M. *Angew. Chem., Int. Ed.*, **2007**, *46*, 7101. (d) Miura, T.; Shimada, M.; de Mendoza, P.; Deutsch, C.; Krause, N.; Murakami, M. *J. Org. Chem.* **2009**, *74*, 6050. (e) Yoshida, M.; Hayashi,

References continued on next page.

enantioenriched propargylic alcohols are readily accessible from the enantioselective addition of terminal alkynes to aldehydes[44] or the reduction of *α,β*-alkynyl ketones,[45] we envisioned a stereoselective Rh-catalyzes synthesis of allenes from propargyl alcohol derivaties. Within Rh catalysis, the addition of boronic acids (or their derivatives) to enones[46] or alkynes[47] is well established. For enones the regioselectivity is governed by the substrate, while the regioselective hydroarylation of alkynes is generally more challenging. For example, the addition of phenylboronic acid to propargylic acetate **136** occurred with 4:1 regioselectivity, as described by *Murakami* and coworkers (Scheme 4.1).[42a] Addition distal to the acetate was followed by elimination to give allene **138** in an overall SN2' process whereas the vinylrhodium intermediate formed through the regioisomeric addition underwent protonation to furnish **139**.[48] The observed regioselectivity was not improved when the corresponding propargylic alcohol (~4:1) or the methyl ether (~2:1) were used.

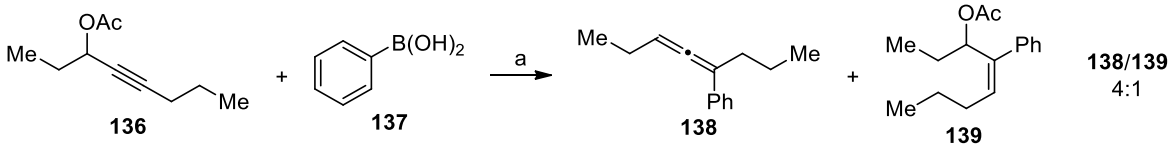

Scheme 4.1 Reaction between phenylboronic acid and propargylic acetate **136** as reported by *Murakami* and coworkers.[42a] Reagents and conditions: (a) **136** (1.0 equiv.), **137** (2.0 equiv.), $NaHCO_3$ (2.0 equiv.), [{Rh(cod)Cl}$_2$] (0.015 equiv.), $P(OEt)_3$ (0.060 equiv.), MeOH (0.10 M), 70 °C, 1 h, **138** and **139** isolated in 94% combined yield, the reaction was run on a 0.30 mmol scale.

When the same reaction was conducted with an enantioenriched starting material, allene **138** was formed with 32% *es* while the hydroarylation product **139** was isolated without detectable loss of optical purity (Scheme 4.2). The latter finding suggests that the reaction proceeds through a vinylrhodium intermediate and no allylic cations are formed.[42a] Using EtOH as solvent yielded the opposite enantiomer with low stereocontrol (-17% *ee*). This result indicates

M.; Matsuda, K.; Shishido, K. *Heterocycles* **2009**, *77*, 193. For the Rh-catalyzed, stereospecific synthesis of allenylsilanes from propargylic carbonates, see: (e) Ohmiya, H.; Ito, H.; Sawamura, M. *Org. Lett.* **2009**, *11*, 5618.

[44] (a) Frantz, D. E.; Fässler, R.; Carreira, E. M. *J. Am. Chem. Soc.* **2000**, *122*, 1806. (b) Anand, N. K.; Carreira, E. M. *J. Am. Chem. Soc.* **2001**, *123*, 9687. (c) Takita, R.; Yakura, K.; Ohshima, T.; Shibasaki, M. *J. Am. Chem. Soc.* **2005**, *127*, 13760. (d) Trost, B. M.; Weiss, A. H.; Jacobi von Wangelin, A. *J. Am. Chem. Soc.* **2006**, *128*, 8. For a selected review, see: (e) Trost, B. M.; Weiss, A. H. *Adv. Synth. Catal.* **2009**, *351*, 963.

[45] (a) Midland, M. M.; McDowell, D. C.; Hatch, R. L.; Tramontano, A. *J. Am. Chem. Soc.* **1980**, *102*, 867. (b) Midland, M. M. *Chem. Rev.* **1989**, *89*, 1553. (c) Matsumura, K.; Hashiguchi, S.; Ikariya, T.; Noyori, R. *J. Am. Chem. Soc.* **1997**, *119*, 8738. (d) a

[46] For the first report on the Rh-catalyzed addition of aryl- and alkenylboronic acids to enones, see: Sakai, M.; Hayashi, H.; Miyaura, N. *Organometallics* **1997**, *16*, 4229.

[47] For the seminal report on the Rh-catalyzed hydroarylation of alkynes with arylboronic acids, see: Hayashi, T.; Inoue, K.; Taniguchi, N.; Ogasawara, M. *J. Am. Chem. Soc.* **2001**, *123*, 9918.

[48] The reagioselectivity was similar when the reaction was done in EtOH (**138/139** 85:15, 60% combined yield).

that both *anti*- and *syn*-elimination are possible and that one pathway is somewhat favored depending on the solvent.

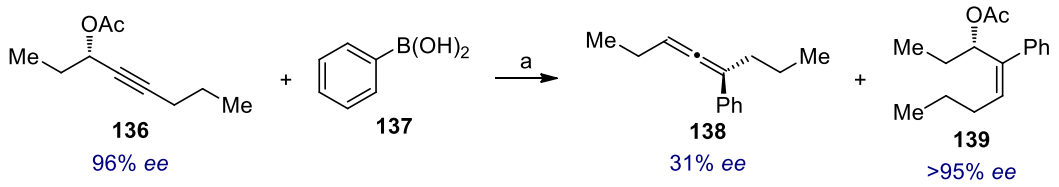

Scheme 4.2 Rh-catalyzed addition of phenylboronic acid to enantioenriched propargylic acetate **136**, followed by elimination to **138** or protonation to **139** reported by *Murakami* and coworkers.[42a] Reagents and conditions: (a) **136** (1.0 equiv.), **137** (2.0 equiv.), $NaHCO_3$ (2.0 equiv.), $[\{Rh(cod)Cl\}_2]$ (0.015 equiv.), $P(OEt)_3$ (0.060 equiv.), MeOH (0.10 M), 70 °C, 1 h, the scale of the reaction, the combined yield and ratio of **138** and **139** was not reported but the latter has to be identical to the one given in Scheme 4.1.

Based on the results described by *Murakami* and coworkers,[42a] a catalytic cycle for the reaction between arylboronic acids and enantioenriched propargylic alcohol derivatives can be proposed (Scheme 4.3). An Rh-catalyst **140** is generated *in situ* from $[\{Rh(cod)Cl\}_2]$ and a ligand. Transmetalation of an arylboronic acid to the formed catalyst then gives **142**.[49] *Syn*-addition of the arylrhodium species across the alkyne of **143** furnishes two vinylrhodium intermediates, **144** as major and **146** as minor regioisomer. The carborhodation of the alkyne may be preceded by a coordination of the arylrhodium complex to the alkyne (**149**). If the aryl group is added proximal to the propargylic stereocenter, compound **146** is formed. This intermediate arrests the catalytic cycle, unless protonation occurs to give the hydroarylation product **147** with release of the catalyst. Regioisomeric vinylrhodium species **144** can either undergo protonation to hydroarylation product **145** or undergo a β-O elimination to furnish an allene. In the latter scenario, enantiomeric allenes **148** are formed through *syn*- (from conformer **151**) or *anti*-elimination (from conformer **150**). The ratio of *syn*- to *anti*-E2-elimination determines the degree of chirality transfer if an enantioenriched benzoate **143** is used as starting material.

[49] Transmetalation of boronic acids to Rh^I complexes has precendent for example in the well studied addition of boronic acids to enones, see: Hayashi, T.; Takahashi, M.; Takaya, Y.; Ogasawara, M. *J. Am. Chem. Soc.* **2002**, *124*, 5052.

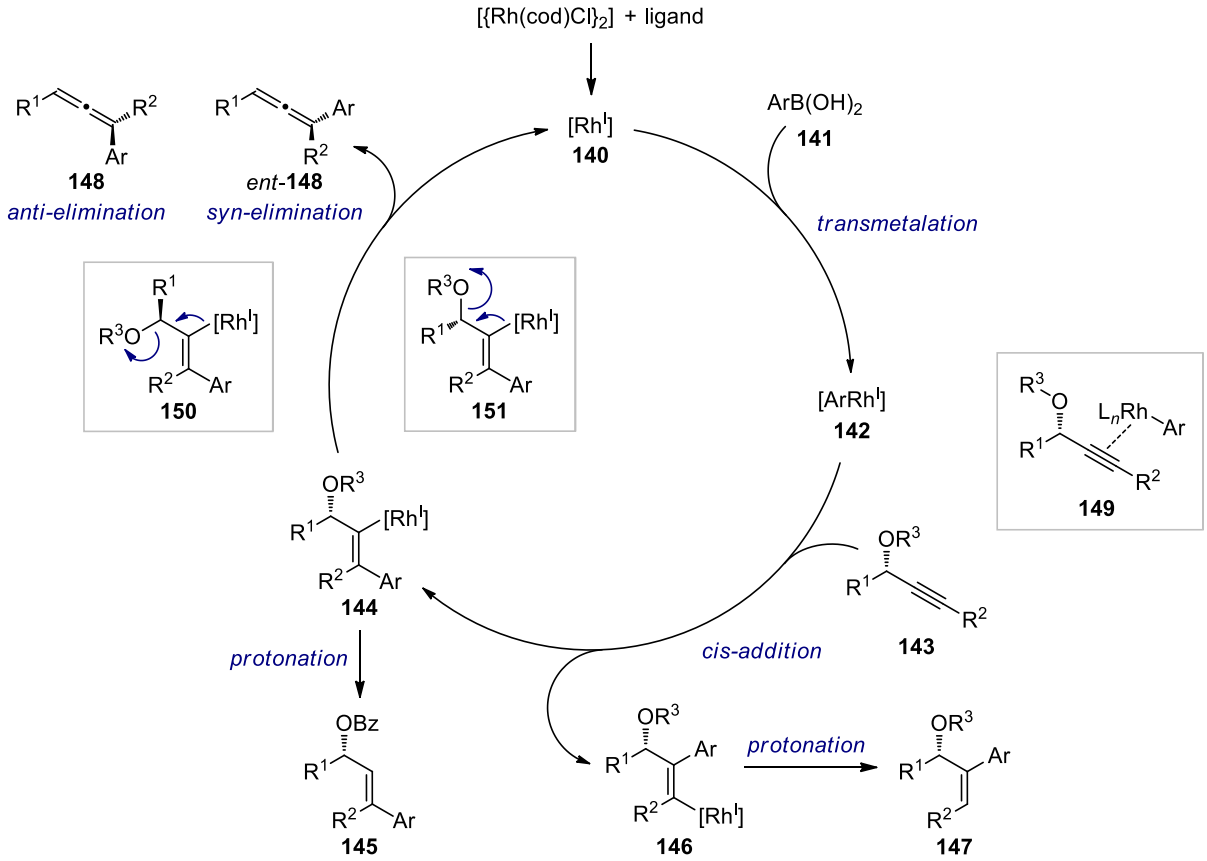

Scheme 4.3 Proposed catalytic cycle of a stereoselective Rh-catalyzed reaction between arylboronic acids and enantioenriched propargylic alcohol derivatives to furnish allenes adapted from work published by *Murakami* and coworkers.[42a]

Alternative mechanisms or variations of the one presented can not be excluded. In that regard, it is noteworthy that some related Pd-catalyzed processes were suggested to proceed through a SN2'-type oxidative addition to give an allenylpalladium intermediate. This species would then undergo transmetalation and reductive elimination to yield the allene.[50] As such the overall reaction furnishes the same product from identical starting materials as the mechanism shown in Scheme 4.3. This mechanism seems to be unlikely since it does not account for the formation of hydroarylation product **139** (Scheme 4.2) observed by *Murakami* and coworkers.[42a]

The catalytic cycle illustrated in Scheme 4.3 would account for the virtual nonexistence of transition-metal catalyzed enantioselective methods to access chiral allenes from racemic propargylic alcohol derivatives and organometallic reagents.[51] This is because an enantioselective process starting from an unsymmetrical propargylic alcohol derivative requires that the reaction proceeds one half each through a *syn*- and *anti*-elimination (Scheme

[50] For a selected example, see ref 41a.
[51] For an example using an achiral propargylic dichloride as substrate, see: Li, H. L.; Müller, D.; Guénée, L.; Alexakis, A. *Org. Lett.* **2012**, *14*, 5880.

4.4). At the same time, this mechanism suggests that enantiospecific transformations should be feasible, which indeed has been realized herein.

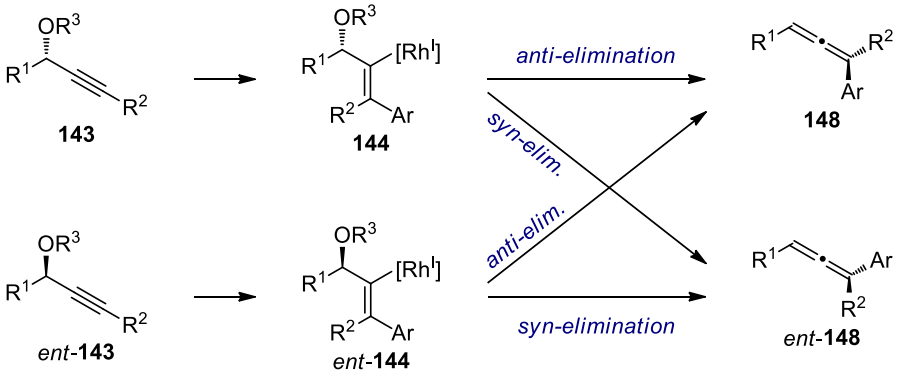

Scheme 4.4 Stereochemical relation between enantiomeric propargylic alcohol derivatives **307**, vinylrhodium intermediates **308** and allenes **312**. Proposed catalytic cycle of a stereoselective Rh-catalyzed reaction between arylboronic acids and enantioenriched.

Presumably, because of the low regio- and stereoselectivity encountered by *Murakami* and coworkers,[42a] the same group set out to employ a different substrate class. When propargyl epoxides were used instead of propargyl acetates the same transformation provided *α*-allenols in complete regio- and high diastereoselectivity (Scheme 4.5).[52] In this case no hydroarylation product arising from the regioisomeric addition to the alkyne was observed. The *α*-allenols were accessed in high to excellent diastereoselectivity with few exceptions. Moreover, in two examples examined, no detectable loss of enantiomeric excess occurred over the course of the reaction. This methodology is to the best of our knowledge the only Rh-catalyzed enantiospecific synthesis of allenes using boronic acids reported to date. However, the use of propargylic epoxides is suboptimal as these starting materials are not as readily accessible in highly enantioenriched form (compared to propargyl alcohols).

[52] Alkynyl oxiranes showed also higher stereo- and regioselectivity (compared to propargylic bromides) in the previously studied Fe-catalyzed reaction, see ref 42b and references therein.

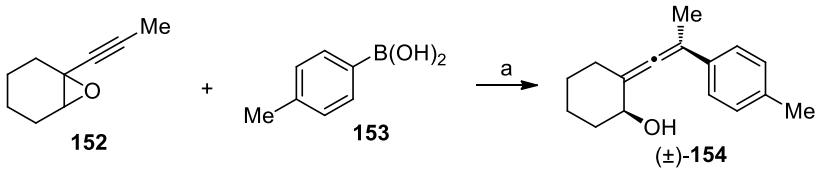

Scheme 4.5 Rh-catalyzed stereoselective synthesis of *α*-allenols reported by *Murakami* and coworkers.[43c] Reagents and conditions: (a) **152** (1.0 equiv.), **153** (1.5 equiv.), KOH (0.50-0.75 equiv.), [{Rh(nbd)Cl}$_2$] (0.025 equiv.), THF (0.10 M), r.t., 3-16 h, reaction carried out on 0.40 mmol scale, (±)-**154** isolated in 77% yield and a 98:2 *syn*/*anti* ratio.

Another Rh-catalyzed enantiospecific synthesis of allenes has been reported by *Sawamura* and coworkers (Scheme 4.6).[43e] They developed a reaction between propargyl carbonates such as **155** and silylboronate **156** to access chiral allenylsilanes (*e.g.* **157**).

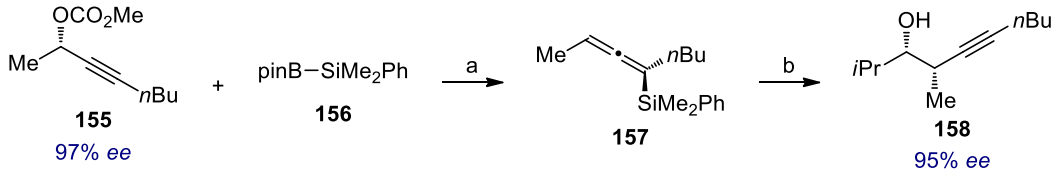

Scheme 4.6 Rh-catalyzed stereospecific synthesis of allenylsilanes described by *Sawamura* and coworkers.[43e] Reagents and conditions: (a) **155** (1.0 equiv.), **156** (1.5 equiv.), Et_3N (2.5 equiv.), $[Rh(cod)_2][BF_4]$ (0.10 equiv.), DMF/CH_3CN 100:1 (0.20 M), 25 °C, 12 h, reaction carried out on 0.20 mmol scale, **157** isolated in 77% yield. (b) **157** (1.0 equiv.),*i*PrCHO (1.5 equiv.), $TiCl_4$ (1.5 equiv.), CH_2Cl_2 (0.10 M), -78 °C, 3 h, the reaction was run on a 0.092 mmol scale, **158** isolated in 74% yield, >20:1 d.r. and in 95% *ee*.

5 Results and Discussion

5.1 Initial Reaction Development

The first goal of this project was the development of a transition metal catalyzed allylic substitution reaction with terminal alkynes as pronucleophiles. While several processes using premetalated alkynes have been described,[53] only one catalytic asymmetric transformation employing terminal alkynes was reported as of October 2014.[54] In this example, *Sawamura* and coworkers accessed chiral 1,4-enynes from primary allylic phosphates and terminal acetylides using a copper catalyst. We envisioned a related transformation using iridium or rhodium catalysis. Likely, such a reaction would employ a branched allylic alcohol derivative and, as such, be complementary to *Sawamura*'s work. Furthermore, it was anticipated that the scope of the reaction would be different from the copper catalyzed process.

In preliminary studies, the desired transformation was observed under the conditions shown in Scheme 5.1. Racemic carbonate **159** reacted with alkyne **160** to give the linear 1,4-enyne **161** with full conversion judged by ^{19}F-NMR analysis of the crude reaction mixture. Notably, no branched product was isolated.[55] In the absence of Rh the starting material was recovered.

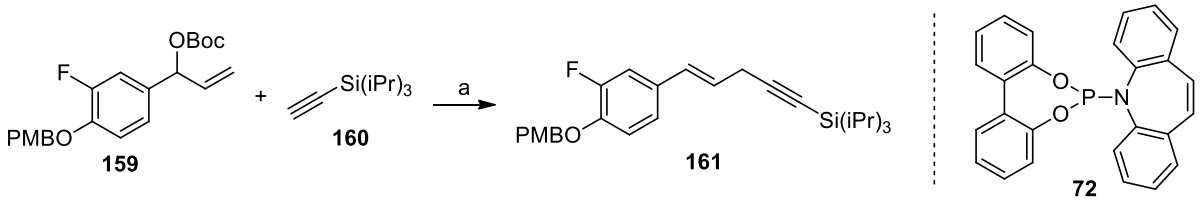

Scheme 5.1 Reagents and conditions: (a) **159** (1.0 equiv.), **160** (2.0 equiv.), [{Rh(cod)Cl}$_2$] (0.020 equiv.), **72** (0.040 equiv.), CuCl (0.20 equiv.), Et_3N (2.0 equiv.), nBu$_4$NCl (0.30 equiv.), 1,4-dioxane (0.20 M), 50 °C to 60 °C, 6 h, >95% convn. as judged by ^{19}F-NMR analysis of the crude material, the reaction was run on a 0.10 mmol scale.

The (triisopropylsilyl)acetylene (**160**) was chosen based on previous work by the group of *Hayashi*.[56] In their enantioselective conjugate alkynylation of enones, they identified **160** as

[53] For catalytic, enantioselective allylic substitution reactions with alkynylaluminum and alkynylboron nucleophiles, see: (a) Dabrowski, J. A.; Gao, F.; Hoveyda, A. H. *J. Am. Chem. Soc.* **2011**, *133*, 4778. (b) Dabrowski, J. A.; Haeffner, F.; Hoveyda, A. H. *Angew. Chem., Int. Ed.* **2013**, *52*, 7694. (c) Hamilton, J. Y.; Sarlah, D.;Carreira, E. M. *Angew. Chem., Int. Ed.* **2013**, *52*, 7532.

[54] Harada, A.; Makida, Y.; Sato, T.; Ohmiya, H.; Sawamura, M. *J. Am. Chem. Soc.* **2014,** *136*, 13932.

[55] The linear product was isolated with a minor side product in a 15:1 ratio as judged by ^{19}F-NMR. The side product was not separated but does not show the spectral properties expected for the branched isomer.

[56] Nishimura, T.; Guo, X.-X.; Uchiyama, N.; Katoh, T.; Hayashi, T. *J. Am. Chem. Soc.* **2008,** *130*, 1576.

optimal reagent. Terminal alkynes with smaller substituents underwent competitive dimerization under the reaction conditions (1,4-dioxane, 80 °C, 24 h). Subsequent efforts were made to obtain the branched product. Scouting experiments were performed using various substrates, bases (*e.g.* Et_3N, Cy_2NMe, Cs_2CO_3, K_2CO_3, LiO*t*Bu, KO*t*Bu, $CsOH \cdot H_2O$), ligands (**72**, $P(OPh)_3$, 2,2′-biphenol, 1,10-phenanthroline), additives (nBu_4NCl, CuCl, $Zn(OTf)_2$, $InBr_3$, $AgNO_3$, AgOTf, MeOH) and organometallic complexes ([{Rh(cod)Cl}$_2$], [{Rh(CO)$_2$Cl}$_2$], [Rh(cod)$_2$]SbF$_6$, [{Ir(cod)Cl}$_2$], [{RuCl$_2$(*p*-cymene)}$_2$]). These reactions were typically run at 50 °C to 75 °C and analyzed by TLC, ^{1}H and ^{19}F-NMR. In general, only the initially employed alkyne **160** in the presence of a Rh^I catalyst resulted in significant amounts of the linear product and no branched product was isolated. Different allylic alcohol derivatives (carbonates and benzoates) were converted into the corresponding alkynylated, linear products. In this event, it was found that aliphatic allylic carbonates such as **162** can be used and that no additives other than the amine base are required (Scheme 5.2). A brief survey of other carbon nucleophiles indicated that the regioselectivity strongly depends on the nature of the nucleophile. Boronic acids yielded the linear regioisomer while sodium dimethyl malonate provided the branched product in good regioselectivity. The latter observation is in accordance with previously reported results obtained under similar conditions.[57]

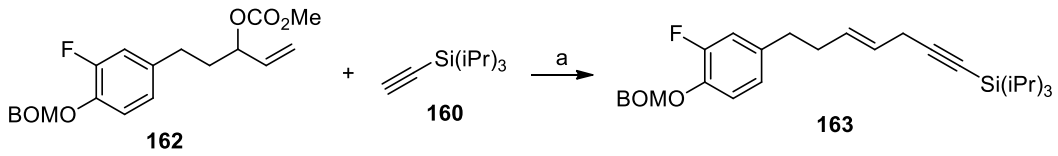

Scheme 5.2 Reagents and conditions: (a) **162** (1.0 equiv.), **160** (2.0 equiv.), [{Rh(cod)Cl}$_2$] (0.020 equiv.), **72** (0.040 equiv.), Et_3N (2.0 equiv.), 1,4-dioxane (0.2.0 M), 50 °C to 70 °C, 3 h, 74% convn. as judged by ^{19}F-NMR analysis of the crude material, the reaction was run on a 0.050 mmol scale.

Allylic alcohol derivatives with a 1,2-disubstituted olefin where also examined (Figure 5.1). While allylic acetate **164** and carbonate **165** gave no conversion (conditions as in Scheme 5.1 and heated up to 90 °C), while phosphate **166** furnished predominantly elimination product **167**.

[57] Evans, P. A.; Nelson, J. D. *Tetrahedron Lett.* **1998**, *39*, 1725.

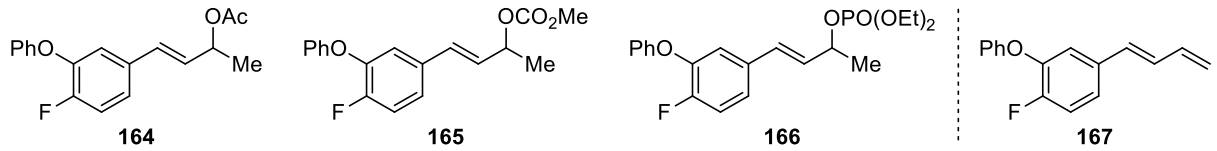

Figure 5.1 Substrates evaluated bearing a 1,2-disubstituted olefin (**164**-**166**) and one observed product (**167**).

With this precedent in mind, we decided to investigate a related propargylic substitution reaction. Since the alkyne moiety was now part of the electrophile, arylboronic acids were chosen as nucleophiles. In an early experiment, good conversion was obtained in the reaction of propargylic carbonate (±)-**168** with 4-cyanophenylboronic acid (**169**) to yield allene **170** (Scheme 5.3). Under these conditions, the product was racemic. Without the addition of water or when using a 2/1 ligand to Rh ratio the conversion was lower (31% and 17%, respectively) and the products were racemic. Recovered starting material accounted for most of the mass balance. Several minor side products were formed but each in less than 5% as judged by ^{19}F-NMR analysis of the crude material. In other words, no substantial amounts of propargylic substitution or hydroarylation products were observed. This finding is in contrast with the work by *Murakami* and coworkers.[42] In their studies, the initial addition of an arylrhodium species across the alkyne occurs with moderate regioselectivity. This leads to a mixture of allene (from the addition of the aryl group distal to the leaving group) along with the hydroarylation product (from the regioisomeric addition of the aryl group) as outlined in the previous chapter.

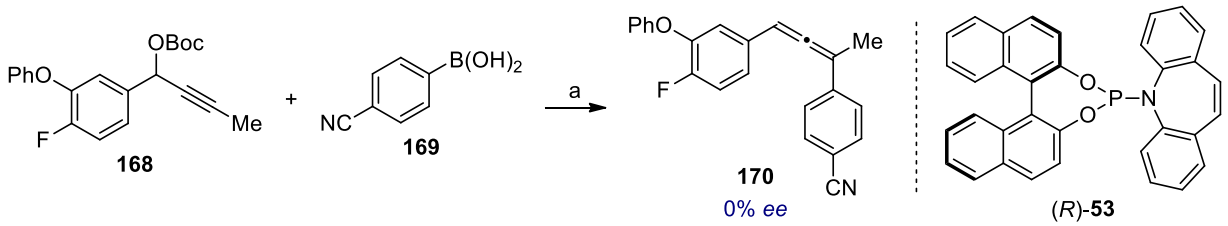

Scheme 5.3 Reagents and conditions: (a) (±)-**168** (1.0 equiv.), **169** (2.0 equiv.), Cs_2CO_3 (2.0 equiv.), [{Rh(cod)Cl}$_2$] (0.040 equiv.), (*R*)-**53** (0.080 equiv.), 1,4-dioxane/H_2O 8:1 (0.18 M), 23 °C to 50 °C, 2 h, 82% convn. as judged by ^{19}F-NMR analysis of the crude material, the reaction was run on a 0.050 mmol scale.

Encouraged by the high regio- and chemoselectivity, we next examined other substrates in order to probe the reactivity and selectivity of this transformation. Two propargylic carbonates with an unsubstituted alkyne were tested but furnished a complex mixture of products. A moderate enantioinduction was found when employing aliphatic propargylic carbonate (±)-**171** (Scheme 5.4). Allene **172**, resulting from addition of phenylboronic acid (**137**) to carbonate **171** and subsequent elimination was isolated in 31% *ee*, as a single regioisomer. Under the same conditions, but in the absence of water, the opposite enantiomer was formed in low

excess (-25% *ee*, 25% convn., 50 °C to 60 °C, 4 h). When the same reaction was carried out at 23 °C with a 1/1 ligand to Rh ratio (90 min, >95% convn.), allene **172** was isolated without any detectable enantiomeric excess.

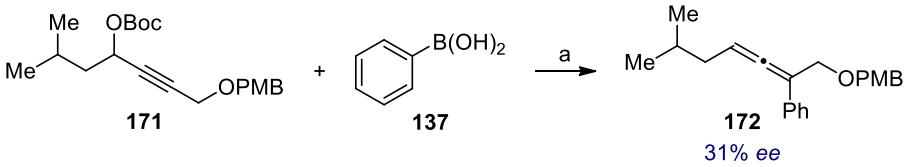

Scheme 5.4 Reagents and conditions: (a) **171** (1.0 equiv.), **137** (2.0 equiv.), Cs_2CO_3 (2.0 equiv.), [{Rh(cod)Cl}$_2$] (0.040 equiv.), (*R*)-**53** (0.18 equiv.), 1,4-dioxane/H_2O 10:1 (0.15 M), 23 °C to 50 °C, 3 h, >95% convn. as judged by ^{1}H-NMR analysis of the crude material, **172** isolated with 31% *ee* and unknown absolute stereochemistry, the reaction was run on a 0.025 mmol scale.

Subjecting (±)-**173** to the same conditions, four different chiral ligands were examined (Table 5.1). The enantiomeric excess was low (6-24% *ee*) but the good reactivity was observed (36-70% convn.) given that all reactions were stopped after 1 h at 50 °C. Since these preliminary runs were stopped before reaching completion, the possibility of a partial kinetic resolution has to been taken into account when interpreting the outcomes. However, because all enantioselectivities obtained were low (<25% *ee*), it can be stated that neither a good enantioinduction nor a strong kinetic resolution was caused by any of the four ligands tested.

Table 5.1 Screening of chiral ligands for the enantioselective synthesis of allenes. Reagents and conditions: (a) (±)-**173** (1.0 equiv.), **174** (2.0 equiv.), Cs_2CO_3 (2.0 equiv.), [{Rh(cod)Cl}$_2$] (0.040 equiv.), ligand (0.080 equiv.; 0.17 equiv. for **177**), 1,4-dioxane/H_2O 10:1 (0.15 M), 50 °C, 1 h, convn. estimated by ^{1}H-NMR analysis of the crude reaction mixture, the absolute stereochemistry of the product was not determined, all reactions were run on a 0.050 mmol scale.

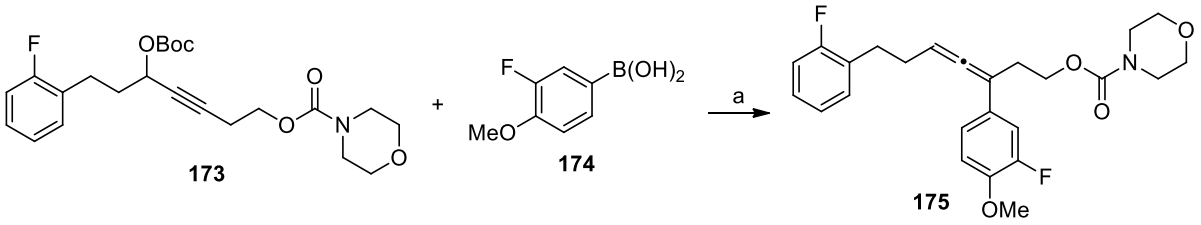

Entry	Ligand	Conversion	*ee* (**175**)
1	(*S*)-**176**	40%	6%
2	(*R*)-**177**	36%	22%
3	(*R*)-**63**	50%	24%
4	(*R*)-**178**	70%	–8%

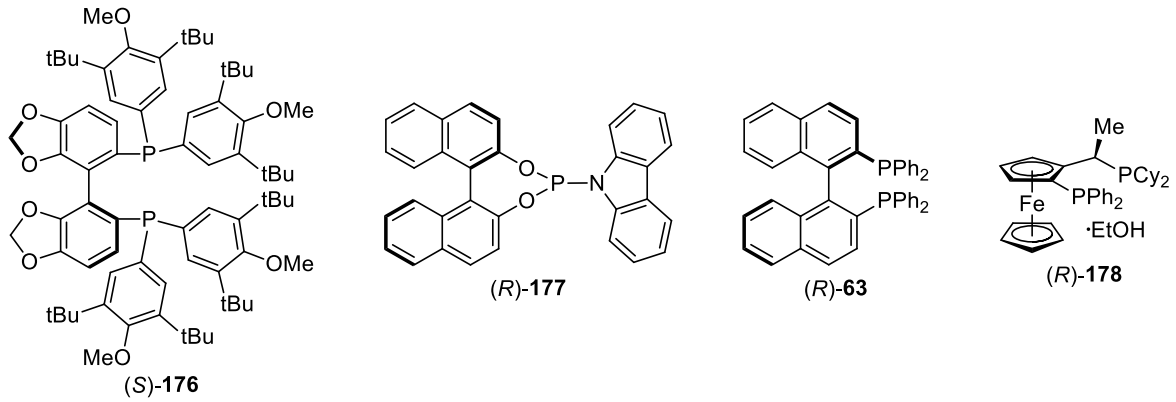

Having examined three different racemic, secondary propargylic carbonates (**168**, **171**, **173**), the challenges of developing an asymmetric variant of this transformation became apparent. Thus far, the nature of the substrate had a greater influence on the observed enantioselectivities than the small set of tested ligands. Therefore, two additional substrates were prepared and subjected to the same reaction conditions (Scheme 5.5). The secondary propargylic carbonate **179** gave the trisubstituted allene **180** with low *ee*, while the tertiary propargylic carbonate **181** yielded the tetrasubstituted allene **182** with minimal enantiomeric excess.

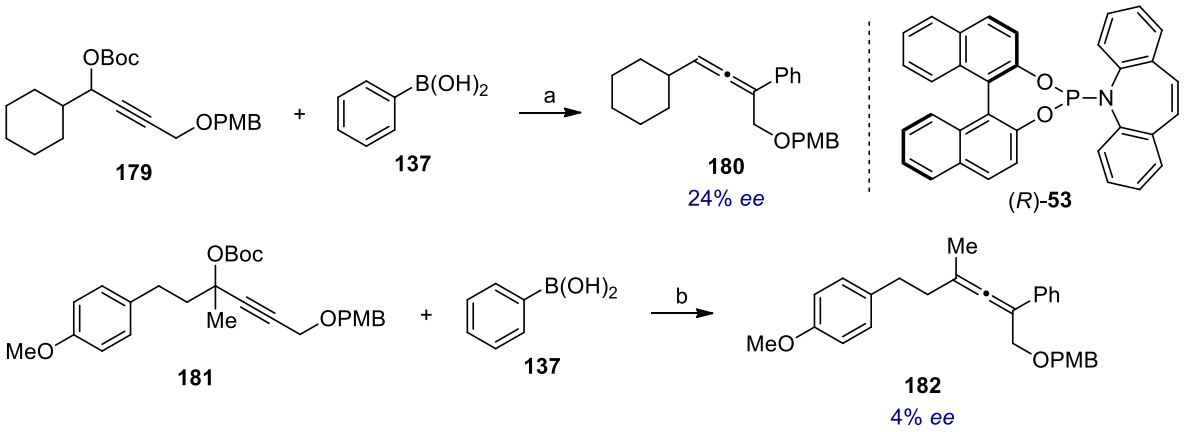

Scheme 5.5 Reagents and conditions: (a) **179** (1.0 equiv.), **137** (2.0 equiv.), 1.5 M aq. Cs_2CO_3 (2.0 equiv.), [{Rh(cod)Cl}$_2$] (0.040 equiv.), (*R*)-**53** (0.18 equiv.), 1,4-dioxane (0.17 M), 50 °C, 5 h, >95% convn. as judged by ^{1}H-NMR analysis of the crude material, **180** isolated with 24% *ee* and undetermined absolute stereochemistry, the reaction was run on a 0.050 mmol scale; (b) **181** (1.0 equiv.), **137** (2.0 equiv.), 1.5 M aq. Cs_2CO_3 (2.0 equiv.), [{Rh(cod)Cl}$_2$] (0.040 equiv.), (*R*)-**53** (0.18 equiv.), 1,4-dioxane (0.17 M), 50 °C, 5 h, 78% convn. as estimated by ^{1}H-NMR analysis of the crude product, **182** isolated with 4% *ee*, the reaction was run on a 0.050 mmol scale.

As discussed in the previous chapter, the difficulty in inducing enantioselectivity is believed to be associated with the mechanism of the reaction. If an addition/elimination pathway is operational, high *ee*'s can only be obtained if there is a selective *syn*- or *anti*-elimination for each diastereomeric vinylrhodium intermediate. This scenario is different from most metal catalyzed substitution reactions, where the chiral catalyst has to differentiate two enantiotopic

sites in order to induce enantioselectivity. The encountered difficulty to change the mode of elimination through catalyst control and the availability of methods for the preparation of chiral secondary propargylic alcohols led us to examine the corresponding enantiospecific reaction. In order to study the extent of chirality transfer, enantioenriched **179** (99% *ee*) was prepared following a known procedure.[58] An initial reaction conducted at room temperature with a 1/1 ligand to Rh ratio led to complete loss of enantiomeric excess (Scheme 5.6). Given the good reactivity and high regio- as well as chemoselectivity observed in this transformation, our next goal was to achieve high enantiospecificity.[59] The development of a stereoselective method for the synthesis of allenes from enantioenriched, propargylic alcohol derivatives is outlined in the following subchapter.

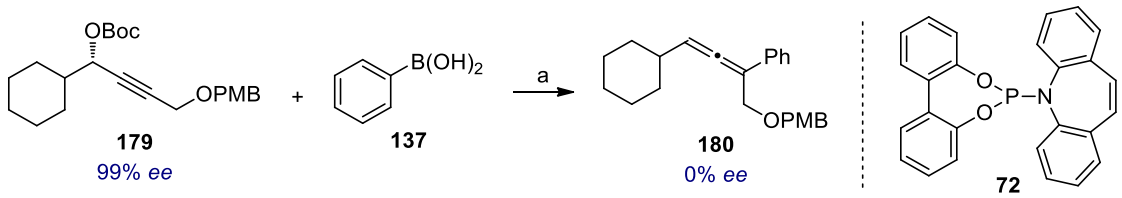

Scheme 5.6 Reagents and conditions: (a) **179** (1.0 equiv.), **137** (2.0 equiv.), 1.5 M aq. Cs_2CO_3 (2.0 equiv.), [{Rh(cod)Cl}$_2$] (0.040 equiv.), **72** (0.080 equiv.), 1,4-dioxane (0.17 M), 22 °C, 2 h, >95% convn. as judged by ^{1}H-NMR analysis of the crude material, the reaction was run on a 0.050 mmol scale.

5.2 Optimization Process

5.2.1 Development of a stereoselective reaction between propargylic alcohol derivatives and electron neutral or electron rich arylboronic acids

At the outset of the optimization process, the desired transformation took place at room temperature. However, the enantiomeric excess of the starting material was lost throughout the reaction (Scheme 5.6). Allene **180** was first isolated with measurable enantiomeric excess when the reaction shown in Scheme 5.6 was conducted with a 2/1 ligand to Rh ratio (24% *ee*,

[58] Frantz, D. E.; Fässler, R.; Carreira, E. M. *J. Am. Chem. Soc.* **2000**, *122*, 1806.
[59] Within this thesis the terms 'enantiospecific' and 'enantiospecificity' refer to a reaction in which the *ee* of the starting material is conserved over the course of the transformation to a measurable degree. It has to be noted, that a more rigid definition of these terms exists. In these cases, it is refered to as no detectable loss of *ee* during the reaction. The enantiospecificity (*es*) is defined as *es* = [*ee* (product)]/[*ee* (starting material)] × 100%, see: Denmark, S. E.; Burk, M. T.; Hoover, A. J. *J. Am. Chem. Soc.* **2010**, *132*, 1232.

50 °C, 2 h, 50% convn.).[60] In line with previous results, the reactivity was significantly diminished under these conditions but the selectivity was higher. A preliminary survey of additives, other than Cs_2CO_3, identified K_3PO_4 as efficient base when the reaction was performed in 1,4-dioxane without additional water. Next, a solvent screening was performed using K_3PO_4 as base and without the addition of water (Table 5.2). Both, reactivity and selectivity, were considerably improved when 1,2-dichloroethane was employed instead of 1,4-dioxane (entry 2 versus 1). THF gave results comparable to 1,4-dioxane (entry 3).

Table 5.2 Screening of solvents for the reaction between benzoate **179** and phenylboronic acid. Reagents and conditions: (a) **179** (1.0 equiv.), **137** (2.0 equiv.), K_3PO_4 (2.0 equiv.), [{Rh(cod)Cl}$_2$] (0.040 equiv.), **72** (0.18 equiv.), solvent (0.17 M), 50 °C, 1 h, then 65 °C, 1 h (entry 1), 50 °C, 1 h (entry 2), 50 °C, 1 h, then 60 °C, 90 min (entry 3), convn. estimated by ^{1}H-NMR analysis of the crude material, all reactions were run on a 0.050 mmol scale. The absolute stereochemistry of the product was assigned based on analogy to compound **214** (*vide infra*).

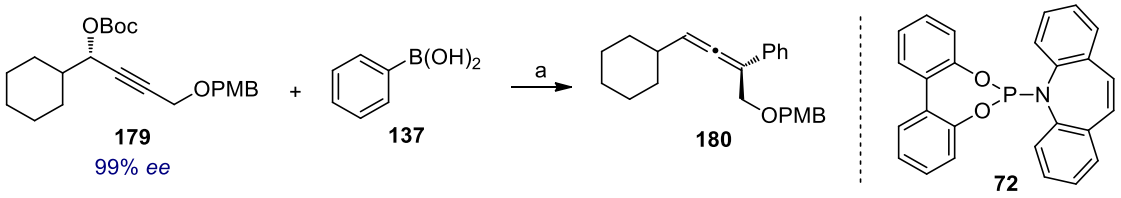

Entry	Solvent	Conversion	*ee* (**180**)
1	1,4-dioxane	41%	79%
2	1,2-dichloroethane	87%	93%
3	THF	43%	83%

It should be noted that the improved selectivity is not only because of the use of K_3PO_4 and 1,2-dichloroethane but also a consequence of removing water. In this regard it, was found that some trends between a specific reaction parameter and the observed selectivity are concurrent for the enantioselective and enantiospecific reaction. A ligand to metal ratio of 2/1 gives, for example, a higher selectivity in both cases. At the same, time the selectivity of the two processes are differently affected *e.g.* by the addition of water.

Besides solvent and base, it was assumed that the leaving group will significantly influence both the rate and selectivity of the transformation. Examination of different propargylic alcohol derivatives identified benzoate as a leaving group slightly superior to the *tert*-butyl carbonate (Scheme 5.7). Specifically, the selectivity was increased from 94% *es* to 95% *es* for the reaction of phenyl boronic acid with **179** and **183**. In addition to this small increase in

[60] The absolute stereochemistry of **180** and all products shown in the following, was assigned by analogy to allene **214**. The absolute configuration of **214** was established by X-ray crystallographic analysis.

selectivity, using benzoates had the advantage that all starting materials were UV active. Thus, facilitating the determination of the enantiomeric excess by SFC or HPLC analysis.

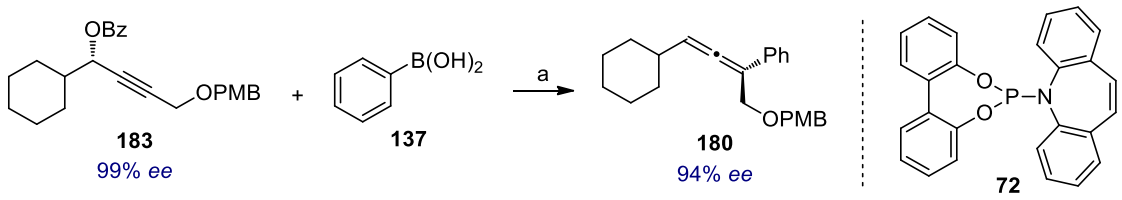

Scheme 5.7 Reagents and conditions: (a) **183** (1.0 equiv.), **137** (2.0 equiv.), K_3PO_4 (2.0 equiv.), [{Rh(cod)Cl}$_2$] (0.040 equiv.), **72** (0.17 equiv.), 1,2-dichloroethane (0.17 M), 50 °C, 1 h, 85% convn. as judged by ^{1}H-NMR analysis of the crude material, the reaction was run on a 0.018 mmol scale.

Having achieved reasonably high conversion and chirality transfer in the reaction of **183** with phenylboronic acid to yield allene **180**, the influence of the ligand was examined next. In this regard, one question to address was, if a commercially available ligand could be identified which gives satisfying result. For this reason, a small set of phosphoramidite, bidentate phosphine, and one phosphite ligand were examined (Table 5.3). In summary, full conversion was observed with various ligands but the selectivity was notably higher for two phosphoramidite ligands (entries 1, 2). Of note, removal of the olefin from ligand **72** led to significantly reduced reactivity (entry 2). The higher reactivity of a phosphine-olefin phosphoramidite ligand versus its counterpart (*i.e.* without an olefin) has been observed in a Rh-catalyzed enantioselective intramolecular hydroacylation reaction.[61] The reaction proceeded with lower enantiospecificity when using phosphine or phosphite ligands (entries 4-7).[62]

Table 5.3 Initial screening for the enantiospecific synthesis of allenes from benzoate **184** and phenylboronic acid. Reagents and conditions: (a) **184** (1.0 equiv.), **137** (2.0 equiv.), K_3PO_4 (2.0 equiv.), [{Rh(cod)Cl}$_2$] (0.040 equiv.), ligand (0.080 equiv. to 0.24 equiv.), 1,2-dichloroethane (0.17 M), 50 °C, 2 h, convn. estimated by ^{1}H-NMR analysis of the crude reaction mixture, all reactions were run on a 0.050 mmol scale.

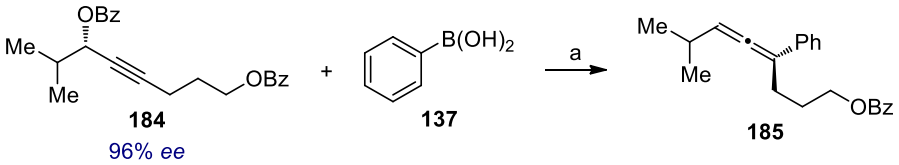

Entry	Ligand	Ligand/Rh	Conversion	*ee* (**185**)
1	**72**	2/1	>95%	94%

[61] Hoffman, T. J.; Carreira, E. M. *Angew. Chem., Int. Ed.* **2011**, *50*, 10670.
[62] For a selected use of ligand **187** (DPEphos) in a Rh^I-catalyzed reaction, see: Lumbroso, A.; Koschker, P.; Vautravers, N. R.; Breit, B. *J. Am. Chem. Soc.* **2011**, *133*, 2386. For a selected use of ligand **188** (DPPF) in a Rh^I-catalyzed reaction, see Li, C.; Breit, B. *J. Am. Chem. Soc.*, **2014**, *136*, 862.

2	**87**	2/1	46%	94%
3	**186**	2/1	<5%	n. d.
4	**187**	1/1	>95%	85%
5	**188**	1/1	>95%	87%
6	**189**	1/1	>95%	90%
7	$P(OMe)_3$	3/1	61%	80%

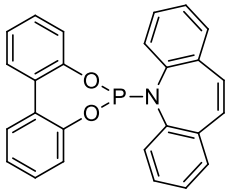

72

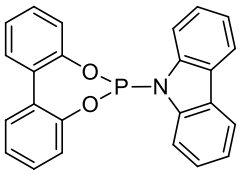

87

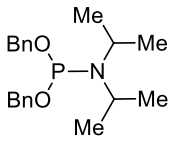

186

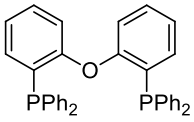

187

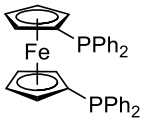

188

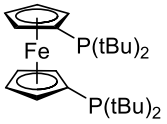

189

In later evaluations of various phosphoramidite ligands, it was found that the olefin ligand derived from TADDOL showed higher reactivity than **72**.[63] This raised the question if the selectivity of the enantiospecific transformation could be improved by using the matching enantiomer of a chiral ligand. Therefore, the TADDOL-derived ligand (*R*,*R*)-**190** and its enantiomer were tested for such a matched case (Table 5.4). Both chiral ligands provided the product in lower *ee* than the racemic ligand **72** (entries 2 and 3 versus 1). This result suggested that only one ligand is bound to the active Rh-catalyst, which could be due to the steric hindrance of the four phenyl substituents only present in **190**. An alternative explanation is that two ligands are coordinated to the Rh-catalyst and the nature of the ligand induces a less selctive *syn*-elimination from the transient vinylrhodium species (compared to **72**).

[63] Specifically, the reaction between **184** and 3-fluorophenylboronic acid showed >95% convn. for **190**, 74% convn. for **72** and 39% convn. for **53** (catalyst generated *in situ* from [{Rh(cod)Cl}$_2$] and the corresponding ligand in a 1/2 Rh to ligand ratio; 6 mol% Rh, 40 °C, 5.5 h, convn. estimated by ^{1}H-NMR analysis of the crude reaction mixture).

Table 5.4 Follow-up ligand screening for the enantiospecific synthesis of allenes from benzoate **184** and phenylboronic acid. Reagents and conditions: (a) **184** (1.0 equiv.), **137** (2.0 equiv.), K_3PO_4 (2.0 equiv.), [{Rh(cod)Cl}$_2$] (0.020 equiv.), ligand (0.080 equiv.), 1,2-dichloroethane (0.17 M), 40 °C, 4 h, convn. estimated by ^{1}H-NMR analysis of the crude reaction mixture, all reactions were run on a 0.025 mmol scale.

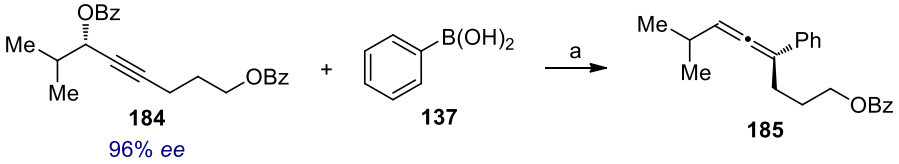

Entry	Ligand	Conversion	*ee* (**185**)
1	**72**	>95%	95%
2	(*R*,*R*)-**190**	>95%	75%
3	(*S*,*S*)-**190**	>95%	80%

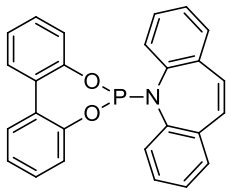

72

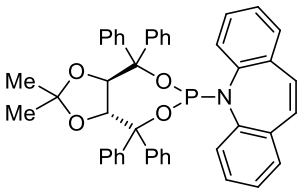

(*R*,*R*)-**190**

This optimization process has led to reaction conditions which showed high selectivity and complete consumption of the benzoate when using phenylboronic acid (8% catalyst loading, 2 h, 50 °C). However, two drawbacks were still evident. Firstly, under these conditions electron poor boronic acids performed sluggishly and often failed to reach full conversion. Secondly, minor amounts of side products were observed. The amount depending on the substrates employed as well as on the exact reaction parameters. Two of these side products are believed to be the regioisomeric hydroarylation products. For the addition of phenylboronic acid to benzoate **184** the hydroarylation products would be **191** and **192** (Figure 5.2).[64]

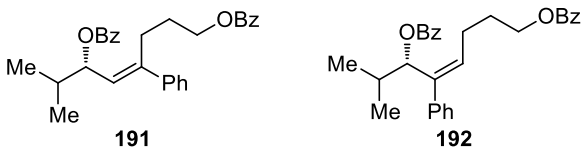

Figure 5.2 Tentatively assigned regioisomeric hydroarylation side products from the addition of phenylboronic acid to benzoate **184** and subsequent protonation.

With the goal of achieving better reactivity while suppressing the formation of side products, the influence of the ligand to rhodium ratio, temperature, and additives was examined

[64] The side products were not fully characterized. **191** and **192** are tentatively assigned structures.

(Table 5.5). As expected, a ligand to Rh ratio of 1/1 increased the conversion and yielded allene **185** with somewhat lower *ee* (entries 1 and 4).

Table 5.5 Initial reaction parameter screening for the enantiospecific synthesis of allenes from benzoate **184** and phenylboronic acid. Reagents and conditions: (a) **184** (1.0 equiv.), **137** (2.0 equiv.), K_3PO_4 (2.0 equiv.), [{Rh(cod)Cl}$_2$] (0.040 equiv.), **72** (0.080 equiv. or 0.18 equiv.), 1,2-dichloroethane (0.17 M), convn. estimated by ^{1}H-NMR analysis of the crude reaction mixture, the reactions were run on a 0.050 mmol scale; (b) ratio of **185** and the sum of **191** and **192** as judged by ^{1}H-NMR analysis of the crude material; (c) 10 equiv. H_2O added; (d) 5.0 equiv. KF instead of K_3PO_4 added.

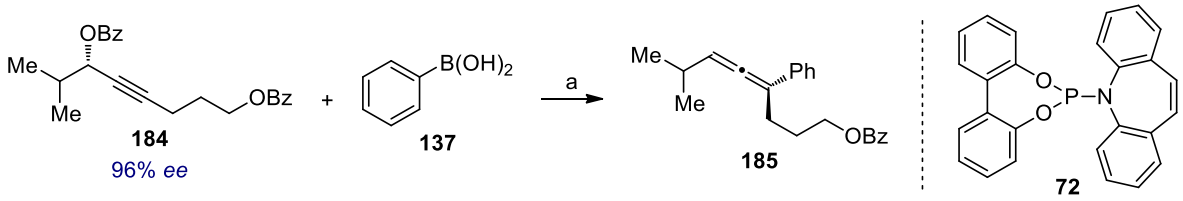

Entry	Additive	Ligand/Rh	Temp.	Time	Prod./Side Prod.[b]	Conversion	*ee* (**185**)
1	none	2/1	50 °C	2 h	4.4	>95%	94%
2	none	2/1	25 °C	16 h	7.1	93%	95%
3	H_2O[c]	2/1	25 °C	3 h	4.3	85%	94%
4	none	1/1	25 °C	1 h	5.1	65%	92%
5	H_2O[c]	1/1	25 °C	1 h	4.1	92%	89%
6	KF[d]	1/1	25 °C	1 h	4.2	69%	93%

The addition of water also led to better conversion, again, at the expense of diminished enantiospecificity (Table 5.5, entries 2 and 3 as well as 4 and 5). Often, additional water led to increased formation of side products. Using K_3PO_4•H_2O instead of K_3PO_4 did not influence the outcome of the transformation.[65] The results in Table 5.5 may suggest that the conditions employed for entry 2 would fulfill all requirements. However, when more challenging substrates were examined, the reactivity was not satisfying, especially with electron poor arylboronic acids as coupling partner. Therefore, the transformation was examined at elevated temperatures (40 °C or 50 °C) and with a 2/1 ligand to Rh ratio (Table 5.6).

Table 5.6 Follow-up reaction parameter screening for the enantiospecific synthesis of allenes from benzoate **184** and phenylboronic acid. Reagents and conditions: (a) **184** (1.0 equiv.), **137** (2.0 equiv.), K_3PO_4 (2.0 equiv.), [{Rh(cod)Cl}$_2$] (0.020 equiv. or 0.030 equiv.), **72** (0.080 equiv. or 0.12 equiv.), 1,2-dichloroethane (0.17 M), convn. estimated by ^{1}H-NMR analysis of the crude reaction mixture, the reactions were run on a 0.050 mmol or a 0.025 mmol scale; (b) 4.0 mol% Rh refers to the use of 2.0 mol% [{Rh(cod)Cl}$_2$]; (c) ratio of **185** and the sum of **191** and **192** as

[65] Under conditions as for entry 2, Table 5.5.

judged by ^{1}H-NMR analysis of the crude material; (d) 10 equiv. H_2O added; (e) 4.0 equiv. H_2O added; (f) 6.0 mol% PPh_3 and 6.0 mol% **72** used.

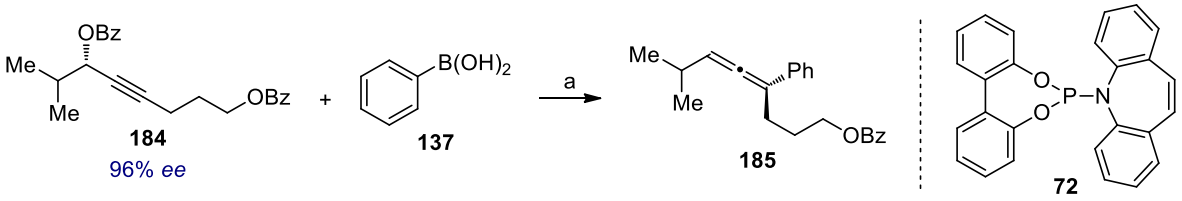

Entry	Additive	mol% Rh[b]	Temp.	Time	Prod./Side Prod.[c]	Conversion (*ee*)
1	H_2O[d]	4.0 mol%	50 °C	14 h	3.7	>95% (93% *ee*)
2	H_2O[e]	4.0 mol%	40 °C	12 h	3.9	64%
3	H_2O[e]	4.0 mol%	50 °C	12 h	3.8	>95%
4	none	6.0 mol%	40 °C	6 h	17	89%
5	PPh_3[f]	6.0 mol%	40 °C	6 h	6.5	>95% (66% *ee*)

Modulating the amount of water present, the temperature, and reaction time did not lead to significantly better results. As noted before, additional water increased the rate of the process but simultaneously reduced the selectivity and led to the formation of side products (Table 5.6). A catalyst generated *in situ* from [{Rh(cod)Cl}$_2$], olefin phosphoramidite ligand **72**, and PPh_3 showed good conversion but a large loss of enantiomeric purity (entry 5).

Various bases were examined for their influence on the efficiency in the synthesis of allene **185** from benzoate **184** (Table 5.7). From all bases tested, only KOH gave somewhat better results than K_3PO_4 (entry 3 compared to entry 1).[66] For practical reasons, the base was not changed. Tribasic potassium phosphate was found to be much easier to handle on smaller scale than KOH which is commonly available as hard pellets. In addition, the outcome using either base was comparable. Other bases were found to be less effective or led to increased amount of side products.

[66] In preliminary experiments, it was found that using NaOMe yielded the product with lower *es* (compared to K_3PO_4).

Table 5.7 Effect of various bases in the synthesis of allenes from benzoate **184** and phenylboronic acid. Reagents and conditions: (a) **184** (1.0 equiv.), **137** (2.0 equiv.), base, [{Rh(cod)Cl}$_2$] (0.030 equiv.), **72** (0.13 equiv.), 1,2-dichloroethane (0.15 M), 50 °C, 10 h, convn. estimated by ^{1}H-NMR analysis of the crude reaction mixture, the reactions were run on a 0.025 mmol; (b) ratio of **185** and the sum of **191** and **192** as judged by ^{1}H-NMR analysis of the crude material.

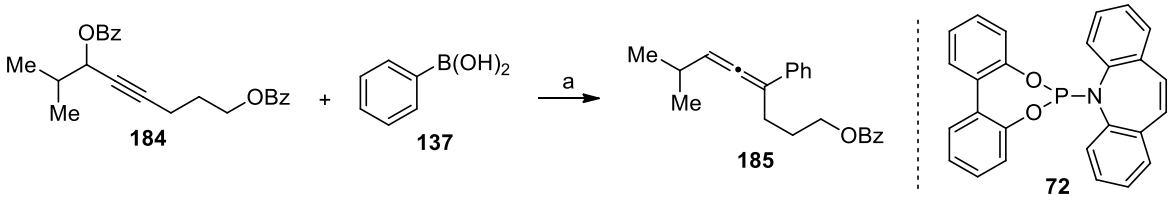

Entry	Base	Prod./Side Prod.[b]	Conversion
1	K_3PO_4 (2.0 equiv.)	14	93%
2	K_2CO_3 (2.7 equiv.)	3.5	>95%
3	KOH (3.7 equiv.)	15	95%
4	KO*t*Bu (2.2 equiv.)	2.2	18%
5	Tl_2CO_3 (2.0 equiv.)	2.0	53%
6	Cs_2CO_3 (2.0 equiv.)	>20	51%

5.2.2 Development of a stereoselective reaction between propargylic alcohol derivatives and electron poor arylboronic acids

This optimization process led to the identification of reaction conditions, which gave good results for a set of propargylic benzoates and electron rich as well as electron neutral arylboronic acids. The reaction of electron deficient arylboronic acids remained challenging, giving only moderate conversions. The last screening was consequently carried out with the goal to increase the rate, especially for electron deficient arylboronic acids. Parameters examined and discussed in the following included additives, solvents, co-solvents, different propargylic alcohol derivatives, ligands, Rh organometallic complexes, or the order of addition. Instead of phenylboronic acid, 4-(ethoxycarbonyl)-benzeneboronic acid (**193**) was chosen as nucleophile for most of the following optimization. A ligand to Rh ratio of 1/1 was utilized in order to gain the higher reactivity required for the electron poor boronic acids. Indeed, with a 2/1 ratio no product was formed with boronic acid **193**.[67]

Early screening with boronic acid **193** and benzoate **184** (96% *ee*) showed that the addition of water (55 equiv.) results in multiple side products. The combination of different amounts of water with THF as co-solvent also increased the amount of undesired compounds. The use of

[67] In the absence of water or other polar additives the starting material was recovered (8 mol% catalyst, 60 °C, 1 h). When 10 equiv. water were added, low conversion was observed at elevated temperatures (28% after 2 h at 70 °C).

an olefin ligand[68] led to significant amounts of side products while allene **194** was isolated with 87% *ee*. Utilization of various polar solvents and additives led to a general increase in the rate of the process but the enantiomeric excess decreased. The effects of a selection of polar co-solvents or additives are given in Table 5.8.

Table 5.8 Additive and co-solvent screening for the synthesis of allenes using boronic acid **193**. Reagents and conditions: (a) **184** (1.0 equiv.), **193** (2.0 equiv.), K_3PO_4 (2.0 equiv.), [{Rh(cod)Cl}$_2$] (0.040 equiv.), **72** (0.080 equiv.), 1,2-dichloroethane (0.17 M), 40 °C, 3 h, convn. estimated by ^{1}H-NMR analysis of the crude reaction mixture, the reactions were run on a 0.025 mmol scale.

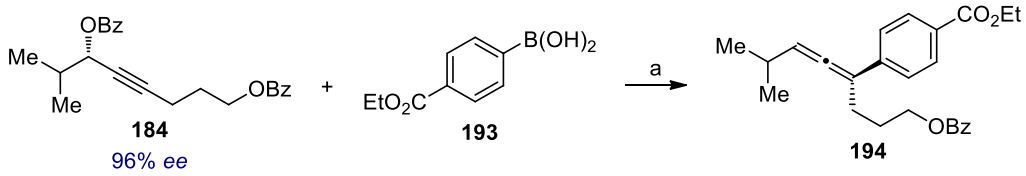

Entry	Additive	Conversion	*ee* (**194**)
1	MeOH (10 equiv.)	>95%	0%
2	DMF (co-solvent)	>95%	12%
3	NMP (co-solvent)	>95%	24%
4	TBAF•3H_2O (2.0 equiv.)	72%	94%
5	KF (2.0 equiv.)	48%	n. d.
6	CsF (6.0 equiv.)	47%	n. d.

Polar, protic, and aprotic solvents were examined as additives and co-solvents because they accelerate the transformation. However, the presence of only 10 equiv. of MeOH led to complete loss of the enantiomeric excess in course of the reaction (Table 5.8, entry 1). Because of this finding and the ones shown in entries 2 and 3, polar solvents were no longer considered as additives despite having a positive effect on reactivity. Of note was the relatively high *ee* observed when TBAF•3H_2O was added while using a 1/1 ligand to Rh ratio (entry 4). When the reaction of **184** to allene **185** was conducted in the presence of TBAF•3H_2O, **185** was enriched in the opposite enantiomer (Scheme 5.8). In other words, this preliminary observation indicated that the transient vinylrhodium species underwent an *anti*-elimination to yield *ent*-**185**. Albeit with lower conversion, the high selectivity for the opposite enantiomer warranted further investigations.

[68] Specifically 2-naphthyl (1*R*,4*R*,7*R*)-7-isopropyl-5-methylbicyclo[2.2.2]octa-2,5-diene-2-carboxylate was used in a 1/1 ligand to Rh ratio. Being interested more in the general reactivity, the existence of matched/mismatched cases were not examined. For a review on the use of chiral olefin ligands in catalysis, see: C. Defieber, H. Grützmacher, E.M. Carreira, *Angew. Chem., Int. Ed.* **2008**, *47*, 4482.

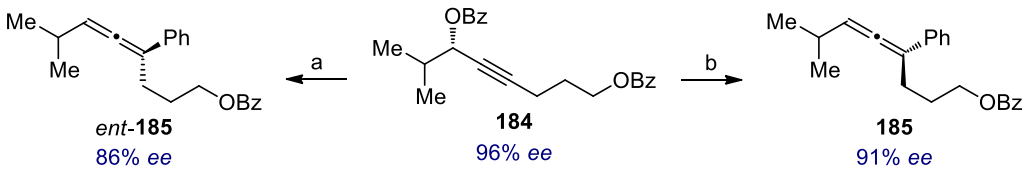

Scheme 5.8 Reagents and conditions: (a) **184** (1.0 equiv.), phenylboronic acid (**137**, 1.8 equiv.), K_3PO_4 (2.0 equiv.), TBAF•$3H_2O$ (2.0 equiv.), [{Rh(cod)Cl}$_2$] (0.020 equiv.), **72** (0.040 equiv.), 1,2-dichloroethane (0.17 M), 24 °C, 2 h, 36% convn. as judged by ^{1}H-NMR analysis of the crude material; (b) **184** (1.0 equiv.), phenylboronic acid (**137**, 1.6 equiv.), K_3PO_4 (2.0 equiv.), [{Rh(cod)Cl}$_2$] (0.020 equiv.), **72** (0.040 equiv.), 1,2-dichloroethane (0.17 M), 24 °C, 2 h, 94% convn. as estimated by ^{1}H-NMR analysis of the crude product, both reactions were run on a 0.025 mmol scale.

The addition of TBAF•$3H_2O$ to the reaction mixture decreased the rate when employing phenylboronic acid and gave the opposite enantiomer of the product (*vide supra*). However, for the addition of 4-(ethoxycarbonyl)-benzeneboronic acid (**193**) to the same starting material (**184**) this additive did not explicitly affect the reactivity.[69] At the same time, the transformation proceeded in a cleaner fashion.[70] Furthermore, the observed chirality transfer was higher when using electron poor arylboronic acid **193** (97% *es* versus 90% *es* for phenylboronic acid, both with benzoate **184**). For these reasons, the role of TBAF•$3H_2O$ was further studied and the transformation was optimized under these new, modified conditions.

So far 2.0 equiv. of TBAF•$3H_2O$ were added as additive in the presence of K_3PO_4 as base. This raised the question if both, the base and the additive, are required in order to achieve turnover and if the amount of the additive could be reduced. These two questions were examined and the results are shown in Table 5.9. No product was formed in the absence of K_3PO_4 (Table 5.9, entry 2). Allene **185** was isolated in considerably lower ee when the amount of TBAF•$3H_2O$ was reduced. This result suggested that the *syn*-elimination to give the opposite enantiomer is competing when using only one equivalent of this additive. Other sources of F^- were less effective than TBAF•$3H_2O$ (entries 3 and 4).

[69] For example 72% conversion was reached in the presence of TBAF•$3H_2O$ after 3 h at 40 °C, whereas 23% conversion was observed without TBAF•$3H_2O$ after 2.5 h at 24 °C under otherwise identical reaction conditions (1/1 ligand to Rh). When conducting the reaction with a 2/1 ligand to Rh ratio at 60 °C in the absence of TBAF•$3H_2O$ no conversion took place after 1 h but a some product was formed when TBAF•$3H_2O$ (2.0 equiv.) was added (32% conversion after 1 h under the same conditions).

[70] As observed for the reaction with phenylboronic acid, the amount of side products increased when employing a 1/1 ligand to metal ratio. Hence additives which lead to a cleaner transformation were of greater importance when using electron poor boronic acids.

Table 5.9 Additive screening for the enantiospecific synthesis of allenes using boronic acid **193**. Reagents and conditions: (a) **184** (1.0 equiv.), **193** (2.0 equiv.), K_3PO_4 (1.0 equiv. or none), [{Rh(cod)Cl}$_2$] (0.020 equiv.), **72** (0.040 equiv.), 1,2-dichloroethane (0.17 M), 50 °C, 2 h, convn. estimated by ^{1}H-NMR analysis of the crude reaction mixture, the reactions were run on a 0.025 mmol scale; (b) 1.4 equiv. TBAF•3H_2O added but no K_3PO_4.

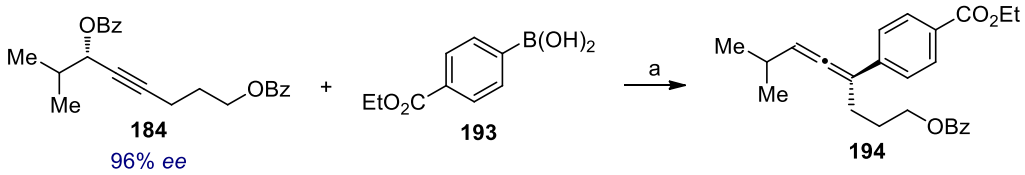

Entry	Additive	Conversion (*ee*)
1	TBAF•3H_2O (1.0 equiv.)	72% (81% *ee*)
2	TBAF•3H_2O, no K_3PO_4[b]	0%
3	TBAT (1.0 equiv.)	57%
4	Et_3N•3HF (1.0 equiv.)	57%

Not surprisingly, the elimination occurred with higher selectivity when the amount of TBAF•3H_2O was increased (Scheme 5.9 and Table 5.8 entry 4). Since the difference in *ee* observed for various amounts of the additive (≥ 2.0 equiv.) were within the experimental error,[71] 2.0 equiv. of TBAF•3H_2O were used henceforth. These reaction parameters selected allowed for a stereoselective and complete transformation when using propargylic benzoate **184** and boronic acid **193**. Since more challenging boronic acids still did not lead to full consumption of **184**, this addition/elimination process was further analyzed. Also, the conditions were somewhat different from the ones used for electron rich or electron neutral boronic acids and it was unclear if changing any parameter will have any effect in this transformation.

[71] The difference in *ee* when using 2.0 or 2.7 equiv. of TBAF•3H_2O was not significant as measured by SFC analysis.

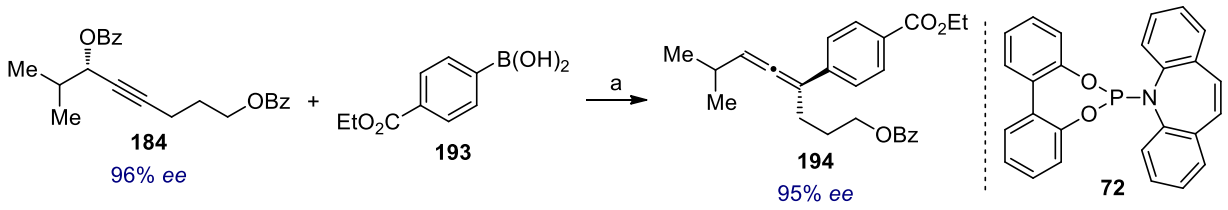

Scheme 5.9 Reagents and conditions: (a) **184** (1.0 equiv.), **193** (1.5 equiv.), K_3PO_4 (2.0 equiv.), TBAF•3H_2O (2.7 equiv.), [{Rh(cod)Cl}$_2$] (0.020 equiv.), **72** (0.040 equiv.), 1,2-dichloroethane (0.17 M), 40 °C, 22 h, >95% convn. as judged by ^{1}H-NMR analysis of the crude material, the reaction was run on 0.025 mmol scale.

For the synthesis of allenes from phenyl boronic acid and propargylic benzoate **184**, phosphoramidite ligand **72** bearing an olefin moiety was found to give best results among all ligands tested. For the evaluation of ligands in the related transformation between **184** and arylboronic acid **193**, a small set of similar phosphoramidite ligands was examined (**195-198**, Table 5.10). Changing one substituent on the nitrogen of the phosphoramidite ligand showed little effect on the rate of the reaction (entries 2-4). Even replacing the olefin from the ligand did not strongly affect the conversion (entry 5). When the enantiomeric excess of the entry with the highest reactivity was measured, ligand **72** proved to give the best selectivity (entry 1 versus 3).[72] Thus, the next series of experiments were conducted with ligand **72**.

Table 5.10 Evaluation of phosphoramidite ligands for the synthesis of allenes using boronic acid **193**. Reagents and conditions: (a) **184** (1.0 equiv.), **193** (2.0 equiv.), K_3PO_4 (2.0 equiv.), TBAF•3H_2O (2.0 equiv.), [{Rh(cod)Cl}$_2$] (0.020 equiv.), ligand (0.040 equiv.), 1,2-dichloroethane (0.17 M), 40 °C, 22 h, convn. estimated by ^{1}H-NMR analysis of the crude reaction mixture, all reactions were run on a 0.025 mmol scale.

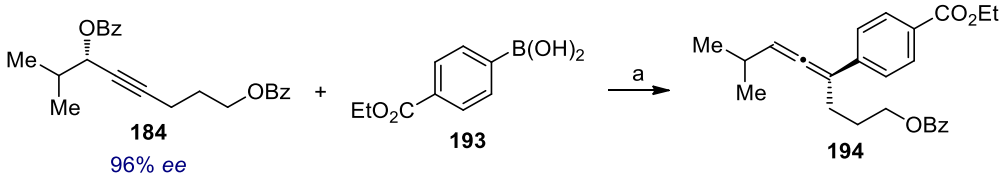

Entry	Ligand	Conversion	*ee* (**194**)
1	**72**	81%	95%
2	**195**	59%	n. d.
3	**196**	86%	93%
4	**197**	62%	n. d.
5	**198**	68%	n. d.

[72] This finding was also true when phenylboronic acid was used instead (79% convn. and 88% *ee* with **72** versus 63% convn. and 81% *ee* with **196**, both after 1 h at 23 °C under otherwise identical conditions).

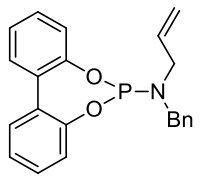

195

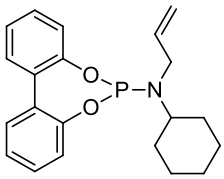

196

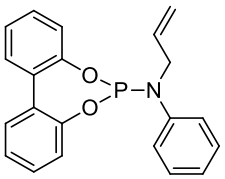

197

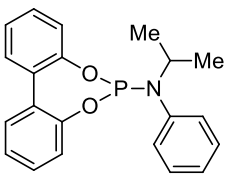

198

The solvent was re-examined and, because of the previous finding that apolar solvents give higher selectivity, no polar solvents were tested (Table 5.11). Both conversion and ee of the product were highest when 1,2-dichloroethane was used as solvent. The enantioselectivity was surprisingly low when the reaction was conducted in toluene (30% *ee*, entry 2). In cyclohexane very little desired product was formed, presumably due to the low solubility of boronic acid as well as catalyst (entry 4).

Table 5.11 Survey of apolar solvents for the synthesis of allenes using boronic acid **193**. Reagents and conditions: (a) **184** (1.0 equiv.), **193** (2.0 equiv.), K_3PO_4 (2.0 equiv.), TBAF•$3H_2O$ (2.0 equiv.), [{Rh(cod)Cl}$_2$] (0.020 equiv.), **72** (0.040 equiv.), solvent (0.17 M), 40 °C, 3 h, convn. estimated by ^{1}H-NMR analysis of the crude material, all reactions were run on a 0.025 mmol scale.

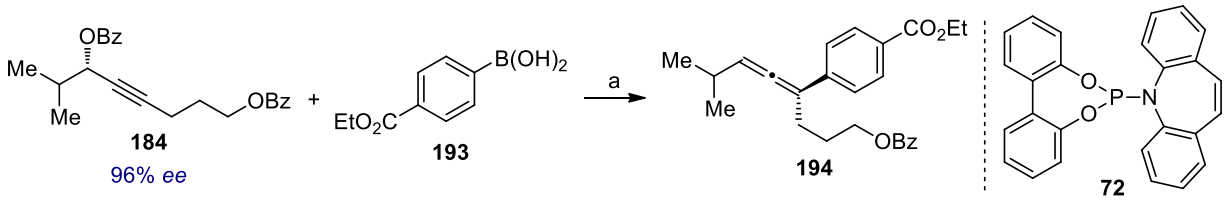

Entry	Solvent	Conversion	*ee* (**194**)
1	1,2-dichloroethane	68%	92%
2	toluene	20%	30%
3	CH_2Cl_2	56%	84%
4	cyclohexane	<5%	n. d.

In one of the last optimization studies, three different benzoates (**184**, **199** and **200**) were reacted with boronic acid **201** under the reaction conditions developed for electron neutral arylboronic acids (Table 5.12). The nitro substituted benzoate **199** proved more reactive than benzoate **184** or the 4-MeO benzoate **200**. However, when other 4-nitro benzoates and arylboronic acids were tested, this trend was found to be substrate dependent. Consequently, it was decided to continue to use unsubstituted benzoates as starting materials. Another advantage of the latter is that they are prepared from more widely available commodity chemicals (BzCl and Bz_2O).

Table 5.12 Examination of different racemic benzoates in the synthesis of allene **202** using boronic acid **201**. Reagents and conditions: (a) benzoate (1.0 equiv.), **201** (2.0 equiv.), K_3PO_4 (2.0 equiv.), [{Rh(cod)Cl}$_2$] (0.030 equiv.), **72** (0.13 equiv.), 1,2-dichloroethane (0.17 M), 40 °C, 3 h, convn. estimated by ^{1}H-NMR analysis of the crude material, all reactions were run on a 0.025 mmol scale.

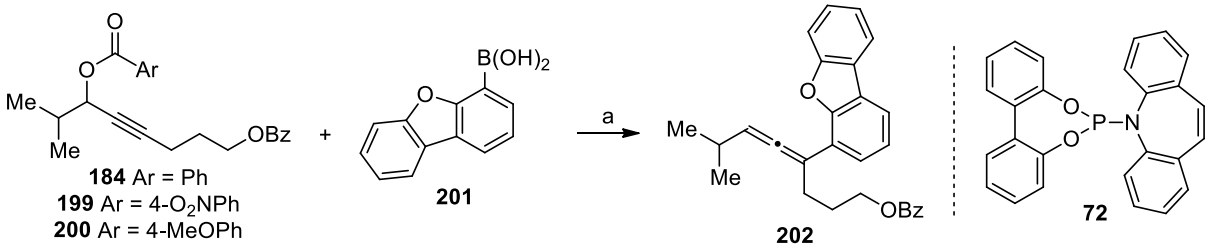

Entry	Benzoate	Conversion
1	**184**	66%
2	**199**	>95%
3	**200**	59%

For many Rh^I-catalyzed reactions it has been observed that Rh^I complexes with a weakly coordinating counterion exhibit greater reactivity.[73] Therefore the influence of a catalyst generated *in situ* from [Rh(cod)$_2$]SbF$_6$ and ligand **72** was examined. Under conditions which showed full conversion when [{Rh(cod)Cl}$_2$] was used, no reaction took place and the starting material was recovered. As a general observation,[74] the effect of water (higher reactivity, increased amount of side products, lower enantiospecificity) was found to be more pronounced when using a 1/1 ligand to Rh ratio (compared to a 2/1 ligand to Rh ratio). With a catalyst generated *in situ* from [{Rh(cod)Cl}$_2$] and phosphoramidite ligand **72** in a 1/4 ratio, water (typically up to about 10 equiv.) did not significantly alter the measured extent of chirality transfer or the ratio of product to side products formed. However, with a catalyst that bears only one phosphoramidite ligand **72**, the addition of water increases the formation of side products and lowers the observed *es*, even when adding water (<10 equiv.). When the reaction was performed in the presence of TBAF•3H$_2$O, a 1/1 ligand to Rh ratio had to be used (*vide supra*). Consequently, direct comparison of the two catalytic systems cannot be made. As expected, TBAF•3H$_2$O could also be replaced with an aq. solution (70-75% by weight in water). For practical reasons, the solid trihydrate was used instead of the viscous aq. solution of TBAF. Premixing the reagents prior to addition of the catalyst (propargylic benzoate, K_3PO_4 and TBAF•3H$_2$O in 1,2-dichloroethane, 40 °C, 15 min) did not influence the outcome.

---

[73] For selected examples, see: (a) Wender, P. A.; Gamber, G. G.; Williams, T. J. In Modern Rhodium-Catalyzed Organic Reactions; Evans, P. A., Ed.; Wiley-VCH: Weinheim, Germany, **2005**; Chapter 13. (b) See also ref 79a.

[74] For reactions conducted in the absence of TBAF•3H$_2$O. For representative conditions, see: Table 5.7, (a), entry 1.

The optimization studies described above changed the conditions under which the reaction is carried out and for this reason the enantioselective variant was re-examined (Scheme 5.10). Conducting the transformation with (*R*)-BINOL-derived phosphoramidite ligand (*R*)-**53** at room temperature in the presence of 10 equiv. water, the product was isolated with 40% *ee*. Without the addition of water, the reaction needed to be heated in order to observe good conversion and **185** was obtained in 33% *ee* (50 °C, 16 h, >95% convn.).

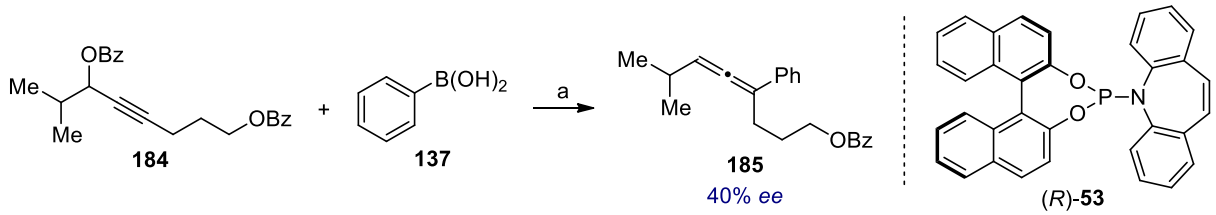

Scheme 5.10 Reagents and conditions: (a) **184** (1.0 equiv.), **137** (2.0 equiv.), K_3PO_4 (2.0 equiv.), [{Rh(cod)Cl}$_2$] (0.040 equiv.), **72** (0.21 equiv.), H_2O (10 equiv.), 1,2-dichloroethane (0.17 M), 24 °C, 17 h, 66% convn. as judged by ^{1}H-NMR analysis of the crude material, **185** isolated with 40% *ee* and undetermined absolute stereochemistry, the reaction was run on a 0.025 mmol scale.

5.3 Scope of the Reaction

In order to study the enantiospecific synthesis of trisubstituted allenes from chiral, propargylic benzoates, a variety of enantiomerically enriched propargylic benzoates were prepared. The benzoates which were successfully used as starting materials are shown below (Figure 5.3). Some propargylic benzoates were found to be challenging substrates and these are discussed later. The majority of substrates shown in Figure 5.3 were prepared by the direct, asymmetric addition of the corresponding terminal alkyne to the appropriate aldehyde.[75] This method proved to be reliable on different scales (0.5-8.0 mmol) and provided access to propargylic alcohols in high enantioselectivity (*ee* ≥ 95%) and good yields.[76] Benzoylation of the chiral alcohols occurred smoothly under standard conditions (BzCl, DMAP, pyridine, CH_2Cl_2). It was noted that more electron deficient benzoates show better reactivity in some cases (see previous subchapter). Therefore **205** was prepared in order to further compare the influence of two different benzoates. One propargylic alcohol was synthesized via Corey-

[75] The procedure described in the following reference was used with few minor changes, as stated in the experimental part: Frantz, D. E.; Fässler, R.; Carreira, E. M. *J. Am. Chem. Soc.* **2000**, *122*, 1806.
[76] In case of UV active propargylic alcohols, the *ee*'s were determined for either the alcohol or the benzoate.

Bakshi-Shibata reduction of the parent alkynyl ketone (**208**).[77] Following benzoylation, the enantiomeric excess was found to be lower (86% *ee*) compared to the other substrates. The absolute stereochemistry of all substrates shown in Figure 5.3 was assigned by analogy to reported transformations.

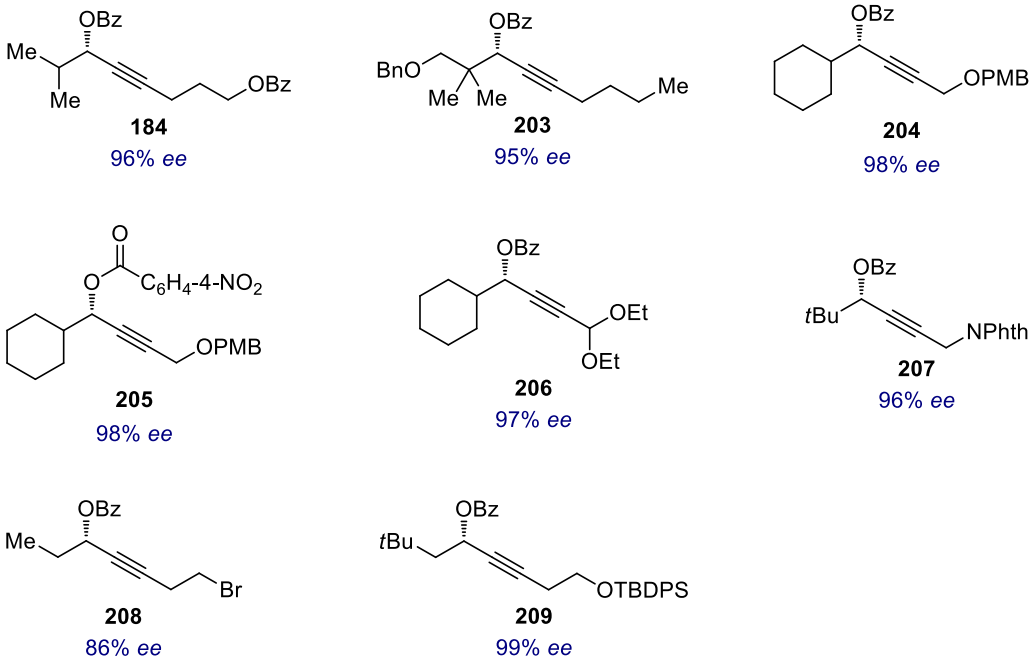

Figure 5.3 Enantioenriched propargylic benzoates prepared which were successfully employed in the enantiospecific synthesis of chiral allenes.

The scope of the enantiospecific reaction between chiral, propargylic benzoates and arylboronic acids is illustrated in Table 5.13. The reaction between the benzoates represented in Figure 5.3 and a variety of arylboronic acids proceeded generally in high yields. Only one substrate gave the allene in low yield (**219**) because of an increased amount of side product formation. The observed selectivities were high (≥90% *es*) in most cases. Almost complete loss of the enantiomeric purity occurred when **203** was employed as substrate. It is speculated that the ether substituent in γ-position to the propargylic benzoate is causing erosion in enantioselectivity. The same observation was made for a different boronic acid.[78] The scope in propargylic benzoates includes a wide array of diverse structures. The secondary benzoate might be in an α-position to either a quaternary (*e.g.* **220**), tertiary (*e.g.* **185**), or secondary carbon substituent (**222**). As noted in the previous subchapter, terminal alkynes do not furnish desired products and are not suitable substrates at the current level of development. However,

[77] A slightly modified literature procedure was followed: Nakayama, A.; Kogure, N.; Kitajima, M.; Takayama, H. *Org. Lett.* **2009**, *11*, 5554.
[78] When 4-(trifluoromethyl)phenylboronic acid was used as nucleophile the measured decrease in *ee* was even higher (14% *es* under otherwise identical conditions).

the alkyne can bear an assortment of different functional groups distal to the propargylic benzoate. Examples include a primary alkyl bromide (**222**), an ether (**218**), a protected amine (**221**), or an ester (**216**). The tolerance of alkyl as well as aryl bromides is noteworthy and likely more difficult to achieve for transformations catalyzed by other transition metals (*e.g.* Pd, Ni). The accessed allenyl-arylbromides allow for functionalization of the products. In general, the rate of the reaction is increased with smaller substituents on the alkyne (opposite to the alcohol derivative). This observation is in agreement with the proposed SN2' mechanism. Typically, alkynes with unbranched substituents work well as substrates. Branched secondary or aromatic substituents give usually full conversion but required higher temperature or longer reaction times. More hindered substituents, such as a trimethylsilyl group, did not yield any product under the reaction conditions examined. A second observation is that heteroatoms in the vicinity of the alkyne (again on the opposite site than the benzoate) generally accelerate the transformation. This effect accounts for the high reactivity observed for substrate **219**. In this case, the increase in reactivity due to the acetal functionality is stronger than the expected decrease due to a more hindered substituent. As stated above, the extent of chirality transfer is generally high. The conditions given in Table 5.13 were slightly modified for some substrates. Specifically the reaction was conducted at 40 °C for 12 h for **213**, **214**, and **222** whereas all other reactions were stirred at 50 °C for 24 h. In the syntheses of **218**, **219**, **220**, and **221** deionized water was added (10 equiv.). Without the addition of water full conversion was not oberseved for these four substrates. An interesting trend in stereoselectivities can be seen from the series of phthalimides **219**, **220**, and **221**. The enantiospecificities were found to decrease with the use of more electrondonating boronic acids. This observation can be rationalized by the assumption that in the synthesis of **221** a more electronrich vinylrhodium intermediate is formed which undergoes a less selective elimination. However, this trend was only seen when water was added to the reaction mixture because the selectivities obtained for substrate **207** were otherwise all uniformly high (while the conversions and isolated yields were siginificantly lower in the absence of water, *e.g.* 79% yield for **220**).

Table 5.13 Scope of the enantiospecific synthesis of allenes from propargylic benzoates and arylboronic acids. Reagents and conditions: (a) benzoate (0.50 mmol, 1.0 equiv.), arylboronic acid (2.0 equiv.), K_3PO_4 (2.0 equiv.), [{Rh(cod)Cl}$_2$] (0.030 equiv.), **72** (0.13 equiv.), 1,2-dichloroethane (0.14 M), 40-50 °C, 12-24 h, yields of purified products.

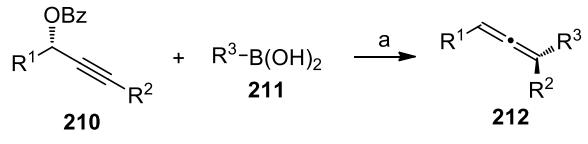

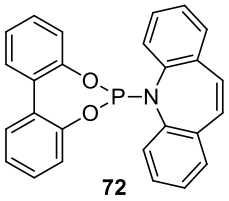

72

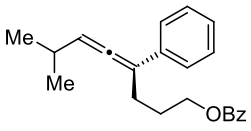

185
98% *es*, 82% yield

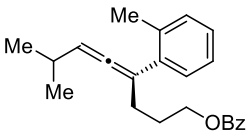

213
97% *es*, 92% yield

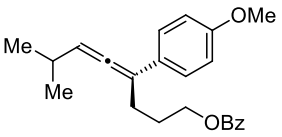

214
98% *es*, 85% yield

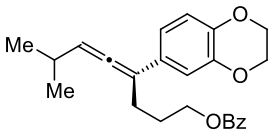

215
98% *es*, 89% yield

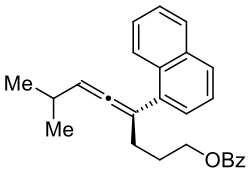

216
97% *es*, 95% yield

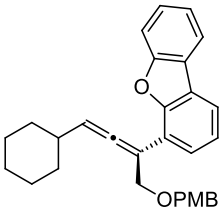

217
93% *es*, 51% yield

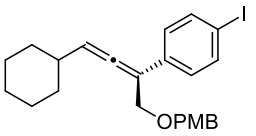

218
93% *es*, 57% yield

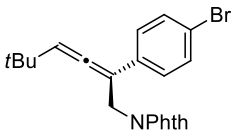

219
>99% *es*, 90% yield

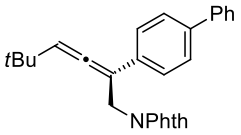

220
95% *es*, 96% yield

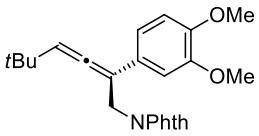

221
90% *es*, 97% yield

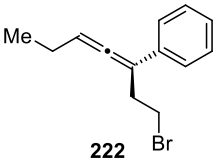

222
97% *es*, 62% yield

The scope, in terms of arylboronic acids, includes a broad variety of electron rich and electron neutral boronic acids. Specifically, arylhalides (**218**, **219**), ethers (*e.g.* **215**), or *ortho*-substitution is well tolerated (**213**, **216**). One heteroarylboronic acid was found to be a good coupling partner (**217**), while other heteroarylboronic acids were not suitable reagents under these conditions (*vide infra*). As outlined in the previous subchapter, electron poor boronic acids are not generally good substrates under the conditions given in Table 5.13. While some electron withdrawing substituents on the arylboronic acid are tolerated (F, CF_3, Br, Cl), other

substituents give typically low or no conversion (SO_2Me, CO_2Et, NO_2). The conditions developed for electron poor arylboronic acids (addition of TBAF•$3H_2O$ and a 1/1 ligand to Rh ratio) increases the reactivity and thus expands the substrate scope for arylboronic acids. However, the selectivity was found to be somewhat lower for some of the examples examined. The full scope under these conditions has not been established. All vinyl boronic acids studied did not give full conversion. This could be due to product inhibition. In other words, that the Rh-catalyst coordinates to the formed allene-ene which may then arrest the catalytic cycle.[79] Alkynyl- and alkylboron reagents were not evaluated as nucleophiles.

The structures of three products were confirmed by X-ray crystallographic analysis (**219**, **220** and **221**, Figure 5.4,) and for allene **219** the absolute configuration was determined. Based on this measurement, the major enantiomer is formed though a *syn*-elimination of the vinylrhodium intermediate. The absolute stereochemistry of all other products was then assigned by analogy to this finding.

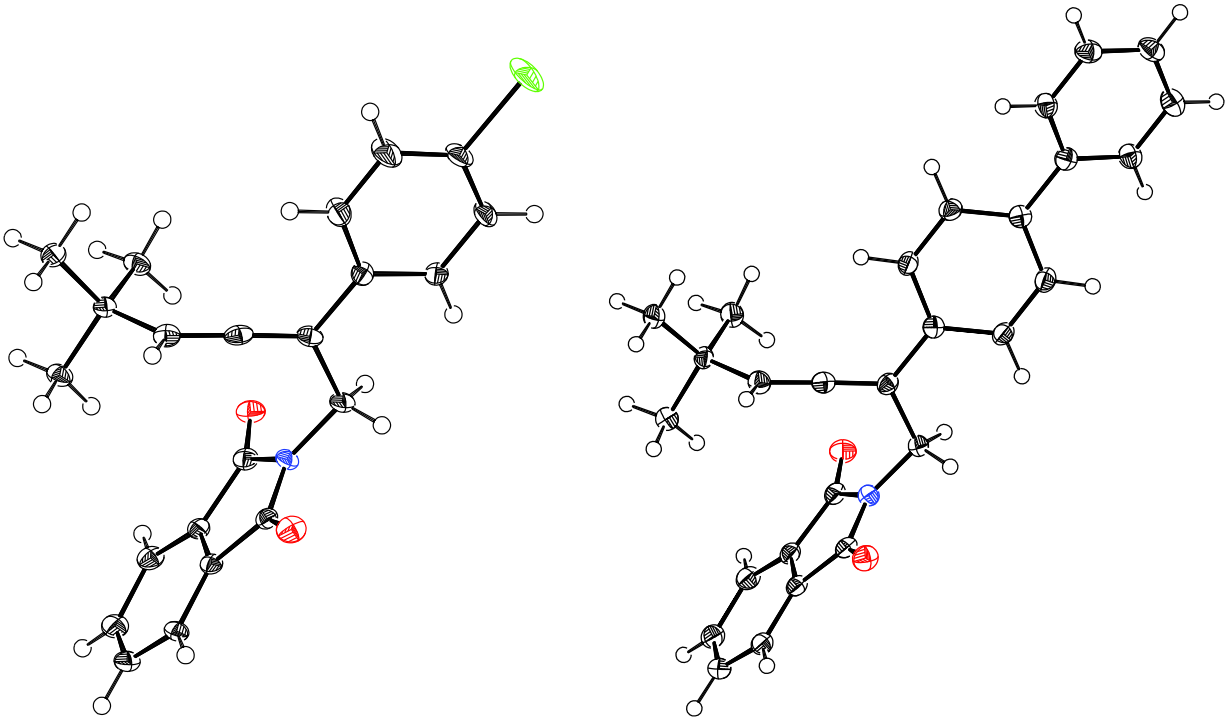

[79] For selected, recent examples of Rh^I-catalyzed reactions using allene-enes as starting materials, see: (a) A. T. Brusoe, E. J. Alexanian, *Angew. Chem., Int. Ed.* **2011**, *50*, 6596. (b) A. T. Brusoe, R. V. Edwankar, E. J. Alexanian, *Org. Lett.* **2012**, *14*, 6096.

Figure 5.4 Structures of allenes **219** (left) and **220** (right) in the solid state (ORTEP view with thermal ellipsoids set at 50% probability). The absolute configuration of **220** has not been established and an arbitrary enantiomer is shown.

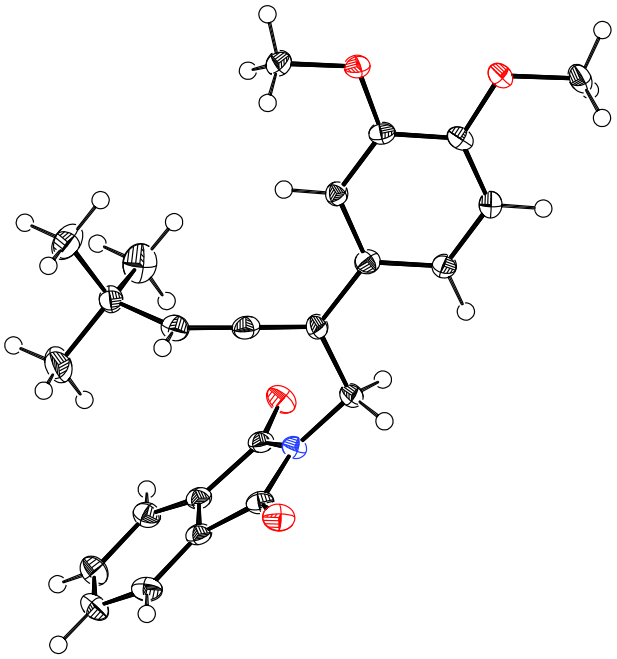

Figure 5.5 Structure of allene **221** in the solid state (ORTEP view with thermal ellipsoids set at 50% probability). Only one molecule of the four independent molecules in the asymmetric unit is shown for clarity. The absolute configuration of **221** has not been established and an arbitrary enantiomer is shown.

A representative selection of propargylic benzoates, which were challenging substrates for the described process, is shown in Figure 5.6. As noted previously, terminal alkynes such as **223** or **224** yield multiple products under the standard reaction conditions. Benzoate **225** bearing a benzyloxyether in α-position provided some allene but the reaction furnished multiple side products. Substrates with a disubstituted (*Z*)-olefin (**226**, **228**) reacted slowly and led to the formation of several side products. When **227**, **229**, or **230** were subjected to the reaction conditions, clean starting material were recovered. In general, aryl substituents were tolerated on the alkyne as well as in the α-position to the benzoate.[80] The challenges observed with 'aryl substrates' is likely associated with the furan (**229**) or benzyl functionality (**230**).

[80] In preliminary experiments, 1-(4-bromophenyl)-4-((4-methoxybenzyl)oxy)but-2-yn-1-yl benzoate and 5-(benzyloxy)-4,4-dimethyl-1-phenylpent-1-yn-3-yl tert-butyl carbonate were found to be viable substrates in terms of reactivity. The stereospecificity of reactions using these substrates was not examined.

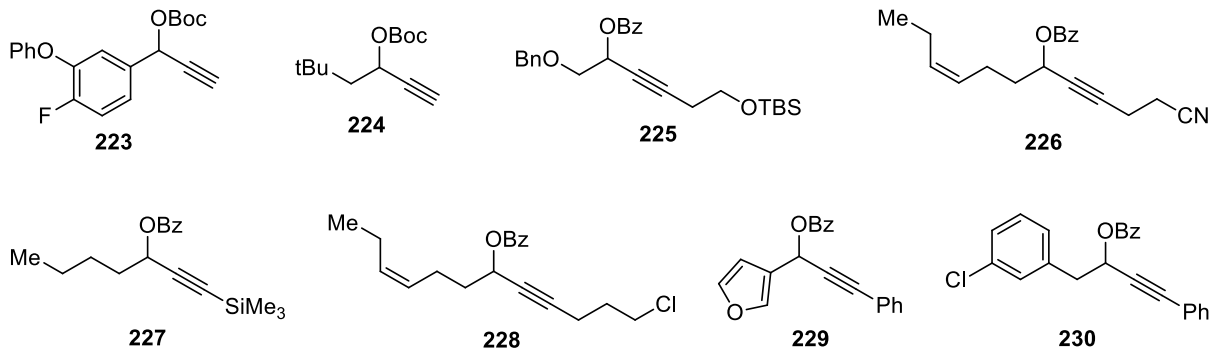

Figure 5.6 Selection of challenging propargylic benzoate substrates in the enantiospecific synthesis of allenes under the conditions given in Table 5.13.

Since a vast number of arylboronic acids are commercially available, only a small fraction of them could be studied. Some aryl-, heteroaryl-, and vinylboronic acids yielded moderate amounts of the allene (Figure 5.7) under the standard reaction conditions and also when increasing the temperature. With these coupling partners the conversion typically reached 20-70% and recovered starting material accounted for the mass balance. As expected, more reactive propargylic benzoates gave higher conversions for a given challenging boronic acid.

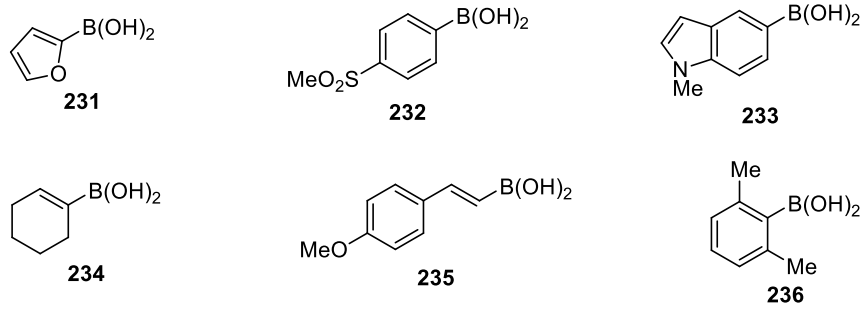

Figure 5.7 Selection of boronic acids which showed a low conversion in the enantiospecific synthesis of allenes under the conditions related to the one given in Table 5.13.

Finally, employing some aryl- and heteroarylboronic acid did not result in the formation of significant amounts of products (convn. < 10%, Figure 5.8). When attempting the transformation with any of those boronic acids, the benzoate was reisolated in good purity.

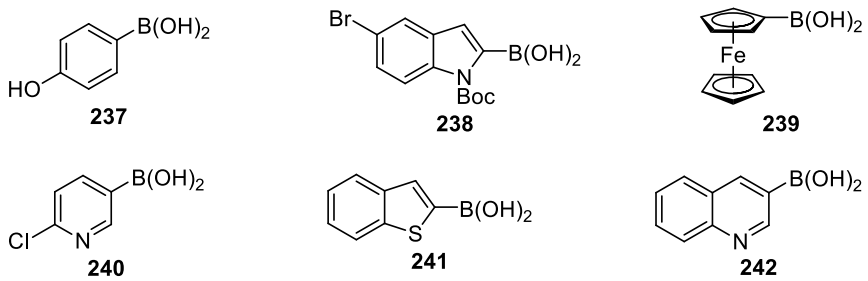

Figure 5.8 Boronic acids which are not suitable coupling partners in the enantiospecific synthesis of allenes under the conditions related to the ones given in Table 5.13.

6 Conclusion and Outlook

In summary, the method developed herein allows for the stereoselective synthesis of structurally diverse, trisubstituted allenes. Readily accessible, chiral propargylic benzoates and widely available arylboronic acids are used as substrates. The transformation occurs under mild conditions employing a catalyst generated *in situ* from a commercially available Rh^{I} organometallic complex and a simple olefin phosphoramidite ligand. The allenes are obtained in high yields and with excellent enantiospecificity. Moreover, no products from a S_N2 substitution are observed and the regioselectivities are generally high. Thus, chiral allenes are accessible in high optical purity without the use of moisture sensitive organometallic reagents or catalysts. This is in contrast to most related approaches where Grignard, zinc, or organocopper reagents are employed as nucleophiles. To the best of our knowledge, this is the first stereoselective Rh-catalyzed synthesis of allenes from propargylic alcohol derivatives and boronic acids. The scope of the method is complementary to Cu- and Pd-catalyzed reactions and the combination of coupling partners is unique among enantiospecific preparations of allenes. Given the high regioselectivity and chirality transfer of the described process, the identified reaction conditions may stimulate the discovery of related transformations in the future.

Experimental Part

7 General Methods

Names and stereochemistry. Names of compounds were generated using the ChemBioDraw 12.0 (Cambridgesoft) software. For racemic compounds and the X-ray diffraction derived plots thereof an arbitrary enantiomer is shown. The absolute stereochemistry of the chiral propargylic alcohols and benzoates is assigned in correlation to reported data.[58] The absolute stereochemistry of the chiral allenes is assigned in analogy to X-ray data obtained for **219**.

Solvents and reagents. 9-Borabicyclo[3.3.1]nonane dimer (9-BBN dimer, stored and handled in a glove box, Sigma-Aldrich), Et_3B (1.0 M in THF, Acros and Sigma-Aldrich), 1-hexene (Sigma-Aldrich), 2-(1*H*-indol-3-yl)ethanol (TCI), [{Ir(cod)Cl}$_2$] (97%, Combi-Blocks), potassium bis(trimethylsilyl)amide (KHMDS, stored and handled in a glove box, Sigma-Aldrich), KO*t*-Bu (ABCR and Acros), tryptamine (TCI), (*S*)-tryptophan (Fisher), (*R*)-tryptophan (Acros), Boc-(*S*)-tryptophan methyl ester (Bachem), 2,2'-biphenol (Fluka), PCl_3 (Aldrich), 5*H*-dibenzo[*b*,*f*]azepine (Combi-Blocks), $Zn(OTf)_2$ (TCI, opened and stored in a glovebox), (−)-*N*-methylephedrine (Fluka), *n*-BuLi in hexanes (1.60 M, Aldrich), 4-bromo-1-butyne (Aldrich), (s)-5,5-diphenyl-2-methyl-3,4-propano-1,3,2-oxazaborolidine ((*S*)-2-Methyl-CBS-oxazaborolidine, CAS 112022-81-8, TCI), BH_3•SMe_2 (Aldrich), *N*,*N*-dimethylpyridin-4-amine (DMAP, Fluka), benzoyl chloride (Aldrich), 1,2-dichloroethane (Fluka, stored under ambient air), K_3PO_4 (Acros), [{Rh(cod)Cl}$_2$] (98%, Combi-Blocks), [{Rh(cod)OH}$_2$] (95%, Aldrich), phenylboronic acid (TCI), 2-methylphenylboronic acid (Combi-Blocks), 4-methoxyphenylboronic acid (Aldrich), 2,3-dihydrobenzo[*b*][1,4]dioxin-6-ylboronic acid (Combi-Blocks), 1-naphthaleneboronic acid (Aldrich), 4-bromophenylboronic acid (Aldrich), 4-biphenylboronic acid (Apollo Scientific), 3,4-dimethoxybenzeneboronic acid (Apollo Scientific), 4-iodophenylboronic acid (Aldrich), 3-bromophenylboronic acid (Combi-Blocks) were used as received. All other chemicals and solvents were purchased from ABCR, Acros, Apollo, Brunschwig, Combi-Blocks, EGT Chemie, Fisher, Fluka, Fluorochem, Hänseler, Lancaster, Merck, Scharlau, Sigma-Aldrich, TCI, Thommen-Furler, Univar and used as such unless otherwise stated and with the exception of dried solvents. CH_2Cl_2, 1,4-dioxane, DMF, THF and toluene were dried by passage over two 4 × 36 inch columns of anhydrous neutral A-2 alumina (Macherey und Nagel; activated for >12 h at 300 °C under a flow of N_2) under an atmosphere of N_2. MeOH was distilled from magnesium turnings under an atmosphere of dry N_2. Et_3N was distilled from CaH_2 under an atmosphere of dry N_2. Pyridine was distilled from

KOH under an atmosphere of dry N_2. Deuterated solvents were obtained from Armar Chemicals, Döttingen, Switzerland.

Reaction handling. All non-aqueous reactions were performed in flame-dried glassware under an atmosphere of N_2 unless stated otherwise. Reactions were magnetically stirred and monitored by analytical thin layer chromatography (TLC) unless otherwise noted. TLC was performed on Merck silica gel 60 F_{254} TLC glass plates and visualized with UV fluorescence quenching and cerium ammonium molybdate (CAM) stain. Column chromatographic purification was performed as flash chromatography on silica gel with 0.2 – 0.5 bar pressure using Fluka silica gel (pore size 60 Å, 230 – 400 mesh particle size) and technical grade solvents. Concentrations under reduced pressure were performed by rotary evaporation at 40 - 44 °C at the appropriate pressure. The yields given refer to the purified products, unless otherwise stated.

Melting points. Melting points were measured on a Büchi SMP-20 and a Büchi B-540 melting point apparatus using open glass capillaries and are uncorrected. The solvent from which the compound was recrystallized is given in parentheses. If no solvent is given, the melting point refers to the solid product as obtained after the workup or purification described in the experimental procedure.

NMR spectroscopy. NMR data was recorded on a Bruker AVIII400 and Bruker DRX400 spectrometer, both operating at 400 MHz for ^{1}H acquisitions. Measurements were carried out at 298 K. Chemical shifts (δ) are reported in parts per million (ppm) with the solvent resonance as internal standard for ^{1}H spectroscopy (chloroform $CHCl_3$ singlet at 7.26 ppm) and for ^{13}C spectroscopy ($CDCl_3$ triplet at 77.16 ppm).[81] *J* is the coupling constant in hertz (Hz); the multiplicities are abbreviated s, singlet; d, doublet; t, triplet; q, quartet; quin, quintet; m, multiplet or unresolved; br, broad signal; app, apparent. All ^{13}C spectra were measured with complete proton decoupling. Service measurements were performed by the NMR service team of the Laboratorium für Organische Chemie at ETH Zurich by R. Arnold, R. Frankenstein and P. Zumbrunnen under direction of Dr. M.-O. Ebert.

IR spectroscopy. Infrared spectra were recorded on a Perkin Elmer UATR Spectrum Two FT-IR spectrometer. Absorptions are given in reciprocal centimeters, and the absorptions are s, strong; m, medium; w, weak; br, broad signal.

[81] Gottlieb, H. E.; Kotlyar, V.; Nudelman, A. *J. Org. Chem.* **1997**, *62*, 7512.

Mass spectrometry. Mass spectrometric analyses were performed by the mass spectrometry service of the Laboratorium für Organische Chemie at ETH Zurich by L. Bertschi, O. Greter and R. Häfliger under direction of Dr. X. Zhang. ESI measurements were carried out on Bruker maXis – ESI-Qq-TOF-MS and Bruker solariX – ESI-FTICR-MS. EI measurements were carried out on a Micromass (Waters) AutoSpec Ultima – EI-Sector-MS. The following abbreviations are used: HRMS is high-resolution mass spectrometry (massspectrometric accurate mass), *m/z* is the mass-to-charge ratio, M is the molecular weight of the molecule itself, $[M]^+$ is the molecular ion.

Specific Rotation. Specific rotations (α) were measured on a Jasco P-2000 polarimeter at the sodium D line with a 100 mm path length cell. Values are reported as follows: $[\alpha]_D^T$ in parentheses concentration (c = 1.00 corresponds to 10.0 mg·mL^{-1}), and solvent. The temperature (T) at which the determination was made is given as the superscript number (/°C).

Elemental analyses. Elemental analyses were performed by the Mikrolabor at the Laboratorium für Organische Chemie at ETH Zurich. All values are given as percentages.

SFC. Supercritical fluid chromatography (SFC) was perfomred on a Jasco 2080 Plus system under the conditions given for each measurement.

X-ray diffraction. X-ray diffraction experiments have been carried out by Dr. N. Trapp and M. Solar from the Small Molecule X ray crystallography analysis Center (SMoCC) at the Department of Chemistry and Applied Biosciences at ETH Zurich.

8 Experimental Procedures and Characterization Data

8.1 Part I. Ir-Catalyzed Reverse Prenylation of 3-Substituted Indoles

8.1.1 Synthesis of Phosphoramidite Ligands **86** and **87**

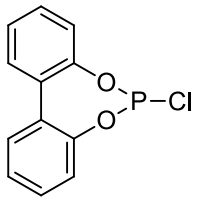

6-Chlorodibenzo[*d*,*f*][1,3,2]dioxaphosphepine.[82] Following a modified literature procedure,[83] 2,2'-biphenol (5.59 g, 30.0 mmol, 1.00 equiv.) was treated with PCl_3 (32 mL, 0.37 mol, 12 equiv.) and 1-methylpyrrolidin-2-one (30 µL, 0.31 mmol, 0.010 equiv.) at 24 °C and the resulting suspension was stirred at that temperature for 40 min. The by then clear solution was heated to 50 °C for 1 h before excess PCl_3 was removed by distillation under reduced pressure (50 °C, 20 mbar). Trace amounts of PCl_3 were azeotropically evaporated with toluene (2 × 10 mL) and the resulting oil was dissolved in toluene to give 45 mL of a chlorophosphite stock solution (0.67 M), which was stored at 24 °C in a sealed Schlenk flask under N_2.

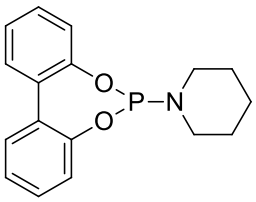

1-(Dibenzo[*d*,*f*][1,3,2]dioxaphosphepin-6-yl)piperidine (86).[84] Following a literature procedure,[83] to a solution of piperidine (0.54 mL, 5.5 mmol, 1.1 equiv.) and Et_3N (1.5 mL, 11 mmol, 2.2 equiv.) in THF (11 mL) at 0 °C was added dropwise a solution of above prepared chlorophosphite (6-chlorodibenzo[*d*,*f*][1,3,2]dioxaphosphepine) in toluene (0.67 M, 7.5 mL,

[82] Li, J.; Lutz, M.; Spek, A. L.; van Klink, G. P. M.; van Koten, G.; Gebbink, R. J. M. K. *J. Organomet. Chem.* **2010**, *695*, 2618.
[83] Bernsmann, H.; van den Berg, M.; Hoen, R.; Minnaard, A. J.; Mehler, G.; Reetz, M. T.; De Vries, J. G.; Feringa, B. L. *J. Org. Chem.* **2005**, *70*, 943.
[84] Lyubimov, S. E.; Rastorguev, E. A.; Ozolin, D. V.; Davankov, V. A. *Russ. Chem. Bull.* **2013**, *62*, 1210.

5.0 mmol, 1.0 equiv.) over 4 min via syringe. The resulting suspension was allowed to warm to 24 °C and stirred at this temperature for 12 h before being diluted with Et_2O (35 mL). The reaction mixture was filtered over a plug of silica gel, washed with Et_2O (35 mL) and concentrated under reduced pressure. The crude product was purified by flash column chromatography on silica gel (pentane/EtOAc 20:1) to yield phosphoramidite **86** as solid (1.23 g, 4.11 mmol, 82%).

TLC: $R_f = 0.34$ (pentane/EtOAc 20:1; UV, CAM); **Melting point**: 68 – 69 °C; **^{1}H-NMR** (400 MHz, $CDCl_3$, 298 K): δ 7.46 (dd, *J* = 7.6, 1.7 Hz, 2H), 7.35 (td, *J* = 7.7, 1.7 Hz, 2H), 7.25 – 7.19 (m, 4H), 3.08 (dt app q, *J* = 6.6 Hz, 4H), 1.62 – 1.57 (m, 2H), 1.49 – 1.43 (m, 4H); **^{13}C-NMR** (101 MHz, $CDCl_3$, 298 K): δ 151.7, 151.6, 131.3, 131.2, 129.73, 129.72, 129.20, 129.19, 124.52, 124.51, 122.12, 122.11, 45.5, 45.3, 27.14, 27.10, 25.1; **^{31}P{^{1}H}-NMR** (162 MHz, $CDCl_3$, 298 K): δ 146.1; **IR** (neat): 3060 (w), 2933 (m), 2851 (w), 1599 (w), 1497 (m), 1474 (m), 1432 (s), 1371 (m), 1333 (m), 1270 (w), 1244 (m), 1208 (s), 1186 (m), 1160 (m), 1119 (m), 1096 (m), 1051 (s), 1028 (m), 1009 (w), 952 (s), 882 (s), 866 (s), 844 (s), 771 (s), 744 (s), 729 (s), 684 (m), 698 (m), 666 (s), 597 (m), 534 (w), 515 (m), 458 (m), 433 (m) cm^{-1}; **HRMS** (ESI-TOF) *m/z*: exact mass calculated for $C_{17}H_{19}NO_2P$ $[M + H]^+$ 300.1148, found 300.1152.

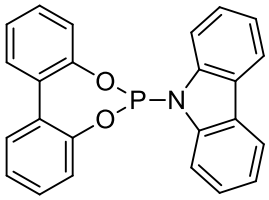

(±)-9-(Dibenzo[*d*,*f*][1,3,2]dioxaphosphepin-6-yl)-9*H*-carbazole (87).[85] Following a modified literature procedure,[86] a solution of 9*H*-carbazole (1.47 g, 8.80 mmol, 1.10 equiv.) in THF (16 mL) at −78 °C was treated with *n*-BuLi in hexanes (1.6 M, 5.25 mL, 8.40 mmol, 1.05 equiv.) over the course of 6 min and the resulting suspension was stirred for 5 min. The reaction mixture was diluted with THF (12 mL) and stirred for 40 min at −78 °C before a solution of the above prepared chlorophosphite (6-chlorodibenzo[*d*,*f*][1,3,2]dioxaphosphepine) in toluene (0.67 M, 12 mL, 8.0 mmol, 1.0 equiv.) was added over 15 min via syringe. The resulting suspension was left to slowly warm to 24 °C over 23 h, then it was concentrated

[85] Diebolt, O.; Tricas, H.; Freixa, Z.; van Leeuwen, P. W. N. M. *ACS Catalysis* **2013**, *3*, 128.
[86] Defieber, C.; Ariger, M. A.; Moriel, P.; Carreira, E. M. *Angew. Chem., Int. Ed.* **2007**, *46*, 3139.

under reduced pressure. Purification by flash column chromatography on silica gel (cyclohexane/toluene 5:1) gave **8** along with a minor impurity. The white solid (1.77 g) was further purified by recrystallization from toluene (10 mL) to afford phosphoramidite **87** (1.09 g, 2.87 mmol, 36%) as a white solid.

TLC: $R_f = 0.33$ (cyclohexane/toluene 5:1; UV, CAM); **Melting point**: 150 – 152 °C; **^{1}H-NMR** (400 MHz, $CDCl_3$, 298 K): δ 8.02 – 8.00 (m, 2H), 7.64 – 7.62 (m, 2H), 7.53 – 7.51 (m, 2H), 7.39 – 7.34 (m, 2H), 7.31 – 7.24 (m, 4H), 7.22 – 7.18 (m, 2H), 7.07 – 7.04 (m, 2H); **^{13}C-NMR** (101 MHz, $CDCl_3$, 298 K): δ 151.4, 151.3, 141.8, 141.7, 131.12, 131.08, 130.27, 130.26, 129.88, 129.87, 126.12, 126.11, 126.00, 125.98, 125.85, 125.84, 122.23, 122.22, 121.7 (two coincident resonances), 119.9 (two coincident resonances), 114.6, 114.4; **^{31}P{^{1}H}-NMR** (162 MHz, $CDCl_3$, 298 K): δ 142.5; **IR** (neat): 1598 (w), 1498 (w), 1473 (m), 1435 (m), 1324 (w), 1298 (w), 1254 (w), 1234 (m), 1194 (s), 1180 (m), 1149 (m), 1117 (m), 1095 (m), 1022 (w), 974 (m), 892 (s) 864 (m), 853 (s), 773 (m), 752 (s), 723 (s), 710 (s), 613 (m), 599 (m), 569 (w), 526 (m), 486 (m), 445 (m) cm^{-1}; **HRMS** (ESI) *m/z*: exact mass calculated for $C_{24}H_{17}NO_2P$ $[M + H]^+$ 382.0991, found 382.0990.

8.1.2 Racemic Reverse Prenylation of 3-Substituted-1*H*-indoles

Typical Procedures used for Preliminary Results

Typical procedure for an allylic alcohol derivative screening: To a solution of sulfonamide **73** (0.70 mmol, 1.0 equiv.), KO*t*-Bu (1.1 equiv.), Et_3B (1.0 M in THF, 1.2 equiv.) in 1,4-dioxane (0.30 M, 1,4-dioxane/THF 2:1) was added at 24 °C a solution of $[\{Ir(cod)Cl\}_2]$ (0.030 equiv.) and ligand **72** (0.060 equiv.) in 1,4-dioxane (1.1 mL). Part of the resulting stock solution (0.50 mL) was then added to a screw-capped vial containing the allylic alcohol derivative (2.0 equiv.) and the resulting mixture was stirred at 50 °C for 3.5 h before it was diluted with Et_2O and filtered through a plug of silica gel with copious washings (Et_2O). Conversion and regioselectivity were determined by ^{19}F NMR of the unpurified reaction mixture.

Typical procedure for a ligand screening: A stock solution of sulfonamide **73** (0.10 mmol, 1.0 equiv.), KO*t*-Bu (1.1 equiv.), Et_3B (1.0 M in THF, 1.2 equiv.) in 1,4-dioxane (0.26 M, 1,4-dioxane/THF 2:1) was added at 24 °C to a screw-capped vial containing a solution of $[\{Ir(cod)Cl\}_2]$ (0.030 equiv.) and ligand (0.060 equiv.) in 1,4-dioxane (0.10 mL). Carbonate **59**

(2.0 equiv.) was added and the resulting mixture was stirred at 50 °C for 1 h before it was diluted with Et_2O and filtered through a plug of silica gel with copious washings (Et_2O). Conversion and regioselectivity were determined by ^{19}F NMR of the unpurified reaction mixture.

Selected Control Experiments

Table S1. Selected Control Experiments for the Racemic Reverse Prenylation

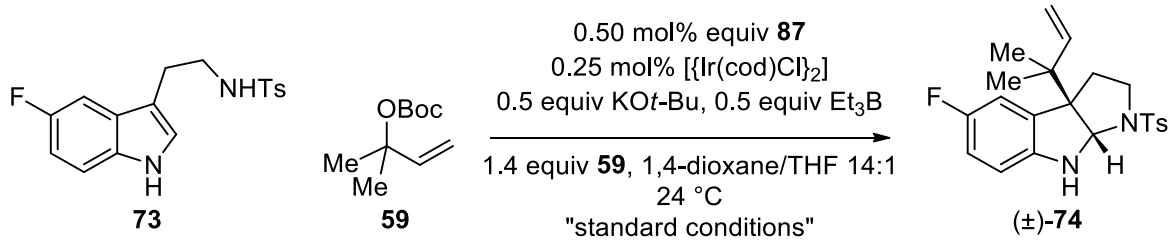

entry	variation from the "standard conditions"	conversion (1 h)	conversion (24 h)
1	none	>98%	-
2	no ligand **87**	<2%	3%
3	no [{Ir(cod)Cl}$_2$], no ligand **87**	<2%	<2%
4	no Et_3B	<2%	<2%
5	no KO*t*-Bu	<2%	<2%
6	0.050 mol% **87**, 0.025 mol% [{Ir(cod)Cl}$_2$]	34%	40%

Typical procedure for the control experiments: A stock solution of sulfonamide **73** (0.05 mmol, 1.0 equiv.), KO*t*-Bu (0.5 equiv.), Et_3B (1.0 M in THF, 0.5 equiv.) in 1,4-dioxane (0.15 M) was added at 24 °C to a screw-capped vial containing a solution of [{Ir(cod)Cl}$_2$] (0.0050 equiv.) and ligand (0.0025 equiv.) in 1,4-dioxane (0.01 M, a stock solution was prepared). Carbonate **59** (1.4 equiv.) was added and the resulting mixture was stirred at 24 °C for the time indicated before it was diluted with EtOAc and filtered through a plug of silica gel with copious washings (EtOAc). Conversion and regioselectivity were determined by ^{19}F NMR of the unpurified reaction mixture.

Synthesis of Carbonates

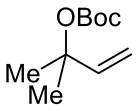

***tert*-Butyl (2-methylbut-3-en-2-yl) carbonate (59).**[87] To a solution of 2-methylbut-3-en-2-ol (5.2 mL, 50 mmol, 1.0 equiv.) in THF (90 mL) was added *n*-BuLi in hexanes (1.6 M, 31 mL, 50 mmol, 1.0 equiv.) at 0 °C over the course of 10 min. The clear solution was stirred at 0 °C for 20 min and then di-*tert*-butyl dicarbonate (10.9 g, 50.0 mmol, 1.00 equiv.) was added as a solid in one portion. The clear solution was allowed to warm to 23 °C and further stirred for 4 h before sat. aq. $NaHCO_3$ (200 mL) was added to the by then thick suspension. The mixture was transferred into a separation funnel, the transfer was assisted with THF (20 mL) and deionized water (30 mL) was added. The organic phase was separated, washed with sat. aq. NaCl (150 mL), dried over $MgSO_4$, filtered, and concentrated under reduced pressure to give carbonate **59** as a clear, pale, light yellow liquid (9.0 g, 48 mmol, 97%), which was used without further purification.

^{1}H-NMR (400 MHz, $CDCl_3$, 298 K): δ 6.10 (dd, *J* = 17.5, 10.9 Hz, 1H), 5.18 (d, *J* = 17.5 Hz, 1H), 5.10 (d, *J* = 10.9 Hz, 1H), 1.52 (s, 6H), 1.46 (s, 9H); **^{13}C-NMR** (101 MHz, $CDCl_3$, 298 K): δ 152.0, 142.5, 113.1, 81.6, 81.5, 28.0, 26.6; **IR** (neat): 2981 (m), 2936 (w), 1737 (s), 1458 (w), 1394 (w), 1368 (m), 1282 (s), 1254 (m), 1175 (m), 1144 (m), 1121 (s), 989 (w), 923 (w), 898 (w), 843 (m) 794 (m), 714 (m) cm^{-1}; **HRMS**: no molecular ion detected due to fragmentation (EI and ESI); **Elemental analysis**: calculated for $C_{10}H_{18}O_3$: C 64.49, H 9.74; found C 64.42, H 9.81.

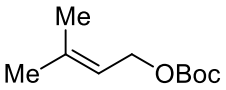

***tert*-Butyl (3-methylbut-2-en-1-yl) carbonate (84).** A solution of 3-methyl-2-buten-1-ol (7.1 mL, 70 mmol, 1.0 equiv.) in THF (130 mL) at 0 °C was treated with *n*-BuLi in hexanes (1.6 M, 44 mL, 70 mmol, 1.0 equiv.). After 90 min. at 0 °C, di-*tert*-butyl dicarbonate (15 g, 70 mmol, 1.0 equiv.) was added as a solid in one portion. The resulting mixture was allowed to stir at 0 °C for 3 h and at 24 °C for 17 h before sat. aq. $NaHCO_3$ (200 mL) and deionized water

[87] (a) Matunas, R.; Lai, A. J.; Lee, C. *Tetrahedron* **2005**, *61*, 6298-6308. (b) Trost, B. M.; Malhotra, S.; Chan, W. H. *J. Am. Chem. Soc.* **2011**, *133*, 7328.

(60 mL) were added to the turbid reaction mixture. The layers were separated, the aqueous phase was extracted with Et_2O (100 mL), the combined organic solutions were washed with sat. aq. NaCl (100 mL), dried over $MgSO_4$, filtered, and concentrated under reduced pressure. Carbonate **84** was obtained as a pale, light yellow, clear liquid (12.8 g, 69 mmol, 99%) and was used without further purification.

^{1}H-NMR (400 MHz, $CDCl_3$, 298 K): δ 5.38 – 5.33 (m, 1H), 4.55 (d, *J* = 7.3 Hz, 2H), 1.74 (s, 3H), 1.70 (s, 3H), 1.47 (s, 9H); **^{13}C-NMR** (101 MHz, $CDCl_3$, 298 K): δ 153.8, 139.5, 118.5, 81.9, 63.8, 27.9, 25.9, 18.2; **IR** (neat): 2980 (m), 2935 (w), 1736 (s), 1455 (w), 1369 (m), 1335 (w), 1272 (s), 1251 (s), 1160 (s), 1126 (m), 1082 (m), 918 (w), 860 (m), 793 (m), 764 (w) cm^{-1}; **HRMS**: no molecular ion detected due to fragmentation (EI and ESI); **Elemental analysis**: calculated for $C_{10}H_{18}O_3$: C 64.49, H 9.74; found C 64.57, H 9.95.

Synthesis and Characterization of Starting Materials

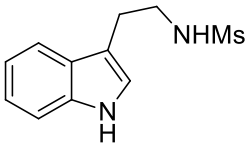

***N*-(2-(1*H*-Indol-3-yl)ethyl)methanesulfonamide (54).** Following a modified literature procedure,[6] a mixture of tryptamine (2.88 g, 18.0 mmol, 1.00 equiv.) and Et_3N (2.8 mL, 20 mmol, 1.1 equiv.) in CH_2Cl_2 (72 mL) at 0 °C was treated with methanesulfonyl chloride (1.47 mL, 18.9 mmol, 1.05 equiv.). The resulting suspension was stirred at 0 °C for 30 min and then was allowed to warm to 24 °C over the course of 1 h before being quenched by the addition of deionized water (20 mL). The mixture was diluted with CH_2Cl_2 (10 mL) as well as EtOAc (30 mL) and the phases were separated. The organic solution was washed with deionized water (2 × 20 mL), dried over $MgSO_4$, filtered and concentrated under reduced pressure to give sulfonamide **54** as pale grey solid (4.08 g, 17.1 mmol, 95%, clean by ^{1}H-NMR). Recrystallization from EtOH (40 mL) gave **54** as pale yellow solid (3.14 g, 13.2 mmol, 73%, used for characterization and as starting material).

TLC: R_f = 0.26 (cyclohexane/EtOAc 1:1; UV, CAM); **Melting point** (EtOH): 132 – 133 °C; **^{1}H-NMR** (400 MHz, $CDCl_3$, 298 K): δ 8.08 (br, 1H), 7.60 (d, *J* = 7.9 Hz, 1H), 7.39 (d, *J* = 8.1 Hz, 1H), 7.25 – 7.21 (m, 1H), 7.17 – 7.13 (m, 1H), 7.09 (d, *J* = 2.3 Hz, 1H), 4.26 (br, 1H), 3.47 (dt app q, *J* = 6.4 Hz, 2H), 3.06 (t, *J* = 6.6 Hz, 2H), 2.83 (s, 3H); **^{13}C-NMR** (101 MHz, $CDCl_3$, 298 K): δ 136.6, 127.1, 122.8, 122.6, 119.9, 118.7, 111.8, 111.6, 43.4, 40.4,

26.3; **IR** (neat): 3388 (m), 3255 (br), 3020 (w), 2937 (w), 1618 (w), 1456 (m), 1443 (m), 1418 (m), 1339 (w), 1294 (s), 1227 (w), 1129 (s), 1070 (m), 1012 (w), 979 (m), 886 (m), 805 (w), 779 (m), 737 (s), 658 (w), 590 (m), 557 (w), 519 (s), 503 (s), 477 (s), 466 (s), 424 (s) cm^{-1}; **HRMS** (ESI-TOF) *m/z*: exact mass calculated for $C_{11}H_{15}N_2O_2S$ $[M + H]^+$ 239.0849, found 239.0851.

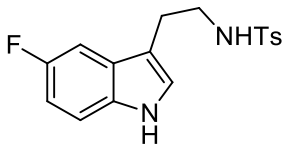

***N*-(2-(5-Fluoro-1*H*-indol-3-yl)ethyl)-4-methylbenzenesulfonamide (73).** To a solution of crude 2-(5-fluoro-1*H*-indol-3-yl)ethanamine[88] (2.04 g, 11.5 mmol, 1.00 equiv.) and Et_3N (1.8 mL, 13 mmol, 1.0 equiv.) in CH_2Cl_2 (20 mL) at 0 °C was added *p*-toluenesulfonyl chloride (2.40 g, 12.6 mmol, 1.10 equiv.). The resulting reaction mixture was allowed to warm to 24 °C and stirred at this temperature for 4 h before being quenched by the addition of 1 M aqueous HCl (20 mL). The phases were separated, the organic solution was washed with 1 M aqueous HCl (20 mL), 5% aqueous NaOH (2 × 20 mL), sat. aq. NaCl (40 mL), dried over $MgSO_4$, filtered, and concentrated under reduced pressure. Purification by flash column chromatography on silica gel (cyclohexane/acetone 3:1 to 2:1 gradient) afforded 3.0 g of a brown oil, which was further purified by recrystallization from hexanes/EtOAc to yield **73** as a beige solid (2.71 g, 8.15 mmol, 71%).

TLC: $R_f = 0.28$ (cyclohexane/acetone 2:1; UV, CAM); **Melting point**: 100 – 101 °C; **^{1}H-NMR** (400 MHz, $CDCl_3$, 298 K): δ 8.15 (br, 1H), 7.62 (d, *J* = 8.3 Hz, 2H), 7.25 (dd, *J* = 8.8, 4.3 Hz, 1H), 7.21 (d, *J* = 8.0 Hz, 2H), 7.01 (d, *J* = 2.4 Hz, 1H), 6.96 (dd, *J* = 9.5, 2.5 Hz, 1H), 6.91 (td, *J* = 9.0, 2.5 Hz, 1H), 4.50 (t, *J* = 6.0 Hz, 1H), 3.24 (dt app q, *J* = 6.6 Hz, 2H), 2.86 (t, *J* = 6.6 Hz, 2H), 2.40 (s, 3H); **^{13}C-NMR** (101 MHz, $CDCl_3$, 298 K): δ 157.8 (d, *J* = 235.0 Hz), 143.6, 136.6, 133.0, 129.8, 127.3 (d, *J* = 9.6 Hz), 127.1, 124.6, 112.1 (d, *J* = 9.6 Hz), 111.7 (d, *J* = 4.8 Hz), 110.7 (d, *J* = 26.3 Hz), 103.5 (d, *J* = 23.5 Hz), 42.9, 25.5, 21.6; **^{19}F{^{1}H}-NMR** (377 MHz, $CDCl_3$, 298 K): δ –124.4; **IR** (neat): 3388 (m), 3291 (m), 1583 (w), 1486 (m), 1459 (m), 1406 (m), 1342 (m), 1313 (m), 1303 (m), 1158 (s), 1095 (m), 1078 (w), 930 (m), 843 (w), 808 (m), 795 (s), 748 (w), 704 (w), 665 (s), 611 (m), 584 (m),

[88] Muratore, M. E.; Holloway, C. A.; Pilling, A. W.; Storer, R. I.; Trevitt, G.; Dixon, D. J. *J. Am. Chem. Soc.* **2009**, *131*, 10796.

552 (s), 540 (s), 479 (m), 433 (m) cm^{-1}; **HRMS** (ESI) *m/z*: exact mass calculated for $C_{17}H_{18}FN_2O_2S$ $[M + H]^+$ 333.1068, found 333.1070.

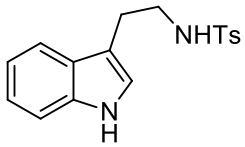

***N*-(2-(1*H*-Indol-3-yl)ethyl)-4-methylbenzenesulfonamide (76).**[89] Sulfonamide **76** was prepared according to a literature procedure[89] and was further purified by recrystallization from EtOAc. The product was obtained as a pale brown solid.

^{1}H-NMR (400 MHz, $CDCl_3$, 298 K): δ 8.06 (br, 1H), 7.64 (d, *J* = 8.3 Hz, 2H), 7.41 (d, *J* = 7.9 Hz, 1H), 7.35 (d, *J* = 8.2 Hz, 1H), 7.23 – 7.17 (m, 3H), 7.06 (ddd, *J* = 7.9, 7.1, 0.9 Hz, 1H), 6.97 (s, 1H), 4.32 (br, 1H), 3.28 (t, *J* = 6.7 Hz, 2H), 2.93 (t, *J* = 6.6 Hz, 2H), 2.40 (s, 3H); **^{13}C-NMR** (101 MHz, $CDCl_3$, 298 K): δ 143.4, 136.9, 136.5, 129.8, 127.1, 127.0, 122.7, 122.4, 119.7, 118.6, 111.7, 111.4, 43.2, 25.6, 21.6. **HRMS** (ESI) *m/z*: exact mass calculated for $C_{17}H_{19}N_2O_2S$ $[M + H]^+$ 315.1162, found 315.1163.

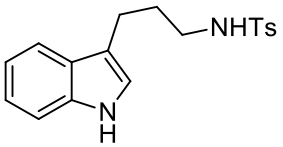

***N*-(3-(1*H*-Indol-3-yl)propyl)-4-methylbenzenesulfonamide (100).**[90] To a solution of crude 3-(1H-indol-3-yl)propan-1-amine[91] (1.04 g, 5.97 mmol, 1.00 equiv.) and Et_3N (0.95 mL, 6.8 mmol, 1.1 equiv.) in CH_2Cl_2 (12 mL) at 0 °C was added and *p*-toluenesulfonyl chloride (1.21 g, 6.35 mmol, 1.06 equiv.). The resulting reaction mixture was allowed to warm to 24 °C, stirred at this temperature for 5 h before being diluted with CH_2Cl_2 (20 mL) and quenched by the addition of 1 M aqueous HCl (10 mL). The organic solution was washed with 1 M aqueous HCl (10 mL), 1 M aqueous NaOH (2 × 10 mL), sat. aq. NaCl (20 mL), dried over $MgSO_4$, filtered, and concentrated under reduced pressure. Purification by flash column

[89] Priebbenow, D. L.; Henderson, L. C.; Pfeffer, F. M.; Stewart, S. G. *J. Org. Chem.* **2010**, *75*, 1787.
[90] Yadav, J. S.; Reddy, B. V. S.; Narasimhulu, G.; Satheesh, G. *Synlett* **2009**, 727.
[91] Mewshaw, R. E.; Zhou, D. H.; Zhou, P.; Shi, X. J.; Hornby, G.; Spangler, T.; Scerni, R.; Smith, D.; Schechter, L. E.; Andree, T. H. *J. Med. Chem.* **2004**, *47*, 3823.

chromatography on silica gel (cyclohexane/EtOAc 3:1 to 5:2 gradient) afforded **100** (1.49 g, 4.54 mmol, 76%) as an off-white solid.

TLC: R_f = 0.29 (cyclohexane/EtOAc 2:1; UV, CAM); **Melting point**: 99 – 100 °C; **^{1}H-NMR** (400 MHz, $CDCl_3$, 298 K): δ 8.00 (br, 1H), 7.71 (d, *J* = 8.3 Hz, 2H), 7.49 – 7.47 (m, 1H), 7.34 (dt, *J* = 8.1, 0.9 Hz, 1H), 7.27 – 7.24 (m, 2H), 7.18 (ddd, *J* = 8.1, 7.1, 1.1 Hz, 1H), 7.09 (ddd, *J* = 8.0, 7.1, 1.0 Hz, 1H), 6.91 – 6.90 (m, 1H), 4.72 (t, *J* = 6.2 Hz, 1H), 2.99 (dt app q, *J* = 6.8 Hz, 2H), 2.74 (t, *J* = 7.3 Hz, 2H), 2.41 (s, 3H), 1.84 (tt app quin, *J* = 7.0 Hz, 2H); **^{13}C-NMR** (101 MHz, $CDCl_3$, 298 K): δ 143.4, 137.0, 136.4, 129.8, 127.3, 127.1, 122.0, 121.8, 119.3, 118.8, 114.9, 111.3, 43.0, 29.7, 22.1, 21.6; **IR** (neat): 3404 (br), 3303 (m), 3049 (w), 2922 (w), 1596 (w), 1458 (m), 1413 (m), 1355 (w), 1317 (m), 1305 (m), 1223 (w), 1152 (s), 1082 (m), 1067 (s), 1037 (w), 952 (m), 891 (w), 849 (w), 816 (s), 778 (w), 732 (s), 704 (w), 732 (s), 704 (w), 667 (br), 609 (m), 579 (m), 526 (br), 492 (s), 476 (m), 422 (m) cm^{-1}; **HRMS** (ESI) *m/z*: exact mass calculated for $C_{18}H_{21}N_2O_2S$ $[M + H]^+$ 329.1318, found 329.1318.

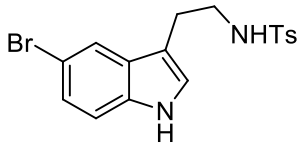

***N*-(2-(5-Bromo-1*H*-indol-3-yl)ethyl)-4-methylbenzenesulfonamide (99).** To a solution of 2-(5-bromo-1*H*-indol-3-yl)ethanamine[88] (964 mg, 4.03 mmol, 1.00 equiv.) and Et_3N (0.62 mL, 4.5 mmol, 1.1 equiv.) in CH_2Cl_2 (8 mL) at 0 °C was added and *p*-toluenesulfonyl chloride (807 mg, 4.23 mmol, 1.05 equiv.). The resulting reaction mixture was allowed to warm to 24 °C, stirred at this temperature for 2 h before being diluted with CH_2Cl_2 (20 mL) and quenched by the addition of 1 M aqueous HCl (10 mL). The organic solution was washed with 1 M aqueous HCl (10 mL), 1 M aqueous NaOH (2 × 10 mL), sat. aq. NaCl (20 mL), dried over $MgSO_4$, filtered, and concentrated under reduced pressure. Purification by flash column chromatography on silica gel (cyclohexane/EtOAc 2:1 to 3:2 gradient) afforded **99** (1.45 g, 3.69 mmol, 91%) as a brown solid.

TLC: R_f = 0.22 (cyclohexane/EtOAc 2:1; UV, CAM); **Melting point**: 91 – 94 °C; **^{1}H-NMR** (400 MHz, $CDCl_3$, 298 K): δ 8.28 (s, 1H), 7.60 (d, *J* = 8.3 Hz, 2H), 7.44 (s, 1H), 7.24 – 7.17 (m, 4H), 6.96 – 6.95 (m, 1H), 4.64 (t, *J* = 5.8 Hz, 1H), 3.22 (dt app q, *J* = 6.5 Hz, 2H), 2.83 (t, *J* = 6.6 Hz, 2H), 2.40 (s, 3H); **^{13}C-NMR** (101 MHz, $CDCl_3$, 298 K): δ 143.6, 136.5, 135.1, 129.8, 128.7, 127.0, 125.0, 124.2, 121.1, 113.0, 112.8, 111.2, 42.9, 25.3, 21.7; **IR** (neat):

3368 (br), 2922 (w), 1597 (w), 1459 (m), 1421 (m), 1317 (m), 1289 (m), 1152 (s), 1091 (m), 882 (m), 812 (m), 795 (m), 749 (w), 663 (s), 576 (m), 548 (s) cm−1; **HRMS** (ESI) *m/z*: exact mass calculated for $C_{17}H_{18}BrN_2O_2S$ $[M + H]^+$ 393.0267, found 393.0266.

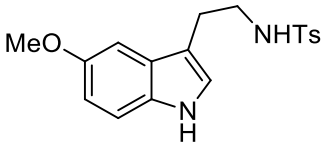

***N*-(2-(5-Methoxy-1*H*-indol-3-yl)ethyl)-4-methylbenzenesulfonamide (98).**[92] 2-(5-methoxy-1*H*-indol-3-yl)ethanamine was prepared according to a procedure used to synthesize 2-(6-chloro-1*H*-indol-3-yl)ethanamine.[93] 2-(5-methoxy-1*H*-indol-3-yl)ethanamine (399 mg, 2.10 mmol, 1.00 equiv.) was dissolved in CH_2Cl_2 (4.2 mL) and Et_3N (0.32 mL, 2.3 mmol, 1.1 equiv.) was added. The solution was cooled to 0 °C and *p*-toluenesulfonyl chloride (419 mg, 2.20 mmol, 1.05 equiv.) was added in one portion. The resulting suspension was allowed to warm to 24 °C and stirred at that temperature for 2 h. The reaction was diluted with CH_2Cl_2 (10 mL) and quenched by the addition of 1 M aqueous HCl (10 mL). The organic solution was washed with 1 M aqueous HCl (10 mL), 1 M aqueous NaOH (2 × 10 mL), sat. aq. NaCl (20 mL), dried over $MgSO_4$, filtered, and concentrated under reduced pressure. Purification by flash column chromatography on silica gel (cyclohexane/EtOAc 2:1 to 1:1 gradient) afforded **98** (547 mg, 1.59 mmol, 76%) as a brown solid.

TLC: $R_f = 0.19$ (cyclohexane/EtOAc 2:1; UV, CAM); **Melting point**: 155 – 156 °C; **^{1}H-NMR** (400 MHz, $CDCl_3$, 298 K): δ 7.99 (br, 1H), 7.61 (d, J = 8.3 Hz, 2H), 7.23 (dd, J = 8.4, 0.9 Hz, 1H), 7.21 – 7.19 (m, 2H), 6.94 (d, J = 2.3 Hz, 1H), 6.86 – 6.83 (m, 2H), 4.47 (t, J = 6.0 Hz, 1H), 3.80 (s, 3H), 3.25 (dt app q, J = 6.5 Hz, 2H), 2.90 (t, J = 6.6 Hz, 2H), 2.39 (s, 3H); **^{13}C-NMR** (101 MHz, $CDCl_3$, 298 K): δ 154.2, 143.4, 136.8, 131.7, 129.7, 127.4, 127.1, 123.5, 112.6, 112.2, 111.3, 100.4, 55.9, 43.0, 25.6, 21.6; **IR** (neat): 3392 (m), 3297 (w), 2939 (w), 1623 (w), 1587 (w), 1486 (m), 1441 (m), 1318 (m), 1292 (m), 1215 (m), 1151 (s), 1092 (m), 1067 (m), 906 (m), 835 (m), 804 (s), 669 (s), 624 (m), 552 (s), 482 (m) cm−1; **HRMS** (ESI) *m/z*: exact mass calculated for $C_{18}H_{21}N_2O_3S$ $[M + H]^+$ 345.1267, found 345.1271.

[92] (a) Wilkinson, S. *J. Chem. Soc.* **1958**, 2079-2081. (b) Amat, M.; Seffar, F.; Llor, N.; Bosch, J. *Synthesis* **2001**, 267.
[93] Hara, T.; Durell, S. R.; Myers, M. C.; Appella, D. H. *J. Am. Chem. Soc.* **2006**, *128*, 1995.

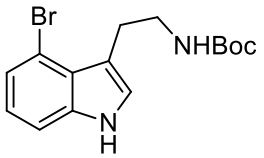

***tert*-Butyl (2-(4-bromo-1*H*-indol-3-yl)ethyl)carbamate (101).**[94] Carbamate **1f** was prepared according to a literature procedure.[94] Purification by flash column chromatography on silica gel (cyclohexane/EtOAc 4:1 to 2:1 gradient) afforded **101** as a pale brown solid.

^{1}H-NMR (400 MHz, $CDCl_3$, 298 K): δ 8.61 (br, 1H), 7.31 – 7.29 (m, 1H), 7.27 – 7.25 (m, 1H), 7.02 – 6.97 (m, 2H), 4.74 (br, 1H), 3.50 (dt app q, J = 6.7 Hz, 2H), 3.20 (t, J = 6.6 Hz, 2H), 1.45 (s, 9H); **^{13}C-NMR** (101 MHz, $CDCl_3$, 298 K): δ 156.3, 137.9, 125.5, 124.3, 124.0, 122.9, 114.3, 113.9, 110.8, 79.3, 42.3, 28.6, 26.7; **HRMS** (ESI) *m/z*: exact mass calculated for $C_{15}H_{20}BrN_2O_2$ $[M + H]^+$ 339.0703, found 339.0704.

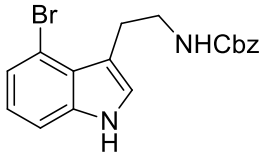

Benzyl (2-(4-bromo-1*H*-indol-3-yl)ethyl)carbamate (102).[95] Carbamate **102** was prepared according to a reported procedure[95] and, after purification by flash column chromatography on silica gel (cyclohexane/EtOAc 2:1 to 3:2 gradient), was obtained as ocher brown, amorphous solid.

^{1}H-NMR (400 MHz, $CDCl_3$, 298 K): δ 8.22 (br, 1H), 7.37 – 7.26 (m, 7H), 7.02 – 6.98 (m, 2H), 5.11 (s, 2H), 4.89 (br, 1H), 3.58 (dt app q, J = 6.6 Hz, 2H), 3.22 (t, J = 6.8 Hz, 2H); **^{13}C-NMR** (101 MHz, $CDCl_3$, 298 K): δ 156.6, 137.9, 136.8, 128.6, 128.24, 128.21, 125.5, 124.3, 124.2, 123.1, 114.3, 113.8, 110.8, 66.7, 42.6, 26.6; **HRMS** (ESI-TOF) *m/z*: exact mass calculated for $C_{18}H_{18}BrN_2O_2$ $[M + H]^+$ 373.0546, found 373.0546.

[94] Delgado, R.; Blakey, S. B. *Eur. J. Org. Chem.* **2009**, 1506.
[95] Davies, J. R.; Kane, P. D.; Moody, C. J. *J. Org. Chem.* **2005**, *70*, 7305.

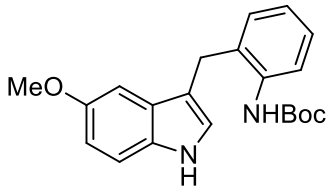

***tert*-Butyl (2-((5-methoxy-1*H*-indol-3-yl)methyl)phenyl)carbamate (103).[96]** Carbamate **103** was prepared following a literature procedure.[96] After flash column chromatography on silica gel (cyclohexane/EtOAc 8:1 to 5:1 gradient), the product was obtained as a white solid.

^{1}H-NMR (400 MHz, $CDCl_3$, 298 K): δ 7.96 (s, 1H), 7.81 (d, *J* = 7.8 Hz, 1H), 7.28 – 7.24 (m, 2H), 7.06 (td, *J* = 7.5, 1.2 Hz, 1H), 6.97 (d, *J* = 2.4 Hz, 1H), 6.88 (dd, *J* = 8.8, 2.4 Hz, 1H), 6.77 (m, 1H), 6.50 (s, 1H), 4.03 (s, 2H), 3.82 (s, 3H), 1.45 (s, 9H); **^{13}C-NMR** (101 MHz, $CDCl_3$, 298 K): δ 154.2, 153.4, 136.6, 131.8, 130.4, 130.3, 127.7, 127.4, 124.0, 123.2, 122.1, 113.4, 112.7, 112.1, 100.9, 80.4, 56.0, 28.5, 28.4; **HRMS** (ESI) *m/z*: exact mass calculated for $C_{21}H_{28}N_3O_3$ $[M + NH_4]^+$ 370.2125, found 370.2120.

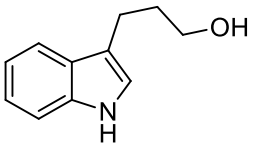

3-(1*H*-Indol-3-yl)propan-1-ol (104).[97] Alcohol **104** was prepared by a literature procedure.[97] The crude product was obtained as a clear, colorless oil and was used without further purification.

^{1}H-NMR (400 MHz, $CDCl_3$, 298 K): δ 8.05 (br, 1H), 7.65 (d, *J* = 7.5 Hz, 1H), 7.35 (d, *J* = 8.1 Hz, 1H), 7.25 – 7.21 (m, 1H), 7.16 (ddd, *J* = 8.0, 7.1, 1.1 Hz, 1H), 6.94 (m, 1H), 3.73 (t, *J* = 6.4 Hz, 2H), 2.88 (t, *J* = 7.8 Hz, 2H), 2.04 – 1.97 (m, 2H), 1.81 (s, 1H); **^{13}C-NMR** (101 MHz, $CDCl_3$, 298 K): δ 136.5, 127.5, 122.0, 121.5, 119.2, 118.9, 115.9, 111.3, 62.7, 33.0, 21.4; **HRMS** (EI) *m/z*: exact mass calculated for $C_{11}H_{13}NO$ $[M]^+$ 175.0992, found 175.0994.

[96] Trost, B. M.; Quancard, J. *J. Am. Chem. Soc.* **2006**, *128*, 6314.
[97] Mamolo, M. G.; Zampieri, D.; Zanette, C.; Florio, C.; Collina, S.; Urbano, M.; Azzolina, O.; Vio, L. *Eur. J. Med. Chem.* **2008**, *43*, 2073.

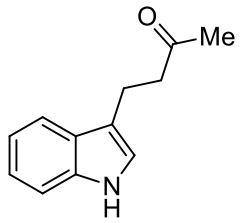

4-(1*H*-Indol-3-yl)butan-2-one (105).[98] Following a literature procedure,[98] ketone **105** was obtained as a pale brown solid after purification by flash column chromatography on silica gel (cyclohexane/EtOAc 3:1).

^{1}H-NMR (400 MHz, $CDCl_3$, 298 K): δ 7.99 (br, 1H), 7.61 – 7.59 (m, 1H), 7.36 (dt, *J* = 8.1, 0.9 Hz, 1H), 7.21 (ddd, *J* = 8.1, 7.1, 1.1 Hz, 1H), 7.13 (ddd, *J* = 8.0, 7.1, 1.1 Hz, 1H), 6.99 – 6.98 (m, 1H), 3.06 (tt, *J* = 6.9, 0.8 Hz, 2H), 2.86 (t, *J* = 7.5 Hz, 2H), 2.15 (s, 3H).; **^{13}C-NMR** (101 MHz, $CDCl_3$, 298 K): δ 208.9, 136.4, 127.3, 122.2, 121.6, 119.4, 118.8, 115.3, 111.3, 44.2, 30.2, 19.5; **HRMS** (ESI) *m/z*: exact mass calculated for $C_{12}H_{13}NNaO$ $[M + Na]^+$ 210.0889, found 210.0893.

General Procedure and Characterization of Products

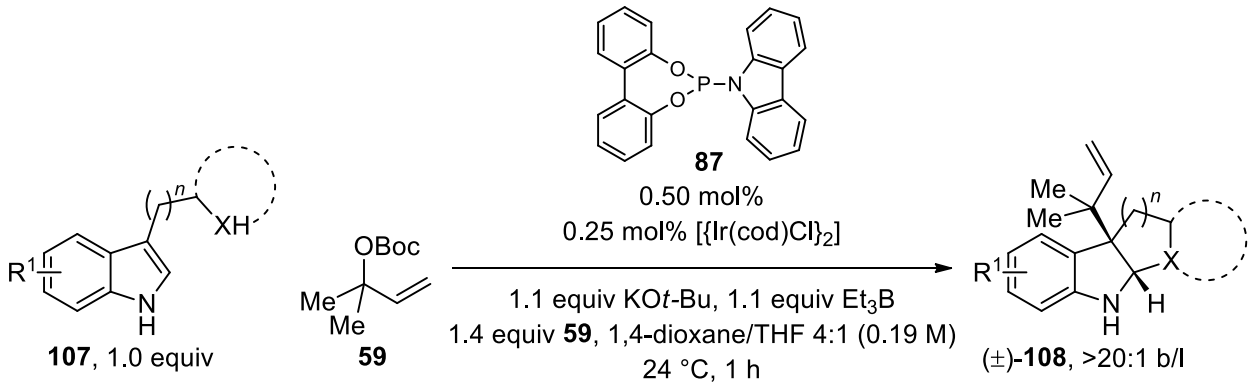

General procedure for the racemic reverse C-3 prenylation of 3-substituted-1*H*-indoles: To a flame-dried 25 mL Schlenk flask equipped with a stir bar were added indole (1.00 mmol, 1.00 equiv.) and KO*t*-Bu (123 mg, 1.10 mmol, 1.10 equiv., stored and handled under air). The flask was sealed with a septum, evacuated and back-filled with N_2 (two cycles). Et_3B in THF (1.0 M, 1.1 mL, 1.1 mmol, 1.1 equiv.) and 1,4-dioxane (3.8 mL) were added at 24 °C and the resulting mixture was stirred at this temperature for 30 min before $[\{Ir(cod)Cl\}_2]$ (1.7 mg, 2.5 µmol, 0.25 mol%) and phosphoramidite **87** (1.9 mg, 5.0 µmol, 0.50 mol%) in

[98] Yadav, J. S.; Abraham, S.; Reddy, B. V. S.; Sabitha, G. *Synthesis* **2001**, 2165.

1,4-dioxane (0.50 mL) – prepared in a screw-capped vial, sparged with N_2 and stirred at 24 °C for 10 min prior to the addition – was added via Pasteur pipette against a flow of N_2. To the stirred mixture was then added carbonate **59** (282 µL, 261 mg, 1.40 mmol, 1.40 equiv.) via syringe and the resulting mixture (often formed a gel, which slowly turned liquid again) was stirred at 24 °C for 1 h before it was diluted with Et_2O (5 mL) and quenched by the addition of sat. aq. NH_4Cl (5 mL). Deionized water (1 mL) was added and the clear solutions were transferred into a separation funnel. Et_2O (10 mL) was used to assist the transfer. The solutions were separated and the organic solution was washed with sat. aq. NaCl (10 mL), dried over $MgSO_4$, filtered, and concentrated under reduced pressure. After purification by flash column chromatography on silica gel the product was isolated as single diastereomer (not applicable for **118** and **119**). The regioselectivity (branched to linear) was found to be >20:1 by ^{1}H NMR analysis of the crude product.

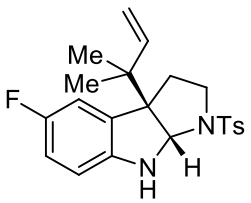

(±)-(3a*S*,8a*R*)-5-Fluoro-3a-(2-methylbut-3-en-2-yl)-1-tosyl-1,2,3,3a,8,8a-hexahydropyrrolo[2,3-*b*]indole (74). The general procedure was followed using 0.50 equiv. KO*t*-Bu (56 mg, 0.50 mmol, stored and handled under air), 0.50 equiv. Et_3B in THF (1.0 M, 0.50 mL, 0.50 mmol) and 4.4 mL 1,4-dioxane. The final concentration of the reaction was unaltered (0.19 M), the ratio of 1,4-dioxane/THF was changed to 10:1. The crude product was purified by flash column chromatography on silica gel (cyclohexane/EtOAc 8:1). The title compound was isolated as a white foam (368 mg, 0.919 mmol, 92%).

TLC: R_f = 0.31 (cyclohexane/EtOAc 5:1; UV, CAM); **Melting point**: 121 – 122 °C; **^{1}H-NMR** (400 MHz, $CDCl_3$, 298 K): δ 7.72 (d, *J* = 8.3 Hz, 2H), 7.30 (d, *J* = 7.9 Hz, 2H), 6.80 – 6.75 (m, 2H), 6.50 – 6.47 (m, 1H), 5.66 (dd, *J* = 17.4, 10.8 Hz, 1H), 5.17 (s, 1H), 4.94 – 4.88 (m, 2H), 4.65 (s, 1H), 3.41 (ddd, *J* = 10.0, 7.9, 1.9 Hz, 1H), 3.04 (ddd app td, *J* = 10.6, 6.0 Hz, 1H), 2.42 (s, 3H), 2.01 (ddd, *J* = 12.4, 10.7, 8.0 Hz, 1H), 1.88 (ddd, *J* = 12.4, 5.9, 1.7 Hz, 1H), 0.95 (s, 3H), 0.84 (s, 3H); **^{13}C-NMR** (101 MHz, $CDCl_3$, 298 K): δ 156.8 (d, *J* = 235.1 Hz), 146.1 (d, *J* = 1.3 Hz), 143.6, 143.5, 136.2, 131.5 (d, *J* = 7.4 Hz), 129.8, 127.2, 114.9 (d, *J* = 23.3 Hz), 114.2, 112.1 (d, *J* = 24.3 Hz), 109.6 (d, *J* = 8.2 Hz), 81.4, 64.9 (d, *J* = 1.8 Hz), 47.8, 41.0, 33.2, 22.7, 22.5, 21.6; **^{19}F{^{1}H}-NMR** (377 MHz, $CDCl_3$, 298 K): δ –

125.8; **IR** (neat): 3388 (br), 2972 (br), 1712 (w), 1598 (w), 1488 (s), 1445 (m), 1415 (w), 1333 (m), 1256 (w), 1183 (w), 1156 (s), 1091 (m), 1042 (m), 1028 (m), 1003 (m), 918 (m), 864 (m), 812 (m), 769 (m), 736 (m), 707 (w), 659 (s), 582 (m), 546 (s), 468 (m) cm^{-1}; **HRMS** (ESI) *m/z*: exact mass calculated for $C_{22}H_{26}FN_2O_2S$ $[M + H]^+$ 401.1694, found 401.1694.

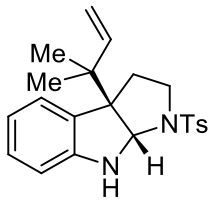

(±)-(3a*S*,8a*R*)-3a-(2-Methylbut-3-en-2-yl)-1-tosyl-1,2,3,3a,8,8a-hexahydropyrrolo[2,3-*b*]indole (109). The general procedure was followed using 0.50 equiv. KO*t*-Bu (56 mg, 0.50 mmol, stored and handled under air), 0.50 equiv. Et_3B in THF (1.0 M, 0.50 mL, 0.50 mmol) and 4.4 mL 1,4-dioxane. The final concentration of the reaction was unaltered (0.19 M), the ratio of 1,4-dioxane/THF was changed to 10:1. The crude product was purified by flash column chromatography on silica gel (cyclohexane/EtOAc 8:1). The title compound was isolated as a white solid (363 mg, 0.949 mmol, 95%). Crystals suitable for X-ray crystallographic analysis were obtained by slow evaporation from $CHCl_3$/*n*-hexane at 24 °C.

TLC: $R_f = 0.31$ (cyclohexane/EtOAc 5:1; UV, CAM); **Melting point**: 115 – 116 °C; **^{1}H-NMR** (400 MHz, $CDCl_3$, 298 K): δ 7.73 (d, *J* = 8.3 Hz, 2H), 7.31 (d, *J* = 8.5 Hz, 2H), 7.08 (td, *J* = 7.6, 1.2 Hz, 1H), 7.05 – 7.03 (m, 1H), 6.72 (td, *J* = 7.5, 1.0 Hz, 1H), 6.58 (d, *J* = 7.8 Hz, 1H), 5.70 (dd, *J* = 17.4, 10.8 Hz, 1H), 5.17 (s, 1H), 4.95 – 4.87 (m, 2H), 4.72 (br, 1H), 3.41 (ddd, *J* = 10.0, 7.9, 1.9 Hz, 1H), 3.05 (ddd app td, *J* = 10.6, 6.0 Hz, 1H), 2.44 (s, 3H), 2.03 (ddd, *J* = 12.3, 10.7, 7.9 Hz, 1H), 1.93 (ddd, *J* = 12.3, 6.0, 1.8 Hz, 1H), 0.98 (s, 3H), 0.84 (s, 3H); **^{13}C-NMR** (101 MHz, $CDCl_3$, 298 K): δ 150.1, 144.0, 143.6, 136.5, 129.8 (two coincident resonances), 128.7, 127.2, 124.9, 118.8, 113.9, 109.4, 80.7, 64.7, 47.9, 41.1, 33.3, 22.8, 22.7, 21.7; **IR** (neat): 3379 (m), 2970 (m), 1714 (w), 1606 (m), 1483 (m), 1466 (m), 1403 (w), 1369 (w), 1333 (s), 1257 (w), 1211 (w), 1157 (s), 1116 (w), 1088 (m), 1059 (m), 1028 (m), 1008 (w), 988 (m), 949 (m), 926 (m), 884 (m), 861 (w), 813 (m), 785 (m), 750 (s), 738 (s), 706 (w), 659 (s), 606 (m), 570 (s), 543 (s) cm^{-1}; **HRMS** (ESI) *m/z*: exact mass calculated for $C_{22}H_{27}N_2O_2S$ $[M + H]^+$ 383.1788, found 383.1783.

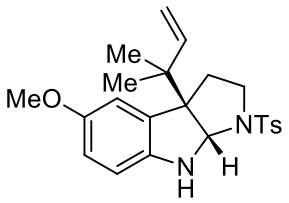

(±)-(3a*S*,8a*R*)-5-Methoxy-3a-(2-methylbut-3-en-2-yl)-1-tosyl-1,2,3,3a,8,8a-hexahydropyrrolo[2,3-*b*]indole (110). The general procedure was followed using 0.50 equiv. KO*t*-Bu (56 mg, 0.50 mmol, stored and handled under air), 0.50 equiv. Et_3B in THF (1.0 M, 0.50 mL, 0.50 mmol) and 4.4 mL 1,4-dioxane. The final concentration of the reaction was unaltered (0.19 M), the ratio of 1,4-dioxane/THF was changed to 10:1. The crude product was purified by flash column chromatography on silica gel (cyclohexane/EtOAc 5:1). The title compound was isolated as a white foam (397 mg, 0.962 mmol, 96%).

TLC: $R_f = 0.23$ (cyclohexane/EtOAc 5:1; UV, CAM); **Melting point**: 105 – 107 °C; **^{1}H-NMR** (400 MHz, $CDCl_3$, 298 K): δ 7.73 (d, *J* = 8.3 Hz, 2H), 7.31 (d, *J* = 7.9 Hz, 2H), 6.68 – 6.65 (m, 2H), 6.53 – 6.50 (m, 1H), 5.69 (dd, *J* = 17.4, 10.8 Hz, 1H), 5.16 (s, 1H), 4.95 – 4.88 (m, 2H), 4.48 (s, 1H), 3.74 (s, 3H), 3.44 – 3.39 (m, 1H), 3.04 (ddd app td, *J* = 10.6, 6.0 Hz, 1H), 2.43 (s, 3H), 2.00 (ddd, *J* = 12.3, 10.7, 7.9 Hz, 1H), 1.90 (ddd, *J* = 12.4, 6.0, 1.7 Hz, 1H), 0.97 (s, 3H), 0.85 (s, 3H); **^{13}C-NMR** (101 MHz, $CDCl_3$, 298 K): δ 153.4, 144.1, 144.0, 143.5, 136.5, 131.6, 129.8, 127.3, 113.9, 113.1, 112.2, 109.9, 81.5, 65.1, 56.1, 47.9, 41.1, 33.2, 22.9, 22.7, 21.7; **IR** (neat): 3381 (br), 2970 (w), 1708 (w), 1598 (w), 1490 (m), 1436 (w), 1334 (m), 1302 (w), 1282 (w), 1207 (w), 1156 (s), 1091 (m), 1038 (m), 914 (m), 859 (w), 812 (m), 766 (m), 736 (m), 707 (w), 659 (s), 568 (m), 546 (s), 461 (w) cm^{-1}; **HRMS** (ESI) *m/z*: exact mass calculated for $C_{23}H_{29}N_2O_3S$ $[M + H]^+$ 413.1893, found 413.1895.

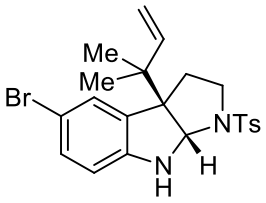

(±)-(3a*S*,8a*R*)-5-Bromo-3a-(2-methylbut-3-en-2-yl)-1-tosyl-1,2,3,3a,8,8a-hexahydropyrrolo[2,3-*b*]indole (111). The general procedure was followed using 0.50 equiv. KO*t*-Bu (56 mg, 0.50 mmol, stored and handled under air), 0.50 equiv. Et_3B in THF (1.0 M, 0.50 mL, 0.50 mmol) and 4.4 mL 1,4-dioxane. The final concentration of the reaction was unaltered (0.19 M), the ratio of 1,4-dioxane/THF was changed to 10:1. The crude product was

purified by flash column chromatography on silica gel (cyclohexane/EtOAc 8:1). The title compound was isolated as a white solid (427 mg, 0.925 mmol, 93%).

TLC: $R_f = 0.35$ (cyclohexane/EtOAc 5:1; UV, CAM); **Melting point**: 121 °C; **^{1}H-NMR** (400 MHz, $CDCl_3$, 298 K): δ 7.72 (d, *J* = 8.3 Hz, 2H), 7.31 (d, *J* = 8.0 Hz, 2H), 7.17 (dd, *J* = 8.3, 2.0 Hz, 1H), 7.13 (d, *J* = 2.0 Hz, 1H), 6.46 (d, *J* = 8.3 Hz, 1H), 5.66 (dd, *J* = 17.4, 10.8 Hz, 1H), 5.16 (s, 1H), 4.96 – 4.89 (m, 2H), 4.76 (s, 1H), 3.40 (ddd, *J* = 10.1, 7.9, 1.9 Hz, 1H), 3.06 (ddd app td, *J* = 10.6, 6.0 Hz, 1H), 2.44 (s, 3H), 2.02 (ddd, *J* = 12.4, 10.6, 8.0 Hz, 1H), 1.89 (ddd, *J* = 12.5, 5.9, 1.7 Hz, 1H), 0.96 (s, 3H), 0.84 (s, 3H); **^{13}C-NMR** (101 MHz, $CDCl_3$, 298 K): δ 149.1, 143.7, 143.4, 136.2, 132.4, 131.4, 129.9, 127.8, 127.2, 114.3, 110.7, 110.3, 80.9, 64.8, 47.8, 41.1, 33.3, 22.7, 22.6, 21.7; **IR** (neat): 3387 (br), 2971 (w), 1600 (m), 1475 (m), 1428 (w), 1333 (m), 1256 (w), 1155 (s), 1122 (w), 1092 (m), 1041 (m), 1006 (m), 919 (m), 882 (w), 811 (m), 754 (m), 737 (m), 659 (s), 619 (m), 576 (s), 544 (s), 460 (m) cm^{-1}; **HRMS** (ESI) *m/z*: exact mass calculated for $C_{22}H_{26}BrN_2O_2S$ $[M + H]^+$ 461.0893, found 461.0893.

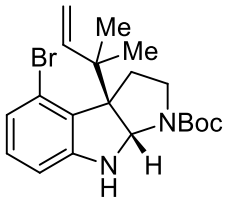

(±)-(3a*S*,8a*R*)-*tert*-butyl 4-bromo-3a-(2-methylbut-3-en-2-yl)-3,3a,8,8a-tetrahydropyrrolo[2,3-*b*]indole-1(2*H*)-carboxylate (112). The catalyst loading was increased to 2 mol% (consequently [{Ir(cod)Cl}$_2$] (6.7 mg, 10 µmol, 1.0 mol%.) and **87** (7.6 mg, 20 µmol, 2.0 mol%) were mixed in 0.50 mL 1,4-dioxane) and the reaction was stirred at 24 °C for 2 h. The crude product was purified by flash column chromatography on silica gel (cyclohexane/EtOAc 20:1 to 12:1 gradient). The title compound was isolated as a colorless solid (365 mg, 0.895 mmol, 90%). Crystals suitable for X-ray crystallographic analysis were obtained by slow evaporation from $CHCl_3$/*n*-hexane at 23 °C.

TLC: $R_f = 0.21$ (cyclohexane/EtOAc 12:1; UV, CAM); **Melting point**: 117 – 118 °C; **^{1}H-NMR** (400 MHz, $CDCl_3$, 298 K, mixture of rotamers, major peaks reported): δ 6.91 – 6.82 (m, 2H), 6.52 – 6.50 (m, 1H), 6.08 (dd, *J* = 17.1, 11.0 Hz, 1H), 5.17 – 5.02 (m, 4H), 3.56 – 3.51 (m, 1H), 3.10 – 2.92 (m, 2H), 2.16 – 2.06 (m, 1H), 1.42 (s, 9H), 1.23 (s, 3H), 1.05 (s, 3H); **^{13}C-NMR** (101 MHz, $CDCl_3$, 298 K, mixture of rotamers, major peaks reported): δ 154.5, 153.6, 145.2, 130.1, 126.9, 124.3, 120.5, 113.5, 108.6, 79.9, 78.8, 65.3, 46.5, 42.9, 28.6, 27.5,

25.6, 23.9; **IR** (neat): 3356 (br), 2974 (w), 2879 (w), 1676 (s), 1598 (m), 1566 (m), 1445 (m), 1393 (s), 1365 (m), 1313 (w), 1298 (w), 1265 (m), 1217 (w), 1159 (s), 1118 (m), 1096 (w), 1060 (w), 1005 (w), 900 (m), 882 (m), 771 (m), 733 (m), 691 (w), 632 (w), 553 (w), 521 (w) cm^{-1}; **HRMS** (ESI) *m/z*: exact mass calculated for $C_{20}H_{28}BrN_2O_2$ $[M + H]^+$ 407.1329, found 407.1328.

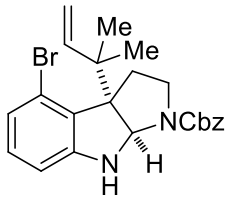

(±)-(3a*S*,8a*R*)-benzyl 4-bromo-3a-(2-methylbut-3-en-2-yl)-3,3a,8,8a-tetrahydropyrrolo[2,3-*b*]indole-1(2*H*)-carboxylate (113). The general procedure was followed using 1.10 equiv. *tert*-BuOK (123 mg, 1.10 mmol), 1.1 equiv. Et_3B in THF (1.0 M, 1.1 mL, 1.1 mmol) and 3.8 mL 1,4-dioxane. The catalyst loading was increased to 2 mol% (consequently $[\{Ir(cod)Cl\}_2]$ (6.7 mg, 10 µmol, 1.0 mol%.) and **87** (7.6 mg, 20 µmol, 2.0 mol%) were mixed in 0.50 mL 1,4-dioxane). The final concentration of the reaction was unaltered (0.19 M), the ratio of solvents was changed to 4:1 (1,4-dioxane/THF). The reaction was stirred at 24 °C for 6 h. NMR analysis of crude **113** showed a complex mixture of rotamers (at 298 K in chloroform-d_1, methanol-d_4 and dimethyl sulfoxide-d_6) and no regioselectivity was determined. The crude product was purified by flash column chromatography on silica gel (cyclohexane/EtOAc 8:1). The title compound was isolated as clear oil (398 mg, 0.901 mmol, 90%).

TLC: R_f = 0.36 (cyclohexane/EtOAc 5:1; UV, CAM); **^{1}H-NMR** (400 MHz, $CDCl_3$, 298 K, mixture of rotamers): δ 7.43 – 7.29 (m, 5H), 6.94 – 6.84 (m, 2H), 6.55 – 6.41 (m, 1H), 6.12 – 6.03 (m, 1H), 5.29 – 5.04 (m, 6H), 3.78 – 3.65 (m, 1H), 3.18 – 3.02 (m, 2H), 2.20 – 2.10 (m, 1H), 1.26 (s, 3H), 1.08 – 1.05 (m, 3H); **^{13}C-NMR** (101 MHz, $CDCl_3$, 298 K, mixture of rotamers, major peaks reported): δ 154.8, 153.3, 145.1, 136.5, 130.1, 128.6, 128.1, 127.9, 126.6, 124.5, 120.5, 113.6, 108.7, 79.2, 66.8, 65.3, 46.3, 42.9, 27.6, 25.6, 23.8; **IR** (neat): 3358 (br), 2970 (w), 2880 (w), 1684 (s), 1598 (m), 1567 (m), 1498 (w), 1444 (m), 1415 (s), 1353 (s), 1312 (w), 1264 (m), 1213 (m), 1196 (m), 1061 (m), 1004 (w), 957 (w), 899 (m), 864 (w), 753 (s), 734 (s), 696 (s), 644 (w), 585 (w) 549 (w) cm^{-1}; **HRMS** (ESI-TOF) *m/z*: exact mass calculated for $C_{23}H_{26}BrN_2O_2$ $[M + H]^+$ 441.1172, found 441.1174.

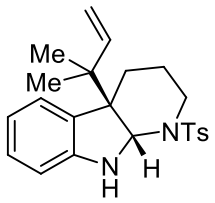

(±)-(4a*S*,9a*R*)-4a-(2-Methylbut-3-en-2-yl)-1-tosyl-2,3,4,4a,9,9a-hexahydro-1*H*-pyrido[2,3-*b*]indole (114). The reaction was stirred at 24 °C for 2 h then 2-aminoethanol (0.12 mL, 2.0 mmol, 2.0 equiv.) was added and the reaction was stirred further at 24 °C for 1 h. The crude product was purified by flash column chromatography on silica gel (cyclohexane/EtOAc 8:1 to 5:1 gradient). The title compound was isolated as a colorless, waxy solid (314 mg, 0.793 mmol, 79%).

TLC: R_f = 0.34 (cyclohexane/EtOAc 5:1; UV, CAM); **^{1}H-NMR** (400 MHz, $CDCl_3$, 298 K): δ 7.75 (d, *J* = 8.3 Hz, 2H), 7.34 (d, *J* = 7.9 Hz, 2H), 7.03 – 6.99 (m, 2H), 6.66 (td, *J* = 7.5, 1.0 Hz, 1H), 6.43 – 6.40 (m, 1H), 5.83 – 5.76 (m, 1H), 5.65 (s, 1H), 5.03 – 5.02 (m, 1H), 5.00 – 4.99 (m, 1H), 3.97 (s, 1H), 3.47 – 3.40 (m, 1H), 2.91 – 2.84 (m, 1H), 2.45 (s, 3H), 1.79 – 1.64 (m, 3H), 1.20 – 1.08 (m, 1H), 1.01 – 1.00 (m, 6H); **^{13}C-NMR** (101 MHz, $CDCl_3$, 298 K): δ 149.9, 144.4, 143.6, 137.3, 129.9, 129.0, 128.2, 127.4, 125.5, 118.0, 113.7, 107.8, 73.1, 55.7, 43.1, 37.2, 24.0, 22.5, 21.7 (two coincident resonances), 18.2; **IR** (neat): 3382 (br), 2964 (br), 2878 (w), 1607 (w), 1485 (w), 1467 (m), 1384 (w), 1334 (m), 1216 (w), 1156 (s), 1091 (m), 1027 (w), 973 (m), 915 (w), 853 (w), 814 (w), 741 (s), 707 (w), 663 (s), 593 (m), 574 (m), 545 (s), 485 (w) cm^{-1}; **HRMS** (ESI) *m/z*: exact mass calculated for $C_{23}H_{29}N_2O_2S$ $[M + H]^+$ 397.1944, found 397.1947.

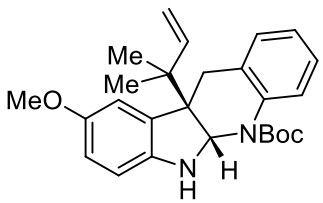

(±)-(5a*R*,10b*S*)-*tert*-Butyl 9-methoxy-10b-(2-methylbut-3-en-2-yl)-5a,6,10b,11-tetrahydro-5*H*-indolo[2,3-*b*]quinoline-5-carboxylate (115). The reaction was stirred at 24 °C for 5 h. The crude product was purified by flash column chromatography on silica gel (cyclohexane/EtOAc 8:1). The title compound was isolated as a pale brown solid (369 mg, 0.877 mmol, 88%).

TLC: R_f = 0.25 (cyclohexane/EtOAc 5:1; UV, CAM); **Melting point**: 131 – 132 °C; **^{1}H-NMR** (400 MHz, $CDCl_3$, 298 K): δ 7.24 (br, 1H), 7.04 – 7.00 (m, 1H), 6.89 – 6.82 (m, 2H), 6.61 (d, *J* = 2.5 Hz, 1H), 6.41 (dd, *J* = 8.4, 2.6 Hz, 1H), 6.23 (d, *J* = 8.4 Hz, 1H), 6.17 (s, 1H), 6.02 (dd, *J* = 17.1, 11.1 Hz, 1H), 5.18 (s, 1H), 5.14 (dd, *J* = 7.9, 1.3 Hz, 1H), 4.03 (br, 1H), 3.66 (s, 3H), 2.99 (d, *J* = 13.7 Hz, 1H), 2.86 (d, *J* = 13.7 Hz, 1H), 1.53 (s, 9H), 1.19 (s, 3H), 1.15 (s, 3H); **^{13}C-NMR** (101 MHz, $CDCl_3$, 298 K): δ 153.4, 152.6, 144.6, 144.5, 137.4, 132.8, 131.6, 128.2, 126.1, 125.0, 124.8, 113.9, 112.6, 112.3, 108.3, 81.1, 74.6, 62.7, 56.0, 43.1, 33.2, 28.5, 22.7, 22.1; **IR** (neat): 3363 (br), 2974 (w), 1683 (s), 1589 (w), 1494 (s), 1454 (w), 1435 (w), 1392 (w), 1367 (m), 1334 (s), 1299 (w), 1279 (w), 1248 (w), 1215 (m), 1160 (s), 1041 (s), 1013 (s), 911 (m), 856 (w), 806 (w), 731 (s), 582 (w), 462 (w) cm^{-1}; **HRMS** (ESI) *m/z*: exact mass calculated for $C_{26}H_{33}N_2O_3$ $[M + H]^+$ 421.2486, found 421.2482.

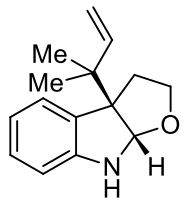

(±)-(3a*S*,8a*R*)-3a-(2-Methylbut-3-en-2-yl)-3,3a,8,8a-tetrahydro-2*H*-furo[2,3-*b*]indole (116).[99] The reaction was stirred at 24 °C for 4 h. The crude product was purified by flash column chromatography on silica gel (cyclohexane/EtOAc 8:1). The title compound was isolated as a white solid (165 mg, 0.719 mmol, 72%).

TLC: R_f = 0.21 (cyclohexane/EtOAc 8:1; UV, CAM); **Melting point**: 44 – 45 °C; **^{1}H-NMR** (400 MHz, $CDCl_3$, 298 K): δ 7.18 – 7.16 (m, 1H), 7.07 (td, *J* = 7.6, 1.3 Hz, 1H), 6.73 (td, *J* = 7.5, 1.0 Hz, 1H), 6.57 (d, *J* = 7.8 Hz, 1H), 6.05 (dd, *J* = 17.4, 10.8 Hz, 1H), 5.44 (s, 1H), 5.11 (dd, *J* = 10.8, 1.3 Hz, 1H), 5.07 (dd, *J* = 17.4, 1.3 Hz, 1H), 4.67 (s, 1H), 3.95 (ddd, *J* = 8.5, 7.3, 1.1 Hz, 1H), 3.48 (ddd, *J* = 11.3, 8.5, 4.9 Hz, 1H), 2.36 (ddd app td, *J* = 11.5, 7.3 Hz, 1H), 1.99 – 1.95 (m, 1H), 1.14 (s, 3H), 1.05 (s, 3H); **^{13}C-NMR** (101 MHz, $CDCl_3$, 298 K): δ 150.5, 144.7, 130.8, 128.1, 125.2, 118.3, 113.3, 108.0, 95.4, 67.7, 64.7, 40.5, 36.0, 23.4, 22.9; **IR** (neat): 3346 (br), 3056 (w), 2970 (m), 2885 (w), 1607 (m), 1469 (s), 1416 (w), 1369 (w), 1340 (w), 1317 (w), 1255 (w), 1184 (w), 1152 (w), 1089 (w), 1071 (w), 1032 (m), 999 (m),

[99] Ideguchi, T.; Yamada, T.; Shirahata, T.; Hirose, T.; Sugawara, A.; Kobayashi, Y.; Omura, S.; Sunazuka, T. *J. Am. Chem. Soc.* **2013**, *135*, 12568.

947 (m), 918 (s), 847 (w), 731 (s), 687 (w), 656 (m), 602 (w), 526 (m), 463 (w) cm^{-1}; **HRMS** (ESI) *m/z*: exact mass calculated for $C_{15}H_{20}NO$ $[M + H]^+$ 230.1539, found 230.1543.

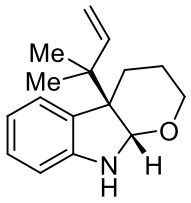

(±)-(4a*S*,9a*R*)-4a-(2-Methylbut-3-en-2-yl)-2,3,4,4a,9,9a-hexahydropyrano[2,3-*b*]indole (117). The reaction was stirred at 24 °C for 4 h. The crude product was purified by flash column chromatography on silica gel (cyclohexane/EtOAc 8:1 to 7:1 gradient). The title compound was isolated as a pale brown solid (148 mg, 0.607 mmol, 62%).

TLC: R_f = 0.24 (cyclohexane/EtOAc 5:1; UV, CAM); **Melting point**: 54 – 56 °C; **^{1}H-NMR** (400 MHz, $CDCl_3$, 298 K): δ 7.10 – 7.04 (m, 2H), 6.72 (td, *J* = 7.4, 1.0 Hz, 1H), 6.58 (d, *J* = 7.7 Hz, 1H), 5.96 (dd, *J* = 17.4, 10.9 Hz, 1H), 5.25 (s, 1H), 5.07 (dd, *J* = 10.9, 1.4 Hz, 1H), 5.00 (dd, *J* = 17.4, 1.4 Hz, 1H), 4.34 (s, 1H), 3.56 – 3.42 (m, 2H), 2.00 – 1.88 (m, 2H), 1.69 – 1.60 (m, 1H), 1.26 – 1.13 (m, 1H), 1.03 (s, 3H), 0.97 (s, 3H); **^{13}C-NMR** (101 MHz, $CDCl_3$, 298 K): δ 150.6, 144.9, 129.6, 128.0, 125.7, 117.8, 113.1, 107.6, 89.5, 57.0, 53.5, 42.2, 22.4, 22.2, 22.0, 19.8; **IR** (neat): 3341 (br), 3081 (w), 2962 (m), 2879 (w), 1635 (w), 1608 (m), 1484 (m), 1467 (s), 1414 (w), 1381 (w), 1364 (w), 1315 (w), 1243 (w),1152 (w), 1076 (s), 1030 (m), 1008 (s), 914 (s), 872 (w), 738 (s), 687 (w), 637 (w), 514 (w) cm^{-1}; **HRMS** (ESI) *m/z*: exact mass calculated for $C_{16}H_{22}NO$ $[M + H]^+$ 244.1696, found 244.1699.

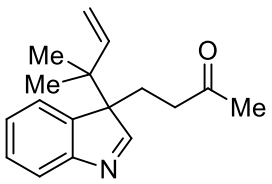

(±)-4-(3-(2-Methylbut-3-en-2-yl)-3*H*-indol-3-yl)butan-2-one (118). The catalyst loading was increased to 2 mol% (consequently $[\{Ir(cod)Cl\}_2]$ (6.7 mg, 10 µmol, 1.0 mol%.) and **87** (7.6 mg, 20 µmol, 2.0 mol%) were mixed in 0.50 mL 1,4-dioxane) and the reaction was stirred at 50 °C for 2 h. The crude product was purified by flash column chromatography on silica gel (cyclohexane/EtOAc 4:1 to 1:1 gradient). The title compound was isolated as a clear, colorless oil (225 mg, 0.883 mmol, 88%).

TLC: R_f = 0.28 (cyclohexane/EtOAc 1:1; UV, CAM); **^{1}H-NMR** (400 MHz, $CDCl_3$, 298 K): δ 8.00 (s, 1H), 7.59 (d, *J* = 7.7 Hz, 1H), 7.35 – 7.31 (m, 1H), 7.27 – 7.25 (m, 1H), 7.20 (t, *J* = 7.5 Hz, 1H), 5.97 (dd, *J* = 17.4, 10.8 Hz, 1H), 5.09 (d, *J* = 10.8 Hz, 1H), 5.02 (d, *J* = 17.4 Hz, 1H), 2.40 (ddd, *J* = 14.0, 9.4, 5.8 Hz, 1H), 2.25 – 2.17 (m, 1H), 1.79 (s, 3H), 1.69 (ddd, *J* = 18.2, 9.6, 5.8 Hz, 1H), 1.48 (ddd, *J* = 18.2, 9.4, 5.6 Hz, 1H), 1.01 (s, 3H), 0.98 (s, 3H); **^{13}C-NMR** (101 MHz, $CDCl_3$, 298 K): δ 208.0, 178.0, 156.2, 144.0, 139.8, 128.2, 126.0, 123.8, 121.3, 114.1, 67.0, 41.3, 37.8, 30.1, 23.7, 23.0 (two coincident resonances); **IR** (neat): 3083 (w), 2969 (m), 2937 (w), 1714 (s), 1637 (w), 1556 (m), 1463 (m), 1452 (m), 1416 (m), 1363 (s), 1277 (w), 1164 (s), 1107 (w), 1006 (m), 917 (s), 849 (w), 777 (m), 754 (s), 691 (w), 563 (m), 549 (w), 482 (w), 438 (m) cm^{-1}; **HRMS** (EI) *m/z*: exact mass calculated for $C_{17}H_{21}NO$ $[M]^+$ 255.1618, found 255.1623.

Synthesis of Linear Prenylated 75

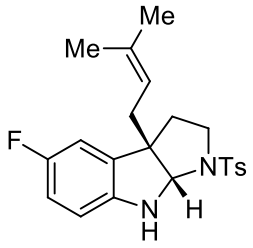

(±)-(3a*R*,8a*R*)-5-Fluoro-3a-(3-methylbut-2-en-1-yl)-1-tosyl-1,2,3,3a,8,8a-hexahydropyrrolo[2,3-*b*]indole (75). To sulfonamide **73** (33 mg, 0.10 mmol, 1.0 equiv.) and KO*t*-Bu (12 mg, 0.11 mmol, 1.1 equiv., stored and handled under air) at 24 °C was added Et_3B in THF (1.0 M, 0.24 mL, 0.12 mmol, 1.2 equiv.) and 1,4-dioxane (0.4 mL) and the resulting mixture was stirred at this temperature for 30 min before being added to tetrakis(triphenylphosphine)palladium(0) (4.5 mg, 3.9 µmol, 3.9 mol%.) in 1,4-dioxane (0.20 mL) – prepared in a screw-capped vial, sparged with N_2 and stirred at 24 °C for 10 min. To the stirred mixture was then added carbonate **84** (40 µL, 37 mg, 0.20 mmol, 2.0 equiv.) via syringe and the resulting mixture was stirred at 50 °C for 2 h before it was diluted with Et_2O, filtered through a plug of silica gel with copious washings (Et_2O), and purified by flash column chromatography on silica gel (cyclohexane/EtOAc 8:1). The title compound was isolated as a clear, colorless oil (23 mg, 0.056 mmol, 56%). The regioselectivity (linear to branched or **75** to **74**, analyzed by $^{19}F\{^1H\}$ NMR) was determined to be 29:1 for the crude product and 33:1 after purification.

TLC: R_f = 0.30 (cyclohexane/EtOAc 5:1; UV, CAM); **^{1}H-NMR** (400 MHz, $CDCl_3$, 298 K): δ 7.72 (d, *J* = 8.3 Hz, 2H), 7.32 (d, *J* = 7.9 Hz, 2H), 6.77 (ddd, *J* = 9.2, 8.5, 2.6 Hz, 1H), 6.70 (dd, *J* = 8.4, 2.5 Hz, 1H), 6.52 (dd, *J* = 8.5, 4.2 Hz, 1H), 5.03 (s, 1H), 4.93 – 4.88 (m, 1H), 4.71 (br, 1H), 3.40 (ddd, *J* = 10.3, 8.0, 2.2 Hz, 1H), 3.12 (ddd app td, *J* = 10.5, 6.0 Hz, 1H), 2.43 (s, 3H), 2.28 – 2.16 (m, 2H), 2.00 (ddd, *J* = 12.5, 6.0, 2.1 Hz, 1H), 1.82 (ddd, *J* = 12.5, 10.5, 8.0 Hz, 1H), 1.62 (s, 3H), 1.46 (s, 3H); **^{13}C-NMR** (101 MHz, $CDCl_3$, 298 K): δ 157.3 (d, *J* = 235.9 Hz) 144.8 (d, *J* = 1.4 Hz), 143.7, 136.2, 135.9, 133.7 (d, *J* = 7.4 Hz), 129.9, 127.2, 118.5, 114.7 (d, *J* = 23.3 Hz), 110.5 (d, *J* = 24.1 Hz), 110.0 (d, *J* = 8.1 Hz), 83.2, 58.8 (d, *J* = 1.9 Hz), 47.6, 35.5, 35.2, 26.0, 21.7, 18.0; **^{19}F{^{1}H}-NMR** (377 MHz, $CDCl_3$, 298 K): δ – 125.6; **IR** (neat): 3389 (br), 2968 (w), 2926 (w), 1598 (w), 1486 (s), 1447 (m), 1378 (w), 1334 (m), 1304 (w), 1292 (w), 1242 (w), 1180 (w), 1157 (s), 1092 (m), 1034 (br), 922 (w), 861 (w), 812 (m), 782 (m), 737 (w), 707 (w), 672 (m), 658 (s), 587 (m), 546 (s), 455 (m) cm^{-1}; **HRMS** (ESI) *m/z*: exact mass calculated for $C_{22}H_{26}FN_2O_2S$ $[M + H]^+$ 401.1694, found 401.1691.

8.1.3 Diastereoselective Reverse Prenylation

Synthesis of (*S*)-Tryptophan methyl ester (23)

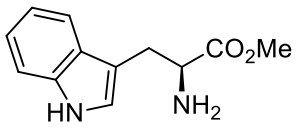

(*S*)-Tryptophan methyl ester ((–)-23).[100] Following modified literature procedures,[100] thionyl chloride (3.1 mL, 43 mmol, 1.4 equiv.) was added dropwise at 0 °C to a suspension of (*S*)-tryptophan (6.30 g, 30.8 mmol, 1.00 equiv.) in MeOH (100 mL). The ice bath was removed and after 30 min the clear solution was heated to 40 °C for 4 h then was allowed to cool to 24 °C. Concentration under reduced pressure afforded an off-white solid, which was dissolved in MeOH (50 mL) and concentrated again under reduced pressure. The flask was cooled in an ice bath and sat. aq. Na_2CO_3 was added. The mixture was transferred into a separation funnel and the transfer was assisted with $CHCl_3$. Deionized water and $CHCl_3$ were added, the phases were separated and the aqueous phase was extracted once with $CHCl_3$. The combined organic solutions were dried over $MgSO_4$, filtered, and concentrated under reduced pressure to afford

[100] (a) Isaacs, N. S.; Coulson, M. *J. Phys. Org. Chem.* **1996**, *9*, 639. (b) Earle, M. J.; Noe, M.; Perosa, A.; Seddon, K. R. *RSC Adv.* **2014**, *4*, 1204.

an oil. Dissolving the oil in CH_2Cl_2 followed by concentration under reduced pressure (40 °C, 20 mbar then 24 °C, <0.1 Torr for 15 h) provided (−)-**23** as an off-white solid (6.14 g, 28.1 mmol, 91%), which was used without further purification.

^{1}H-NMR (400 MHz, $CDCl_3$, 298 K): δ 8.30 (br, 1H), 7.62 (d, *J* = 7.9 Hz, 1H), 7.36 – 7.33 (m, 1H), 7.22 – 7.18 (m, 1H), 7.15 – 7.11 (m, 1H), 7.04 – 7.03 (m, 1H), 3.85 (dd, *J* = 7.7, 4.8 Hz, 1H), 3.72 (s, 3H), 3.29 (dd, *J* = 14.4, 4.8 Hz, 1H), 3.06 (dd, *J* = 14.4, 7.7 Hz, 1H), 1.55 (s, 2H); **^{13}C-NMR** (101 MHz, $CDCl_3$, 298 K): δ 175.9, 136.4, 127.6, 123.1, 122.3, 119.6, 118.9, 111.35, 111.26, 55.1, 52.1, 30.9; **HRMS** (ESI) *m/z*: exact mass calculated for $C_{12}H_{15}N_2O_2$ $[M + H]^+$ 219.1128, found 219.1130.

Synthesis of Boc-protected Hexahydropyrroloindole 90 and 91

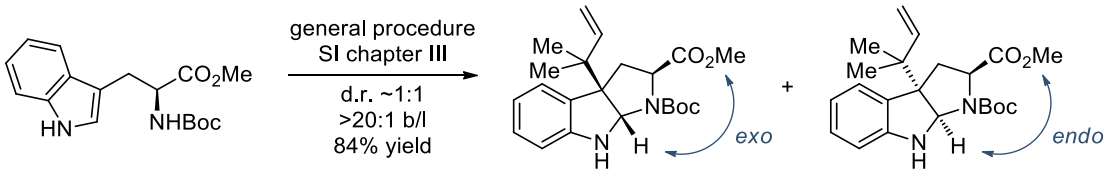

To a flame-dried 25 mL Schlenk flask equipped with a stir bar was added Boc-(*S*)-tryptophan methyl ester (318 mg, 1.00 mmol, 1.00 equiv.) and KO*t*-Bu (123 mg, 1.10 mmol, 1.10 equiv., stored and handled under air). The flask was sealed with a septum, evacuated and back-filled with N_2 (two cycles). Et_3B in THF (1.0 M, 1.1 mL, 1.1 mmol, 1.1 equiv.) and 1,4-dioxane (3.8 mL) were added at 24 °C and the resulting mixture was stirred at this temperature for 25 min before [{Ir(cod)Cl}$_2$] (1.7 mg, 2.5 µmol, 0.25 mol%) and phosphoramidite **87** (1.9 mg, 5.0 µmol, 0.50 mol%) in 1,4-dioxane (0.50 mL) – prepared in a screw-capped vial, sparged with N_2 and stirred at 24 °C for 10 min prior to the addition – was added via Pasteur pipette against a flow of N_2. To the stirred mixture was then added carbonate **59** (282 µL, 261 mg, 1.40 mmol, 1.40 equiv.) via syringe and the resulting mixture was stirred at 24 °C for 4 h before it was diluted with Et_2O (5 mL) and quenched by the addition of sat. aq. NH_4Cl (5 mL). Deionized water (1 mL) was added and the clear solutions were transferred into a separation funnel. Et_2O (10 mL) was used to assist the transfer. The solutions were separated and the organic solution was washed with sat. aq. NaCl (10 mL), dried over $MgSO_4$, filtered, and concentrated under reduced pressure. Purification by flash column chromatography on silica gel (cyclohexane/EtOAc 8:1 to 5:1 gradient) afforded the product as a clear, colorless, sticky oil (327 mg, 0.846 mmol, 84%). The *exo* to *endo* diastereoselectivity was determined to be ~1:1 by ^{13}C NMR analysis; both in the crude and purified product. The regioselectivity

(branched to linear) was found to be >20:1 by ^{1}H NMR analysis of the crude product. An analytical sample of the *exo*-diastereomer was obtained by partial separation by flash column chromatography on silica gel (pentane/Et_2O 6:1 to 5:1 gradient, the *exo*-diastereomer elutes first). Crystals of the *exo*-diastereomer suitable for X-ray crystallographic analysis were obtained by slow evaporation from CH_2Cl_2/*n*-hexane at 23 °C.

Analytical data for the *exo*-diastereomer **(–)-(2*S*,3a*R*,8a*S*)-1-*tert*-butyl 2-methyl 3a-(2-methylbut-3-en-2-yl)-3,3a,8,8a-tetrahydropyrrolo[2,3-*b*]indole-1,2(2*H*)-dicarboxylate ((–)-*exo*-90)**: **TLC**: R_f = 0.33 (pentane/Et_2O 5:1; UV, CAM); **Melting point**: 135 – 137 °C; **Specific Rotation**: $[\alpha]_D^{23}$ –333.4 (c = 1.00, $CHCl_3$); **^{1}H-NMR** (400 MHz, $CDCl_3$, 298 K, mixture of rotamers, all peaks reported): δ 7.11 – 7.07 (m, 2H), 6.77 – 6.72 (m, 1H), 6.61 – 6.57 (m, 1H), 6.04 – 5.96 (m, 1H), 5.41 – 5.29 (m, 2H), 5.13 – 5.00 (m, 2H), 3.94 (dd, *J* = 9.1, 7.7 Hz, 1H), 3.72 – 3.71 (m, 3H), 2.46 – 2.32 (m, 2H), 1.52 – 1.36 (m, 9H), 1.06 – 0.98 (m, 6H); **^{13}C-NMR** (101 MHz, $CDCl_3$, 298 K, mixture of rotamers, all peaks reported): δ 173.5, 172.9, 153.8, 153.3, 150.0, 149.4, 144.0, 130.3, 130.1, 128.8, 128.7, 125.11, 125.05, 118.9, 118.3, 114.0, 109.5, 109.3, 81.3, 80.9, 79.3, 78.6, 63.0, 61.8, 59.49, 59.45, 52.2, 52.0, 41.1, 37.3, 36.6, 28.7, 28.3, 23.1, 23.0, 22.5, 22.4; **IR** (neat): 3414 (w), 2974 (w), 1744 (m), 1684 (s), 1610 (w), 1483 (w), 1468 (w), 1435 (w), 1391 (m), 1355 (s), 1328 (w), 1302 (w), 1276 (w), 1256 (w), 1201 (s), 1170 (s), 1150 (s), 1131 (m), 1087 (w), 1053 (m), 1005 (m), 924 (m), 890 (m), 873 (m), 849 (w), 785 (m), 775 (m), 754 (m), 744 (s), 693 (w), 640 (m), 596 (w), 539 (w), 515 (w), 463 (m), 431 (w) cm^{-1}; **HRMS** (ESI) *m/z*: exact mass calculated for $C_{22}H_{30}N_2NaO_4$ $[M + Na]^+$ 409.2098, found 409.2098.

Generation of 9-BBN-*n*-C_6H_{13}

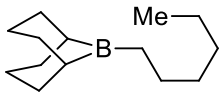

(1*s*,5*s*)-9-Hexyl-9-borabicyclo[3.3.1]nonane. In a glove box, 9-borabicyclo[3.3.1]nonane dimer (4.27 g, 35.0 mmol of monomer, 1.00 equiv.) was added to a flame-dried Schlenk flask. The flask was sealed with a septum and removed from the glove box. To the solid was subsequently added 1,4-dioxane (20 mL) and 1-hexene (4.56 mL, 36.8 mmol, 1.05 equiv.) at 24 °C. Additional 1,4-dioxane (6.5 mL) was added to give a total volume of 35 mL. The suspension was stirred at 24 °C for 12 h and the resulting solution of 9-BBN-*n*-C_6H_{13} (1.0 M in

1,4-dioxane) was kept in the sealed Schlenk flask under N_2 at 24 °C. In the same manner a 0.50 M stock solution of 9-BBN-*n*-C_6H_{13} in 1,4-dioxane was prepared.

Synthesis of Hexahydropyrroloindole (–)-33

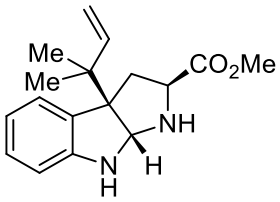

(–)-(2*S*,3a*R*,8a*R*)-methyl 3a-(2-methylbut-3-en-2-yl)-1,2,3,3a,8,8a-hexahydropyrrolo[2,3-*b*]indole-2-carboxylate ((–)-*exo*-33).[101] To a flame-dried 25 mL Schlenk flask equipped with a stir bar and a septum was added (*S*)-tryptophan methyl ester (**23**) (218 mg, 1.00 mmol, 1.00 equiv.) and subsequently in a glove box was added KHMDS (199 mg, 1.00 mmol, 1.00 equiv.). The flask was removed from the glove box, immersed in an ice bath before 9-BBN-*n*-C_6H_{13} in 1,4-dioxane (0.50 M, 5.0 mL, 2.5 mmol, 2.5 equiv.) and THF (1.0 mL) were added via syringe. The resulting suspension was stirred at 0 °C for 10 min before a solution of [{Ir(cod)Cl}$_2$] (3.4 mg, 5.0 µmol, 0.50 mol%) and **87** (3.8 mg, 10 µmol, 1.0 mol%) in THF (0.67 mL) – prepared in a screw-capped vial, sparged with N_2 and stirred at 24 °C for 40 min prior to the addition – was added via Pasteur pipette against a flow of N_2. The mixture was stirred at 0 °C for 6 min before carbonate **59** (211 µL, 196 mg, 1.05 mmol, 1.05 equiv.) was added via syringe and the resulting mixture was stirred at 0 °C for 3 h. The reaction was diluted with EtOAc (5 mL) and quenched with by the addition of sat. aq. NH_4Cl (10 mL) at 0 °C. Deionized water (1 mL) was added, the mixture was allowed to warm to 24 °C and then was transferred into a separation funnel. The transfer was assisted with EtOAc (10 mL). The layers were separated and the aqueous phase was extracted with EtOAc (10 mL). The combined organic solutions were washed with sat. aq. NaCl (20 mL), dried over $MgSO_4$, filtered, and concentrated under reduced pressure. Purification by flash column chromatography on silica gel (cyclohexane/EtOAc 3:1 to 1:2 gradient) afforded hexahydropyrroloindole (−)-*exo*-**33** as a pale yellow, clear oil (167 mg, 0.584 mmol, 58%). The regioselectivity (branched to linear) was found to be >20:1 by ^{1}H NMR analysis of the crude product. The product was isolated as single diastereomer and there was no detectable racemization by SFC analysis.

[101] (a) Depew, K. M.; Marsden, S. P.; Zatorska, D.; Zatorski, A.; Bornmann, W. G.; Danishefsky, S. J. *J. Am. Chem. Soc.* **1999**, *121*, 11953. (b) Wang, Y.; Kong, C.; Du, Y.; Song, H.; Zhang, D.; Qin, Y. *Org. Biomol. Chem.* **2012**, *10*, 2793.

Notes: Combining the reagents as solutions (H-Trp-OMe 0.4 M in 1,4-dioxane, KHMDS 1.0 M in THF and 9-BBN-*n*-C_6H_{13} 1.0 M in 1,4-dioxane) led to a comparable result (56 – 60% yield). When KO*t*-Bu (1.0 equiv.) was used instead of KHMDS under otherwise identical conditions, the yield was lower (48 – 50% for KO*t*-Bu handled and stored under air as well as for KO*t*-Bu handled and stored in a glove box).

TLC: R_f = 0.56 (EtOAc; UV, CAM); **Specific Rotation**: $[\alpha]_D^{22}$ –84.0 (c = 1.00, $CHCl_3$); **^{1}H-NMR** (400 MHz, $CDCl_3$, 298 K): δ 7.13 – 7.11 (m, 1H), 7.05 (td, *J* = 7.6, 1.3 Hz, 1H), 6.71 (td, *J* = 7.5, 1.1 Hz, 1H), 6.56 – 6.54 (m, 1H), 6.00 (dd, *J* = 17.4, 10.8 Hz, 1H), 5.09 (dd, *J* = 10.8, 1.3 Hz, 1H), 5.04 (dd, *J* = 17.4, 1.3 Hz, 1H), 4.99 (s, 1H), 3.69 (s, 3H), 3.58 (dd, *J* = 10.9, 5.6 Hz, 1H), 2.26 (dd, *J* = 11.9, 5.5 Hz, 1H), 2.14 (dd, *J* = 11.9, 11.0 Hz, 1H), 1.10 (s, 3H), 1.00 (s, 3H); **^{13}C-NMR** (101 MHz, $CDCl_3$, 298 K): δ 174.3, 151.1, 144.6, 131.0, 128.4, 125.4, 118.5, 113.7, 109.0, 80.0, 65.9, 60.0, 52.2, 41.6, 41.1, 23.4, 23.0; **IR** (neat): 3316 (br), 2966 (m), 1734 (s), 1636 (w), 1605 (m), 1484 (m), 1467 (m), 1437 (w), 1414 (w), 1381 (w), 1363 (w), 1315 (m), 1251 (m), 1211 (m), 1198 (m), 1182 (m), 1152 (w), 1112 (w), 1092 (w), 1074 (w), 1023 (w), 1010 (w), 915 (m), 821 (w), 739 (s), 688 (w), 595 (w) 485 (w) cm^{-1}; **HRMS** (ESI) *m/z*: exact mass calculated for $C_{17}H_{23}N_2O_2$ $[M + H]^+$ 287.1754, found 287.1757; **SFC** (Daicel Chiralpak IA, 93% CO_2, 7% MeOH at 100 bar, flow rate 2.0 mL·min^{-1}, 25 °C, detection 204 nm): t_R 17.2 min.

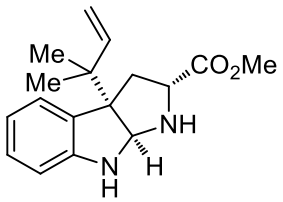

(+)-(2*R*,3a*S*,8a*S*)-methyl 3a-(2-methylbut-3-en-2-yl)-1,2,3,3a,8,8a-hexahydropyrrolo[2,3-*b*]indole-2-carboxylate ((+)-*exo*-33). Hexahydropyrroloindole (+)-*exo*-**33** was prepared from (*R*)-tryptophan methyl ester according to the procedure described above for (−)-*exo*-**33**.

Specific Rotation: $[\alpha]_D^{23}$ +80.3 (c = 1.00, $CHCl_3$); **SFC** (Daicel Chiralpak IA, 93% CO_2, 7% MeOH at 100 bar, flow rate 2.0 mL·min^{-1}, 25 °C, detection 204 nm): t_R .14.0 min.

Synthesis of Hexahydropyrroloindole (+)-*endo*-97

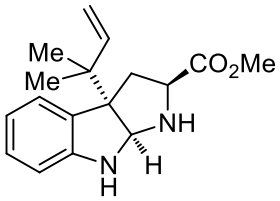

(+)-(2*S*,3a*S*,8a*S*)-methyl 3a-(2-methylbut-3-en-2-yl)-1,2,3,3a,8,8a-hexahydropyrrolo[2,3-*b*]indole-2-carboxylate ((+)-*endo*-97). The *endo*-diastereomer **97** can be ontained by using Et_3B instead of 9-BBN-*n*-C_6H_{13} and subsequent separation of the two diastereomers: To a flame-dried 25 mL Schlenk flask equipped with a stir bar and a septum was added (*S*)-tryptophan methyl ester (**23**) (218 mg, 1.00 mmol, 1.00 equiv.) and subsequently in a glove box was added KHMDS (199 mg, 1.00 mmol, 1.00 equiv.). The flask was removed from the glove box, immersed in an ice bath before 1,4-dioxane (3.5 mL) and after 2 min Et_3B in THF (1.0 M, 2.5 mL, 2.5 mmol, 2.5 equiv.) were added via syringe. The resulting suspension was stirred at 0 °C for 15 min, then a solution of [{Ir(cod)Cl}$_2$] (3.4 mg, 5.0 µmol, 0.50 mol%) and **87** (4.0 mg, 10 µmol, 1.0 mol%) in 1,4-dioxane (0.70 mL) – prepared in a screw-capped vial, sparged with N_2 and stirred at 24 °C for 60 min prior to the addition – was added via Pasteur pipette against a flow of N_2 to the by then clear solution. The reaction mixture was stirred at 0 °C for 6 min before carbonate **59** (211 µL, 196 mg, 1.05 mmol, 1.05 equiv.) was added via syringe and the resulting mixture was stirred at 0 °C for 1 h. The ice bath was removed and the reaction was further stired at 24 °C for 1 h before it was diluted with EtOAc (10 mL) and quenched with by the addition of sat. aq. NH_4Cl (10 mL) at 0 °C. The mixture was transferred into a separation funnel. The transfer was assisted with EtOAc (10 mL). The layers were separated and the aqueous phase was extracted with EtOAc (10 mL). The combined organic solutions were washed with sat. aq. NaCl (20 mL), dried over $MgSO_4$, filtered, and concentrated under reduced pressure. Purification by flash column chromatography on silica gel (cyclohexane/EtOAc 5:1 to 100% EtOAc gradient) afforded hexahydropyrroloindole (−)-*exo*-**33** as a yellow, clear oil (88 mg, 0.31 mmol, 31%) and (+)-*endo*-**97** as pale yellow, clear oil (35 mg, 0.12 mmol, 12%). Both products were isolated substantially racemized, therefore only the sign of the specific roation is given for (+)-*endo*-**97**.

Analytical data for (+)-*endo*-**97**: **TLC**: R_f = 0.22 (EtOAc; UV, CAM); **^{1}H-NMR** (400 MHz, $CDCl_3$, 298 K): δ 7.08 – 7.06 (m, 1H), 7.02 (td, *J* = 7.6, 1.2 Hz, 1H), 6.67 (td, *J* = 7.5, 1.0 Hz, 1H), 6.54 (d, *J* = 7.8 Hz, 1H), 5.99 (dd, *J* = 17.4, 10.8 Hz, 1H), 5.10 – 5.02 (m, 2H), 4.91 (s, 1H), 3.83 (dd, *J* = 7.9, 2.6 Hz, 1H), 3.25 (s, 3H), 2.56 (dd, *J* = 12.7, 8.0 Hz, 1H), 2.40 (dd,

J = 12.7, 2.7 Hz, 1H), 1.10 (s, 3H), 0.98 (s, 3H); **^{13}C-NMR** (101 MHz, $CDCl_3$, 298 K): δ 174.5, 150.9, 144.7, 131.1, 128.5, 126.2, 118.4, 113.6, 109.6, 80.2, 64.0, 60.7, 51.9, 41.2, 38.5, 23.1, 22.7; **IR** (neat): 3355 (br), 3081 (w), 2958 (m), 1732 (s), 1636 (w), 1605 (m), 1484 (m), 1467 (m), 1434 (w), 1414 (w), 1381 (w), 1365 (w), 1316 (w), 1246 (m), 1211 (s), 1154 (m), 1116 (m), 1087 (m), 1017 (m), 981 (w), 914 (m), 877 (w), 821 (w), 741 (s), 687 (w), 616 (w), 522 (w), 464 (w) cm^{-1}; **HRMS** (ESI) *m/z*: exact mass calculated for $C_{17}H_{23}N_2O_2$ $[M + H]^+$ 287.1754, found 287.1754.

Synthesis of (+)-Aszonalenin (130)

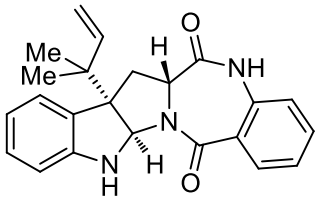

(+)-Aszonalenin ((+)-130).[102] To a solution of (+)-**33** (48.0 mg, 0.168 mmol, 1.00 equiv.) in CH_2Cl_2 (1.7 mL) at 25 °C was subsequently added 2-aminobenzoic acid (32.2 mg, 0.235 mmol, 1.40 equiv.), Et_3N (47 µL, 0.34 mmol, 2.0 equiv.) and HATU (89.1 mg, 0.234 mmol, 1.40 equiv.). The resulting mixture was stirred at 25 °C for 30 h before EtOAc (5 mL), sat. aq. NH_4Cl (5 mL) and deionized water (1 mL) were added. The organic phase was washed with sat. aq. $NaHCO_3$ (2 × 5 mL), sat. aq. NaCl (5 mL) and dried over $MgSO_4$. Filtration and concentration under reduced pressure yielded brown oil, which was azeotropically evaporated with toluene (2 × 4 mL). The crude product was dissolved in toluene (1.7 mL) and at 0 °C a solution of $AlMe_3$ in toluene (2.0 M, 0.34 mL, 0.67 mmol, 4.0 equiv.) was added dropwise. The mixture was stirred at 0 °C for 1 h, then MeOH (0.58 mL) was added dropwise to the clear solution and the resulting suspension was allowed to warm to 25 °C over 1 h. EtOAc (5 mL) and sat. aq. $NaHCO_3$ (5 mL) were added, the mixture was stirred at 25 °C for 30 min before it was filtered through a pad of celite. The filter cake was washed with EtOAc (4 × 5 mL), sat. aq. $NaHCO_3$ (10 mL) was added to the filtrate and the phases were separated. The organic solution was washed with sat. aq. NaCl (10 mL), dried over $MgSO_4$, filtered, and concentrated under reduced pressure. The crude product was purified by flash column chromatography on silica gel (cyclohexane/acetone 3:1) to give synthetic

[102] (a) Kimura, Y.; Hamasaki, T.; Nakajima, H.; Isogai, A. *Tetrahedron Lett.* **1982**, *23*, 225. (b) Yin, W.-B.; Cheng, J.; Li, S.-M. *Org. Biomol. Chem.* **2009**, *7*, 2202.

(+)-aszonalenin (40.4 mg, 0.108 mmol, 64% over two steps) as an off-white solid. The product was isolated as single diastereomer. Crystals suitable for X-ray crystallographic analysis were obtained by slow evaporation from acetone/*n*-hexane at 24 °C.

TLC: $R_f = 0.24$ (cyclohexane/acetone 3:1; UV, CAM); **Melting point**: 246 – 247 °C; **Specific Rotation**: $[\alpha]_D^{23}$ +55.3 (c = 1.00, $CHCl_3$); **^{1}H-NMR** (400 MHz, $CDCl_3$, 298 K): δ 8.92 (s, 1H), 7.83 (dd, *J* = 7.9, 1.5 Hz, 1H), 7.43 (td, *J* = 7.9, 1.6 Hz, 1H), 7.23 – 7.18 (m, 1H), 7.16 (d, *J* = 7.4 Hz, 1H), 7.08 (td, *J* = 7.7, 1.1 Hz, 1H), 6.97 (d, *J* = 8.0 Hz, 1H), 6.72 (td, *J* = 7.4, 0.8 Hz, 1H), 6.63 (d, *J* = 7.8 Hz, 1H), 6.18 (s, 1H), 6.11 (dd, *J* = 17.2, 10.9 Hz, 1H), 5.58 (s, 1H), 5.12 (d, *J* = 2.3 Hz, 1H), 5.08 (dd, *J* = 9.8, 1.1 Hz, 1H), 4.02 – 3.98 (m, 1H), 3.48 (dd, *J* = 13.9, 7.5 Hz, 1H), 2.42 (dd, *J* = 13.9, 9.0 Hz, 1H), 1.14 (s, 3H), 1.05 (s, 3H); **^{13}C-NMR** (101 MHz, $CDCl_3$, 298 K): δ 170.4, 167.0, 149.2, 143.9, 134.4, 132.7, 131.32, 131.27, 128.7, 126.9, 125.2, 125.0, 120.8, 118.4, 114.3, 109.3, 81.8, 60.8, 57.2, 41.6, 33.5, 22.8, 22.6; **IR** (neat): 3413 (w), 3231 (w), 3171 (w), 2982 (w), 1694 (s), 1611 (s), 1598 (s), 1573 (m), 1482 (m), 1464 (m), 1406 (s), 1391 (s), 1324 (m), 1251 (w), 1204 (m), 1138 (m), 1091 (w), 1061 (w), 1012 (w), 924 (m), 874 (w), 856 (w), 802 (w), 763 (s), 748 (s), 717 (m), 692 (w), 669 (m), 644 (w), 603 (w), 514 (m), 465 (m) cm^{-1}; **HRMS** (ESI) *m/z*: exact mass calculated for $C_{23}H_{24}N_3O_2$ $[M + H]^+$ 374.1863, found 374.1863.

Synthesis of (–)-Brevicompanine B (132)

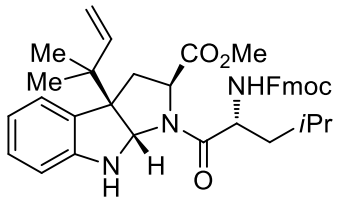

(–)-(2*S*,3a*R*,8a*S*)-methyl 1-((*R*)-2-((((9*H*-fluoren-9-yl)methoxy)carbonyl)amino)-4-methylpentanoyl)-3a-(2-methylbut-3-en-2-yl)-1,2,3,3a,8,8a-hexahydropyrrolo[2,3-*b*]indole-2-carboxylate (131). Following a modified literature procedure,[103] a solution of (−)-**33** (69.0 mg, 0.241 mmol, 1.00 equiv.) in CH_2Cl_2 (2.4 mL) at 0 °C was subsequently treated with *N*-Fmoc-(*R*)-Leu (128 mg, 0.361 mmol, 1.50 equiv.), HATU (101 mg, 0.265 mmol, 1.10 equiv.) and Et_3N (67 µL, 0.48 mmol, 2.0 equiv.). The resulting mixture was allowed to warm slowly to 19 °C over 20 h before the reaction was quenched with sat. aq.

[103] Sun, Y.; Li, R.; Zhang, W.; Li, A. *Angew. Chem., Int. Ed.* **2013**, *52*, 9201.

NH_4Cl (6 mL) and diluted with EtOAc (5 mL). The organic phase was extracted with EtOAc (2× 5 mL), the combined organic solutions were washed with sat. aq. NaCl (10 mL), dried over $MgSO_4$, filtrated and concentrated under reduced pressure. Purification by flash column chromatography on silica gel (cyclohexane/EtOAc 4:1) afforded (−)-**131** as a white foam (123 mg, 0.198 mmol, 82%). The product was isolated as single diastereomer.

TLC: $R_f = 0.32$ (cyclohexane/EtOAc 3:1; UV, CAM); **Melting point**: 119 – 120 °C; **Specific Rotation**: $[\alpha]_D^{25}$ –140.5 (c = 1.00, $CHCl_3$); **^{1}H-NMR** (400 MHz, $CDCl_3$, 298 K, mixture of rotamers, all peaks reported): δ 7.79 – 7.76 (m, 2H), 7.63 (dd, *J* = 7.3, 3.7 Hz, 1H), 7.51 (d, *J* = 7.4 Hz, 1H), 7.43 – 7.33 (m, 4H), 7.17 – 6.87 (m, 2H), 6.76 – 6.19 (m, 2H), 5.98 – 5.82 (m, 1H), 5.80 – 5.59 (m, 1H), 5.52 – 4.41 (m, 6H), 4.29 – 3.95 (m, 3H), 3.78 – 3.69 (m, 3H), 2.68 – 2.33 (m, 2H), 1.78 – 1.42 (m, 3H), 1.02 – 1.00 (m, 6H), 0.93 – 0.84 (m, 6H); **^{13}C-NMR** (101 MHz, $CDCl_3$, 298 K, mixture of rotamers, all peaks reported): δ 174.0, 173.5, 172.3, 172.2, 156.6, 155.9, 149.5, 148.8, 144.1, 144.0, 143.9, 143.8, 143.8, 143.4, 141.4, 141.4, 141.4, 135.3, 132.3, 129.8, 129.1, 128.6, 127.9, 127.8, 127.3, 127.2, 127.2, 127.1, 125.3, 125.2, 125.1, 125.0, 120.9, 120.1, 120.1, 118.4, 114.3, 114.3, 112.4, 109.1, 80.9, 78.3, 67.4, 67.2, 64.7, 60.9, 59.5, 59.2, 52.8, 52.2, 51.0, 50.6, 47.3, 47.2, 41.5, 41.3, 41.1, 39.6, 38.2, 35.2, 32.3, 26.5, 24.6, 24.2, 23.7, 23.5, 23.0, 22.9, 22.5, 22.4, 22.1, 21.3; **IR** (neat): 3281 (br), 2956 (m), 1748 (m), 1714 (m), 1634 (m), 1607 (w), 1521 (w), 1484 (w), 1466 (w), 1449 (w), 1433 (w), 1365 (w), 1317 (m), 1247 (m), 1203 (m), 1173 (m), 1108 (w), 1092 (w), 1046 (w), 1006 (w), 920 (m), 757 (m), 739 (s), 645 (w), 621 (w), 541 (w) cm^{-1}; **HRMS** (ESI) *m/z*: exact mass calculated for $C_{38}H_{44}N_3O_5$ $[M + H]^+$ 622.3275, found 622.3266.

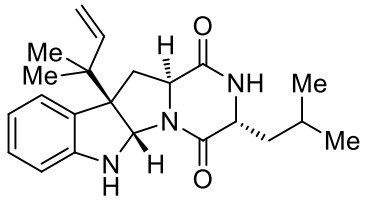

(–)-Brevicompanine B ((–)-132).[104] Following a modified literature procedure,[103] to a solution of (−)-**131** (98.0 mg, 0.158 mmol, 1.00 equiv.) in THF (7.9 mL) at 0 °C was added Et_2NH (0.57 mL, 5.5 mmol, 35 equiv.) over 5 min. The resulting mixture was allowed to warm slowly to 22 °C over 14 h before it was concentrated under reduced pressure. The crude

[104] (a) Kusano, M.; Sotoma, G.; Koshino, H.; Uzawa, J.; Chijimatsu, M.; Fujioka, S.; Kawano, T.; Kimura, Y. *J. Chem. Soc., Perkin Trans. 1* **1998**, 2823. (b) Matsumura, K.; Kitahara, T. *Heterocycles* **2001**, *54*, 727.

product was purified by flash column chromatography on silica gel (cyclohexane/EtOAc 2:1 to 1:2 gradient) to afford synthetic (−)-brevicompanine B (47.8 mg, 0.130 mmol, 83%) as a white solid. The product was isolated as single diastereomer.

TLC: R_f = 0.26 (cyclohexane/EtOAc 1:1; UV, CAM); **Melting point**: 96 – 98 °C; **Specific Rotation**: $[\alpha]_D^{23}$ –363.2 (c = 1.00, $CHCl_3$); **^{1}H-NMR** (400 MHz, $CDCl_3$, 298 K): δ 7.16 (d, *J* = 7.5 Hz, 1H), 7.10 (td, *J* = 7.7, 1.1 Hz, 1H), 6.96 (br, 1H), 6.76 (td, *J* = 7.5, 0.8 Hz, 1H), 6.59 (d, *J* = 7.6 Hz, 1H), 5.97 (dd, *J* = 17.3, 10.8 Hz, 1H), 5.56 (s, 1H), 5.13 – 5.05 (m, 2H), 4.93 (s, 1H), 3.92 – 3.87 (m, 2H), 2.55 (dd, *J* = 12.6, 6.2 Hz, 1H), 2.45 – 2.39 (m, 1H), 1.74 – 1.63 (m, 1H), 1.59 – 1.46 (m, 2H), 1.11 (s, 3H), 1.00 (s, 3H), 0.91 – 0.89 (m, 6H); **^{13}C-NMR** (101 MHz, $CDCl_3$, 298 K): δ 169.6, 166.8, 150.1, 143.6, 129.04, 128.97, 125.2, 118.9, 114.7, 109.2, 77.8, 61.3, 57.9, 56.1, 43.0, 41.1, 36.8, 24.4, 23.2, 23.0, 22.6, 21.4; **IR** (neat): 3243 (br), 2959 (m), 2871 (w), 1659 (s), 1606 (m), 1483 (w), 1466 (m), 1431 (m), 1385 (w), 1366 (w), 1315 (m), 1295 (w), 1249 (w), 1213 (m), 1180 (w), 1139 (m), 1079 (m), 1069 (w), 1007 (w), 917 (m), 877 (w), 743 (s), 670 (w), 556 (w), 488 (w), 445 (w) cm^{-1}; **HRMS** (ESI) *m/z*: exact mass calculated for $C_{22}H_{30}N_3O_2$ $[M + H]^+$ 368.2333, found 368.2333.

8.2 Part II. Rh-Catalyzed Stereoselective Synthesis of Allenes

8.2.1 Selected Optimization Studies

Table 1. Selected Ligand Screening.

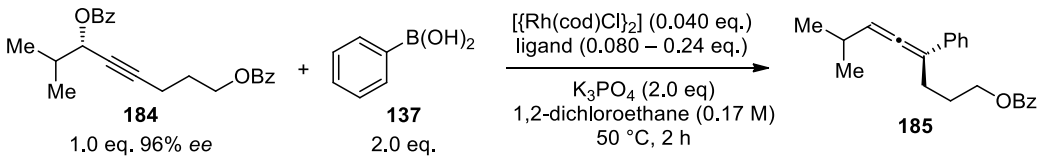

Entry	Ligand	Ligand/Rh	Conversion	*ee* (**185**)	*es*
1	**72**	2/1	>95%	94%	98%
2	**87**	2/1	46%	94%	98%
3	**186**	2/1	<5%	n. d.	n. d.
4	**187**	1/1	>95%	85%	89%
5	**188**	1/1	>95%	87%	91%
6	**189**	1/1	>95%	90%	94%
7	$P(OMe)_3$	3/1	61%	80%	83%

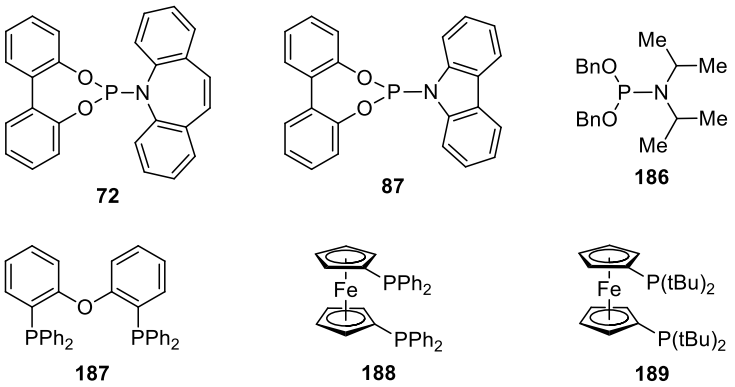

Typical procedure for the ligand screening: To a suspension of benzoate **184** (18 mg, 0.050 mmol, 1.0 equiv.), phenylboronic acid (12 mg, 0.10 mmol, 2.0 equiv.), K_3PO_4 (21 mg, 0.10 mmol, 2.0 equiv.) in 1,2-dichloroethane (0.20 mL) was added a solution of [{Rh(cod)Cl}$_2$] (1.0 mg, 2.0 µmol, 0.040 equiv.), the appropriate ligand (0.080 equiv., 0.16 equiv., or 0.24 equiv.) in 1,2-dichloroethane (0.10 mL). The resulting suspension was stirred in a screw-capped vial at 50 °C for 2 h before it was diluted with Et_2O and filtered through a plug of silica gel with copious washings (Et_2O). The solution was concentrated and the conversion was determined by ^{1}H NMR of the unpurified reaction mixture. After purification by flash column chromatography on silica gel the enantiomeric excess was determined by supercritical fluid chromatography (SFC) on a chiral stationary phase.

Reaction with Other Phenyl Boron Nucleophiles.[a]

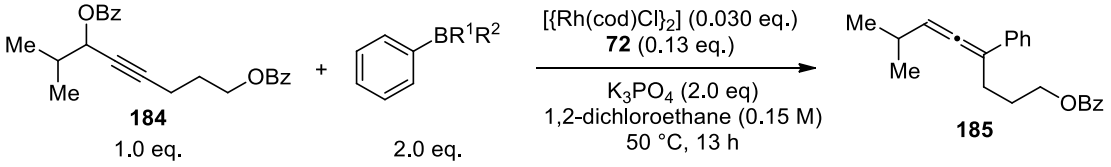

Entry	PhBR^{1}R^2	Conversion
1	$PhB(OH)_2$	>95%
2	$PhBF_3K$	<5%
3	PhBpin	24%
4	PhBneop	35%
5	$(PhBO)_3$	81%

[a]PhBpin = phenyl pinacol boronic ester, PhBneop = phenyl boronic acid neopentylglycol ester, $(PhBO)_3$ = phenylboroxine.

Procedure for the reaction with various phenyl boron nucleophiles: To a suspension of benzoate **184** (9.1 mg, 0.025 mmol, 1.0 equiv.), the corresponding phenyl boron reagent

(0.050 mmol, 2.0 equiv.), K_3PO_4 (11 mg, 0.050 mmol, 2.0 equiv.) in 1,2-dichloroethane (0.12 mL) was added 50 µL of a stock solution of [{Rh(cod)Cl}$_2$] (2.2 mg, 4.5 µmol – 0.75 µmol, 0.030 equiv. per reaction), **72** (7.6 mg, 0.019 mmol – 3.1 µmol, 0.13 equiv. per reaction) in 1,2-dichloroethane (0.30 mL). The resulting suspension was sparged with N_2 and stirred in a screw-capped vial at 50 °C for 13 h. It was then diluted with Et_2O and filtered through a plug of silica gel with copious washings (Et_2O). The solution was concentrated and the conversion was determined by ^{1}H NMR of the unpurified reaction mixture.

8.2.2 Synthesis and Characterization of Starting Materials and Ligand **72**

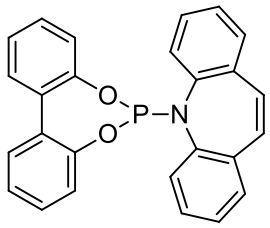

5-(Dibenzo[*d*,*f*][1,3,2]dioxaphosphepin-6-yl)-5H-dibenzo[*b*,*f*]azepine (72). Following a modified literature procedure,[105] a 50 mL Schlenk flask was charged with 2,2'-biphenol (1.86 g, 10.0 mmol, 1.00 equiv.). PCl_3 (8.60 mL, 98.6 mmol, 9.86 equiv.) and DMF (50 µL, 0.65 mmol, 0.065 equiv.) were added at 23 °C and the resulting brown suspension was was heated to 50 °C for 1 h. The now brown solution was left stirring at 50 °C while excess PCl_3 was removed through short path distillation into a flask cooled to –78 °C (PCl_3 was later quenched with sat. aq. $NaHCO_3$). To the remaining oil was added toluene (2 × 2.0 mL) which was removed under reduced pressure. The Schlenk flask was evacuated for 10 min and 30 min after the first and second cycle respectively. The flask was allowed to cool to 23 °C and the oil was dissolved in THF (20 mL). In a separate 200 mL, single-necked, round-bottomed flask a solution of 5*H*-dibenzo[*b*,*f*]azepine (2.03 g, 10.5 mmol, 1.05 equiv.) in THF (20 mL) was treated with *n*-BuLi in hexanes (1.60 M, 6.25 mL, 10.0 mmol, 1.00 equiv.) at –78 °C. The resulting dark violet mixture was stirred at –78 °C for 2 h before the solution of the phosphorchloridite in THF was added via cannula. The Schlenk flask was rinsed with THF (10 mL). The dark green mixture was allowed to warm to 14 °C over 18 h. The now orange solution was concentrated to give an orange gum. The crude product was suspended in 30 mL cyclohexane/toluene 2:1 containing 0.5% Et_3N. Celite (18 g) was added and the volatiles were removed under reduced

[105] Defieber, C.; Ariger, M. A.; Moriel, P.; Carreira, E. M. *Angew. Chem., Int. Ed.* **2007**, *46*, 3139.

pressure. The solid was loaded onto a column and the product was obtained after flash column chromatography on silica gel (cyclohexane/toluene 2:1 with 0.5% Et_3N) as a white solid (3.15 g, 7.73 mmol, 77%). The title compound was stored under an inert atmosphere in a freezer (–20 °C).

TLC: $R_f = 0.51$ (cyclohexane/toluene 2:1 with 0.5% Et_3N; UV, CAM); **Melting point**: 164 – 165 °C; **^{1}H-NMR** (400 MHz, $CDCl_3$, 298 K): δ 7.39 – 7.36 (m, 2H), 7.29 – 7.09 (m, 12H), 7.03 – 7.02 (m, 2H), 6.97 (s, 2H); **^{13}C-NMR** (101 MHz, $CDCl_3$, 298 K): δ 151.0, 150.9, 142.8, 142.7, 136.14, 136.12, 131.5 (two coincident resonances), 130.62, 130.59, 129.64, 129.63, 129.2 (two coincident resonances), 129.05, 128.99, 128.96 (four coincident resonances), 126.7 (two coincident resonances), 124.44, 124.43, 122.12, 122.11; **^{31}P{^{1}H}-NMR** (162 MHz, $CDCl_3$, 298 K): δ 137.8; **IR** (neat): 3024 (w), 1599 (w), 1567 (w), 1497 (w), 1486 (m), 1475 (w), 1459 (w), 1435 (m), 1281 (w), 1243 (m), 1196 (s), 1185 (m), 1165 (w), 1153 (w), 1117 (w), 1105 (w), 1095 (m), 1040 (w), 1008 (w), 984 (m), 946 (w), 920 (w), 891 (s), 885 (s), 861 (m), 848 (m), 836 (m), 800 (m), 774 (s), 769 (s), 760 (s), 747 (s), 731 (m), 711 (m), 699 (m), 678 (m), 623 (w), 596 (m), 553 (m), 542 (m), 519 (m), 511 (m), 485 (s), 474 (m), 462 (m) cm^{-1}; **HRMS** (ESI) *m/z*: exact mass calculated for $C_{26}H_{19}NO_2P$ $[M + H]^+$ 408.1148, found 408.1148.

General Procedure A: Enantioselective Addition of Terminal Alkynes to Aldehydes. Following a slightly modified reported procedure,[106] a 100 mL, single-necked, round-bottomed flask containing a magnetic stir bar, was charged in a glovebox with $Zn(OTf)_2$ (2.40 g, 6.60 mmol, 1.10 equiv.). The flask was removed from the glovebox and heated to 140 °C for 2 h under vacuum (the initial pressure of 0.6 mbar decreased to 0.1 mbar within the first 20 min). The flask was allowed to cool to 24 °C before (−)-*N*-methylephedrine (1.29 g, 7.20 mmol, 1.20 equiv.) was added in a glovebox. The flask was sealed with a septum and removed from the glovebox. Toluene (18.0 mL, 0.333 M) and Et_3N (1.00 mL, 7.20 mmol, 1.20 equiv.) were added under N_2 at 24 °C. The white suspension was stirred at 24 °C for 2 h, then the corresponding alkyne (6.00 mmol, 1.00 equiv.) was added in one portion. After 15 min the appropriate aldehyde (7.20 mmol, 1.20 equiv.) was added, again in one portion. The resulting suspension was stirred at 24 °C for the time indicated for each substrate. The reaction was quenched at 24 °C by addition of sat. aq. NH_4Cl (60 mL). The mixture was diluted with

[106] Frantz, D. E.; Fassler, R.; Carreira, E. M. *J. Am. Chem. Soc.* **2000**, *122*, 1806.

Et_2O (180 mL), the layers were separated and the aqueous layer was extracted with Et_2O (50 mL). The combined organic layers were washed with sat. aq. NaCl (120 mL), dried over $MgSO_4$, and filtered. The solution was concentrated, and the residue was purified by flash column chromatography on silica gel.

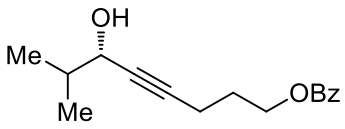

(+)-(*S*)-6-Hydroxy-7-methyloct-4-yn-1-yl benzoate (243). General procedure A was followed on a 10.0 mmol scale. The reaction was stirred at 24 °C for 15 h. The crude product was purified by flash column chromatography on silica gel (cyclohexane/EtOAc 8:1 to 2:1 gradient). The title compound was isolated as a clear, colorless oil (2.29 g, 8.79 mmol, 88%).

TLC: $R_f = 0.32$ (cyclohexane/EtOAc 3:1; UV, CAM); **Specific Rotation**: $[\alpha]_D^{22}$ +1.0 (c = 2.00, $CHCl_3$); **^{1}H-NMR** (400 MHz, $CDCl_3$, 298 K): δ 8.06 – 8.03 (m, 2H), 7.56 (tt, *J* = 6.9, 1.3 Hz, 1H), 7.46 – 7.42 (m, 2H), 4.42 (t, *J* = 6.3 Hz, 2H), 4.16 – 4.12 (m, 1H), 2.42 (td, *J* = 7.0, 2.0 Hz, 2H), 1.99 (app p, *J* = 6.7 Hz, 2H), 1.87 – 1.79 (m, 2H), 0.98 (app t, *J* = 7.0 Hz, 6H); **^{13}C-NMR** (101 MHz, $CDCl_3$, 298 K): δ 166.7, 133.1, 130.4, 129.7, 128.5, 84.6, 81.0, 68.2, 63.7, 34.8, 28.1, 18.2, 17.6, 15.8; **IR** (neat): 3424 (br), 3064 (w), 2960 (w), 2873 (w), 1717 (s), 1602 (w), 1584 (w), 1468 (w), 1452 (w), 1386 (w), 1366 (w), 1353 (w), 1315 (w), 1271 (s), 1177 (w), 1147 (w), 1115 (m), 1070 (w), 1026 (m), 980 (w), 935 (w), 912 (w), 844 (w), 806 (w), 749 (w), 710 (s), 687 (w), 675 (w) cm^{-1}; **HRMS** (EI) *m/z*: exact mass calculated for $C_{13}H_{13}O_3$ $[M - C_3H_7]^+$ 217.0860, found 217.0856; **SFC** (Jasco 2080 Plus, Daicel Chiralpak AS-H, 98% CO_2, 2% MeOH at 100 bar, flow rate 2.0 mL·min^{-1}, 25 °C, detection 219 nm): 96% *ee*, t_R (minor enantiomer) 9.1 min, t_R (major enantiomer) 9.4 min.

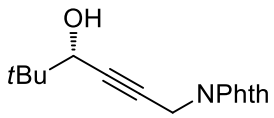

(–)-(*S*)-2-(4-Hydroxy-5,5-dimethylhex-2-yn-1-yl)isoindoline-1,3-dione (244). General procedure A was followed on a 6.00 mmol scale. The reaction was stirred at 24 °C for 12 h. The crude product was purified by flash column chromatography on silica gel

(cyclohexane/EtOAc 4:1 to 2:1 gradient). The title compound was isolated as a white solid (1.37 g, 5.05 mmol, 84%).

TLC: R_f = 0.36 (cyclohexane/EtOAc 2:1; UV, CAM); **Melting point**: 94 – 95 °C; **Specific Rotation**: $[\alpha]_D^{22}$ –0.7 (c = 1.00, $CHCl_3$); **^{1}H-NMR** (400 MHz, $CDCl_3$, 298 K): δ 7.89 – 7.84 (m, 2H), 7.75 – 7.70 (m, 2H), 4.48 (d, *J* = 1.8 Hz, 2H), 3.98 (dt, *J* = 6.1, 1.8 Hz, 1H), 1.91 (d, *J* = 6.1 Hz, 1H), 0.95 (s, 9H); **^{13}C-NMR** (101 MHz, $CDCl_3$, 298 K): δ 167.2, 134.3, 132.1, 123.7, 83.1, 79.2, 71.4, 36.0, 27.4, 25.4; **IR** (neat): 3446 (m), 2961 (w), 2869 (w), 1770 (m), 1708 (s), 1611 (w), 1478 (w), 1465 (w), 1429 (m), 1401 (m), 1352 (m), 1328 (m), 1319 (m), 1242 (w), 1181 (w), 1134 (m), 1122 (m), 1088 (w), 1050 (m), 1011 (m), 946 (m), 900 (w), 850 (w), 798 (w), 761 (w), 710 (s), 724 (s), 639 (m), 601 (w), 544 (w), 529 (m), 463 (w) cm^{-1}; **HRMS** (EI) *m/z*: exact mass calculated for $C_{12}H_9NO_3$ $[M - C_4H_8]^+$ 215.0577, found 215.0579; **SFC** (Jasco 2080 Plus, Daicel Chiralcel OJ-H, 98% CO_2, 2% MeOH at 100 bar, flow rate 2.0 mL·min^{-1}, 25 °C, detection 218 nm): 96% *ee*, t_R (minor enantiomer) 13.7 min, t_R (major enantiomer) 15.0 min.

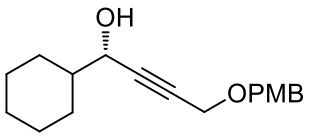

(+)-(*S*)-1-Cyclohexyl-4-((4-methoxybenzyl)oxy)but-2-yn-1-ol (245). General procedure A was followed on a 4.00 mmol scale. The reaction was stirred at 24 °C for 12 h. The crude product was purified by flash column chromatography on silica gel (cyclohexane/EtOAc 12:1 to 3:1 gradient). The title compound was isolated as a clear, pale light yellow oil (1.07 g, 3.70 mmol, 92%).

TLC: R_f = 0.30 (cyclohexane/EtOAc 3:1; UV, CAM); **Specific Rotation**: $[\alpha]_D^{27}$ +2.5 (c = 1.00, $CHCl_3$); **^{1}H-NMR** (400 MHz, $CDCl_3$, 298 K): δ 7.30 – 7.27 (m, 2H), 6.90 – 6.86 (m, 2H), 4.53 (s, 2H), 4.23 – 4.18 (m, 3H), 3.80 (s, 3H), 1.88 – 1.85 (m, 3H), 1.80 – 1.76 (m, 2H), 1.71 – 1.64 (m, 1H), 1.61 – 1.55 (m, 1H), 1.32 – 1.03 (m, 5H); **^{13}C-NMR** (101 MHz, $CDCl_3$, 298 K): δ 159.5, 129.9, 129.6, 114.0, 86.7, 81.8, 71.3, 67.4, 57.2, 55.4, 44.2, 28.7, 28.3, 26.5, 26.01, 25.99; **IR** (neat): 3410 (br), 3000 (w), 2924 (m), 2851 (m), 1612 (m), 1586 (w), 1513 (s), 1450 (m), 1385 (w), 1350 (w), 1302 (m), 1247 (s), 1174 (m), 1112 (w), 1070 (s), 1033 (s), 1011 (s), 941 (w), 920 (w), 893 (w), 846 (w), 819 (s), 758 (w), 710 (w), 674 (w), 577 (m), 516 (m) cm^{-1}; **HRMS** (EI) *m/z*: exact mass calculated for $C_{18}H_{24}O_3$ $[M]^+$ 288.1720,

found 288.1723; **SFC** (Jasco 2080 Plus, Daicel Chiralcel OJ-H, 90% CO_2, 10% MeOH at 100 bar, flow rate 2.0 mL·min^{-1}, 25 °C, detection 226 nm): 98% *ee*, t_R (major enantiomer) 12.9 min, t_R (minor enantiomer) 14.4 min.

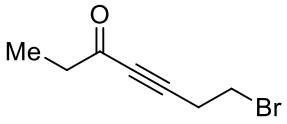

7-Bromohept-4-yn-3-one (246). Following a modified literature procedure,[107] to a solution of 4-bromo-1-butyne (0.930 mL, 9.91 mmol, 1.00 equiv.) in THF (33.0 mL) at –78 °C was added *n*-BuLi in hexanes (1.60 M, 6.20 mL, 9.92 mmol, 1.00 equiv.) over 4 min. The resulting solution was stirred at –78 °C for 15 min before a solution of *N*-methoxy-*N*-methylpropionamide[108] (1.16 g, 9.90 mmol, 1.00 equiv.) in THF (10 mL) was added via cannula at –78 °C over 7 min. The cooling bath was removed and the clear, yellow solution was allowed to warm to 0 °C over 1 h. The brown suspension was quenched at 0 °C by the addition of sat. aq. NH_4Cl (80 mL). Deionized water (2 mL) was added and the clear solution was transferred into a separation funnel. EtOAc (60 mL) was used to assist the transfer. The solutions were separated and the aqueous solution was extracted with EtOAc (60 mL). The EtOAc solutions were washed with sat. aq. NaCl (75 mL), dried over $MgSO_4$, filtered, and concentrated under reduced pressure. Purification by flash column chromatography on silica gel (cyclohexane/EtOAc 12:1 to 8:1 gradient) afforded the title compound as a clear, colorless oil (1.06 g, 5.62 mmol, 57%).

TLC: $R_f = 0.24$ (cyclohexane/EtOAc 8:1; UV, $KMnO_4$); **^{1}H-NMR** (400 MHz, $CDCl_3$, 298 K): δ 3.46 (t, *J* = 7.0 Hz, 2H), 2.94 (t, *J* = 7.0 Hz, 2H), 2.57 (q, *J* = 7.4 Hz, 2H), 1.14 (t, *J* = 7.4 Hz, 3H); **^{13}C-NMR** (101 MHz, $CDCl_3$, 298 K): δ 188.5, 89.5, 81.8, 38.9, 27.9, 23.4, 8.1; **IR** (film, $CDCl_3$): 2979 (w), 2939 (w), 2905 (w), 1672 (s), 1459 (w), 1437 (w), 1409 (w), 1379 (w), 1349 (w), 1330 (w), 1270 (m), 1216 (m), 1174 (s), 1141 (w), 1073 (w), 1023 (m), 991 (w), 934 (m), 897 (w), 842 (w), 797 (w), 743 (w), 724 (w), 695 (w), 670 (w), 632 (w), 561 (m), 518 (w) cm^{-1}; **HRMS** (EI) *m/z*: exact mass calculated for C_7H_9BrO $[M]^+$ 187.9832, found 187.9829.

[107] Higo, T.; Ukegawa, T.; Yokoshima, S.; Fukuyama, T. *Angew. Chem.* **2015**, *127*, 7475.
[108] Kerr, W. J.; Morrison, A. J.; Pazicky, M.; Weber, T. *Org. Lett.* **2012**, *14*, 2250.

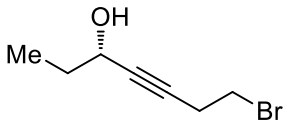

(–)-(*S*)-7-Bromohept-4-yn-3-ol (247). Following a modified literature procedure,[109] to a stirred solution of (s)-2-Methyl-CBS-oxazaborolidine (750 mg, 2.71 mmol, 1.01 equiv.) in THF (26.0 mL) was added 7-bromohept-4-yn-3-one (508 mg, 2.69 mmol, 1.00 equiv.) at 24 °C. The solution was cooled to –40 °C and BH_3•SMe_2 (1.50 mL, 15.8 mmol, 5.88 equiv.) was added dropwise over 10 min. The resulting clear, pale light yellow solution was stirred at –40 °C for 2 h before MeOH (5.0 mL) was added. The solution was allowed to warm to –30 °C over 1 h and was then partitioned between sat. aq. NH_4Cl (60 mL) and Et_2O (120 mL). The phases were separated, the aqueous phase was extracted with Et_2O (60 mL), and the combined organic solutions were washed with sat. aq. NaCl (60 mL), dried over $MgSO_4$, and concentrated under reduced pressure. Purification by flash column chromatography on silica gel (cyclohexane/EtOAc 8:1 to 4:1 gradient) afforded the title compound as a clear, colorless oil (438 mg, 2.29 mmol, 85%).

TLC: $R_f = 0.30$ (cyclohexane/EtOAc 3:1; UV, $KMnO_4$); **Specific Rotation**: $[\alpha]_D^{23}$ –6.1 (c = 1.00, $CHCl_3$); **^{1}H-NMR** (400 MHz, $CDCl_3$, 298 K): δ 4.34 – 4.28 (m, 1H), 3.43 (t, *J* = 7.2 Hz, 2H), 2.78 (td, *J* = 7.2, 1.9 Hz, 2H), 1.83 (d, *J* = 5.5 Hz, 1H), 1.76 – 1.65 (m, 2H), 1.00 (t, *J* = 7.4 Hz, 3H); **^{13}C-NMR** (101 MHz, $CDCl_3$, 298 K): δ 83.3, 82.2, 64.0, 31.1, 29.7, 23.3, 9.5; **IR** (neat): 3339 (br), 2967 (m), 2934 (m), 2877 (w), 1456 (w), 1434 (w), 1418 (w), 1378 (w), 1333 (w), 1271 (s), 1239 (w), 1212 (s), 1154 (w), 1096 (w), 1073 (w), 1040 (m), 1006 (s), 962 (s), 924 (w), 889 (w), 859 (w), 832 (w), 814 (w), 749 (w), 702 (w), 659 (m), 557 (m) cm^{-1}; **HRMS** (EI) *m/z*: exact mass calculated for C_5H_6BrO $[M - C_2H_5]^+$ 160.9597, found 160.9596.

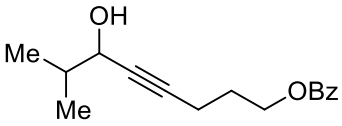

Typical procedure for the synthesis of racemic, secondary propargylic alcohols using LDA. A solution of LDA in THF was prepared by the dropwise addition of *n*-BuLi in hexanes (1.60 M, 3.28 mL, 5.28 mmol, 1.05 equiv.) to a solution of *i*-Pr_2NH (0.775 mL, 1.10 equiv.,

[109] Nakayama, A.; Kogure, N.; Kitajima, M.; Takayama, H. *Org. Lett.* **2009**, *11*, 5554.

5.53 mmol) in THF (6.45 mL) at –78 °C. The fresh LDA solution was allowed to stir at 25 °C for 20 min and then added via cannula to a solution of pent-4-yn-1-yl benzoate[110] (946 mg, 5.03 mmol, 1.00 equiv.) in THF (12.5 mL) at –78 °C. The resulting reaction mixture was stirred at –78 °C for 15 min before isobutyraldehyde (0.640 mL, 7.05 mmol, 1.40 equiv.) was added via syringe. The reaction was stirred at –78 °C for 30 min and then quenched at –78 °C by the addition of sat. aq. NH_4Cl (25 mL). The cooling bath was removed and the mixture was allowed to warm to 25 °C. Deionized water (2 mL) was added and the clear solution was transferred into a separation funnel. EtOAc (100 mL) was used to assist the transfer. The solutions were separated and the organic solution was washed with sat. aq. NaCl (100 mL), dried over $MgSO_4$, filtered, and concentrated under reduced pressure. Purification by flash column chromatography on silica gel (cyclohexane/EtOAc 8:1 to 3:1 gradient) afforded (±)-6-hydroxy-7-methyloct-4-yn-1-yl benzoate (1.05 g, 4.03 mmol, 80%) as a clear, colorless oil. Characterization data were in accordance with (+)-(*S*)-6-hydroxy-7-methyloct-4-yn-1-yl benzoate (**243**).

General Procedure B: Benzoylation of Propargylic Alcohols. To a solution of propargylic alcohol (4.0 mmol, 1.0 equiv.) in CH_2Cl_2 (22 mL, 0.18 M) at 24 °C was added pyridine (0.65 mL, 8.0 mmol, 2.0 equiv.), DMAP (24 mg, 0.20 mmol, 0.050 equiv.) and benzoyl chloride (0.70 mL, 6.0 mmol, 1.5 equiv.). The solution was stirred at 24 °C for the time indicated for each compound before Et_2O (30 mL) and sat. aq. $NaHCO_3$ (30 mL) were added. The resulting biphasic mixture was stirred at 24 °C then transferred to a separation funnel. The transfer was assisted with Et_2O (100 mL). The phases were separated, the organic solution was washed with 1.0 M aq. HCl (20 mL) and sat. aq. NaCl (60 mL), then dried over $MgSO_4$ and filtered. The solvent was evaporated, and the residue was purified by flash column chromatography on silica gel.

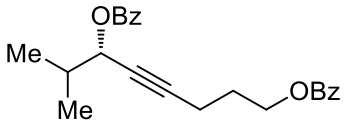

(–)-(*S*)-7-Methyloct-4-yne-1,6-diyl dibenzoate (184). General procedure B was followed on a 8.60 mmol scale. The reaction was stirred at 24 °C for 20 h. The crude product was

[110] Stevens, B. D.; Nelson, S. G. *J. Org. Chem.* **2005**, *70*, 4375.

purified by flash column chromatography on silica gel (cyclohexane/EtOAc 20:1 to 8:1 gradient). The title compound was isolated as a clear, colorless oil (2.90 g, 7.96 mmol, 92%).

TLC: R_f = 0.34 (cyclohexane/EtOAc 8:1; UV, CAM); **Specific Rotation**: $[\alpha]_D^{22}$ –27.6 (c = 1.00, $CHCl_3$); **^{1}H-NMR** (400 MHz, $CDCl_3$, 298 K): δ 8.09 – 8.02 (m, 4H), 7.58 – 7.53 (m, 2H), 7.46 – 7.41 (m, 4H), 5.45 (dt, *J* = 5.5, 2.0 Hz, 1H), 4.41 (t, *J* = 6.3 Hz, 2H), 2.43 (td, *J* = 7.1, 2.0 Hz, 2H), 2.17 – 2.08 (m, 1H), 2.00 (app p, *J* = 6.7 Hz, 2H), 1.08 (app dd, *J* = 10.8, 6.8 Hz, 6H).; **^{13}C-NMR** (101 MHz, $CDCl_3$, 298 K): δ 166.6, 165.8, 133.1, 133.1, 130.4 (two coincident resonances), 129.9, 129.7, 128.5 (two coincident resonances), 85.4, 77.3, 70.0, 63.7, 32.9, 28.0, 18.4, 17.9, 15.9; **IR** (neat): 3063 (w), 2965 (w), 2932 (w), 1717 (s), 1602 (w), 1584 (w), 1491 (w), 1451 (m), 1387 (w), 1361 (w), 1335 (w), 1314 (w), 1264 (s), 1176 (m), 1158 (w), 1107 (s), 1096 (s), 1069 (s), 1026 (m), 973 (m), 936 (w), 915 (w), 805 (w), 750 (w), 708 (s), 687 (m), 674 (w), 595 (w) cm^{-1}; **HRMS** (ESI) *m/z*: exact mass calculated for $C_{23}H_{28}NO_4$ $[M + NH_4]^+$ 382.2013, found 382.2011; **SFC** (Jasco 2080 Plus, Daicel Chiralcel OJ-H, 98% CO_2, 2% MeOH at 100 bar, flow rate 2.0 mL·min^{-1}, 25 °C, detection 225 nm): 96% *ee*, t_R (major enantiomer) 14.9 min, t_R (minor enantiomer) 16.9 min.

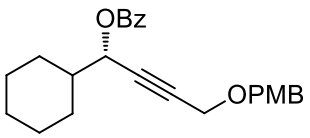

(–)-(*S*)-1-Cyclohexyl-4-((4-methoxybenzyl)oxy)but-2-yn-1-yl benzoate (204). General procedure B was followed on a 3.57 mmol scale. The reaction was stirred at 24 °C for 18 h. The crude product was purified by flash column chromatography on silica gel (pentane/Et_2O 8:1 to 5:1 gradient). The title compound was isolated as a clear, colorless oil (1.22 g, 3.10 mmol, 87%). The enantiomeric excess was determined for the starting material ((+)-(*S*)-1-cyclohexyl-4-((4-methoxybenzyl)oxy)but-2-yn-1-ol (**SI-3**), 98% *ee*).

TLC: R_f = 0.33 (pentane/Et_2O 5:1; UV, CAM); **Specific Rotation**: $[\alpha]_D^{22}$ –32.6 (c = 1.00, $CHCl_3$); **^{1}H-NMR** (400 MHz, $CDCl_3$, 298 K): δ 8.12 – 8.10 (m, 2H), 7.62 – 7.58 (m, 1H), 7.50 – 7.46 (m, 2H), 7.31 – 7.27 (m, 2H), 6.90 – 6.86 (m, 2H), 5.56 (dt, *J* = 5.9, 1.6 Hz, 1H), 4.56 (s, 2H), 4.21 (d, *J* = 1.7 Hz, 2H), 3.82 (s, 3H), 2.01 – 1.81 (m, 5H), 1.75 – 1.72 (m, 1H), 1.38 – 1.17 (m, 5H); **^{13}C-NMR** (101 MHz, $CDCl_3$, 298 K): δ 165.7, 159.5, 133.2, 130.2, 130.0, 129.9, 129.5, 128.5, 114.0, 83.3, 82.4, 71.2, 69.0, 57.1, 55.4, 42.2, 28.8, 28.5, 26.4, 25.94, 25.89; **IR** (neat): 2929 (m), 2853 (w), 1719 (s), 1612 (w), 1585 (w), 1513 (m), 1451 (m), 1347 (w),

1315 (w), 1248 (s), 1175 (m), 1155 (w), 1106 (m), 1096 (m), 1068 (s), 1035 (m), 1026 (m), 971 (m), 950 (w), 891 (w), 846 (w), 819 (m), 758 (w), 710 (s), 688 (w), 661 (w), 576 (w), 517 (w) cm^{-1}; **HRMS** (ESI) *m/z*: exact mass calculated for $C_{25}H_{32}NO_4$ $[M + NH_4]^+$ 410.2326, found 410.2335.

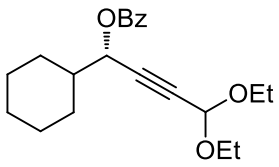

(–)-(*S*)-1-cyclohexyl-4,4-diethoxybut-2-yn-1-yl benzoate (206).[44a] The title compound was synthesized according to general procedure B from (*S*)-1-cyclohexyl-4,4-diethoxybut-2-yn-1-ol[44a] on a 4.0 mmol scale. The reaction was stirred for 11 h and the crude product was purified by flash column chromatography on silica gel (cyclohexane/EtOAc 20:1 to 12:1 gradient). The title compound was isolated as a colorless oil (1.28 g, 3.72 mmol, 93%).

TLC: $R_f = 0.30$ (cyclohexane/ EtOAc 12:1; UV, CAM); **Specific Rotation**: $[\alpha]_D^{23}$ –27.8 (c = 1.00, $CHCl_3$); **^{1}H-NMR** (400 MHz, $CDCl_3$, 298 K): δ 8.07 – 8.04 (m, 2H), 7.59 – 7.54 (m, 1H), 7.47 – 7.42 (m, 2H), 5.55 (dd, *J* = 5.9, 1.2 Hz, 1H), 5.31 (d, *J* = 1.3 Hz, 1H), 3.77 – 3.69 (m, 2H), 3.62 – 3.54 (m, 2H), 1.95 – 1.77 (m, 5H), 1.71 – 1.68 (m, 1H), 1.30 – 1.15 (m, 11H); **^{13}C-NMR** (101 MHz, $CDCl_3$, 298 K): δ 165.5, 133.2, 130.1, 129.9, 128.5, 91.4, 81.9, 81.6, 68.5, 61.1, 61.0, 42.1, 28.7, 28.5, 26.3, 25.9, 25.8, 15.2; **IR** (neat): 2976 (w), 2929 (m), 2855 (w), 1722 (s), 1602 (w), 1585 (w), 1451 (m), 1328 (m), 1315 (m), 1261 (s), 1176 (w), 1152 (m), 1138 (m), 1096 (s), 1067 (s), 1050 (s), 1025 (s), 973 (m), 892 (w), 710 (s), 688 (w), 585 (w), 527 (w) cm^{-1}; **HRMS** (ESI) *m/z*: exact mass calculated for $C_{21}H_{32}NO_4$ $[M + NH_4]^+$ 362.2326, found 362.2331; **SFC** (Daicel Chiralpak IA, 99% CO_2, 1% MeOH at 100 bar, flow rate 2.0 mL·min^{-1}, 25 °C, detection 226 nm): 97% *ee*, t_R (major enantiomer) 9.4 min, t_R (minor enantiomer) 11.3 min.

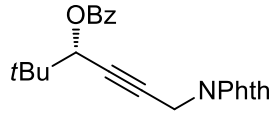

(–)-(*S*)-6-(1,3-Dioxoisoindolin-2-yl)-2,2-dimethylhex-4-yn-3-yl benzoate (207). General procedure B was followed on a 4.89 mmol scale. The reaction was stirred at 24 °C for 18 h.

The crude product was purified by recrystallization from EtOAc/*n*-hexanes. Therefore the crude product was dissolved in 7 mL of hot EtOAc and 60 mL *n*-hexanes were added. The solution was allowed to cool to 24 °C and then placed in a freezer (–20 °C) for 15 h. The title compound was isolated as a white solid (1.68 g, 4.46 mmol, 91%) in one crop.

TLC: $R_f = 0.36$ (cyclohexane/EtOAc 3:1; UV, CAM); **Melting point**: 123 – 125 °C (EtOAc/*n*-hexane); **Specific Rotation**: $[\alpha]_D^{22}$ –39.2 (c = 1.00, $CHCl_3$); **^{1}H-NMR** (400 MHz, $CDCl_3$, 298 K): δ 8.09 – 8.06 (m, 2H), 7.92 – 7.87 (m, 2H), 7.78 – 7.73 (m, 2H), 7.61 – 7.56 (m, 1H), 7.48 – 7.44 (m, 2H), 5.36 (t, *J* = 1.8 Hz, 1H), 4.52 (d, *J* = 1.8 Hz, 2H), 1.09 (s, 9H); **^{13}C-NMR** (101 MHz, $CDCl_3$, 298 K): δ 167.1, 165.6, 134.3, 133.2, 132.1, 130.1, 129.9, 128.5, 123.7, 79.7, 79.6, 72.2, 35.8, 27.5, 25.8; **IR** (neat): 2979 (w), 2963 (w), 1771 (m), 1713 (s), 1618 (w), 1599 (w), 1474 (m), 1449 (w), 1423 (m), 1394 (m), 1367 (w), 1339 (m), 1322 (m), 1299 (m), 1259 (s), 1248 (m), 1188 (w), 1175 (w), 1141 (m), 1121 (m), 1105 (s), 1095 (m), 1067 (m), 1024 (m), 972 (m), 944 (m), 923 (w), 793 (w), 727 (w), 706 (s), 685 (m), 633 (m), 570 (w), 530 (m), 471 (w) cm^{-1}; **HRMS** (ESI) *m/z*: exact mass calculated for $C_{23}H_{25}N_2O_4$ $[M + NH_4]^+$ 393.1809, found 393.1812; **SFC** (Waters Acquity UPC^2, Trefoil CEL2, 85% CO_2, 15% MeOH, flow rate 2.0 mL·min^{-1}, 40 °C, detection 254 nm): 97% *ee*, t_R (major enantiomer) 1.1 min, t_R (minor enantiomer) 1.5 min.

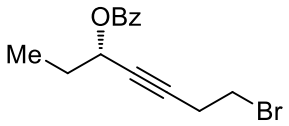

(–)-(*S*)-7-Bromohept-4-yn-3-yl benzoate (208). General procedure B was followed on a 2.10 mmol scale. The reaction was stirred at 24 °C for 11 h. The crude product was purified by flash column chromatography on silica gel (cyclohexane/EtOAc 20:1). The title compound was isolated as a clear, colorless oil (556 mg, 1.89 mmol, 90%).

TLC: $R_f = 0.25$ (cyclohexane/EtOAc 12:1; UV, CAM); **Specific Rotation**: $[\alpha]_D^{21}$ –26.2 (c = 1.00, $CHCl_3$); **^{1}H-NMR** (400 MHz, $CDCl_3$, 298 K): δ 8.08 – 8.06 (m, 2H), 7.59 – 7.55 (m, 1H), 7.47 – 7.43 (m, 2H), 5.55 (tt, *J* = 6.4, 1.9 Hz, 1H), 3.43 (t, *J* = 7.3 Hz, 2H), 2.79 (td, *J* = 7.3, 1.9 Hz, 2H), 1.95 – 1.88 (m, 2H), 1.09 (t, *J* = 7.4 Hz, 3H); **^{13}C-NMR** (101 MHz, $CDCl_3$, 298 K): δ 165.7, 133.2, 130.2, 129.9, 128.5, 82.9, 79.8, 66.0, 29.4, 28.4, 23.4, 9.6; **IR** (neat): 2972 (w), 2937 (w), 2879 (w), 1718 (s), 1601 (w), 1585 (w), 1491 (w), 1451 (m), 1382 (w), 1341 (w), 1314 (w), 1299 (m), 1264 (s), 1213 (m), 1176 (w), 1176 (w), 1167 (w), 1106 (m), 1069 (m), 1042 (w), 1025 (m), 999 (w), 959 (w), 927 (m), 896 (w), 804 (w), 709 (s),

687 (m), 674 (w), 591 (w), 568 (w) cm^{-1}; **HRMS** (ESI) *m/z*: exact mass calculated for $C_{14}H_{15}BrNaO_2$ $[M + Na]^+$ 317.0148, found 317.0153; **SFC** (Jasco 2080 Plus, Daicel Chiralcel OB-H, 99% CO_2, 1% MeOH at 100 bar, flow rate 2.0 mL·min^{-1}, 25 °C, detection 215 nm): 86% *ee*, t_R (minor enantiomer) 7.4 min, t_R (major enantiomer) 8.6 min.

8.2.3 Synthesis and Characterization of Products

General procedure C: Stereoselective synthesis of allenes from propargylic benzoates and arylboronic acids. To a non-dried two necked 25 mL round bottomed flask equipped with a stir bar was added the propargylic benzoate (0.500 mmol, 1.00 equiv.). The side neck was connected to a gas inlet adapter and the flask was purged with N_2 for 5 min, then the top neck sealed with a glass stopper. To the flask were subsequently added 1,2-dichloroethane (2.50 mL), the corresponding arylboronic acid (1.00 mmol, 2.00 equiv.), and K_3PO_4 (212 mg, 1.00 mmol, 2.00 equiv.) against a flow of N_2 (while replacing the glass stopper). Finally a clear, red solution of $[\{Rh(cod)Cl\}_2]$ (7.4 mg, 0.015 mmol, 3.0 mol%) and phosphoramidite **72** (25.5 mg, 0.0625 mmol, 12.5 mol%) in 1,2-dichloroethane (1.00 mL) – prepared in a screw-capped vial, sparged with N_2 for 1 min and stirred at 24 °C for 30 min prior to the addition – was added via Pasteur pipette against a flow of N_2. The flask was sealed and immersed in an oil bath. The orange heterogeneous mixture was stirred at 50 °C for 24 h. The mixture was allowed to cool to 24 °C and partitioned between Et_2O (100 mL) and sat. aq. $NaHCO_3$ (50 mL). The aqueous layer was extracted with Et_2O (50 mL). The combined organic layers were washed with sat. aq. NaCl (50 mL), dried over $MgSO_4$, and filtered. The solution was concentrated and the residue was purified by flash column chromatography on silica gel. All deviations from the general procedure, and the solvent system for chromatography are given below for each substrate.

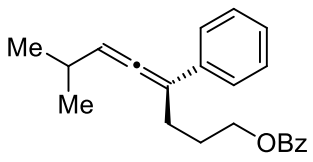

(+)-(*S*)-7-Methyl-4-phenylocta-4,5-dien-1-yl benzoate (185). General procedure C was followed. (–)-(*S*)-7-methyloct-4-yne-1,6-diyl dibenzoate (**184**) (182 mg, 0.500 mmol, 96% *ee*) and phenylboronic acid (122 mg, 1.00 mmol) were used. The crude product was purified by

flash column chromatography on silica gel (cyclohexane/EtOAc 50:1 to 20:1 gradient). The title compound was isolated as a light yellow, clear oil (132 mg, 0.412 mmol, 82%).

TLC: R_f = 0.25 (cyclohexane/EtOAc 20:1; UV, CAM); **Specific Rotation**: $[\alpha]_D^{22}$ +75.6 (c = 1.00, $CHCl_3$); **^{1}H-NMR** (400 MHz, $CDCl_3$, 298 K): δ 8.08 – 8.05 (m, 2H), 7.58 – 7.54 (m, 1H), 7.47 – 7.42 (m, 4H), 7.34 – 7.29 (m, 2H), 7.22 – 7.18 (m, 1H), 5.60 – 5.57 (m, 1H), 4.43 (app td, *J* = 6.4, 1.5 Hz, 2H), 2.63 – 2.58 (m, 2H), 2.50 – 2.39 (m, 1H), 2.08 – 2.00 (m, 2H), 1.09 (d, *J* = 6.8 Hz, 6H); **^{13}C-NMR** (101 MHz, $CDCl_3$, 298 K): δ 202.1, 166.8, 137.3, 133.0, 130.6, 129.7, 128.5, 128.5, 126.7, 125.8, 106.0, 102.8, 64.8, 28.9, 27.4, 26.6, 22.9; **IR** (neat): 3061 (w), 2958 (m), 2925 (w), 2868 (w), 1946 (w), 1717 (s), 1600 (w), 1493 (m), 1451 (m), 1381 (w), 1363 (w), 1314 (w), 1270 (s), 1176 (m), 1113 (s), 1070 (m), 1027 (m), 977 (w), 935 (w), 813 (w), 754 (m), 710 (s), 693 (s), 676 (w), 648 (w), 617 (w) cm^{-1}; **HRMS** (ESI) *m/z*: exact mass calculated for $C_{22}H_{24}NaO_2$ $[M + Na]^+$ 343.1669, found 343.1671; **SFC** (Jasco 2080 Plus, Daicel Chiralpak IB, 99% CO_2, 1% MeOH at 100 bar, flow rate 2.0 mL·min^{-1}, 25 °C, detection 253 nm): 94% *ee*, t_R (minor enantiomer) 15.0 min, t_R (major enantiomer) 15.8 min.

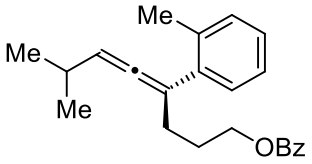

(+)-(*S*)-7-Methyl-4-(o-tolyl)octa-4,5-dien-1-yl benzoate (213). General procedure C was followed but the reaction was stirred at 40 °C for 12 h. (–)-(*S*)-7-methyloct-4-yne-1,6-diyl dibenzoate (**184**) (182 mg, 0.500 mmol, 96% *ee*) and 2-methylphenylboronic acid (136 mg, 1.00 mmol) were used. The crude product was purified by flash column chromatography on silica gel (cyclohexane/EtOAc 20:1). The title compound was isolated as a light yellow, clear oil (153 mg, 0.457 mmol, 91%).

TLC: R_f = 0.33 (cyclohexane/EtOAc 20:1; UV, CAM); **Specific Rotation**: $[\alpha]_D^{28}$ +40.7 (c = 1.00, $CHCl_3$); **^{1}H-NMR** (400 MHz, $CDCl_3$, 298 K): δ 8.06 – 8.03 (m, 2H), 7.58 – 7.54 (m, 1H), 7.46 – 7.42 (m, 2H), 7.23 – 7.15 (m, 4H), 5.28 – 5.25 (m, 1H), 4.43 – 4.37 (m, 2H), 2.49 – 2.44 (m, 2H), 2.40 – 2.32 (m, 4H), 2.00 – 1.93 (m, 2H), 1.04 (app dd, *J* = 6.8, 0.8 Hz, 6H); **^{13}C-NMR** (101 MHz, $CDCl_3$, 298 K): δ 200.8, 166.8, 138.5, 135.9, 133.0, 130.6 (two coincident resonances), 129.7, 128.5, 128.3, 126.9, 125.9, 105.0, 99.9, 64.7, 30.5, 28.6, 27.2, 22.9, 22.8, 20.5; **IR** (neat): 3063 (w), 2957 (m), 2925 (w), 2868 (w), 1958 (w), 1718 (s), 1602 (w), 1585 (w), 1489 (w), 1451 (m), 1380 (w), 1363 (w), 1314 (w), 1270 (s), 1176 (w),

1112 (m), 1070 (w), 1027 (w), 975 (w), 936 (w), 806 (w), 756 (w), 710 (s), 675 (w) cm^{-1}; **HRMS** (ESI) *m/z*: exact mass calculated for $C_{23}H_{26}NaO_2$ $[M + Na]^+$ 357.1825, found 357.1825; **SFC** (Jasco 2080 Plus, Daicel Chiralpak IB, 98% CO_2, 2% MeOH at 100 bar, flow rate 2.0 mL·min^{-1}, 25 °C, detection 209 nm): 93% *ee*, t_R (minor enantiomer) 9.0 min, t_R (major enantiomer) 10.3 min.

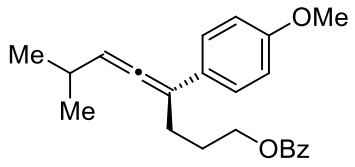

(+)-(*S*)-4-(4-Methoxyphenyl)-7-methylocta-4,5-dien-1-yl benzoate (214). General procedure C was followed but the reaction was stirred at 40 °C for 12 h. (–)-(*S*)-7-methyloct-4-yne-1,6-diyl dibenzoate (**184**) (182 mg, 0.500 mmol, 96% *ee*) and 4-methoxyphenylboronic acid (152 mg, 1.00 mmol) were used. The crude product was purified by flash column chromatography on silica gel (cyclohexane/EtOAc 20:1). The title compound was isolated as a light yellow, clear oil (150 mg, 0.427 mmol, 85%).

TLC: R_f = 0.30 (cyclohexane/EtOAc 12:1; UV, CAM); **Specific Rotation**: $[\alpha]_D^{28}$ +77.2 (c = 1.00, $CHCl_3$); **^{1}H-NMR** (400 MHz, $CDCl_3$, 298 K): δ 8.07 – 8.05 (m, 2H), 7.58 – 7.54 (m, 1H), 7.46 – 7.42 (m, 2H), 7.37 – 7.34 (m, 2H), 6.88 – 6.85 (m, 2H), 5.57 – 5.54 (m, 1H), 4.45 – 4.39 (m, 2H), 3.80 (s, 3H), 2.59 – 2.55 (m, 2H), 2.47 – 2.39 (m, 1H), 2.06 – 1.99 (m, 2H), 1.08 (d, *J* = 6.8 Hz, 6H); **^{13}C-NMR** (101 MHz, $CDCl_3$, 298 K): δ 201.5, 166.8, 158.6, 133.0, 130.6, 129.7, 129.6, 128.5, 126.9, 114.0, 105.5, 102.7, 64.8, 55.4, 28.9, 27.3, 26.8, 22.9; **IR** (neat): 2957 (m), 2867 (w), 2836 (w), 1717 (s), 1605 (m), 1589 (w), 1509 (s), 1451 (m), 1381 (w), 1363 (w), 1314 (w), 1271 (s), 1246 (s), 1176 (s), 1112 (s), 1070 (w), 1027 (m), 978 (w), 833 (m), 805 (w), 710 (s), 687 8w), 594 (w) cm^{-1}; **HRMS** (ESI) *m/z*: exact mass calculated for $C_{23}H_{26}NaO_3$ $[M + Na]^+$ 373.1774, found 373.1770; **SFC** (Jasco 2080 Plus, Daicel Chiralpak IB, 98% CO_2, 2% MeOH at 100 bar, flow rate 2.0 mL·min^{-1}, 25 °C, detection 253 nm): 94% *ee*, t_R (minor enantiomer) 15.7 min, t_R (major enantiomer) 17.1 min.

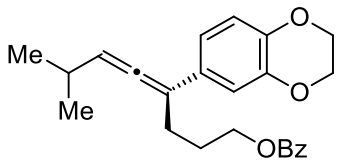

(+)-(*S*)-4-(2,3-Dihydrobenzo[*b*][1,4]dioxin-6-yl)-7-methylocta-4,5-dien-1-yl benzoate (215). General procedure C was followed. (–)-(*S*)-7-methyloct-4-yne-1,6-diyl dibenzoate (**184**) (182 mg, 0.500 mmol, 96% *ee*) and 2,3-dihydrobenzo[*b*][1,4]dioxin-6-ylboronic acid (180 mg, 1.00 mmol) were used. The crude product was purified by flash column chromatography on silica gel (cyclohexane/EtOAc 12:1). The title compound was isolated as a light yellow, clear oil (168 mg, 0.443 mmol, 89%).

TLC: R_f = 0.35 (cyclohexane/EtOAc 5:1; UV, CAM); **Specific Rotation**: $[\alpha]_D^{22}$ +39.4 (c = 1.00, $CHCl_3$); **^{1}H-NMR** (400 MHz, $CDCl_3$, 298 K): δ 8.07 – 8.05 (m, 2H), 7.58 – 7.53 (m, 1H), 7.46 – 7.42 (m, 2H), 6.95 – 6.91 (m, 2H), 6.81 (d, *J* = 8.3 Hz, 1H), 5.56 – 5.53 (m, 1H), 4.41 (app td, *J* = 6.4, 1.6 Hz, 2H), 4.25 (s, 4H), 2.56 – 2.51 (m, 2H), 2.46 – 2.36 (m, 1H), 2.01 – 1.98 (m, 2H), 1.07 (d, *J* = 6.8 Hz, 6H); **^{13}C-NMR** (101 MHz, $CDCl_3$, 298 K): δ 201.6, 166.8, 143.5, 142.5, 133.0, 130.8, 130.6, 129.7, 128.5, 119.1, 117.2, 114.6, 105.4, 102.8, 64.8, 64.6, 64.5, 28.9, 27.3, 26.7, 22.8, 22.8; **IR** (neat): 3062 (w), 2958 (w), 2871 (w), 1945 (w), 1715 (s), 1602 (w), 1583 (m), 1504 (s), 1451 (m), 1430 (w), 1382 (w), 1304 (m), 1272 (s), 1175 (m), 1114 (s), 1068 (s), 1027 (m), 1001 (w), 930 (w), 891 (m), 873 (w), 811 (m), 749 (w), 711 (s), 687 (w), 675 (w), 631 (w), 602 (w) cm^{-1}; **HRMS** (ESI) *m/z*: exact mass calculated for $C_{24}H_{27}O_4$ $[M + H]^+$ 379.1904, found 379.1907; **SFC** (Jasco 2080 Plus, Daicel Chiralpak IB, 95% CO_2, 5% MeOH at 100 bar, flow rate 2.0 mL·min^{-1}, 25 °C, detection 271 nm): 94% *ee*, t_R (major enantiomer) 21.7 min, t_R (minor enantiomer) 23.8 min.

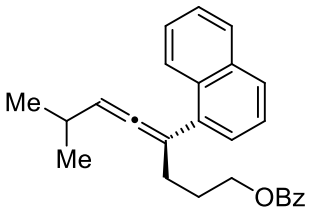

(+)-(*S*)-7-Methyl-4-(naphthalen-1-yl)octa-4,5-dien-1-yl benzoate (216). General procedure C was followed. (–)-(*S*)-7-methyloct-4-yne-1,6-diyl dibenzoate (**184**) (182 mg, 0.500 mmol, 96% *ee*) and 1-naphthaleneboronic acid (172 mg, 1.00 mmol) were used. The crude product was purified by flash column chromatography on silica gel (cyclohexane/EtOAc

50:1 to 20:1 gradient). The title compound was isolated as a yellow, clear oil (176 mg, 0.476 mmol, 95%).

TLC: R_f = 0.25 (cyclohexane/EtOAc 20:1; UV, CAM); **Specific Rotation**: $[\alpha]_D^{22}$ +54.7 (c = 1.00, $CHCl_3$); **^{1}H-NMR** (400 MHz, $CDCl_3$, 298 K): δ 8.19 – 8.15 (m, 1H), 8.05 – 8.02 (m, 2H), 7.88 – 7.84 (m, 1H), 7.77 (d, *J* = 7.8 Hz, 1H), 7.58 – 7.53 (m, 1H), 7.51 – 7.40 (m, 6H), 5.38 – 5.35 (m, 1H), 4.44 (app td, *J* = 6.5, 0.9 Hz, 2H), 2.65 – 2.61 (m, 2H), 2.47 – 2.35 (m, 1H), 2.06 – 1.99 (m, 2H), 1.07 (app dd, *J* = 6.8, 2.8 Hz, 6H); **^{13}C-NMR** (101 MHz, $CDCl_3$, 298 K): δ 201.5, 166.8, 137.1, 134.1, 133.0, 131.4, 130.5, 129.7, 128.5, 128.4, 127.5, 125.9, 125.8, 125.7, 125.7, 125.6, 104.3, 99.9, 64.6, 31.3, 28.6, 27.4, 22.9, 22.7; **IR** (neat): 3060 (w), 2957 (w), 2925 (w), 2867 (w), 1957 (w), 1717 (s), 1602 (w), 1583 (w), 1506 (w), 1492 (w), 1451 (w), 1392 (w), 1363 (w), 1314 (w), 1270 (s), 1175 (w), 1112 (m), 1070 (m), 1027 (m), 968 (w), 933 (w), 862 (w), 800 (m), 777 (s), 735 (w), 710 (s), 687 (w), 675 (w), 635 (w), 526 (w) cm^{-1}; **HRMS** (ESI) *m/z*: exact mass calculated for $C_{26}H_{26}NaO_2$ $[M + H]^+$ 393.1825, found 393.1828; **SFC** (Jasco 2080 Plus, Daicel Chiralpak IB, 90% CO_2, 10% MeOH at 100 bar, flow rate 2.0 mL·min^{-1}, 25 °C, detection 225 nm): 93% *ee*, t_R (major enantiomer) 11.1 min, t_R (minor enantiomer) 14.5 min.

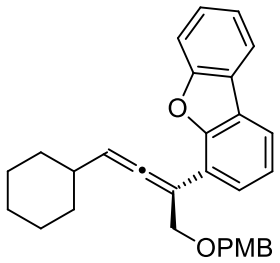

(+)-(*R*)-4-(4-cyclohexyl-1-((4-methoxybenzyl)oxy)buta-2,3-dien-2-yl)dibenzo[*b*,*d*]furan (217). General procedure C was followed. (–)-(*S*)-1-cyclohexyl-4-((4-methoxybenzyl)oxy)but-2-yn-1-yl benzoate (**204**) (196 mg, 0.500 mmol, 98% *ee*) and 4-dibenzofuranboronic acid (212 mg, 1.00 mmol) were used. The crude product was purified by flash column chromatography on silica gel (cyclohexane/EtOAc 20:1). The title compound was isolated as a light yellow, clear oil (112 mg, 0.255 mmol, 51%).

TLC: R_f = 0.16 (cyclohexane/EtOAc 20:1; UV, CAM); **Specific Rotation**: $[\alpha]_D^{22}$ +89.5 (c = 1.00, $CHCl_3$); **^{1}H-NMR** (400 MHz, $CDCl_3$, 298 K): δ 7.96 – 7.94 (m, 1H), 7.84 (dd, *J* = 7.6, 1.1 Hz, 1H), 7.58 – 7.52 (m, 3H), 7.47 – 7.43 (m, 1H), 7.36 – 7.30 (m, 2H), 7.24 – 7.20 (m, 2H), 6.85 – 6.81 (m, 2H), 5.59 – 5.57 (m, 1H), 4.72 – 4.63 (m, 2H), 4.56 (s, 2H), 3.78 (s,

3H), 2.31 – 2.23 (m, 1H), 1.97 – 1.93 (m, 2H), 1.81 – 1.67 (m, 3H), 1.42 – 1.19 (m, 5H); **^{13}C-NMR** (101 MHz, $CDCl_3$, 298 K): δ 206.1, 159.2, 156.1, 153.7, 130.6, 129.6, 127.1, 126.2, 124.7, 124.4, 123.0, 122.7, 121.0, 120.7, 119.2, 113.8, 111.8, 99.8, 98.9, 71.2, 70.9, 55.4, 38.1, 33.3, 33.1, 26.33, 26.25, 26.23; **IR** (neat): 3061 (w), 2998 (w), 2922 (m), 2849 (m), 1947 (w), 1612 (w), 1585 (w), 1512 (m), 1450 (m), 1424 (w), 1397 (w), 1348 (w), 1301 (w), 1246 (s), 1189 (s), 1173 (m), 1104 (w), 1071 (m), 1035 (m), 1011 (w), 951 (w), 891 (w), 844 (m), 811 (m), 795 (w), 748 (s), 702 (w), 627 (w), 604 (w), 572 (m), 517 (w) cm^{-1}; **HRMS** (ESI) *m/z*: exact mass calculated for $C_{30}H_{31}O_3$ $[M + H]^+$ 439.2268, found 439.2267; **SFC** (Waters Acquity UPC^2, Daicel Chiralcel OD3, 90% CO_2, 10% MeOH at 100 bar, flow rate 2.0 mL·min^{-1}, 40 °C, detection 258 nm): 91% *ee*, t_R (major enantiomer) 5.8 min, t_R (major enantiomer) 6.1 min.

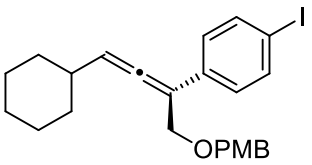

(+)-(*R*)-1-(4-Cyclohexyl-1-((4-methoxybenzyl)oxy)buta-2,3-dien-2-yl)-4-iodobenzene (218). General procedure C was followed but [{Rh(cod)OH}$_2$] (6.8 mg, 0.015 mmol, 3.0 mol%) was used instead of [{Rh(cod)Cl}$_2$] and deionized water (90.0 µL, 5.00 mmol, 10.0 equiv.) was added subsequent to the addition of K_3PO_4. (–)-(*S*)-1-cyclohexyl-4-((4-methoxybenzyl)oxy)but-2-yn-1-yl benzoate (**204**) (196 mg, 0.500 mmol, 98% *ee*) and 4-iodophenylboronic acid (248 mg, 1.00 mmol) were used. The crude product was purified by flash column chromatography on silica gel (cyclohexane/EtOAc 30:1 to 20:1 gradient). The title compound was isolated as a yellow, clear oil (134 mg, 0.282 mmol, 57%).

TLC: R_f = 0.22 (cyclohexane/EtOAc 20:1; UV, CAM); **Specific Rotation**: $[\alpha]_D^{22}$ +99.6 (c = 1.00, $CHCl_3$); **^{1}H-NMR** (400 MHz, $CDCl_3$, 298 K): δ 7.64 – 7.60 (m, 2H), 7.25 – 7.21 (m, 4H), 6.89 – 6.85 (m, 2H), 5.57 – 5.56 (m, 1H), 4.47 (s, 2H), 4.41 (d, *J* = 1.2 Hz, 2H), 3.81 (s, 3H), 2.19 – 2.10 (m, 1H), 1.85 – 1.81 (m, 2H), 1.75 – 1.71 (m, 2H), 1.66 – 1.62 (m, 1H), 1.36 – 1.11 (m, 5H); **^{13}C-NMR** (101 MHz, $CDCl_3$, 298 K): δ 204.4, 159.4, 137.5, 135.3, 130.3, 129.7, 128.3, 113.9, 102.9, 100.7, 92.0, 71.2, 69.7, 55.4, 37.9, 33.4, 33.3, 26.2, 26.14, 26.13; **IR** (neat): 2999 (w), 2922 (m), 2849 (m), 1945 (w), 1612 (m), 1585 (w), 1512 (s), 1484 (m), 1463 (w), 1447 (m), 1381 (w), 1348 (w), 1302 (w), 1246 (s), 1172 (m), 1076 (s), 1063 (s), 1036 (s), 1003 (s), 949 (w), 910 (w), 890 (w), 823 (s), 807 (s), 757 (m), 738 (m), 709 (w), 637 (w), 629 (w), 580 (m), 518 (m) cm^{-1}; **HRMS** (ESI) *m/z*: exact mass calculated for

$C_{24}H_{31}INO_2$ $[M + NH_4]^+$ 492.1394, found 492.1392; **SFC** (Jasco 2080 Plus, Daicel Chiralcel OJ-H, 80% CO_2, 20% MeOH at 100 bar, flow rate 2.0 mL·min^{-1}, 25 °C, detection 254 nm): 91% *ee*, t_R (major enantiomer) 23.4 min, t_R (minor enantiomer) 30.1 min.

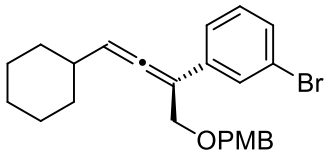

(+)-(*R*)-1-Bromo-3-(4-cyclohexyl-1-((4-methoxybenzyl)oxy)buta-2,3-dien-2-yl)benzene (248). General procedure C was followed but deionized water (90.0 µL, 5.00 mmol, 10.0 equiv.) was added subsequent to the addition of K_3PO_4. (–)-(*S*)-1-cyclohexyl-4-((4-methoxybenzyl)oxy)but-2-yn-1-yl benzoate (**204**) (196 mg, 0.500 mmol, 98% *ee*) and 3-bromophenylboronic acid (201 mg, 1.00 mmol) were used. The crude product was purified by flash column chromatography on silica gel (cyclohexane/EtOAc 30:1 to 20:1 gradient). The title compound was isolated as a yellow, clear oil (134 mg, 0.314 mmol, 63%).

TLC: R_f = 0.34 (cyclohexane/EtOAc 12:1; UV, CAM); **Specific Rotation**: $[\alpha]_D^{22}$ +88.8 (c = 1.00, $CHCl_3$); **^{1}H-NMR** (400 MHz, $CDCl_3$, 298 K): δ 7.62 (t, *J* = 1.8 Hz, 1H), 7.43 – 7.62 (m, 1H), 7.34 – 7.31 (m, 1H), 7.27 – 7.24 (m, 2H), 7.17 (t, *J* = 7.9 Hz, 1H), 6.90 – 6.86 (m, 2H), 5.61 – 5.60 (m, 1H), 4.49 (s, 2H), 4.40 (d, *J* = 1.2 Hz, 2H), 3.81 (s, 3H), 2.21 – 2.12 (m, 1H), 1.87 – 1.82 (m, 2H), 1.77 – 1.72 (m, 2H), 1.67 – 1.63 (m, 1H), 1.37 – 1.13 (m, 5H).; **^{13}C-NMR** (101 MHz, $CDCl_3$, 298 K): δ 204.6, 159.4, 138.0, 130.3, 129.9, 129.7, 129.7, 129.3, 124.9, 122.7, 113.9, 102.6, 100.8, 71.3, 69.6, 55.4, 37.9, 33.4, 33.3, 26.2, 26.1 (two coincident resonances); **IR** (neat): 2999 (w), 2911 (s), 2849 (m), 1945 (w), 1612 (m), 1589 (m), 1559 (m), 1512 (s), 1474 (m), 1464 (m), 1448 (m), 1381 (w), 1348 (w), 1302 (m), 1246 (s), 1172 (m), 1070 (s), 1036 (s), 995 (w), 948 (w), 890 (w), 819 (m), 784 (m), 756 (w), 733 (w), 690 (m), 665 (w), 575 (w), 517 (w) cm^{-1}; **HRMS** (ESI) *m/z*: exact mass calculated for $C_{24}H_{31}BrNO_2$ $[M + NH_4]^+$ 444.1533, found 444.1534; **SFC** (Jasco 2080 Plus, Daicel Chiralpak AS-H, 99% CO_2, 1% MeOH at 100 bar, flow rate 2.0 mL·min^{-1}, 25 °C, detection 254 nm): 90% *ee*, t_R (minor enantiomer) 29.7 min, t_R (major enantiomer) 31.3 min.

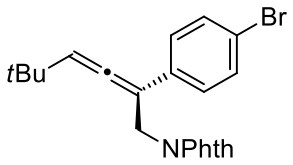

(+)-(*R*)-2-(2-(4-Bromophenyl)-5,5-dimethylhexa-2,3-dien-1-yl)isoindoline-1,3-dione (219). General procedure C was followed but deionized water (90.0 µL, 5.00 mmol, 10.0 equiv.) was added subsequent to the addition of K_3PO_4. (–)-(*S*)-6-(1,3-dioxoisoindolin-2-yl)-2,2-dimethylhex-4-yn-3-yl benzoate (**207**) (188 mg, 0.500 mmol, 97% *ee*) and 4-bromophenylboronic acid (201 mg, 1.00 mmol) were used. The crude product was purified by flash column chromatography on silica gel (cyclohexane/EtOAc 12:1 to 8:1 gradient). The title compound was isolated as a light yellow solid (185 mg, 0.451 mmol, 90%). Crystals suitable for X-ray crystallographic analysis were obtained by slow evaporation from CH_2Cl_2/*n*-hexane at 24 °C.

TLC: $R_f = 0.32$ (cyclohexane/EtOAc 5:1; UV, CAM); **Melting point**: 126 – 128 °C (CH_2Cl_2/*n*-hexane); **Specific Rotation**: $[\alpha]_D^{22}$ +85.8 (c = 1.00, $CHCl_3$); **^{1}H-NMR** (400 MHz, $CDCl_3$, 298 K): δ 7.89 – 7.84 (m, 2H), 7.74 – 7.70 (m, 2H), 7.47 – 7.43 (m, 2H), 7.29 – 7.26 (m, 2H), 5.51 (t, *J* = 3.6 Hz, 1H), 4.73 (dd, *J* = 15.4, 3.5 Hz, 1H), 4.61 (dd, *J* = 15.4, 3.8 Hz, 1H), 0.84 (s, 9H); **^{13}C-NMR** (101 MHz, $CDCl_3$, 298 K): δ 199.4, 167.9, 134.2, 134.1, 132.3, 131.7, 127.3, 123.4, 121.0, 110.7, 103.7, 37.6, 33.2, 29.8; **IR** (neat): 2964 (w), 2928 (w), 1953 (w), 1769 (m), 1710 (s), 1615 (w), 1489 (m), 1466 (m), 1430 (m), 1418 (m), 1395 (s), 1362 (m), 1327 (m), 1248 (w), 1207 (w), 1190 (w), 1168 (w), 1111 (s), 1089 (w), 1073 (m), 1001 (m), 954 (m), 938 (w), 899 (w), 850 (w), 836 (m), 806 (s), 770 (m), 752 (w), 725 (s), 708 (s), 693 (m), 686 (m), 611 (m), 584 (m), 540 (m), 529 (s), 498 (w), 486 (m) cm^{-1}; **HRMS** (ESI) *m/z*: exact mass calculated for $C_{22}H_{20}BrNNaO_2$ $[M + Na]^+$ 432.0570, found 432.0569; **SFC** (Jasco 2080 Plus, Daicel Chiralcel OJ-H, 95% CO_2, 5% MeOH at 100 bar, flow rate 2.0 mL·min^{-1}, 25 °C, detection 218 nm): 98% *ee*, t_R (major enantiomer) 8.8 min, t_R (minor enantiomer) 9.9 min.

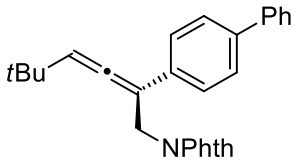

(+)-(*R*)-2-(2-([1,1'-Biphenyl]-4-yl)-5,5-dimethylhexa-2,3-dien-1-yl)isoindoline-1,3-dione (220). General procedure C was followed but deionized water (90.0 µL, 5.00 mmol,

10.0 equiv.) was added subsequent to the addition of K_3PO_4. (–)-(*S*)-6-(1,3-dioxoisoindolin-2-yl)-2,2-dimethylhex-4-yn-3-yl benzoate (**207**) (188 mg, 0.500 mmol, 97% *ee*) and 4-biphenylboronic acid (198 mg, 1.00 mmol) were used. The crude product was purified by flash column chromatography on silica gel (cyclohexane/EtOAc 12:1 to 8:1 gradient). The title compound was isolated as an orange solid (195 mg, 0.479 mmol, 96%). Crystals suitable for X-ray crystallographic analysis were obtained by slow evaporation from $CHCl_3$/*n*-hexane at 24 °C.

TLC: $R_f = 0.32$ (cyclohexane/EtOAc 5:1; UV, CAM); **Melting point**: 152 – 154 °C ($CHCl_3$/*n*-hexane); **Specific Rotation**: $[\alpha]_D^{22}$ +99.4 (c = 1.00, $CHCl_3$); **^{1}H-NMR** (400 MHz, $CDCl_3$, 298 K): δ 7.90 – 7.85 (m, 2H), 7.75 – 7.70 (m, 2H), 7.62 – 7.57 (m, 4H), 7.51 – 7.48 (m, 2H), 7.44 – 7.42 (m, 2H), 7.37 – 7.33 (m, 1H), 5.56 (t, *J* = 3.7 Hz, 1H), 4.81 (dd, *J* = 15.4, 3.5 Hz, 1H), 4.70 (dd, *J* = 15.4, 3.9 Hz, 1H), 0.87 (s, 9H); **^{13}C-NMR** (101 MHz, $CDCl_3$, 298 K): δ 199.4, 168.0, 140.8, 139.9, 134.1 (two coincident resonances), 132.4, 128.9, 127.4, 127.3, 127.1, 126.1, 123.4, 110.5, 104.2, 37.8, 33.2, 29.9; **IR** (neat): 3033 (w), 2959 (w), 2926 (w), 2867 (w), 1952 (w), 1770 (m), 1712 (s), 1614 (w), 1598 (w), 1486 (m), 1466 (m), 1430 (m), 1417 (w), 1393 (s), 1384 (m), 1362 (w), 1328 (m), 1249 (w), 1202 (w), 1189 (w), 1168 (w), 1109 (s), 1089 (w), 1072 (w), 1003 (w), 955 (m), 941 (w), 925 (w), 850 (m), 838 (m), 814 (w), 760 (s), 741 (m), 709 (s), 692 (s), 648 (w), 607 (m), 583 (m), 556 (w), 531 (s), 516 (w), 480 (w) cm^{-1}; **HRMS** (ESI) *m/z*: exact mass calculated for $C_{28}H_{26}NO_2$ $[M + H]^+$ 408.1958, found 408.1957; **SFC** (Jasco 2080 Plus, Daicel Chiralcel OJ-H, 90% CO_2, 10% MeOH at 100 bar, flow rate 2.0 mL·min^{-1}, 25 °C, detection 271 nm): 92% *ee*, t_R (major enantiomer) 20.5 min, t_R (minor enantiomer) 25.1 min.

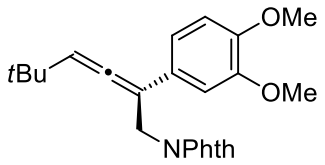

(+)-(*R*)-2-(2-(3,4-Dimethoxyphenyl)-5,5-dimethylhexa-2,3-dien-1-yl)isoindoline-1,3-dione (221). General procedure C was followed but deionized water (90.0 µL, 5.00 mmol, 10.0 equiv.) was added subsequent to the addition of K_3PO_4. (–)-(*S*)-6-(1,3-dioxoisoindolin-2-yl)-2,2-dimethylhex-4-yn-3-yl benzoate (**207**) (188 mg, 0.500 mmol, 97% *ee*) and 3,4-dimethoxybenzeneboronic acid (182 mg, 1.00 mmol) were used. The crude product was purified by flash column chromatography on silica gel (cyclohexane/EtOAc 12:1 to 2:1

gradient). The title compound was isolated as a light yellow foam (191 mg, 0.487 mmol, 97%). Crystals suitable for X-ray crystallographic analysis were obtained by slow evaporation from CH_2Cl_2/*n*-hexane at 24 °C.

TLC: $R_f = 0.29$ (cyclohexane/EtOAc 3:1; UV, CAM); **Melting point**: 117 – 118 °C (CH_2Cl_2/*n*-hexane); **Specific Rotation**: $[\alpha]_D^{21}$ +85.7 (c = 1.00, $CHCl_3$); **^{1}H-NMR** (400 MHz, $CDCl_3$, 298 K): δ 7.88 – 7.84 (m, 2H), 7.74 – 7.68 (m, 2H), 7.00 – 6.95 (m, 2H), 6.85 (d, *J* = 8.2 Hz, 1H), 5.51 (t, *J* = 3.6 Hz, 1H), 4.75 (dd, *J* = 15.4, 3.5 Hz, 1H), 4.64 (dd, *J* = 15.4, 3.7 Hz, 1H), 3.88 – 3.87 (m, 6H), 0.86 (s, 9H); **^{13}C-NMR** (101 MHz, $CDCl_3$, 298 K): δ 198.9, 168.0, 149.1, 148.5, 134.1, 132.4, 127.7, 123.4, 117.7, 111.2, 110.3, 109.5, 104.3, 56.1, 55.9, 37.9, 33.1, 29.9; **IR** (neat): 2953 (m), 2861 (w), 1772 (m), 1713 (s), 1605 (w), 1587 (w), 1514 (m), 1469 (m), 1455 (w), 1433 (w), 1410 (m), 1393 (m), 1363 (w), 1342 (w), 1323 (m), 1259 (m), 1241 (m), 1205 (w), 1192 (w), 1166 (w), 1147 (m), 1110 (m), 1089 (w), 1045 (w), 1023 (m), 975 (w), 952 (m), 857 (m), 824 (w), 798 (m), 760 (m), 748 (m), 714 (s), 633 (m), 615 (m), 596 (w), 527 (m), 482 (w) cm^{-1}; **HRMS** (ESI) *m/z*: exact mass calculated for $C_{24}H_{26}NO_4$ $[M + H]^+$ 392.1856, found 392.1858; **SFC** (Waters Acquity UPC^2, Trefoil, 95% CO_2, 5% MeOH, flow rate 2.0 mL·min^{-1}, 40 °C, detection 254 nm): 87% *ee*, t_R (minor enantiomer) 8.4 min, t_R (major enantiomer) 9.1 min.

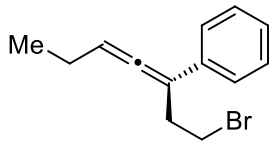

(+)-(*S*)-(1-Bromohepta-3,4-dien-3-yl)benzene (222). General procedure C was followed but the reaction was conducted on a 0.200 mmol scale and stirred at 40 °C for 12 h. (–)-(*S*)-7-bromohept-4-yn-3-yl benzoate (**208**) (59.0 mg, 0.200 mmol, 86% *ee*) and phenylboronic acid (49.0 mg, 0.400 mmol) were used. The crude product was purified by flash column chromatography on silica gel (cyclohexane/EtOAc 80:1). The title compound was isolated as a pale brown, clear oil (31.0 mg, 0.123 mmol, 62%).

TLC: $R_f = 0.42$ (cyclohexane/EtOAc 30:1; UV, CAM); **Specific Rotation**: $[\alpha]_D^{22}$ +32.0 (c = 1.00, $CHCl_3$); **^{1}H-NMR** (400 MHz, $CDCl_3$, 298 K): δ 7.40 – 7.31 (m, 4H), 7.24 – 7.20 (m, 1H), 5.67 (tt, *J* = 6.1, 3.0 Hz, 1H), 3.55 (t, *J* = 7.6 Hz, 2H), 3.04 – 2.95 (m, 2H), 2.21 – 2.14 (m, 2H), 1.10 (t, *J* = 7.4 Hz, 3H).; **^{13}C-NMR** (101 MHz, $CDCl_3$, 298 K): δ 203.4, 136.5, 128.6, 126.9, 125.8, 104.4, 97.9, 33.7, 30.8, 22.3, 13.7; **IR** (film, $CHCl_3$): 3060 (w), 3028 (w),

2964 (m), 2930 (w), 2872 (w), 1946 (w), 1597 (w), 1494 (m), 1451 (m), 1374 (w), 1323 (w), 1269 (w), 1204 (m), 1069 (w), 1031 (w), 812 (w), 754 (m), 730 (w), 692 (s), 597 (m) cm^{-1}; **HRMS** (EI) *m/z*: exact mass calculated for $C_{13}H_{14}Br$ $[M]^+$ 250.0352, found 250.0351; **SFC** (Jasco 2080 Plus, Daicel Chiralcel OB-H, 100% CO_2 at 100 bar, flow rate 2.0 $mL \cdot min^{-1}$, 25 °C, detection 221 nm): 83% *ee*, t_R (major enantiomer) 12.6 min, t_R (minor enantiomer) 13.4 min.

Appendix

9 X-Ray Crystallographic Data

9.1 X-Ray Crystallographic Data for Sulfonamide (±)-**109**

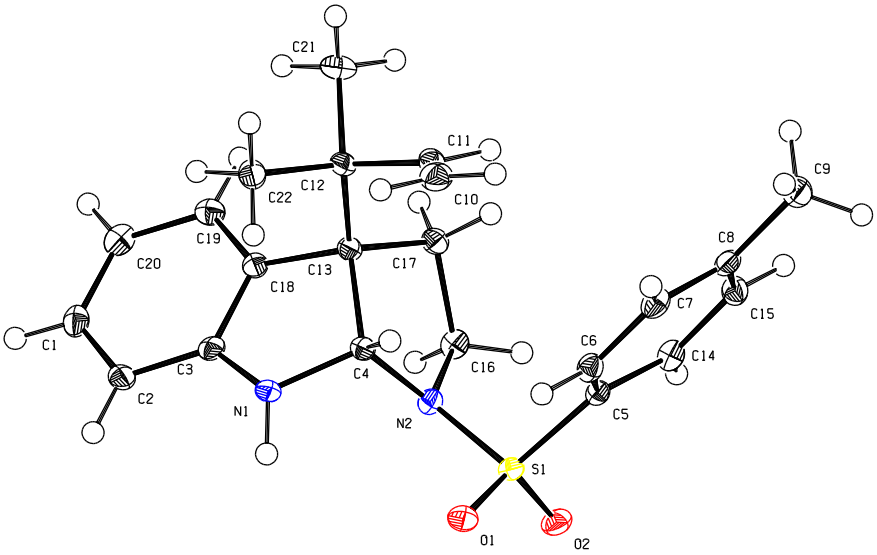

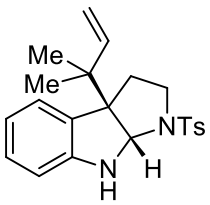

ORTEP view[111] of (±)-**109**, the thermal ellipsoids are drawn at the 50% probability level.

Database Reference. Crystallographic data have been deposited with the Cambridge Crystallographic Data Centre (CCDC) as supplementary publication no. CCDC-1019992. Data can be obtained free of charge on application to CCDC.

Experimental. A suitable clear, colorless prism was selected, mounted in perfluoroalkyl polyether oil on polyimide Micromounts (supplied by MiTeGen) and measured on a Bruker/Nonius Kappa Apex II diffractometer with a Bruker Apex II area detector. The detector type was a CCD area detector. The crystal was kept at 100.0(2) K during data collection. Using Olex2,[112] the structure was solved with the XS structure solution program[113] using Direct Methods and refined with the XL refinement package[113] using Least Squares minimization.

Table A2. Crystal data and structure refinement.

Empirical formula	$C_{22}H_{26}N_2O_2S$
Formula weight	382.51
Temperature/K	100.0(2)
Crystal system	monoclinic

[111] All ORTEP views were generated using the Platon software (version 70414) by A. L. Spek, see: Spek, A. L. *Acta Crystallogr., Sect. D: Biol. Crystallogr.* **2009**, *65*, 148.
[112] Dolomanov, O. V.; Bourhis, L. J.; Gildea, R. J.; Howard, J. A. K.; Puschmann, H. *J. Appl. Crystallogr.* **2009**, *42*, 339.
[113] Sheldrick, G. M. *Acta Crystallogr., Sect. A: Found. Crystallogr.* **2008**, *64*, 112.

Space group	$P2_1/c$
a/Å	13.5108(6)
b/Å	10.3083(4)
c/Å	16.0724(7)
α/°	90
β/°	121.932(3)
γ/°	90
Volume/Å^3	1899.73(15)
Z	4
ρ_{calc}mg/mm^3	1.337
m/mm^{-1}	0.191
F(000)	816.0
Crystal size/mm^3	0.28 × 0.24 × 0.08
Radiation	MoKα (λ = 0.71073)
2Θ range for data collection	4.954 to 55.204°
Index ranges	$-17 \leq h \leq 17$, $-13 \leq k \leq 13$, $-17 \leq l \leq 20$
Reflections collected	32625
Independent reflections	4397 [R_{int} = 0.0391, R_{sigma} = 0.0310]
Data/restraints/parameters	4397/1/250
Goodness-of-fit on F^2	1.042
Final R indexes [I>=2σ (I)]	R_1 = 0.0372, wR_2 = 0.0856
Final R indexes [all data]	R_1 = 0.0510, wR_2 = 0.0933
Largest diff. peak/hole / e Å^{-3}	0.38/-0.42

Table A3. Fractional Atomic Coordinates (×10^4) and Equivalent Isotropic Displacement Parameters (Å^2×10^3). U_{eq} is defined as 1/3 of the trace of the orthogonalised U_{IJ} tensor.

Atom	***x***	***y***	***z***	**U(eq)**
S1	4366.7(3)	7105.2(3)	3013.8(3)	12.94(10)
O1	5322.7(9)	6307.9(10)	3695.8(8)	17.8(2)
O2	4443.8(9)	7847.6(10)	2295.0(8)	17.3(2)
N1	3435.7(11)	3834.6(12)	2871.1(10)	14.1(3)
N2	3264.8(11)	6129.0(12)	2414.1(9)	12.7(3)
C1	1382.0(14)	1601.9(15)	895.5(12)	17.9(3)
C2	2452.2(14)	2073.5(14)	1630.0(12)	15.8(3)
C3	2472.4(13)	3219.7(14)	2090.0(11)	13.1(3)
C4	3083.8(13)	5116.4(14)	2982.1(11)	12.0(3)
C5	4040.2(13)	8178.8(14)	3687.9(11)	13.3(3)
C6	4419.7(13)	7901.1(15)	4653.4(11)	15.5(3)
C7	4096.1(14)	8713.2(15)	5158.0(12)	16.9(3)
C8	3394.7(13)	9789.3(15)	4710.6(12)	16.0(3)
C9	3034.7(15)	10653.6(16)	5259.6(13)	20.8(4)
C10	2635.9(14)	5787.7(17)	4964.3(13)	20.8(3)

C11	1861.9(14)	5907.8(15)	4020.7(12)	17.1(3)
C12	1367.8(13)	4836.8(14)	3265.1(11)	13.8(3)
C13	1730.0(12)	5052.5(14)	2491.7(11)	12.3(3)
C14	3359.8(13)	9271.0(14)	3229.0(11)	15.4(3)
C15	3042.7(13)	10061.3(15)	3743.5(12)	17.0(3)
C16	2140.1(13)	6628.2(15)	1604.8(11)	14.9(3)
C17	1282.2(13)	6327.0(14)	1916.1(11)	14.6(3)
C18	1445.8(13)	3882.5(14)	1824.3(11)	12.7(3)
C19	388.6(13)	3420.8(15)	1065.9(11)	16.0(3)
C20	358.2(14)	2267.2(15)	605.0(12)	18.1(3)
C21	32.6(14)	4891.8(17)	2754.9(13)	21.1(4)
C22	1780.3(15)	3505.3(14)	3747.0(12)	18.1(3)

Table A4. Anisotropic Displacement Parameters ($Å^2 \times 10^3$). The Anisotropic displacement factor exponent takes the form: $-2\pi^2[h^2a^{*2}U_{11}+2hka^*b^*U_{12}+\ldots]$.

Atom	**U_{11}**	**U_{22}**	**U_{33}**	**U_{23}**	**U_{13}**	**U_{12}**
S1	11.68(18)	13.97(18)	14.4(2)	-0.13(14)	7.76(15)	-0.89(14)
O1	12.3(5)	18.7(6)	21.2(6)	0.7(4)	8.1(5)	1.5(4)
O2	18.4(6)	19.3(6)	18.5(6)	0.0(4)	12.7(5)	-3.4(4)
N1	10.7(6)	13.6(6)	19.0(7)	0.9(5)	8.5(6)	1.5(5)
N2	12.2(6)	12.5(6)	12.2(6)	0.6(5)	5.6(5)	-0.6(5)
C1	28.3(9)	13.8(7)	18.6(8)	-1.7(6)	17.2(7)	-3.5(6)
C2	20.6(8)	14.0(7)	19.9(8)	3.4(6)	15.6(7)	2.3(6)
C3	14.9(7)	13.9(7)	13.6(8)	3.2(6)	9.7(6)	-0.3(6)
C4	12.3(7)	12.4(7)	12.1(7)	1.6(6)	7.1(6)	1.5(5)
C5	13.1(7)	12.6(7)	14.9(8)	-1.5(6)	7.9(6)	-2.4(6)
C6	14.9(7)	13.3(7)	16.2(8)	2.0(6)	6.8(6)	-0.3(6)
C7	20.2(8)	17.4(8)	14.3(8)	-0.1(6)	10.0(7)	-4.4(6)
C8	16.4(8)	15.2(7)	19.3(8)	-3.9(6)	11.4(7)	-5.8(6)
C9	24.6(9)	19.0(8)	23.4(9)	-2.9(7)	15.8(8)	-1.9(7)
C10	21.6(8)	23.7(8)	22.3(9)	-4.3(7)	15.1(7)	-3.5(7)
C11	22.6(8)	14.1(7)	21.0(9)	0.2(6)	15.9(7)	1.0(6)
C12	15.1(7)	13.5(7)	16.3(8)	-0.1(6)	10.6(7)	1.2(6)
C13	11.8(7)	12.6(7)	13.2(8)	0.1(6)	7.0(6)	0.9(5)
C14	16.5(7)	15.0(7)	11.9(8)	1.0(6)	5.6(6)	-1.7(6)
C15	14.6(7)	13.4(7)	20.1(8)	0.8(6)	7.3(7)	0.9(6)
C16	14.7(7)	15.7(7)	11.4(7)	2.4(6)	5.1(6)	0.1(6)
C17	12.8(7)	14.4(7)	15.4(8)	1.8(6)	6.6(6)	2.4(6)
C18	15.8(7)	12.8(7)	12.2(7)	1.6(6)	9.3(6)	0.2(6)
C19	14.4(7)	18.2(8)	15.7(8)	1.9(6)	8.2(7)	1.3(6)
C20	19.7(8)	20.3(8)	13.7(8)	-1.0(6)	8.5(7)	-4.1(6)
C21	16.0(8)	27.4(9)	24.0(9)	-0.4(7)	13.3(7)	1.7(7)

C22	25.4(8)	14.6(7)	21.1(9)	0.8(6)	17.0(7)	0.4(6)

Table A5. Bond Lengths.

Atom	Atom	Length/Å	Atom	Atom	Length/Å
S1	O1	1.4310(11)	C6	C7	1.387(2)
S1	O2	1.4347(11)	C7	C8	1.387(2)
S1	N2	1.6249(13)	C8	C9	1.504(2)
S1	C5	1.7604(15)	C8	C15	1.392(2)
N1	C3	1.394(2)	C10	C11	1.316(2)
N1	C4	1.4469(19)	C11	C12	1.510(2)
N2	C4	1.4896(18)	C12	C13	1.574(2)
N2	C16	1.4747(19)	C12	C21	1.538(2)
C1	C2	1.384(2)	C12	C22	1.529(2)
C1	C20	1.385(2)	C13	C17	1.535(2)
C2	C3	1.386(2)	C13	C18	1.522(2)
C3	C18	1.395(2)	C14	C15	1.381(2)
C4	C13	1.564(2)	C16	C17	1.518(2)
C5	C6	1.382(2)	C18	C19	1.382(2)
C5	C14	1.393(2)	C19	C20	1.390(2)

Table A6. Bond Angles.

Atom	Atom	Atom	Angle/°	Atom	Atom	Atom	Angle/°
O1	S1	O2	120.17(6)	C7	C8	C15	118.42(14)
O1	S1	N2	105.74(7)	C15	C8	C9	120.66(14)
O1	S1	C5	107.94(7)	C10	C11	C12	127.00(15)
O2	S1	N2	106.66(7)	C11	C12	C13	109.99(12)
O2	S1	C5	107.99(7)	C11	C12	C21	107.26(12)
N2	S1	C5	107.77(7)	C11	C12	C22	111.17(13)
C3	N1	C4	108.37(12)	C21	C12	C13	109.92(13)
C4	N2	S1	117.80(10)	C22	C12	C13	110.15(12)
C16	N2	S1	120.03(10)	C22	C12	C21	108.28(13)
C16	N2	C4	111.00(11)	C4	C13	C12	112.16(12)
C2	C1	C20	121.35(15)	C17	C13	C4	104.52(11)
C1	C2	C3	118.11(14)	C17	C13	C12	114.13(12)
N1	C3	C18	110.88(13)	C18	C13	C4	100.39(11)
C2	C3	N1	127.83(14)	C18	C13	C12	112.13(12)
C2	C3	C18	121.21(14)	C18	C13	C17	112.41(12)
N1	C4	N2	113.15(12)	C15	C14	C5	119.13(14)
N1	C4	C13	105.80(11)	C14	C15	C8	121.26(14)
N2	C4	C13	104.36(11)	N2	C16	C17	104.37(12)
C6	C5	S1	119.73(12)	C16	C17	C13	104.33(12)
C6	C5	C14	120.72(14)	C3	C18	C13	109.44(13)

C14	C5	S1	119.49(12)	C19	C18	C3	119.84(14)
C5	C6	C7	119.13(14)	C19	C18	C13	130.70(13)
C6	C7	C8	121.30(15)	C18	C19	C20	119.34(14)
C7	C8	C9	120.91(14)	C1	C20	C19	120.08(15)

Table A7. Torsion Angles.

A	**B**	**C**	**D**	**Angle/°**	**A**	**B**	**C**	**D**	**Angle/°**
S1	N2	C4	N1	-104.06(13)	C4	C13	C18	C3	13.46(15)
S1	N2	C4	C13	141.40(10)	C4	C13	C18	C19	-167.79(15)
S1	N2	C16	C17	-120.59(11)	C5	S1	N2	C4	-72.39(11)
S1	C5	C6	C7	-176.09(11)	C5	S1	N2	C16	68.21(12)
S1	C5	C14	C15	175.71(11)	C5	C6	C7	C8	0.5(2)
O1	S1	N2	C4	42.85(12)	C5	C14	C15	C8	0.3(2)
O1	S1	N2	C16	-176.55(11)	C6	C5	C14	C15	-1.6(2)
O1	S1	C5	C6	-19.22(14)	C6	C7	C8	C9	179.14(14)
O1	S1	C5	C14	163.48(12)	C6	C7	C8	C15	-1.7(2)
O2	S1	N2	C4	171.86(10)	C7	C8	C15	C14	1.3(2)
O2	S1	N2	C16	-47.54(12)	C9	C8	C15	C14	-179.53(14)
O2	S1	C5	C6	-150.57(12)	C10	C11	C12	C13	-115.93(17)
O2	S1	C5	C14	32.13(14)	C10	C11	C12	C21	124.55(17)
N1	C3	C18	C13	-0.64(17)	C10	C11	C12	C22	6.3(2)
N1	C3	C18	C19	-179.54(13)	C11	C12	C13	C4	57.57(16)
N1	C4	C13	C12	98.08(13)	C11	C12	C13	C17	-61.06(16)
N1	C4	C13	C17	-137.76(12)	C11	C12	C13	C18	169.66(12)
N1	C4	C13	C18	-21.15(14)	C12	C13	C17	C16	154.59(12)
N2	S1	C5	C6	94.56(13)	C12	C13	C18	C3	-105.79(14)
N2	S1	C5	C14	-82.74(13)	C12	C13	C18	C19	73.0(2)
N2	C4	C13	C12	-142.29(12)	C13	C18	C19	C20	-175.87(14)
N2	C4	C13	C17	-18.13(14)	C14	C5	C6	C7	1.2(2)
N2	C4	C13	C18	98.48(12)	C16	N2	C4	N1	112.00(14)
N2	C16	C17	C13	-33.18(15)	C16	N2	C4	C13	-2.54(15)
C1	C2	C3	N1	176.78(14)	C17	C13	C18	C3	124.03(13)
C1	C2	C3	C18	0.1(2)	C17	C13	C18	C19	-57.2(2)
C2	C1	C20	C19	-1.3(2)	C18	C13	C17	C16	-76.27(14)
C2	C3	C18	C13	176.57(13)	C18	C19	C20	C1	-1.0(2)
C2	C3	C18	C19	-2.3(2)	C20	C1	C2	C3	1.7(2)
C3	N1	C4	N2	-91.34(14)	C21	C12	C13	C4	175.46(12)
C3	N1	C4	C13	22.32(15)	C21	C12	C13	C17	56.83(16)
C3	C18	C19	C20	2.8(2)	C21	C12	C13	C18	-72.46(15)
C4	N1	C3	C2	168.96(14)	C22	C12	C13	C4	-65.31(16)
C4	N1	C3	C18	-14.06(16)	C22	C12	C13	C17	176.06(13)
C4	N2	C16	C17	22.44(15)	C22	C12	C13	C18	46.78(17)

C4 C13 C17 C16 31.70(15)

Table A8. Hydrogen Atom Coordinates (Å×10^4) and Isotropic Displacement Parameters (Å^2×10^3).

Atom	***x***	***y***	***z***	**U(eq)**
H1	4112(13)	3791(17)	2913(13)	17
H1A	1349	822	591	21
H2	3139	1634	1810	19
H4	3469	5357	3675	14
H6	4886	7179	4961	19
H7	4355	8533	5809	20
H9A	3395	10357	5924	31
H9B	2202	10628	4950	31
H9C	3277	11527	5255	31
H10A	2937	4975	5228	25
H10B	2882	6516	5367	25
H11	1590	6742	3795	20
H14	3122	9465	2584	19
H15	2585	10789	3438	20
H16A	1916	6195	994	18
H16B	2182	7555	1523	18
H17A	500	6222	1349	18
H17B	1277	7013	2327	18
H19	-296	3877	866	19
H20	-350	1942	101	22
H21A	-181	4775	3232	32
H21B	-311	4215	2273	32
H21C	-244	5719	2441	32
H22A	2612	3447	4060	27
H22B	1418	2841	3257	27
H22C	1570	3391	4227	27

9.2 X-Ray Crystallographic Data for Carbamate (±)-**112**

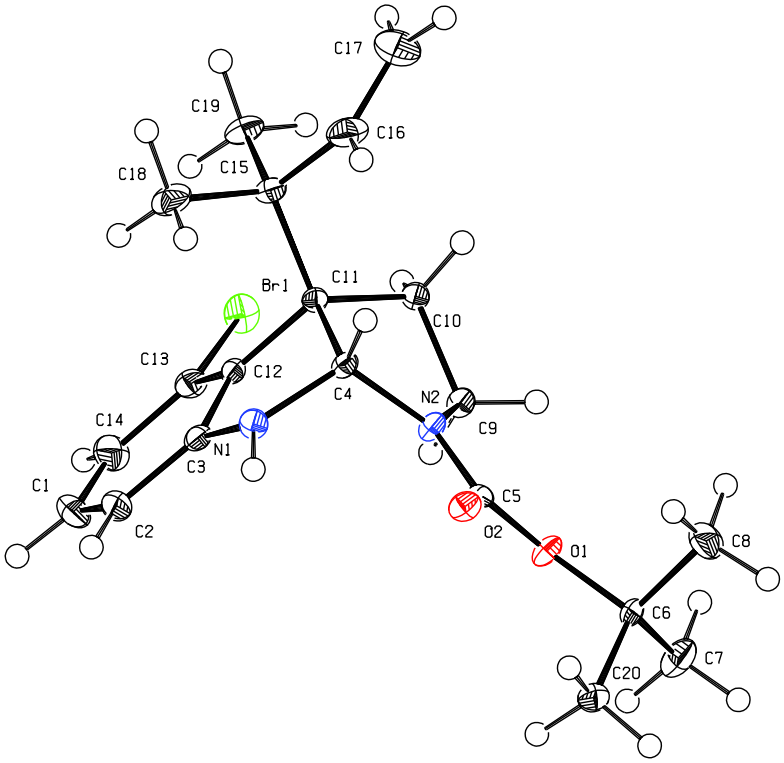

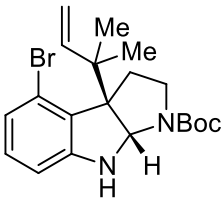

ORTEP view[111] of (±)-**112**, the thermal ellipsoids are drawn at the 50% probability level.

Database Reference. Crystallographic data have been deposited with the Cambridge Crystallographic Data Centre (CCDC) as supplementary publication no. CCDC-1433588. Data can be obtained free of charge on application to CCDC.

Experimental. A suitable clear, colorless plate was selected, mounted in perfluoroalkyl polyether oil on polyimide Micromounts (supplied by MiTeGen) and measured on a Bruker/Nonius Kappa Apex II diffractometer with a Bruker Apex II area detector. The detector type was a CCD area detector. The crystal was kept at 100.0(2) K during data collection. Using Olex2,[112] the structure was solved with the XS structure solution program[113] using Direct Methods and refined with the XL refinement package[113] using Least Squares minimization. The absolute stereochemistry was not determined by X-Ray diffraction.

Table A9. Crystal data and structure refinement.

Empirical formula	$C_{20}H_{27}BrN_2O_2$
Formula weight	407.34
Temperature/K	100.0(2)
Crystal system	monoclinic
Space group	$P2_1/c$
a/Å	7.6804(4)
b/Å	20.7205(11)

c/Å	12.2782(7)
α/°	90
β/°	97.1240(10)
γ/°	90
Volume/Å^3	1938.89(18)
Z	4
ρ_{calc}g/cm^3	1.395
μ/mm^{-1}	2.135
F(000)	848.0
Crystal size/mm^3	0.2 × 0.18 × 0.08
Radiation	MoKα (λ = 0.71073)
2Θ range for data collection/°	3.878 to 55.074
Index ranges	-9 ≤ h ≤ 9, -23 ≤ k ≤ 26, -15 ≤ l ≤ 15
Reflections collected	31551
Independent reflections	4442 [R_{int} = 0.0318, R_{sigma} = 0.0209]
Data/restraints/parameters	4442/1/234
Goodness-of-fit on F^2	1.015
Final R indexes [I>=2σ (I)]	R_1 = 0.0240, wR_2 = 0.0554
Final R indexes [all data]	R_1 = 0.0313, wR_2 = 0.0580
Largest diff. peak/hole / e Å^{-3}	0.38/-0.31

Table A10. Fractional Atomic Coordinates (×10^4) and Equivalent Isotropic Displacement Parameters (Å^2×10^3). U_{eq} is defined as 1/3 of the trace of the orthogonalised U_{IJ} tensor.

Atom	***x***	***y***	***z***	**U(eq)**
Br1	3999.8(2)	3220.6(2)	9767.1(2)	20.83(6)
O1	4085.1(13)	4096.9(5)	4629.3(8)	15.0(2)
O2	1162.0(14)	4336.6(5)	4217.0(8)	15.4(2)
N1	40.0(17)	4375.8(6)	6625.4(10)	15.2(3)
N2	2227.1(16)	3769.7(6)	5743(1)	12.7(2)
C1	1960(2)	5053.0(8)	9292.3(14)	25.8(4)
C2	991(2)	5050.2(7)	8261.2(13)	20.1(3)
C3	876.5(19)	4474.2(7)	7675.7(12)	14.5(3)
C4	569.8(19)	3758.9(7)	6231.3(11)	12.1(3)
C5	2385.5(19)	4088.0(6)	4798.7(11)	11.8(3)
C6	4684(2)	4241.5(7)	3560.4(11)	14.2(3)
C7	6665(2)	4193.1(9)	3847.2(14)	24.5(4)
C8	3996(3)	3725.5(8)	2753.5(14)	27.3(4)
C9	3626.8(19)	3390.4(7)	6362.4(12)	13.8(3)
C10	2599.6(19)	2934.8(7)	7012.0(12)	13.3(3)
C11	1062.8(19)	3346.9(7)	7297.2(11)	11.4(3)
C12	1611.3(19)	3892.4(7)	8115.3(11)	12.5(3)
C13	2637(2)	3930.4(7)	9125.7(12)	16.3(3)

C14	2820(2)	4504.6(8)	9721.1(13)	23.4(3)
C15	-530(2)	2940.0(7)	7630.1(12)	15.3(3)
C16	-1246(2)	2507.0(8)	6686.5(14)	24.3(4)
C17	-1224(3)	1871.8(9)	6659.4(18)	35.5(5)
C18	-2041(2)	3381.3(8)	7877.4(16)	25.1(4)
C19	42(2)	2543.3(8)	8664.4(13)	21.3(3)
C20	4169(2)	4917.6(7)	3161.6(13)	18.8(3)

Table A11. Anisotropic Displacement Parameters ($Å^2 \times 10^3$). The Anisotropic displacement factor exponent takes the form: $-2\pi^2[h^2a^{*2}U_{11}+2hka^*b^*U_{12}+\ldots]$.

Atom	**U_{11}**	**U_{22}**	**U_{33}**	**U_{23}**	**U_{13}**	**U_{12}**
Br1	24.26(9)	23.92(9)	13.18(8)	3.43(6)	-2.18(6)	4.89(7)
O1	12.9(5)	21.1(5)	11.4(5)	4.7(4)	3.4(4)	-0.2(4)
O2	14.9(5)	16.7(5)	14.6(5)	5.0(4)	0.8(4)	1.7(4)
N1	18.5(7)	12.3(6)	15.2(6)	4.7(5)	3.6(5)	5.5(5)
N2	10.7(6)	15.1(6)	12.7(6)	4.8(5)	3.1(5)	3.6(5)
C1	38.5(10)	14.9(8)	25.2(9)	-5.7(6)	8.4(7)	-3.6(7)
C2	26.3(9)	12.8(7)	22.5(8)	1.2(6)	8.7(7)	2.0(6)
C3	14.3(7)	13.8(7)	16.4(7)	2.6(6)	6.4(6)	0.2(6)
C4	11.1(7)	13.2(7)	12.3(6)	3.1(5)	3.0(5)	1.2(5)
C5	14.8(7)	7.9(6)	12.7(7)	-1.1(5)	2.3(5)	-1.4(5)
C6	18.6(8)	15.0(7)	10.2(7)	0.3(5)	6.8(6)	-0.9(6)
C7	18.8(8)	30.8(9)	25.6(9)	7.3(7)	9.5(7)	4.1(7)
C8	41.2(11)	21.1(8)	20.2(8)	-7.3(7)	6.4(7)	-5.5(8)
C9	12.6(7)	14.5(7)	14.5(7)	3.8(5)	2.4(5)	3.9(5)
C10	15.0(7)	11.6(7)	13.4(7)	2.6(5)	2.1(5)	2.5(6)
C11	13.2(7)	10.5(7)	10.6(6)	2.0(5)	2.0(5)	0.8(5)
C12	13.6(7)	11.8(7)	12.8(7)	1.3(5)	5.0(5)	0.8(5)
C13	18.3(8)	15.9(7)	14.7(7)	3.9(6)	2.4(6)	0.0(6)
C14	31.0(9)	23.3(8)	15.4(8)	-3.2(6)	0.6(7)	-4.6(7)
C15	14.7(7)	14.6(7)	16.9(7)	3.1(6)	3.5(6)	-2.2(6)
C16	25.1(9)	26.1(9)	21.7(8)	1.5(7)	2.2(7)	-11.8(7)
C17	37.3(11)	27.8(10)	41.2(11)	-8.1(8)	4.0(9)	-12.8(8)
C18	14.2(8)	24.1(9)	38.8(10)	5.7(7)	9.9(7)	-0.4(6)
C19	22.2(8)	21.4(8)	20.8(8)	8.3(6)	5.0(6)	-3.8(6)
C20	22.7(8)	15.1(7)	19.7(8)	3.0(6)	7.2(6)	-0.3(6)

Table A12. Bond Lengths.

Atom	**Atom**	**Length/Å**	**Atom**	**Atom**	**Length/Å**
Br1	C13	1.9167(15)	C6	C7	1.522(2)
O1	C5	1.3472(17)	C6	C8	1.508(2)
O1	C6	1.4743(16)	C6	C20	1.520(2)

O2	C5	1.2215(17)	C9	C10	1.518(2)
N1	C3	1.3826(19)	C10	C11	1.5321(19)
N1	C4	1.4431(18)	C11	C12	1.5359(19)
N2	C4	1.4729(18)	C11	C15	1.581(2)
N2	C5	1.3526(18)	C12	C13	1.387(2)
N2	C9	1.4659(18)	C13	C14	1.394(2)
C1	C2	1.387(2)	C15	C16	1.514(2)
C1	C14	1.385(2)	C15	C18	1.537(2)
C2	C3	1.391(2)	C15	C19	1.531(2)
C3	C12	1.410(2)	C16	C17	1.317(3)
C4	C11	1.5691(19)			

Table A13. Bond Angles.

Atom	**Atom**	**Atom**	**Angle/°**	**Atom**	**Atom**	**Atom**	**Angle/°**
C5	O1	C6	123.73(11)	N2	C9	C10	102.15(11)
C3	N1	C4	109.00(12)	C9	C10	C11	103.81(11)
C5	N2	C4	122.03(12)	C4	C11	C15	113.04(11)
C5	N2	C9	124.62(12)	C10	C11	C4	103.04(11)
C9	N2	C4	113.33(11)	C10	C11	C12	113.77(12)
C14	C1	C2	121.35(15)	C10	C11	C15	113.87(11)
C1	C2	C3	117.90(15)	C12	C11	C4	99.40(11)
N1	C3	C2	126.94(14)	C12	C11	C15	112.44(11)
N1	C3	C12	110.41(13)	C3	C12	C11	108.33(12)
C2	C3	C12	122.64(14)	C13	C12	C3	116.75(13)
N1	C4	N2	114.64(12)	C13	C12	C11	134.92(13)
N1	C4	C11	104.54(11)	C12	C13	Br1	123.00(11)
N2	C4	C11	102.49(11)	C12	C13	C14	121.76(14)
O1	C5	N2	109.32(12)	C14	C13	Br1	115.16(11)
O2	C5	O1	126.44(13)	C1	C14	C13	119.25(15)
O2	C5	N2	124.23(13)	C16	C15	C11	109.73(12)
O1	C6	C7	101.18(11)	C16	C15	C18	107.00(14)
O1	C6	C8	108.56(12)	C16	C15	C19	110.88(13)
O1	C6	C20	112.13(12)	C18	C15	C11	111.18(12)
C8	C6	C7	111.35(14)	C19	C15	C11	110.43(12)
C8	C6	C20	112.70(13)	C19	C15	C18	107.56(13)
C20	C6	C7	110.35(13)	C17	C16	C15	127.38(17)

Table A14. Torsion Angles.

A	**B**	**C**	**D**	**Angle/°**	**A**	**B**	**C**	**D**	**Angle/°**
Br1	C13	C14	C1	176.52(13)	C5	O1	C6	C20	61.71(17)
N1	C3	C12	C11	-5.10(16)	C5	N2	C4	N1	-66.55(17)
N1	C3	C12	C13	174.00(13)	C5	N2	C4	C11	-179.17(12)

N1	C4	C11	C10	-144.84(11)
N1	C4	C11	C12	-27.60(13)
N1	C4	C11	C15	91.80(13)
N2	C4	C11	C10	-24.92(14)
N2	C4	C11	C12	92.32(12)
N2	C4	C11	C15	-148.28(12)
N2	C9	C10	C11	-36.14(14)
C1	C2	C3	N1	-177.28(15)
C1	C2	C3	C12	3.9(2)
C2	C1	C14	C13	-3.1(3)
C2	C3	C12	C11	173.89(14)
C2	C3	C12	C13	-7.0(2)
C3	N1	C4	N2	-84.43(14)
C3	N1	C4	C11	26.97(15)
C3	C12	C13	Br1	-171.42(11)
C3	C12	C13	C14	5.1(2)
C4	N1	C3	C2	166.76(15)
C4	N1	C3	C12	-14.30(16)
C4	N2	C5	O1	171.11(12)
C4	N2	C5	O2	-7.4(2)
C4	N2	C9	C10	21.01(15)
C4	C11	C12	C3	20.06(14)
C4	C11	C12	C13	-158.80(16)
C4	C11	C15	C16	56.72(16)
C4	C11	C15	C18	-61.44(16)
C4	C11	C15	C19	179.25(12)
C5	O1	C6	C7	179.29(13)
C5	O1	C6	C8	-63.47(17)
C5	N2	C9	C10	-157.22(13)
C6	O1	C5	O2	-18.7(2)
C6	O1	C5	N2	162.81(12)
C9	N2	C4	N1	115.17(13)
C9	N2	C4	C11	2.55(15)
C9	N2	C5	O1	-10.81(19)
C9	N2	C5	O2	170.65(13)
C9	C10	C11	C4	38.26(14)
C9	C10	C11	C12	-68.32(14)
C9	C10	C11	C15	161.07(12)
C10	C11	C12	C3	128.90(13)
C10	C11	C12	C13	-50.0(2)
C10	C11	C15	C16	-60.43(16)
C10	C11	C15	C18	-178.59(13)
C10	C11	C15	C19	62.09(16)
C11	C12	C13	Br1	7.4(2)
C11	C12	C13	C14	-176.12(15)
C11	C15	C16	C17	114.38(19)
C12	C11	C15	C16	168.30(13)
C12	C11	C15	C18	50.14(16)
C12	C11	C15	C19	-69.18(15)
C12	C13	C14	C1	-0.2(2)
C14	C1	C2	C3	1.3(3)
C15	C11	C12	C3	-99.78(14)
C15	C11	C12	C13	81.4(2)
C18	C15	C16	C17	-124.9(2)
C19	C15	C16	C17	-7.9(2)

Table A15. Hydrogen Atom Coordinates (Å×10^4) and Isotropic Displacement Parameters (Å^2×10^3).

Atom	***x***	***y***	***z***	**U(eq)**
H1	-200(20)	4693(8)	6192(13)	18
H1A	2035	5439	9713	31
H2	424	5430	7964	24
H4	-396	3553	5728	14
H7A	7064	4518	4402	37
H7B	7233	4268	3187	37
H7C	6973	3762	4137	37
H8A	4306	3299	3066	41
H8B	4518	3780	2070	41
H8C	2717	3762	2600	41

H9A	4425	3668	6854	17
H9B	4317	3150	5866	17
H10A	3329	2783	7685	16
H10B	2174	2556	6564	16
H14	3526	4519	10413	28
H16	-1771	2717	6040	29
H17A	-715	1636	7282	43
H17B	-1716	1650	6017	43
H18A	-2427	3646	7231	38
H18B	-1637	3662	8500	38
H18C	-3023	3117	8059	38
H19A	-940	2276	8837	32
H19B	402	2835	9280	32
H19C	1031	2266	8539	32
H20A	2905	4932	2920	28
H20B	4811	5031	2547	28
H20C	4460	5226	3761	28

9.3 X-Ray Crystallographic Data for Dicarboxylate (–)-*exo*-**90**

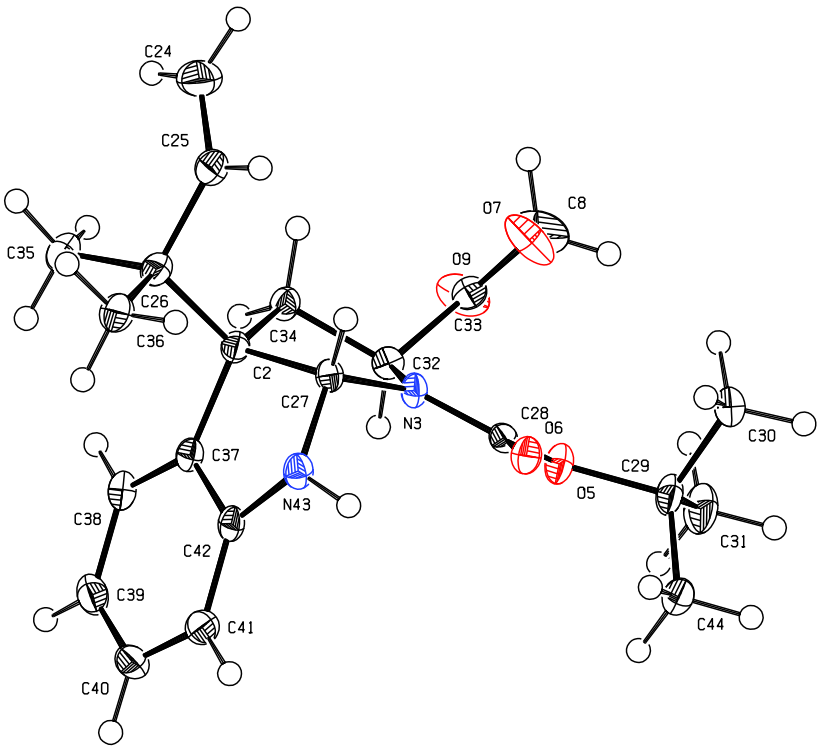

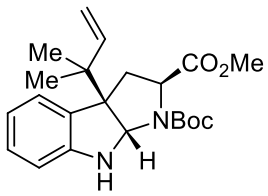

ORTEP view[111] of (–)-*exo*-**90**, the thermal ellipsoids are drawn at the 50% probability level.

Database Reference. Crystallographic data have been deposited with the Cambridge Crystallographic Data Centre (CCDC) as supplementary publication no. CCDC-1433589. Data can be obtained free of charge on application to CCDC.

Experimental. A suitable clear, colorless block was selected, mounted in perfluoroalkyl polyether oil on polyimide Micromounts (supplied by MiTeGen) and measured on a Bruker/Nonius Kappa Apex II diffractometer with a Bruker Apex II area detector. The detector type was a CCD area detector. The crystal was kept at 100.0(2) K during data collection. Using Olex2,[112] the structure was solved with the XS structure solution program[113] using Direct Methods and refined with the XL refinement package[113] using Least Squares minimization. The absolute stereochemistry was not determined by X-Ray diffraction.

Table A16. Crystal data and structure refinement.

Empirical formula	$C_{22}H_{30}N_2O_4$
Formula weight	386.48
Temperature/K	100.0(2)
Crystal system	monoclinic
Space group	$P2_1$
a/Å	9.1201(2)
b/Å	10.9513(3)
c/Å	20.9141(6)
α/°	90
β/°	96.6170(10)
γ/°	90
Volume/Å^3	2074.92(9)
Z	4
ρ_{calc}g/cm^3	1.237
μ/mm^{-1}	0.686
F(000)	832.0
Crystal size/mm^3	0.2 × 0.14 × 0.06
Radiation	CuKα (λ = 1.54178)
2Θ range for data collection/°	4.254 to 133.264
Index ranges	$-10 \leq h \leq 10$, $-13 \leq k \leq 12$, $-17 \leq l \leq 17$
Reflections collected	36373
Independent reflections	6181 [R_{int} = 0.0279, R_{sigma} = 0.0190]
Data/restraints/parameters	6181/636/533
Goodness-of-fit on F^2	1.043
Final R indexes [I>=2σ (I)]	R_1 = 0.0245, wR_2 = 0.0630
Final R indexes [all data]	R_1 = 0.0247, wR_2 = 0.0633
Largest diff. peak/hole / e Å^{-3}	0.12/-0.17

Flack parameter -0.02(3)

Table A17. Fractional Atomic Coordinates ($\times 10^4$) and Equivalent Isotropic Displacement Parameters ($Å^2 \times 10^3$). U_{eq} is defined as 1/3 of the trace of the orthogonalised U_{IJ} tensor.

Atom	***x***	***y***	***z***	**U(eq)**
O1	-1007.5(13)	5233.3(12)	6629.1(6)	20.7(3)
O2	-1635.6(15)	7232.8(13)	6427.6(8)	31.1(4)
O3	2096.0(16)	5626.9(12)	7269.2(7)	28.8(3)
O4	2255.1(14)	3787.0(12)	6818.6(7)	25.2(3)
O5	4639.9(13)	5333.8(11)	1708.2(7)	20.8(3)
O6	4142.0(13)	7376.3(11)	1586.0(6)	19.7(3)
O7	7863.8(17)	5501.0(14)	2154.3(8)	37.2(4)
C8	8795(3)	3222(2)	2183.6(14)	42.8(7)
N1	429.6(16)	6396.2(14)	6100.2(8)	18.3(3)
C2	7308.3(17)	7003.9(16)	250.1(9)	16.8(4)
N3	5982.8(15)	6465.3(13)	1120.0(8)	16.4(3)
O9	8095.1(16)	3793.0(12)	1602.8(8)	31.8(4)
C1	-3633(2)	5281(2)	6812.0(11)	33.6(5)
C3	-2059.4(19)	5001.5(18)	7102.2(10)	23.3(4)
C4	-817.8(19)	6361.4(17)	6396.3(10)	20.0(4)
C5	760.5(19)	7451.3(16)	5705.9(10)	19.1(4)
C6	2140.8(18)	7002.4(17)	5395.8(10)	18.9(4)
C7	3259(2)	8058.2(18)	5280.9(11)	26.2(5)
C9	4465(3)	7526(2)	4938.2(15)	46.8(7)
C10	5783(3)	7337(4)	5126(2)	45.4(12)
C11	-1603(2)	5742(2)	7701.2(11)	28.7(5)
C12	1494.2(18)	5397.6(16)	6122.5(9)	17.5(4)
C13	2818.8(18)	6003.8(18)	5853.7(10)	21.5(4)
N12	-341.6(17)	7673.7(15)	5160.0(8)	22.8(4)
C14	-48(2)	6898.0(17)	4659.7(10)	22.0(4)
C15	1396.8(19)	6456.6(17)	4773.7(10)	18.8(4)
C16	1918(2)	5631.4(17)	4353(1)	23.6(4)
C17	1010(2)	5277.5(19)	3805.9(11)	30.0(5)
C18	-394(2)	5773(2)	3678.0(11)	32.6(5)
C19	-944(2)	6581(2)	4103.5(11)	30.4(5)
C1A	2477(3)	9049(2)	4845.5(12)	35.2(5)
C20	3889(2)	8665(2)	5912.3(11)	32.4(5)
C21	1952.6(18)	4978.2(17)	6802.7(10)	18.6(4)
C22	2746(2)	3290.6(19)	7445.9(12)	34.1(5)
C23	-1850(2)	3642.5(19)	7230.8(12)	30.8(5)
C24	10798(2)	8194(2)	802.2(12)	37.8(6)
C25	9392(2)	8441.0(19)	632.6(11)	26.6(5)

C26	8429.7(19)	7980.5(17)	38.9(10)	21.0(4)
C27	6220.0(18)	7524.7(16)	707.8(9)	15.9(4)
C28	4853.3(18)	6466.5(16)	1487.8(9)	16.6(4)
C29	3716(2)	5129.0(18)	2236(1)	23.0(4)
C30	4356(2)	5842.3(18)	2824.4(10)	24.4(4)
C31	3884(2)	3760(2)	2347.2(12)	32.4(5)
C32	6907.4(18)	5408.3(16)	1029.7(9)	17.0(4)
C33	7650.1(18)	4934.5(16)	1665.3(10)	18.7(4)
C34	8072.0(18)	5924.2(17)	625.2(10)	18.5(4)
C35	9365(2)	7414.3(19)	-445(1)	26.7(5)
C36	7599(2)	9086.7(17)	-279.6(11)	24.5(5)
C37	6205.8(18)	6562.6(16)	-305.6(10)	16.9(4)
C38	6370.1(19)	5748.2(16)	-794.6(10)	20.0(4)
C39	5168(2)	5489.0(18)	-1247.3(10)	25.2(4)
C40	3810(2)	6040.4(19)	-1200(1)	26.2(5)
C41	3620.5(19)	6841.3(18)	-699.5(10)	23.1(4)
C42	4825.8(18)	7087.7(15)	-251.2(10)	17.0(4)
N43	4914.2(16)	7864.1(13)	280.1(8)	18.4(4)
C44	2116(2)	5462(2)	2013.1(11)	28.0(5)
C1B	5098(8)	7444(8)	4485(4)	44(2)

Table A18. Anisotropic Displacement Parameters ($Å^2 \times 10^3$). The Anisotropic displacement factor exponent takes the form: $-2\pi^2[h^2a^{*2}U_{11}+2hka^*b^*U_{12}+\ldots]$.

Atom	**U_{11}**	**U_{22}**	**U_{33}**	**U_{23}**	**U_{13}**	**U_{12}**
O1	22.4(6)	20.6(6)	20.4(9)	3.3(6)	8.6(5)	-1.0(5)
O2	30.3(7)	27.3(7)	38.8(11)	9.5(7)	18.1(6)	10.6(6)
O3	42.8(8)	25.2(7)	16.6(10)	-3.2(6)	-4.0(6)	5.1(6)
O4	34.5(7)	17.6(6)	22.1(9)	1.8(6)	-2.8(6)	4.6(6)
O5	27.1(6)	16.9(6)	20.1(9)	1.1(6)	10.1(5)	-2.0(5)
O6	21.7(6)	19.2(6)	19.1(9)	0.3(5)	6.6(5)	1.9(5)
O7	51.8(9)	35.5(8)	21.0(11)	-7.2(7)	-10.5(7)	18.3(7)
C8	44.1(12)	24.6(11)	54.1(19)	18.6(11)	-17.9(11)	1.0(9)
N1	18.9(7)	18.9(7)	17.8(10)	5.0(7)	5.3(6)	3.8(6)
C2	16.4(8)	18.4(8)	16.0(12)	1.9(8)	3.4(7)	0.0(6)
N3	18.7(7)	17.0(7)	14.1(10)	3.5(6)	4.6(6)	2.6(6)
O9	39.6(8)	15.8(6)	36.3(11)	1.2(6)	-11.7(6)	6.3(6)
C1	22.0(9)	51.5(13)	28.0(15)	8.1(11)	6.4(8)	-5.0(9)
C3	22.5(9)	28.4(10)	20.2(13)	3.6(8)	7.6(8)	-4.0(7)
C4	20.4(8)	22.2(9)	17.9(13)	2.5(8)	4.5(7)	1.5(7)
C5	22.3(8)	17.3(8)	18.9(13)	3.7(8)	7.1(7)	1.5(7)
C6	18.5(8)	20.8(9)	18.4(13)	-0.3(8)	6.9(7)	-1.3(7)
C7	27.5(9)	27.1(10)	24.9(14)	-1.8(9)	7.5(8)	-9.4(8)

C9	41.7(13)	43.4(13)	61(2)	-17.4(13)	31.8(12)	-20.1(11)
C10	26.1(16)	55(2)	58(3)	-5.7(19)	14.6(15)	-3.2(14)
C11	29.6(10)	35.4(11)	22.6(14)	2.0(9)	9.9(8)	-3.0(8)
C12	18.1(8)	17.5(8)	16.9(13)	-0.8(8)	1.6(7)	1.8(7)
C13	15.9(8)	28.2(10)	20.7(13)	0.4(8)	2.9(7)	1.2(7)
N12	21.7(7)	25.9(8)	21.9(12)	7.6(7)	7.5(6)	7.5(6)
C14	23.8(9)	22.5(9)	20.2(13)	9.7(8)	4.8(8)	-1.4(7)
C15	21.3(8)	18.5(8)	17.2(13)	2.9(8)	4.9(7)	-3.1(7)
C16	29.5(9)	22.6(10)	20.3(14)	1.2(8)	10.0(8)	-2.8(7)
C17	45.8(11)	26(1)	19.5(14)	-1.9(9)	9.8(9)	-10.3(9)
C18	42.9(11)	38.9(12)	14.8(14)	5.7(9)	-1.7(9)	-17.6(9)
C19	27.2(10)	37.5(12)	25.4(15)	12.8(10)	-2.2(8)	-5.2(8)
C1A	48.5(12)	28.7(11)	28.6(15)	4.4(9)	6.2(10)	-16.2(9)
C20	34.0(11)	33.0(11)	30.4(15)	-4.3(10)	4.2(9)	-12.2(9)
C21	17.5(8)	18.2(9)	20.0(13)	-0.2(8)	1.3(7)	0.1(7)
C22	40.2(12)	25.9(11)	33.6(16)	10(1)	-7(1)	4.0(9)
C23	35.0(11)	28.3(11)	29.9(16)	6.3(9)	8.0(9)	-8.9(8)
C24	30.7(11)	45.3(13)	35.1(17)	9.7(11)	-5.5(10)	-14.5(10)
C25	27.9(9)	30.6(10)	21.5(14)	3.3(9)	3.4(8)	-11.4(8)
C26	18.6(8)	23.8(9)	21.1(14)	3.6(8)	3.7(7)	-3.3(7)
C27	18.7(8)	14.8(8)	14.3(13)	2.2(7)	2.6(7)	0.6(6)
C28	17.9(8)	18.5(8)	13.2(12)	1.1(7)	0.4(6)	-2.5(7)
C29	28.5(9)	23.2(10)	19.2(13)	3.2(8)	10.5(8)	-4.5(7)
C30	26.9(9)	28.6(10)	18.2(13)	2.4(9)	5.4(8)	-1.2(8)
C31	45.1(12)	25.5(10)	28.9(16)	6.9(9)	13.6(10)	-6.7(9)
C32	18.1(8)	15.0(8)	18.0(12)	-0.2(7)	2.2(7)	1.3(6)
C33	18.5(8)	15.1(8)	22.6(14)	0.8(8)	2.8(7)	-0.6(6)
C34	16.3(8)	21.5(9)	18.1(13)	2.5(8)	4.2(7)	2.6(7)
C35	22.0(9)	32.4(11)	27.1(15)	2.9(9)	8.7(8)	-2.7(8)
C36	26.9(9)	22.5(10)	24.5(14)	6.2(8)	4.3(8)	-4.3(7)
C37	18.3(8)	17.2(8)	15.8(12)	2.7(7)	4.6(7)	-0.5(6)
C38	24.2(8)	19.4(9)	17.6(13)	1.8(8)	7.8(7)	0.6(7)
C39	34.9(10)	24.7(10)	16.4(13)	-1.4(8)	4.5(8)	-6.1(8)
C40	26.8(9)	32.9(11)	17.7(14)	3.9(9)	-2.2(8)	-8.2(8)
C41	19.5(8)	27.9(10)	21.5(14)	7.3(9)	0.9(7)	0.0(7)
C42	20.0(8)	16.4(8)	15.3(13)	5.4(7)	4.8(7)	1.4(7)
N43	18.8(7)	19.9(8)	17.0(11)	1.4(7)	4.7(6)	5.3(6)
C44	26.0(9)	37.3(11)	21.8(14)	-1.2(9)	7.4(8)	-9.9(8)
C1B	33(4)	55(5)	46(6)	-2(4)	18(3)	-5(3)

Table A19. Bond Lengths.

Atom	Atom	Length/Å	Atom	Atom	Length/Å
O1	C3	1.477(2)	C7	C1A	1.538(3)
O1	C4	1.346(2)	C7	C20	1.530(3)
O2	C4	1.218(2)	C9	C10	1.238(4)
O3	C21	1.202(2)	C9	C1B	1.168(9)
O4	C21	1.333(2)	C12	C13	1.540(2)
O4	C22	1.443(3)	C12	C21	1.508(3)
O5	C28	1.345(2)	N12	C14	1.398(3)
O5	C29	1.481(2)	C14	C15	1.398(3)
O6	C28	1.219(2)	C14	C19	1.386(3)
O7	C33	1.193(2)	C15	C16	1.383(3)
C8	O9	1.447(3)	C16	C17	1.388(3)
N1	C4	1.357(2)	C17	C18	1.388(3)
N1	C5	1.471(2)	C18	C19	1.389(3)
N1	C12	1.460(2)	C24	C25	1.319(3)
C2	C26	1.578(2)	C25	C26	1.522(3)
C2	C27	1.564(2)	C26	C35	1.528(3)
C2	C34	1.540(2)	C26	C36	1.539(3)
C2	C37	1.525(3)	C27	N43	1.453(2)
N3	C27	1.476(2)	C29	C30	1.517(3)
N3	C28	1.355(2)	C29	C31	1.522(3)
N3	C32	1.457(2)	C29	C44	1.524(3)
O9	C33	1.325(2)	C32	C33	1.513(3)
C1	C3	1.524(3)	C32	C34	1.539(2)
C3	C11	1.510(3)	C37	C38	1.378(3)
C3	C23	1.521(3)	C37	C42	1.400(2)
C5	C6	1.560(2)	C38	C39	1.393(3)
C5	N12	1.452(3)	C39	C40	1.391(3)
C6	C7	1.578(2)	C40	C41	1.392(3)
C6	C13	1.536(3)	C41	C42	1.387(3)
C6	C15	1.519(3)	C42	N43	1.394(2)
C7	C9	1.499(3)			

Table A20. Bond Angles.

Atom	Atom	Atom	Angle/°	Atom	Atom	Atom	Angle/°
C4	O1	C3	121.35(14)	C19	C14	C15	120.6(2)
C21	O4	C22	115.66(16)	C14	C15	C6	109.22(17)
C28	O5	C29	120.82(14)	C16	C15	C6	130.53(17)
C4	N1	C5	120.99(15)	C16	C15	C14	120.23(18)
C4	N1	C12	123.64(15)	C15	C16	C17	119.40(18)
C12	N1	C5	115.32(14)	C18	C17	C16	119.9(2)
C27	C2	C26	113.69(14)	C17	C18	C19	121.2(2)

C34	C2	C26	113.16(13)	C14	C19	C18	118.41(19)
C34	C2	C27	104.47(15)	O3	C21	O4	123.74(19)
C37	C2	C26	113.15(16)	O3	C21	C12	125.34(17)
C37	C2	C27	99.95(13)	O4	C21	C12	110.84(17)
C37	C2	C34	111.38(15)	C24	C25	C26	127.1(2)
C28	N3	C27	120.20(14)	C25	C26	C2	109.13(16)
C28	N3	C32	124.30(15)	C25	C26	C35	111.20(15)
C32	N3	C27	115.01(14)	C25	C26	C36	107.52(16)
C33	O9	C8	115.78(18)	C35	C26	C2	109.86(15)
O1	C3	C1	110.69(16)	C35	C26	C36	108.49(17)
O1	C3	C11	108.97(15)	C36	C26	C2	110.63(14)
O1	C3	C23	102.03(16)	N3	C27	C2	102.53(13)
C11	C3	C1	112.30(18)	N43	C27	C2	104.45(15)
C11	C3	C23	111.23(18)	N43	C27	N3	113.31(13)
C23	C3	C1	111.13(17)	O5	C28	N3	110.07(15)
O1	C4	N1	109.89(15)	O6	C28	O5	126.51(16)
O2	C4	O1	126.49(16)	O6	C28	N3	123.41(16)
O2	C4	N1	123.60(18)	O5	C29	C30	109.13(14)
N1	C5	C6	102.30(14)	O5	C29	C31	101.96(16)
N12	C5	N1	113.85(14)	O5	C29	C44	110.05(16)
N12	C5	C6	104.15(16)	C30	C29	C31	111.14(18)
C5	C6	C7	113.50(15)	C30	C29	C44	112.98(17)
C13	C6	C5	104.55(15)	C31	C29	C44	111.01(17)
C13	C6	C7	113.32(15)	N3	C32	C33	111.46(15)
C15	C6	C5	100.24(14)	N3	C32	C34	103.06(14)
C15	C6	C7	113.00(16)	C33	C32	C34	109.96(14)
C15	C6	C13	111.22(16)	O7	C33	O9	123.61(19)
C9	C7	C6	108.09(16)	O7	C33	C32	125.98(17)
C9	C7	C1A	107.9(2)	O9	C33	C32	110.37(17)
C9	C7	C20	110.98(18)	C32	C34	C2	105.16(13)
C1A	C7	C6	110.09(16)	C38	C37	C2	130.70(16)
C20	C7	C6	111.85(17)	C38	C37	C42	120.12(17)
C20	C7	C1A	107.87(18)	C42	C37	C2	109.13(16)
C10	C9	C7	130.8(3)	C37	C38	C39	119.46(17)
C1B	C9	C7	151.2(5)	C40	C39	C38	120.0(2)
N1	C12	C13	102.26(14)	C39	C40	C41	121.07(18)
N1	C12	C21	111.68(15)	C42	C41	C40	118.26(17)
C21	C12	C13	109.38(14)	C41	C42	C37	121.00(18)
C6	C13	C12	104.96(14)	C41	C42	N43	128.76(16)
C14	N12	C5	108.15(15)	N43	C42	C37	110.20(15)
N12	C14	C15	109.93(18)	C42	N43	C27	107.62(14)
C19	C14	N12	129.42(18)				

Table A21. Torsion Angles.

A	B	C	D	Angle/°	A	B	C	D	Angle/°
C8	O9	C33	O7	3.8(3)	C16	C17	C18	C19	-3.0(3)
C8	O9	C33	C32	-178.56(16)	C17	C18	C19	C14	0.8(3)
N1	C5	C6	C7	-147.28(16)	C19	C14	C15	C6	176.94(17)
N1	C5	C6	C13	-23.31(18)	C19	C14	C15	C16	-4.4(3)
N1	C5	C6	C15	91.96(16)	C1A	C7	C9	C10	130.9(4)
N1	C5	N12	C14	-82.45(18)	C1A	C7	C9	C1B	-5.4(10)
N1	C12	C13	C6	-28.88(19)	C20	C7	C9	C10	12.9(4)
N1	C12	C21	O3	-35.0(2)	C20	C7	C9	C1B	-123.4(9)
N1	C12	C21	O4	148.13(15)	C21	C12	C13	C6	-147.39(15)
C2	C27	N43	C42	29.49(17)	C22	O4	C21	O3	1.5(3)
C2	C37	C38	C39	179.46(18)	C22	O4	C21	C12	178.40(15)
C2	C37	C42	C41	179.70(17)	C24	C25	C26	C2	107.7(2)
C2	C37	C42	N43	1.6(2)	C24	C25	C26	C35	-13.6(3)
N3	C27	N43	C42	-81.29(18)	C24	C25	C26	C36	-132.2(2)
N3	C32	C33	O7	-21.8(3)	C26	C2	C27	N3	-147.33(14)
N3	C32	C33	O9	160.62(14)	C26	C2	C27	N43	94.25(17)
N3	C32	C34	C2	-27.07(18)	C26	C2	C34	C32	155.95(15)
C3	O1	C4	O2	-16.0(3)	C26	C2	C37	C38	77.2(2)
C3	O1	C4	N1	165.28(15)	C26	C2	C37	C42	-105.58(17)
C4	O1	C3	C1	63.4(2)	C27	C2	C26	C25	62.08(19)
C4	O1	C3	C11	-60.6(2)	C27	C2	C26	C35	-175.77(15)
C4	O1	C3	C23	-178.27(17)	C27	C2	C26	C36	-56.0(2)
C4	N1	C5	C6	-172.27(17)	C27	C2	C34	C32	31.77(18)
C4	N1	C5	N12	-60.5(2)	C27	C2	C37	C38	-161.60(19)
C4	N1	C12	C13	-167.75(17)	C27	C2	C37	C42	15.67(18)
C4	N1	C12	C21	-50.9(2)	C27	N3	C28	O5	166.38(15)
C5	N1	C4	O1	169.11(16)	C27	N3	C28	O6	-12.6(3)
C5	N1	C4	O2	-9.6(3)	C27	N3	C32	C33	130.46(15)
C5	N1	C12	C13	14.8(2)	C27	N3	C32	C34	12.58(19)
C5	N1	C12	C21	131.62(16)	C28	O5	C29	C30	-58.6(2)
C5	C6	C7	C9	-175.79(19)	C28	O5	C29	C31	-176.27(16)
C5	C6	C7	C1A	-58.2(2)	C28	O5	C29	C44	65.9(2)
C5	C6	C7	C20	61.7(2)	C28	N3	C27	C2	-165.41(15)
C5	C6	C13	C12	32.93(19)	C28	N3	C27	N43	-53.5(2)
C5	C6	C15	C14	17.50(19)	C28	N3	C32	C33	-57.6(2)
C5	C6	C15	C16	-161.03(19)	C28	N3	C32	C34	-175.48(16)
C5	N12	C14	C15	-17.5(2)	C29	O5	C28	O6	-15.2(3)
C5	N12	C14	C19	164.52(19)	C29	O5	C28	N3	165.93(15)
C6	C5	N12	C14	28.15(18)	C32	N3	C27	C2	6.89(18)

C6	C7	C9	C10	-110.1(3)
C6	C7	C9	C1B	113.7(9)
C6	C15	C16	C17	-179.48(19)
C7	C6	C13	C12	157.02(16)
C7	C6	C15	C14	-103.62(18)
C7	C6	C15	C16	77.8(2)
C12	N1	C4	O1	-8.2(3)
C12	N1	C4	O2	173.03(18)
C12	N1	C5	C6	5.3(2)
C12	N1	C5	N12	117.01(17)
C13	C6	C7	C9	65.2(2)
C13	C6	C7	C1A	-177.22(18)
C13	C6	C7	C20	-57.3(2)
C13	C6	C15	C14	127.62(17)
C13	C6	C15	C16	-50.9(3)
C13	C12	C21	O3	77.5(2)
C13	C12	C21	O4	-99.40(17)
N12	C5	C6	C7	93.92(18)
N12	C5	C6	C13	-142.11(15)
N12	C5	C6	C15	-26.84(17)
N12	C14	C15	C6	-1.2(2)
N12	C14	C15	C16	177.50(17)
N12	C14	C19	C18	-179.42(19)
C14	C15	C16	C17	2.1(3)
C15	C6	C7	C9	-62.5(2)
C15	C6	C7	C1A	55.1(2)
C15	C6	C7	C20	175.02(17)
C15	C6	C13	C12	-74.40(18)
C15	C14	C19	C18	2.8(3)
C15	C16	C17	C18	1.5(3)
C32	N3	C27	N43	118.85(16)
C32	N3	C28	O5	-5.2(2)
C32	N3	C28	O6	175.90(17)
C33	C32	C34	C2	-146.00(15)
C34	C2	C26	C25	-56.9(2)
C34	C2	C26	C35	65.3(2)
C34	C2	C26	C36	-174.99(17)
C34	C2	C27	N3	-23.50(16)
C34	C2	C27	N43	-141.91(14)
C34	C2	C37	C38	-51.7(3)
C34	C2	C37	C42	125.61(16)
C34	C32	C33	O7	91.9(2)
C34	C32	C33	O9	-85.74(18)
C37	C2	C26	C25	175.21(15)
C37	C2	C26	C35	-62.63(19)
C37	C2	C26	C36	57.1(2)
C37	C2	C27	N3	91.81(15)
C37	C2	C27	N43	-26.60(17)
C37	C2	C34	C32	-75.24(18)
C37	C38	C39	C40	-0.7(3)
C37	C42	N43	C27	-20.06(19)
C38	C37	C42	C41	-2.7(3)
C38	C37	C42	N43	179.16(16)
C38	C39	C40	C41	-0.9(3)
C39	C40	C41	C42	0.7(3)
C40	C41	C42	C37	1.1(3)
C40	C41	C42	N43	178.87(18)
C41	C42	N43	C27	161.98(18)
C42	C37	C38	C39	2.4(3)

Table A22. Hydrogen Atom Coordinates (Å×10^4) and Isotropic Displacement Parameters (Å^2×10^3).

Atom	***x***	***y***	***z***	**U(eq)**
H8A	9024	2369	2093	64
H8B	8125	3251	2518	64
H8C	9708	3658	2333	64
H1A	-3739	6161	6736	50
H1B	-4325	5018	7110	50
H1C	-3848	4843	6403	50
H5	977	8202	5972	23
H9A	4169	7295	4505	56

H9B	4967	6980	5242	56
H10A	6169	7542	5554	55
H10B	6408	6986	4842	55
H11A	-579	5549	7864	43
H11B	-2249	5545	8030	43
H11C	-1686	6614	7598	43
H12	1101	4702	5844	21
H13A	3504	6363	6205	26
H13B	3365	5402	5619	26
H12A	-1240(20)	7790(20)	5253(11)	27
H16	2888	5310	4438	28
H17	1349	4697	3519	36
H18	-990	5556	3292	39
H19	-1910	6909	4016	36
H1AA	2033	8678	4443	53
H1AB	3196	9669	4751	53
H1AC	1704	9432	5066	53
H20A	3079	8980	6135	49
H20B	4538	9341	5820	49
H20C	4455	8064	6187	49
H22A	2050	3523	7748	51
H22B	3727	3613	7597	51
H22C	2794	2398	7418	51
H23A	-2111	3187	6830	46
H23B	-2486	3383	7552	46
H23C	-816	3482	7392	46
H24A	11316	7676	541	45
H24B	11293	8534	1186	45
H25	8929	8964	911	32
H27	6651	8236	964	19
H30A	5397	5623	2933	37
H30B	3809	5645	3188	37
H30C	4275	6719	2733	37
H31A	3501	3323	1954	49
H31B	3329	3515	2701	49
H31C	4930	3562	2458	49
H32	6319	4749	790	20
H34A	8376	5297	326	22
H34B	8956	6205	906	22
H35A	9871	6689	-255	40
H35B	10097	8010	-555	40
H35C	8726	7181	-835	40

H36A	6944	8815	-657	37
H36B	8312	9677	-414	37
H36C	7014	9473	29	37
H38	7296	5367	-823	24
H39	5275	4935	-1588	30
H40	3000	5867	-1514	31
H41	2689	7210	-666	28
H43	4130(20)	7970(20)	469(10)	22
H44A	2054	6330	1899	42
H44B	1508	5301	2361	42
H44C	1757	4969	1636	42
H1BA	4792	7913	4112	52
H1BB	5919	6909	4491	52

9.4 X-Ray Crystallographic Data for Aszonalenin (+)-**130**

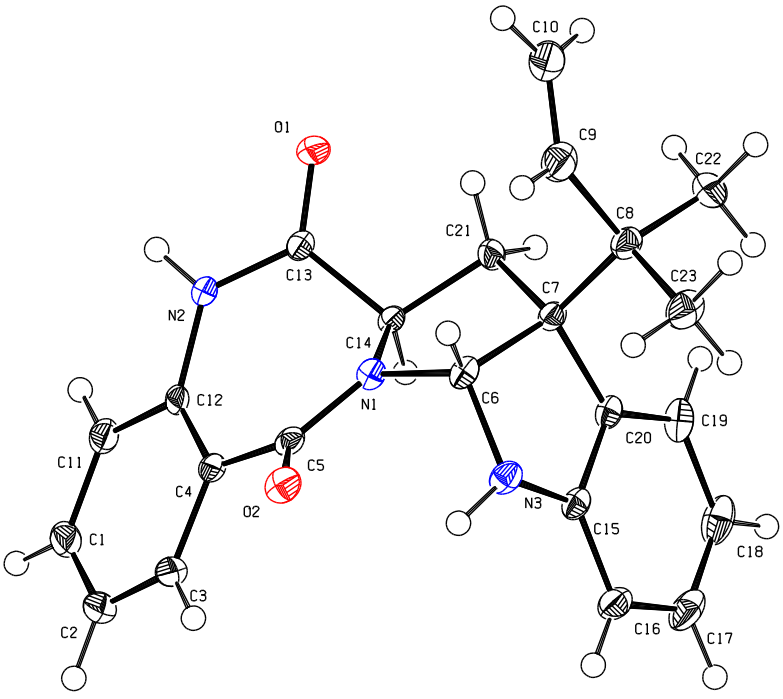

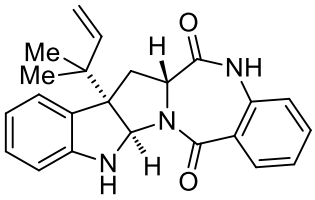

ORTEP view[111] of (+)-**130**, the thermal ellipsoids are drawn at the 50% probability level.

Database Reference. Crystallographic data have been deposited with the Cambridge Crystallographic Data Centre (CCDC) as supplementary publication no. CCDC-1019993. Data can be obtained free of charge on application to CCDC.

Experimental. A suitable clear, colorless prism was selected, mounted in perfluoroalkyl polyether oil on polyimide Micromounts (supplied by MiTeGen) and measured on a Bruker/Nonius Kappa Apex II diffractometer with a Bruker Apex II area detector. The detector

type was a CCD area detector. The crystal was kept at 100.0(2) K during data collection. Using Olex2,[112] the structure was solved with the XS structure solution program[113] using Direct Methods and refined with the XL refinement package[113] using Least Squares minimization. The absolute stereochemistry was not determined by X-Ray diffraction.

Table A23. Crystal data and structure refinement.

Empirical formula	$C_{23}H_{23}N_3O_2$
Formula weight	373.44
Temperature/K	100.0(2)
Crystal system	monoclinic
Space group	$P2_1$
a/Å	9.0926(7)
b/Å	10.6133(8)
c/Å	9.8276(8)
α/°	90
β/°	96.206(2)
γ/°	90
Volume/Å^3	942.83(13)
Z	2
ρ_{calc}g/cm^3	1.315
μ/mm^{-1}	0.085
F(000)	396.0
Crystal size/mm^3	0.32 × 0.2 × 0.12
Radiation	MoKα (λ = 0.71073)
2Θ range for data collection/°	4.168 to 61.114
Index ranges	$-12 \leq h \leq 12$, $-15 \leq k \leq 6$, $-13 \leq l \leq 14$
Reflections collected	11450
Independent reflections	3893 [R_{int} = 0.0178, R_{sigma} = 0.0190]
Data/restraints/parameters	3893/3/261
Goodness-of-fit on F^2	1.052
Final R indexes [I>=2σ (I)]	R_1 = 0.0341, wR_2 = 0.0898
Final R indexes [all data]	R_1 = 0.0356, wR_2 = 0.0911
Largest diff. peak/hole / e Å^{-3}	0.47/-0.20
Flack parameter	0.1(4)

Table A24. Fractional Atomic Coordinates (×10^4) and Equivalent Isotropic Displacement Parameters (Å^2×10^3). U_{eq} is defined as 1/3 of the trace of the orthogonalised U_{IJ} tensor.

Atom	***x***	***y***	***z***	**U(eq)**
O1	1930.4(13)	5318.4(15)	3283.8(13)	24.1(3)
O2	6480.3(13)	8473.0(13)	3554.5(12)	20.2(2)

N1	4614.2(14)	7362.6(14)	2434.7(13)	13.9(2)
N2	4283.0(14)	5076.7(14)	4203.0(13)	14.6(3)
N3	5363.7(16)	8932.8(14)	816.1(14)	17.1(3)
C1	8183.7(19)	4179(2)	4997.9(17)	25.5(4)
C2	8928.9(18)	5259(2)	4655.0(18)	27.0(4)
C3	8129.2(18)	6282(2)	4125.0(17)	21.9(3)
C4	6573.9(17)	6259.4(17)	3901.0(15)	15.1(3)
C5	5872.4(16)	7437.4(17)	3309.4(15)	15.0(3)
C6	4168.6(17)	8471.0(15)	1545.0(15)	15.0(3)
C7	3022.5(16)	7902.7(16)	412.7(15)	14.5(3)
C8	1722.4(18)	8838.8(18)	-65.7(17)	19.7(3)
C9	960(2)	9261(2)	1172.4(19)	26.1(4)
C10	-313(2)	8878(2)	1531(2)	32.8(5)
C11	6648.9(18)	4136.4(18)	4802.8(16)	19.8(3)
C12	5837.1(16)	5168.7(16)	4255.1(14)	14.1(3)
C13	3240.5(16)	5510.0(16)	3218.6(15)	14.4(3)
C14	3799.9(16)	6206.2(15)	2010.1(15)	12.6(3)
C15	5383.3(17)	8222.8(16)	-375.6(15)	15.5(3)
C16	6520.5(18)	8117.9(18)	-1212.1(17)	20.8(3)
C17	6276(2)	7363(2)	-2377.2(18)	26.5(4)
C18	4951(2)	6734.2(19)	-2686.6(18)	25.9(4)
C19	3813(2)	6853.0(17)	-1842.6(17)	20.6(3)
C20	4028.0(17)	7617.7(15)	-694.0(15)	14.8(3)
C21	2488.3(17)	6688.0(17)	1043.9(16)	16.7(3)
C22	643.2(18)	8207(2)	-1163.7(19)	26.7(4)
C23	2329(2)	10032.4(19)	-690(2)	25.5(4)

Table A25. Anisotropic Displacement Parameters ($Å^2 \times 10^3$). The Anisotropic displacement factor exponent takes the form: $-2\pi^2[h^2a^{*2}U_{11}+2hka^*b^*U_{12}+\ldots]$.

Atom	**U_{11}**	**U_{22}**	**U_{33}**	**U_{23}**	**U_{13}**	**U_{12}**
O1	15.0(5)	34.4(8)	23.2(6)	11.8(6)	3.9(4)	-0.9(5)
O2	23.7(6)	20.4(6)	16.6(5)	-6.9(5)	3.6(4)	-6.1(5)
N1	17.1(6)	11.9(6)	12.8(6)	-0.9(5)	2.1(4)	-1.7(5)
N2	14.9(5)	17.4(6)	11.6(5)	2.9(5)	2.2(4)	-0.1(5)
N3	20.5(6)	15.5(6)	15.8(6)	-1.2(5)	4.0(5)	-5.5(5)
C1	20.0(7)	39.4(11)	17.1(7)	2.9(7)	2.0(6)	11.4(8)
C2	15.7(7)	46.2(13)	19.1(7)	2.8(8)	2.0(6)	5.4(8)
C3	15.2(7)	35.1(10)	15.4(7)	-0.2(7)	2.2(5)	-2.7(7)
C4	14.6(6)	21.4(8)	9.7(6)	-2.5(6)	2.6(5)	-0.2(6)
C5	16.3(6)	18.2(7)	11.1(6)	-3.3(6)	4.7(5)	-2.0(6)
C6	20.0(7)	12.4(7)	13.1(6)	0.4(5)	4.6(5)	0.1(6)
C7	15.2(6)	15.2(7)	13.5(6)	2.8(5)	3.4(5)	0.1(5)

C8	19.3(7)	21.6(8)	18.8(7)	7.8(6)	5.7(6)	5.4(6)
C9	27.7(8)	28.8(10)	22.7(8)	5.4(7)	6.3(6)	9.6(8)
C10	27.8(9)	48.4(14)	22.7(8)	7.2(9)	4.9(7)	8.8(9)
C11	21.4(7)	24.2(9)	14.1(7)	2.0(6)	3.4(5)	5.2(7)
C12	14.7(6)	19.7(8)	7.9(6)	-1.0(5)	1.2(5)	2.7(6)
C13	16.3(6)	14.9(7)	12.5(6)	1.3(5)	3.3(5)	0.6(6)
C14	13.8(6)	13.3(6)	10.8(6)	-0.3(5)	2.9(5)	-2.3(5)
C15	19.1(7)	14.1(7)	13.7(6)	2.6(5)	4.1(5)	1.1(6)
C16	20.7(7)	22.0(8)	20.8(7)	6.4(7)	7.7(6)	4.1(6)
C17	34.5(9)	27.0(9)	20.4(8)	6.8(7)	14.1(7)	13.9(8)
C18	44.3(11)	19.2(8)	15.1(7)	-1.4(6)	6.6(7)	7.8(8)
C19	30.9(8)	15.5(7)	14.5(7)	0.5(6)	-0.8(6)	0.4(6)
C20	19.5(7)	13.0(7)	12.2(6)	1.7(5)	2.7(5)	1.3(6)
C21	15.0(6)	18.9(7)	15.6(7)	5.9(6)	-0.9(5)	-2.8(6)
C22	17.9(7)	35.8(11)	25.7(8)	9.1(8)	-0.9(6)	2.2(7)
C23	28.6(8)	21.2(9)	28.1(8)	10.7(7)	9.1(7)	7.8(7)

Table A26. Bond Lengths.

Atom	Atom	Length/Å	Atom	Atom	Length/Å
O1	C13	1.2170(19)	C7	C8	1.577(2)
O2	C5	1.242(2)	C7	C20	1.525(2)
N1	C5	1.3569(19)	C7	C21	1.532(2)
N1	C6	1.495(2)	C8	C9	1.531(2)
N1	C14	1.470(2)	C8	C22	1.532(3)
N2	C12	1.4118(19)	C8	C23	1.536(3)
N2	C13	1.3593(19)	C9	C10	1.310(3)
N3	C6	1.450(2)	C11	C12	1.396(2)
N3	C15	1.394(2)	C13	C14	1.532(2)
C1	C2	1.391(3)	C14	C21	1.530(2)
C1	C11	1.389(2)	C15	C16	1.393(2)
C2	C3	1.377(3)	C15	C20	1.395(2)
C3	C4	1.408(2)	C16	C17	1.396(3)
C4	C5	1.493(2)	C17	C18	1.382(3)
C4	C12	1.400(2)	C18	C19	1.400(3)
C6	C7	1.561(2)	C19	C20	1.387(2)

Table A27. Bond Angles.

Atom	Atom	Atom	Angle/°	Atom	Atom	Atom	Angle/°
C5	N1	C6	118.75(13)	C22	C8	C7	109.68(15)
C5	N1	C14	126.36(14)	C22	C8	C23	108.07(14)
C14	N1	C6	113.22(12)	C23	C8	C7	110.40(13)

C13	N2	C12	128.36(13)	C10	C9	C8	127.8(2)
C15	N3	C6	108.10(13)	C1	C11	C12	120.60(17)
C11	C1	C2	120.13(18)	C4	C12	N2	123.51(15)
C3	C2	C1	119.35(16)	C11	C12	N2	116.43(15)
C2	C3	C4	121.73(18)	C11	C12	C4	119.83(14)
C3	C4	C5	115.23(15)	O1	C13	N2	121.15(14)
C12	C4	C3	118.36(16)	O1	C13	C14	122.04(14)
C12	C4	C5	126.41(14)	N2	C13	C14	116.78(13)
O2	C5	N1	120.11(16)	N1	C14	C13	112.45(12)
O2	C5	C4	120.21(14)	N1	C14	C21	103.42(13)
N1	C5	C4	119.55(15)	C21	C14	C13	109.91(12)
N1	C6	C7	103.34(12)	N3	C15	C20	110.24(13)
N3	C6	N1	112.62(13)	C16	C15	N3	128.06(16)
N3	C6	C7	104.87(12)	C16	C15	C20	121.66(15)
C6	C7	C8	112.98(13)	C15	C16	C17	117.87(17)
C20	C7	C6	100.34(11)	C18	C17	C16	121.02(16)
C20	C7	C8	113.60(12)	C17	C18	C19	120.58(17)
C20	C7	C21	111.26(14)	C20	C19	C18	119.12(17)
C21	C7	C6	104.65(12)	C15	C20	C7	109.38(13)
C21	C7	C8	113.00(13)	C19	C20	C7	130.84(15)
C9	C8	C7	109.67(13)	C19	C20	C15	119.71(15)
C9	C8	C22	112.15(15)	C14	C21	C7	105.81(12)
C9	C8	C23	106.82(16)				

Table A28. Torsion Angles.

A	**B**	**C**	**D**	**Angle/°**	**A**	**B**	**C**	**D**	**Angle/°**
O1	C13	C14	N1	119.66(18)	C6	C7	C20	C19	163.44(17)
O1	C13	C14	C21	5.0(2)	C6	C7	C21	C14	-31.03(15)
N1	C6	C7	C8	144.26(12)	C7	C8	C9	C10	-103.5(2)
N1	C6	C7	C20	-94.44(13)	C8	C7	C20	C15	107.48(15)
N1	C6	C7	C21	20.94(15)	C8	C7	C20	C19	-75.7(2)
N1	C14	C21	C7	28.49(15)	C8	C7	C21	C14	-154.34(13)
N2	C13	C14	N1	-62.36(18)	C11	C1	C2	C3	0.2(3)
N2	C13	C14	C21	-176.99(14)	C12	N2	C13	O1	177.09(17)
N3	C6	C7	C8	-97.57(14)	C12	N2	C13	C14	-0.9(2)
N3	C6	C7	C20	23.72(15)	C12	C4	C5	O2	149.56(15)
N3	C6	C7	C21	139.10(13)	C12	C4	C5	N1	-34.5(2)
N3	C15	C16	C17	-178.79(17)	C13	N2	C12	C4	42.3(2)
N3	C15	C20	C7	-2.43(18)	C13	N2	C12	C11	-143.25(17)
N3	C15	C20	C19	-179.65(15)	C13	C14	C21	C7	148.75(13)
C1	C2	C3	C4	-0.9(3)	C14	N1	C5	O2	177.82(13)
C1	C11	C12	N2	-174.81(15)	C14	N1	C5	C4	1.9(2)

C1	C11	C12	C4	-0.1(2)
C2	C1	C11	C12	0.4(3)
C2	C3	C4	C5	-179.45(16)
C2	C3	C4	C12	1.2(2)
C3	C4	C5	O2	-29.8(2)
C3	C4	C5	N1	146.17(14)
C3	C4	C12	N2	173.67(14)
C3	C4	C12	C11	-0.6(2)
C5	N1	C6	N3	50.26(18)
C5	N1	C6	C7	162.88(13)
C5	N1	C14	C13	60.94(19)
C5	N1	C14	C21	179.46(14)
C5	C4	C12	N2	-5.6(2)
C5	C4	C12	C11	-179.92(15)
C6	N1	C5	O2	13.6(2)
C6	N1	C5	C4	-162.38(13)
C6	N1	C14	C13	-134.06(13)
C6	N1	C14	C21	-15.55(15)
C6	N3	C15	C16	-163.23(16)
C6	N3	C15	C20	18.97(18)
C6	C7	C8	C9	-55.90(18)
C6	C7	C8	C22	-179.48(13)
C6	C7	C8	C23	61.55(18)
C6	C7	C20	C15	-13.37(16)
C14	N1	C6	N3	-115.98(14)
C14	N1	C6	C7	-3.36(15)
C15	N3	C6	N1	84.73(16)
C15	N3	C6	C7	-26.95(17)
C15	C16	C17	C18	-0.4(3)
C16	C15	C20	C7	179.61(15)
C16	C15	C20	C19	2.4(2)
C16	C17	C18	C19	0.8(3)
C17	C18	C19	C20	0.4(3)
C18	C19	C20	C7	-178.47(16)
C18	C19	C20	C15	-1.9(2)
C20	C7	C8	C9	-169.36(15)
C20	C7	C8	C22	67.06(17)
C20	C7	C8	C23	-51.91(19)
C20	C7	C21	C14	76.48(15)
C20	C15	C16	C17	-1.2(2)
C21	C7	C8	C9	62.68(19)
C21	C7	C8	C22	-60.90(17)
C21	C7	C8	C23	-179.88(15)
C21	C7	C20	C15	-123.66(14)
C21	C7	C20	C19	53.1(2)
C22	C8	C9	C10	18.6(3)
C23	C8	C9	C10	136.8(2)

Table A29. Hydrogen Atom Coordinates (Å×10^4) and Isotropic Displacement Parameters (Å^2×10^3).

Atom	***x***	***y***	***z***	**U(eq)**
H2	3950(20)	4580(20)	4810(20)	18
H3	6180(20)	9100(20)	1340(20)	21
H1	8726	3470	5366	31
H2A	9979	5291	4785	32
H3A	8641	7023	3905	26
H6	3726	9157	2067	18
H9	1471	9873	1750	31
H10A	-876	8267	994	39
H10B	-674	9213	2328	39
H11	6147	3398	5044	24
H14	4431	5636	1508	15
H16	7433	8546	-996	25
H17	7032	7280	-2967	32
H18	4811	6217	-3479	31

H19	2905	6416	-2054	25
H21A	1630	6861	1555	20
H21B	2193	6058	323	20
H22A	1165	7986	-1952	40
H22B	-167	8790	-1455	40
H22C	241	7442	-787	40
H23A	3037	10444	-9	38
H23B	1512	10611	-968	38
H23C	2827	9804	-1491	38

9.5 X-Ray Crystallographic Data for Allene (+)-**219**

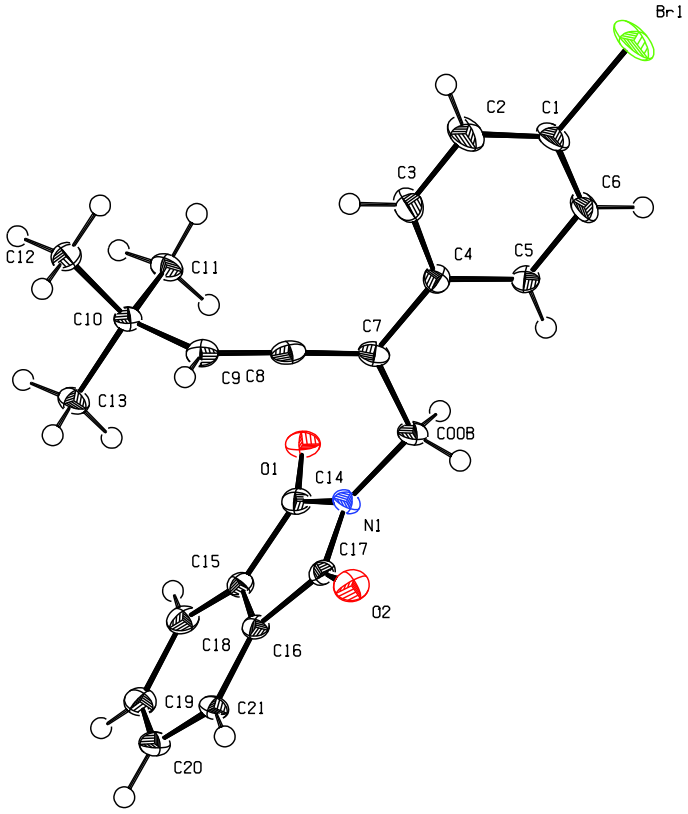

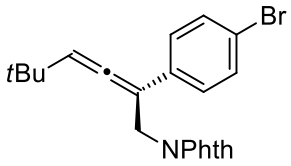

ORTEP view[111] of (+)-**219**, the thermal ellipsoids are drawn at the 50% probability level.

Database Reference. Crystallographic data have been deposited with the Cambridge Crystallographic Data Centre (CCDC) as supplementary publication no. CCDC-1437268. Data can be obtained free of charge on application to CCDC.

Experimental. A suitable clear, colorless block was selected, mounted in perfluoroalkyl polyether oil on polyimide Micromounts (supplied by MiTeGen) and measured on a Bruker/Nonius Kappa Apex II diffractometer with a Bruker Apex II area detector. The detector

type was a CCD area detector. The crystal was kept at 100.0(2) K during data collection. Using Olex2,[112] the structure was solved with the XS structure solution program[113] using Direct Methods and refined with the XL refinement package[113] using Least Squares minimization. The absolute stereochemistry was not determined by X-Ray diffraction.

Table A30. Crystal data and structure refinement.

Empirical formula	$C_{22}H_{20}BrNO_2$
Formula weight	410.30
Temperature/K	100.0(2)
Crystal system	monoclinic
Space group	$P2_1$
a/Å	8.6651(6)
b/Å	5.8524(3)
c/Å	18.9495(10)
α/°	90
β/°	93.712(5)
γ/°	90
Volume/Å^3	958.94(10)
Z	2
ρ_{calc}g/cm^3	1.421
μ/mm^{-1}	2.159
F(000)	420.0
Crystal size/mm^3	0.28 × 0.11 × 0.07
Radiation	MoKα (λ = 0.71073)
2Θ range for data collection/°	4.71 to 61.33
Index ranges	$-12 \leq h \leq 12$, $-8 \leq k \leq 8$, $-26 \leq l \leq 25$
Reflections collected	5272
Independent reflections	5272 [R_{int} = 0.0688, R_{sigma} = 0.0274]
Data/restraints/parameters	5272/73/239
Goodness-of-fit on F^2	1.091
Final R indexes [I>=2σ (I)]	R_1 = 0.0589, wR_2 = 0.1301
Final R indexes [all data]	R_1 = 0.0720, wR_2 = 0.1410
Largest diff. peak/hole / e Å^{-3}	0.47/-0.66
Flack parameter	0.047(15)

Table A31. Fractional Atomic Coordinates (×10^4) and Equivalent Isotropic Displacement Parameters (Å^2×10^3). U_{eq} is defined as 1/3 of the trace of the orthogonalised U_{IJ} tensor.

Atom	***x***	***y***	***z***	**U(eq)**
Br1	1991.3(12)	-927.0(15)	5502.3(4)	43.3(3)
O1	3650(5)	3681(8)	1127(2)	21.4(11)

O2	106(5)	8881(11)	1816(2)	23.8(10)
N1	1751(6)	5888(9)	1596(3)	17.4(11)
C00B	1498(7)	4479(11)	2208(3)	20.9(15)
C1	2163(9)	941(12)	4687(4)	24.8(14)
C2	3115(10)	2832(14)	4729(4)	33.2(18)
C3	3211(8)	4191(17)	4134(3)	28.2(15)
C4	2379(7)	3669(11)	3497(3)	17.1(12)
C5	1435(8)	1726(12)	3475(3)	18.0(12)
C6	1331(8)	339(12)	4075(3)	22.0(14)
C7	2519(8)	5114(11)	2859(3)	17.9(12)
C8	3482(8)	6842(12)	2846(3)	18.7(13)
C9	4460(7)	8512(10)	2793(3)	18.9(13)
C10	6083(7)	8323(11)	2546(3)	17.5(12)
C11	6566(8)	5828(11)	2484(4)	20.7(13)
C12	7201(8)	9546(11)	3079(4)	22.5(15)
C13	6111(8)	9492(11)	1820(3)	19.4(14)
C14	2821(8)	5350(11)	1101(3)	18.5(13)
C15	2658(7)	7178(11)	552(3)	16.5(12)
C16	1584(6)	8732(11)	762(3)	15.1(12)
C17	1020(7)	7964(11)	1450(3)	16.1(12)
C18	3377(8)	7401(12)	-77(3)	20.3(13)
C19	2954(8)	9314(18)	-493(3)	23.8(16)
C20	1888(8)	10892(12)	-279(3)	22.3(13)
C21	1161(8)	10622(11)	354(3)	17.5(13)

Table A32. Anisotropic Displacement Parameters ($Å^2 \times 10^3$). The Anisotropic displacement factor exponent takes the form: $-2\pi^2[h^2a^{*2}U_{11}+2hka^*b^*U_{12}+\ldots]$.

Atom	**U_{11}**	**U_{22}**	**U_{33}**	**U_{23}**	**U_{13}**	**U_{12}**
Br1	77.0(6)	37.1(4)	14.9(3)	10.3(4)	-5.7(3)	-21.7(5)
O1	24(2)	22(3)	18(2)	-1.1(19)	-3.5(17)	3.1(19)
O2	25(2)	31(3)	15.6(19)	-4(2)	2.5(16)	2(2)
N1	21(3)	19(3)	12(2)	4(2)	-1(2)	-2(2)
C00B	24(3)	24(4)	14(3)	5(2)	-5(2)	-3(3)
C1	35(4)	25(3)	14(3)	7(2)	-2(3)	-4(3)
C2	51(5)	34(4)	14(3)	5(3)	-5(3)	-13(3)
C3	38(4)	28(3)	18(3)	2(3)	-5(2)	-15(3)
C4	17(3)	20(3)	14(2)	-1(2)	2.9(19)	-1(2)
C5	20(3)	24(3)	10(3)	-1(2)	-1(2)	-4(2)
C6	29(3)	24(3)	14(3)	5(2)	2(2)	-7(3)
C7	22(3)	21(3)	11(3)	1(2)	0(2)	2(2)
C8	19(3)	27(3)	10(3)	-2(2)	-1(2)	6(3)
C9	22(3)	19(3)	15(3)	-3(2)	-1(2)	2(2)

C10	18(3)	19(3)	15(3)	2(2)	-2(2)	-1(2)
C11	26(3)	14(3)	21(3)	2(2)	-1(3)	3(2)
C12	25(3)	23(4)	18(3)	0(2)	-6(2)	-6(3)
C13	27(3)	18(4)	14(3)	1(2)	-2(2)	-1(2)
C14	20(3)	22(3)	13(3)	-1(2)	-2(2)	-1(3)
C15	18(3)	16(3)	14(3)	-1(2)	-4(2)	-3(2)
C16	16(3)	19(3)	10(2)	-1(2)	-1(2)	-1(2)
C17	14(3)	19(3)	15(3)	0(2)	-1(2)	-1(2)
C18	19(3)	28(3)	14(3)	-2(3)	0(2)	1(3)
C19	22(3)	38(5)	12(3)	5(3)	0.9(19)	-2(3)
C20	24(3)	24(3)	18(3)	5(2)	-6(3)	-2(3)
C21	21(3)	18(3)	12(3)	2(2)	-1(2)	1(2)

Table A33. Bond Lengths.

Atom	**Atom**	**Length/Å**	**Atom**	**Atom**	**Length/Å**
Br1	C1	1.907(7)	C7	C8	1.312(10)
O1	C14	1.212(8)	C8	C9	1.302(9)
O2	C17	1.211(8)	C9	C10	1.515(9)
N1	C00B	1.451(8)	C10	C11	1.525(9)
N1	C14	1.396(9)	C10	C12	1.531(9)
N1	C17	1.390(8)	C10	C13	1.538(9)
C00B	C7	1.518(9)	C14	C15	1.493(9)
C1	C2	1.379(10)	C15	C16	1.378(9)
C1	C6	1.371(10)	C15	C18	1.386(9)
C2	C3	1.387(10)	C16	C17	1.492(9)
C3	C4	1.398(8)	C16	C21	1.385(9)
C4	C5	1.400(9)	C18	C19	1.404(11)
C4	C7	1.487(9)	C19	C20	1.386(11)
C5	C6	1.403(9)	C20	C21	1.400(9)

Table A34. Bond Angles.

Atom	**Atom**	**Atom**	**Angle/°**	**Atom**	**Atom**	**Atom**	**Angle/°**
C14	N1	C00B	123.4(6)	C9	C10	C13	108.2(5)
C17	N1	C00B	124.4(6)	C11	C10	C12	109.5(5)
C17	N1	C14	112.1(5)	C11	C10	C13	109.7(5)
N1	C00B	C7	113.6(5)	C12	C10	C13	109.6(5)
C2	C1	Br1	119.3(5)	O1	C14	N1	124.9(6)
C6	C1	Br1	118.3(5)	O1	C14	C15	129.4(6)
C6	C1	C2	122.4(6)	N1	C14	C15	105.7(6)
C1	C2	C3	118.6(7)	C16	C15	C14	107.8(6)
C2	C3	C4	121.5(7)	C16	C15	C18	122.4(6)
C3	C4	C5	118.1(6)	C18	C15	C14	129.8(6)

C3	C4	C7	120.8(6)	C15	C16	C17	108.7(6)
C5	C4	C7	121.1(6)	C15	C16	C21	121.7(6)
C4	C5	C6	120.9(6)	C21	C16	C17	129.7(6)
C1	C6	C5	118.6(6)	O2	C17	N1	125.4(6)
C4	C7	C00B	116.6(5)	O2	C17	C16	129.1(6)
C8	C7	C00B	120.7(6)	N1	C17	C16	105.5(5)
C8	C7	C4	122.6(6)	C15	C18	C19	116.3(6)
C9	C8	C7	176.3(7)	C20	C19	C18	121.5(6)
C8	C9	C10	126.2(6)	C19	C20	C21	121.4(6)
C9	C10	C11	111.0(5)	C16	C21	C20	116.8(6)
C9	C10	C12	108.8(5)				

Table A35. Torsion Angles.

A	**B**	**C**	**D**	**Angle/°**	**A**	**B**	**C**	**D**	**Angle/°**
Br1	C1	C2	C3	-179.1(7)	C8	C9	C10	C11	-10.0(9)
Br1	C1	C6	C5	179.1(5)	C8	C9	C10	C12	-130.5(7)
O1	C14	C15	C16	-179.1(6)	C8	C9	C10	C13	110.4(7)
O1	C14	C15	C18	2.1(12)	C14	N1	C00B	C7	90.4(7)
N1	C00B	C7	C4	-177.1(5)	C14	N1	C17	O2	-175.9(6)
N1	C00B	C7	C8	2.1(9)	C14	N1	C17	C16	5.0(7)
N1	C14	C15	C16	2.9(7)	C14	C15	C16	C17	0.0(7)
N1	C14	C15	C18	-175.8(6)	C14	C15	C16	C21	-179.0(6)
C00B	N1	C14	O1	-0.4(10)	C14	C15	C18	C19	178.8(7)
C00B	N1	C14	C15	177.6(5)	C15	C16	C17	O2	178.0(7)
C00B	N1	C17	O2	1.4(10)	C15	C16	C17	N1	-2.9(7)
C00B	N1	C17	C16	-177.7(5)	C15	C16	C21	C20	-0.6(9)
C1	C2	C3	C4	-0.6(13)	C15	C18	C19	C20	0.6(11)
C2	C1	C6	C5	-1.2(12)	C16	C15	C18	C19	0.2(10)
C2	C3	C4	C5	0.2(12)	C17	N1	C00B	C7	-86.7(7)
C2	C3	C4	C7	-178.7(8)	C17	N1	C14	O1	176.9(6)
C3	C4	C5	C6	-0.2(10)	C17	N1	C14	C15	-5.0(7)
C3	C4	C7	C00B	-176.6(6)	C17	C16	C21	C20	-179.4(6)
C3	C4	C7	C8	4.2(10)	C18	C15	C16	C17	178.9(6)
C4	C5	C6	C1	0.7(11)	C18	C15	C16	C21	-0.2(10)
C5	C4	C7	C00B	4.6(9)	C18	C19	C20	C21	-1.3(11)
C5	C4	C7	C8	-174.6(6)	C19	C20	C21	C16	1.3(10)
C6	C1	C2	C3	1.2(13)	C21	C16	C17	O2	-3.1(11)
C7	C4	C5	C6	178.7(6)	C21	C16	C17	N1	176.0(6)

Table A36. Hydrogen Atom Coordinates ($Å \times 10^4$) and Isotropic Displacement Parameters ($Å^2 \times 10^3$).

Atom	***x***	***y***	***z***	**U(eq)**
H00A	1687	2895	2090	25
H00B	423	4610	2318	25
H2	3682	3188	5149	40
H3	3841	5478	4159	34
H5	869	1349	3058	22
H6	712	-960	4057	26
H9	4130	9960	2918	23
H11A	6618	5132	2943	31
H11B	7562	5749	2292	31
H11C	5821	5034	2177	31
H12A	6892	11113	3121	34
H12B	8229	9482	2918	34
H12C	7184	8811	3531	34
H13A	5457	8668	1480	29
H13B	7150	9506	1673	29
H13C	5744	11033	1854	29
H18	4098	6343	-216	24
H19	3400	9527	-922	29
H20	1649	12158	-562	27
H21	430	11662	495	21

9.6 X-Ray Crystallographic Data for Allene (+)-**220**

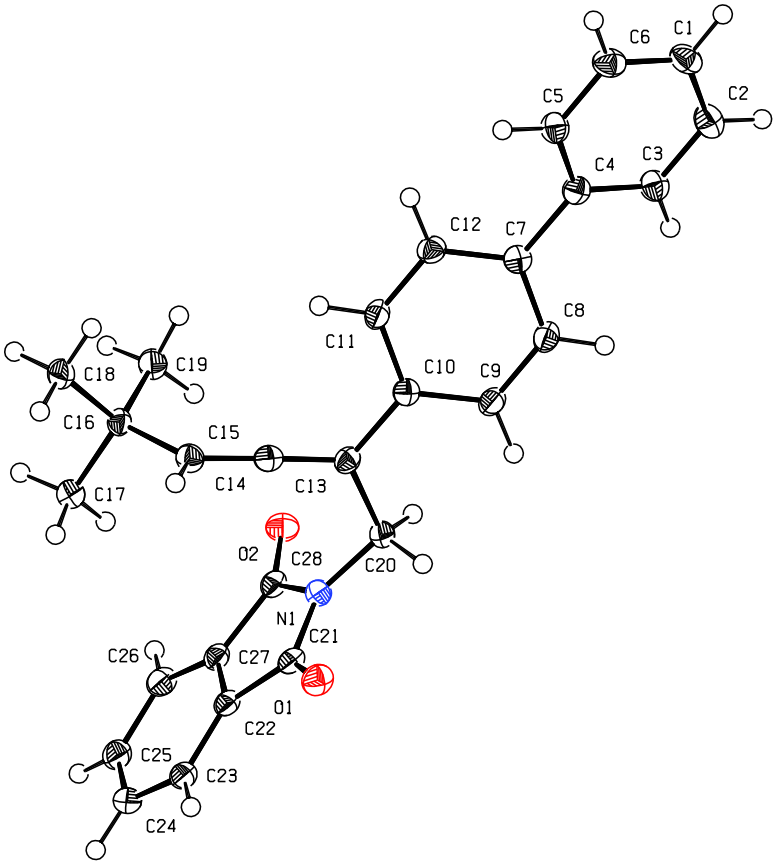

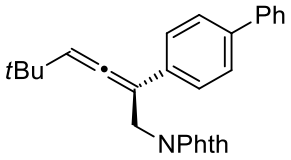

ORTEP view[111] of (+)-**220**, the thermal ellipsoids are drawn at the 50% probability level.

Database Reference. Crystallographic data have been deposited with the Cambridge Crystallographic Data Centre (CCDC) as supplementary publication no. CCDC-1446561. Data can be obtained free of charge on application to CCDC.

Experimental. A suitable clear, colorless block was selected, mounted in perfluoroalkyl polyether oil on polyimide Micromounts (supplied by MiTeGen) and measured on a Bruker/Nonius Kappa Apex II diffractometer with a Bruker Apex II area detector. The detector type was a CCD area detector. The crystal was kept at 100.0(2) K during data collection. Using Olex2,[112] the structure was solved with the XS structure solution program[113] using Direct Methods and refined with the XL refinement package[113] using Least Squares minimization. The absolute stereochemistry was not determined by X-Ray diffraction.

Table A37. Crystal data and structure refinement.

Empirical formula	$C_{28}H_{25}NO_2$
Formula weight	407.49
Temperature/K	100.0(2)
Crystal system	orthorhombic

Space group	$P2_12_12_1$
a/Å	5.99770(10)
b/Å	8.66900(10)
c/Å	42.0392(7)
α/°	90
β/°	90
γ/°	90
Volume/Å^3	2185.79(6)
Z	4
ρ_{calc}g/cm^3	1.238
μ/mm^{-1}	0.607
F(000)	864.0
Crystal size/mm^3	0.14 × 0.13 × 0.06
Radiation	CuKα (λ = 1.54178)
2Θ range for data collection/°	4.204 to 133.2
Index ranges	$-7 \leq h \leq 4$, $-10 \leq k \leq 10$, $-50 \leq l \leq 49$
Reflections collected	28660
Independent reflections	3862 [R_{int} = 0.0430, R_{sigma} = 0.0225]
Data/restraints/parameters	3862/0/283
Goodness-of-fit on F^2	1.075
Final R indexes [I>=2σ (I)]	R_1 = 0.0299, wR_2 = 0.0721
Final R indexes [all data]	R_1 = 0.0317, wR_2 = 0.0732
Largest diff. peak/hole / e Å^{-3}	0.10/-0.18
Flack parameter	-0.01(10)

Table A38. Fractional Atomic Coordinates (×10^4) and Equivalent Isotropic Displacement Parameters (Å^2×10^3). U_{eq} is defined as 1/3 of the trace of the orthogonalised U_{IJ} tensor.

Atom	*x*	*y*	*z*	U(eq)
O1	-3094(2)	7697.6(15)	4188.9(3)	25.6(3)
O2	1915(2)	4031.2(15)	4506.2(3)	25.3(3)
N1	-201(3)	6009.7(17)	4292.9(3)	19.6(3)
C1	9731(3)	5803(2)	2146.3(4)	25.9(4)
C2	10305(4)	6483(2)	2433.8(5)	27.0(4)
C3	8846(3)	6403(2)	2689.7(4)	23.4(4)
C4	6793(3)	5662(2)	2663.6(4)	20.4(4)
C5	6232(3)	5001(2)	2370.2(4)	23.3(4)
C6	7706(4)	5070(2)	2115.5(4)	25.9(4)
C7	5239(3)	5565(2)	2939.1(4)	19.4(4)
C8	5266(3)	6675(2)	3180.4(4)	22.7(4)
C9	3809(3)	6601(2)	3434.8(4)	22.1(4)
C10	2237(3)	5422(2)	3459.8(4)	18.2(4)
C11	2211(3)	4303(2)	3219.6(4)	21.1(4)

C12	3684(3)	4372(2)	2967.0(4)	21.5(4)
C13	700(3)	5310(2)	3734.5(4)	18.6(4)
C14	-1025(3)	4379(2)	3740.6(4)	19.8(4)
C15	-2751(3)	3465(2)	3752.4(4)	21.1(4)
C16	-2746(3)	1804(2)	3869.3(4)	18.8(4)
C17	-3826(3)	1754(2)	4200.4(4)	24.4(4)
C18	-4150(3)	832(2)	3640.3(4)	25.0(4)
C19	-384(3)	1167(2)	3884.1(5)	23.5(4)
C20	1201(3)	6337(2)	4019.0(4)	21.2(4)
C21	-2236(3)	6719(2)	4354.6(4)	19.3(4)
C22	-3046(3)	6044(2)	4659.4(4)	18.8(4)
C23	-4919(3)	6393(2)	4835.9(4)	21.5(4)
C24	-5220(4)	5569(2)	5118.9(4)	25.2(4)
C25	-3693(4)	4464(2)	5216.6(4)	26.1(4)
C26	-1806(3)	4123(2)	5037.0(4)	23.5(4)
C27	-1520(3)	4936(2)	4756.5(4)	18.9(4)
C28	298(3)	4866(2)	4516.7(4)	19.3(4)

Table A39. Anisotropic Displacement Parameters ($Å^2 \times 10^3$). The Anisotropic displacement factor exponent takes the form: $-2\pi^2[h^2a^{*2}U_{11}+2hka^*b^*U_{12}+\ldots]$.

Atom	U_{11}	U_{22}	U_{33}	U_{23}	U_{13}	U_{12}
O1	30.4(8)	21.0(7)	25.4(7)	3.5(6)	-1.0(6)	2.8(6)
O2	24.3(7)	24.4(7)	27.1(7)	-1.0(6)	0.3(6)	5.0(6)
N1	22.0(8)	18.5(7)	18.4(7)	0.0(6)	2.3(6)	-1.0(7)
C1	26.9(10)	27(1)	23.8(9)	5.9(8)	6.3(8)	5.7(9)
C2	21.7(10)	30.3(10)	29.1(10)	5.8(8)	1.7(8)	0.5(9)
C3	24.5(10)	25(1)	20.7(9)	2.4(8)	-0.2(8)	-0.7(8)
C4	23(1)	17.4(8)	20.7(9)	3.3(7)	-0.2(7)	2.5(8)
C5	23.9(10)	23.6(9)	22.2(9)	2.3(8)	0.2(8)	-1.2(8)
C6	31.6(11)	25.9(10)	20.1(9)	1.3(8)	2.3(8)	3.9(9)
C7	20.9(9)	19.9(9)	17.3(8)	2.0(7)	-1.7(7)	1.3(8)
C8	26.9(10)	18.5(9)	22.8(9)	0.8(8)	-0.7(8)	-4.7(9)
C9	29(1)	17.0(9)	20.3(9)	-1.4(7)	0.5(8)	-3.5(8)
C10	19.7(9)	17.3(9)	17.5(8)	2.7(7)	-1.2(7)	1.4(8)
C11	24.4(10)	18.4(9)	20.5(9)	0.0(7)	-1.1(7)	-5.2(8)
C12	25.7(10)	20.8(9)	18.0(8)	-2.2(7)	-0.6(7)	-1.2(8)
C13	22.2(10)	14.9(9)	18.8(8)	1.1(7)	-0.9(7)	0.1(8)
C14	23.3(10)	18.8(9)	17.1(8)	0.9(7)	-0.1(7)	2.9(8)
C15	18.0(9)	22.0(9)	23.4(9)	0.7(8)	-0.5(8)	1.2(8)
C16	16.4(9)	17.6(9)	22.3(9)	-0.8(7)	-0.3(7)	-2.5(8)
C17	25.6(10)	23.2(10)	24.5(9)	-1.2(8)	3.8(8)	-2.2(9)
C18	21.9(10)	27.4(10)	25.7(9)	-4.5(8)	1.8(8)	-6.3(9)

C19	20.1(10)	21.4(9)	29(1)	2.9(8)	0.8(8)	1.5(8)
C20	24.0(9)	19.4(9)	20.0(9)	-1.3(7)	4.2(8)	-4.1(8)
C21	23.2(10)	15.0(8)	19.5(8)	-2.6(7)	-1.6(8)	-0.8(8)
C22	21.7(9)	16.0(9)	18.8(8)	-2.9(7)	-1.4(7)	-1.7(8)
C23	20.6(10)	18.8(9)	25.1(9)	-3.2(7)	0.4(8)	-0.6(8)
C24	27.8(11)	22.4(9)	25.3(9)	-4.6(8)	7.4(8)	-2.3(9)
C25	37.5(11)	20.6(9)	20.1(9)	0.8(8)	4.9(8)	-4.0(9)
C26	30.7(11)	19.3(9)	20.7(9)	-0.4(7)	-0.6(8)	-0.4(8)
C27	21.8(10)	16.4(8)	18.6(8)	-2.2(7)	-1.1(7)	-2.8(7)
C28	21.3(10)	17.2(9)	19.6(8)	-2.2(7)	-1.9(7)	-2.3(8)

Table A40. Bond Lengths.

Atom	Atom	Length/Å	Atom	Atom	Length/Å
O1	C21	1.213(2)	C10	C13	1.481(2)
O2	C28	1.211(2)	C11	C12	1.383(3)
N1	C20	1.454(2)	C13	C14	1.312(3)
N1	C21	1.391(2)	C13	C20	1.522(2)
N1	C28	1.399(2)	C14	C15	1.305(3)
C1	C2	1.388(3)	C15	C16	1.521(3)
C1	C6	1.377(3)	C16	C17	1.536(3)
C2	C3	1.388(3)	C16	C18	1.531(3)
C3	C4	1.393(3)	C16	C19	1.522(3)
C4	C5	1.401(3)	C21	C22	1.490(3)
C4	C7	1.489(2)	C22	C23	1.380(3)
C5	C6	1.389(3)	C22	C27	1.388(3)
C7	C8	1.398(3)	C23	C24	1.399(3)
C7	C12	1.398(3)	C24	C25	1.387(3)
C8	C9	1.383(3)	C25	C26	1.393(3)
C9	C10	1.395(3)	C26	C27	1.384(3)
C10	C11	1.400(2)	C27	C28	1.486(3)

Table A41. Bond Angles.

Atom	Atom	Atom	Angle/°	Atom	Atom	Atom	Angle/°
C21	N1	C20	124.68(15)	C14	C15	C16	125.85(17)
C21	N1	C28	112.03(14)	C15	C16	C17	108.57(15)
C28	N1	C20	123.19(15)	C15	C16	C18	108.46(15)
C6	C1	C2	119.79(18)	C15	C16	C19	110.97(15)
C1	C2	C3	119.79(19)	C18	C16	C17	108.81(15)
C2	C3	C4	121.28(18)	C19	C16	C17	110.22(15)
C3	C4	C5	118.05(17)	C19	C16	C18	109.76(15)
C3	C4	C7	121.20(16)	N1	C20	C13	113.19(15)
C5	C4	C7	120.75(17)	O1	C21	N1	125.07(17)

C6	C5	C4	120.53(19)	O1	C21	C22	129.06(18)
C1	C6	C5	120.56(18)	N1	C21	C22	105.86(15)
C8	C7	C4	121.19(17)	C23	C22	C21	129.95(17)
C12	C7	C4	121.64(16)	C23	C22	C27	122.01(16)
C12	C7	C8	117.17(16)	C27	C22	C21	108.02(16)
C9	C8	C7	121.45(17)	C22	C23	C24	116.77(18)
C8	C9	C10	121.29(17)	C25	C24	C23	121.27(19)
C9	C10	C11	117.47(16)	C24	C25	C26	121.50(18)
C9	C10	C13	121.86(15)	C27	C26	C25	117.03(18)
C11	C10	C13	120.63(16)	C22	C27	C28	108.20(15)
C12	C11	C10	121.10(18)	C26	C27	C22	121.41(18)
C11	C12	C7	121.51(17)	C26	C27	C28	130.38(18)
C10	C13	C20	116.84(15)	O2	C28	N1	124.76(17)
C14	C13	C10	123.14(16)	O2	C28	C27	129.54(17)
C14	C13	C20	120.02(16)	N1	C28	C27	105.70(15)
C15	C14	C13	178.8(2)				

Table A42. Torsion Angles.

A	B	C	D	Angle/°	A	B	C	D	Angle/°
O1	C21	C22	C23	-2.6(3)	C13	C10	C11	C12	-178.05(18)
O1	C21	C22	C27	178.57(18)	C14	C13	C20	N1	7.6(2)
N1	C21	C22	C23	176.47(18)	C14	C15	C16	C17	105.0(2)
N1	C21	C22	C27	-2.34(19)	C14	C15	C16	C18	-136.87(19)
C1	C2	C3	C4	-0.7(3)	C14	C15	C16	C19	-16.2(2)
C2	C1	C6	C5	-0.2(3)	C20	N1	C21	O1	-0.1(3)
C2	C3	C4	C5	-0.2(3)	C20	N1	C21	C22	-179.21(15)
C2	C3	C4	C7	179.47(18)	C20	N1	C28	O2	-0.5(3)
C3	C4	C5	C6	0.9(3)	C20	N1	C28	C27	179.01(15)
C3	C4	C7	C8	26.8(3)	C21	N1	C20	C13	-90.6(2)
C3	C4	C7	C12	-153.66(18)	C21	N1	C28	O2	176.11(17)
C4	C5	C6	C1	-0.7(3)	C21	N1	C28	C27	-4.37(19)
C4	C7	C8	C9	179.21(17)	C21	C22	C23	C24	-178.89(18)
C4	C7	C12	C11	-178.60(17)	C21	C22	C27	C26	178.87(17)
C5	C4	C7	C8	-153.53(18)	C21	C22	C27	C28	-0.24(19)
C5	C4	C7	C12	26.0(3)	C22	C23	C24	C25	0.4(3)
C6	C1	C2	C3	0.9(3)	C22	C27	C28	O2	-177.80(18)
C7	C4	C5	C6	-178.79(17)	C22	C27	C28	N1	2.72(19)
C7	C8	C9	C10	-0.6(3)	C23	C22	C27	C26	-0.1(3)
C8	C7	C12	C11	1.0(3)	C23	C22	C27	C28	-179.16(16)
C8	C9	C10	C11	0.9(3)	C23	C24	C25	C26	-0.3(3)
C8	C9	C10	C13	178.63(17)	C24	C25	C26	C27	0.0(3)
C9	C10	C11	C12	-0.3(3)	C25	C26	C27	C22	0.2(3)

C9	C10	C13	C14	168.39(18)	C25	C26	C27	C28	179.04(18)
C9	C10	C13	C20	-11.7(3)	C26	C27	C28	O2	3.2(3)
C10	C11	C12	C7	-0.7(3)	C26	C27	C28	N1	-176.28(18)
C10	C13	C20	N1	-172.30(15)	C27	C22	C23	C24	-0.2(3)
C11	C10	C13	C14	-13.9(3)	C28	N1	C20	C13	85.6(2)
C11	C10	C13	C20	165.93(17)	C28	N1	C21	O1	-176.63(18)
C12	C7	C8	C9	-0.3(3)	C28	N1	C21	C22	4.23(19)

Table A43. Hydrogen Atom Coordinates (Å×10^4) and Isotropic Displacement Parameters (Å^2×10^3).

Atom	***x***	***y***	***z***	**U(eq)**
H1	10732	5843	1971	31
H2	11691	7003	2455	32
H3	9256	6861	2886	28
H5	4833	4502	2345	28
H6	7313	4607	1919	31
H8	6309	7498	3169	27
H9	3881	7369	3596	27
H11	1163	3482	3230	25
H12	3638	3590	2809	26
H15	-4135	3873	3682	25
H17A	-2852	2272	4354	37
H17B	-4045	678	4265	37
H17C	-5271	2281	4194	37
H18A	-5667	1249	3631	38
H18B	-4199	-237	3716	38
H18C	-3481	863	3428	38
H19A	237	1112	3669	35
H19B	-410	132	3978	35
H19C	544	1847	4015	35
H20A	2783	6202	4080	25
H20B	992	7428	3956	25
H23	-5955	7155	4769	26
H24	-6494	5770	5247	30
H25	-3941	3928	5411	31
H26	-761	3366	5104	28

9.7 X-Ray Crystallographic Data for Allene (+)-**221**

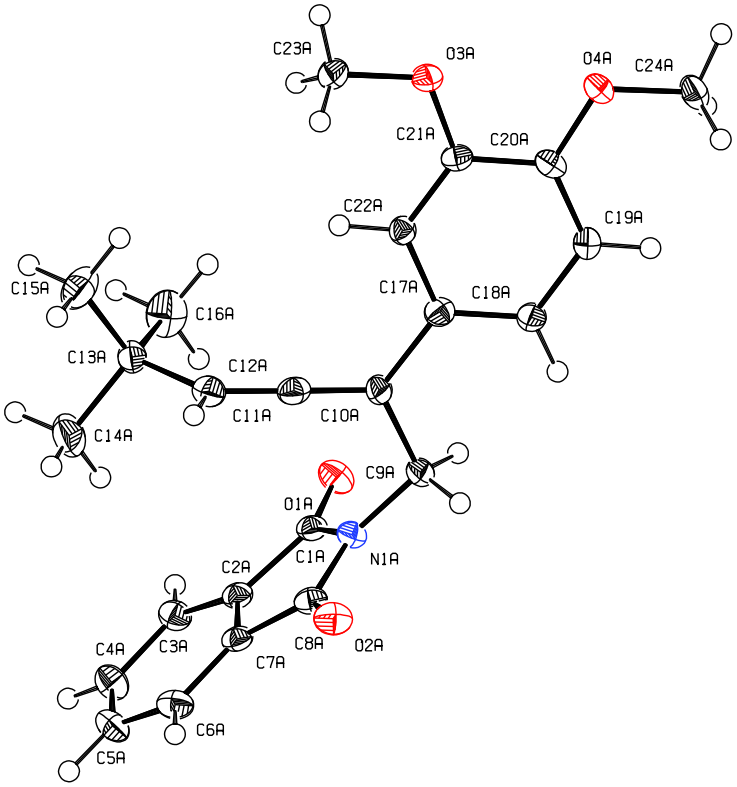

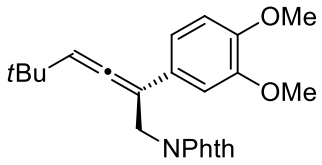

ORTEP view[111] of (+)-**221**, the thermal ellipsoids are drawn at the 50% probability level.

Database Reference. Crystallographic data have been deposited with the Cambridge Crystallographic Data Centre (CCDC) as supplementary publication no. CCDC-1437269. Data can be obtained free of charge on application to CCDC.

Experimental. A suitable clear, colorless block was selected, mounted in perfluoroalkyl polyether oil on polyimide Micromounts (supplied by MiTeGen) and measured on a Bruker/Nonius Kappa Apex II diffractometer with a Bruker Apex II area detector. The detector type was a CCD area detector. The crystal was kept at 100.0(2) K during data collection. Using Olex2,[112] the structure was solved with the XS structure solution program[113] using Direct Methods and refined with the XL refinement package[113] using Least Squares minimization. The absolute stereochemistry was not determined by X-Ray diffraction.

Table A44. Crystal data and structure refinement.

Empirical formula	$C_{24}H_{25}NO_4$
Formula weight	391.45
Temperature/K	100.0
Crystal system	triclinic
Space group	P1
a/Å	12.7971(3)

b/Å	12.8656(3)
c/Å	14.0933(3)
α/°	88.9680(10)
β/°	86.1080(10)
γ/°	66.5820(10)
Volume/Å^3	2124.21(8)
Z	4
ρ_{calc}g/cm^3	1.224
μ/mm^{-1}	0.671
F(000)	832.0
Crystal size/mm^3	0.15 × 0.13 × 0.07
Radiation	CuKα (λ = 1.54178)
2Θ range for data collection/°	6.286 to 133.496
Index ranges	-11 ≤ h ≤ 14, -14 ≤ k ≤ 15, -16 ≤ l ≤ 16
Reflections collected	36886
Independent reflections	11081 [R_{int} = 0.0261, R_{sigma} = 0.0255]
Data/restraints/parameters	11081/3/1065
Goodness-of-fit on F^2	1.020
Final R indexes [I>=2σ (I)]	R_1 = 0.0307, wR_2 = 0.0827
Final R indexes [all data]	R_1 = 0.0313, wR_2 = 0.0833
Largest diff. peak/hole / e Å^{-3}	0.27/-0.20
Flack parameter	0.12(6)

Table A45. Fractional Atomic Coordinates (×10^4) and Equivalent Isotropic Displacement Parameters (Å^2×10^3). U_{eq} is defined as 1/3 of the trace of the orthogonalised U_{IJ} tensor.

Atom	***x***	***y***	***z***	**U(eq)**
O1C	3936.0(16)	2732.8(15)	4309.0(12)	30.1(4)
O2C	4439.5(15)	5154.2(14)	6397.9(12)	27.6(4)
O3C	-1422.4(14)	9066.3(14)	4621.7(11)	22.6(4)
O4C	-471.1(15)	9954.7(14)	3356.9(12)	24.6(4)
N1C	4032.5(17)	4170.1(17)	5214.9(14)	20.5(4)
C1C	4209(2)	3059(2)	5018.7(16)	20.7(5)
C2C	4798(2)	2383(2)	5836.8(16)	18.7(5)
C3C	5152(2)	1235(2)	6016.7(17)	24.2(5)
C4C	5676(2)	844(2)	6860.7(17)	24.8(5)
C5C	5828(2)	1571(2)	7499.2(17)	23.0(5)
C6C	5454(2)	2733(2)	7318.8(17)	21.3(5)
C7C	4944(2)	3110(2)	6474.9(17)	19.6(5)
C8C	4465(2)	4279(2)	6074.3(17)	20.6(5)
C9C	3410(2)	5133(2)	4629.4(17)	23.1(5)
C10C	2217(2)	5831(2)	5065.1(17)	21.7(5)
C11C	1896(2)	5575.5(19)	5906.4(17)	24.2(5)

C12C	1645(2)	5320.8(19)	6769.0(16)	26.0(5)
C13C	1040(2)	4548(2)	7041.1(17)	26.1(6)
C14C	-81(3)	5241(3)	7599(2)	48.3(8)
C15C	810(3)	4021(3)	6166(2)	45.3(7)
C16C	1798(3)	3609(2)	7674(2)	44.6(7)
C17C	1521(2)	6866(2)	4545.8(16)	18.0(5)
C18C	366(2)	7461.4(19)	4839.4(16)	18.6(5)
C19C	-285(2)	8467.7(19)	4415.8(15)	18.3(5)
C20C	230(2)	8930(2)	3708.9(16)	19.0(5)
C21C	1354(2)	8331(2)	3394.5(17)	20.5(5)
C22C	1995(2)	7294(2)	3801.7(16)	20.5(5)
C23C	-2003(2)	8524(2)	5220.5(17)	25.1(6)
C24C	28(2)	10451(2)	2644.3(19)	28.7(6)
O1A	5734.3(15)	7488.8(14)	-128.2(12)	27.2(4)
O2A	2034.4(15)	8627.6(15)	1066.6(12)	26.9(4)
O3A	6548.4(14)	4608.4(13)	4790.0(11)	22.0(4)
O4A	6725.4(15)	2710.7(14)	4057.9(12)	24.6(4)
N1A	3949.7(18)	7798.7(16)	562.9(13)	19.9(4)
C1A	4744(2)	8114(2)	54.6(16)	19.4(5)
C2A	4121(2)	9323(2)	-203.0(16)	19.2(5)
C3A	4511(2)	10060(2)	-687.7(17)	22.6(5)
C4A	3712(2)	11166(2)	-812.8(18)	26.8(6)
C5A	2585(2)	11495(2)	-456.2(18)	26.4(6)
C6A	2207(2)	10750(2)	36.9(17)	24.7(6)
C7A	2999(2)	9661(2)	154.1(15)	19.3(5)
C8A	2864(2)	8691(2)	653.4(15)	20.5(5)
C9A	4257(2)	6718(2)	1041.1(16)	21.7(5)
C10A	4610(2)	6770.4(19)	2040.2(16)	21.2(5)
C11A	4365(2)	7758.5(19)	2448.3(15)	22.3(5)
C12A	4145(2)	8740.4(19)	2842.6(16)	23.8(5)
C13A	4951(2)	9344(2)	2823.3(17)	22.2(5)
C14A	4425(3)	10463(2)	2288(2)	41.5(7)
C15A	5073(3)	9611(2)	3853.8(18)	38.7(7)
C16A	6104(3)	8619(2)	2353(2)	40.4(7)
C17A	5175(2)	5678(2)	2536.2(16)	20.0(5)
C18A	5258(2)	4662(2)	2161.9(17)	22.0(5)
C19A	5776(2)	3648(2)	2651.9(17)	22.0(5)
C20A	6214(2)	3649(2)	3520.1(16)	19.4(5)
C21A	6133(2)	4680(2)	3910.6(16)	18.1(5)
C22A	5634(2)	5672(2)	3418.1(16)	18.0(5)
C23A	6350(2)	5667(2)	5250.4(17)	24.2(5)
C24A	6844(2)	1644(2)	3667.0(18)	26.7(6)

O1D	-132.4(15)	10976.9(15)	9306.8(12)	25.8(4)
O2D	-515.3(16)	8576.1(14)	7131.1(12)	25.9(4)
O3D	4307.9(16)	3700.3(14)	10110.1(12)	25.0(4)
O4D	5272.3(14)	4683.6(13)	8938.4(11)	21.7(4)
N1D	-183.9(17)	9545.1(16)	8361.2(13)	19.4(4)
C1D	-362(2)	10657(2)	8578.1(16)	20.4(5)
C2D	-899(2)	11338(2)	7741.3(17)	19.9(5)
C3D	-1235(2)	12479(2)	7572.4(17)	23.7(5)
C4D	-1728(2)	12885(2)	6716.9(18)	26.3(6)
C5D	-1865(2)	12167(2)	6054.6(17)	24.7(6)
C6D	-1507(2)	11016(2)	6226.4(17)	23.5(5)
C7D	-1023(2)	10614(2)	7081.8(16)	18.7(5)
C8D	-566(2)	9450(2)	7470.6(16)	19.7(5)
C9D	394(2)	8568(2)	8944.7(17)	21.4(5)
C10D	1673(2)	8042.1(19)	8704.6(15)	18.4(5)
C11D	2174.1(19)	8598.9(17)	8190.2(14)	18.5(5)
C12D	2665(2)	9156.5(18)	7689.4(15)	21.1(5)
C13D	2928(2)	9079(2)	6620.4(17)	26.6(6)
C14D	2479(3)	8292(3)	6160.3(19)	43.2(7)
C15D	2400(3)	10275(3)	6215(2)	49.1(8)
C16D	4227(3)	8616(2)	6448(2)	38.6(7)
C17D	2321(2)	6889(2)	9081.1(16)	19.2(5)
C18D	1824(2)	6366(2)	9722.0(17)	21.0(5)
C19D	2461(2)	5297(2)	10078.1(17)	21.9(5)
C20D	3602(2)	4737(2)	9795.3(16)	20.0(5)
C21D	4116(2)	5267.4(19)	9144.2(16)	18.3(5)
C22D	3482(2)	6319(2)	8787.6(15)	18.0(5)
C23D	5832(2)	5235(2)	8336.7(17)	23.4(5)
C24D	3827(3)	3192(2)	10835.4(19)	29.7(6)
O1B	8175.6(16)	6209.2(15)	3767.7(12)	27.3(4)
O2B	11793.0(16)	5069.4(16)	2378.6(13)	31.8(4)
O3B	7326.2(14)	9115.8(13)	-1263(1)	19.3(4)
O4B	7209.5(15)	11005.8(13)	-545.3(11)	21.3(4)
N1B	9914.1(18)	5899.2(17)	2971.5(13)	21.3(4)
C1B	9144(2)	5584(2)	3520.3(16)	21.3(5)
C2B	9772(2)	4358(2)	3731.7(16)	21.5(5)
C3B	9413(2)	3602(2)	4213.4(17)	25.9(6)
C4B	10222(3)	2500(2)	4299.6(18)	29.7(6)
C5B	11336(3)	2180(2)	3928.2(19)	30.9(6)
C6B	11692(2)	2947(2)	3439.6(18)	26.7(6)
C7B	10883(2)	4030(2)	3344.1(16)	22.4(5)
C8B	10978(2)	5022(2)	2832.5(16)	22.2(5)

C9B	9590(2)	6978(2)	2491.9(17)	23.5(5)
C10B	8917(2)	7021(2)	1628.3(16)	20.8(5)
C11B	8588.5(19)	6195.9(17)	1475.4(14)	18.4(4)
C12B	8210(2)	5406.3(18)	1394.2(15)	20.0(5)
C13B	8755(2)	4343.3(19)	784.1(16)	20.6(5)
C14B	7967(2)	4437(2)	-12.2(17)	29.9(6)
C15B	8872(3)	3309(2)	1397.2(18)	30.8(6)
C16B	9925(2)	4218(2)	352.8(19)	33.2(6)
C17B	8562(2)	8059.1(19)	1042.9(16)	18.2(5)
C18B	8130(2)	8066(2)	151.4(16)	18.3(5)
C19B	7712(2)	9046(2)	-369.8(16)	17.1(5)
C20B	7679(2)	10068.7(19)	5.2(16)	18.2(5)
C21B	8130(2)	10058(2)	872.8(16)	21.0(5)
C22B	8578(2)	9060(2)	1385.0(16)	21.2(5)
C23B	7045(2)	12072(2)	-133.6(19)	26.8(6)
C24B	7493(2)	8071(2)	-1715.8(17)	22.1(5)

Table A46. Anisotropic Displacement Parameters ($Å^2 \times 10^3$). The Anisotropic displacement factor exponent takes the form: $-2\pi^2[h^2a^{*2}U_{11}+2hka^*b^*U_{12}+\ldots]$.

Atom	**U_{11}**	**U_{22}**	**U_{33}**	**U_{23}**	**U_{13}**	**U_{12}**
O1C	31.8(11)	31.3(10)	24.8(9)	-1.3(7)	-9.1(8)	-8.7(8)
O2C	29.4(10)	21.0(9)	31.7(9)	0.9(7)	-3.1(8)	-9.1(8)
O3C	17.5(9)	21.6(9)	23.6(9)	0.9(7)	-0.8(7)	-2.4(7)
O4C	26.2(10)	18.8(8)	25.3(8)	5.7(7)	-5.3(7)	-5.1(8)
N1C	17.8(11)	20.2(11)	20.4(10)	3.8(8)	-1.7(8)	-4.2(9)
C1C	14.4(12)	22.8(13)	20.6(12)	-0.3(10)	0.3(9)	-3.2(10)
C2C	14.9(12)	21.7(12)	16.8(11)	0.7(9)	-0.3(9)	-4.3(10)
C3C	25.7(14)	22.4(13)	23.1(12)	-2.5(10)	-3.8(10)	-7.7(11)
C4C	26.5(14)	19.9(12)	24.3(12)	3.8(10)	-4.1(10)	-5.2(11)
C5C	19.6(13)	25.7(13)	21.4(11)	4.3(9)	-3.7(10)	-6.5(10)
C6C	20.3(13)	23.7(12)	19.7(11)	-0.7(9)	-3.0(9)	-8.3(11)
C7C	15.4(12)	19.4(12)	21.9(11)	0.0(9)	1.1(9)	-4.9(10)
C8C	15.7(12)	20.8(13)	23.2(12)	2.5(10)	0.9(10)	-5.3(10)
C9C	17.5(13)	24.1(13)	21.9(12)	7.4(10)	-0.4(10)	-2.5(11)
C10C	17.7(12)	21.7(12)	22.4(11)	2.6(9)	1.7(9)	-4.8(10)
C11C	19.3(12)	19.3(11)	30.5(12)	1.3(9)	-3.3(9)	-3.8(9)
C12C	28.0(13)	24.2(12)	21.6(11)	2.0(9)	-1.5(10)	-5.8(10)
C13C	27.8(14)	30.7(13)	19.2(11)	2.4(10)	3.5(10)	-11.8(11)
C14C	43.6(19)	43.7(17)	50.7(18)	5.0(14)	17.8(14)	-13.5(14)
C15C	61(2)	57.2(18)	33.4(14)	0.4(13)	1.2(14)	-40.2(17)
C16C	54(2)	31.9(15)	44.5(17)	15.9(12)	-2.4(14)	-14.4(14)
C17C	18.2(12)	19.6(11)	16.2(10)	0.4(9)	-2.6(9)	-7.3(10)

C18C	21.0(13)	17.2(11)	17.7(10)	0.1(9)	-0.8(9)	-7.7(10)
C19C	18.1(13)	19.1(12)	16.2(11)	-3.4(9)	-2.1(9)	-5.5(10)
C20C	23.9(13)	15.3(11)	17.6(11)	1.4(9)	-7.7(9)	-6.6(10)
C21C	21.0(13)	23.2(12)	19.4(11)	3.1(9)	-2.7(9)	-11.1(10)
C22C	18.7(13)	21.9(12)	20.1(11)	-0.1(9)	-0.8(10)	-7.2(10)
C23C	19.7(13)	27.5(14)	25.3(13)	-0.1(10)	1.3(10)	-6.8(11)
C24C	31.7(15)	22.3(13)	35.7(14)	12.4(11)	-8.6(11)	-13.9(12)
O1A	22.7(10)	22.2(9)	31.2(9)	2.0(7)	-0.3(7)	-3.4(8)
O2A	24.1(10)	32.6(10)	23.8(8)	4.8(7)	-0.8(7)	-11.4(8)
O3A	25.6(10)	21.9(9)	17.5(8)	1.6(7)	-5.6(7)	-7.9(8)
O4A	28.2(10)	16.4(8)	26.9(9)	3.5(7)	-7.0(7)	-5.7(7)
N1A	21.8(11)	17.8(10)	19.1(9)	2.8(8)	-4.6(8)	-6.2(9)
C1A	19.7(13)	21.1(12)	15.7(11)	0.1(9)	-4.5(9)	-5.9(11)
C2A	20.3(13)	21.8(12)	14.4(10)	-0.7(9)	-3.7(9)	-6.8(10)
C3A	22.8(14)	22.7(12)	20.4(11)	1.9(9)	-1.2(10)	-7.2(11)
C4A	28.3(14)	22.5(13)	28.6(13)	4.2(10)	0.2(11)	-9.4(11)
C5A	26.4(14)	18.2(12)	28.5(13)	3.3(10)	-2.3(11)	-2.6(11)
C6A	19.6(13)	27.8(14)	22.2(12)	1.4(10)	-2.2(10)	-4.8(11)
C7A	20.0(13)	23.2(12)	13.9(10)	-0.6(9)	-4.2(9)	-7.3(10)
C8A	21.5(14)	25.6(13)	14.2(11)	0.9(9)	-3.3(10)	-8.8(11)
C9A	27.9(14)	17.1(12)	20.6(12)	3.7(9)	-6.1(10)	-8.9(11)
C10A	29.4(14)	17.4(11)	20.7(11)	4.3(9)	-6.3(10)	-12.8(10)
C11A	22.8(12)	26.8(12)	20.2(10)	5.5(9)	-5.6(9)	-12.3(10)
C12A	23.6(12)	23.5(12)	22.0(11)	1.2(9)	-1.8(9)	-7(1)
C13A	27.5(14)	19.7(12)	20.4(11)	0.1(9)	-1.5(10)	-10.5(11)
C14A	66(2)	24.5(13)	37.7(15)	6.2(11)	-10.4(14)	-20.2(14)
C15A	56.6(19)	47.0(16)	27.1(13)	1.5(11)	-8.0(12)	-35.4(15)
C16A	35.5(16)	42.7(16)	45.3(16)	-5.3(13)	7.3(13)	-19.4(13)
C17A	22.0(13)	22.9(12)	17.5(11)	3.1(9)	-2.2(9)	-11.4(10)
C18A	28.0(14)	21.0(12)	19.7(11)	4.0(9)	-6.5(10)	-11.8(11)
C19A	24.4(14)	18.8(12)	23.6(12)	-1.5(9)	-1.9(10)	-9.4(11)
C20A	15.8(12)	18.2(12)	22.4(12)	4.9(9)	-0.2(10)	-5.1(10)
C21A	13.7(12)	22.4(12)	17.0(11)	-0.1(9)	-0.3(9)	-6(1)
C22A	20.1(12)	17.8(11)	17.9(11)	1.2(9)	-1.3(9)	-9.6(10)
C23A	29.7(15)	23.9(13)	20.6(12)	-0.7(10)	-5.4(11)	-11.6(11)
C24A	30.4(15)	14.9(12)	30.9(13)	-0.5(10)	-3.3(11)	-4.5(11)
O1D	24.9(10)	29.4(10)	22.3(8)	1.1(7)	-7.2(7)	-9.1(8)
O2D	30(1)	19.3(9)	27.5(9)	-0.5(7)	-2.3(7)	-8.6(8)
O3D	26.7(10)	16.3(8)	27.9(9)	6.0(7)	-3.2(7)	-4.2(7)
O4D	16.7(9)	19.8(9)	23.2(8)	-0.5(7)	0.2(7)	-1.7(7)
N1D	15.5(11)	19.3(10)	20.2(10)	4.2(8)	-2.5(8)	-3.3(8)
C1D	15.0(12)	24.1(13)	20.3(12)	2.1(10)	-0.7(10)	-5.9(10)

C2D	14.7(12)	22.3(12)	21.1(11)	1.2(9)	0.2(9)	-5.9(10)
C3D	25.7(14)	20.1(12)	22.8(12)	0(1)	-0.6(10)	-6.6(11)
C4D	25.9(14)	20.4(12)	28.9(13)	6.1(10)	-0.7(11)	-5.7(11)
C5D	23.2(14)	28.3(13)	19.8(11)	6.3(10)	-1.6(10)	-7.6(11)
C6D	22.6(14)	28.1(13)	20.5(12)	2.7(10)	-2.4(10)	-10.9(11)
C7D	14.8(12)	21.0(12)	19.4(11)	2.1(9)	-0.2(9)	-6.4(10)
C8D	15.2(12)	23.7(13)	19.6(11)	-0.4(10)	1.1(9)	-7.3(10)
C9D	16.2(12)	20.4(12)	23.8(12)	6.5(9)	-1.1(10)	-3.7(10)
C10D	18.9(12)	19.0(11)	14.6(10)	2.3(8)	0.3(9)	-4.9(10)
C11D	16.7(11)	16.5(10)	17.2(10)	-1.2(8)	-3.5(8)	-0.6(9)
C12D	22.4(12)	19.6(11)	21.4(11)	1.3(8)	-1.2(9)	-8.6(9)
C13D	32.3(15)	28.1(13)	20.0(12)	4.4(10)	1.3(10)	-13.4(12)
C14D	52.5(19)	64.1(19)	23.4(13)	-8.5(12)	3.1(12)	-34.5(16)
C15D	59(2)	42.7(17)	34.3(15)	17.2(13)	4.4(14)	-10.3(16)
C16D	38.5(17)	42.0(15)	33.2(14)	1.8(12)	9.5(12)	-15.6(13)
C17D	19.4(13)	18.2(12)	18.4(11)	-0.2(9)	-1.9(9)	-5.6(10)
C18D	16.8(13)	22.2(13)	22.7(12)	3.1(9)	-1(1)	-6.5(10)
C19D	25.0(13)	22.0(12)	21.3(11)	4.6(9)	-2.7(10)	-12.2(10)
C20D	23.2(13)	17.5(12)	18.5(11)	0.0(9)	-4.2(10)	-6.8(10)
C21D	16.2(12)	17.8(12)	17.9(11)	-4.8(9)	-2.5(9)	-3.1(10)
C22D	19.3(13)	21.5(12)	13.5(10)	0.5(9)	-1.8(9)	-8.3(10)
C23D	16.2(13)	25.4(13)	25.1(12)	-1.2(10)	0.8(10)	-4.8(10)
C24D	32.9(16)	21.4(13)	35.1(14)	9.5(11)	-7.0(12)	-10.8(12)
O1B	24.9(10)	24.1(9)	27.0(9)	0.8(7)	1.5(8)	-4.0(8)
O2B	29.0(11)	38.1(11)	29.9(9)	3.9(8)	1.5(8)	-15.8(9)
O3B	21.9(9)	17.3(8)	17.2(8)	-1.2(6)	-5.1(7)	-5.6(7)
O4B	24.4(9)	14.4(8)	23.4(8)	1.8(6)	-7.2(7)	-5.0(7)
N1B	23.5(11)	24.4(11)	17.1(9)	3.1(8)	-4.0(8)	-10.5(9)
C1B	27.6(15)	22.2(12)	15.8(11)	0.3(9)	-4.1(10)	-11.1(11)
C2B	25.4(14)	22.3(12)	15.8(11)	0.0(9)	-4.3(10)	-8.2(11)
C3B	25.8(14)	28.2(14)	22.2(12)	3.6(10)	-1.2(10)	-9.4(11)
C4B	37.3(16)	25.6(14)	24.2(12)	6.5(10)	-2.3(11)	-10.5(12)
C5B	32.6(16)	23.7(14)	29.4(13)	4.9(10)	-7.8(11)	-3.1(12)
C6B	23.7(14)	28.3(14)	24.4(12)	0.2(10)	-3.6(10)	-5.9(11)
C7B	24.5(14)	25.8(13)	16.7(11)	1.8(9)	-6.2(10)	-9.2(11)
C8B	23.8(14)	28.7(13)	15.8(11)	0.5(9)	-5.2(10)	-11.7(11)
C9B	31.9(15)	22.3(13)	20.0(11)	2.4(10)	-6.3(10)	-14.0(11)
C10B	24.0(13)	20.3(11)	19.2(11)	0.4(9)	-4.0(9)	-9.5(10)
C11B	18.6(11)	18.3(10)	14.8(9)	2.6(8)	-1.3(8)	-3.8(9)
C12B	22.1(12)	20.1(11)	18.5(10)	0.8(8)	-2.0(9)	-9.1(9)
C13B	25.2(13)	18.0(12)	20.7(11)	-1.8(9)	-1.9(10)	-10.8(10)
C14B	39.5(16)	24.7(12)	27.8(12)	-0.4(9)	-11.1(11)	-13.9(11)

C15B	42.8(16)	19.5(12)	30.7(13)	3.5(10)	-7.5(12)	-12.3(12)
C16B	28.8(14)	31.2(13)	37.9(14)	-8.0(11)	7.9(11)	-11.2(11)
C17B	17.1(12)	17.6(12)	20.1(11)	1.1(9)	-2.4(9)	-7(1)
C18B	17.1(12)	16.9(11)	21.2(11)	-3.1(9)	0.3(9)	-7.2(9)
C19B	13.4(12)	21.3(12)	16.9(11)	-0.4(9)	0.6(9)	-7.3(10)
C20B	15.5(12)	16.7(12)	20.6(11)	1.2(9)	-0.5(9)	-4.6(10)
C21B	24.6(14)	18.8(12)	21.7(12)	-1.9(9)	-2.9(10)	-10.6(11)
C22B	24.0(14)	23.5(13)	18.7(12)	-1.2(10)	-3.8(10)	-11.5(11)
C23B	27.4(15)	15.1(12)	33.1(14)	-0.7(10)	-6.0(11)	-2.7(11)
C24B	28.2(14)	20.5(12)	19.2(11)	-1.9(9)	-2.3(10)	-11.1(11)

Table A47. Bond Lengths.

Atom	**Atom**	**Length/Å**	**Atom**	**Atom**	**Length/Å**
O1C	C1C	1.215(3)	O1D	C1D	1.210(3)
O2C	C8C	1.211(3)	O2D	C8D	1.206(3)
O3C	C19C	1.362(3)	O3D	C20D	1.366(3)
O3C	C23C	1.434(3)	O3D	C24D	1.436(3)
O4C	C20C	1.373(3)	O4D	C21D	1.379(3)
O4C	C24C	1.428(3)	O4D	C23D	1.427(3)
N1C	C1C	1.386(3)	N1D	C1D	1.393(3)
N1C	C8C	1.397(3)	N1D	C8D	1.402(3)
N1C	C9C	1.455(3)	N1D	C9D	1.453(3)
C1C	C2C	1.488(3)	C1D	C2D	1.491(3)
C2C	C3C	1.386(3)	C2D	C3D	1.377(3)
C2C	C7C	1.382(3)	C2D	C7D	1.387(3)
C3C	C4C	1.391(3)	C3D	C4D	1.394(4)
C4C	C5C	1.387(4)	C4D	C5D	1.393(4)
C5C	C6C	1.400(4)	C5D	C6D	1.387(4)
C6C	C7C	1.382(3)	C6D	C7D	1.388(3)
C7C	C8C	1.497(3)	C7D	C8D	1.485(3)
C9C	C10C	1.521(3)	C9D	C10D	1.517(3)
C10C	C11C	1.308(3)	C10D	C11D	1.317(3)
C10C	C17C	1.488(3)	C10D	C17D	1.492(3)
C11C	C12C	1.306(3)	C11D	C12D	1.299(3)
C12C	C13C	1.515(4)	C12D	C13D	1.518(3)
C13C	C14C	1.525(4)	C13D	C14D	1.520(4)
C13C	C15C	1.518(4)	C13D	C15D	1.532(4)
C13C	C16C	1.531(4)	C13D	C16D	1.530(4)
C17C	C18C	1.404(3)	C17D	C18D	1.383(3)
C17C	C22C	1.388(3)	C17D	C22D	1.406(3)
C18C	C19C	1.382(3)	C18D	C19D	1.395(3)
C19C	C20C	1.408(3)	C19D	C20D	1.380(4)

C20C	C21C	1.380(4)	C20D	C21D	1.411(4)
C21C	C22C	1.396(3)	C21D	C22D	1.378(3)
O1A	C1A	1.214(3)	O1B	C1B	1.210(3)
O2A	C8A	1.207(3)	O2B	C8B	1.208(3)
O3A	C21A	1.369(3)	O3B	C19B	1.372(3)
O3A	C23A	1.441(3)	O3B	C24B	1.430(3)
O4A	C20A	1.366(3)	O4B	C20B	1.368(3)
O4A	C24A	1.435(3)	O4B	C23B	1.430(3)
N1A	C1A	1.389(3)	N1B	C1B	1.391(3)
N1A	C8A	1.406(3)	N1B	C8B	1.384(3)
N1A	C9A	1.452(3)	N1B	C9B	1.450(3)
C1A	C2A	1.490(3)	C1B	C2B	1.493(3)
C2A	C3A	1.386(4)	C2B	C3B	1.380(4)
C2A	C7A	1.386(4)	C2B	C7B	1.386(4)
C3A	C4A	1.400(4)	C3B	C4B	1.393(4)
C4A	C5A	1.391(4)	C4B	C5B	1.384(4)
C5A	C6A	1.390(4)	C5B	C6B	1.395(4)
C6A	C7A	1.380(3)	C6B	C7B	1.377(4)
C7A	C8A	1.484(3)	C7B	C8B	1.497(3)
C9A	C10A	1.518(3)	C9B	C10B	1.527(3)
C10A	C11A	1.315(3)	C10B	C11B	1.313(3)
C10A	C17A	1.487(3)	C10B	C17B	1.484(3)
C11A	C12A	1.306(3)	C11B	C12B	1.298(3)
C12A	C13A	1.516(4)	C12B	C13B	1.516(3)
C13A	C14A	1.534(3)	C13B	C14B	1.531(3)
C13A	C15A	1.531(3)	C13B	C15B	1.535(3)
C13A	C16A	1.511(4)	C13B	C16B	1.524(4)
C17A	C18A	1.381(3)	C17B	C18B	1.405(3)
C17A	C22A	1.409(3)	C17B	C22B	1.391(3)
C18A	C19A	1.400(3)	C18B	C19B	1.378(3)
C19A	C20A	1.380(3)	C19B	C20B	1.411(3)
C20A	C21A	1.407(3)	C20B	C21B	1.384(3)
C21A	C22A	1.379(3)	C21B	C22B	1.391(3)

Table A48. Bond Angles.

Atom	**Atom**	**Atom**	**Angle/°**	**Atom**	**Atom**	**Atom**	**Angle/°**
C19C	O3C	C23C	116.61(19)	C20D	O3D	C24D	116.5(2)
C20C	O4C	C24C	116.8(2)	C21D	O4D	C23D	116.70(18)
C1C	N1C	C8C	112.3(2)	C1D	N1D	C8D	112.21(19)
C1C	N1C	C9C	124.5(2)	C1D	N1D	C9D	125.2(2)
C8C	N1C	C9C	123.1(2)	C8D	N1D	C9D	122.5(2)
O1C	C1C	N1C	125.4(2)	O1D	C1D	N1D	125.7(2)

O1C	C1C	C2C	128.6(2)	O1D	C1D	C2D	128.7(2)
N1C	C1C	C2C	105.9(2)	N1D	C1D	C2D	105.58(19)
C3C	C2C	C1C	130.2(2)	C3D	C2D	C1D	130.0(2)
C7C	C2C	C1C	108.3(2)	C3D	C2D	C7D	121.6(2)
C7C	C2C	C3C	121.4(2)	C7D	C2D	C1D	108.3(2)
C2C	C3C	C4C	117.1(2)	C2D	C3D	C4D	117.2(2)
C5C	C4C	C3C	121.5(2)	C5D	C4D	C3D	121.5(2)
C4C	C5C	C6C	121.0(2)	C6D	C5D	C4D	120.7(2)
C7C	C6C	C5C	116.9(2)	C5D	C6D	C7D	117.7(2)
C2C	C7C	C6C	122.0(2)	C2D	C7D	C6D	121.2(2)
C2C	C7C	C8C	108.0(2)	C2D	C7D	C8D	108.21(19)
C6C	C7C	C8C	130.0(2)	C6D	C7D	C8D	130.6(2)
O2C	C8C	N1C	125.3(2)	O2D	C8D	N1D	124.6(2)
O2C	C8C	C7C	129.2(2)	O2D	C8D	C7D	129.8(2)
N1C	C8C	C7C	105.4(2)	N1D	C8D	C7D	105.68(19)
N1C	C9C	C10C	112.3(2)	N1D	C9D	C10D	112.3(2)
C11C	C10C	C9C	119.8(2)	C11D	C10D	C9D	120.5(2)
C11C	C10C	C17C	123.0(2)	C11D	C10D	C17D	122.3(2)
C17C	C10C	C9C	116.8(2)	C17D	C10D	C9D	117.2(2)
C12C	C11C	C10C	175.7(3)	C12D	C11D	C10D	179.4(2)
C11C	C12C	C13C	126.4(2)	C11D	C12D	C13D	126.6(2)
C12C	C13C	C14C	108.5(2)	C12D	C13D	C14D	111.5(2)
C12C	C13C	C15C	111.1(2)	C12D	C13D	C15D	108.2(2)
C12C	C13C	C16C	108.5(2)	C12D	C13D	C16D	107.0(2)
C14C	C13C	C16C	109.3(2)	C14D	C13D	C15D	111.0(3)
C15C	C13C	C14C	110.0(3)	C14D	C13D	C16D	109.6(2)
C15C	C13C	C16C	109.3(2)	C16D	C13D	C15D	109.4(2)
C18C	C17C	C10C	119.5(2)	C18D	C17D	C10D	122.2(2)
C22C	C17C	C10C	121.8(2)	C18D	C17D	C22D	118.7(2)
C22C	C17C	C18C	118.7(2)	C22D	C17D	C10D	119.0(2)
C19C	C18C	C17C	121.0(2)	C17D	C18D	C19D	120.9(2)
O3C	C19C	C18C	124.8(2)	C20D	C19D	C18D	120.6(2)
O3C	C19C	C20C	115.7(2)	O3D	C20D	C19D	125.4(2)
C18C	C19C	C20C	119.5(2)	O3D	C20D	C21D	115.7(2)
O4C	C20C	C19C	115.4(2)	C19D	C20D	C21D	118.9(2)
O4C	C20C	C21C	124.9(2)	O4D	C21D	C20D	115.4(2)
C21C	C20C	C19C	119.7(2)	C22D	C21D	O4D	124.2(2)
C20C	C21C	C22C	120.4(2)	C22D	C21D	C20D	120.4(2)
C17C	C22C	C21C	120.5(2)	C21D	C22D	C17D	120.6(2)
C21A	O3A	C23A	116.27(18)	C19B	O3B	C24B	116.70(17)
C20A	O4A	C24A	116.83(18)	C20B	O4B	C23B	116.82(17)
C1A	N1A	C8A	112.1(2)	C1B	N1B	C9B	123.3(2)

C1A	N1A	C9A	122.9(2)	C8B	N1B	C1B	112.7(2)
C8A	N1A	C9A	124.6(2)	C8B	N1B	C9B	123.6(2)
O1A	C1A	N1A	124.5(2)	O1B	C1B	N1B	125.1(2)
O1A	C1A	C2A	129.4(2)	O1B	C1B	C2B	129.1(2)
N1A	C1A	C2A	106.1(2)	N1B	C1B	C2B	105.8(2)
C3A	C2A	C1A	130.2(2)	C3B	C2B	C1B	130.8(2)
C3A	C2A	C7A	122.0(2)	C3B	C2B	C7B	121.5(2)
C7A	C2A	C1A	107.8(2)	C7B	C2B	C1B	107.7(2)
C2A	C3A	C4A	116.9(2)	C2B	C3B	C4B	116.9(3)
C5A	C4A	C3A	120.7(2)	C5B	C4B	C3B	121.6(3)
C6A	C5A	C4A	121.9(2)	C4B	C5B	C6B	121.2(3)
C7A	C6A	C5A	117.1(2)	C7B	C6B	C5B	116.8(3)
C2A	C7A	C8A	108.8(2)	C2B	C7B	C8B	108.2(2)
C6A	C7A	C2A	121.5(2)	C6B	C7B	C2B	122.0(2)
C6A	C7A	C8A	129.7(2)	C6B	C7B	C8B	129.8(3)
O2A	C8A	N1A	124.6(2)	O2B	C8B	N1B	126.0(2)
O2A	C8A	C7A	130.1(2)	O2B	C8B	C7B	128.5(2)
N1A	C8A	C7A	105.2(2)	N1B	C8B	C7B	105.6(2)
N1A	C9A	C10A	111.79(19)	N1B	C9B	C10B	111.56(19)
C11A	C10A	C9A	119.8(2)	C11B	C10B	C9B	119.6(2)
C11A	C10A	C17A	122.7(2)	C11B	C10B	C17B	122.3(2)
C17A	C10A	C9A	117.44(19)	C17B	C10B	C9B	117.8(2)
C12A	C11A	C10A	178.5(3)	C12B	C11B	C10B	175.0(2)
C11A	C12A	C13A	125.7(2)	C11B	C12B	C13B	126.6(2)
C12A	C13A	C14A	109.2(2)	C12B	C13B	C14B	107.8(2)
C12A	C13A	C15A	107.5(2)	C12B	C13B	C15B	109.11(19)
C15A	C13A	C14A	108.6(2)	C12B	C13B	C16B	111.1(2)
C16A	C13A	C12A	111.2(2)	C14B	C13B	C15B	109.4(2)
C16A	C13A	C14A	110.0(2)	C16B	C13B	C14B	109.6(2)
C16A	C13A	C15A	110.2(2)	C16B	C13B	C15B	109.9(2)
C18A	C17A	C10A	121.9(2)	C18B	C17B	C10B	120.0(2)
C18A	C17A	C22A	118.6(2)	C22B	C17B	C10B	121.2(2)
C22A	C17A	C10A	119.5(2)	C22B	C17B	C18B	118.6(2)
C17A	C18A	C19A	120.8(2)	C19B	C18B	C17B	120.9(2)
C20A	C19A	C18A	120.4(2)	O3B	C19B	C18B	124.7(2)
O4A	C20A	C19A	124.9(2)	O3B	C19B	C20B	115.4(2)
O4A	C20A	C21A	115.6(2)	C18B	C19B	C20B	119.9(2)
C19A	C20A	C21A	119.4(2)	O4B	C20B	C19B	115.84(19)
O3A	C21A	C20A	115.5(2)	O4B	C20B	C21B	125.0(2)
O3A	C21A	C22A	124.6(2)	C21B	C20B	C19B	119.1(2)
C22A	C21A	C20A	119.9(2)	C20B	C21B	C22B	120.6(2)
C21A	C22A	C17A	121.0(2)	C17B	C22B	C21B	120.6(2)

Table A49. Torsion Angles.

A	B	C	D	Angle/°	A	B	C	D	Angle/°
O1C	C1C	C2C	C3C	-2.2(5)	O1D	C1D	C2D	C3D	2.1(5)
O1C	C1C	C2C	C7C	179.4(3)	O1D	C1D	C2D	C7D	-178.6(3)
O3C	C19C	C20C	O4C	3.3(3)	O3D	C20D	C21D	O4D	-2.1(3)
O3C	C19C	C20C	C21C	-174.2(2)	O3D	C20D	C21D	C22D	-179.6(2)
O4C	C20C	C21C	C22C	180.0(2)	O4D	C21D	C22D	C17D	-175.90(19)
N1C	C1C	C2C	C3C	178.5(3)	N1D	C1D	C2D	C3D	-178.7(3)
N1C	C1C	C2C	C7C	0.0(3)	N1D	C1D	C2D	C7D	0.6(3)
N1C	C9C	C10C	C11C	4.5(3)	N1D	C9D	C10D	C11D	14.7(3)
N1C	C9C	C10C	C17C	177.4(2)	N1D	C9D	C10D	C17D	-165.76(19)
C1C	N1C	C8C	O2C	178.5(2)	C1D	N1D	C8D	O2D	-179.2(2)
C1C	N1C	C8C	C7C	-1.4(3)	C1D	N1D	C8D	C7D	0.5(3)
C1C	N1C	C9C	C10C	103.7(3)	C1D	N1D	C9D	C10D	-88.7(3)
C1C	C2C	C3C	C4C	-179.2(2)	C1D	C2D	C3D	C4D	-179.5(2)
C1C	C2C	C7C	C6C	179.0(2)	C1D	C2D	C7D	C6D	179.7(2)
C1C	C2C	C7C	C8C	-0.9(3)	C1D	C2D	C7D	C8D	-0.3(3)
C2C	C3C	C4C	C5C	0.6(4)	C2D	C3D	C4D	C5D	-0.7(4)
C2C	C7C	C8C	O2C	-178.5(3)	C2D	C7D	C8D	O2D	179.5(3)
C2C	C7C	C8C	N1C	1.4(3)	C2D	C7D	C8D	N1D	-0.1(3)
C3C	C2C	C7C	C6C	0.5(4)	C3D	C2D	C7D	C6D	-0.9(4)
C3C	C2C	C7C	C8C	-179.4(2)	C3D	C2D	C7D	C8D	179.1(2)
C3C	C4C	C5C	C6C	0.3(4)	C3D	C4D	C5D	C6D	-0.3(4)
C4C	C5C	C6C	C7C	-0.8(4)	C4D	C5D	C6D	C7D	0.8(4)
C5C	C6C	C7C	C2C	0.5(4)	C5D	C6D	C7D	C2D	-0.2(4)
C5C	C6C	C7C	C8C	-179.7(2)	C5D	C6D	C7D	C8D	179.9(2)
C6C	C7C	C8C	O2C	1.6(5)	C6D	C7D	C8D	O2D	-0.5(5)
C6C	C7C	C8C	N1C	-178.5(2)	C6D	C7D	C8D	N1D	179.9(2)
C7C	C2C	C3C	C4C	-1.0(4)	C7D	C2D	C3D	C4D	1.3(4)
C8C	N1C	C1C	O1C	-178.5(2)	C8D	N1D	C1D	O1D	178.5(2)
C8C	N1C	C1C	C2C	0.9(3)	C8D	N1D	C1D	C2D	-0.6(3)
C8C	N1C	C9C	C10C	-72.4(3)	C8D	N1D	C9D	C10D	87.2(3)
C9C	N1C	C1C	O1C	5.0(4)	C9D	N1D	C1D	O1D	-5.2(4)
C9C	N1C	C1C	C2C	-175.6(2)	C9D	N1D	C1D	C2D	175.6(2)
C9C	N1C	C8C	O2C	-5.0(4)	C9D	N1D	C8D	O2D	4.5(4)
C9C	N1C	C8C	C7C	175.2(2)	C9D	N1D	C8D	C7D	-175.9(2)
C9C	C10C	C17C	C18C	171.5(2)	C9D	C10D	C17D	C18D	-8.2(3)
C9C	C10C	C17C	C22C	-11.4(3)	C9D	C10D	C17D	C22D	172.9(2)
C10C	C17C	C18C	C19C	175.5(2)	C10D	C17D	C18D	C19D	-178.5(2)
C10C	C17C	C22C	C21C	-173.1(2)	C10D	C17D	C22D	C21D	177.9(2)
C11C	C10C	C17C	C18C	-15.8(4)	C11D	C10D	C17D	C18D	171.3(2)

C11C	C10C	C17C	C22C	161.3(2)
C11C	C12C	C13C	C14C	-117.5(3)
C11C	C12C	C13C	C15C	3.6(4)
C11C	C12C	C13C	C16C	123.8(3)
C17C	C18C	C19C	O3C	176.3(2)
C17C	C18C	C19C	C20C	-2.9(3)
C18C	C17C	C22C	C21C	4.0(3)
C18C	C19C	C20C	O4C	-177.4(2)
C18C	C19C	C20C	C21C	5.1(3)
C19C	C20C	C21C	C22C	-2.7(3)
C20C	C21C	C22C	C17C	-1.9(4)
C22C	C17C	C18C	C19C	-1.6(3)
C23C	O3C	C19C	C18C	-9.2(3)
C23C	O3C	C19C	C20C	170.1(2)
C24C	O4C	C20C	C19C	179.5(2)
C24C	O4C	C20C	C21C	-3.1(3)
O1A	C1A	C2A	C3A	-2.3(4)
O1A	C1A	C2A	C7A	179.0(2)
O3A	C21A	C22A	C17A	-176.7(2)
O4A	C20A	C21A	O3A	-1.8(3)
O4A	C20A	C21A	C22A	179.7(2)
N1A	C1A	C2A	C3A	178.2(2)
N1A	C1A	C2A	C7A	-0.5(2)
N1A	C9A	C10A	C11A	15.6(3)
N1A	C9A	C10A	C17A	-167.4(2)
C1A	N1A	C8A	O2A	-179.7(2)
C1A	N1A	C8A	C7A	-0.3(2)
C1A	N1A	C9A	C10A	87.0(3)
C1A	C2A	C3A	C4A	-179.3(2)
C1A	C2A	C7A	C6A	179.3(2)
C1A	C2A	C7A	C8A	0.3(2)
C2A	C3A	C4A	C5A	0.4(4)
C2A	C7A	C8A	O2A	179.4(2)
C2A	C7A	C8A	N1A	0.0(2)
C3A	C2A	C7A	C6A	0.5(3)
C3A	C2A	C7A	C8A	-178.5(2)
C3A	C4A	C5A	C6A	0.2(4)
C4A	C5A	C6A	C7A	-0.4(4)
C5A	C6A	C7A	C2A	0.1(3)
C5A	C6A	C7A	C8A	178.9(2)
C6A	C7A	C8A	O2A	0.5(4)
C6A	C7A	C8A	N1A	-179.0(2)

C11D	C10D	C17D	C22D	-7.6(3)
C11D	C12D	C13D	C14D	3.3(4)
C11D	C12D	C13D	C15D	125.7(3)
C11D	C12D	C13D	C16D	-116.5(3)
C17D	C18D	C19D	C20D	-0.2(4)
C18D	C17D	C22D	C21D	-1.0(3)
C18D	C19D	C20D	O3D	178.8(2)
C18D	C19D	C20D	C21D	0.4(3)
C19D	C20D	C21D	O4D	176.5(2)
C19D	C20D	C21D	C22D	-1.0(3)
C20D	C21D	C22D	C17D	1.3(3)
C22D	C17D	C18D	C19D	0.5(3)
C23D	O4D	C21D	C20D	-175.58(19)
C23D	O4D	C21D	C22D	1.7(3)
C24D	O3D	C20D	C19D	-3.8(3)
C24D	O3D	C20D	C21D	174.7(2)
O1B	C1B	C2B	C3B	3.8(4)
O1B	C1B	C2B	C7B	-176.2(2)
O3B	C19B	C20B	O4B	3.5(3)
O3B	C19B	C20B	C21B	-175.3(2)
O4B	C20B	C21B	C22B	179.3(2)
N1B	C1B	C2B	C3B	-177.0(2)
N1B	C1B	C2B	C7B	3.0(2)
N1B	C9B	C10B	C11B	8.0(3)
N1B	C9B	C10B	C17B	-177.8(2)
C1B	N1B	C8B	O2B	179.4(2)
C1B	N1B	C8B	C7B	0.3(2)
C1B	N1B	C9B	C10B	-73.2(3)
C1B	C2B	C3B	C4B	-179.3(2)
C1B	C2B	C7B	C6B	178.2(2)
C1B	C2B	C7B	C8B	-2.8(2)
C2B	C3B	C4B	C5B	0.6(4)
C2B	C7B	C8B	O2B	-177.5(2)
C2B	C7B	C8B	N1B	1.7(2)
C3B	C2B	C7B	C6B	-1.8(4)
C3B	C2B	C7B	C8B	177.2(2)
C3B	C4B	C5B	C6B	-0.8(4)
C4B	C5B	C6B	C7B	-0.2(4)
C5B	C6B	C7B	C2B	1.5(4)
C5B	C6B	C7B	C8B	-177.2(2)
C6B	C7B	C8B	O2B	1.4(4)
C6B	C7B	C8B	N1B	-179.5(2)

C7A	C2A	C3A	C4A	-0.8(3)	C7B	C2B	C3B	C4B	0.6(4)
C8A	N1A	C1A	O1A	-179.0(2)	C8B	N1B	C1B	O1B	177.3(2)
C8A	N1A	C1A	C2A	0.5(2)	C8B	N1B	C1B	C2B	-2.0(2)
C8A	N1A	C9A	C10A	-84.8(3)	C8B	N1B	C9B	C10B	98.0(3)
C9A	N1A	C1A	O1A	8.3(3)	C9B	N1B	C1B	O1B	-10.7(3)
C9A	N1A	C1A	C2A	-172.24(19)	C9B	N1B	C1B	C2B	170.1(2)
C9A	N1A	C8A	O2A	-7.2(4)	C9B	N1B	C8B	O2B	7.4(4)
C9A	N1A	C8A	C7A	172.29(19)	C9B	N1B	C8B	C7B	-171.7(2)
C9A	C10A	C17A	C18A	-7.7(4)	C9B	C10B	C17B	C18B	168.3(2)
C9A	C10A	C17A	C22A	172.8(2)	C9B	C10B	C17B	C22B	-16.0(3)
C10A	C17A	C18A	C19A	-178.8(2)	C10B	C17B	C18B	C19B	174.8(2)
C10A	C17A	C22A	C21A	178.0(2)	C10B	C17B	C22B	C21B	-173.1(2)
C11A	C10A	C17A	C18A	169.1(3)	C11B	C10B	C17B	C18B	-17.7(4)
C11A	C10A	C17A	C22A	-10.3(4)	C11B	C10B	C17B	C22B	158.0(2)
C11A	C12A	C13A	C14A	116.8(3)	C11B	C12B	C13B	C14B	-112.6(3)
C11A	C12A	C13A	C15A	-125.6(3)	C11B	C12B	C13B	C15B	128.7(2)
C11A	C12A	C13A	C16A	-4.8(3)	C11B	C12B	C13B	C16B	7.4(3)
C17A	C18A	C19A	C20A	0.0(4)	C17B	C18B	C19B	O3B	176.7(2)
C18A	C17A	C22A	C21A	-1.5(4)	C17B	C18B	C19B	C20B	-2.1(4)
C18A	C19A	C20A	O4A	179.4(2)	C18B	C17B	C22B	C21B	2.7(4)
C18A	C19A	C20A	C21A	0.2(4)	C18B	C19B	C20B	O4B	-177.5(2)
C19A	C20A	C21A	O3A	177.5(2)	C18B	C19B	C20B	C21B	3.6(4)
C19A	C20A	C21A	C22A	-1.0(4)	C19B	C20B	C21B	C22B	-2.0(4)
C20A	C21A	C22A	C17A	1.7(4)	C20B	C21B	C22B	C17B	-1.2(4)
C22A	C17A	C18A	C19A	0.6(4)	C22B	C17B	C18B	C19B	-1.0(4)
C23A	O3A	C21A	C20A	-172.8(2)	C23B	O4B	C20B	C19B	172.9(2)
C23A	O3A	C21A	C22A	5.6(3)	C23B	O4B	C20B	C21B	-8.3(3)
C24A	O4A	C20A	C19A	2.2(4)	C24B	O3B	C19B	C18B	-7.3(3)
C24A	O4A	C20A	C21A	-178.6(2)	C24B	O3B	C19B	C20B	171.7(2)

Table A50. Hydrogen Atom Coordinates ($Å \times 10^4$) and Isotropic Displacement Parameters ($Å^2 \times 10^3$).

Atom	***x***	***y***	***z***	**U(eq)**
H3C	5042	737	5583	29
H4C	5935	61	7003	30
H5C	6193	1277	8068	28
H6C	5547	3238	7756	26
H9CA	3350	4855	3993	28
H9CB	3841	5622	4546	28
H12C	1863	5653	7275	31
H14A	-447	4738	7834	72
H14B	-587	5810	7182	72

H14C	71	5619	8138	72
H15A	1535	3571	5816	68
H15B	332	4621	5756	68
H15C	414	3530	6362	68
H16A	1951	3947	8238	67
H16B	2520	3164	7318	67
H16C	1408	3113	7872	67
H18C	27	7168	5337	22
H21C	1694	8626	2898	25
H22C	2761	6877	3568	25
H23A	-1900	7799	4933	38
H23B	-2818	9011	5291	38
H23C	-1687	8390	5847	38
H24A	246	9977	2068	43
H24B	708	10508	2879	43
H24C	-525	11209	2496	43
H3A	5284	9826	-924	27
H4A	3942	11697	-1145	32
H5A	2059	12250	-552	32
H6A	1438	10982	283	30
H9AA	4894	6131	667	26
H9AB	3597	6498	1074	26
H12A	3418	9108	3170	29
H14D	3649	10897	2560	62
H14E	4401	10303	1615	62
H14F	4891	10904	2348	62
H15D	5582	10013	3864	58
H15E	5394	8903	4207	58
H15F	4322	10088	4149	58
H16D	6017	8469	1689	61
H16E	6428	7900	2691	61
H16F	6615	9017	2372	61
H18A	4959	4650	1565	26
H19A	5827	2955	2385	26
H22A	5600	6363	3677	22
H23D	6737	6069	4869	36
H23E	6649	5520	5883	36
H23F	5528	6132	5312	36
H24D	7282	1515	3051	40
H24E	6086	1655	3580	40
H24F	7244	1035	4103	40
H3D	-1135	12970	8020	28

H4D	-1976	13670	6583	32
H5D	-2208	12468	5479	30
H6D	-1590	10519	5774	28
H9DA	76	7992	8852	26
H9DB	247	8801	9623	26
H12D	2881	9665	8026	25
H14G	2705	8222	5478	65
H14H	1644	8604	6252	65
H14I	2797	7544	6454	65
H15G	2698	10767	6525	74
H15H	1568	10576	6331	74
H15I	2597	10248	5529	74
H16G	4519	9100	6776	58
H16H	4429	8607	5764	58
H16I	4565	7844	6694	58
H18D	1039	6739	9922	25
H19D	2106	4951	10519	26
H22D	3833	6662	8340	22
H23G	5500	5376	7717	35
H23H	6647	4751	8252	35
H23I	5732	5957	8628	35
H24G	3187	3066	10591	45
H24H	3554	3696	11392	45
H24I	4411	2465	11018	45
H3B	8651	3824	4474	31
H4B	10003	1955	4621	36
H5B	11868	1423	4008	37
H6B	12456	2733	3185	32
H9BA	10286	7104	2285	28
H9BB	9121	7595	2942	28
H12B	7521	5504	1753	24
H14J	7891	5098	-403	45
H14K	7214	4523	266	45
H14L	8291	3751	-409	45
H15J	8122	3408	1692	46
H15K	9396	3234	1894	46
H15L	9172	2625	997	46
H16J	10238	3552	-68	50
H16K	10438	4126	862	50
H16L	9849	4897	-13	50
H18B	8126	7386	-96	22
H21B	8133	10738	1121	25

H22B	8897	9062	1974	25
H23J	6646	12682	-569	40
H23K	7787	12083	-20	40
H23L	6587	12181	471	40
H24J	7264	8216	-2371	33
H24K	7030	7722	-1366	33
H24L	8301	7558	-1721	33

10 SFC and HPLC Traces

10.1 Part I. Ir-Catalyzed Reverse Prenylation of 3-Substituted Indoles

SFC trace for (–)-33

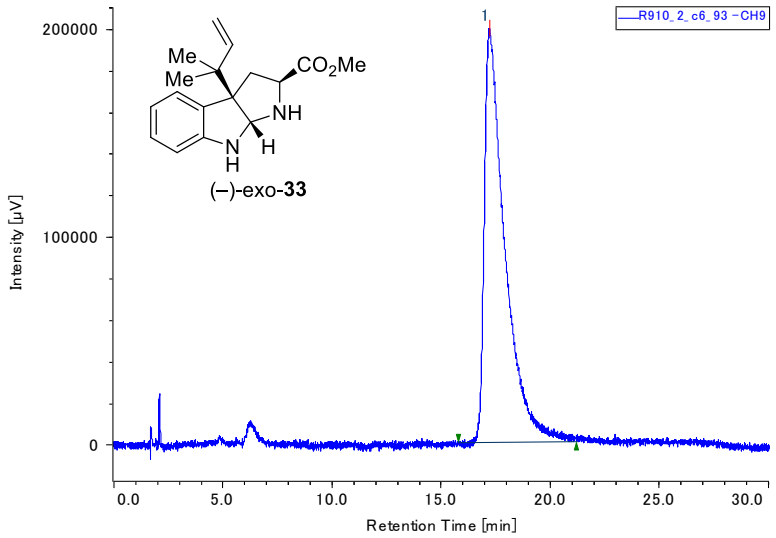

CH	tR / min	Area / µV·sec	Height / µV	Area%	Height%	NTP	Symmetry Factor
9	17.187	13012933	198726	100.000	100.000	1982	2.764

SFC trace for (+)-33

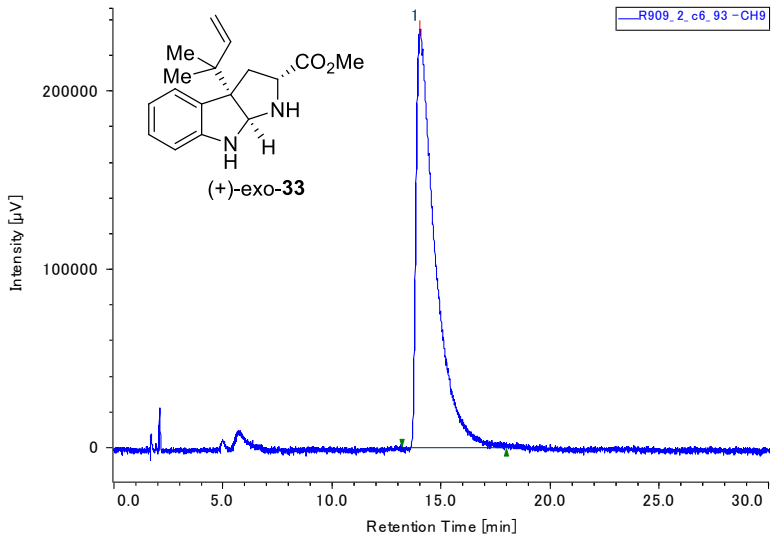

CH	tR / min	Area / µV·sec	Height / µV	Area%	Height%	NTP	Symmetry Factor
9	14.013	14161452	234491	100.000	100.000	1548	3.572

SFC trace for (±)-33

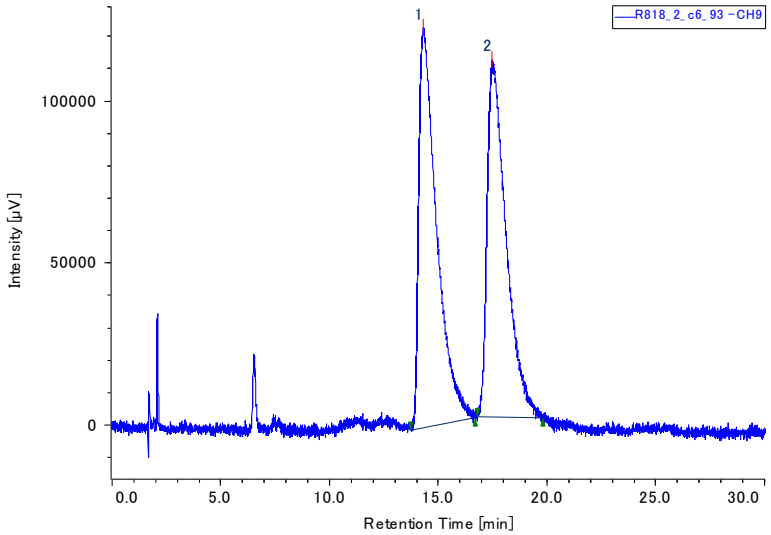

CH	tR / min	Area / µV·sec	Height / µV	Area%	Height%	NTP	Symmetry Factor
9	14.280	6983678	123233	51.227	52.910	1664	2.864
9	17.453	6649093	109676	48.773	47.090	2033	2.168

SFC traces for (–)-33, (+)-33 and (±)-33 superimposed

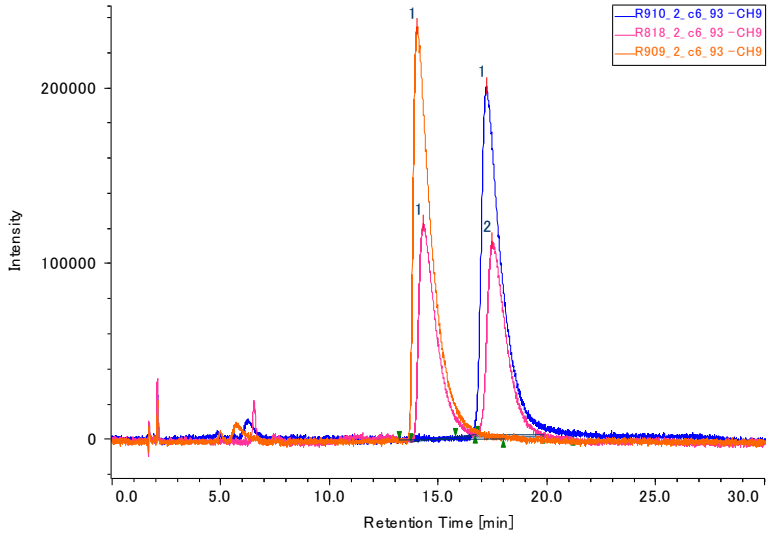

10.2 Part II. Rh-Catalyzed Stereoselective Synthesis of Allenes

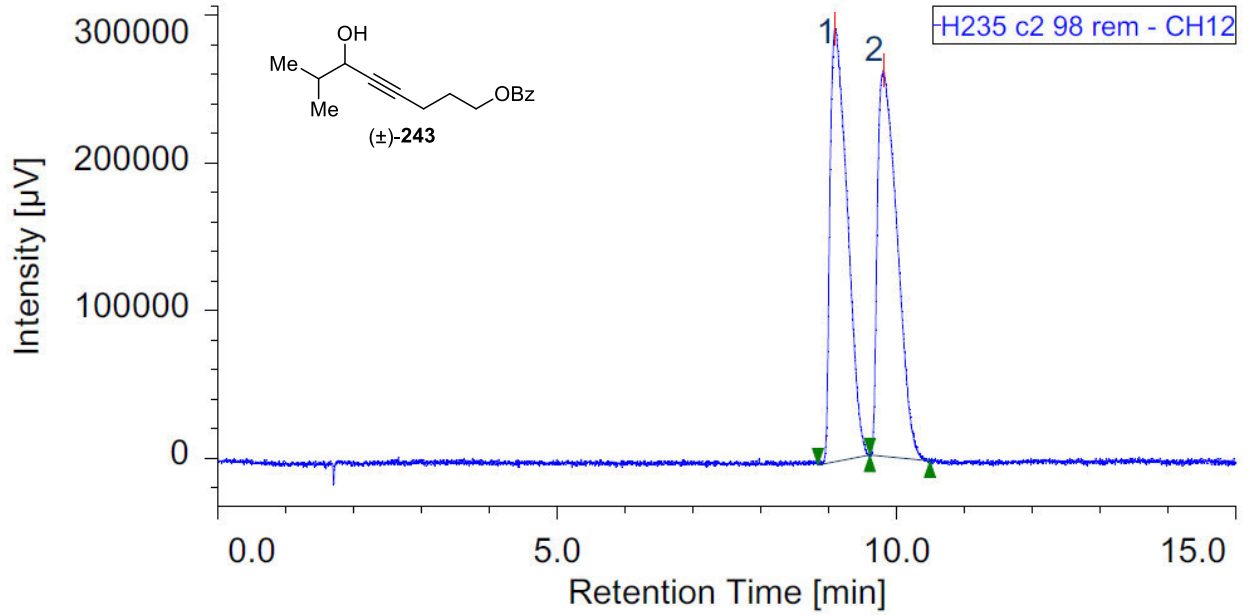

#	Peak Name	CH	tR [min]	Area [µV·sec]	Height [µV]	Area%	Height%	Quantity	NTP	Resolution	Symmetry Factor
1	Unknown	12	9.093	5160990	293138	49.526	52.881	N/A	5394	1.338	1.933
2	Unknown	12	9.800	5259778	261197	50.474	47.119	N/A	4831	N/A	2.018

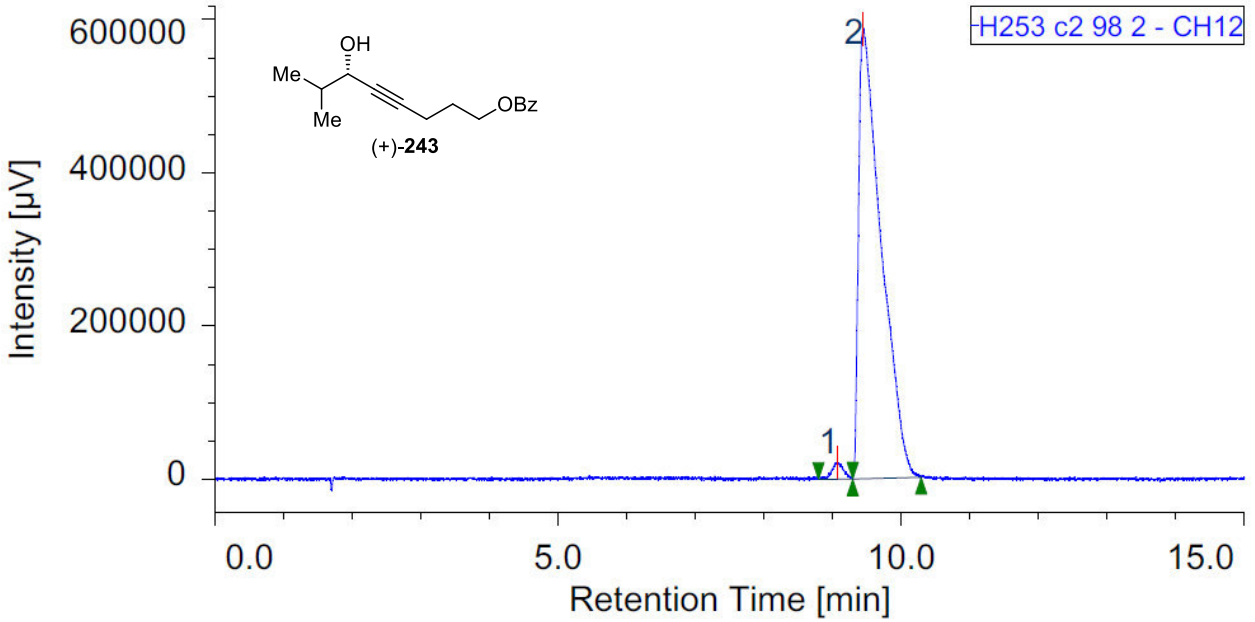

#	Peak Name	CH	tR [min]	Area [µV·sec]	Height [µV]	Area%	Height%	Quantity	NTP	Resolution	Symmetry Factor
1	Unknown	12	9.073	267298	21737	1.963	3.572	N/A	13248	0.832	0.893
2	Unknown	12	9.447	13349165	586821	98.037	96.428	N/A	4171	N/A	3.046

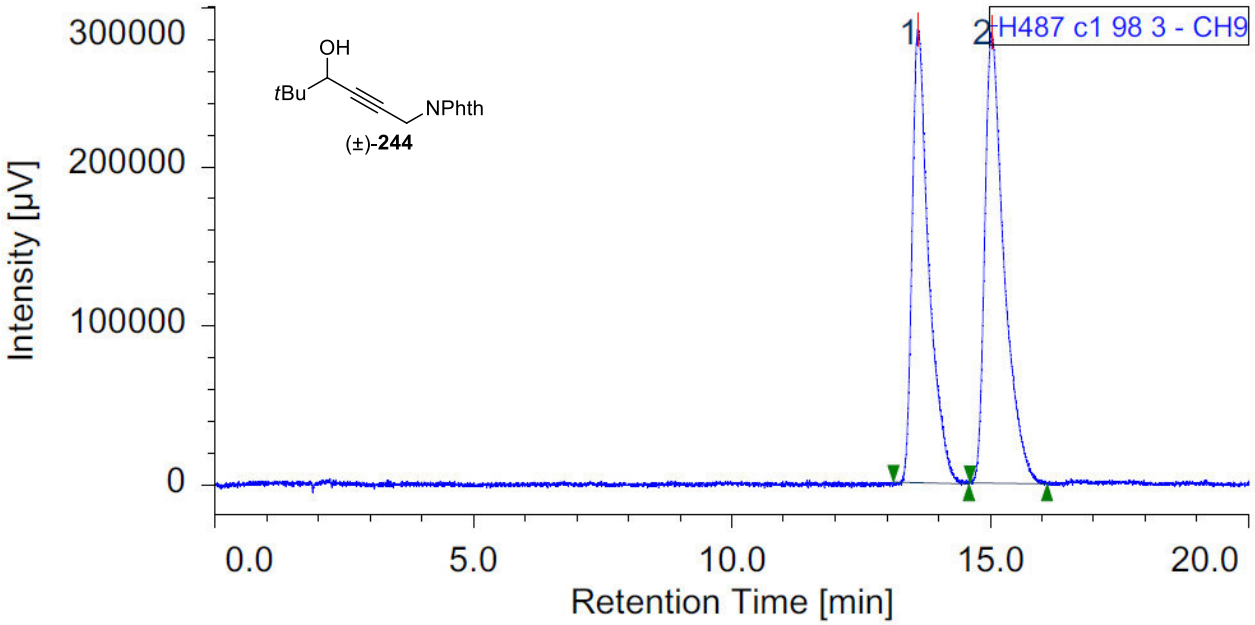

#	Peak Name	CH	tR [min]	Area [µV·sec]	Height [µV]	Area%	Height%	Quantity	NTP	Resolution	Symmetry Factor
1	Unknown	9	13.593	6467741	284591	46.765	50.159	N/A	9517	2.396	1.736
2	Unknown	9	15.027	7362670	282788	53.235	49.841	N/A	8759	N/A	1.723

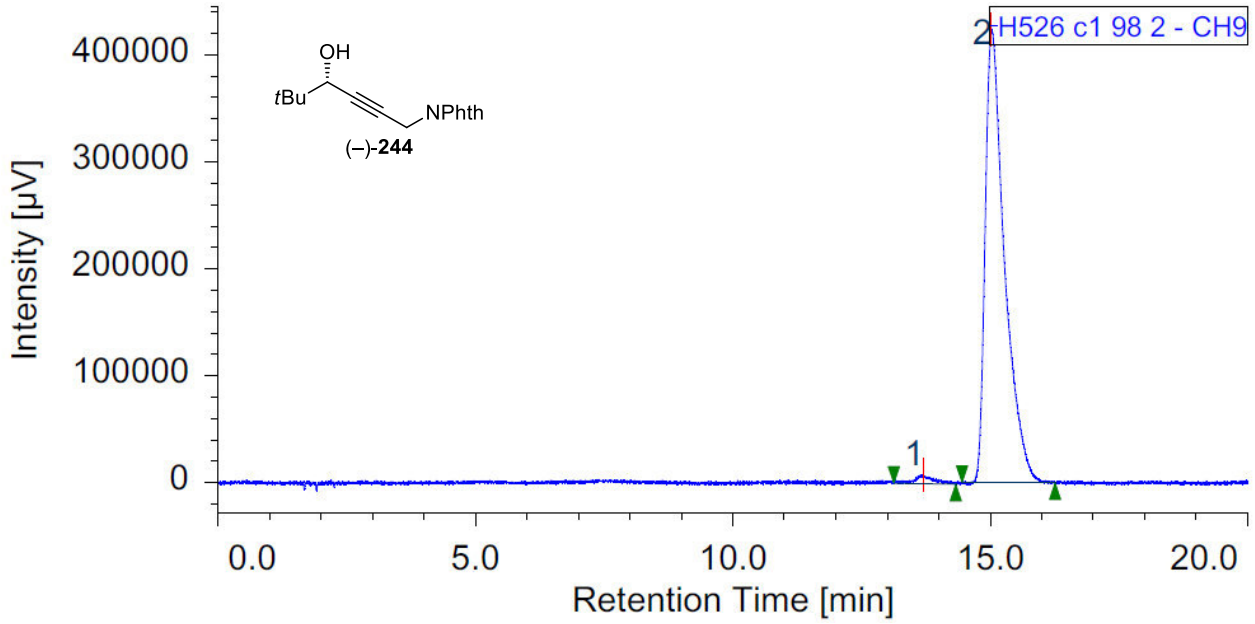

#	Peak Name	CH	tR [min]	Area [µV·sec]	Height [µV]	Area%	Height%	Quantity	NTP	Resolution	Symmetry Factor
1	Unknown	9	13.687	213882	8441	1.900	1.954	N/A	6196	1.999	1.065
2	Unknown	9	15.020	11045085	423586	98.100	98.046	N/A	8748	N/A	1.832

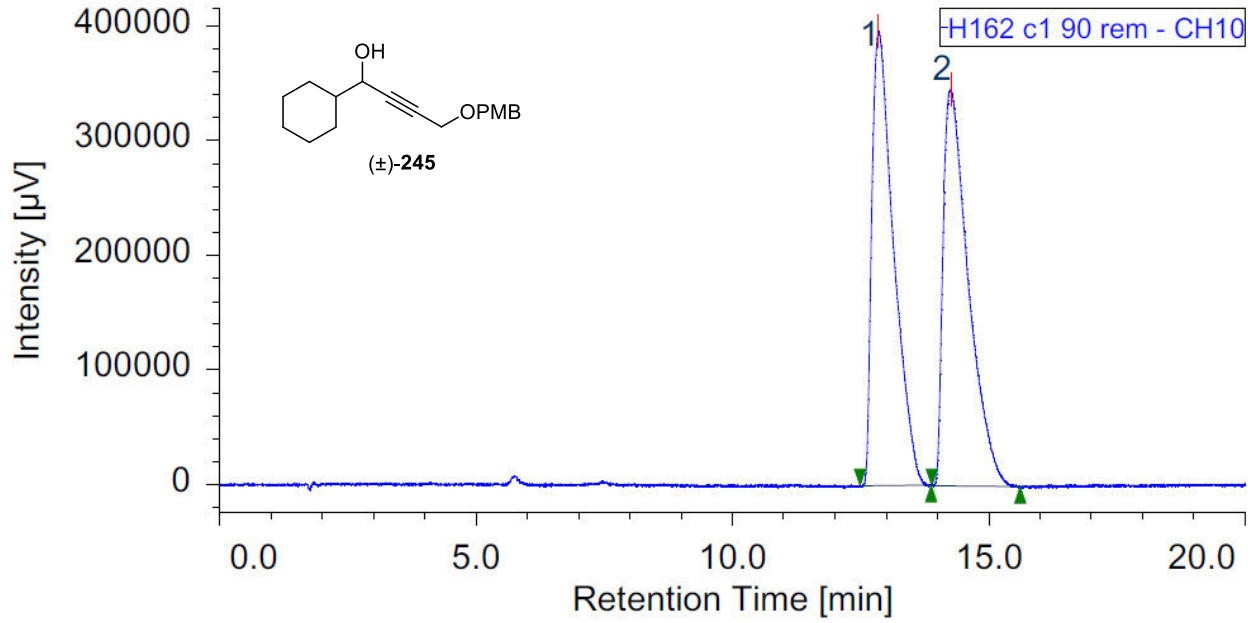

#	Peak Name	CH	tR [min]	Area [µV·sec]	Height [µV]	Area%	Height%	Quantity	NTP	Resolution	Symmetry Factor
1	Unknown	10	12.847	11658589	396001	49.731	53.416	N/A	4431	1.709	2.042
2	Unknown	10	14.260	11784701	345357	50.269	46.584	N/A	4141	N/A	2.160

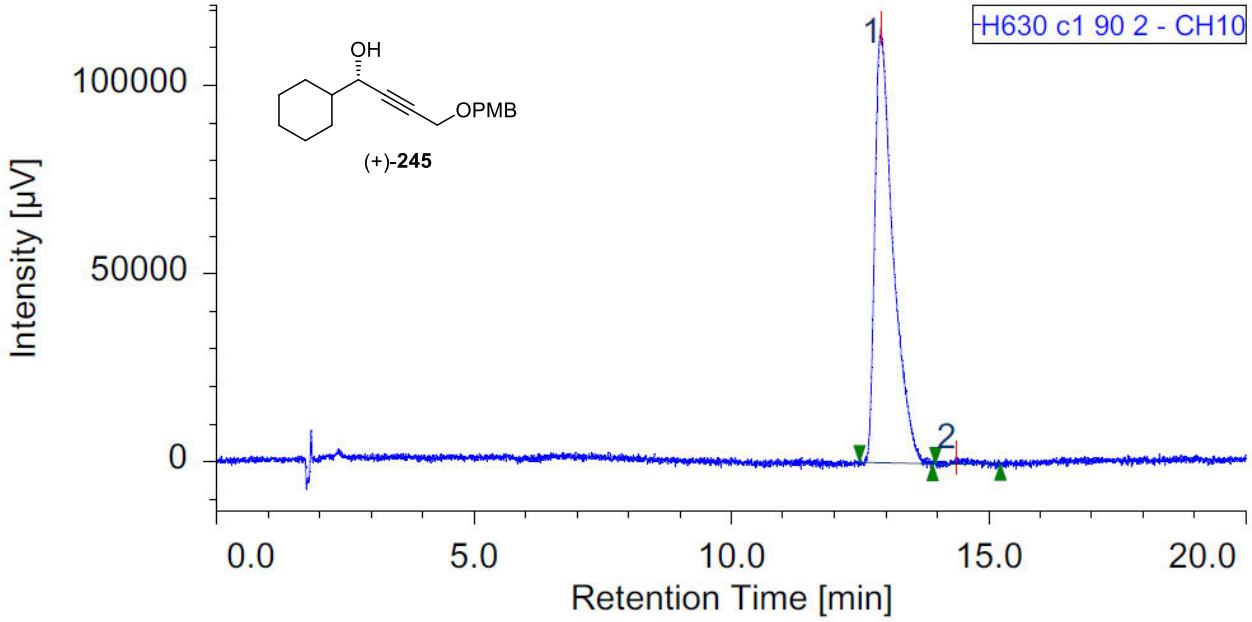

#	Peak Name	CH	tR [min]	Area [µV·sec]	Height [µV]	Area%	Height%	Quantity	NTP	Resolution	Symmetry Factor
1	Unknown	10	12.900	2829767	115374	98.984	98.477	N/A	7308	1.676	1.865
2	Unknown	10	14.353	29056	1784	1.016	1.523	N/A	2559	N/A	1.592

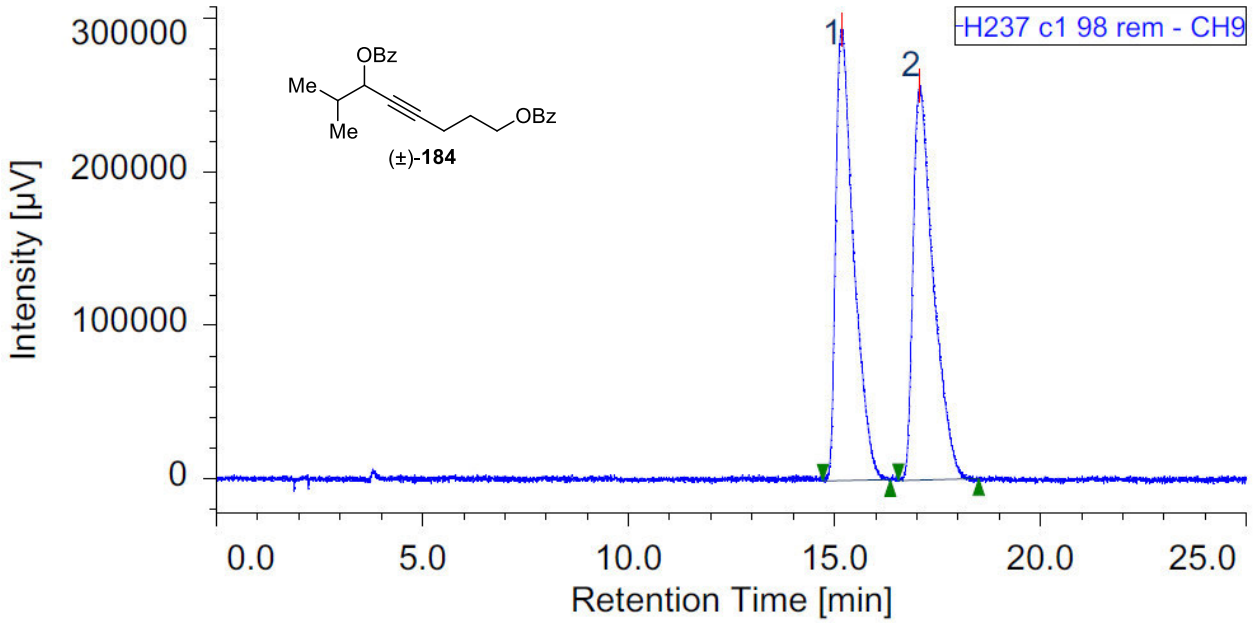

#	Peak Name	CH	tR [min]	Area [µV·sec]	Height [µV]	Area%	Height%	Quantity	NTP	Resolution	Symmetry Factor
1	Unknown	9	15.167	8882478	293888	50.120	53.362	N/A	6144	2.307	1.893
2	Unknown	9	17.067	8840032	256857	49.880	46.638	N/A	6052	N/A	1.857

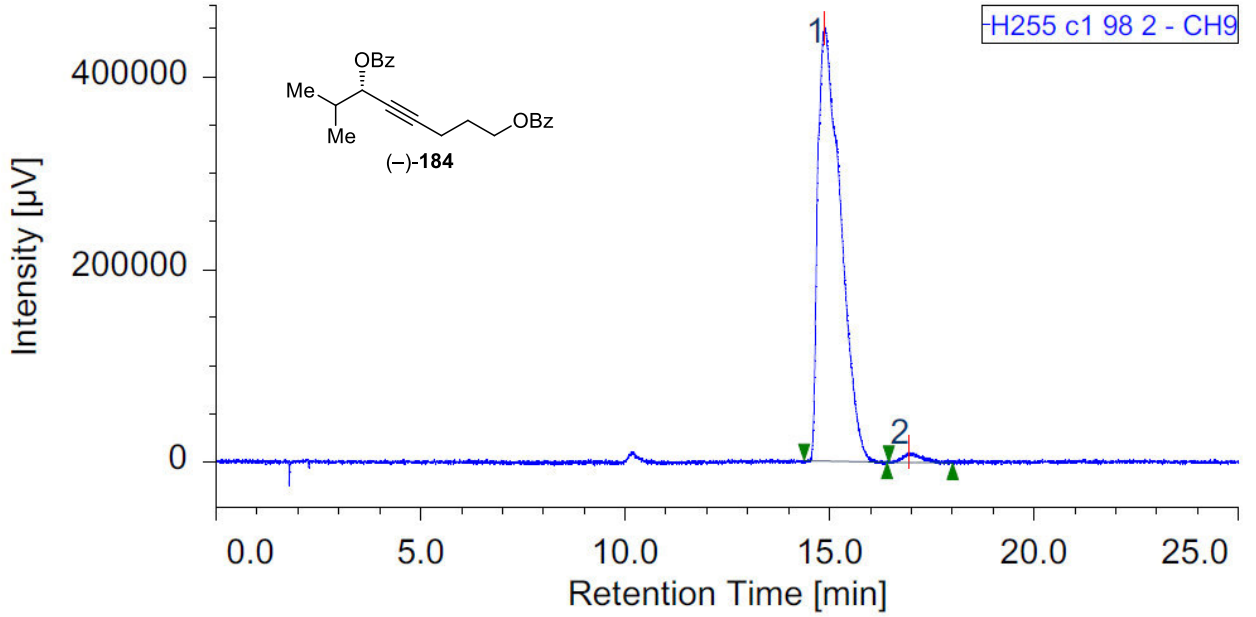

#	Peak Name	CH	tR [min]	Area [µV·sec]	Height [µV]	Area%	Height%	Quantity	NTP	Resolution	Symmetry Factor
1	Unknown	9	14.880	17270165	449445	98.083	97.666	N/A	2954	2.112	2.031
2	Unknown	9	16.940	337611	10743	1.917	2.334	N/A	6198	N/A	1.597

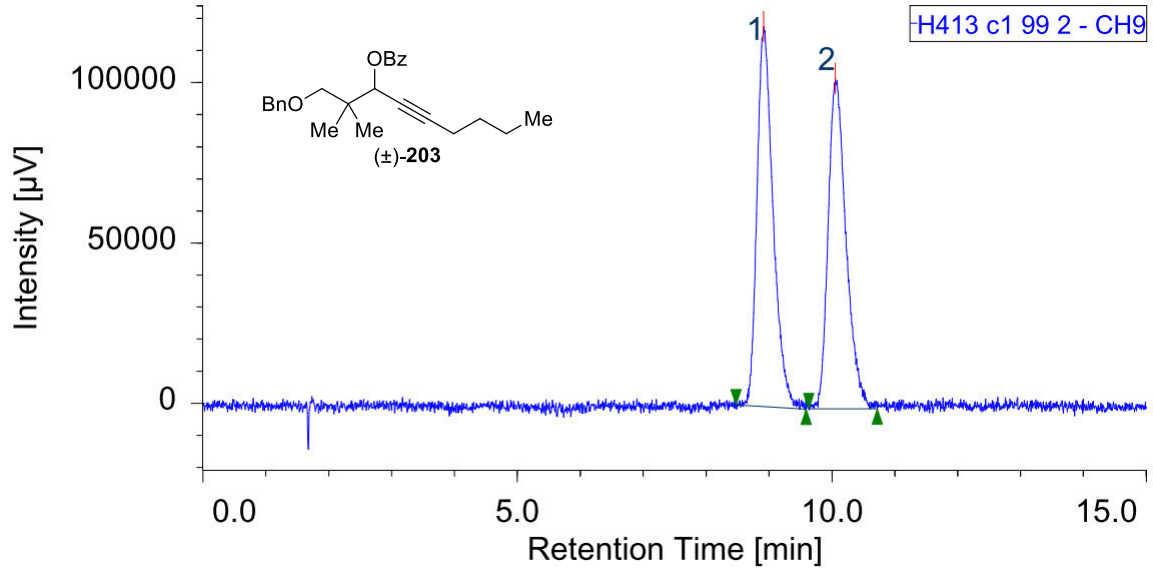

#	Peak Name	CH	tR [min]	Area [µV·sec]	Height [µV]	Area%	Height%	Quantity	NTP	Resolution	Symmetry Factor
1	Unknown	9	8.913	2102199	118465	50.503	53.485	N/A	6133	2.353	1.366
2	Unknown	9	10.047	2060317	103027	49.497	46.515	N/A	6191	N/A	1.440

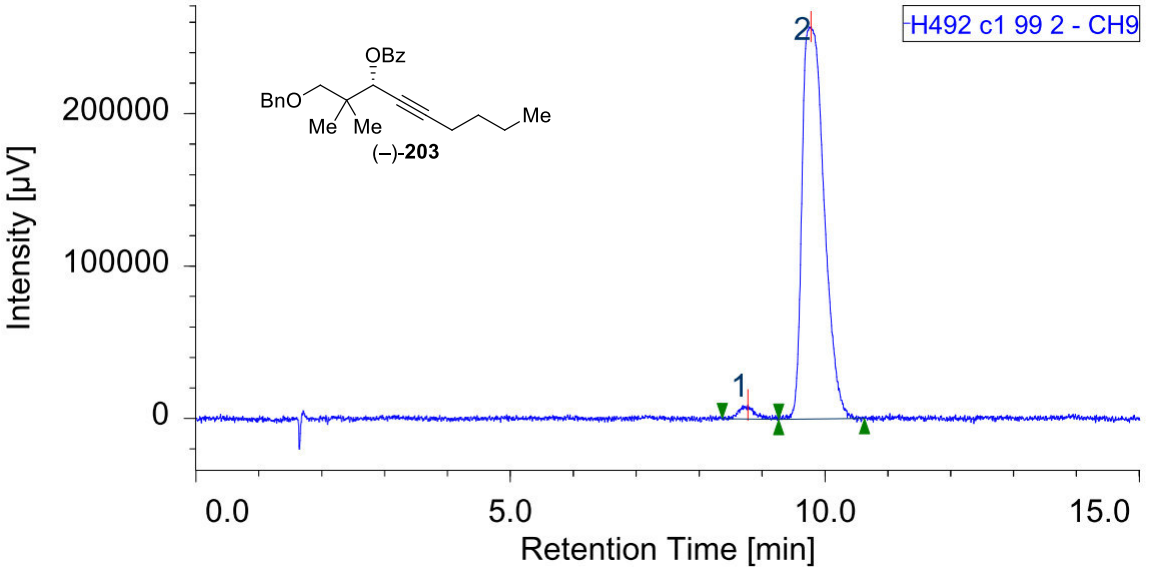

#	Peak Name	CH	tR [min]	Area [µV·sec]	Height [µV]	Area%	Height%	Quantity	NTP	Resolution	Symmetry Factor
1	Unknown	9	8.773	156021	9232	2.430	3.463	N/A	5408	1.787	1.108
2	Unknown	9	9.773	6264404	257373	97.570	96.537	N/A	3674	N/A	1.450

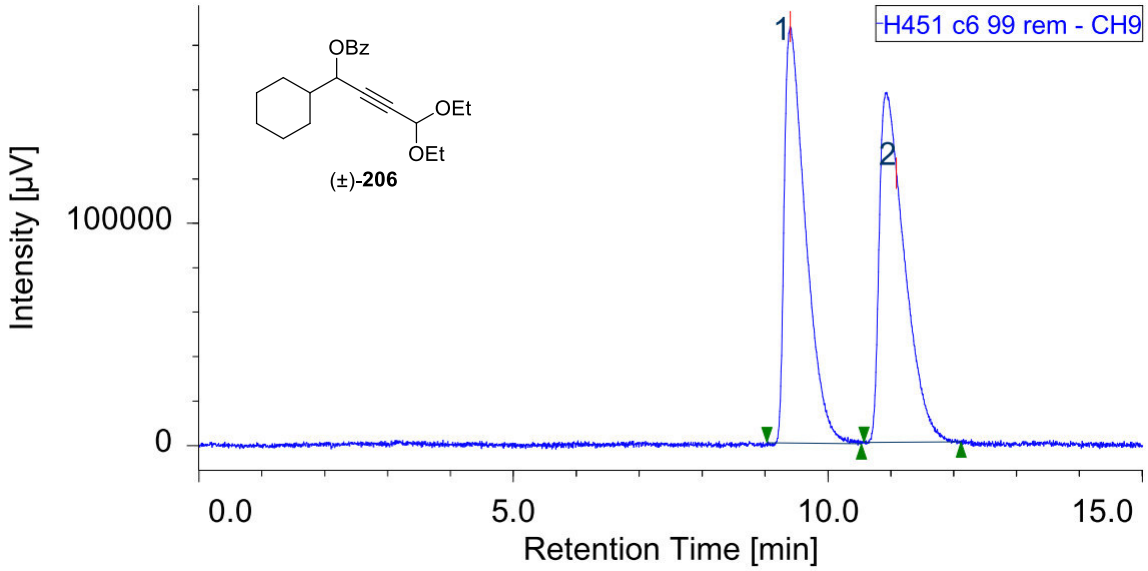

#	Peak Name	CH	tR [min]	Area [µV·sec]	Height [µV]	Area%	Height%	Quantity	NTP	Resolution	Symmetry Factor
1	Unknown	9	9.400	4375457	187188	50.117	60.757	N/A	3858	2.295	2.278
2	Unknown	9	11.087	4355026	120905	49.883	39.243	N/A	2607	N/A	1.317

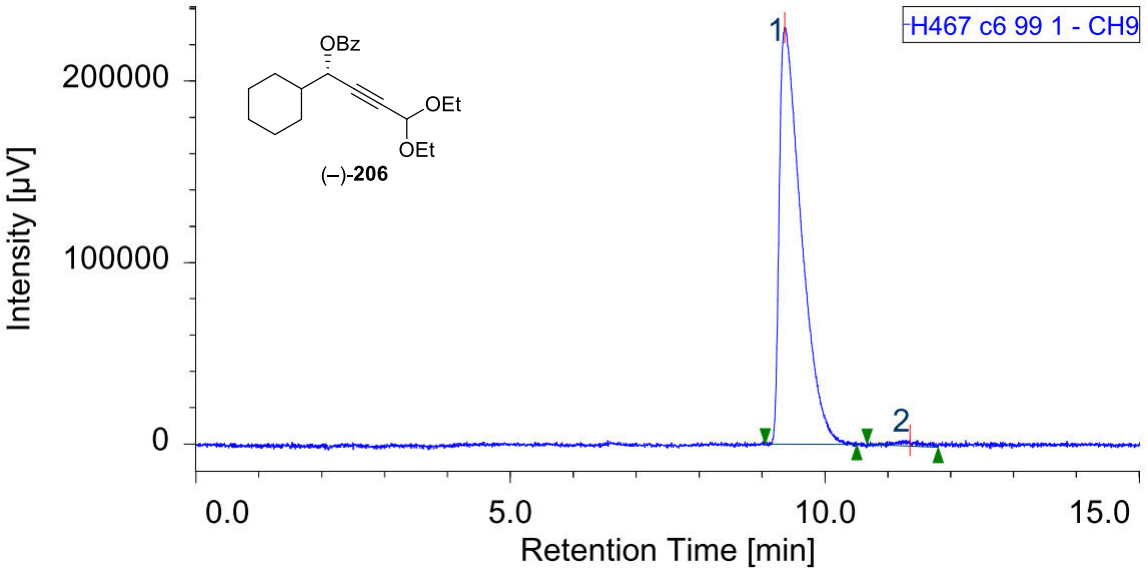

#	Peak Name	CH	tR [min]	Area [µV·sec]	Height [µV]	Area%	Height%	Quantity	NTP	Resolution	Symmetry Factor
1	Unknown	9	9.360	5527578	229414	98.628	98.542	N/A	3609	2.046	2.547
2	Unknown	9	11.347	76891	3395	1.372	1.458	N/A	1175	N/A	0.833

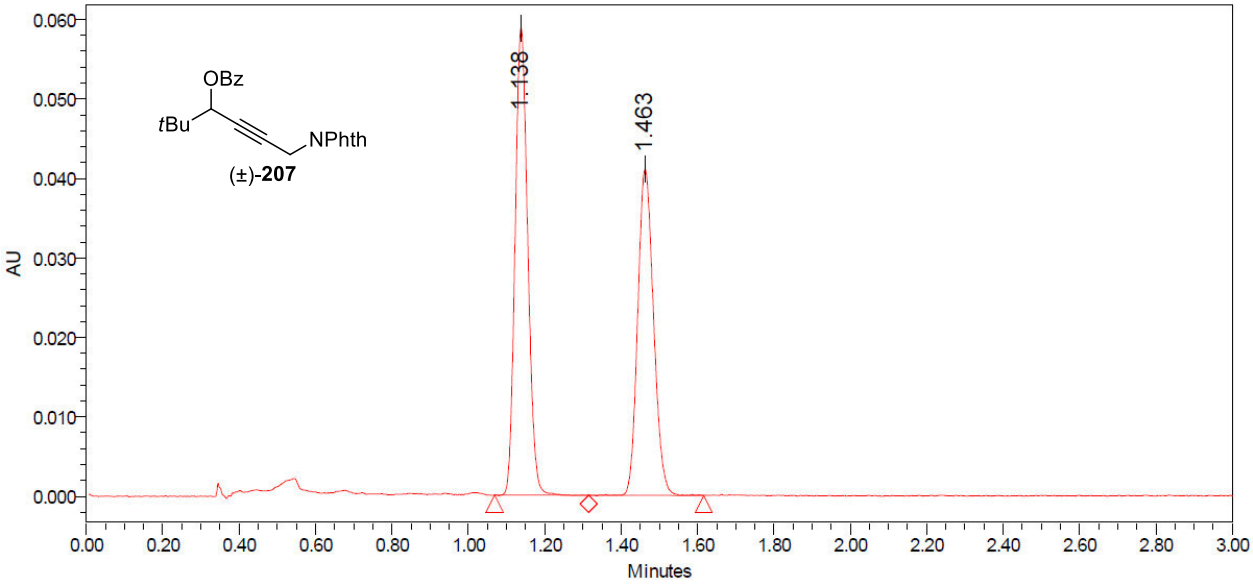

	Processed Channel	Retention Time (min)	Area	% Area
1	PDA Ch1 254nm@1.2nm -Compens.	1.138	135718	53.42
2	PDA Ch1 254nm@1.2nm -Compens.	1.463	118364	46.58

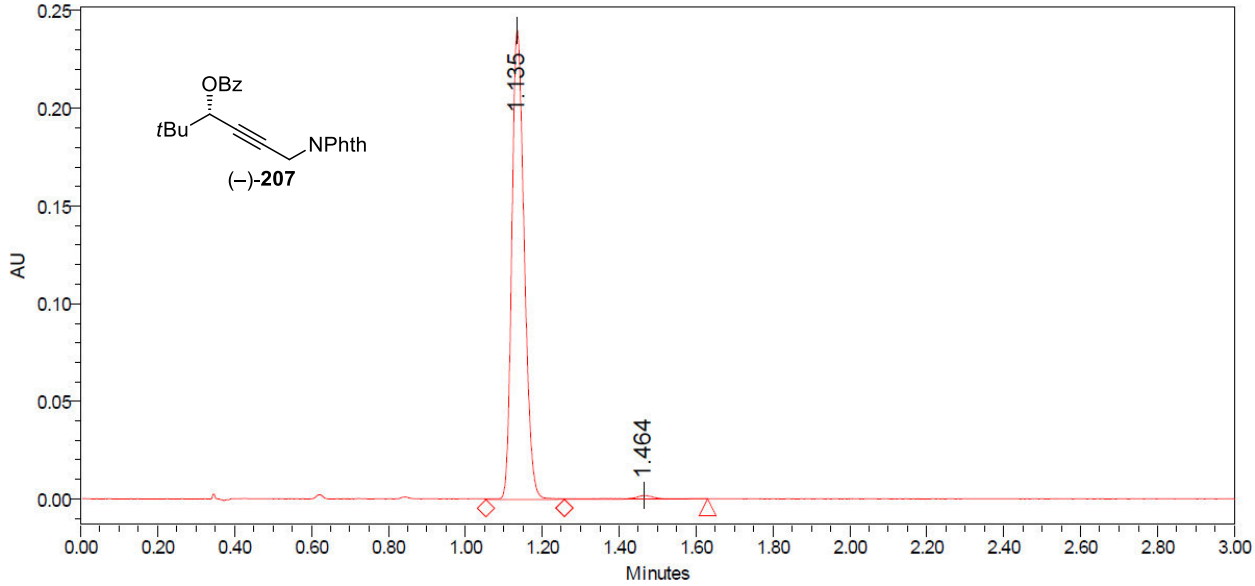

	Processed Channel	Retention Time (min)	Area	% Area
1	PDA Ch1 254nm@1.2nm -Compens.	1.135	541841	98.40
2	PDA Ch1 254nm@1.2nm -Compens.	1.464	8823	1.60

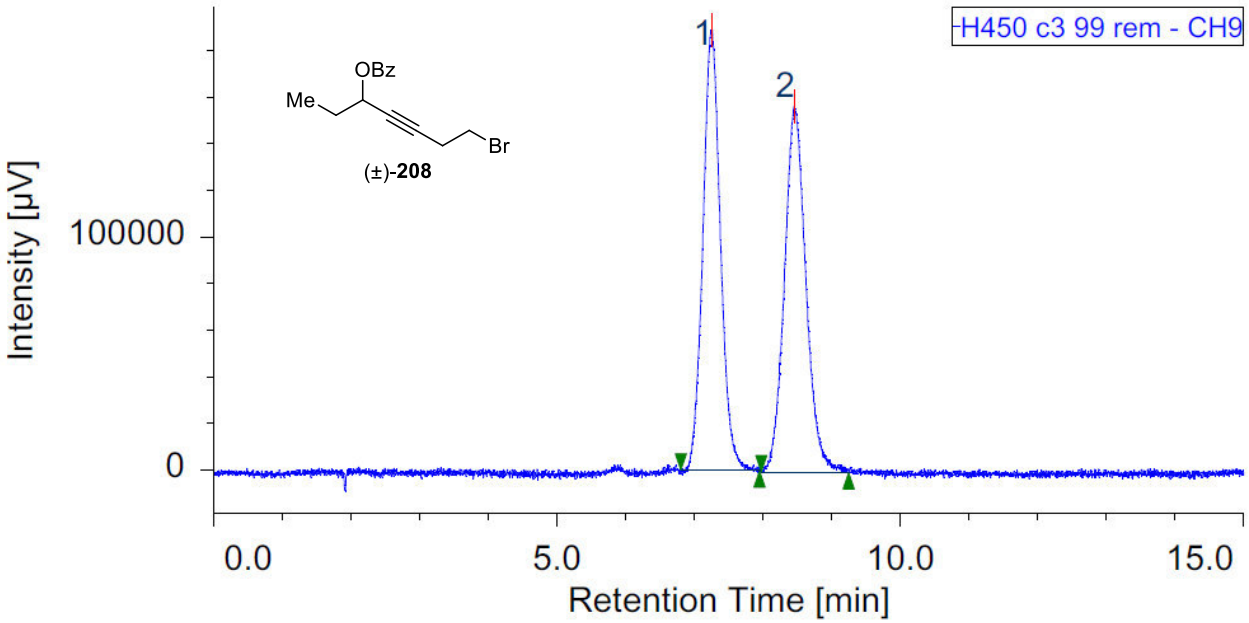

#	Peak Name	CH	tR [min]	Area [µV·sec]	Height [µV]	Area%	Height%	Quantity	NTP	Resolution	Symmetry Factor
1	Unknown	9	7.260	3360009	188947	49.562	54.663	N/A	4117	2.378	1.055
2	Unknown	9	8.453	3419425	156711	50.438	45.337	N/A	3727	N/A	1.115

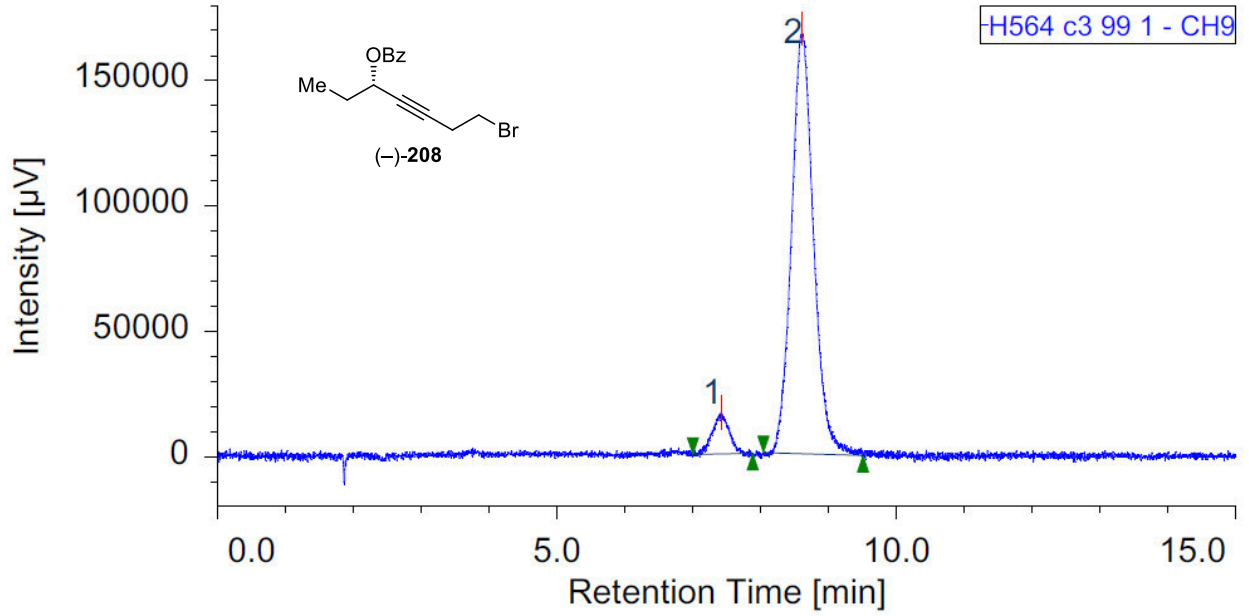

#	Peak Name	CH	tR [min]	Area [µV·sec]	Height [µV]	Area%	Height%	Quantity	NTP	Resolution	Symmetry Factor
1	Unknown	9	7.420	281140	16573	6.914	8.901	N/A	4294	2.337	1.050
2	Unknown	9	8.607	3785265	169619	93.086	91.099	N/A	3708	N/A	1.130

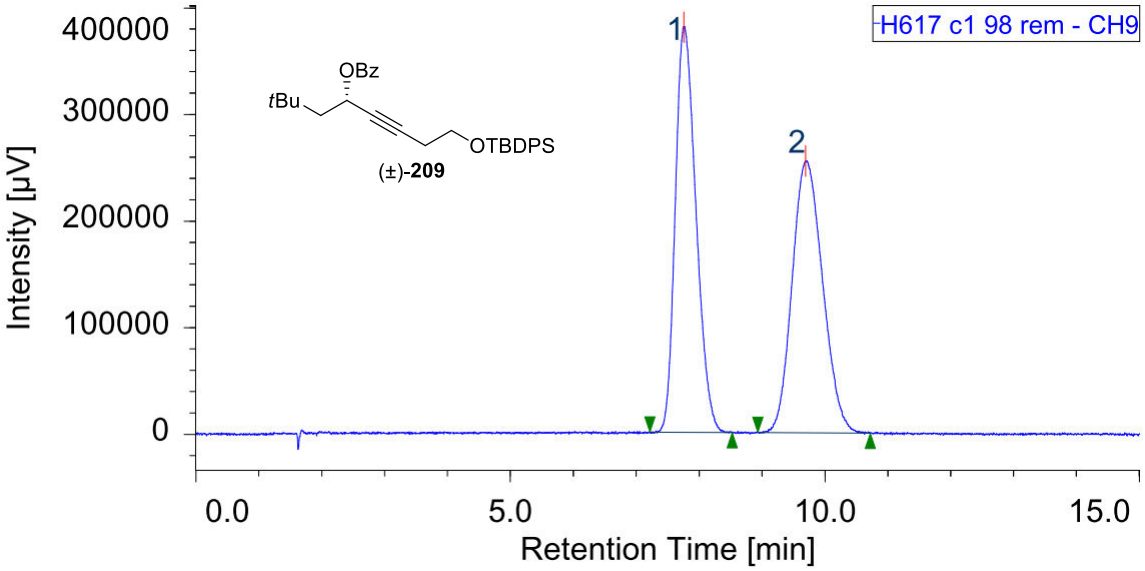

#	Peak Name	CH	tR [min]	Area [µV·sec]	Height [µV]	Area%	Height%	Quantity	NTP	Resolution	Symmetry Factor
1	Unknown	9	7.753	8671674	379925	50.287	59.857	N/A	2617	2.578	1.292
2	Unknown	9	9.687	8572802	254795	49.713	40.143	N/A	1863	N/A	1.181

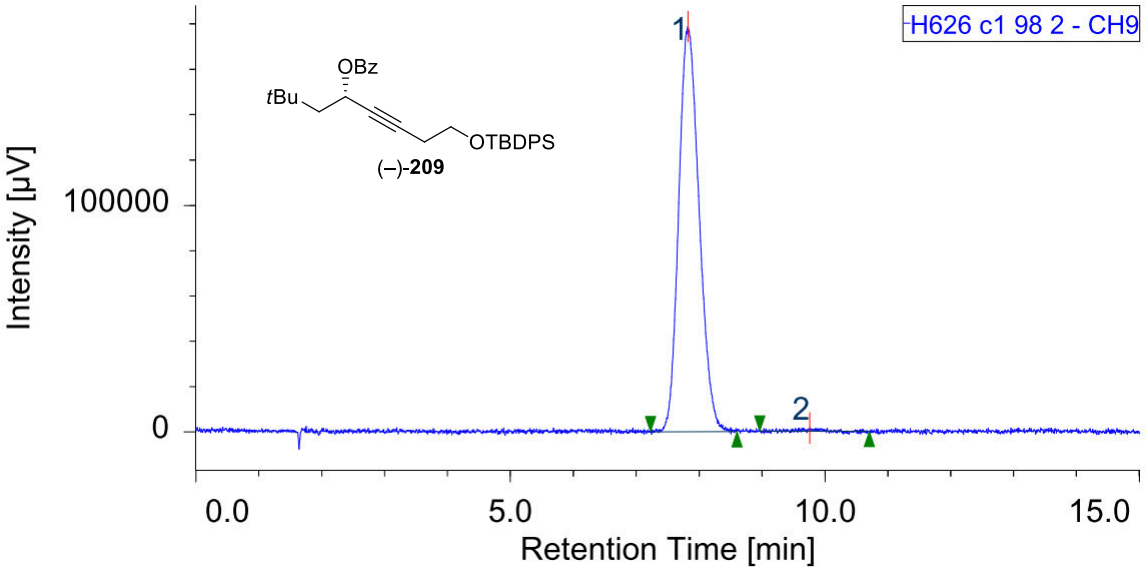

#	Peak Name	CH	tR [min]	Area [µV·sec]	Height [µV]	Area%	Height%	Quantity	NTP	Resolution	Symmetry Factor
1	Unknown	9	7.820	4021224	178669	99.250	99.274	N/A	2759	1.182	1.188
2	Unknown	9	9.753	30381	1306	0.750	0.726	N/A	211	N/A	1.079

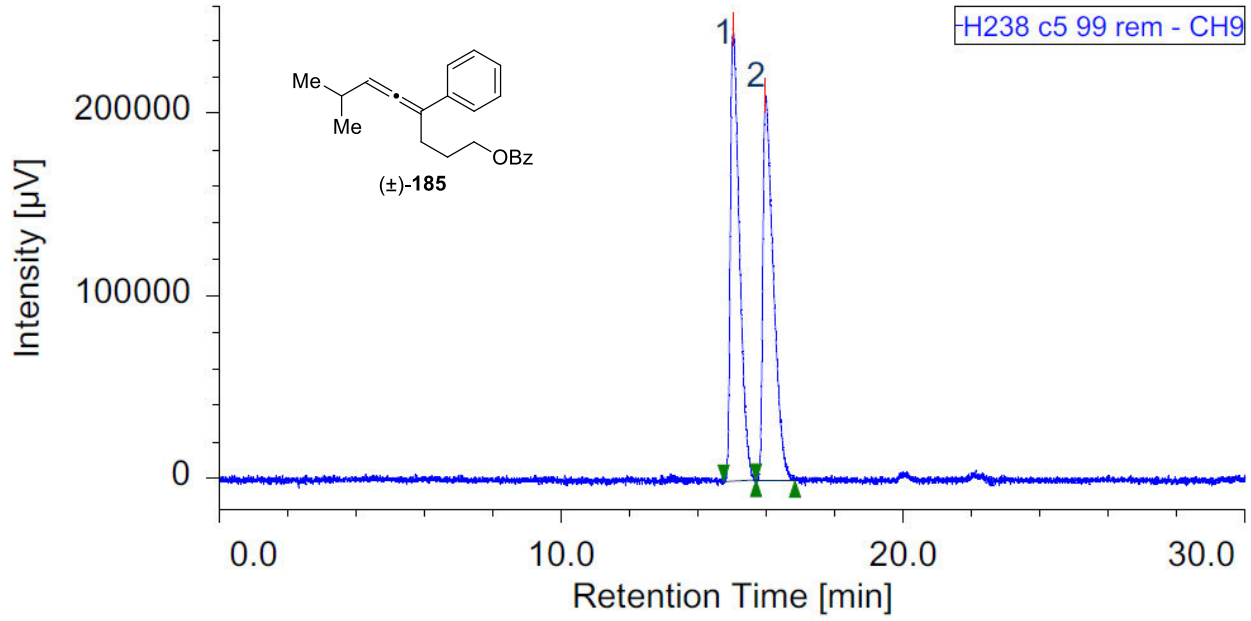

#	Peak Name	CH	tR [min]	Area [µV·sec]	Height [µV]	Area%	Height%	Quantity	NTP	Resolution	Symmetry Factor
1	Unknown	9	15.020	4518708	247615	49.925	54.023	N/A	15827	1.838	1.978
2	Unknown	9	15.967	4532315	210740	50.075	45.977	N/A	13217	N/A	2.320

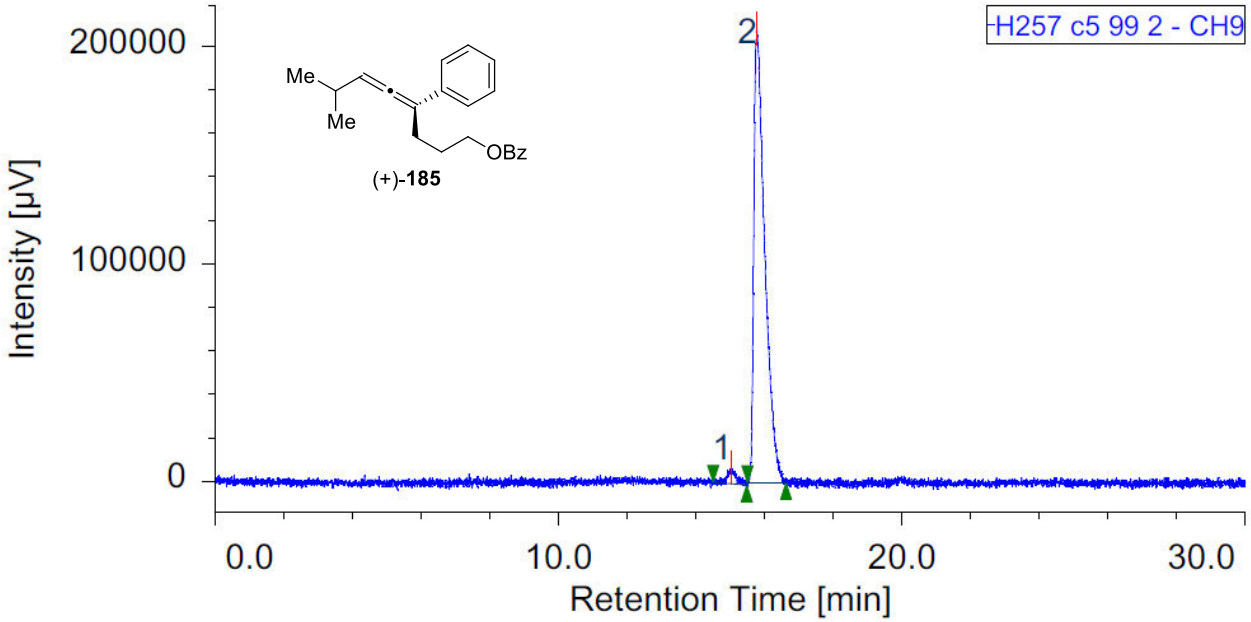

#	Peak Name	CH	tR [min]	Area [µV·sec]	Height [µV]	Area%	Height%	Quantity	NTP	Resolution	Symmetry Factor
1	Unknown	9	15.027	132255	7218	2.816	3.339	N/A	17097	1.456	0.955
2	Unknown	9	15.767	4564425	208961	97.184	96.661	N/A	12692	N/A	2.385

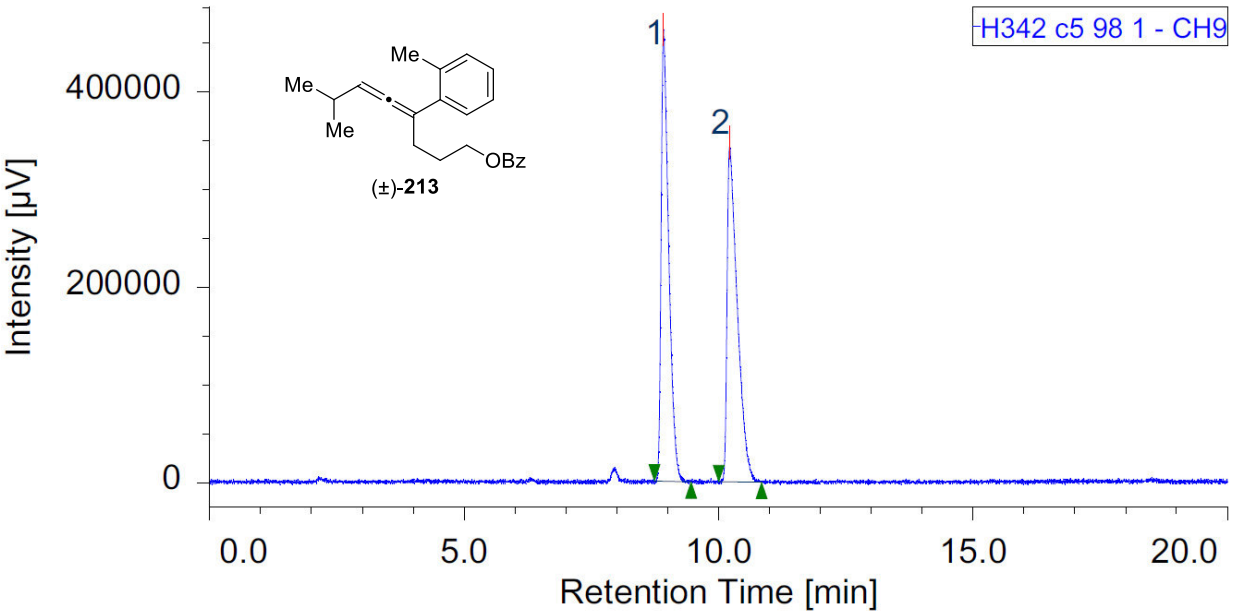

#	Peak Name	CH	tR [min]	Area [µV·sec]	Height [µV]	Area%	Height%	Quantity	NTP	Resolution	Symmetry Factor
1	Unknown	9	8.920	4851250	462156	50.026	57.110	N/A	17338	4.091	1.752
2	Unknown	9	10.213	4846116	347089	49.974	42.890	N/A	12670	N/A	2.362

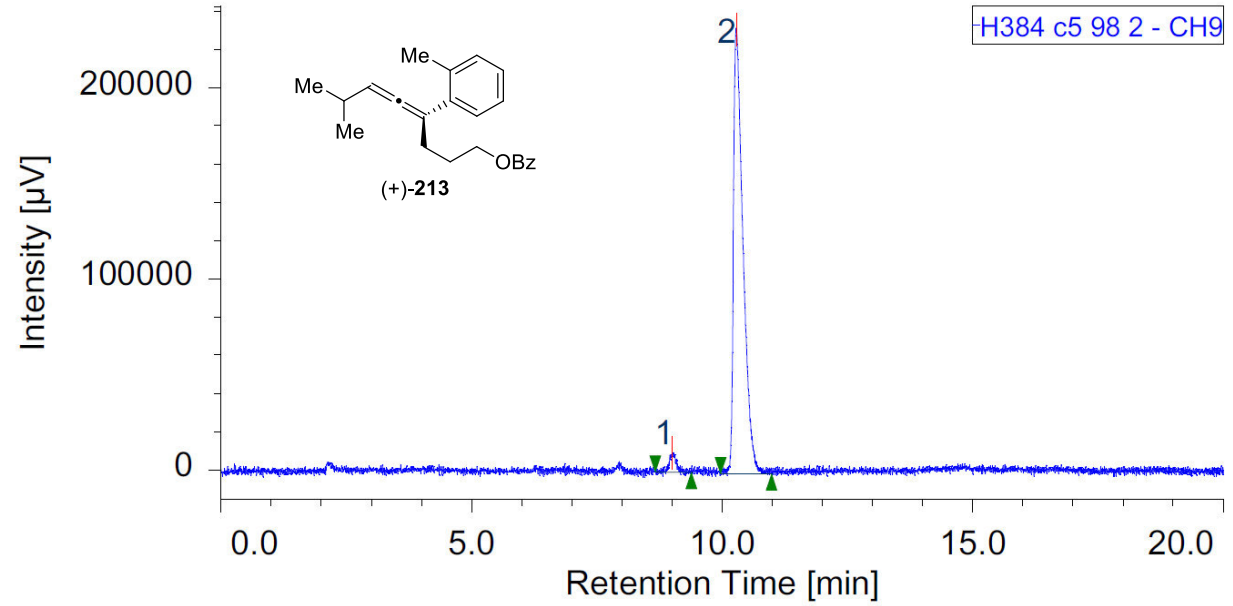

#	Peak Name	CH	tR [min]	Area [µV·sec]	Height [µV]	Area%	Height%	Quantity	NTP	Resolution	Symmetry Factor
1	Unknown	9	9.007	109464	10256	3.440	4.233	N/A	21281	4.341	1.061
2	Unknown	9	10.280	3072385	232048	96.560	95.767	N/A	14520	N/A	1.987

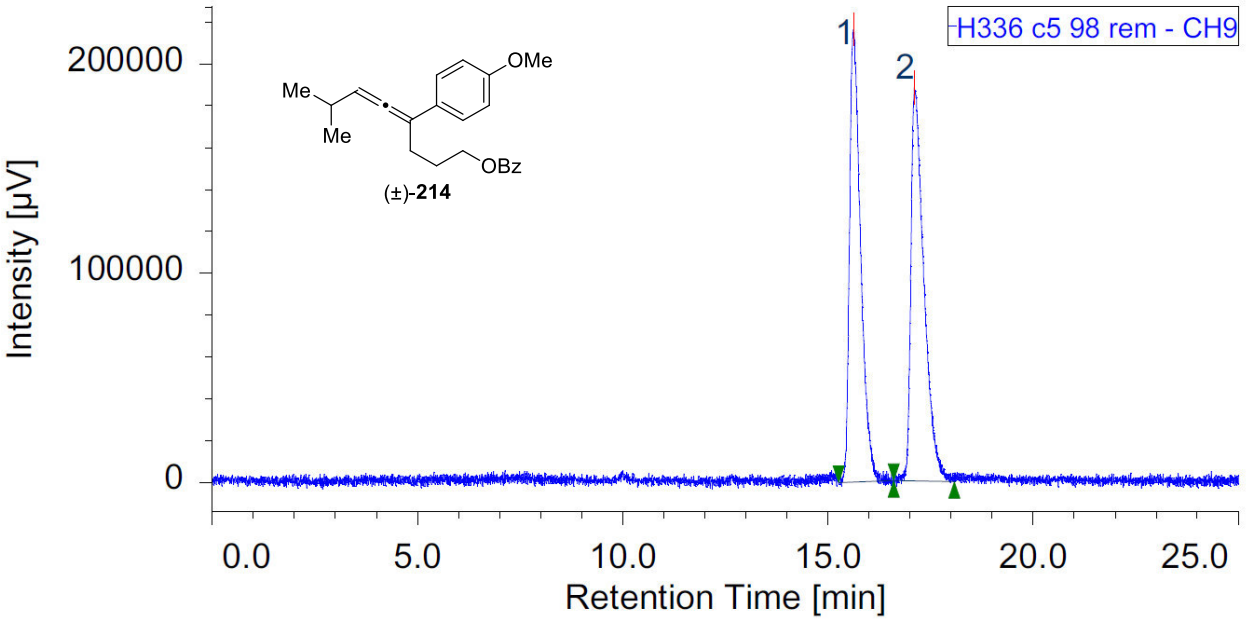

#	Peak Name	CH	tR [min]	Area [µV·sec]	Height [µV]	Area%	Height%	Quantity	NTP	Resolution	Symmetry Factor
1	Unknown	9	15.620	4079345	216174	49.486	53.523	N/A	16595	2.850	1.649
2	Unknown	9	17.100	4164109	187719	50.514	46.477	N/A	15116	N/A	2.179

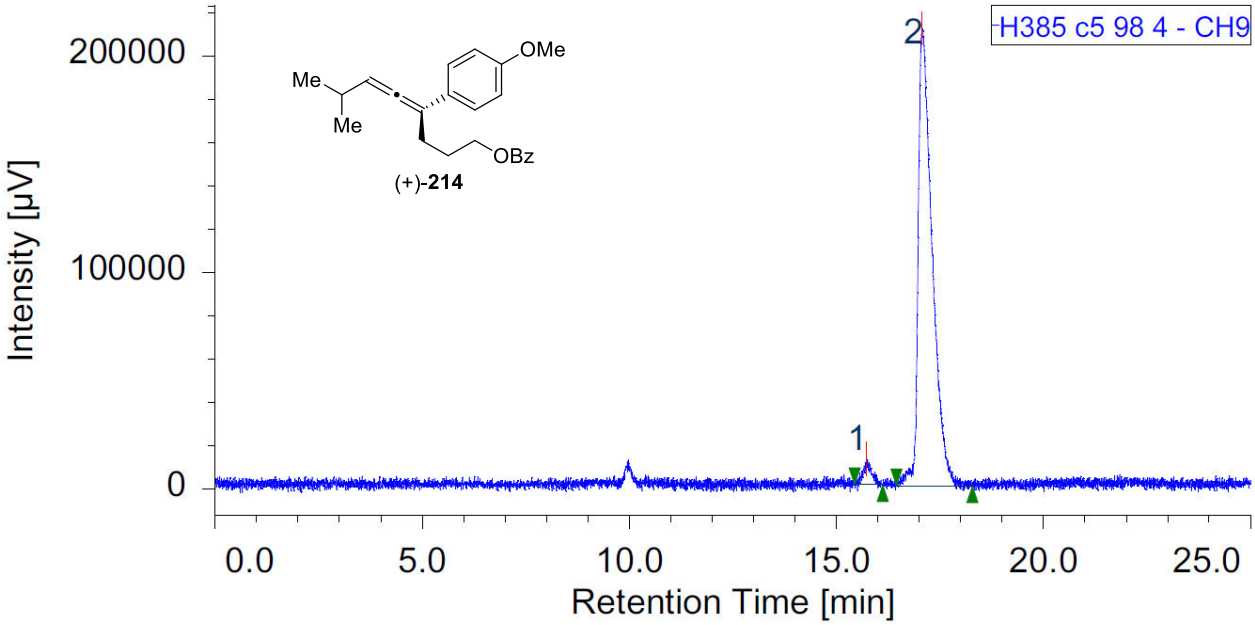

#	Peak Name	CH	tR [min]	Area [µV·sec]	Height [µV]	Area%	Height%	Quantity	NTP	Resolution	Symmetry Factor
2	Unknown	9	15.727	161148	11975	3.143	5.374	N/A	24235	2.684	1.103
1	Unknown	9	17.067	4966245	210880	96.857	94.626	N/A	13074	N/A	2.011

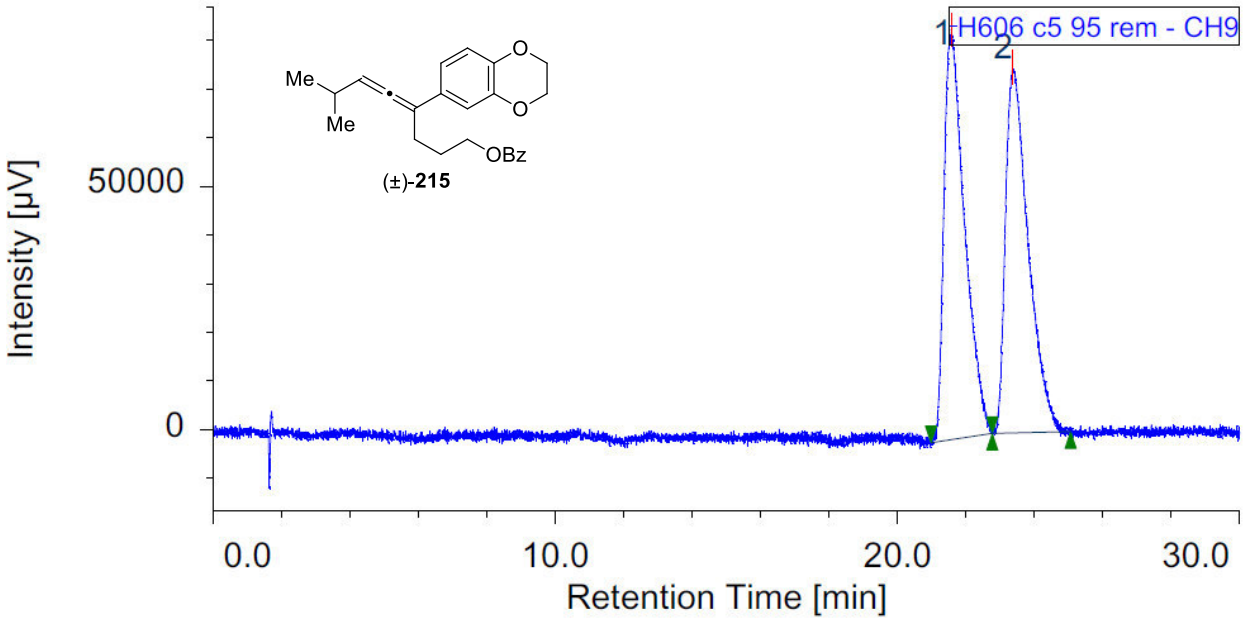

#	Peak Name	CH	tR [min]	Area [µV·sec]	Height [µV]	Area%	Height%	Quantity	NTP	Resolution	Symmetry Factor
1	Unknown	9	21.573	3512786	84196	50.311	52.866	N/A	6327	1.562	1.760
2	Unknown	9	23.360	3469375	75066	49.689	47.134	N/A	5970	N/A	1.923

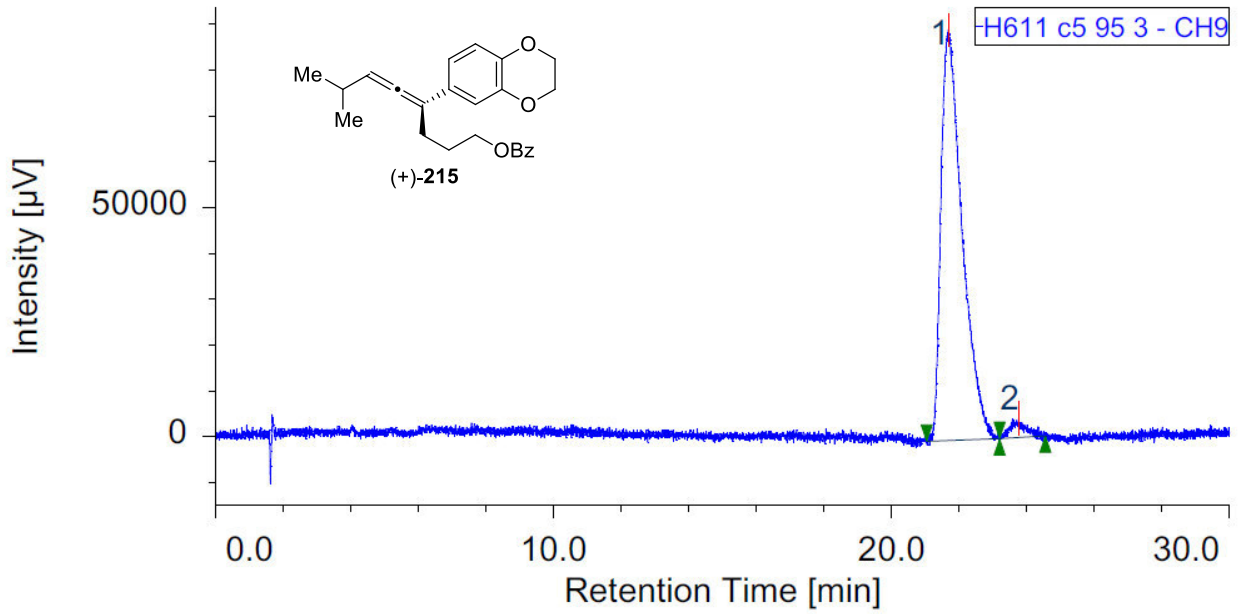

#	Peak Name	CH	tR [min]	Area [µV·sec]	Height [µV]	Area%	Height%	Quantity	NTP	Resolution	Symmetry Factor
1	Unknown	9	21.680	3889076	89703	96.833	95.551	N/A	6106	1.978	1.857
2	Unknown	9	23.760	127212	4177	3.167	4.449	N/A	9054	N/A	1.199

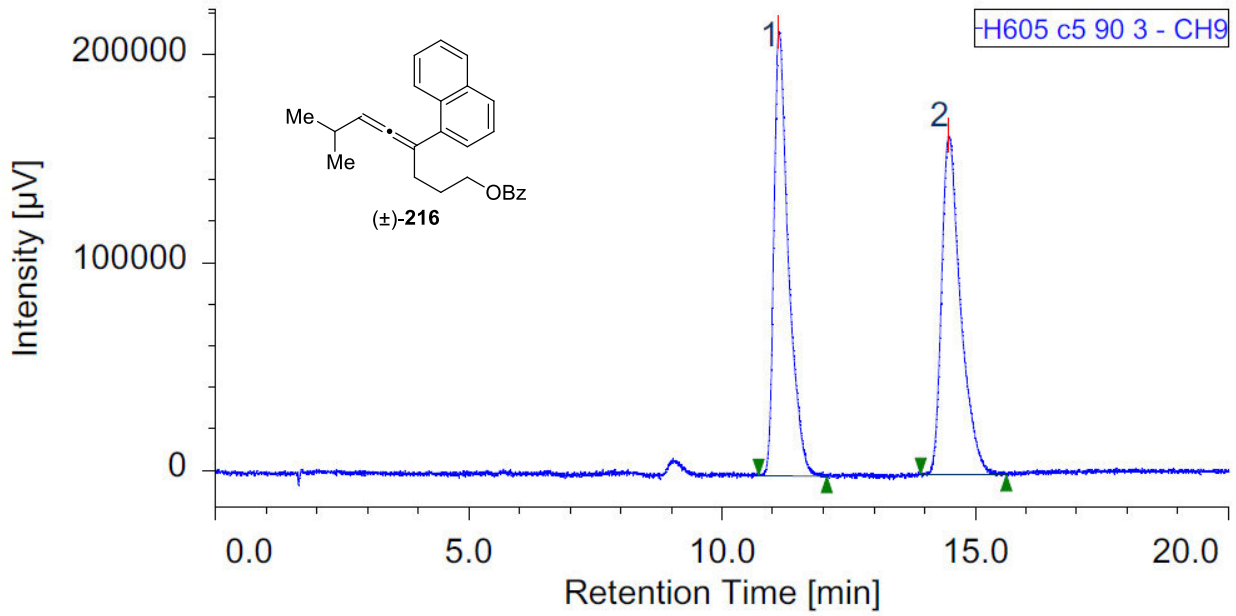

#	Peak Name	CH	tR [min]	Area [µV·sec]	Height [µV]	Area%	Height%	Quantity	NTP	Resolution	Symmetry Factor
1	Unknown	9	11.120	4293038	213661	50.271	56.714	N/A	8151	5.871	1.680
2	Unknown	9	14.460	4246701	163075	49.729	43.286	N/A	7962	N/A	1.610

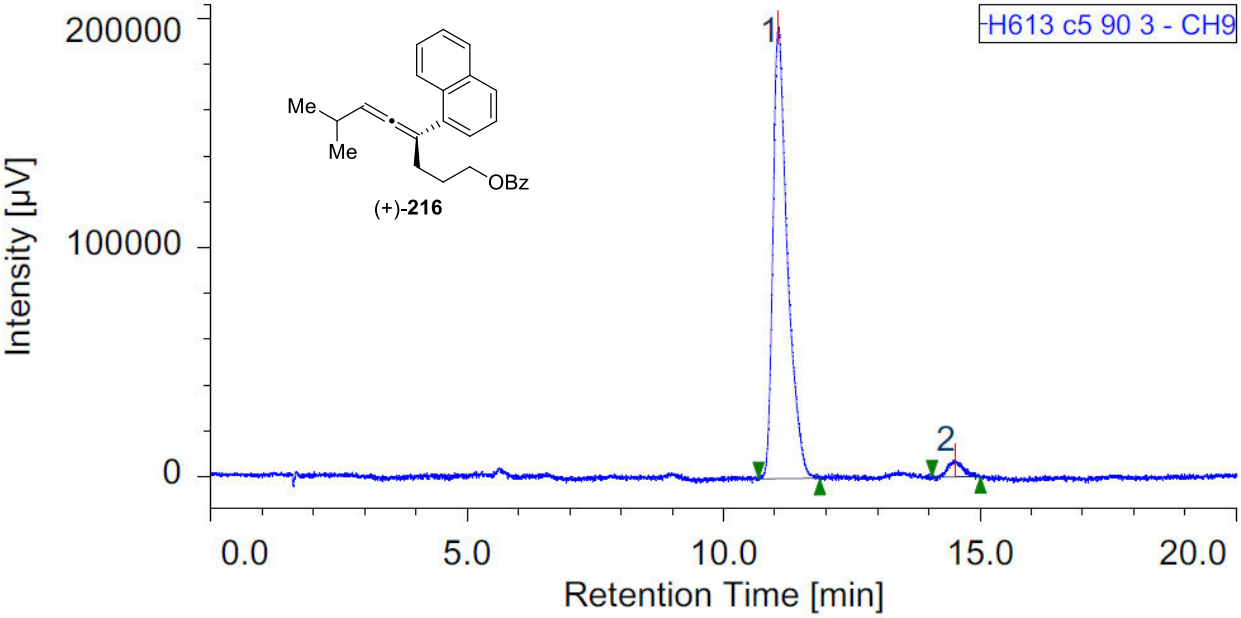

#	Peak Name	CH	tR [min]	Area [µV·sec]	Height [µV]	Area%	Height%	Quantity	NTP	Resolution	Symmetry Factor
1	Unknown	9	11.067	3931243	197010	96.532	96.447	N/A	7929	6.471	1.551
2	Unknown	9	14.507	141241	7257	3.468	3.553	N/A	10405	N/A	1.030

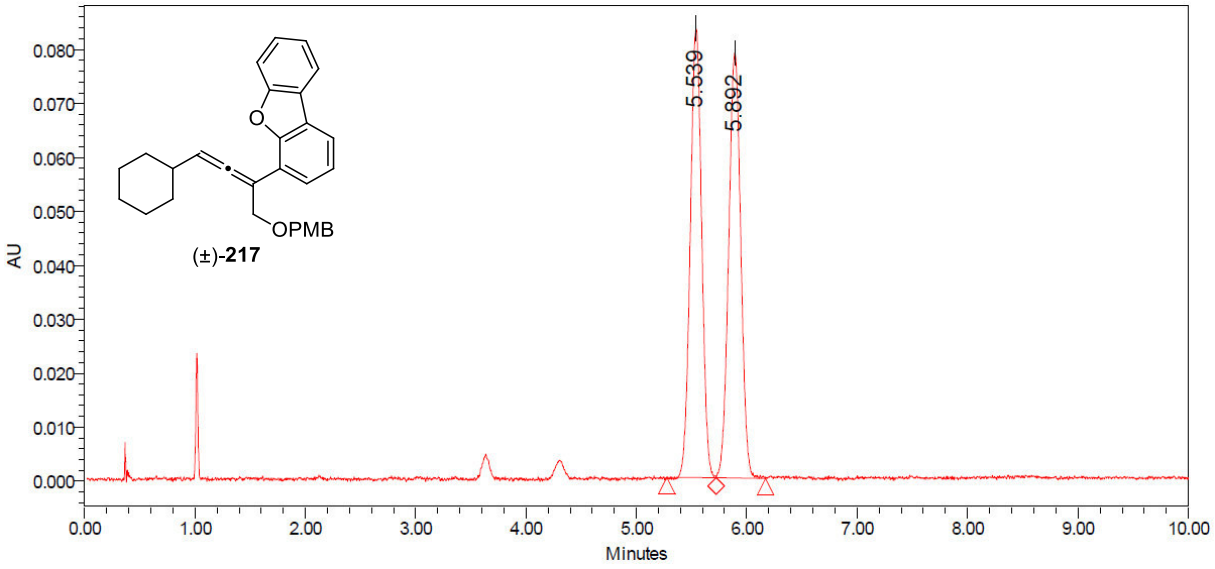

	Processed Channel	Retention Time (min)	Area	% Area	Height
1	PDA 258.0 nm (190-400)nm	5.539	598909	49.94	83274
2	PDA 258.0 nm (190-400)nm	5.892	600394	50.06	78817

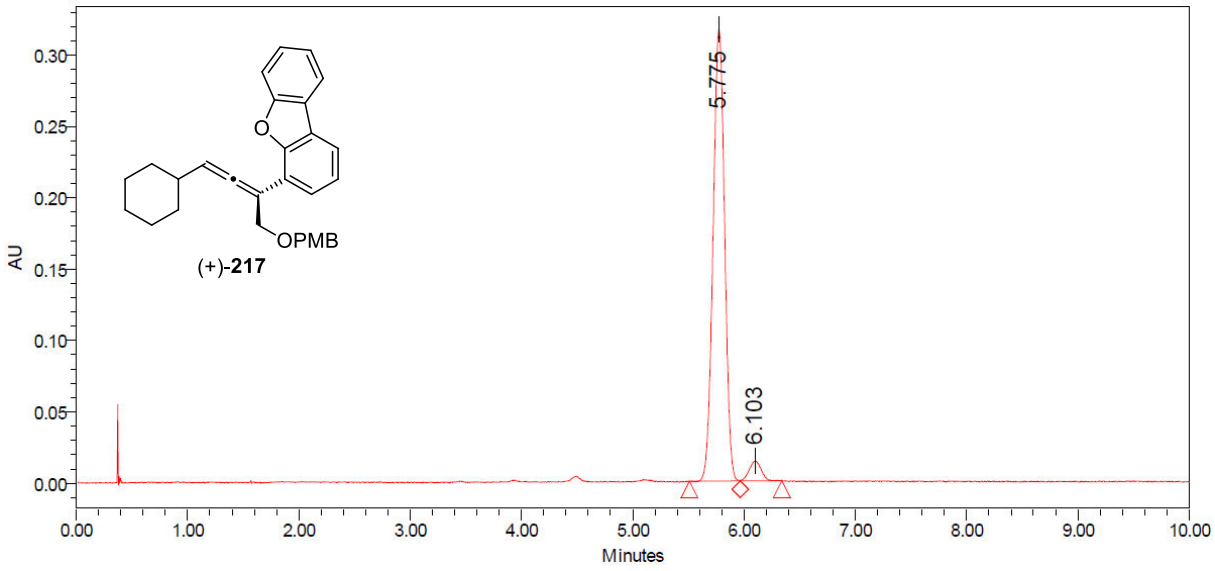

	Processed Channel	Retention Time (min)	Area	% Area	Height
1	PDA 258.0 nm (190-400)nm	5.775	2279533	95.69	316344
2	PDA 258.0 nm (190-400)nm	6.103	102767	4.31	13915

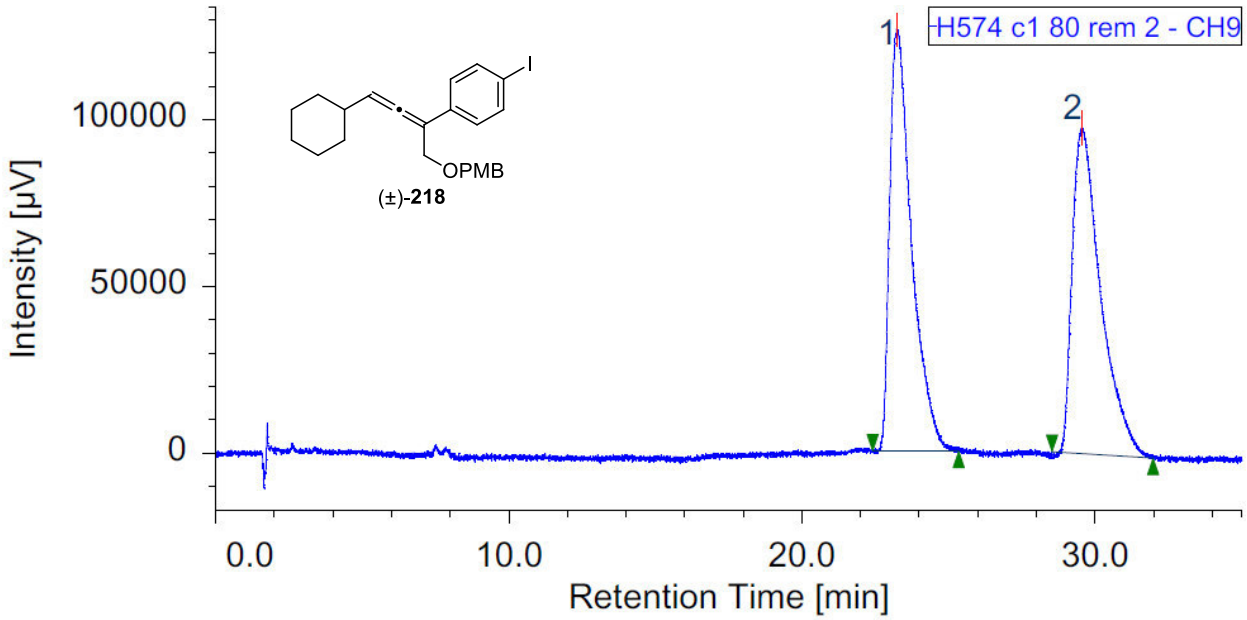

#	Peak Name	CH	tR [min]	Area [µV·sec]	Height [µV]	Area%	Height%	Quantity	NTP	Resolution	Symmetry Factor
1	Unknown	9	23.213	6587449	126352	50.135	56.410	N/A	5100	4.244	1.986
2	Unknown	9	29.540	6552020	97636	49.865	43.590	N/A	4891	N/A	1.942

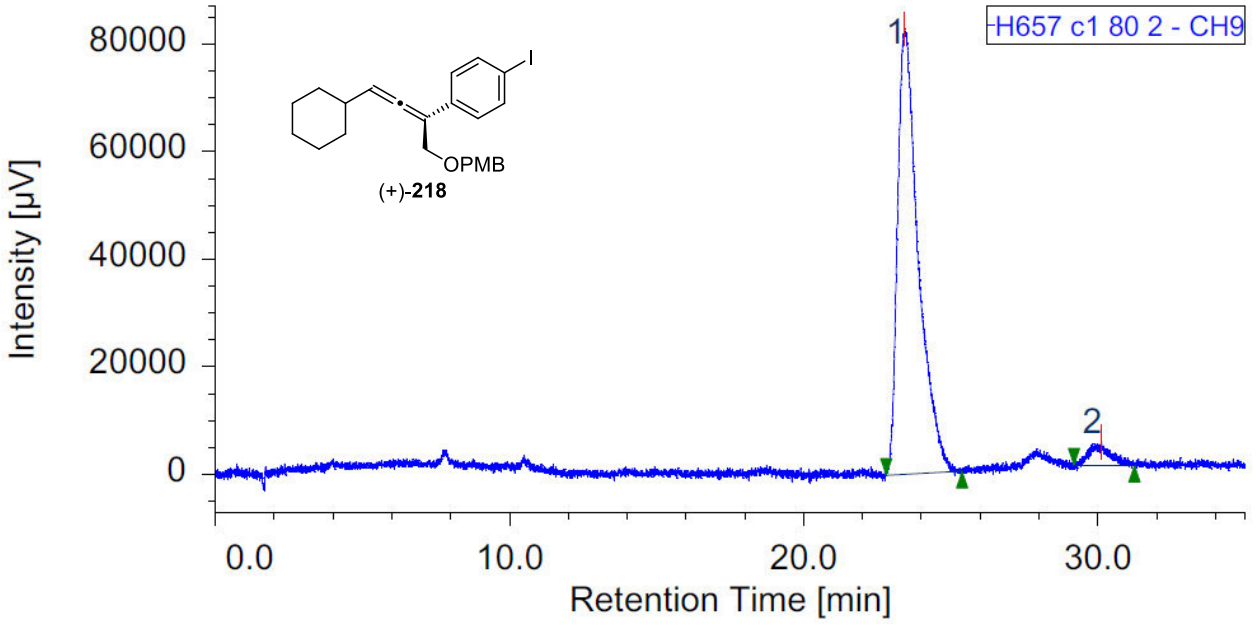

#	Peak Name	CH	tR [min]	Area [µV·sec]	Height [µV]	Area%	Height%	Quantity	NTP	Resolution	Symmetry Factor
1	Unknown	9	23.420	4089549	82833	95.415	94.977	N/A	5863	4.702	1.843
2	Unknown	9	30.120	196496	4381	4.585	5.023	N/A	5438	N/A	1.114

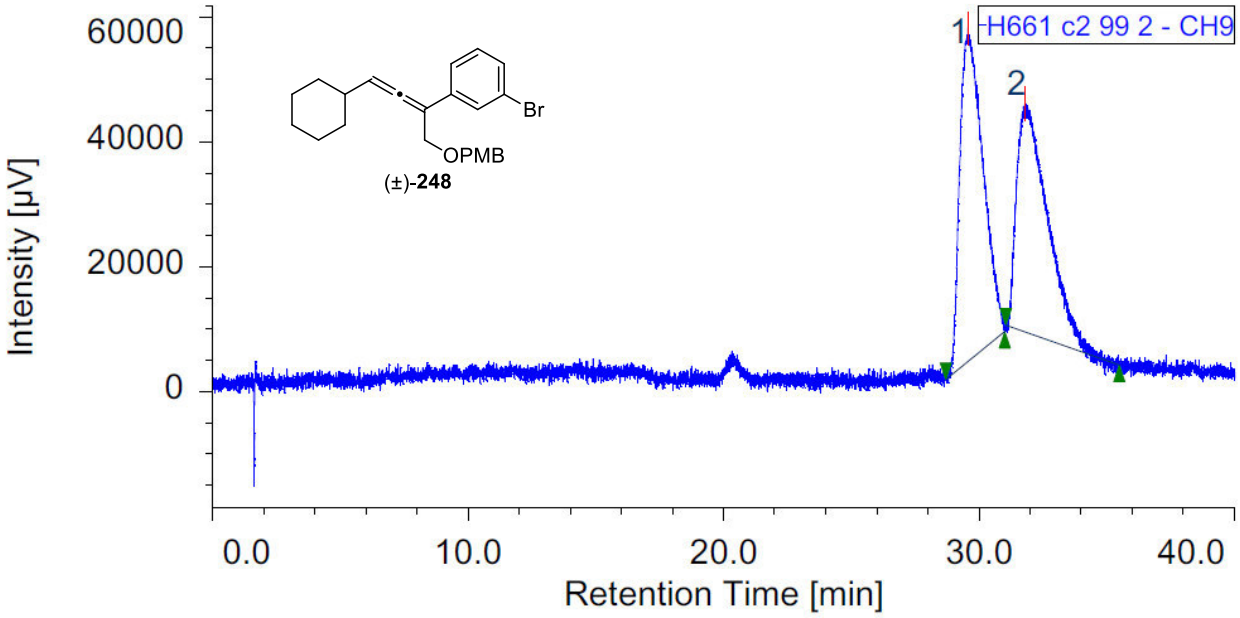

#	Peak Name	CH	tR [min]	Area [µV·sec]	Height [µV]	Area%	Height%	Quantity	NTP	Resolution	Symmetry Factor
1	Unknown	9	29.553	3316863	53385	51.609	59.302	N/A	4671	1.116	1.625
2	Unknown	9	31.813	3109987	36637	48.391	40.698	N/A	2977	N/A	2.342

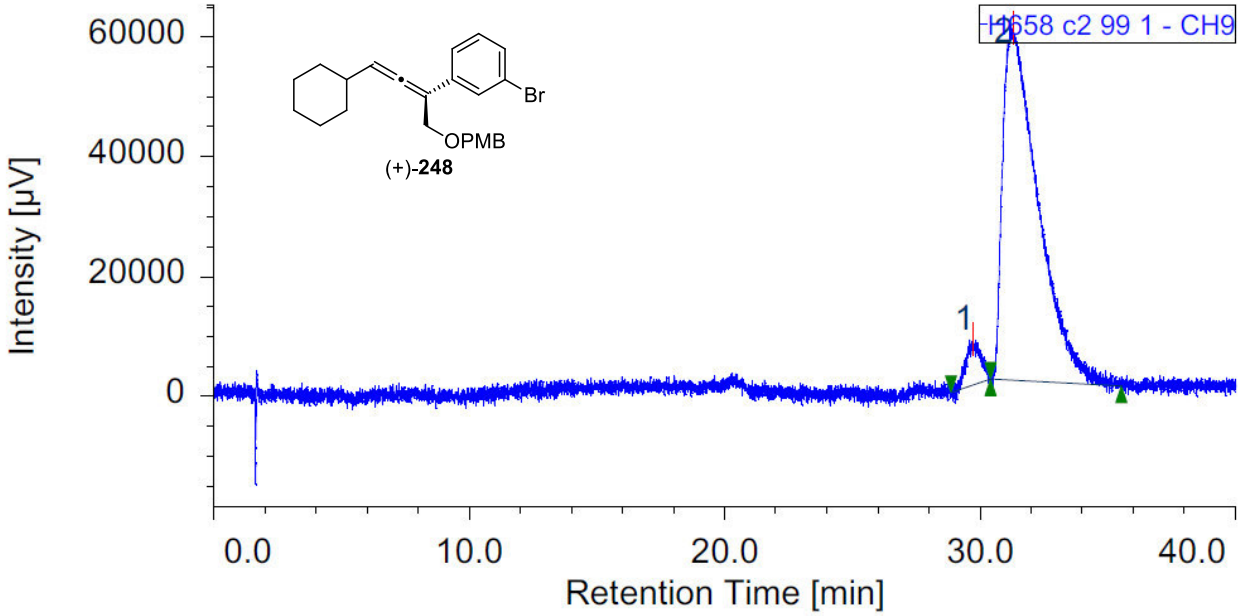

#	Peak Name	CH	tR [min]	Area [µV·sec]	Height [µV]	Area%	Height%	Quantity	NTP	Resolution	Symmetry Factor
1	Unknown	9	29.720	301006	7671	5.046	11.530	N/A	7956	0.805	0.896
2	Unknown	9	31.273	5663954	58860	94.954	88.470	N/A	2432	N/A	2.617

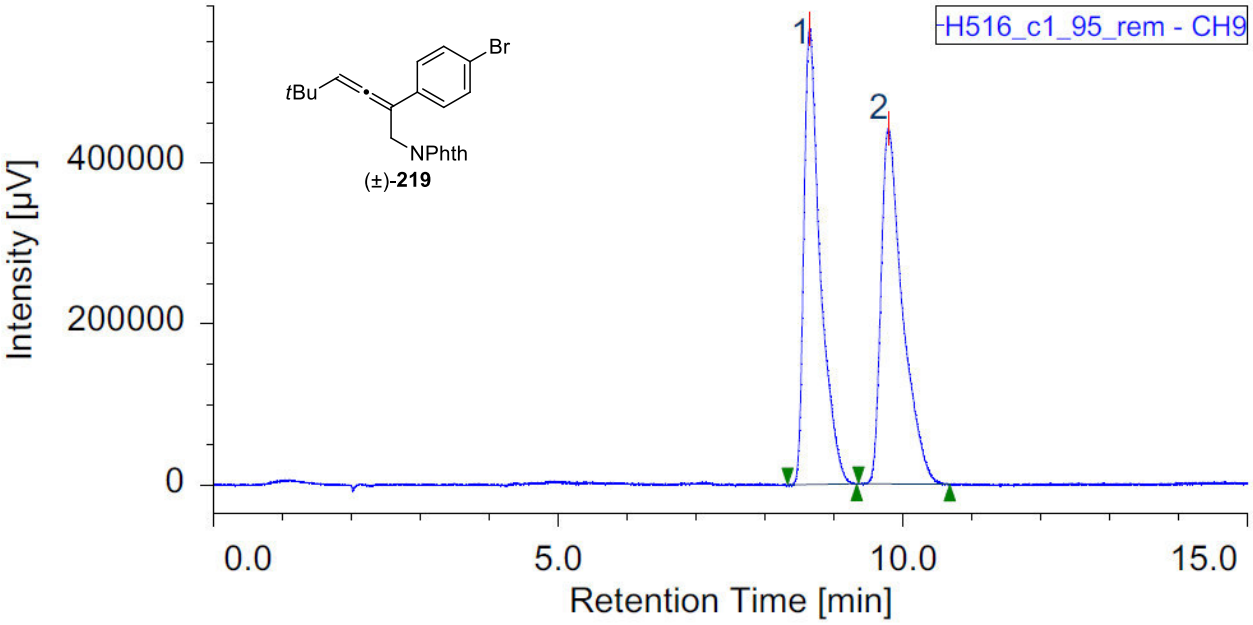

#	Peak Name	CH	tR [min]	Area [µV·sec]	Height [µV]	Area%	Height%	Quantity	NTP	Resolution	Symmetry Factor
1	Unknown	9	8.647	9303466	565794	49.226	56.209	N/A	7638	2.454	1.787
2	Unknown	9	9.787	9595896	440793	50.774	43.791	N/A	5335	N/A	1.770

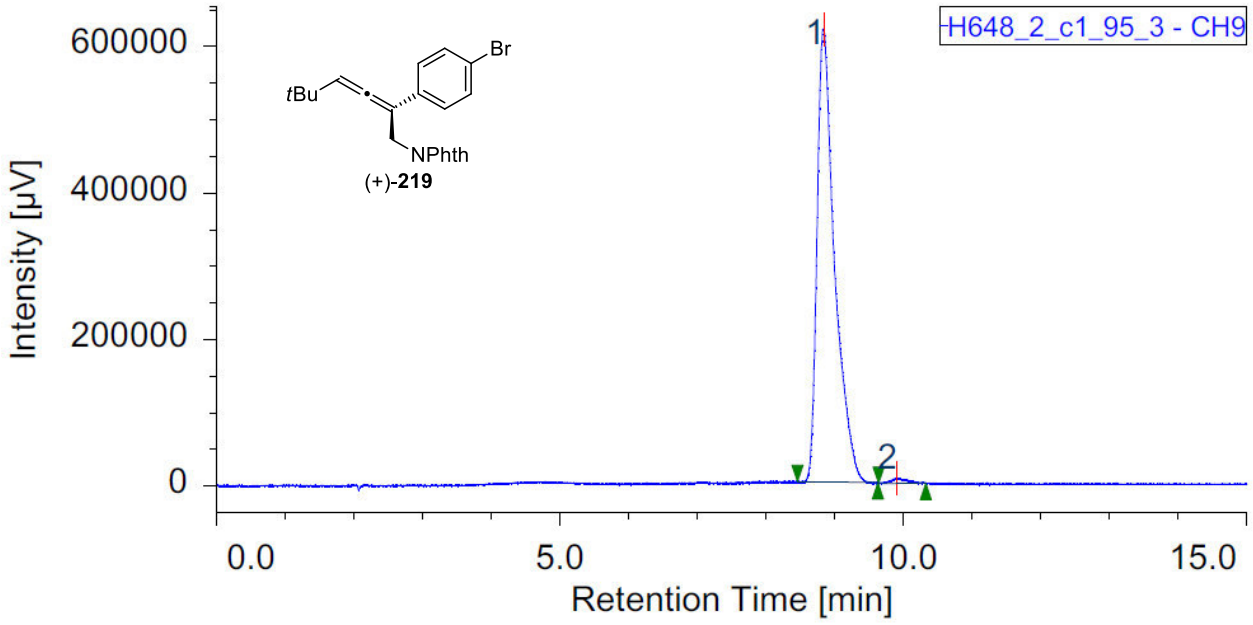

#	Peak Name	CH	tR [min]	Area [µV·sec]	Height [µV]	Area%	Height%	Quantity	NTP	Resolution	Symmetry Factor
1	Unknown	9	8.840	10917057	617655	99.002	98.826	N/A	6757	2.340	1.644
2	Unknown	9	9.900	110025	7338	0.998	1.174	N/A	6853	N/A	1.247

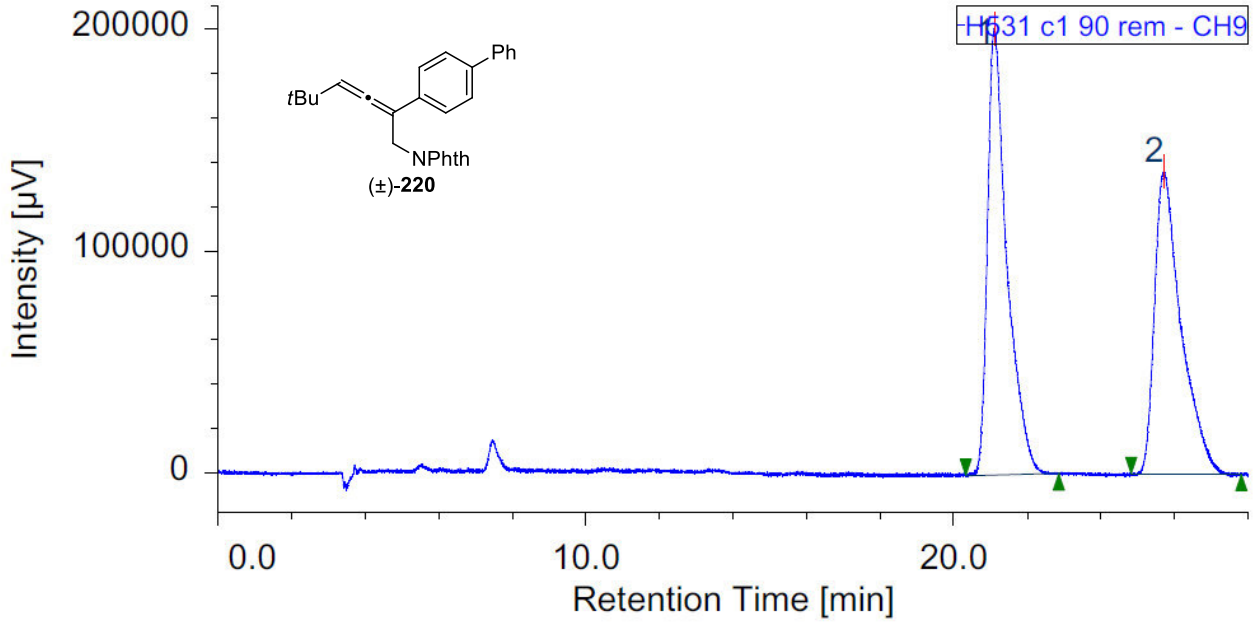

#	Peak Name	CH	tR [min]	Area [µV·sec]	Height [µV]	Area%	Height%	Quantity	NTP	Resolution	Symmetry Factor
1	Unknown	9	21.100	7404778	201253	51.986	59.613	N/A	9186	4.341	1.715
2	Unknown	9	25.700	6838935	136346	48.014	40.387	N/A	6825	N/A	1.717

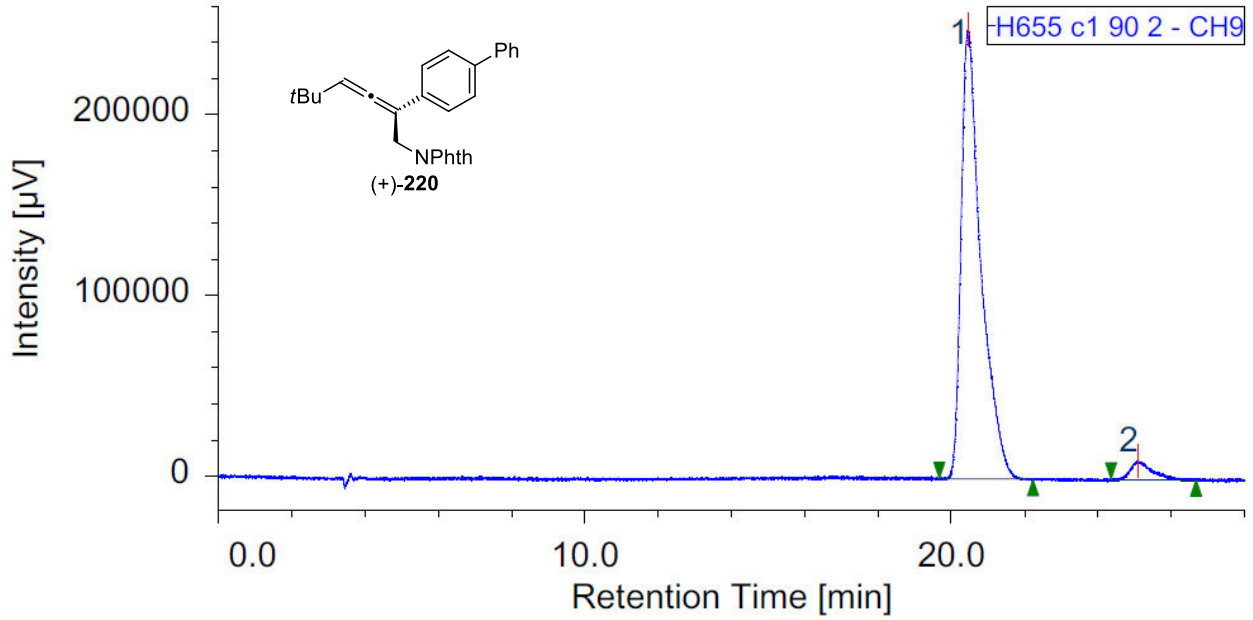

#	Peak Name	CH	tR [min]	Area [µV·sec]	Height [µV]	Area%	Height%	Quantity	NTP	Resolution	Symmetry Factor
1	Unknown	9	20.453	9340140	248778	95.845	96.062	N/A	8233	4.842	1.744
2	Unknown	9	25.080	404917	10199	4.155	3.938	N/A	9777	N/A	1.528

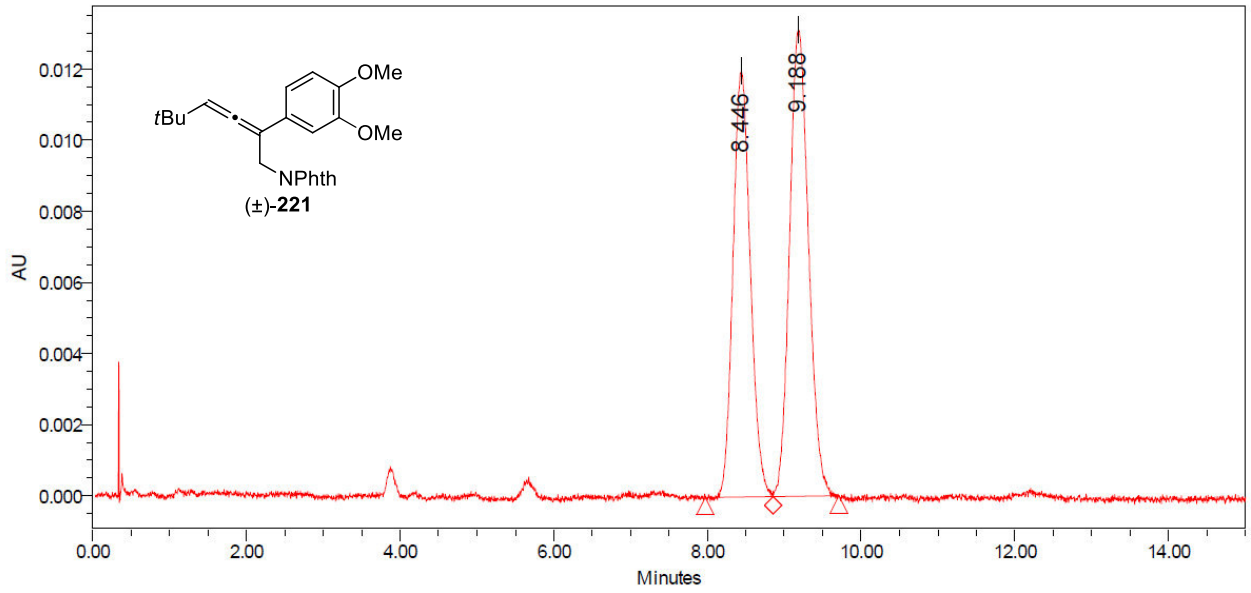

	Processed Channel	Retention Time (min)	Area	% Area
1	PDA Ch1 254nm@1.2nm - Compens.	8.446	188396	45.59
2	PDA Ch1 254nm@1.2nm - Compens.	9.188	224828	54.41

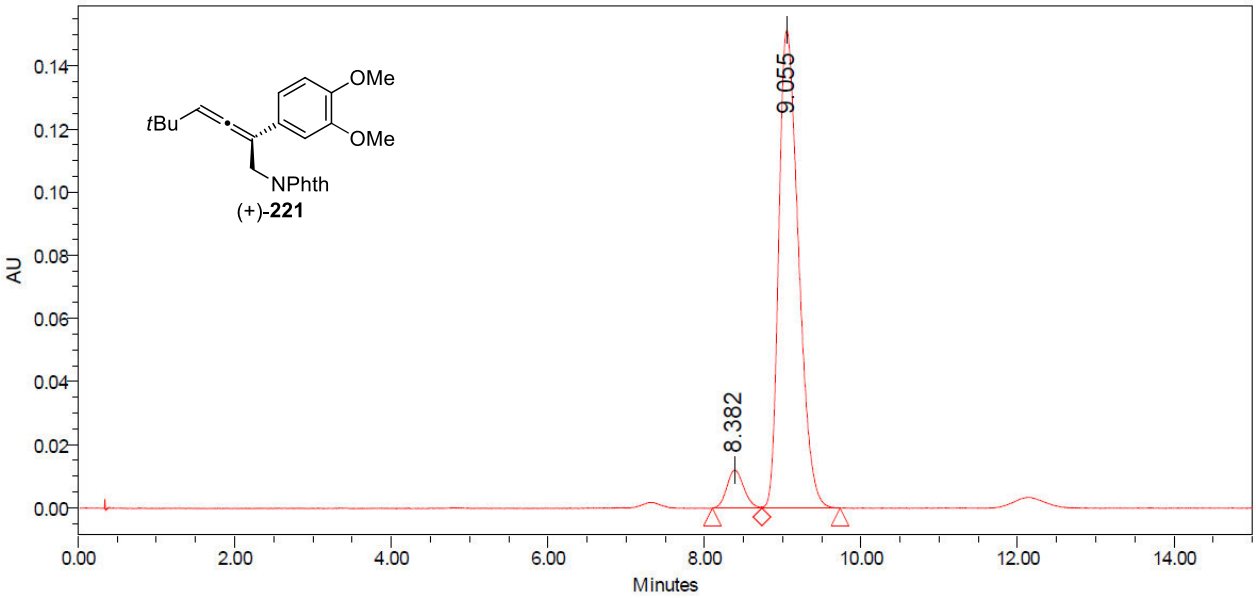

	Processed Channel	Retention Time (min)	Area	% Area
1	PDA Ch1 254nm@1.2nm - Compens.	8.382	181708	6.41
2	PDA Ch1 254nm@1.2nm - Compens.	9.055	2651802	93.59

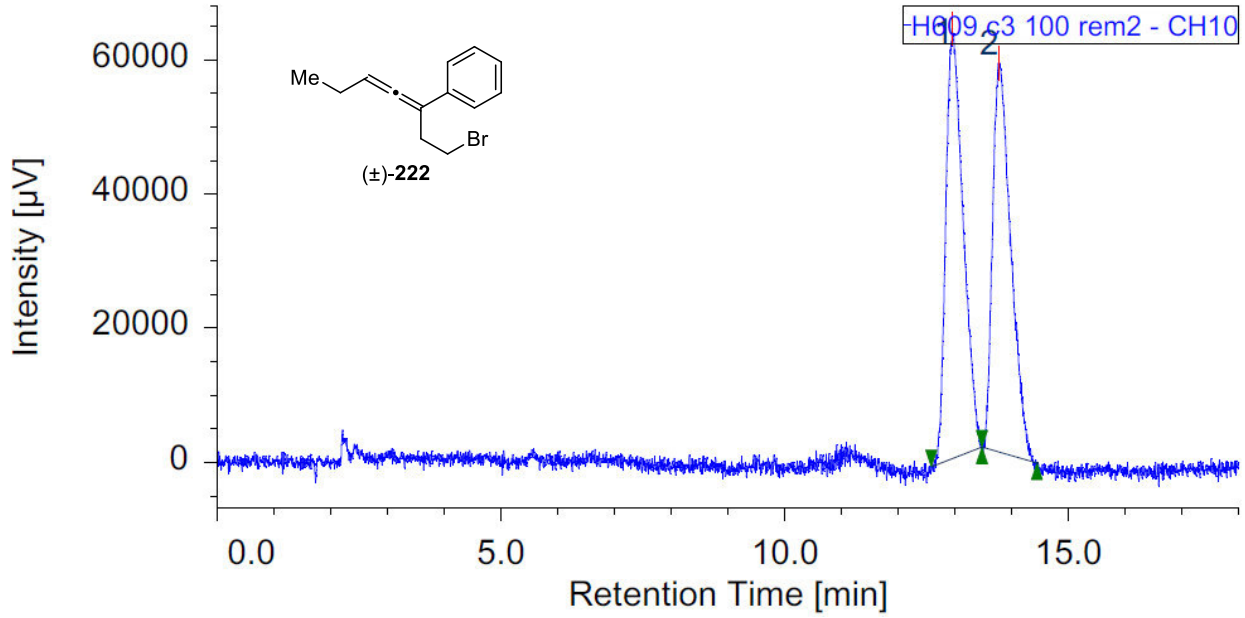

#	Peak Name	CH	tR [min]	Area [µV·sec]	Height [µV]	Area%	Height%	Quantity	NTP	Resolution	Symmetry Factor
1	Unknown	10	12.947	1352694	64051	51.192	52.551	N/A	8485	1.423	1.481
2	Unknown	10	13.767	1289716	57833	48.808	47.449	N/A	8611	N/A	1.622

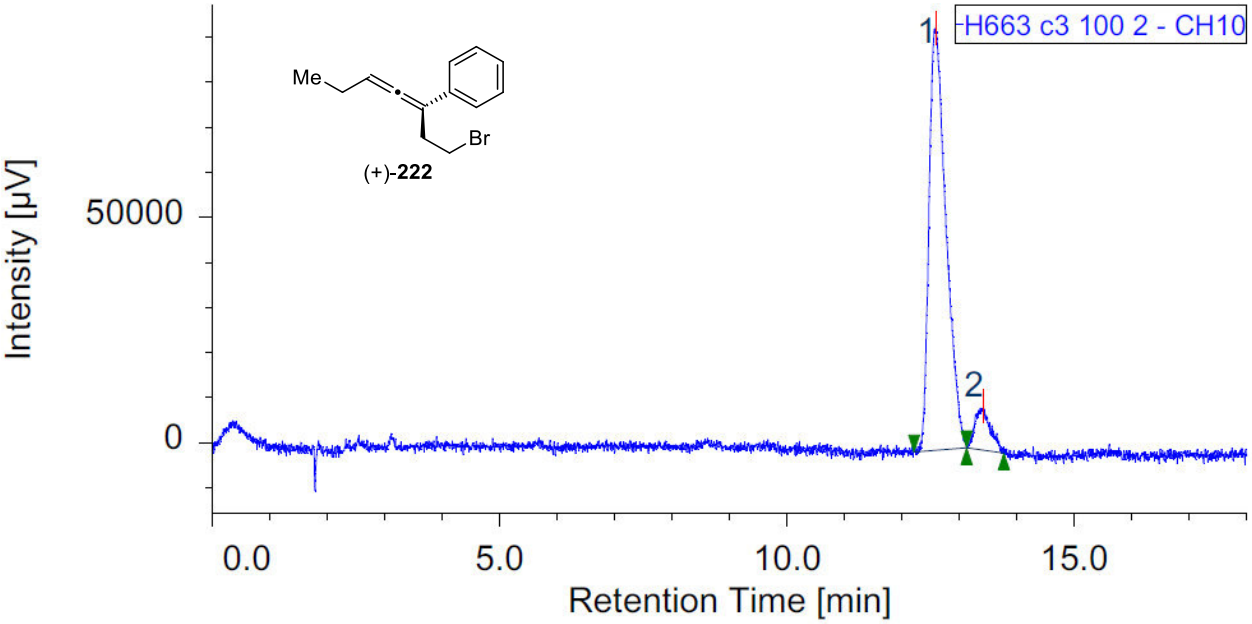

#	Peak Name	CH	tR [min]	Area [µV·sec]	Height [µV]	Area%	Height%	Quantity	NTP	Resolution	Symmetry Factor
1	Unknown	10	12.587	1921346	93854	91.490	90.536	N/A	8653	1.552	1.493
2	Unknown	10	13.420	178722	9811	8.510	9.464	N/A	10046	N/A	1.105

11 NMR Spectroscopic Data

11.1 Part I. Ir-Catalyzed Reverse Prenylation of 3-Substituted Indoles

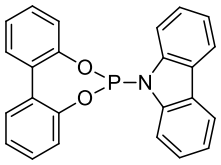

87

^{1}H NMR, 400 MHz
$CDCl_3$, 298 K

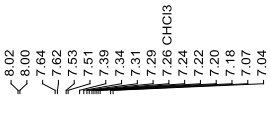

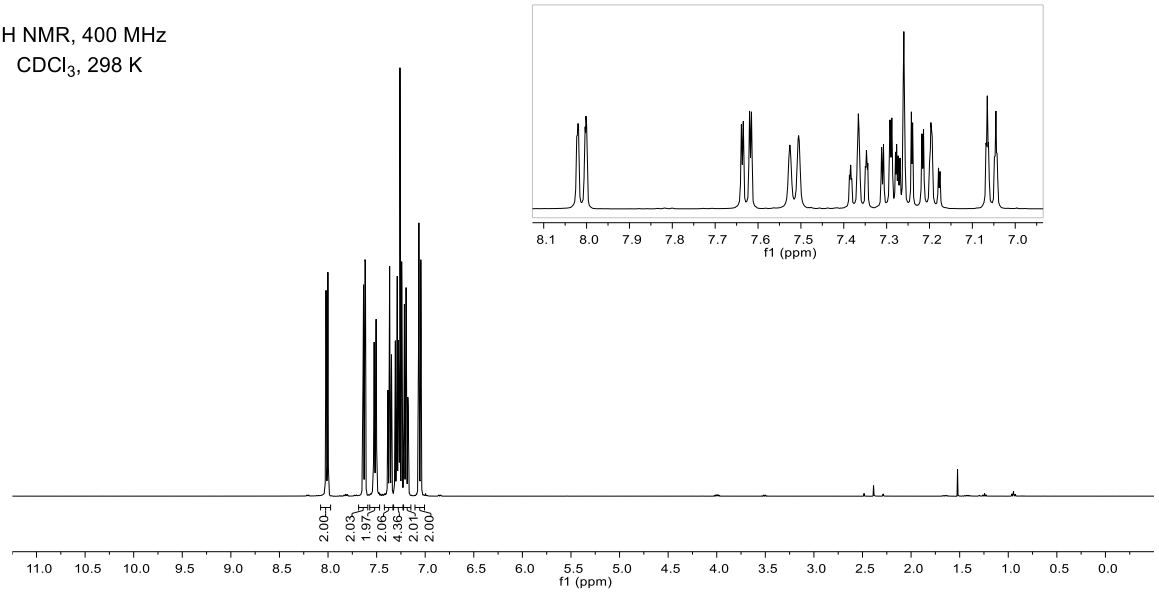

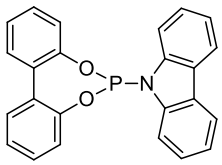

87

^{13}C NMR, 101 MHz, $CDCl_3$, 298 K

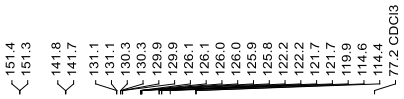

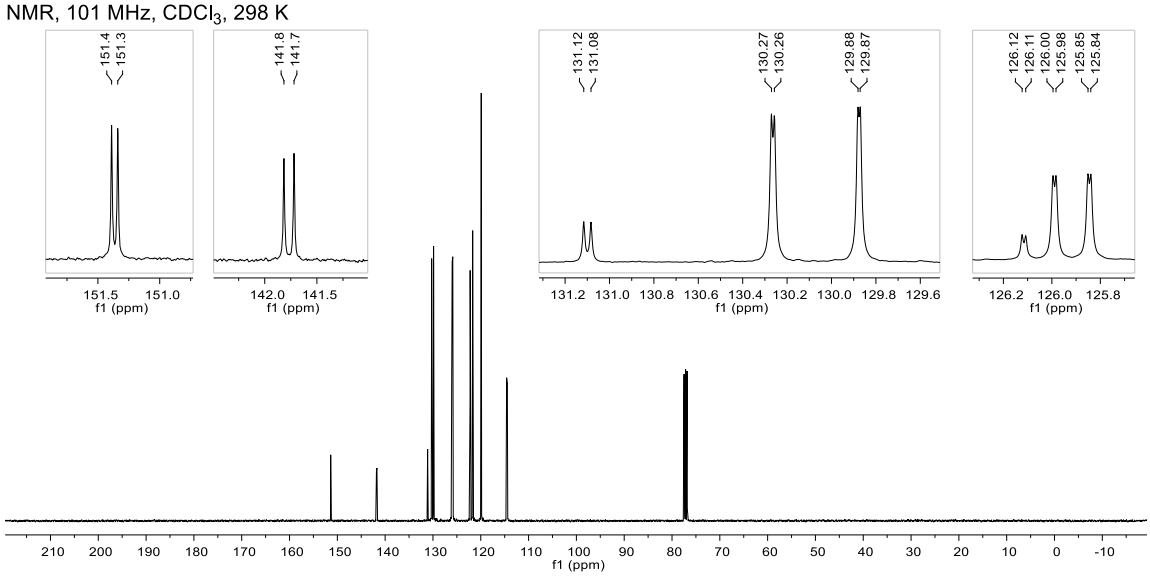

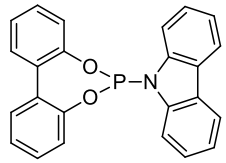

87

$^{31}P\{^{1}H\}$ NMR, 162 MHz
$CDCl_3$, 298 K

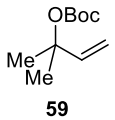

59

^{1}H NMR, 400 MHz
$CDCl_3$, 298 K

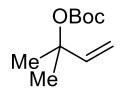

59

^{13}C NMR, 101 MHz
$CDCl_3$, 298 K

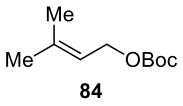

84

^{1}H NMR, 400 MHz
$CDCl_3$, 298 K

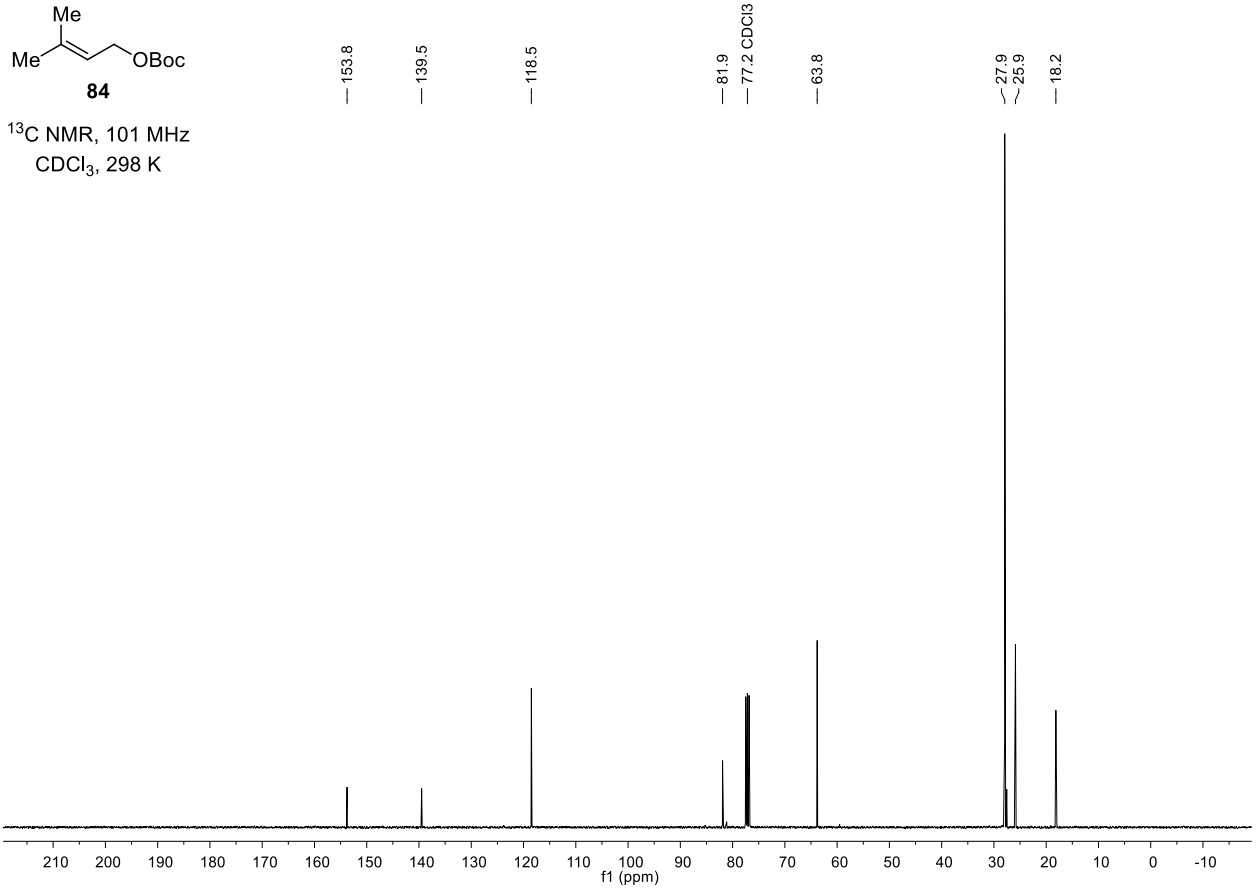
Me
Me
OBoc
84
153.8
139.5
118.5
81.9
77.2 CDCl3
63.8
27.9
25.9
18.2
13C NMR, 101 MHz
CDCl3, 298 K
f1 (ppm)

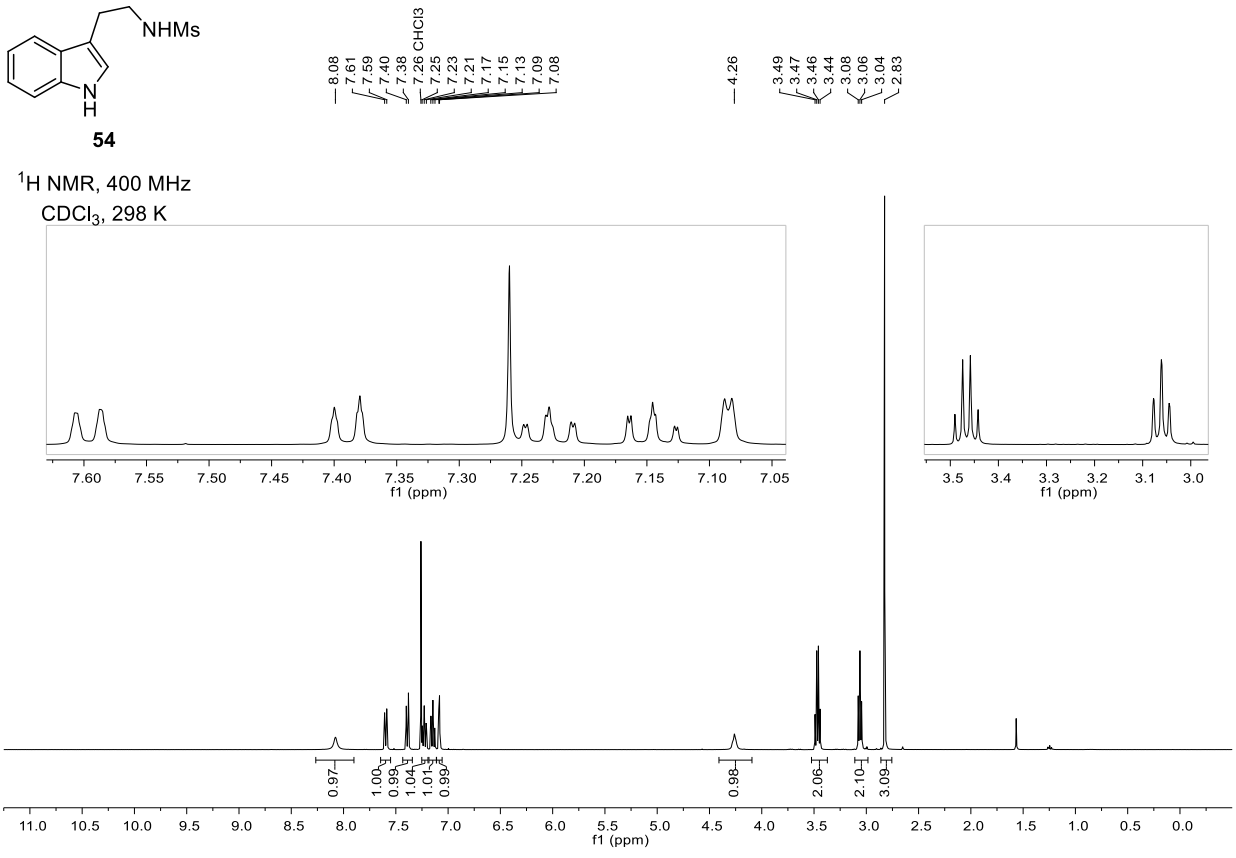
NHMs
N
H
54
8.08
7.61
7.59
7.40
7.38
7.26 CHCl3
7.25
7.23
7.21
7.17
7.15
7.13
7.09
7.08
4.26
3.49
3.47
3.46
3.44
3.08
3.06
3.04
2.83
1H NMR, 400 MHz
CDCl3, 298 K
0.97
1.00
0.99
1.04
1.01
0.99
0.98
2.06
2.10
3.09
f1 (ppm)

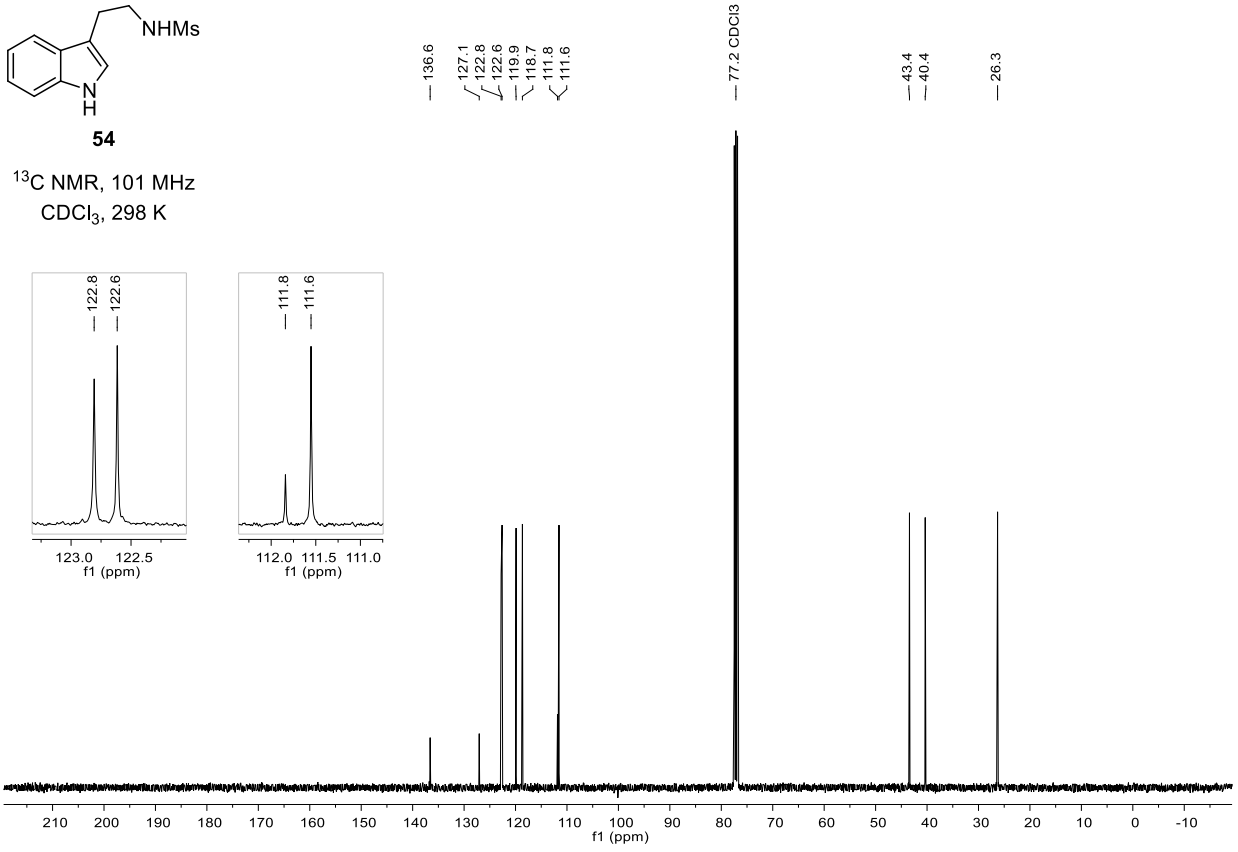

54

^{13}C NMR, 101 MHz
$CDCl_3$, 298 K

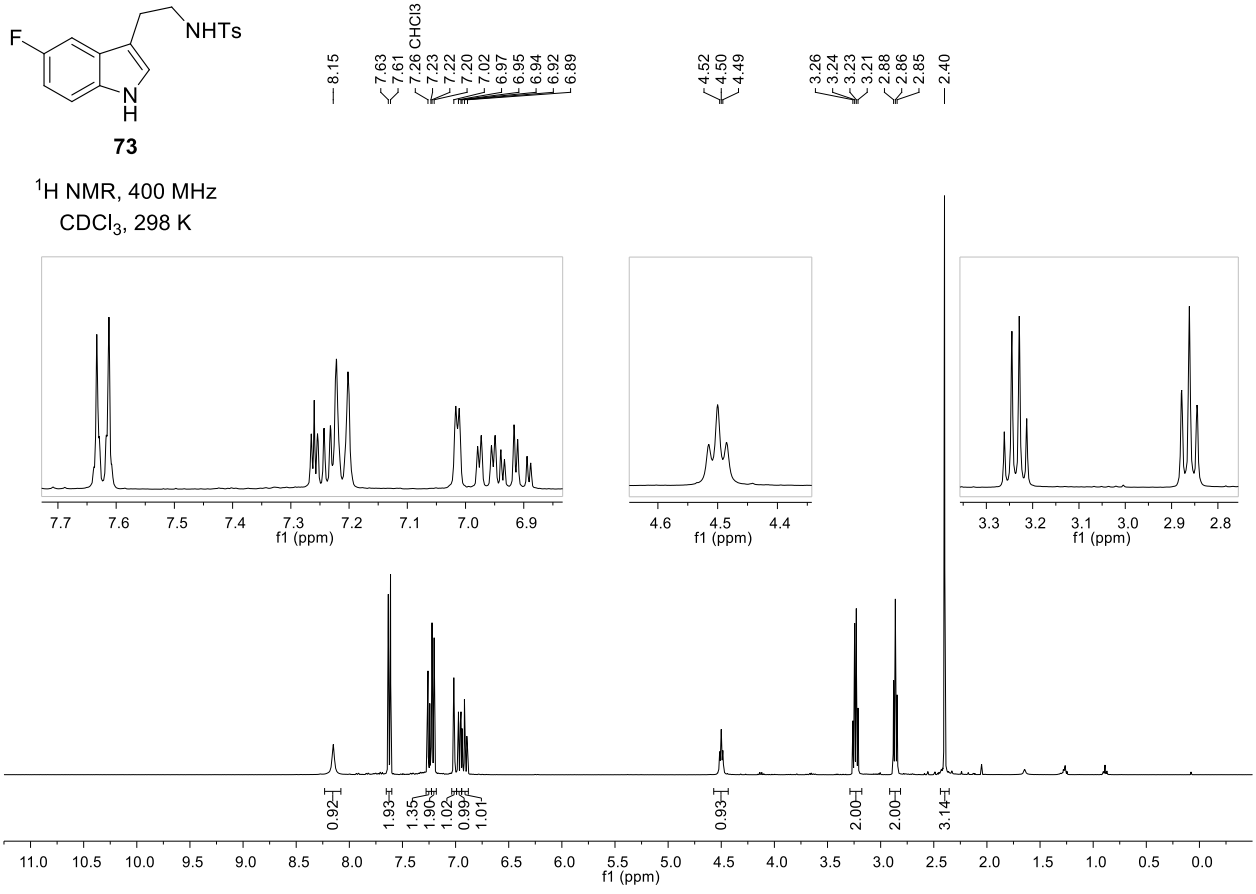

73

^{1}H NMR, 400 MHz
$CDCl_3$, 298 K

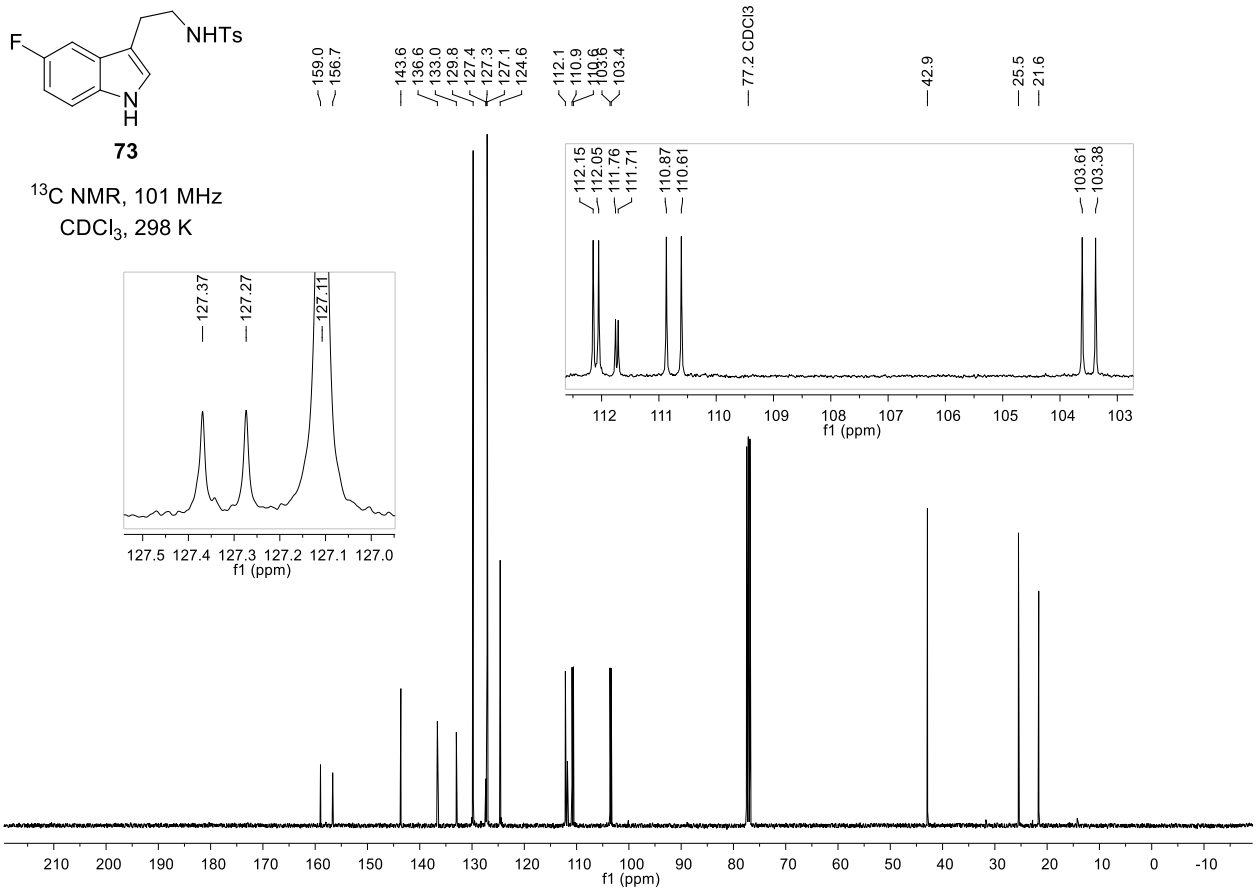

^{13}C NMR, 101 MHz
$CDCl_3$, 298 K

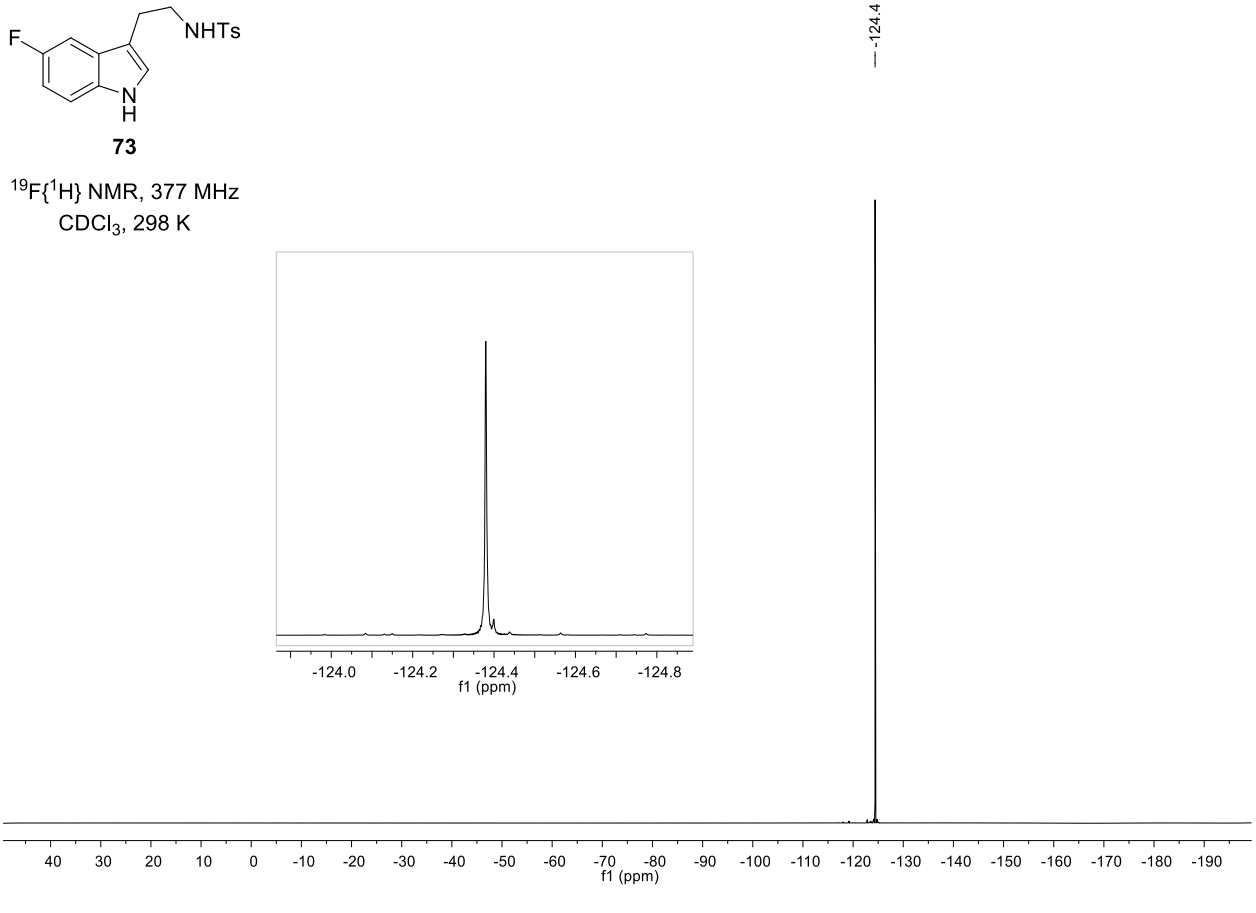

$^{19}F\{^{1}H\}$ NMR, 377 MHz
$CDCl_3$, 298 K

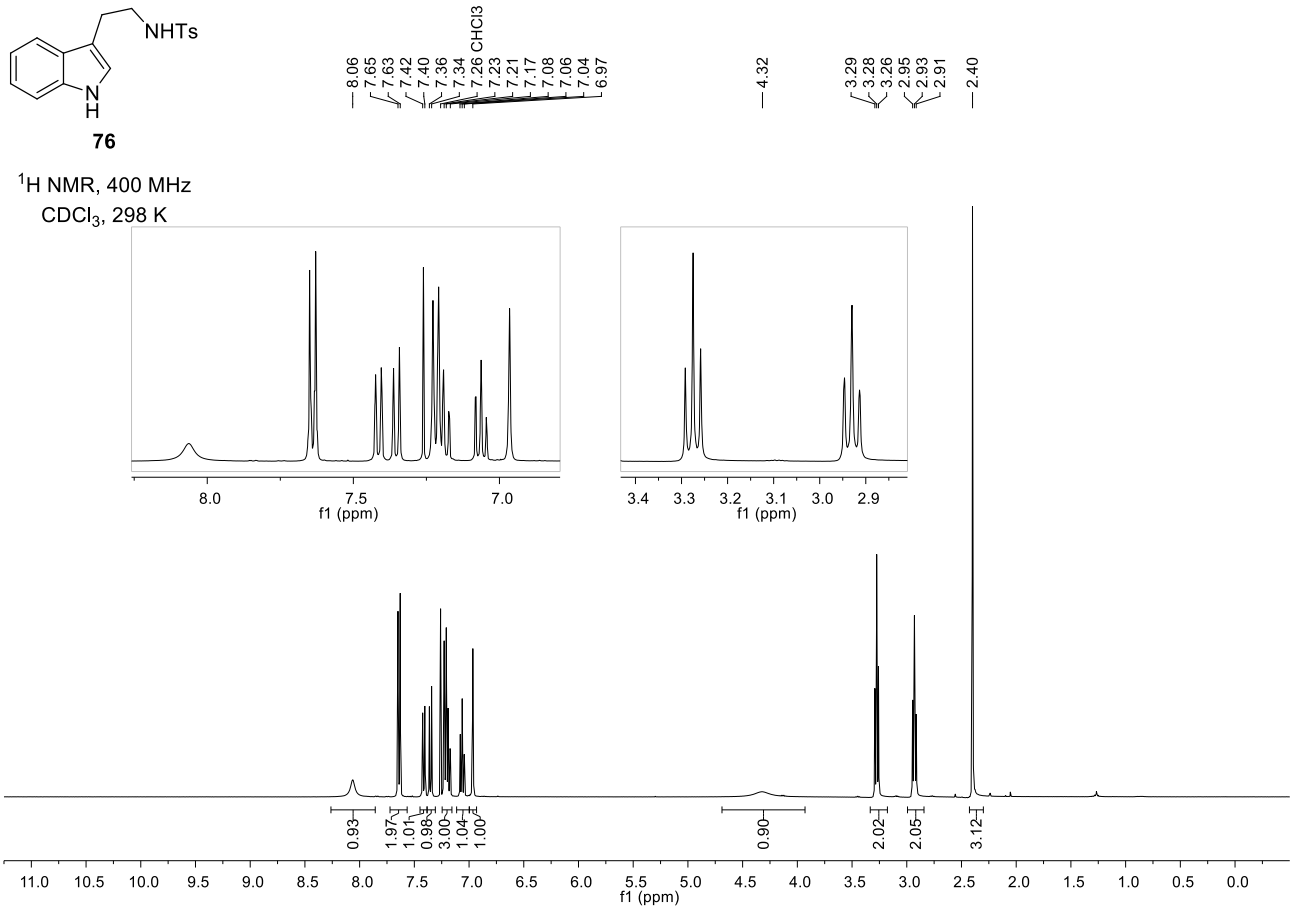
NHTs
N
H
76
1H NMR, 400 MHz
CDCl3, 298 K
8.06
7.65
7.63
7.42
7.40
7.36
7.34
7.26 CHCl3
7.23
7.21
7.17
7.08
7.06
7.04
6.97
4.32
3.29
3.28
3.26
2.95
2.93
2.91
2.40
0.93
1.97
1.01
0.98
3.00
1.04
1.00
0.90
2.02
2.05
3.12
f1 (ppm)

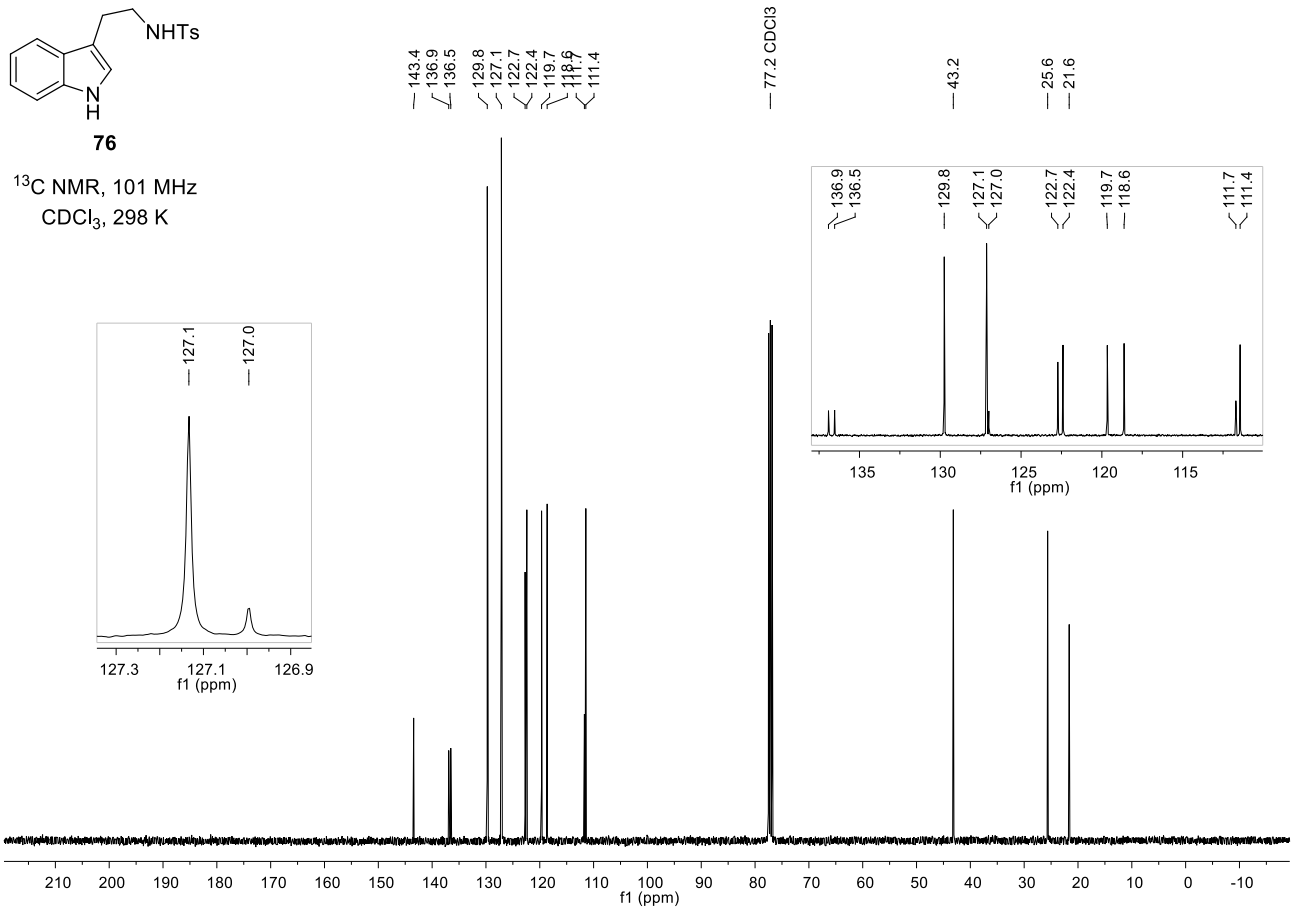
NHTs
N
H
76
13C NMR, 101 MHz
CDCl3, 298 K
143.4
136.9
136.5
129.8
127.1
122.7
122.4
119.7
118.6
111.7
111.4
77.2 CDCl3
43.2
25.6
21.6
127.1
127.0
f1 (ppm)

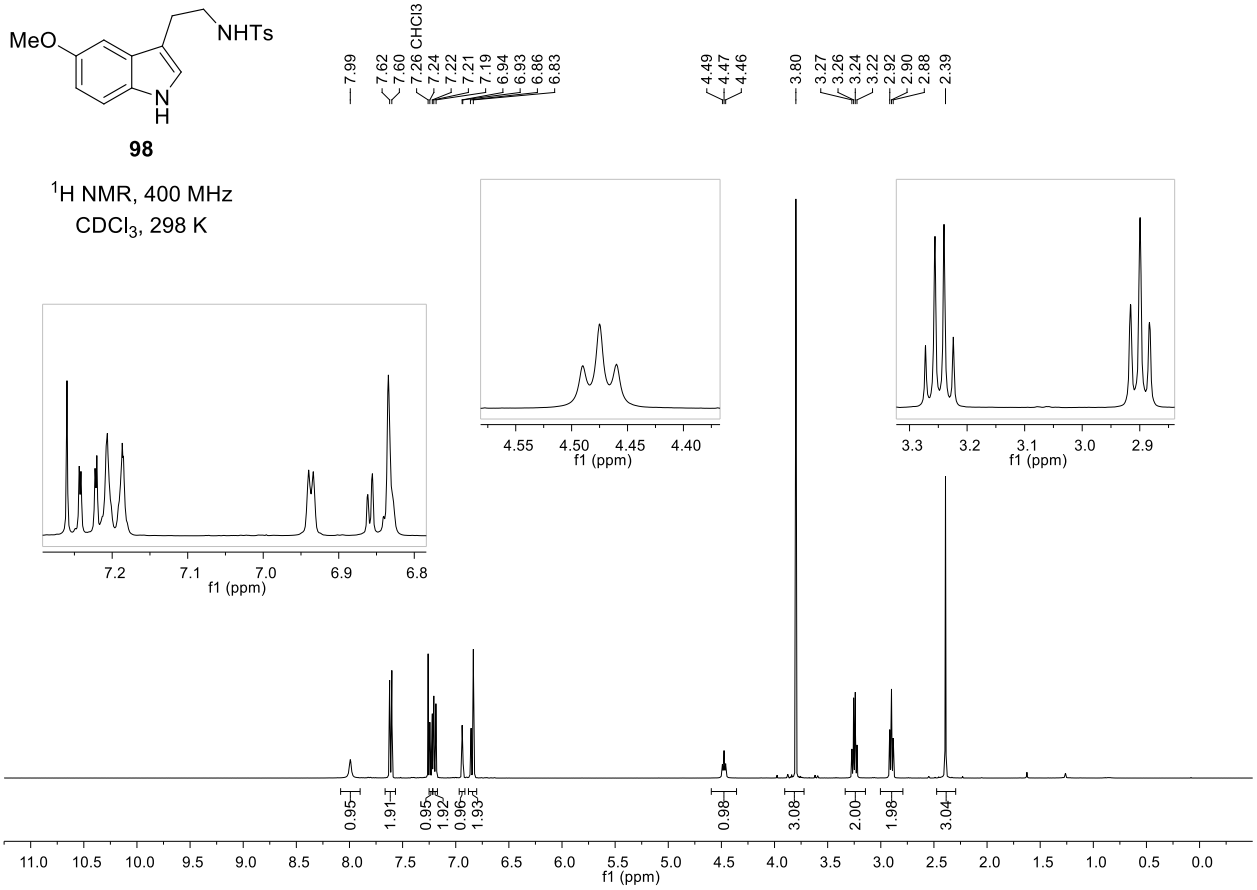
MeO
NHTs
N
H
98
^{1}H NMR, 400 MHz
$CDCl_3$, 298 K
7.99
7.62
7.60
7.26 CHCl3
7.24
7.22
7.21
7.19
6.94
6.93
6.86
6.83
4.49
4.47
4.46
3.80
3.27
3.26
3.24
3.22
2.92
2.90
2.88
2.39
0.95
1.91
0.95
1.92
0.96
1.93
0.98
3.08
2.00
1.98
3.04
f1 (ppm)

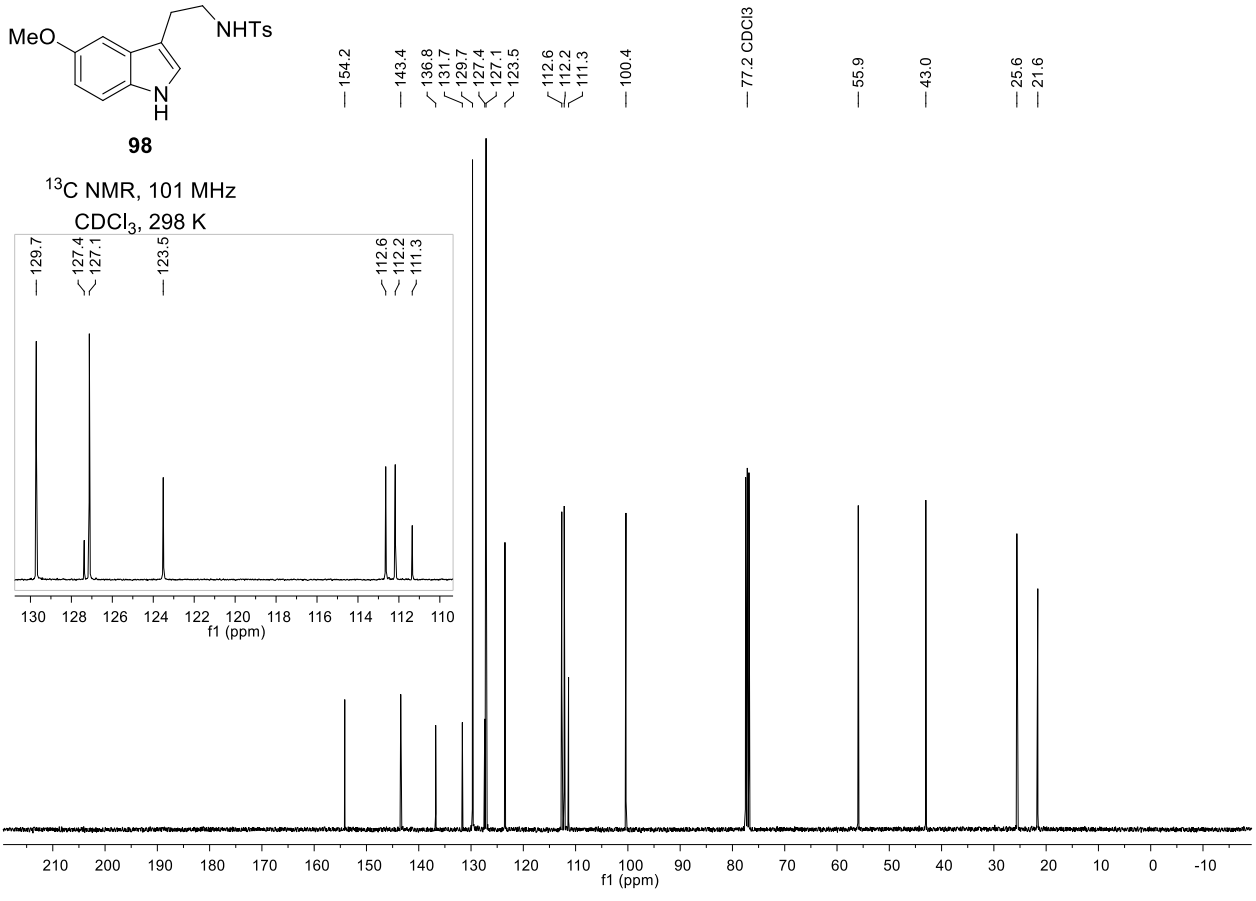
MeO
NHTs
N
H
98
^{13}C NMR, 101 MHz
$CDCl_3$, 298 K
154.2
143.4
136.8
131.7
129.7
127.4
127.1
123.5
112.6
112.2
111.3
100.4
77.2 CDCl3
55.9
43.0
25.6
21.6
f1 (ppm)

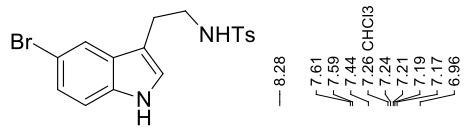

99

^{1}H NMR, 400 MHz, $CDCl_3$, 298 K

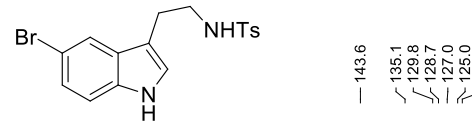

99

^{13}C NMR, 101 MHz, $CDCl_3$, 298 K

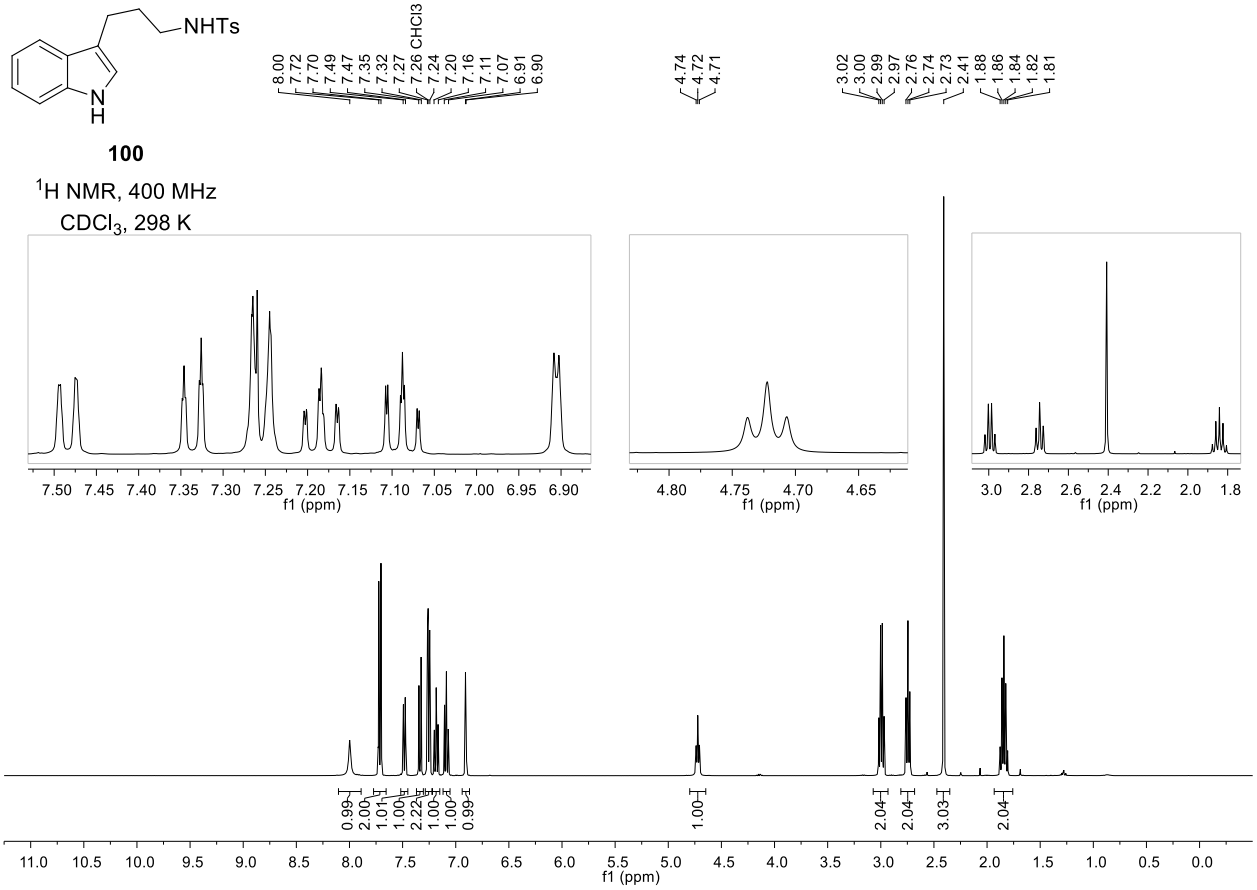
NHTs
N
H
100
1H NMR, 400 MHz
CDCl3, 298 K
8.00
7.72
7.70
7.49
7.47
7.35
7.32
7.27
7.26 CHCl3
7.24
7.20
7.16
7.11
7.07
6.91
6.90
4.74
4.72
4.71
3.02
3.00
2.99
2.97
2.76
2.74
2.73
2.41
1.88
1.86
1.84
1.82
1.81
f1 (ppm)

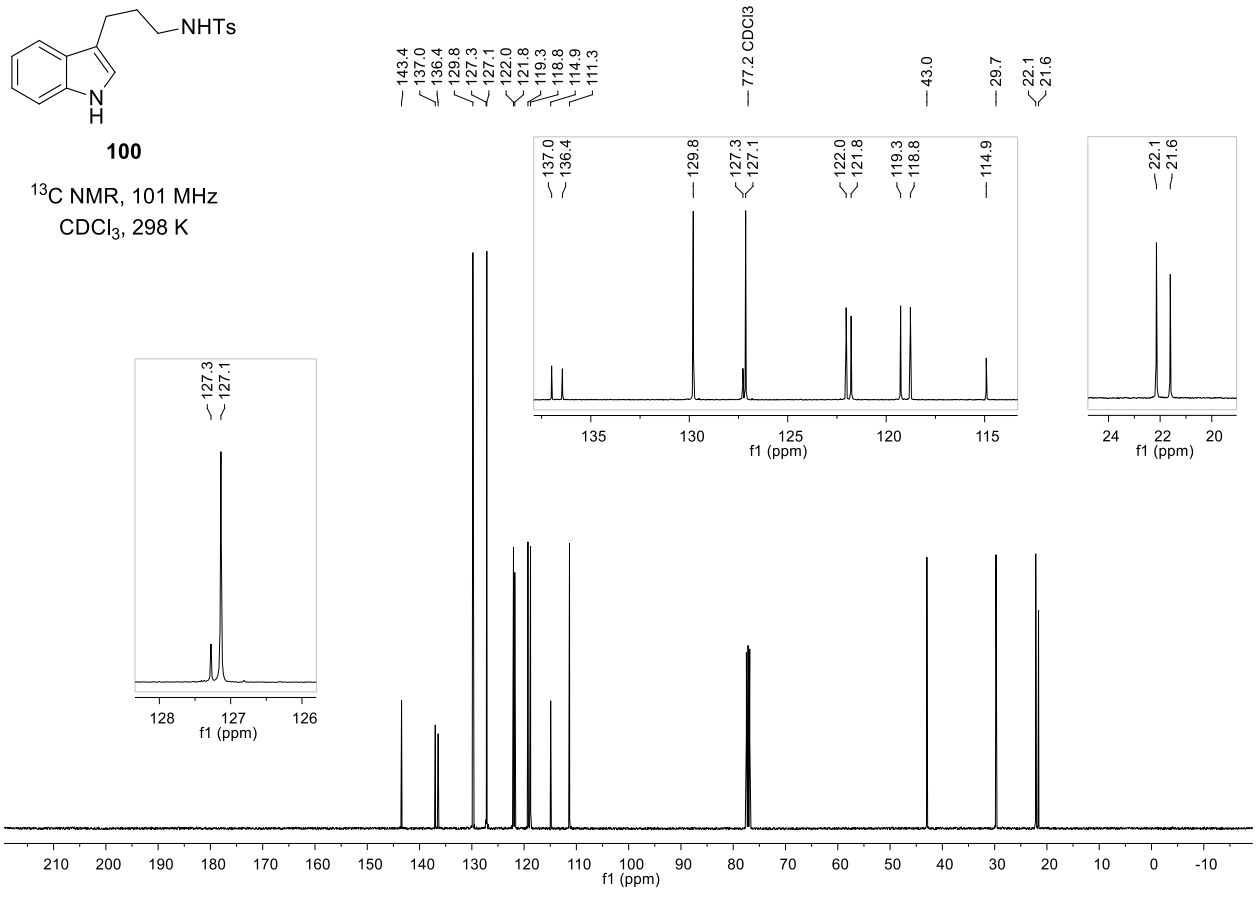
NHTs
N
H
100
13C NMR, 101 MHz
CDCl3, 298 K
143.4
137.0
136.4
129.8
127.3
127.1
122.0
121.8
119.3
118.8
114.9
111.3
77.2 CDCl3
43.0
29.7
22.1
21.6
f1 (ppm)

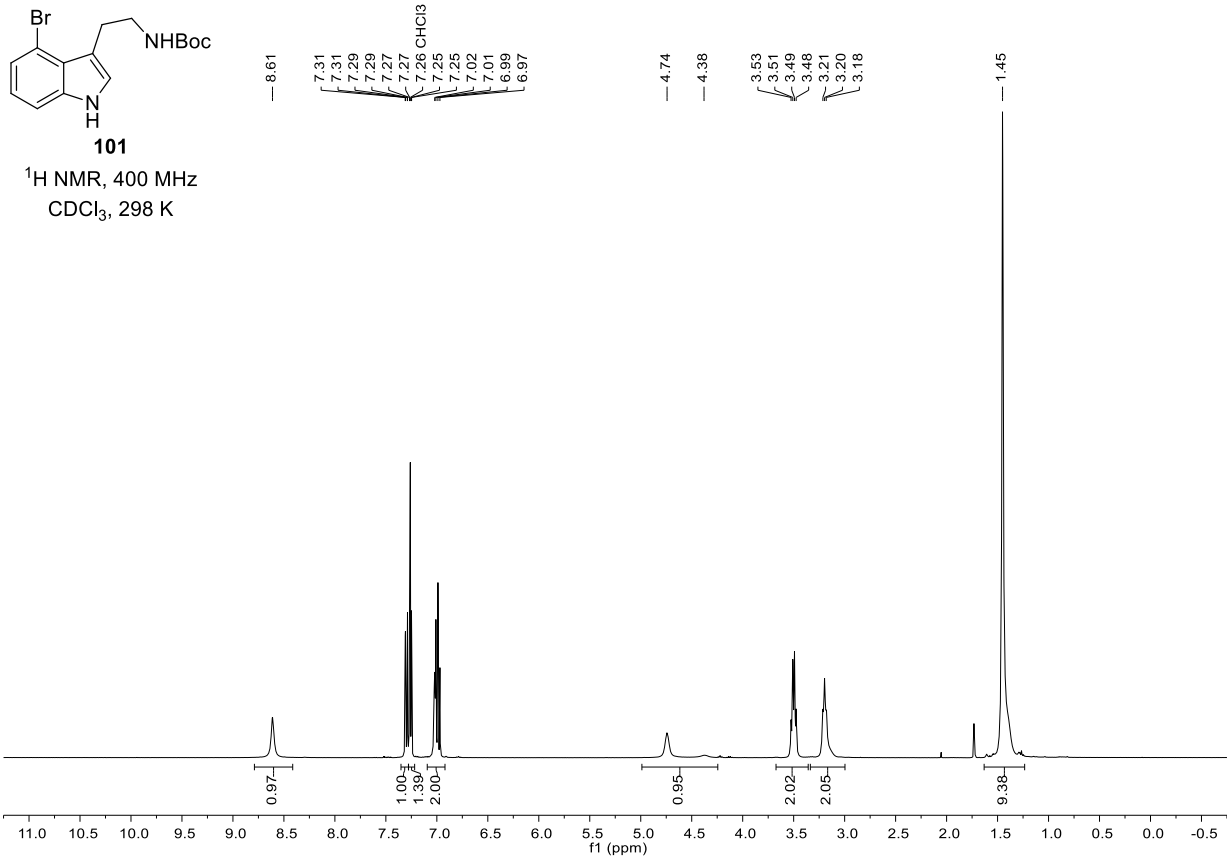

101

^{1}H NMR, 400 MHz

$CDCl_3$, 298 K

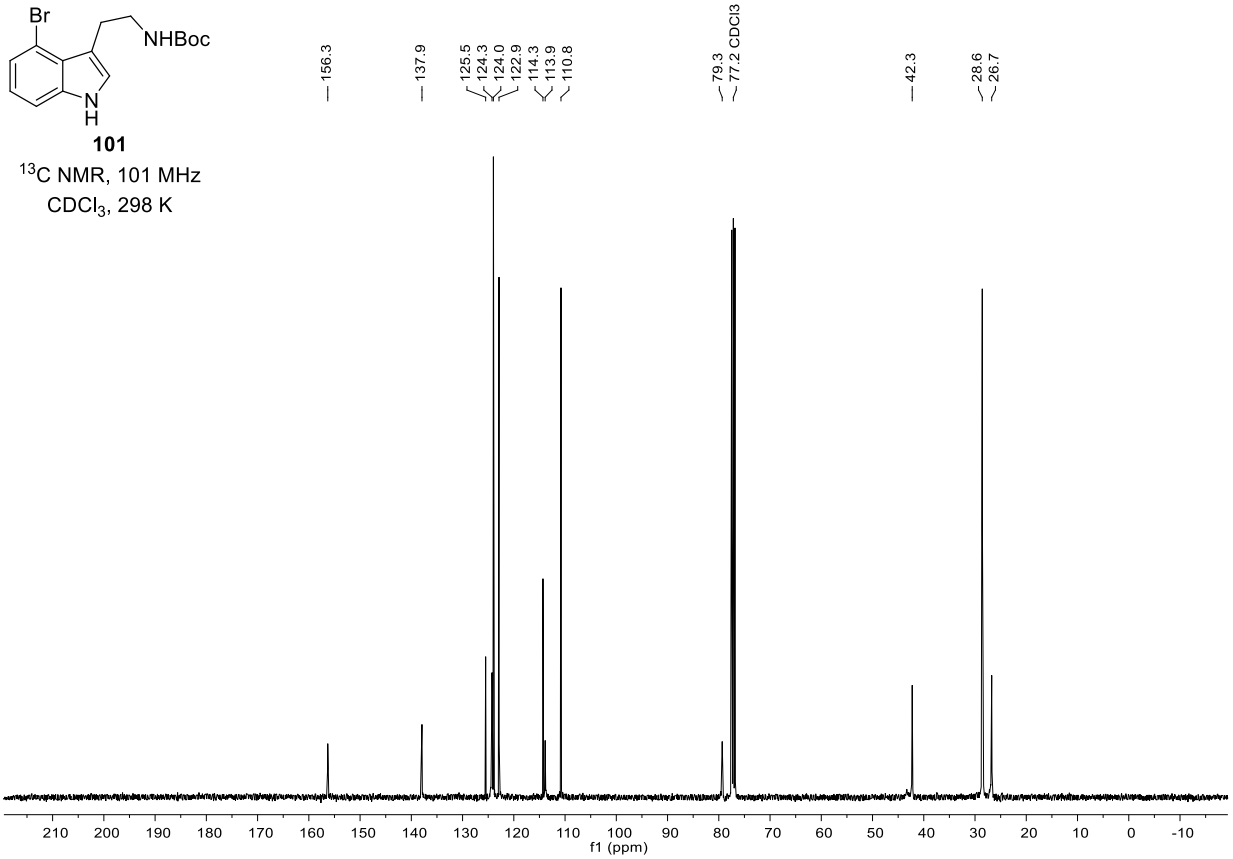

101

^{13}C NMR, 101 MHz

$CDCl_3$, 298 K

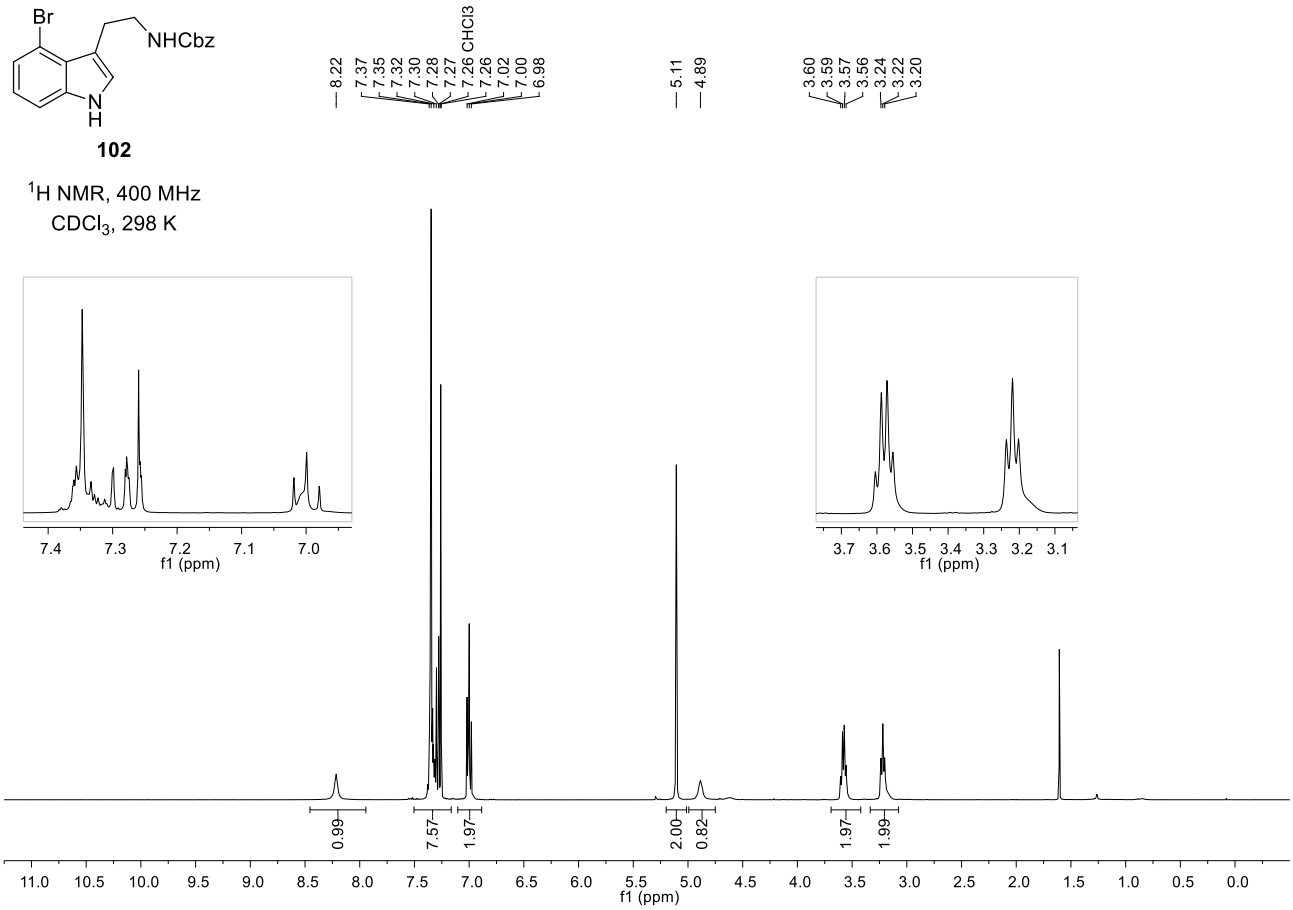
Br
NHCbz
N
H
102
8.22
7.37
7.35
7.32
7.30
7.28
7.27
7.26 CHCl3
7.26
7.02
7.00
6.98
5.11
4.89
3.60
3.59
3.57
3.56
3.24
3.22
3.20
1H NMR, 400 MHz
CDCl3, 298 K
f1 (ppm)
0.99
7.57
1.97
2.00
0.82
1.97
1.99

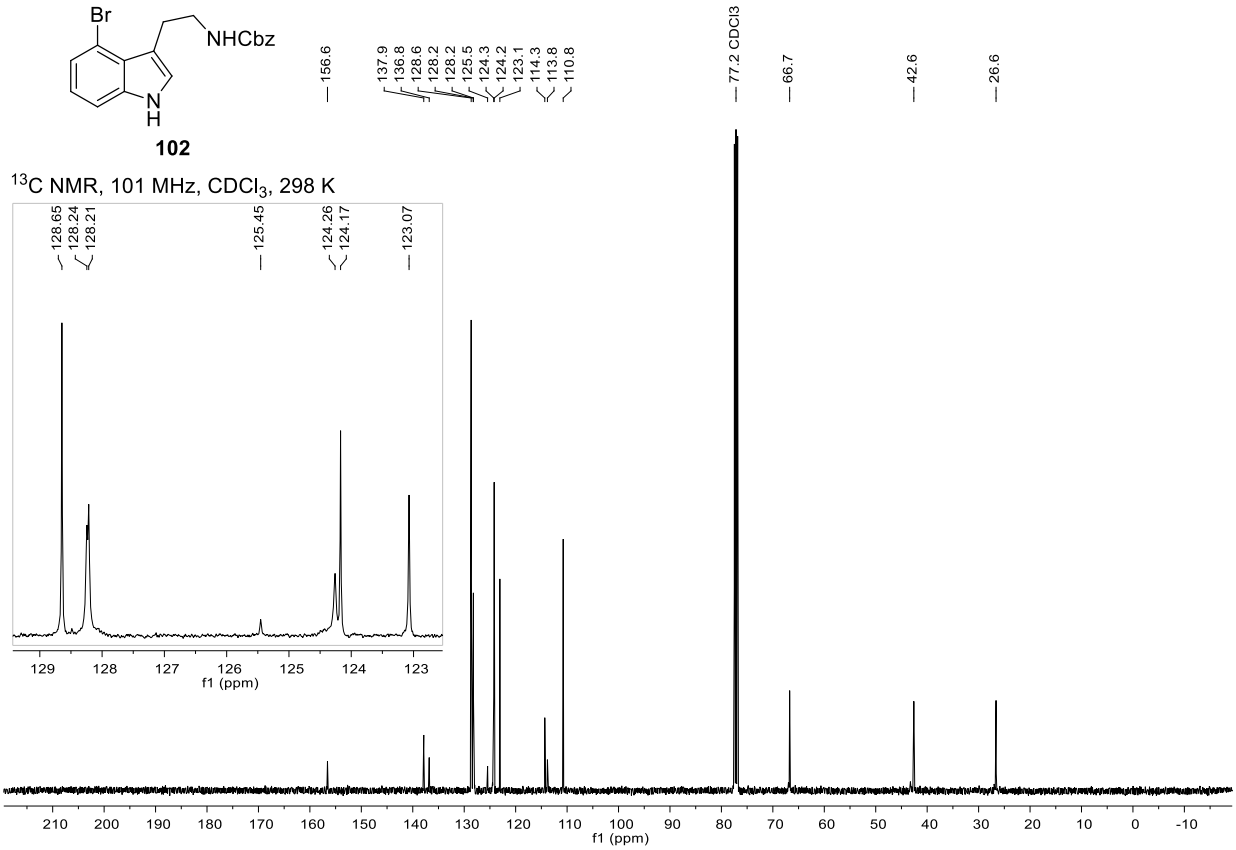
Br
NHCbz
N
H
102
156.6
137.9
136.8
128.6
128.2
128.2
125.5
124.3
124.2
123.1
114.3
113.8
110.8
77.2 CDCl3
66.7
42.6
26.6
13C NMR, 101 MHz, CDCl3, 298 K
128.65
128.24
128.21
125.45
124.26
124.17
123.07
f1 (ppm)

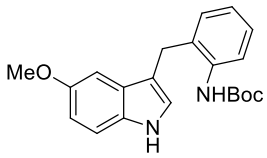

103

^{1}H NMR, 400 MHz
$CDCl_3$, 298 K

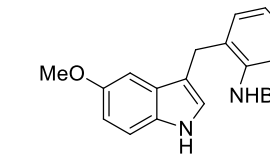

103

^{13}C NMR, 101 MHz, $CDCl_3$, 298 K

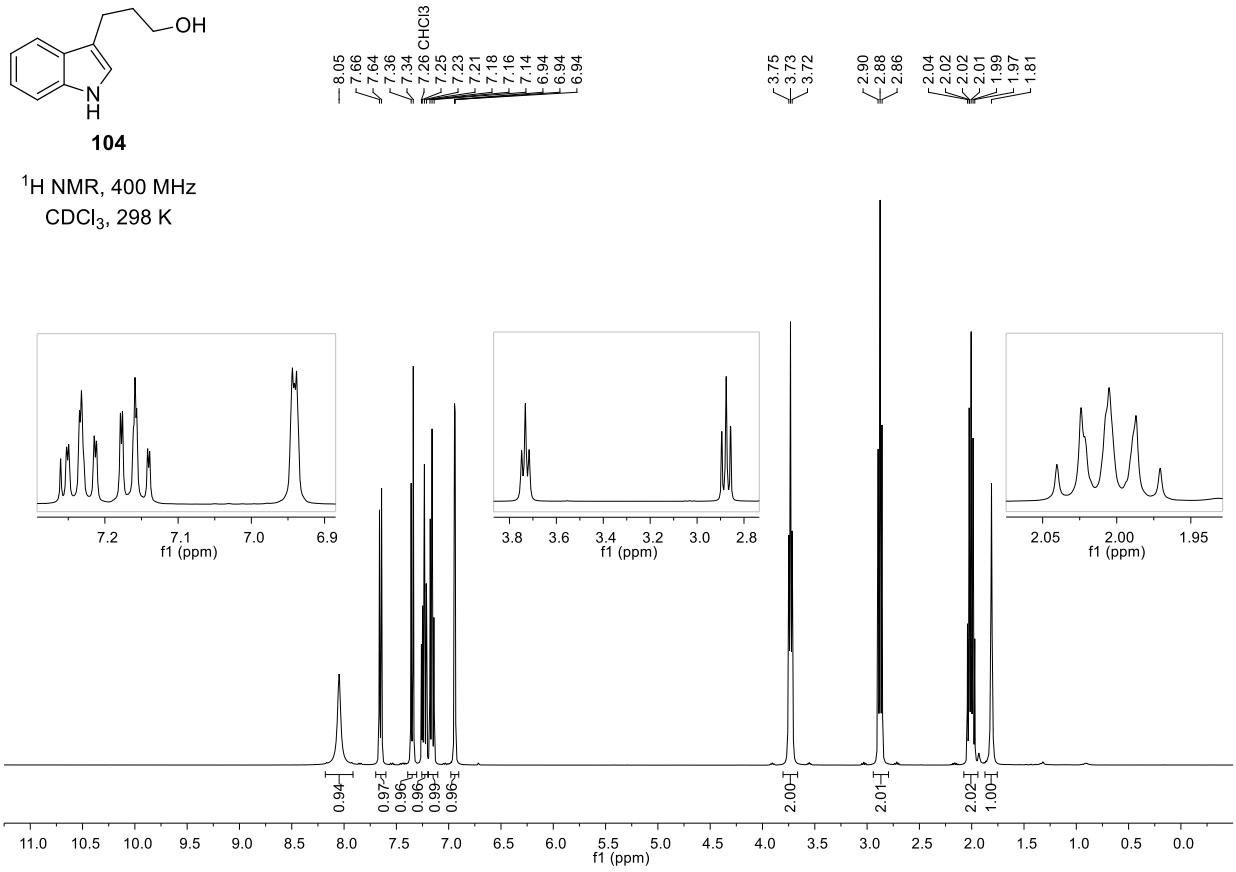

^{1}H NMR, 400 MHz
$CDCl_3$, 298 K

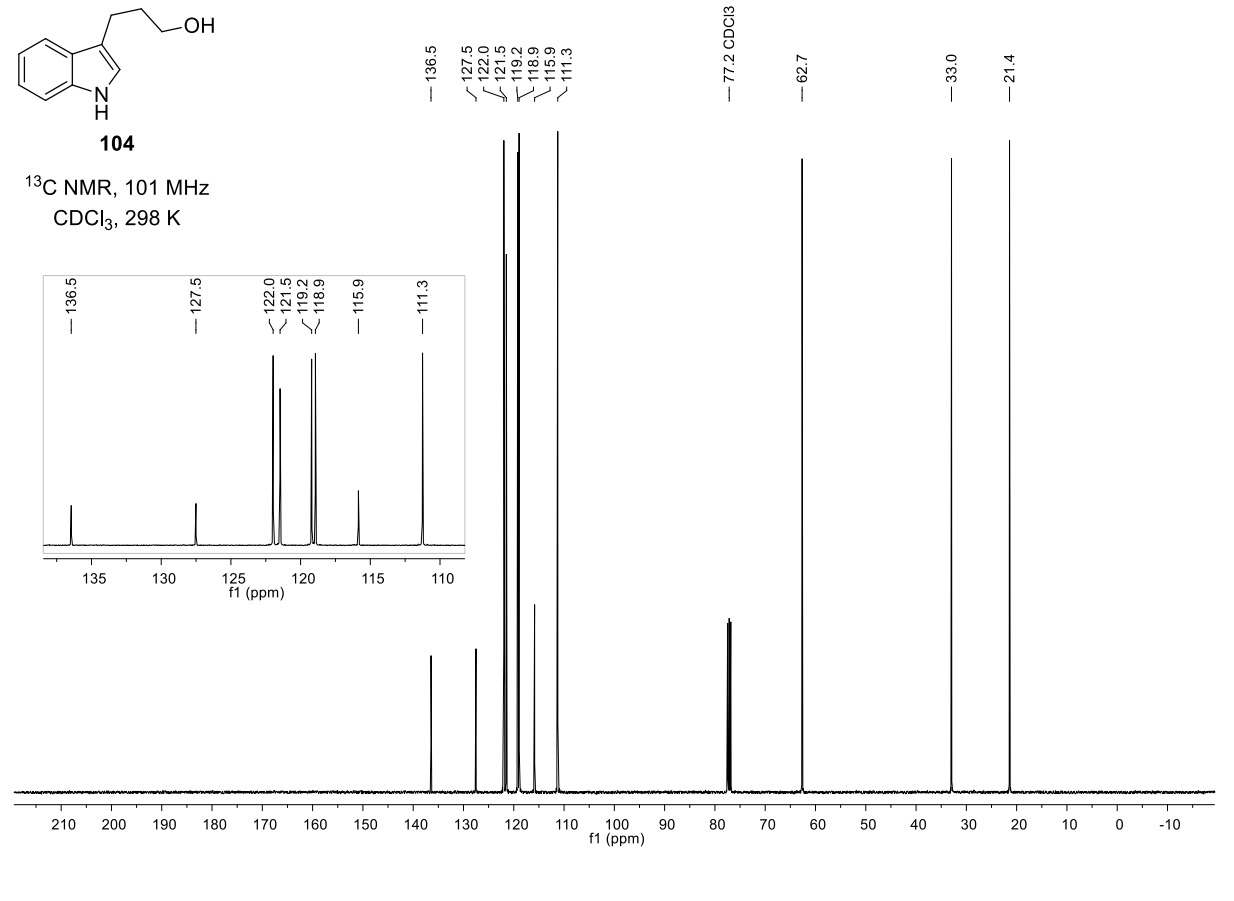

^{13}C NMR, 101 MHz
$CDCl_3$, 298 K

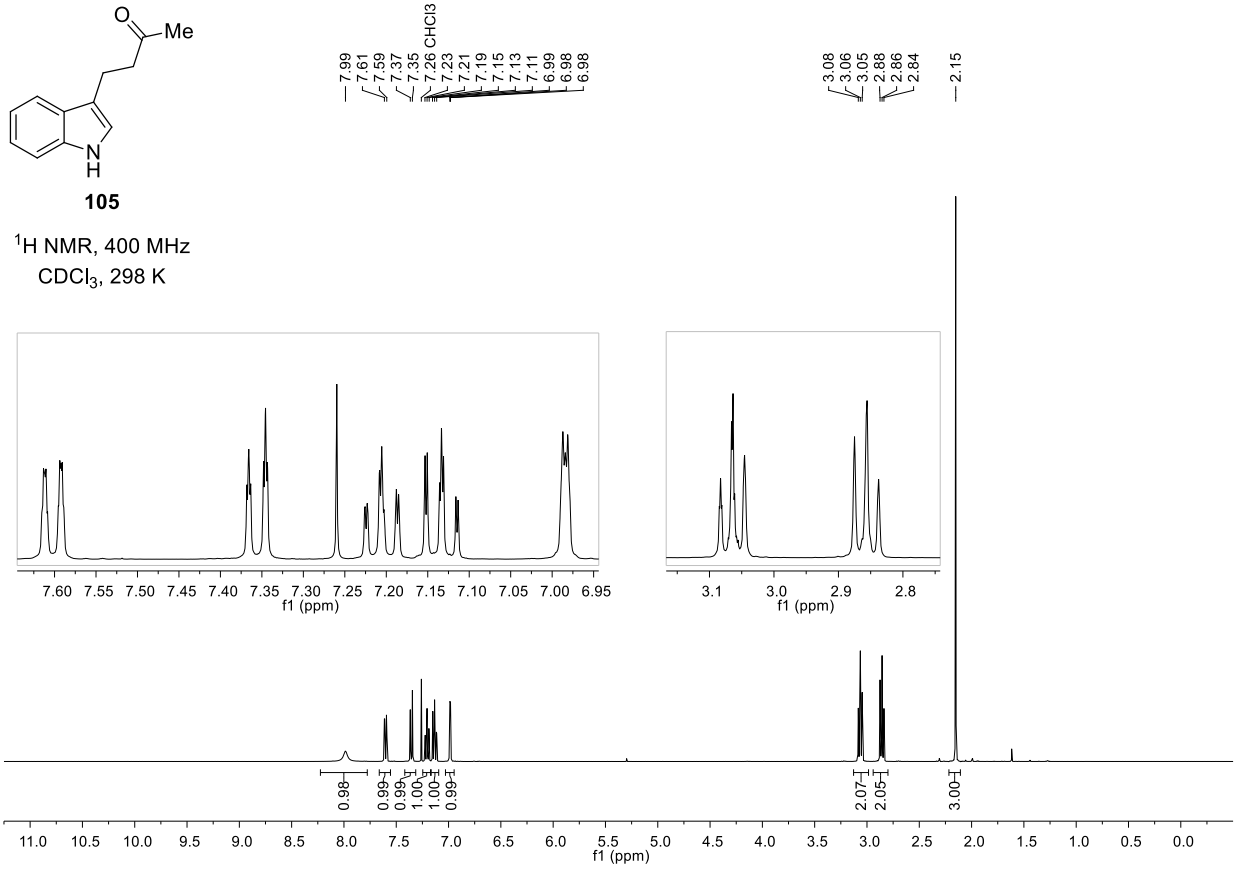
O
Me
N
H
105
7.99
7.61
7.59
7.37
7.35
7.26 CHCl3
7.23
7.21
7.19
7.15
7.13
7.11
6.99
6.98
6.98
3.08
3.06
3.05
2.88
2.86
2.84
2.15
1H NMR, 400 MHz
CDCl3, 298 K
f1 (ppm)
0.98
0.99
0.99
1.00
1.00
0.99
2.07
2.05
3.00

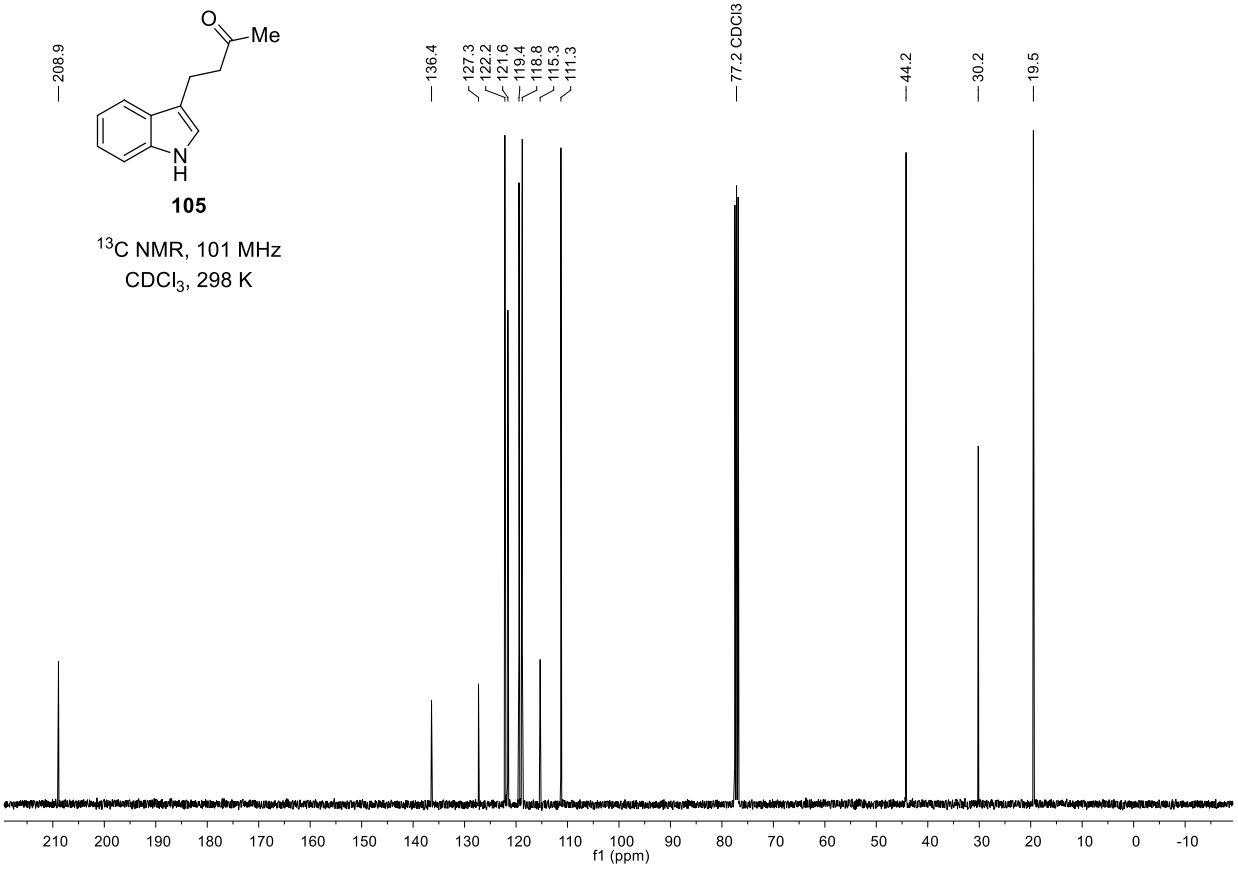
O
Me
N
H
105
208.9
136.4
127.3
122.2
121.6
119.4
118.8
115.3
111.3
77.2 CDCl3
44.2
30.2
19.5
13C NMR, 101 MHz
CDCl3, 298 K
f1 (ppm)

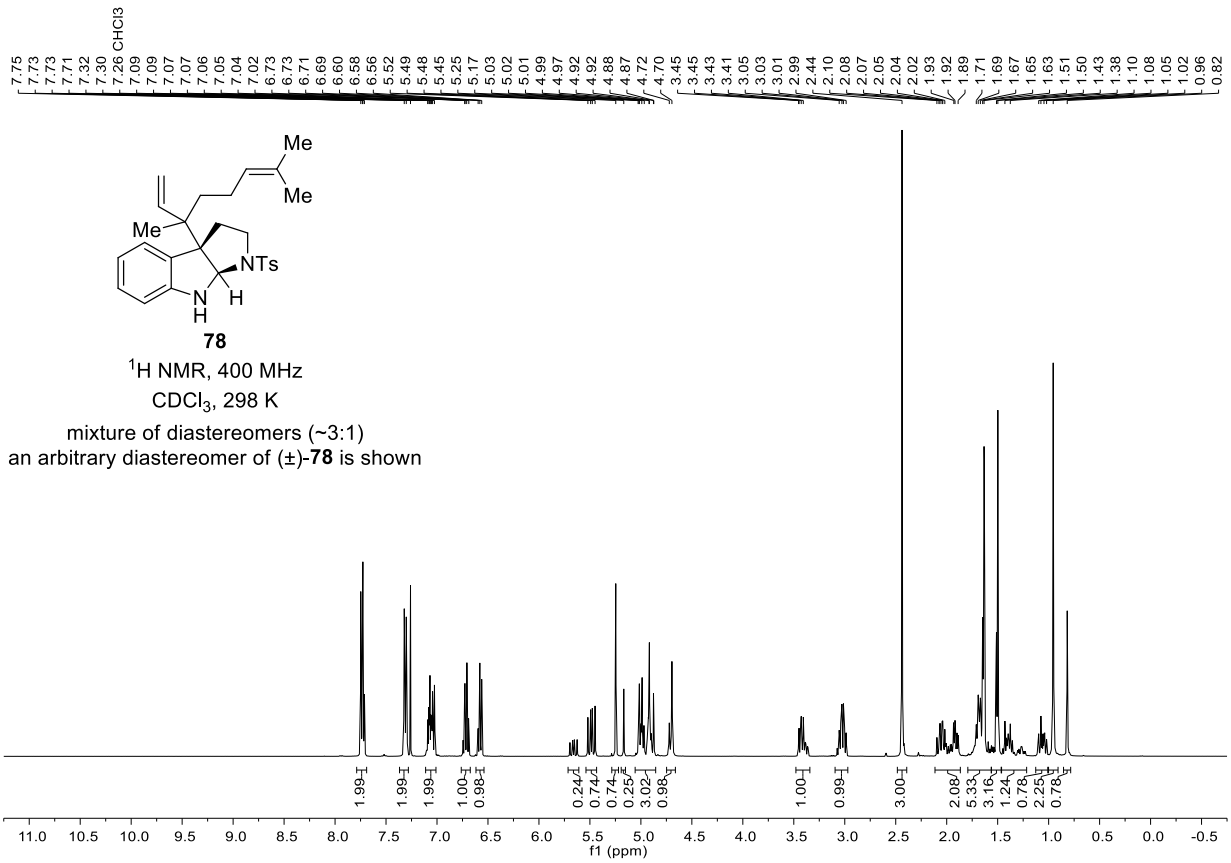
Me
Me
Me
NTs
N H
H
78
1H NMR, 400 MHz
CDCl3, 298 K
mixture of diastereomers (~3:1)
an arbitrary diastereomer of (±)-78 is shown
f1 (ppm)

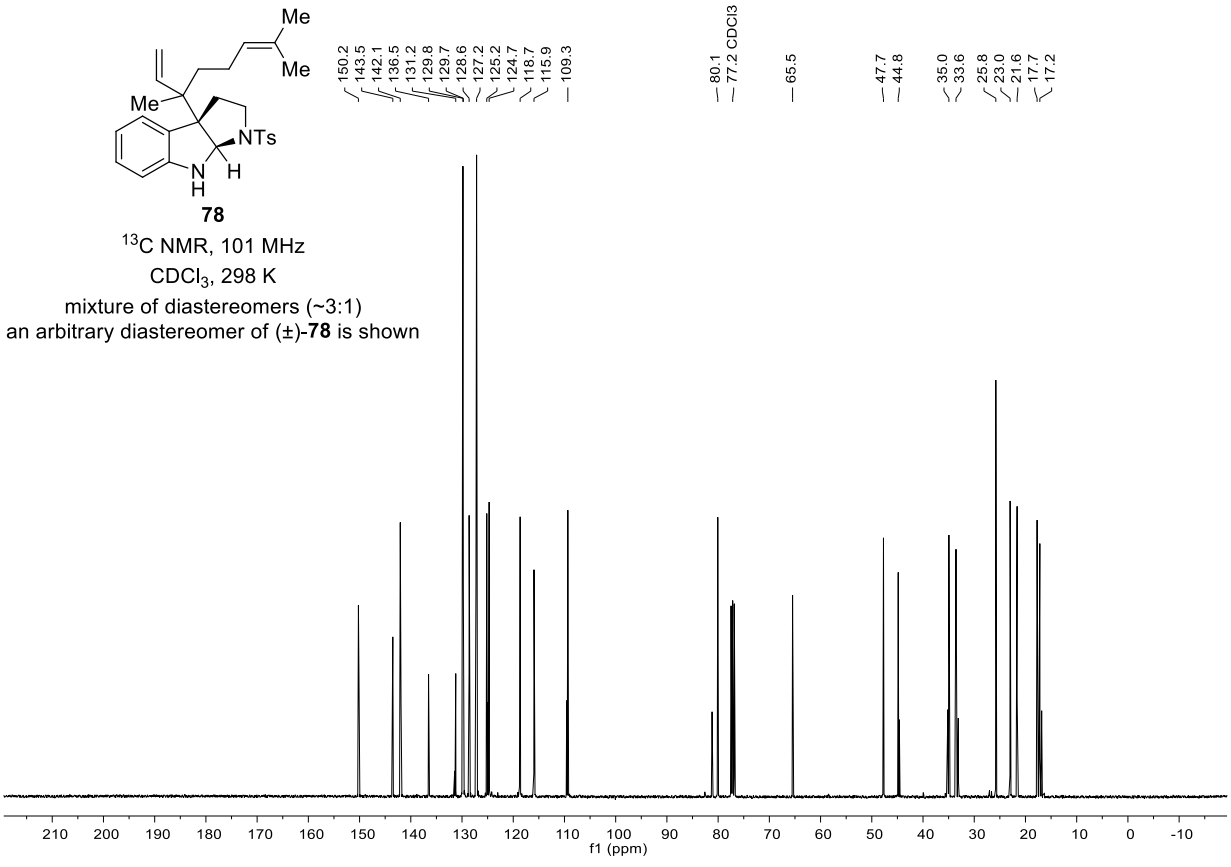
Me
Me
Me
NTs
N H
H
78
13C NMR, 101 MHz
CDCl3, 298 K
mixture of diastereomers (~3:1)
an arbitrary diastereomer of (±)-78 is shown
f1 (ppm)

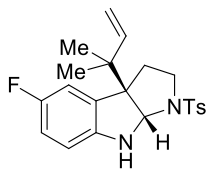

74

^{1}H NMR, 400 MHz
$CDCl_3$, 298 K

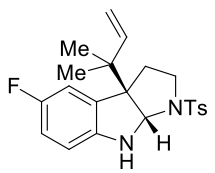

74

^{13}C NMR, 101 MHz
$CDCl_3$, 298 K

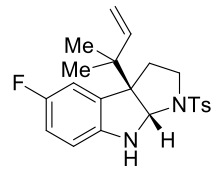

74

$^{19}F\{^{1}H\}$ NMR, 377 MHz
$CDCl_3$, 298 K

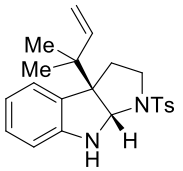

109

^{1}H NMR, 400 MHz, $CDCl_3$, 298 K

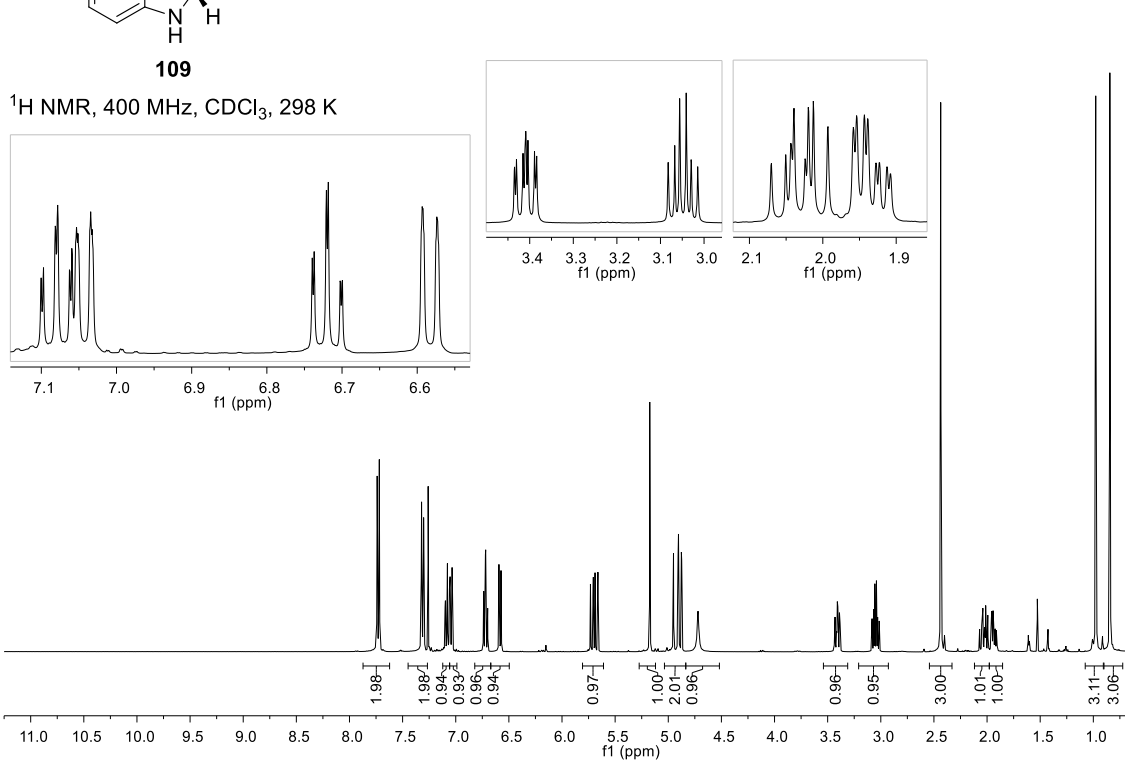

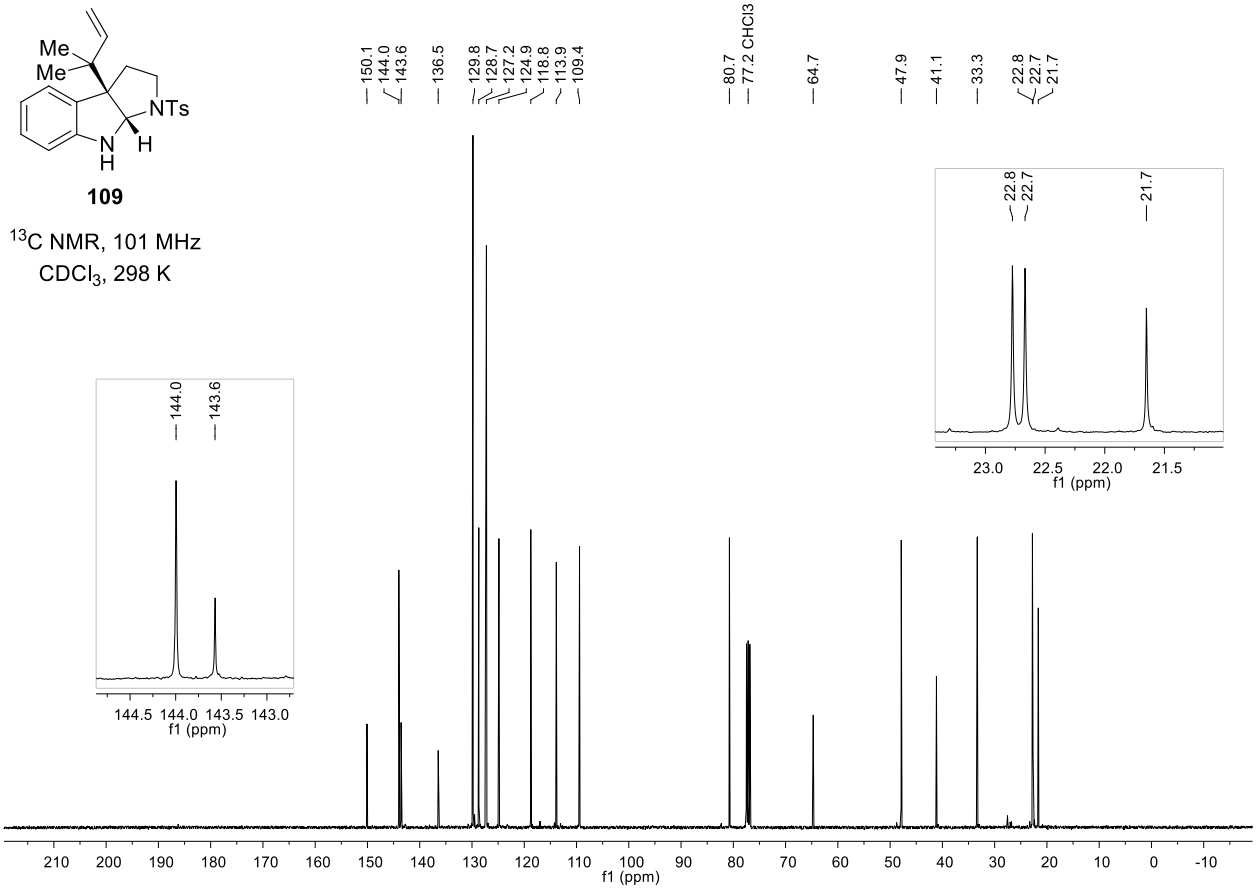
Me
Me
NTs
N
H
H
109
13C NMR, 101 MHz
CDCl3, 298 K
150.1
144.0
143.6
136.5
129.8
128.7
127.2
124.9
118.8
113.9
109.4
80.7
77.2 CHCl3
64.7
47.9
41.1
33.3
22.8
22.7
21.7
f1 (ppm)

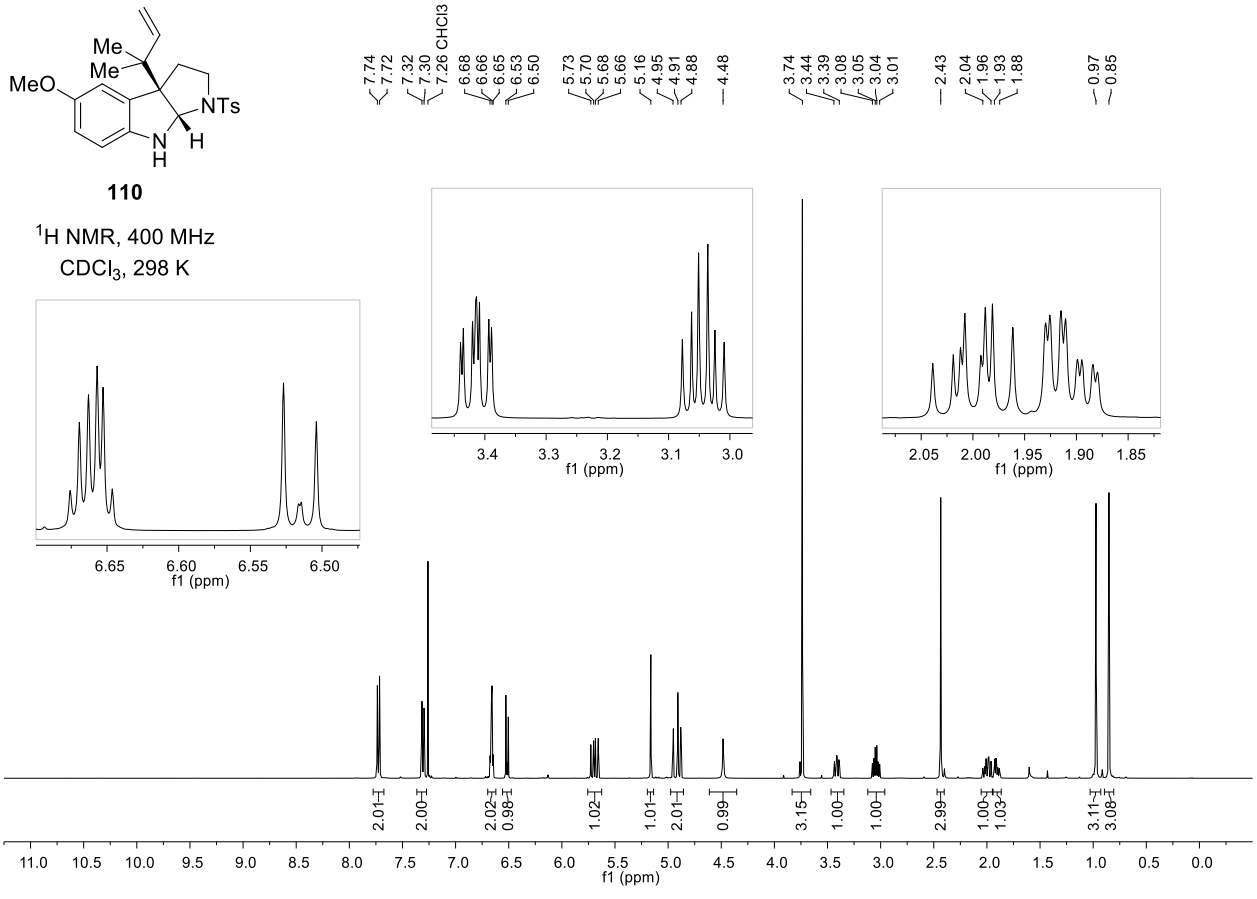
Me
Me
MeO
NTs
N
H
H
110
1H NMR, 400 MHz
CDCl3, 298 K
7.74
7.72
7.32
7.30
7.26 CHCl3
6.68
6.66
6.65
6.53
6.50
5.73
5.70
5.68
5.66
5.16
4.95
4.91
4.88
4.48
3.74
3.44
3.39
3.08
3.05
3.04
3.01
2.43
2.04
1.96
1.93
1.88
0.97
0.85
2.01
2.00
2.02
0.98
1.02
1.01
2.01
0.99
3.15
1.00
1.00
2.99
1.00
1.03
3.11
3.08
f1 (ppm)

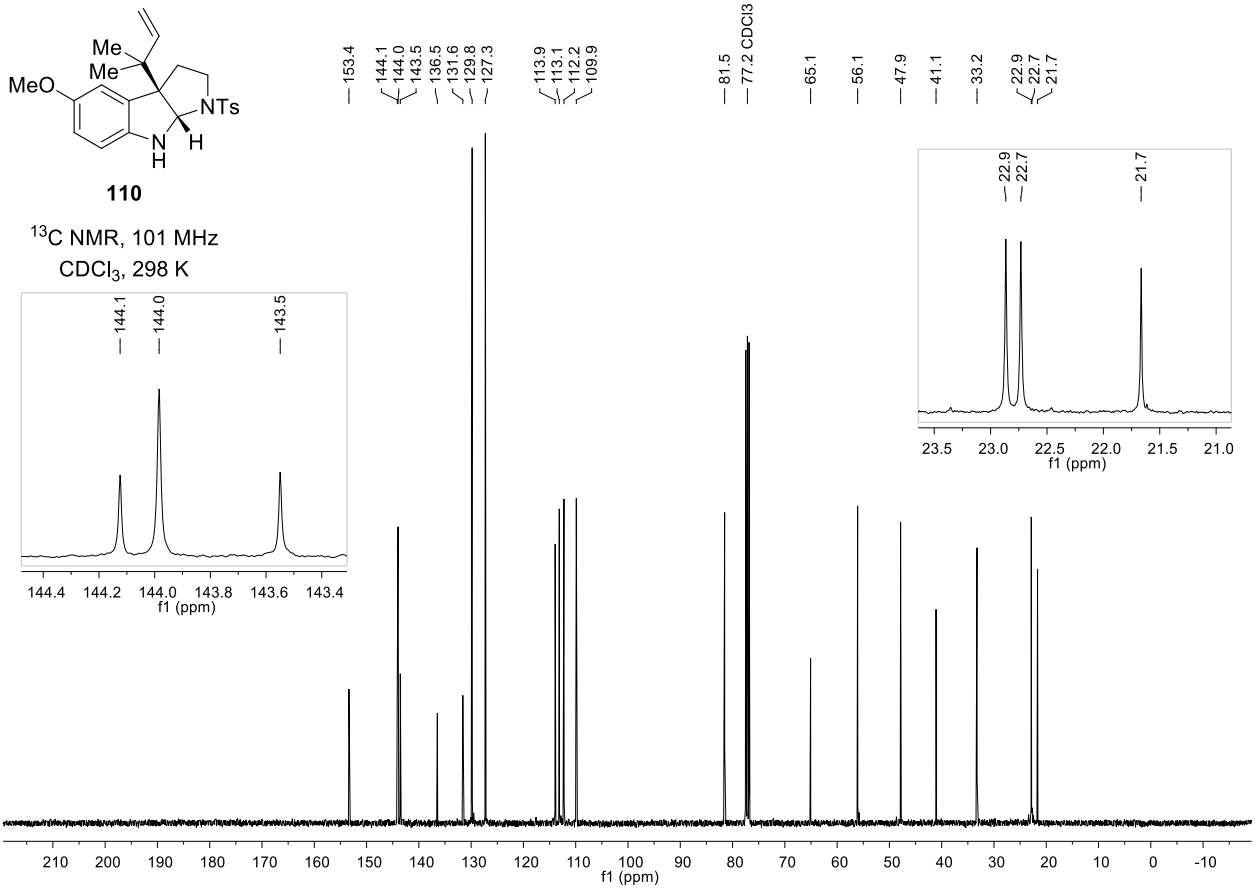

^{13}C NMR, 101 MHz
$CDCl_3$, 298 K

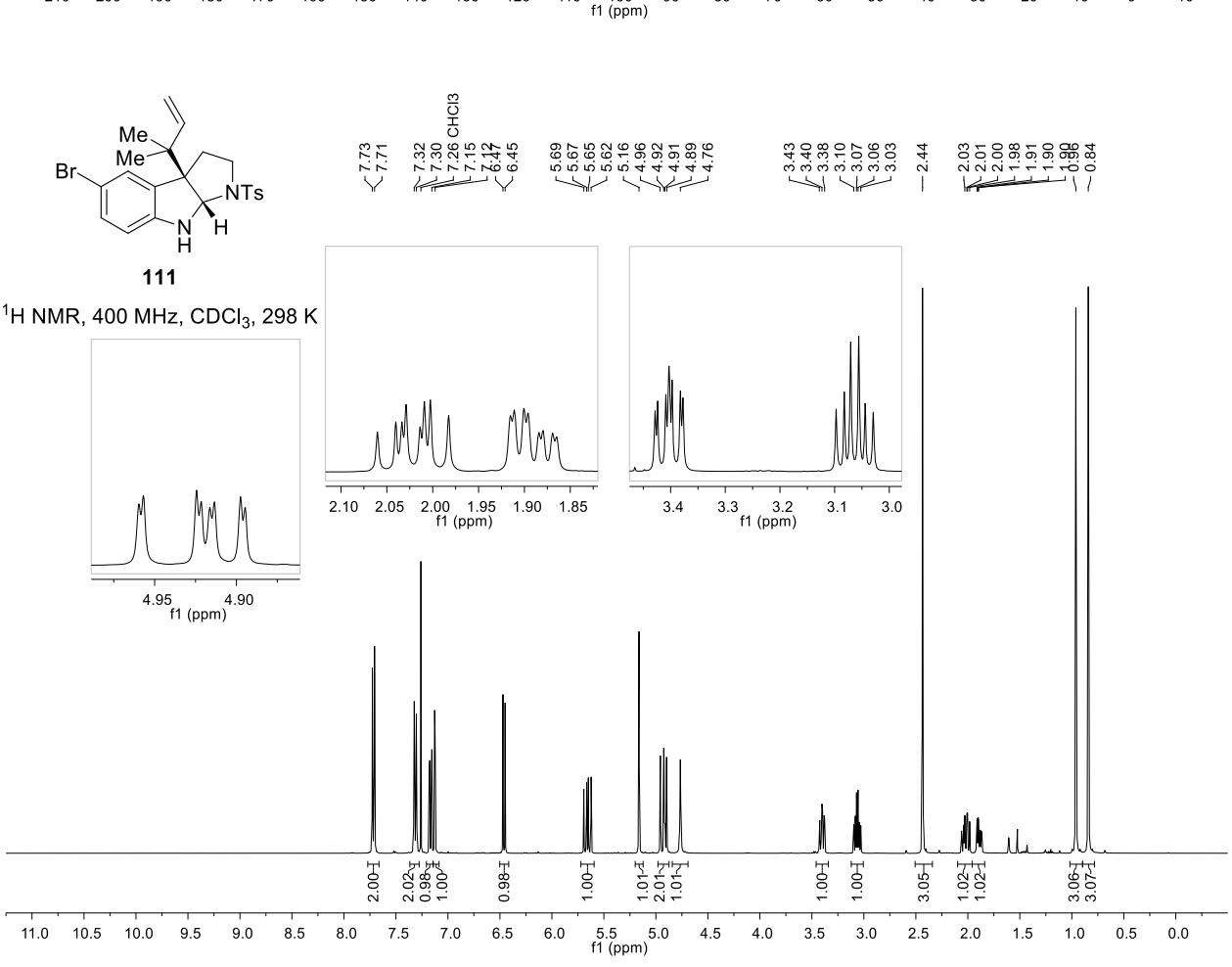

^{1}H NMR, 400 MHz, $CDCl_3$, 298 K

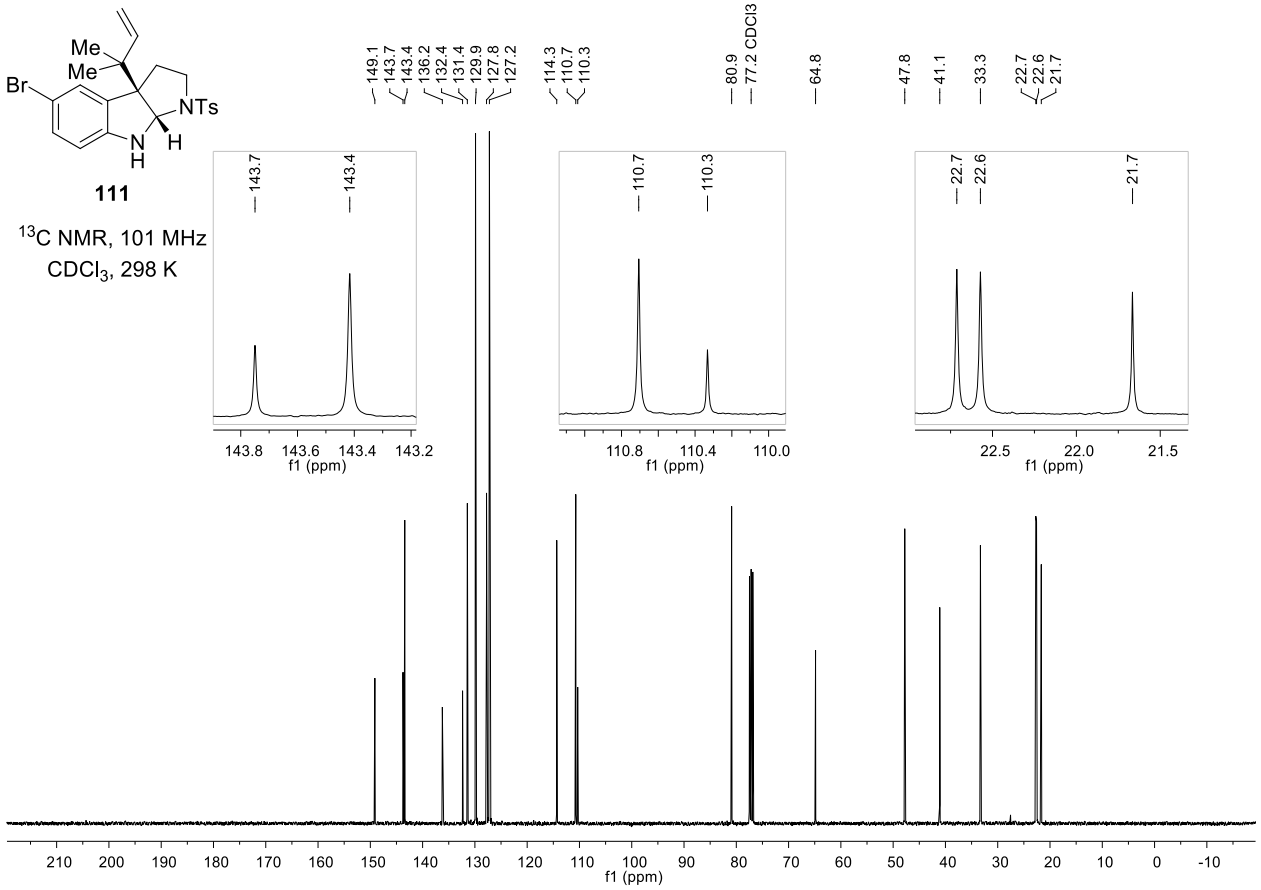
Me
Me
Br
NTs
N
H
H
111
13C NMR, 101 MHz
CDCl3, 298 K
149.1
143.7
143.4
136.2
132.4
131.4
129.9
127.8
127.2
114.3
110.7
110.3
80.9
77.2 CDCl3
64.8
47.8
41.1
33.3
22.7
22.6
21.7
f1 (ppm)

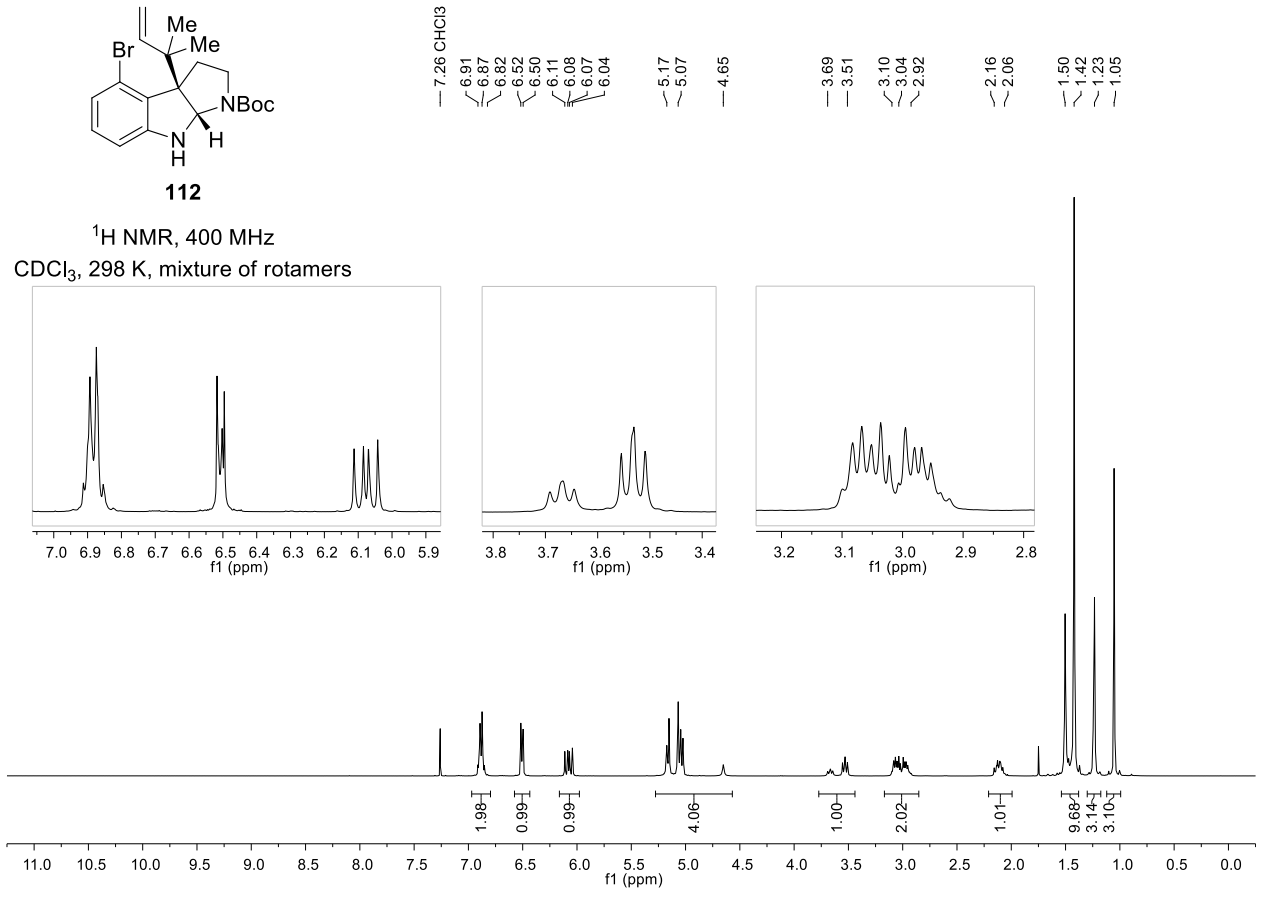
Me
Me
Br
NBoc
N
H
H
112
1H NMR, 400 MHz
CDCl3, 298 K, mixture of rotamers
7.26 CHCl3
6.91
6.87
6.82
6.52
6.50
6.11
6.08
6.07
6.04
5.17
5.07
4.65
3.69
3.51
3.10
3.04
2.92
2.16
2.06
1.50
1.42
1.23
1.05
1.98
0.99
0.99
4.06
1.00
2.02
1.01
9.68
3.14
3.10
f1 (ppm)

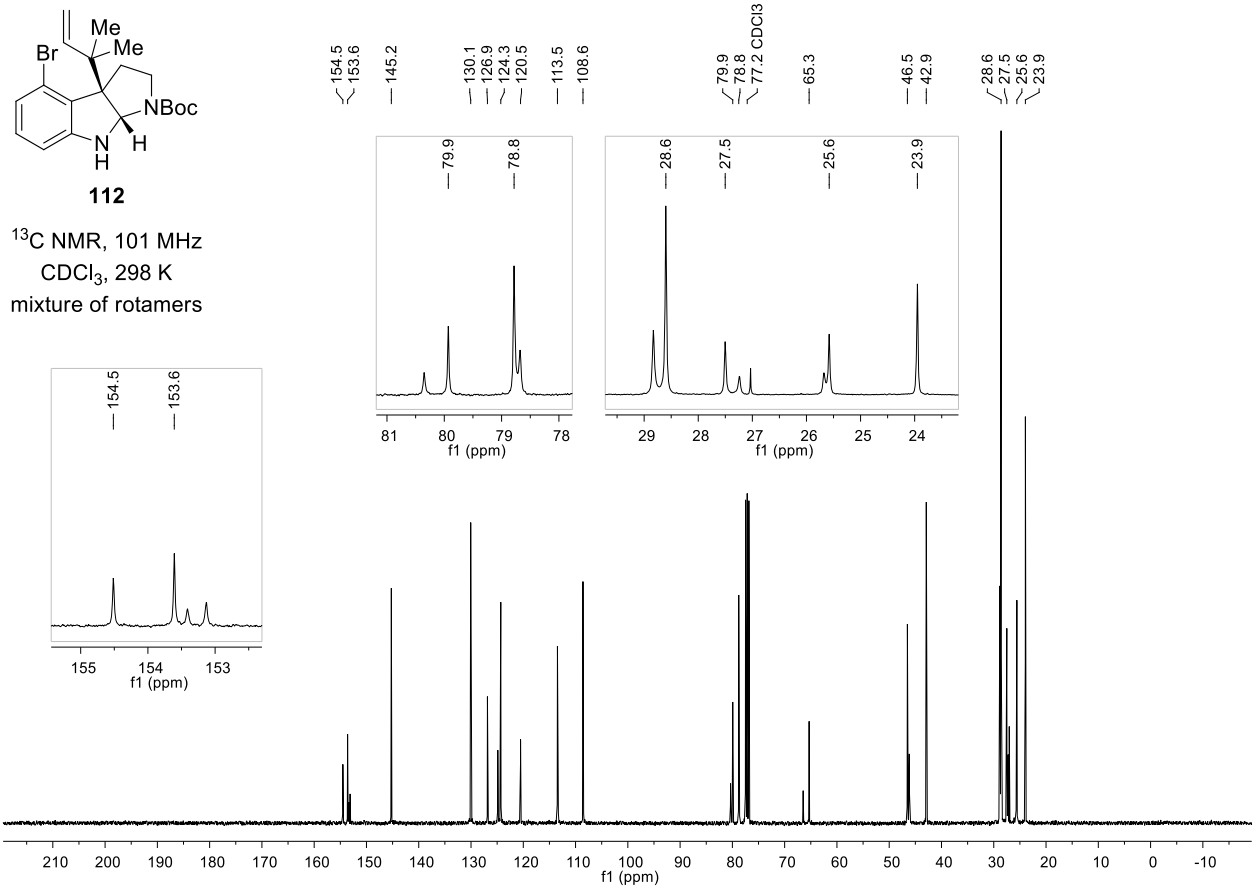
Me
Me
Br
NBoc
N
H
H
112
^{13}C NMR, 101 MHz
$CDCl_3$, 298 K
mixture of rotamers
154.5
153.6
145.2
130.1
126.9
124.3
120.5
113.5
108.6
79.9
78.8
77.2 CDCl3
65.3
46.5
42.9
28.6
27.5
25.6
23.9
f1 (ppm)

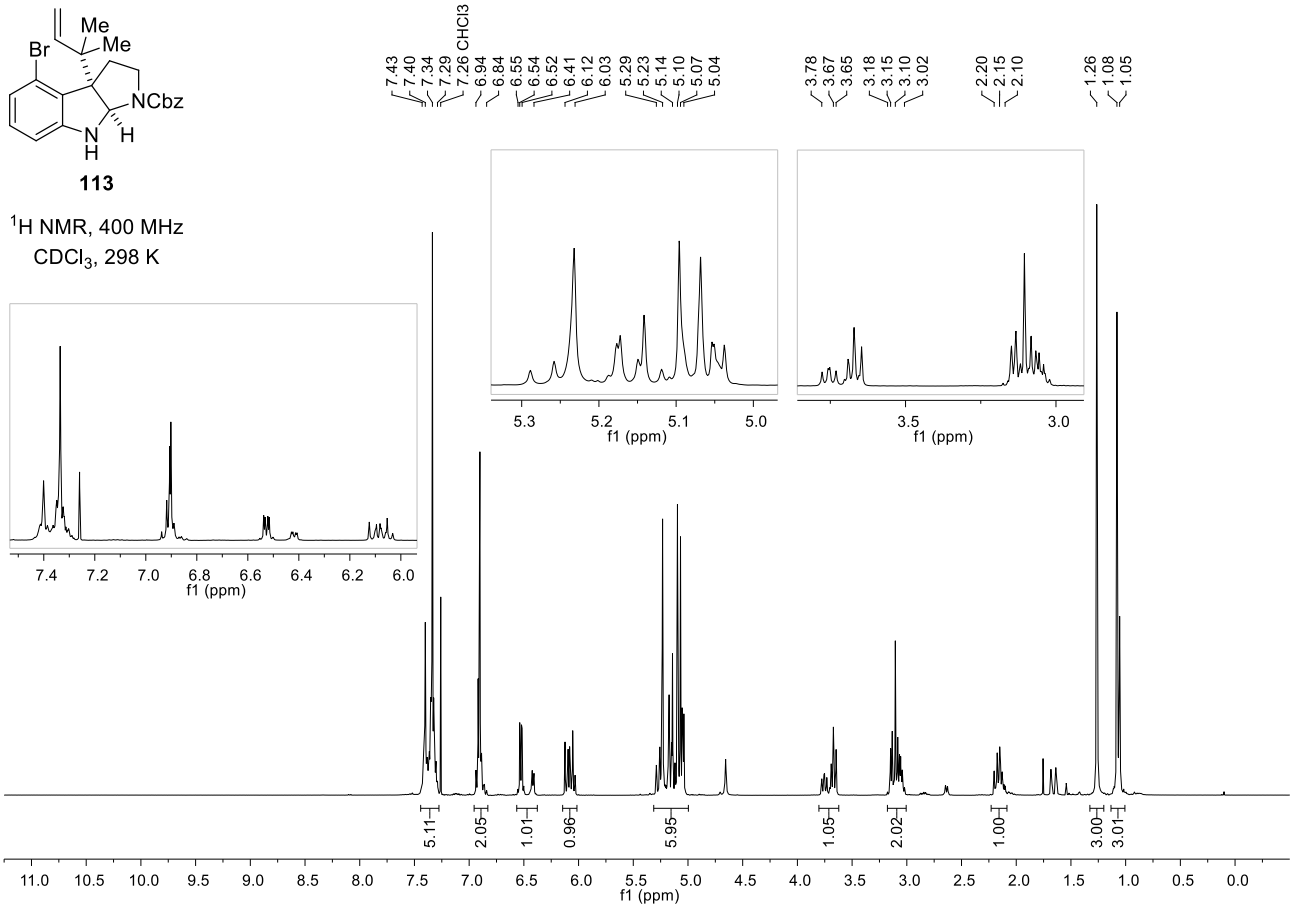
Me
Me
Br
NCbz
N
H
H
113
^{1}H NMR, 400 MHz
$CDCl_3$, 298 K
7.43
7.40
7.34
7.29
7.26 CHCl3
6.94
6.84
6.55
6.54
6.52
6.41
6.12
6.03
5.29
5.23
5.14
5.10
5.07
5.04
3.78
3.67
3.65
3.18
3.15
3.10
3.02
2.20
2.15
2.10
1.26
1.08
1.05
5.11
2.05
1.01
0.96
5.95
1.05
2.02
1.00
3.00
3.01
f1 (ppm)

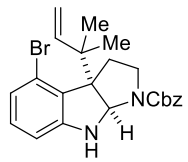

113

^{13}C NMR, 101 MHz
$CDCl_3$, 298 K

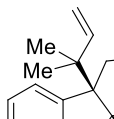

114

^{1}H NMR, 400 MHz, $CDCl_3$, 298 K

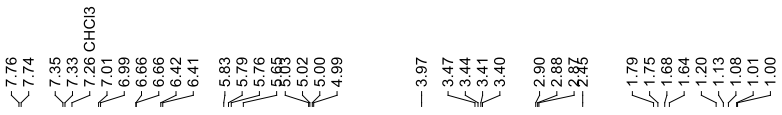

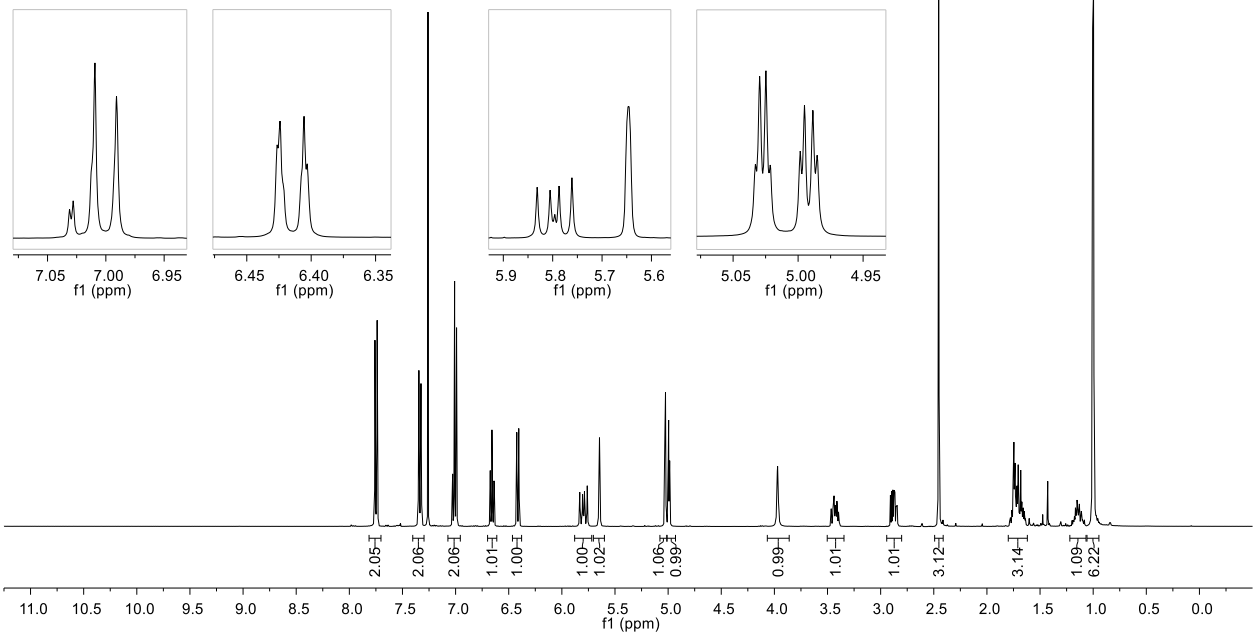

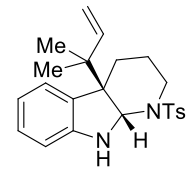

114

^{13}C NMR, 101 MHz
$CDCl_3$, 298 K

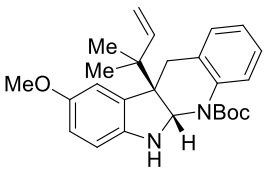

115

^{1}H NMR, 400 MHz
$CDCl_3$, 298 K

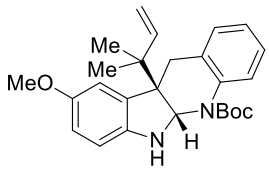

115

^{13}C NMR, 101 MHz, $CDCl_3$, 298 K

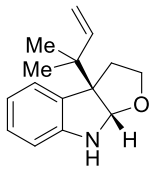

116

^{1}H NMR, 400 MHz, $CDCl_3$, 298 K

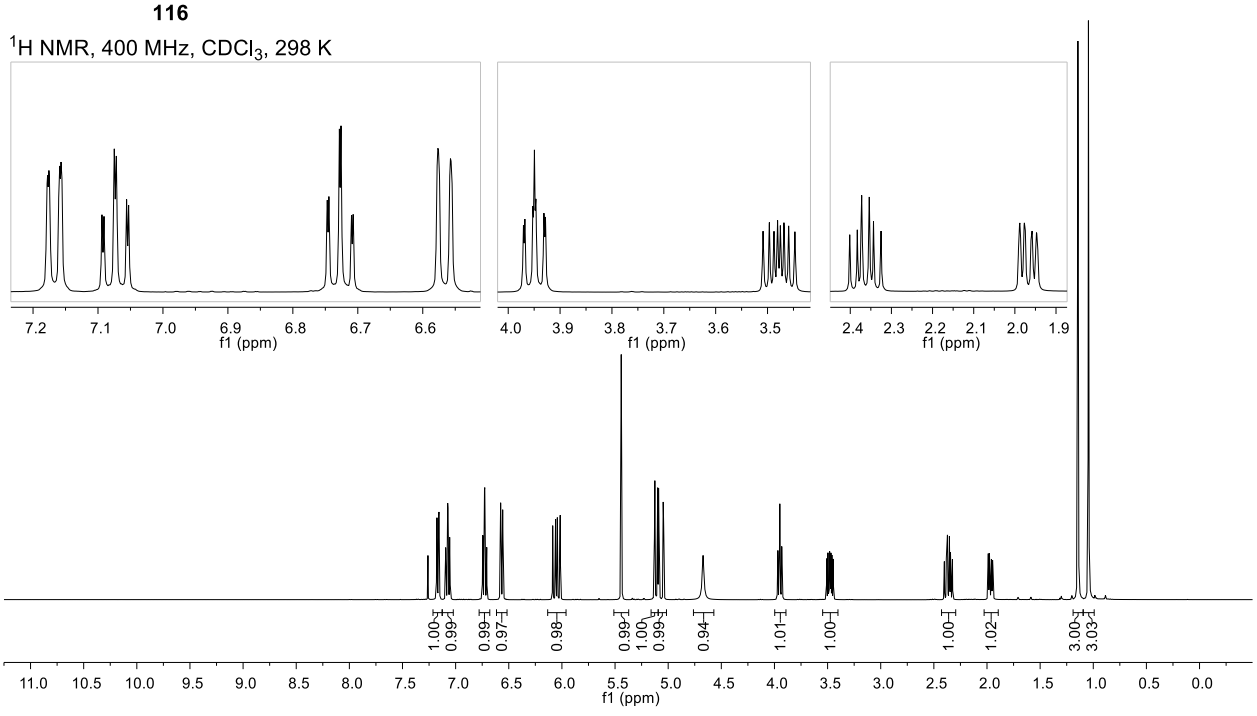

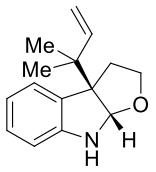

116

^{13}C NMR, 101 MHz
$CDCl_3$, 298 K

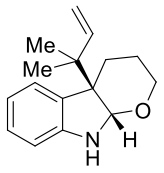

117

^{1}H NMR, 400 MHz, $CDCl_3$, 298 K

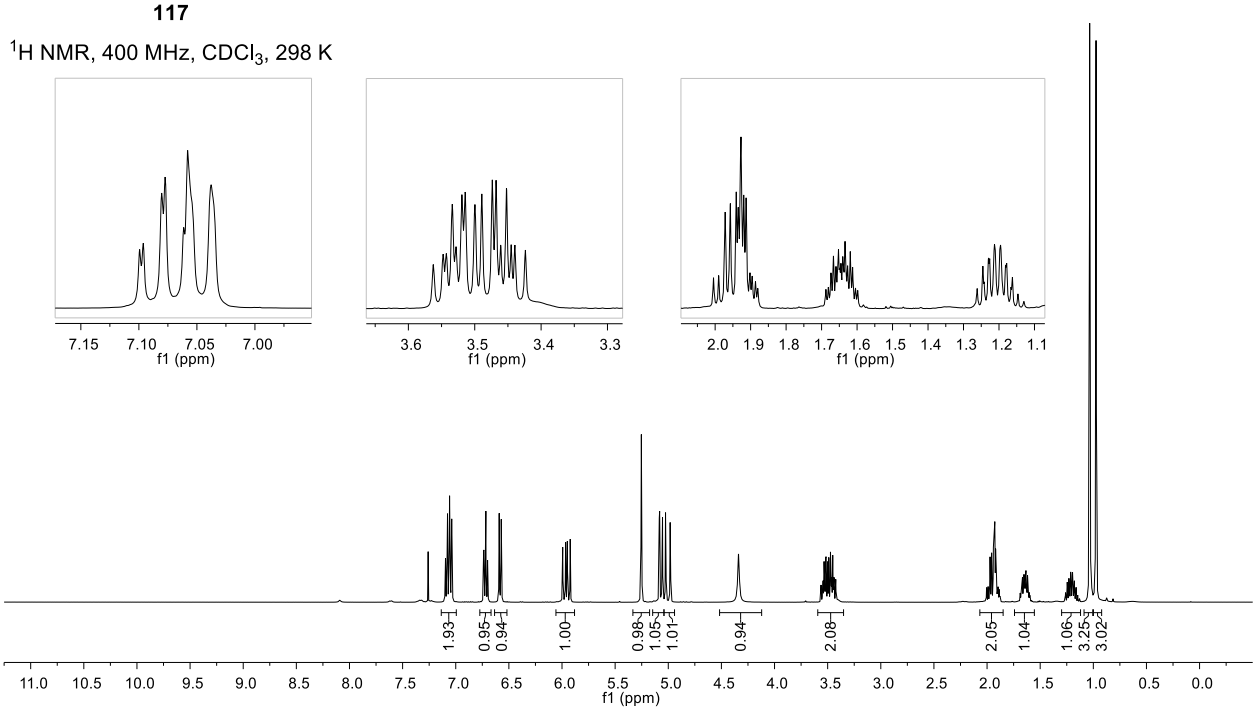

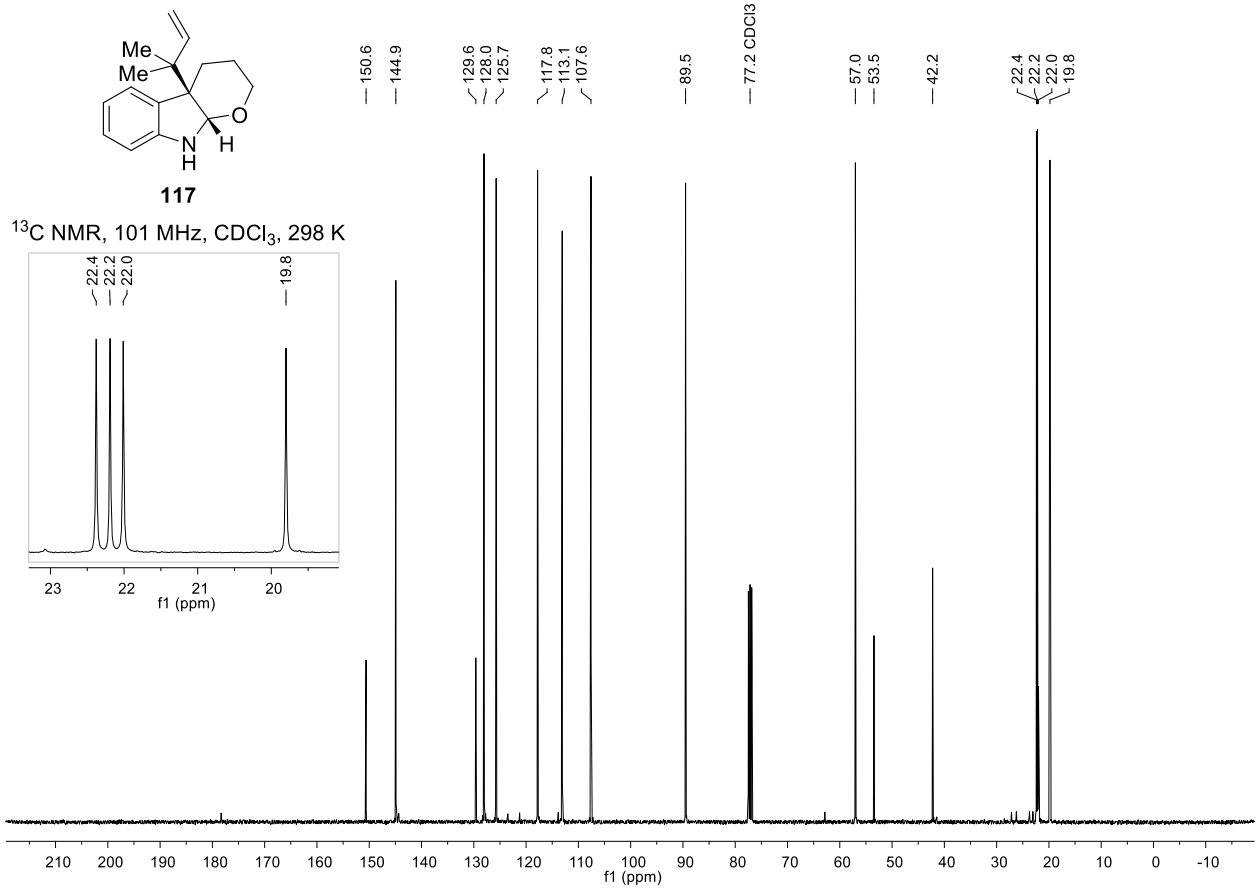
Me
Me
O
N
H
H
117
150.6
144.9
129.6
128.0
125.7
117.8
113.1
107.6
89.5
77.2 CDCl3
57.0
53.5
42.2
22.4
22.2
22.0
19.8
13C NMR, 101 MHz, CDCl3, 298 K
f1 (ppm)

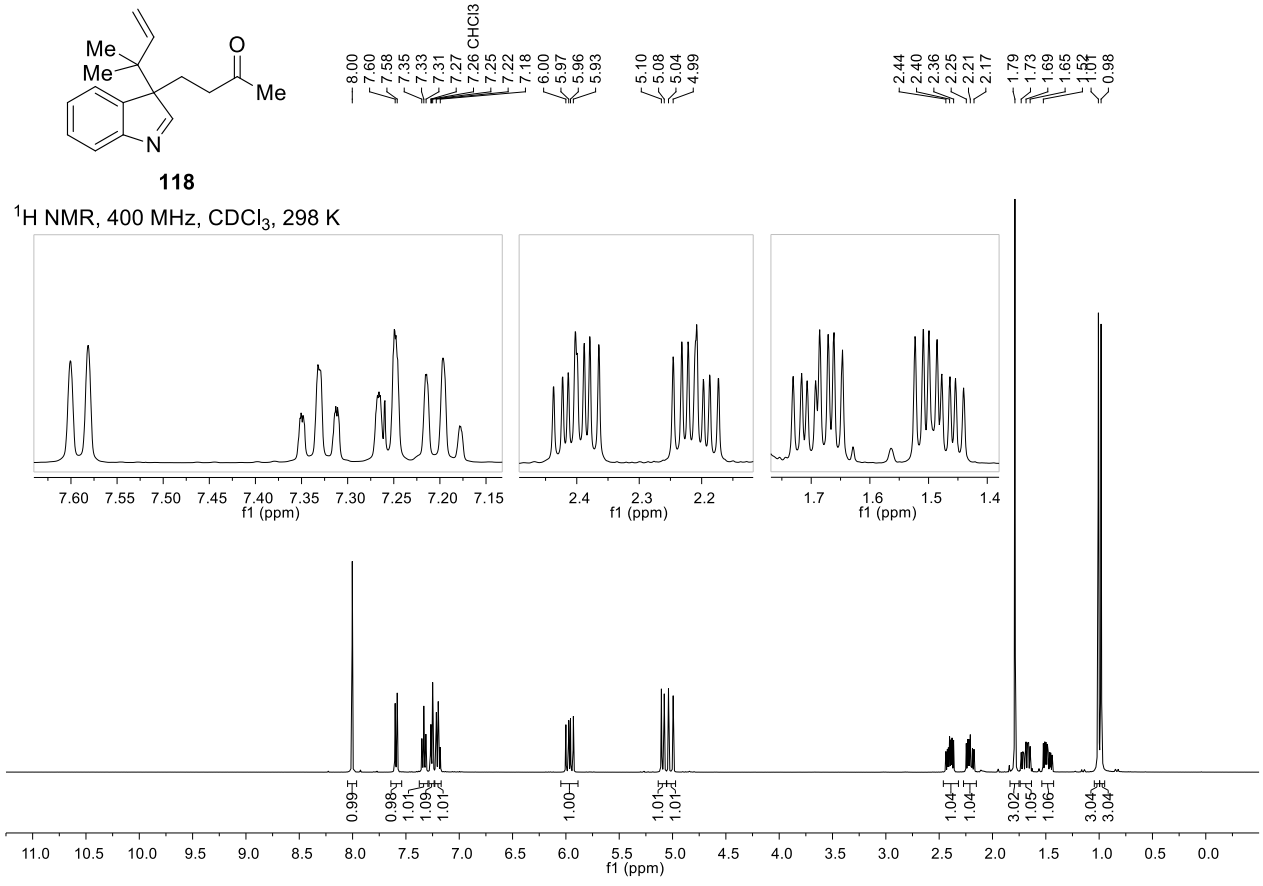
Me
Me
O
Me
N
118
8.00
7.60
7.58
7.35
7.33
7.31
7.27
7.26 CHCl3
7.25
7.22
7.18
6.00
5.97
5.96
5.93
5.10
5.08
5.04
4.99
2.44
2.40
2.36
2.25
2.21
2.17
1.79
1.73
1.69
1.65
1.52
1.01
0.98
1H NMR, 400 MHz, CDCl3, 298 K
f1 (ppm)

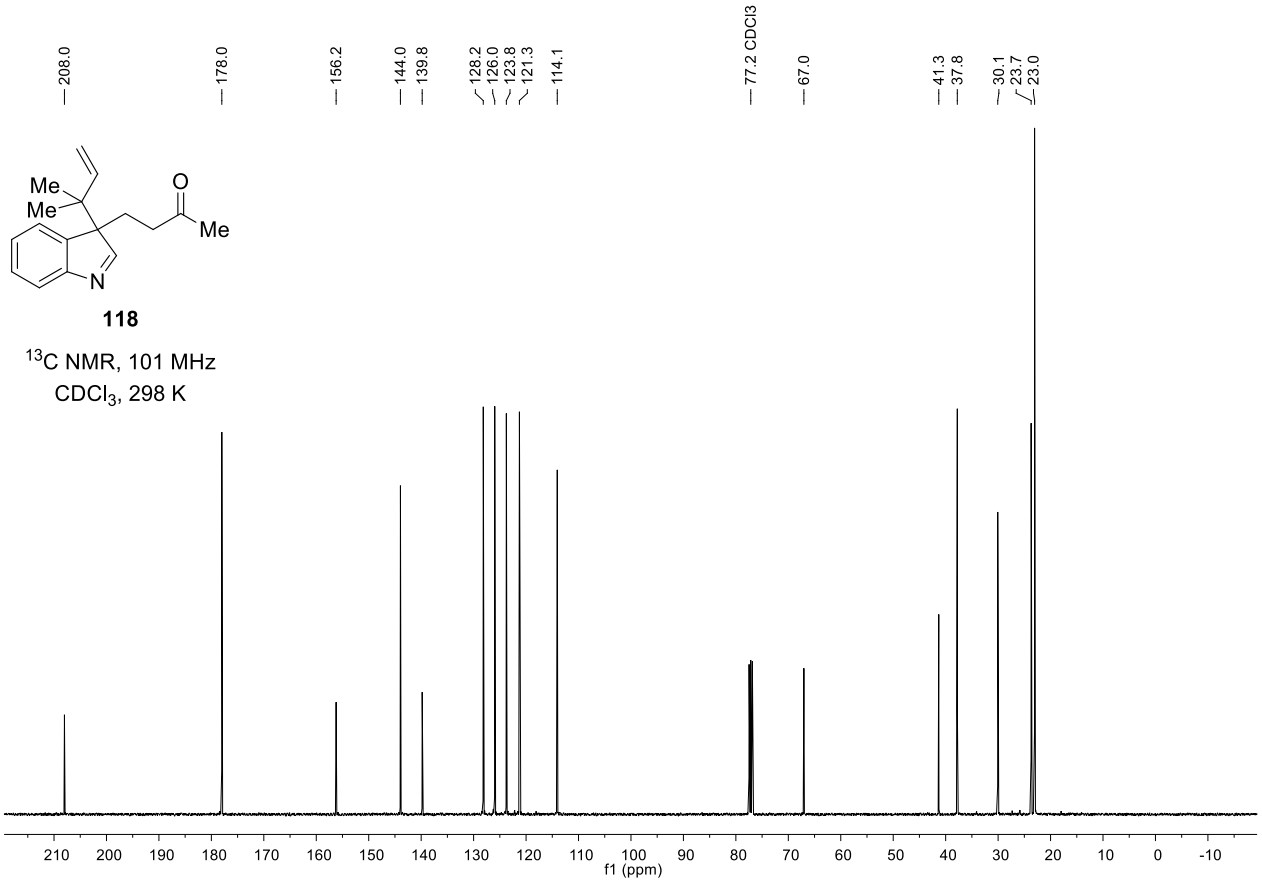

118

^{13}C NMR, 101 MHz
$CDCl_3$, 298 K

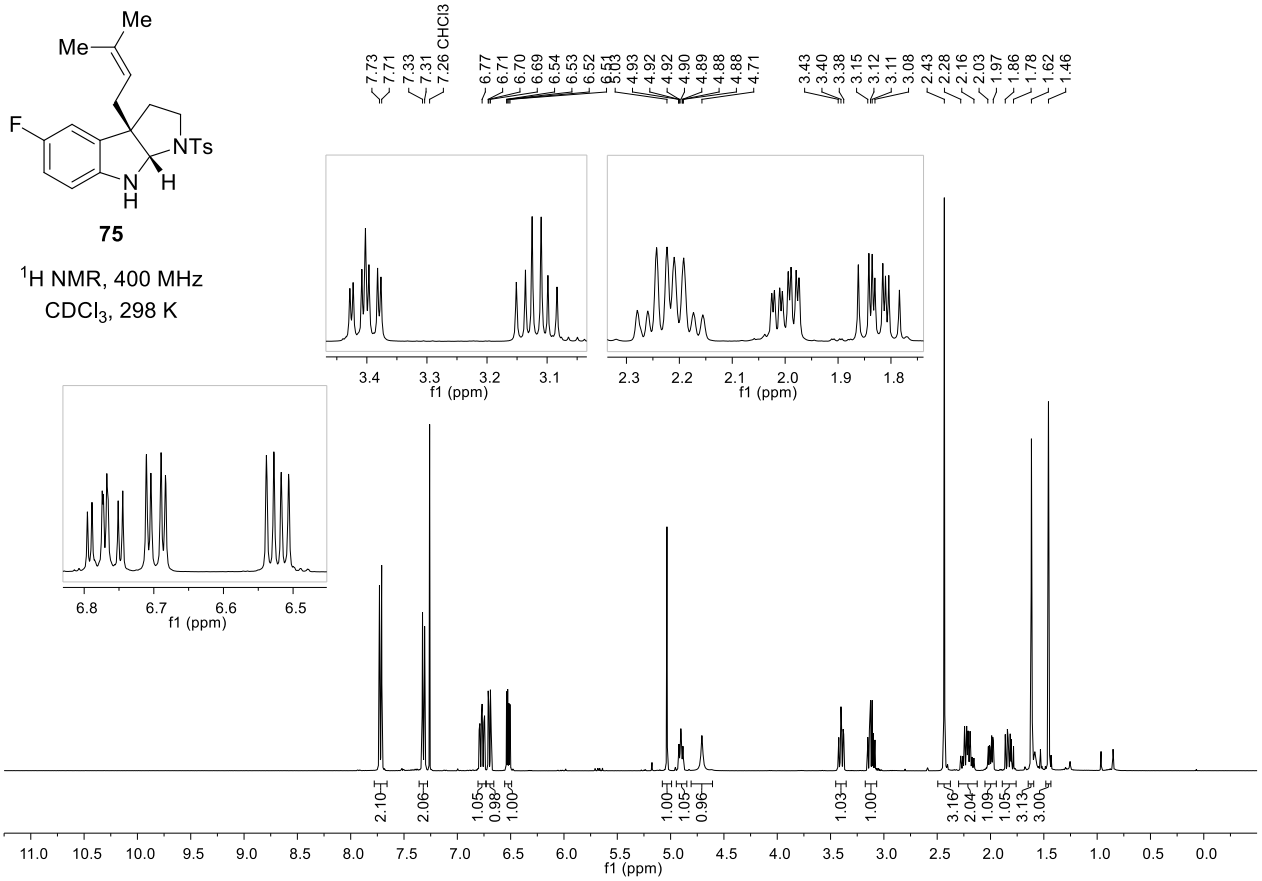

75

^{1}H NMR, 400 MHz
$CDCl_3$, 298 K

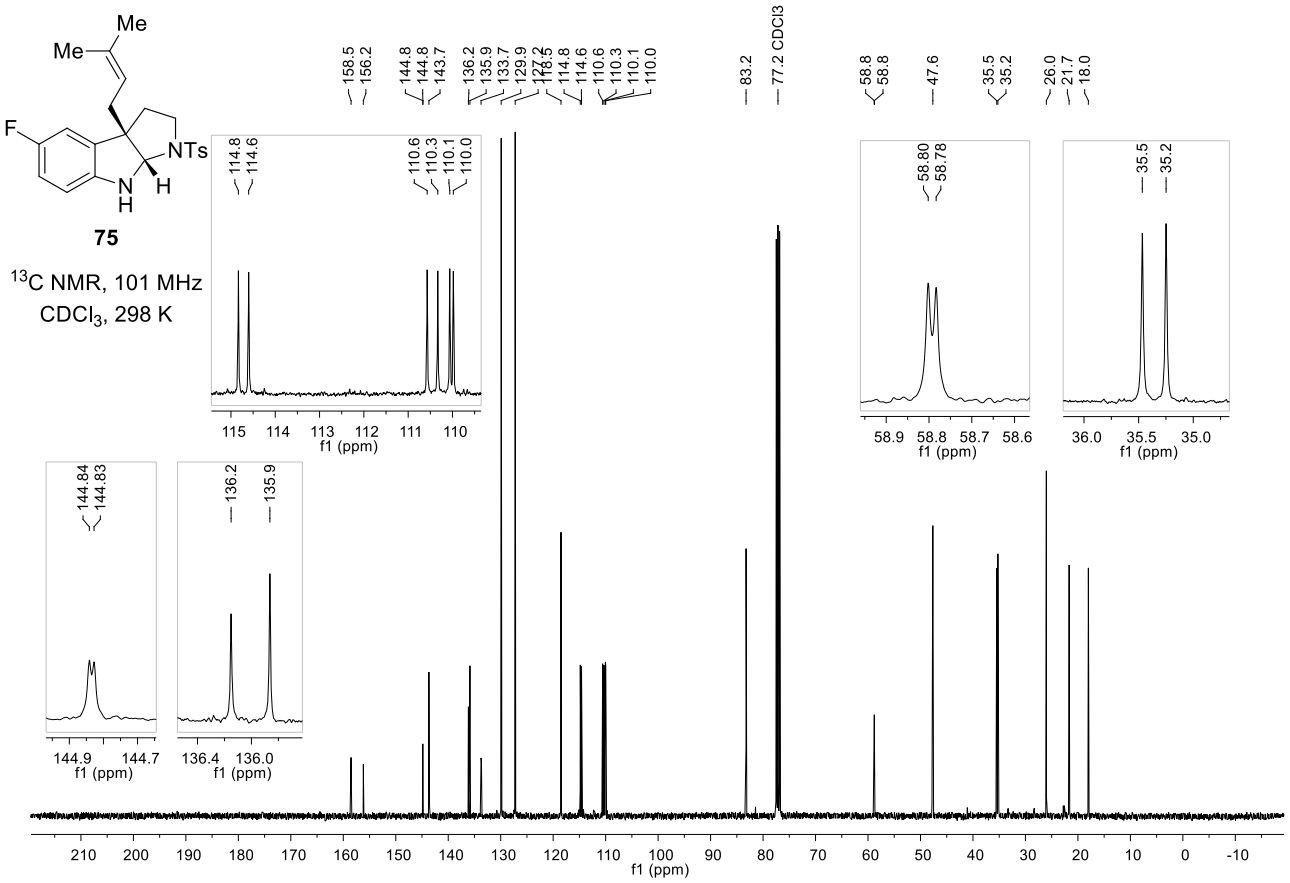

^{13}C NMR, 101 MHz
$CDCl_3$, 298 K

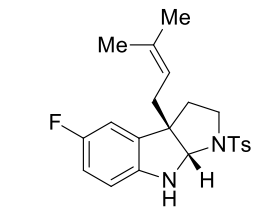

^{19}F{^{1}H} NMR, 377 MHz
$CDCl_3$, 298 K

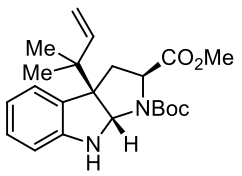

90

^{1}H NMR
400 MHz
$CDCl_3$, 298 K
mixture of
rotamers

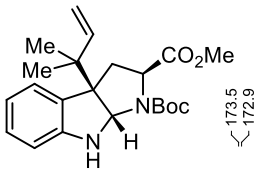

90

^{13}C NMR, 101 MHz, $CDCl_3$
298 K, mixture of rotamers

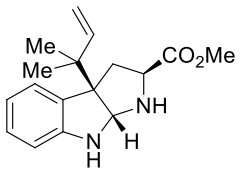

33

^{1}H NMR, 400 MHz, $CDCl_3$, 298 K

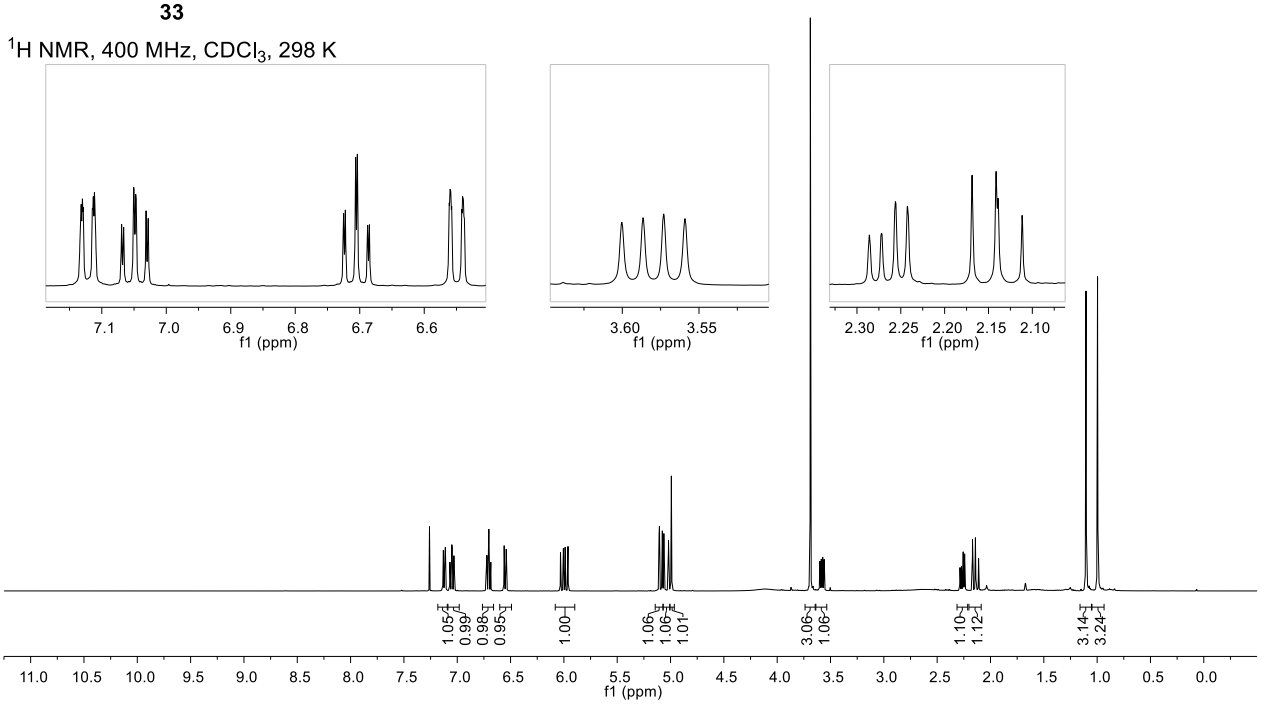

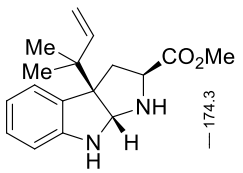

33

^{13}C NMR, 101 MHz, $CDCl_3$, 298 K

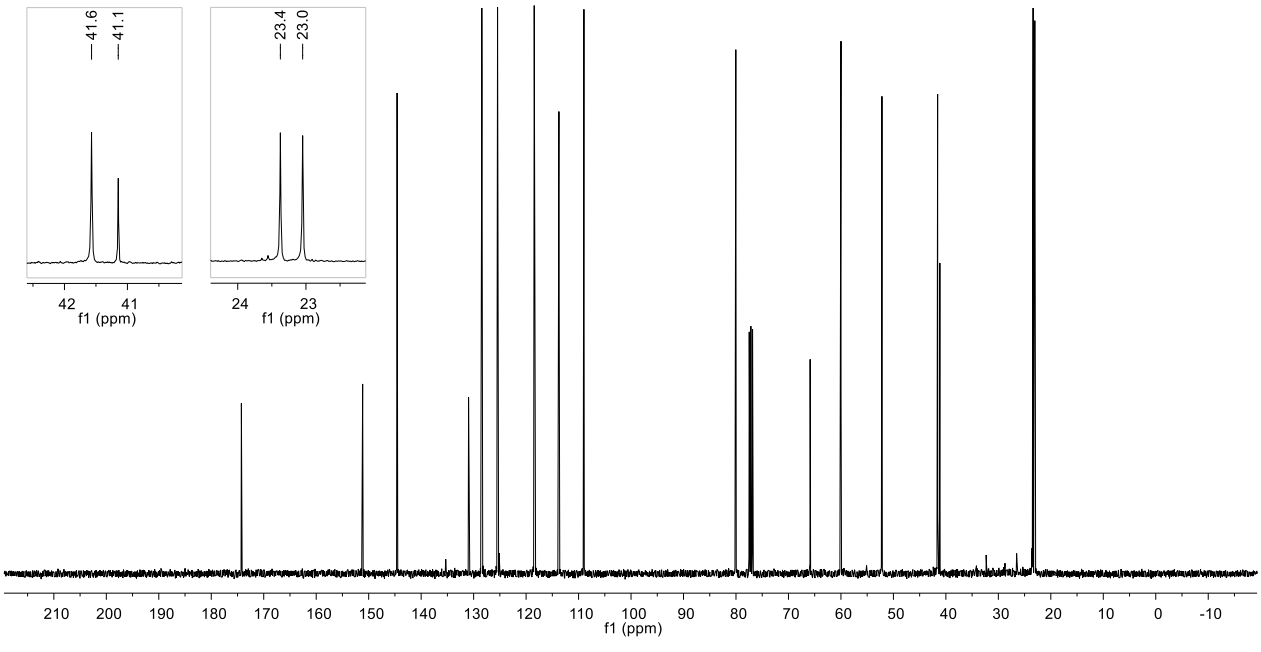

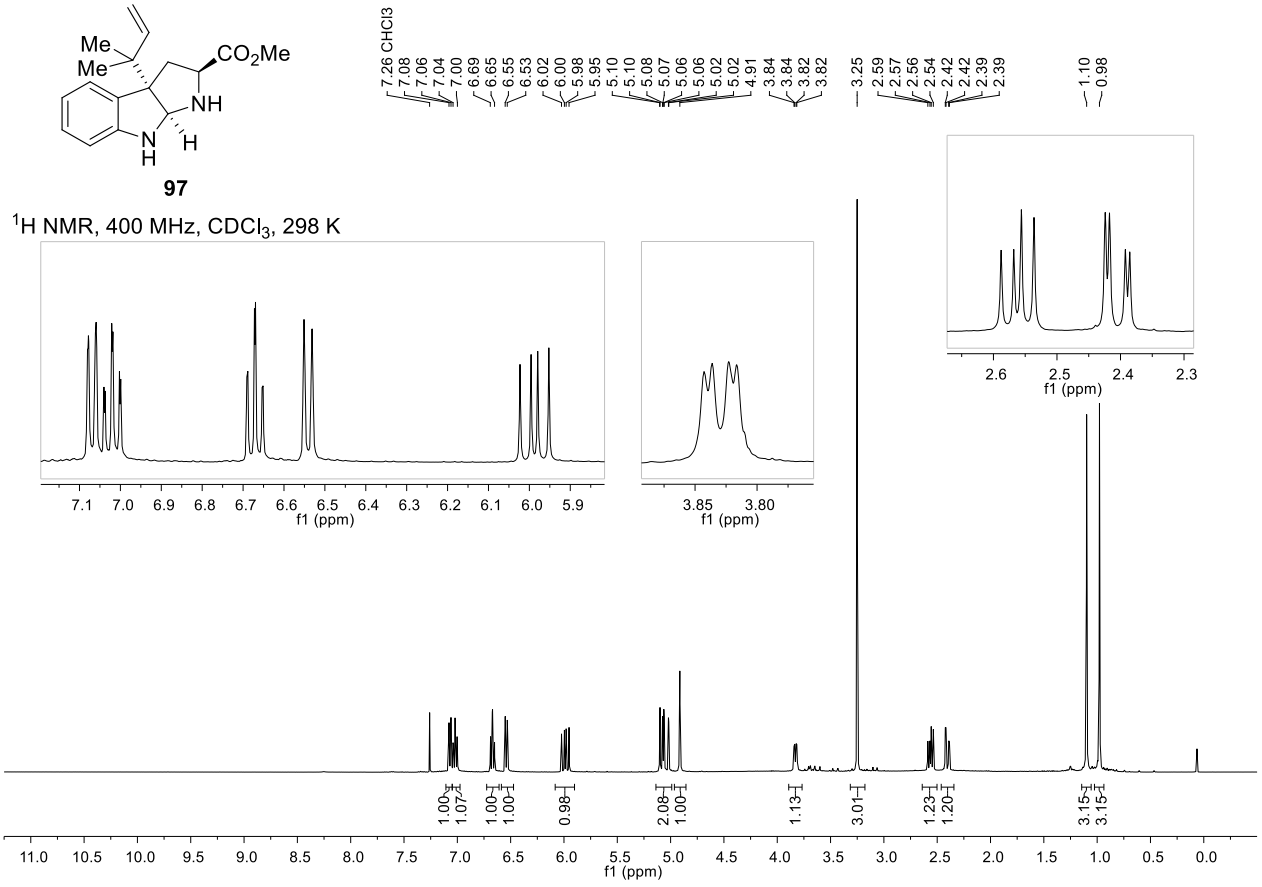
Me
Me
CO2Me
NH
N
H
H
97
1H NMR, 400 MHz, CDCl3, 298 K
7.26 CHCl3
7.08
7.06
7.04
7.00
6.69
6.65
6.55
6.53
6.02
6.00
5.98
5.95
5.10
5.10
5.08
5.07
5.06
5.06
5.02
5.02
4.91
3.84
3.84
3.82
3.82
3.25
2.59
2.57
2.56
2.54
2.42
2.42
2.39
2.39
1.10
0.98
f1 (ppm)
1.00
1.07
1.00
1.00
0.98
2.08
1.00
1.13
3.01
1.23
1.20
3.15
3.15

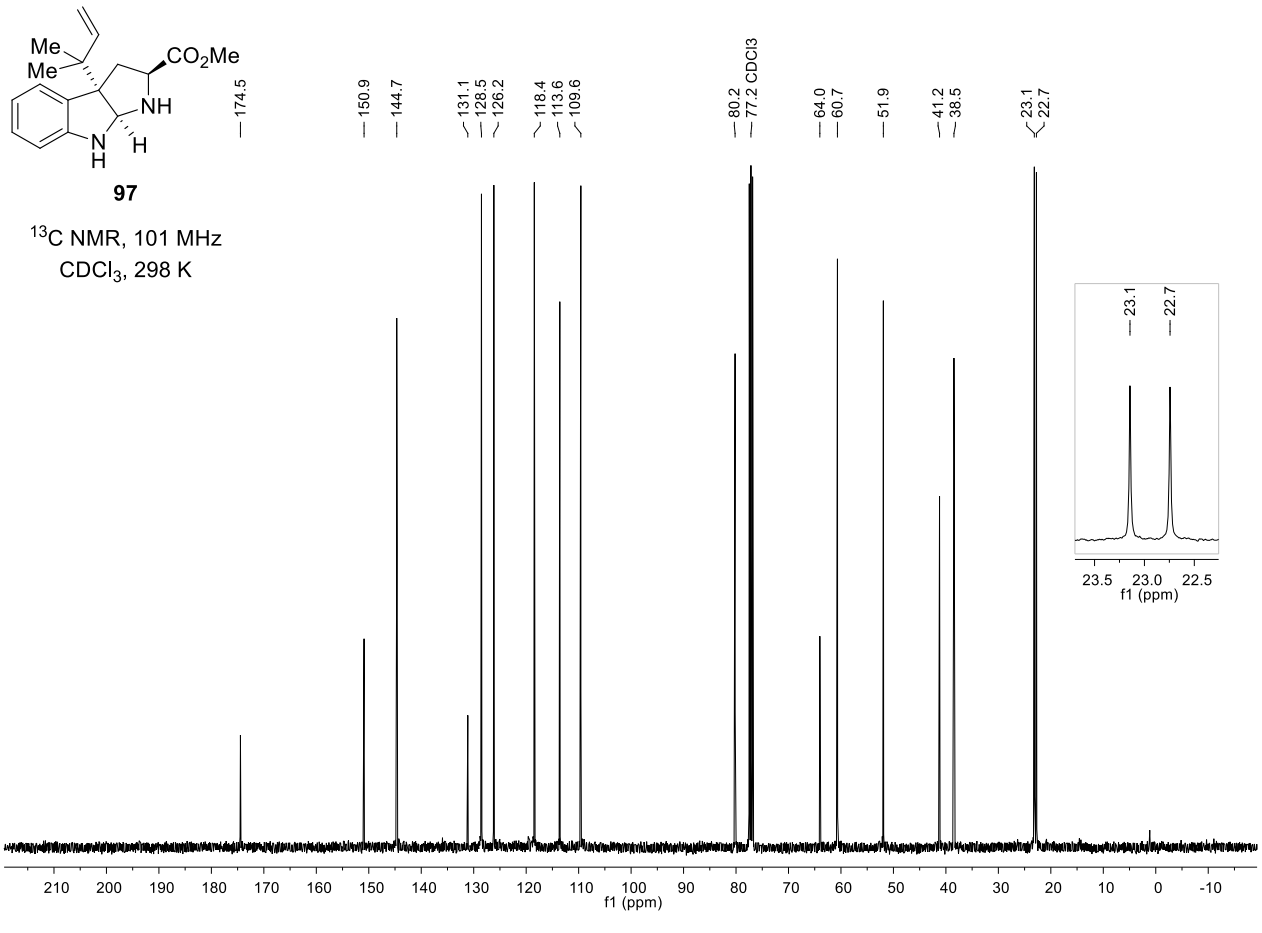
Me
Me
CO2Me
NH
N
H
H
97
13C NMR, 101 MHz
CDCl3, 298 K
174.5
150.9
144.7
131.1
128.5
126.2
118.4
113.6
109.6
80.2
77.2 CDCl3
64.0
60.7
51.9
41.2
38.5
23.1
22.7
f1 (ppm)

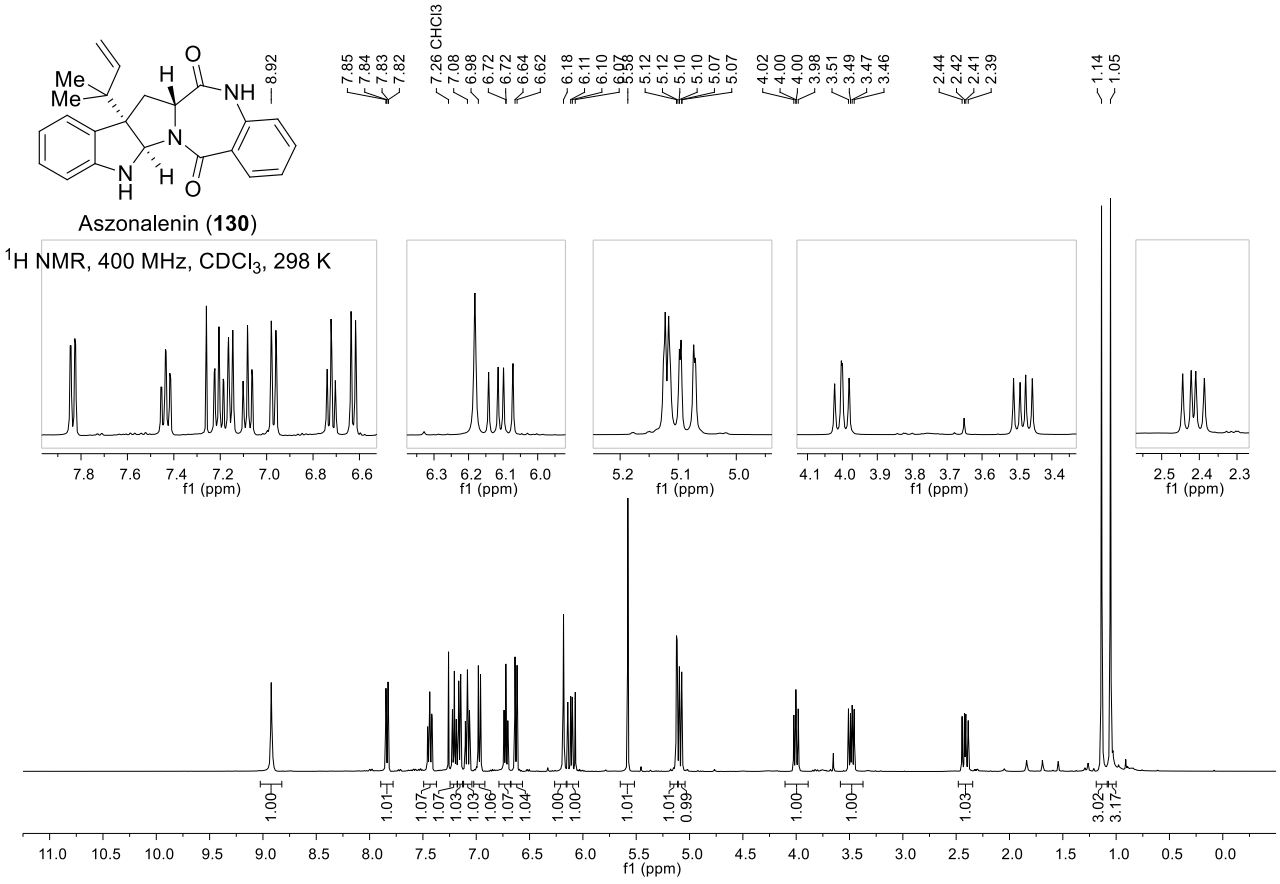
Aszonalenin (130)
1H NMR, 400 MHz, CDCl3, 298 K
f1 (ppm)

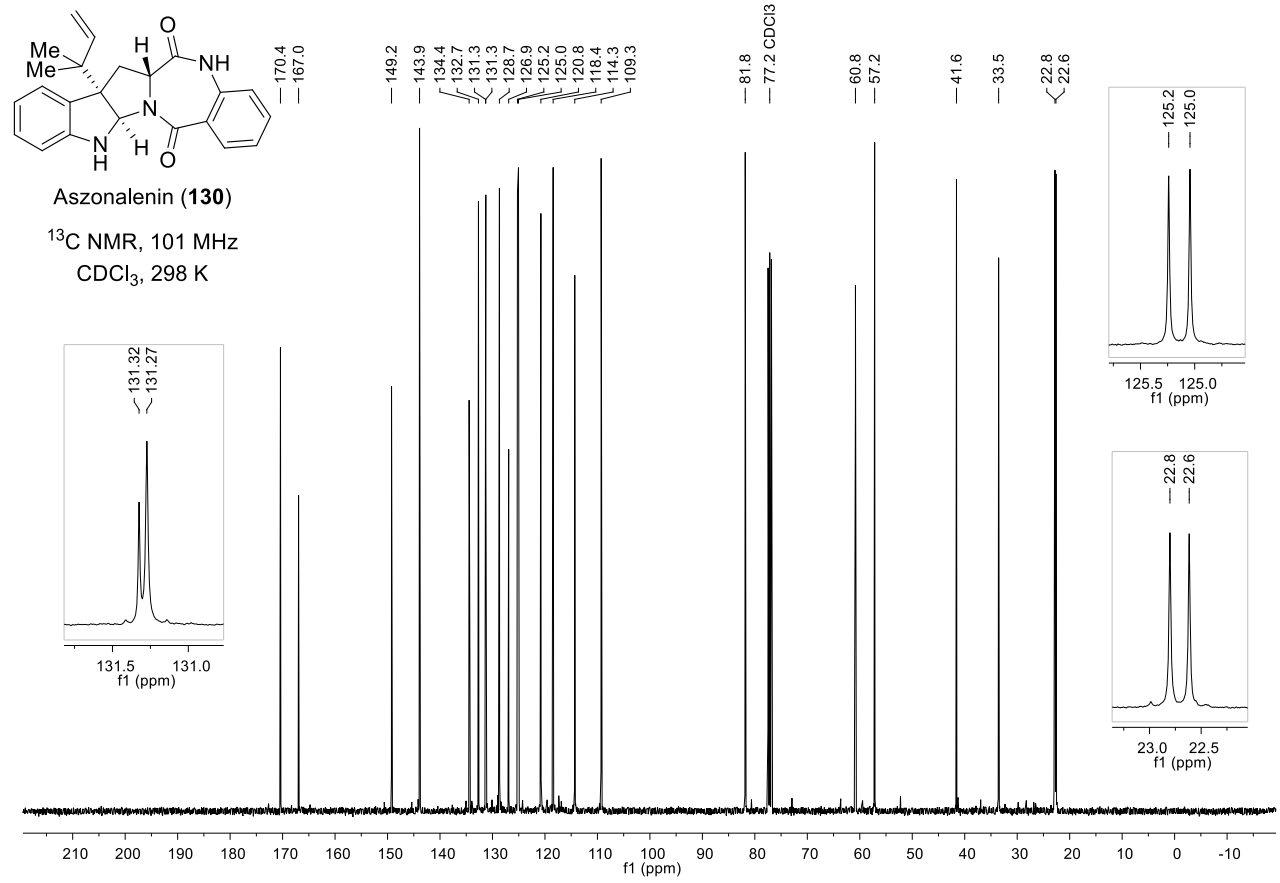
Aszonalenin (130)
13C NMR, 101 MHz
CDCl3, 298 K
f1 (ppm)

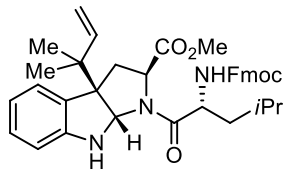

131

^{1}H NMR, 400 MHz
$CDCl_3$, 298 K
mixture of rotamers

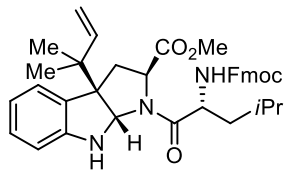

131

^{13}C NMR, 101 MHz
$CDCl_3$, 298 K
mixture of rotamers

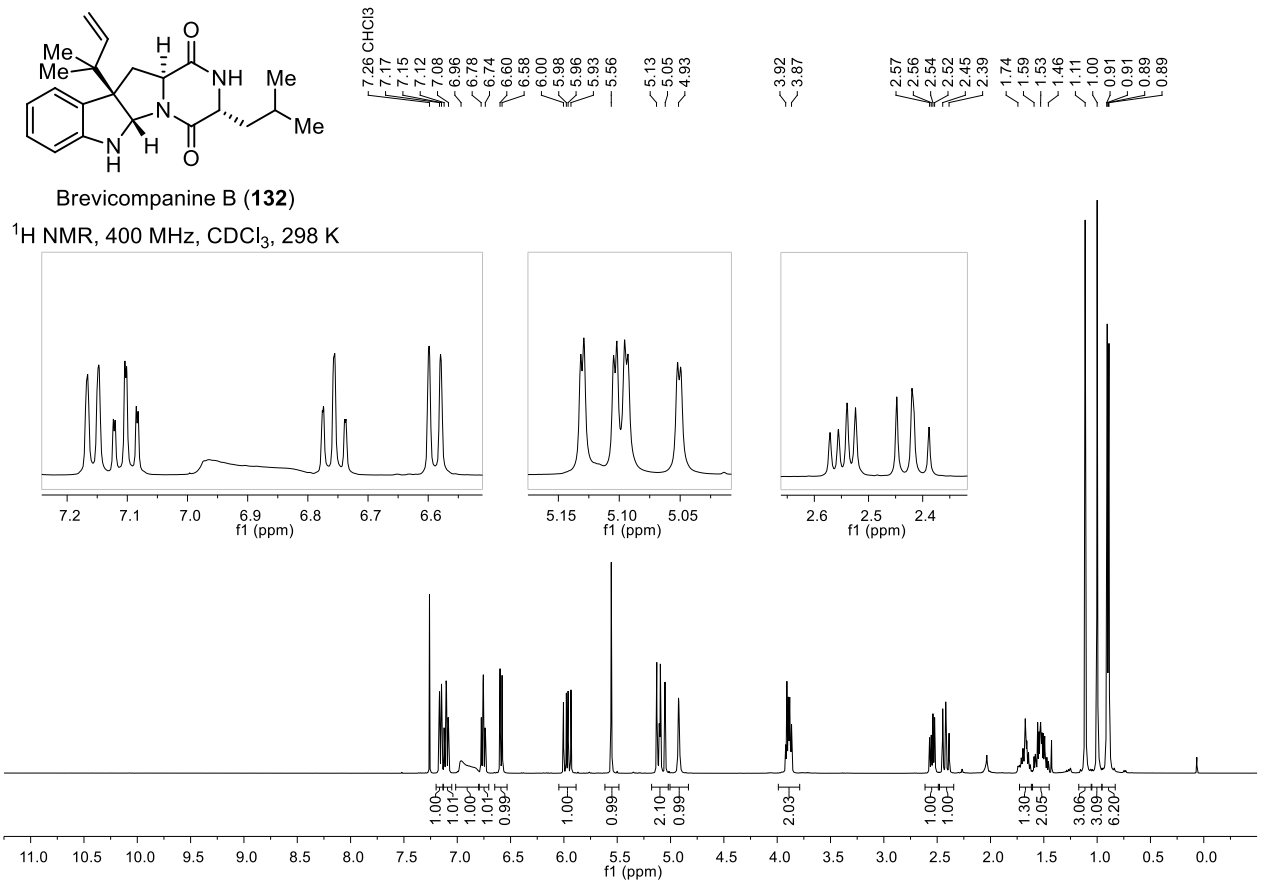
Brevicompanine B (132)
1H NMR, 400 MHz, CDCl3, 298 K
f1 (ppm)

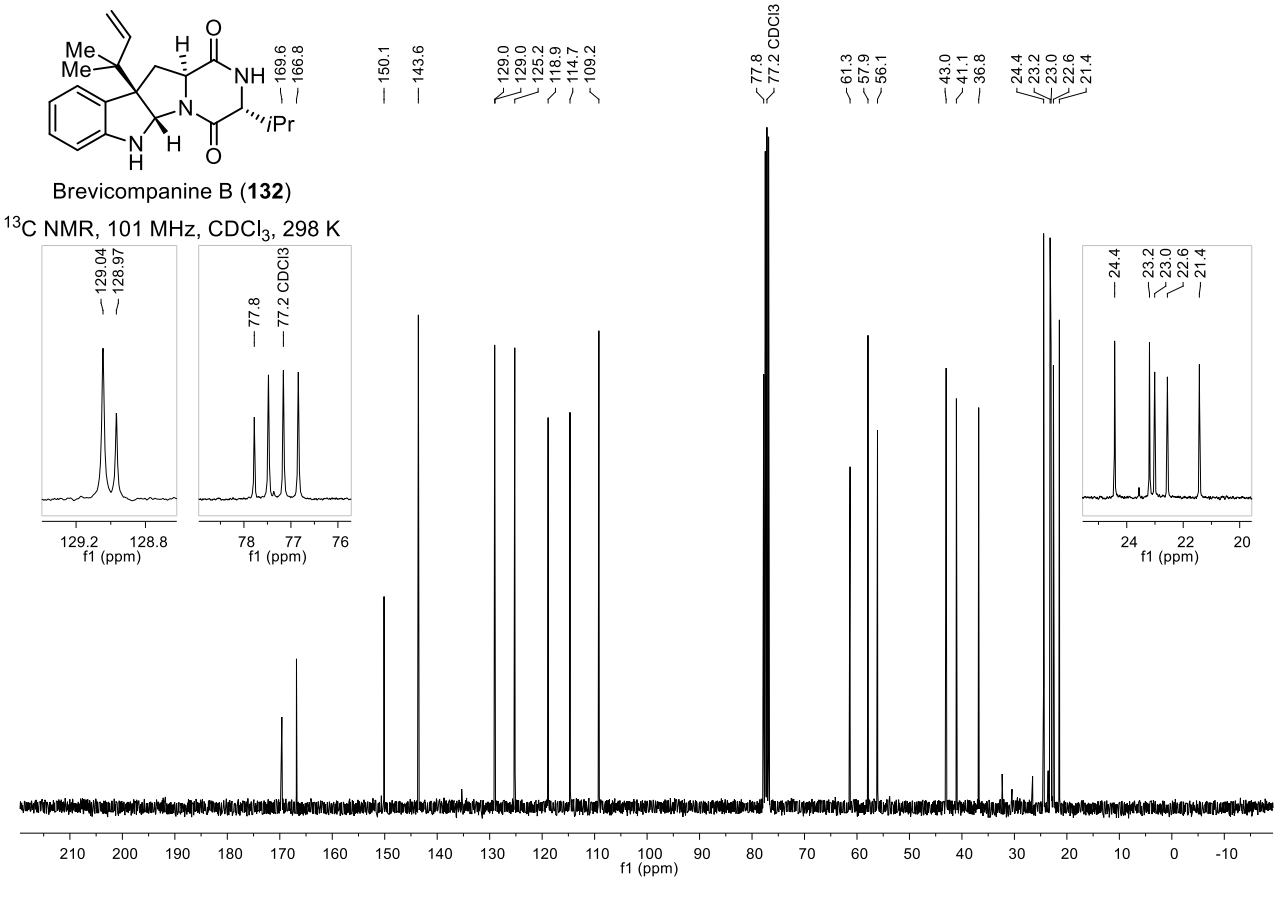
Brevicompanine B (132)
13C NMR, 101 MHz, CDCl3, 298 K
f1 (ppm)

11.2 Part II. Rh-Catalyzed Stereoselective Synthesis of Allenes

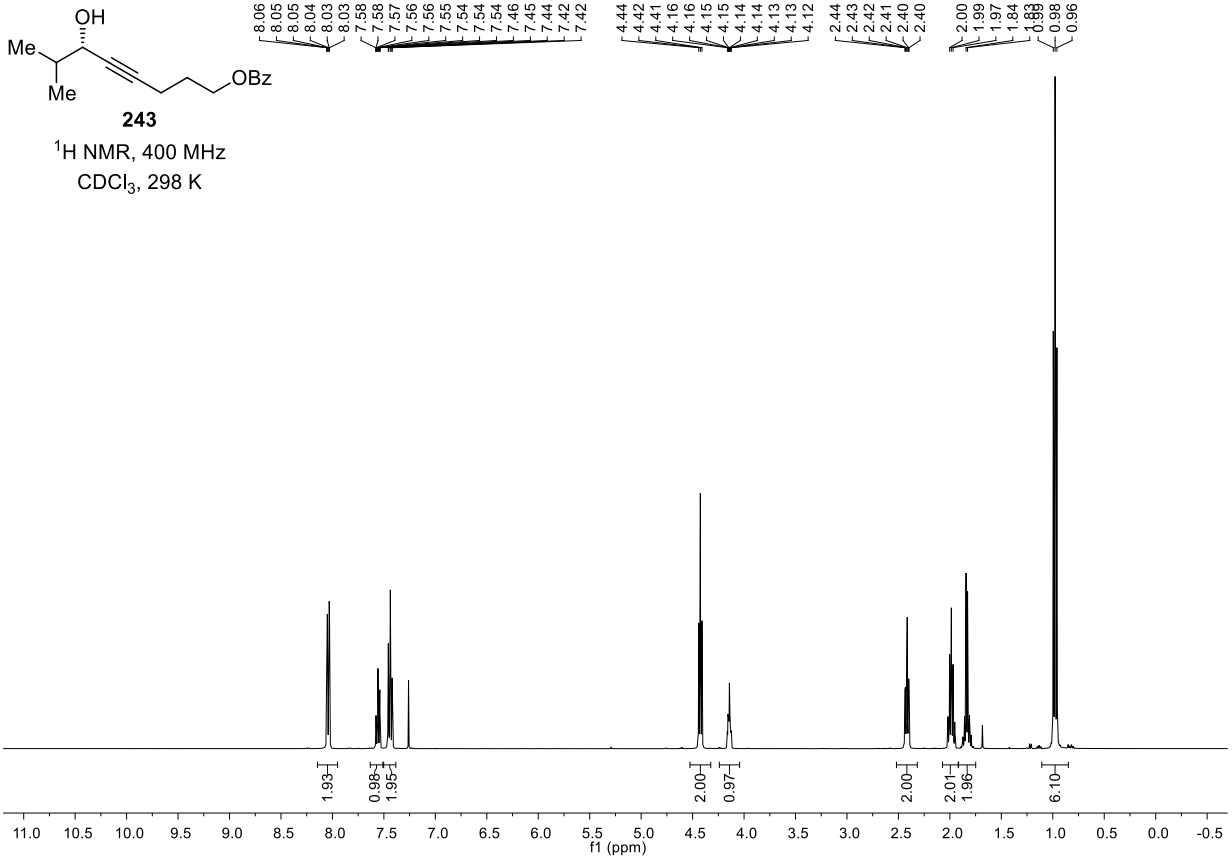

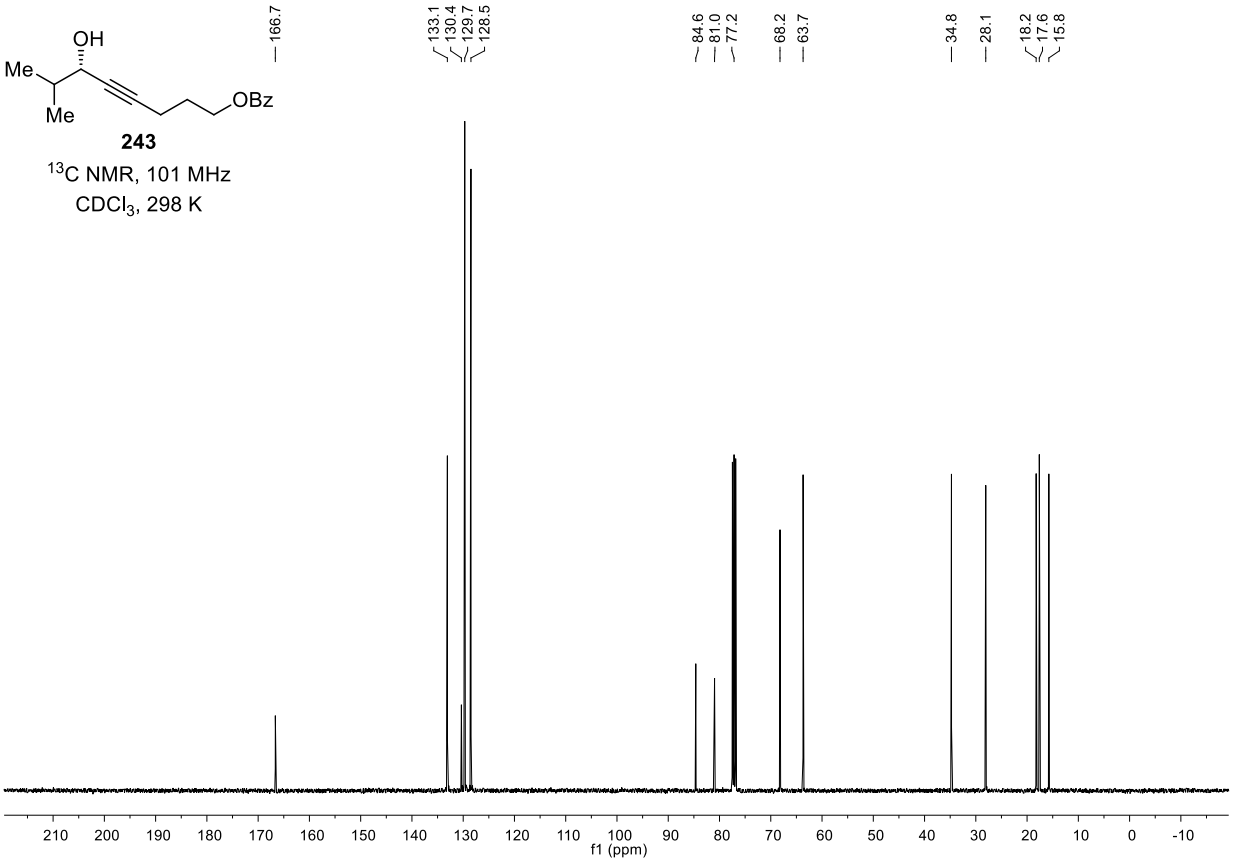

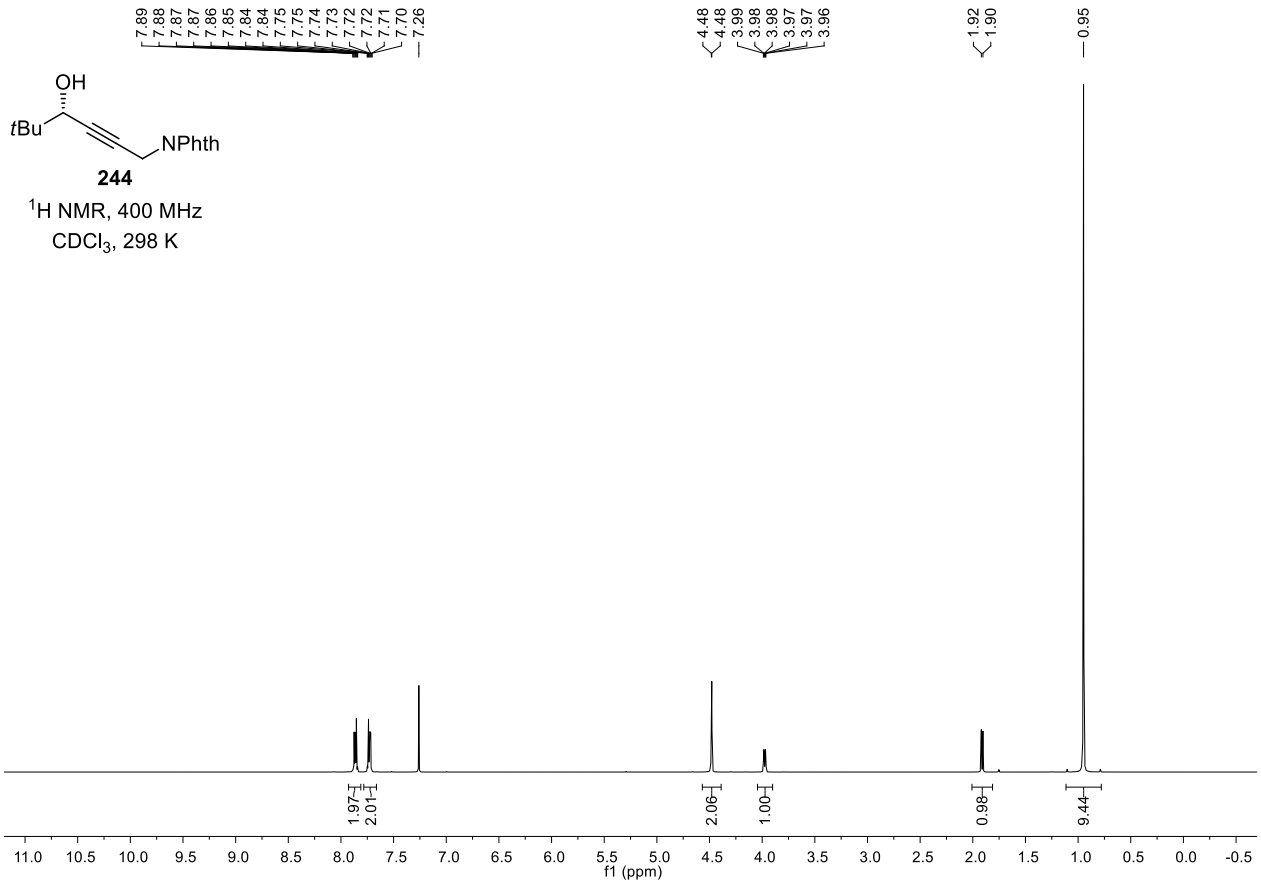
7.89
7.88
7.87
7.87
7.86
7.85
7.84
7.84
7.75
7.75
7.74
7.73
7.72
7.72
7.71
7.70
7.26
4.48
4.48
3.99
3.98
3.98
3.97
3.97
3.96
1.92
1.90
0.95
OH
tBu
NPhth
244
1H NMR, 400 MHz
CDCl3, 298 K
1.97
2.01
2.06
1.00
0.98
9.44
11.0 10.5 10.0 9.5 9.0 8.5 8.0 7.5 7.0 6.5 6.0 5.5 5.0 4.5 4.0 3.5 3.0 2.5 2.0 1.5 1.0 0.5 0.0 -0.5
f1 (ppm)

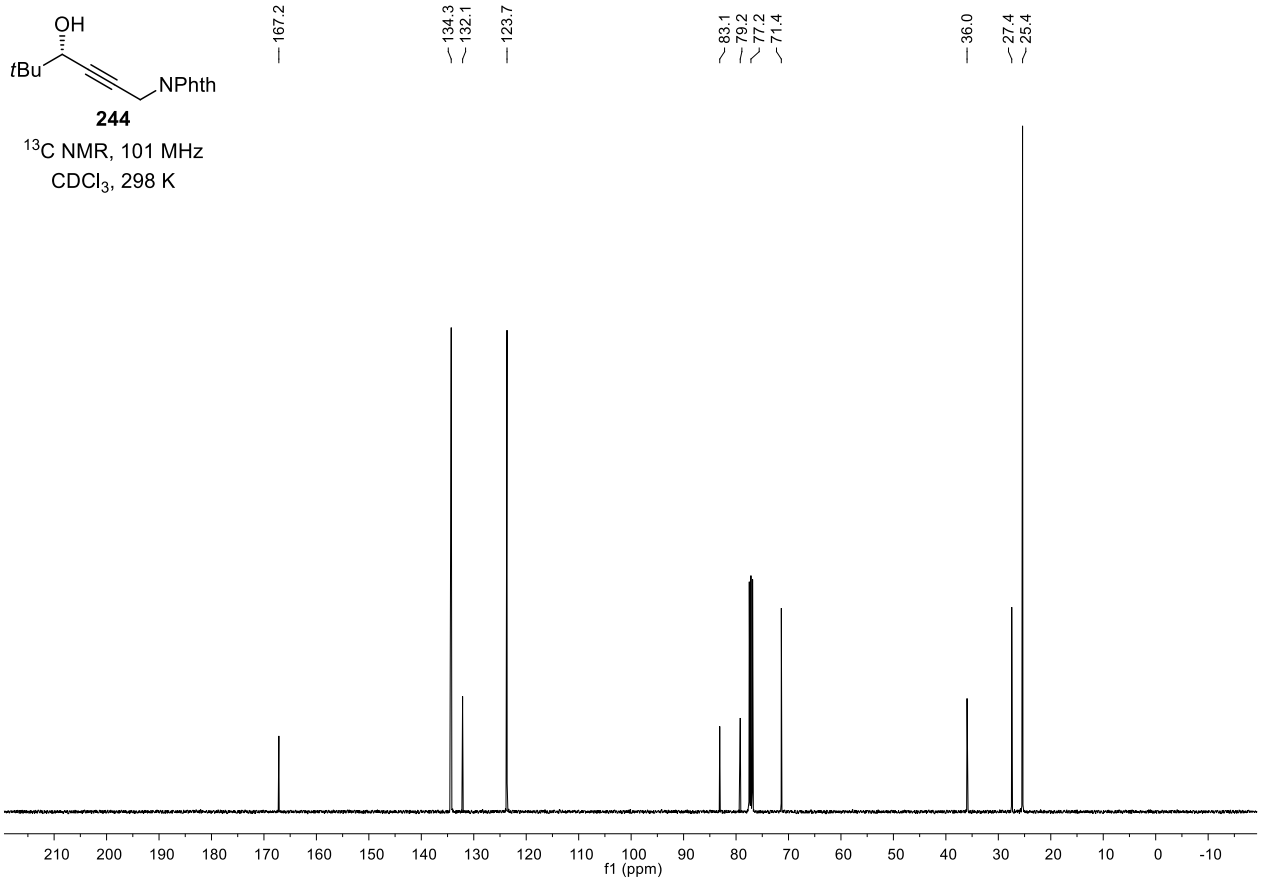
OH
tBu
NPhth
244
13C NMR, 101 MHz
CDCl3, 298 K
167.2
134.3
132.1
123.7
83.1
79.2
77.2
71.4
36.0
27.4
25.4
210 200 190 180 170 160 150 140 130 120 110 100 90 80 70 60 50 40 30 20 10 0 -10
f1 (ppm)

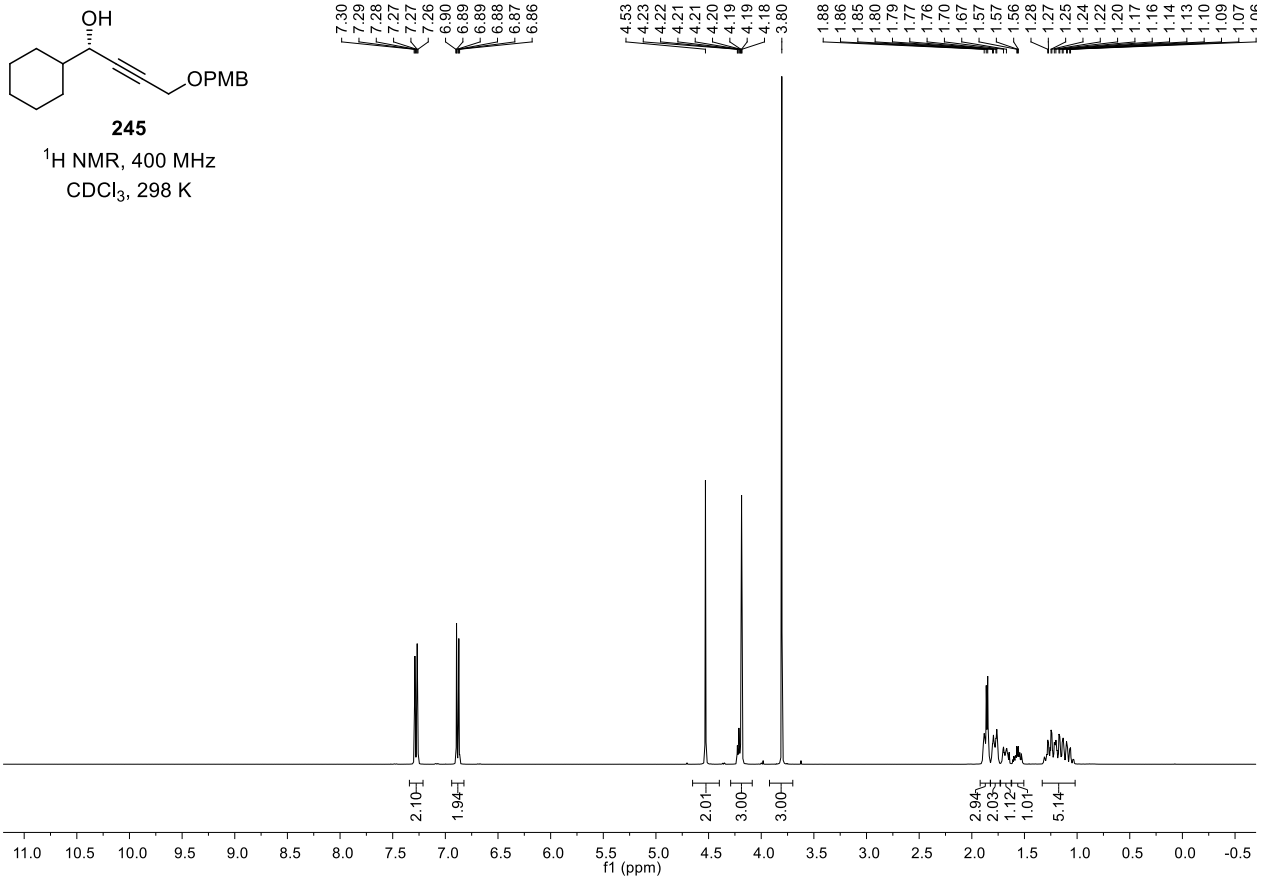
OH
OPMB
245
1H NMR, 400 MHz
CDCl3, 298 K
f1 (ppm)

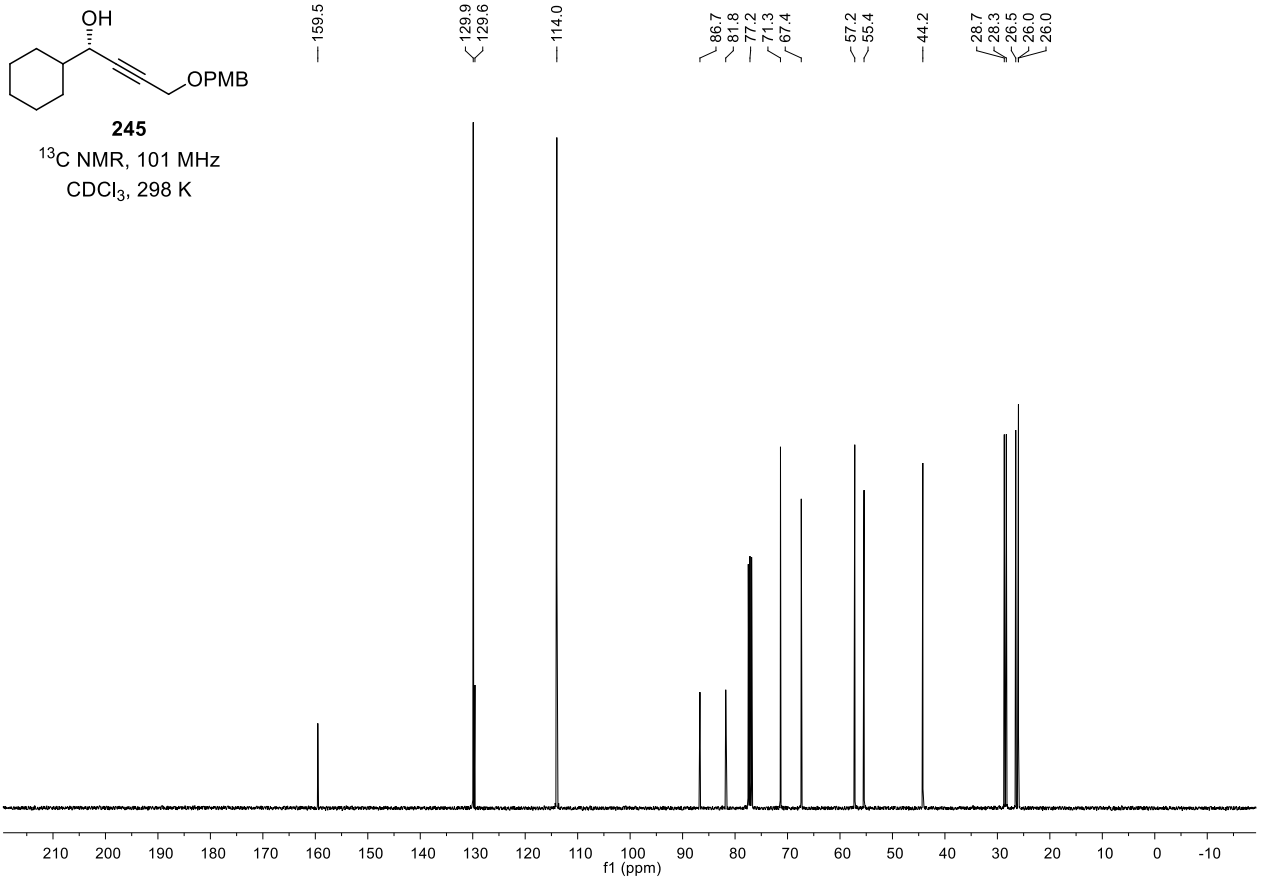
OH
OPMB
245
13C NMR, 101 MHz
CDCl3, 298 K
f1 (ppm)

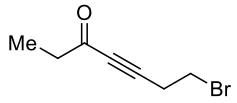

246

^{1}H NMR, 400 MHz

$CDCl_3$, 298 K

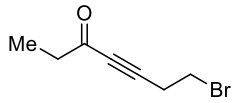

246

^{13}C NMR, 101 MHz

$CDCl_3$, 298 K

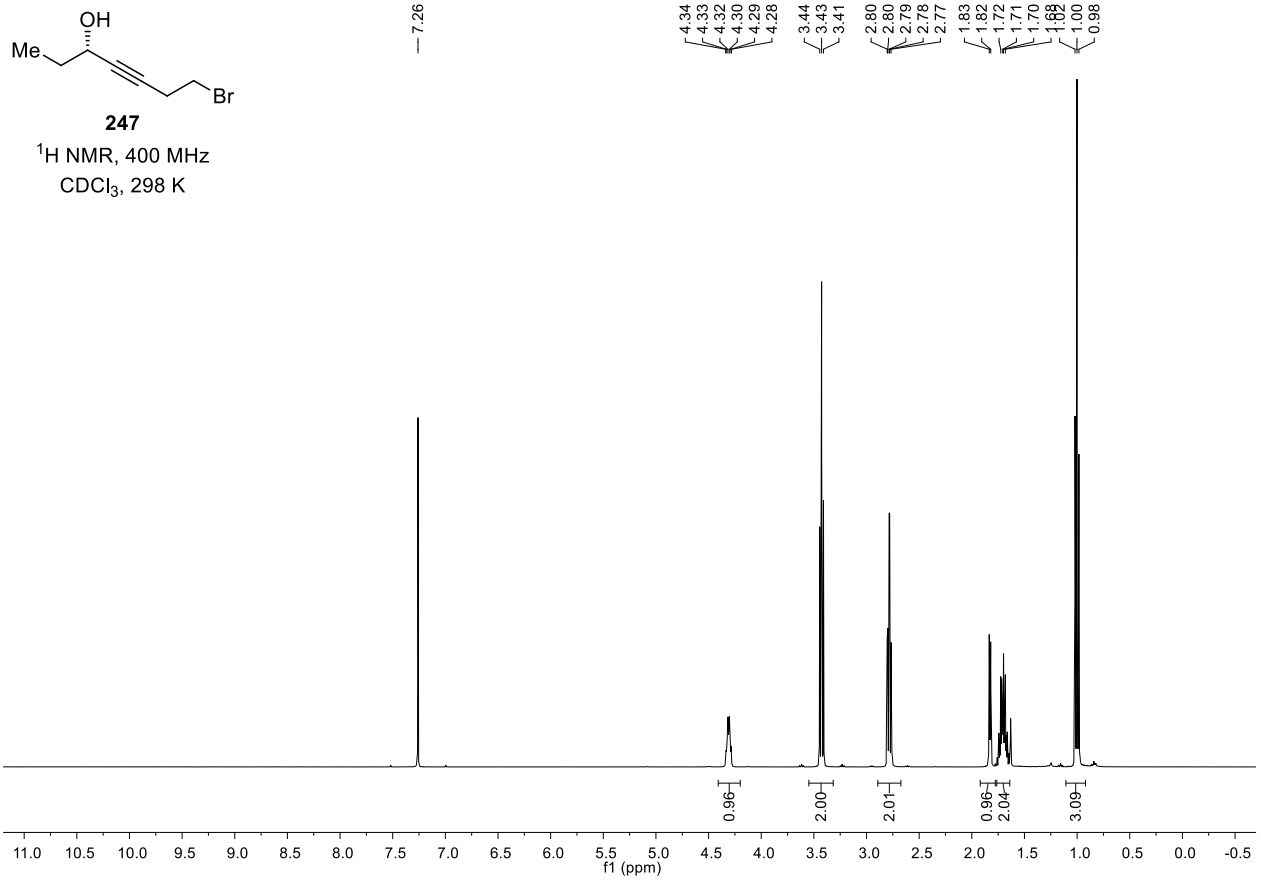
OH
Me
Br
247
1H NMR, 400 MHz
CDCl3, 298 K
7.26
4.34
4.33
4.32
4.30
4.29
4.28
3.44
3.43
3.41
2.80
2.80
2.79
2.78
2.77
1.83
1.82
1.72
1.71
1.70
1.68
1.00
0.98
0.96
2.00
2.01
0.96
2.04
3.09
f1 (ppm)

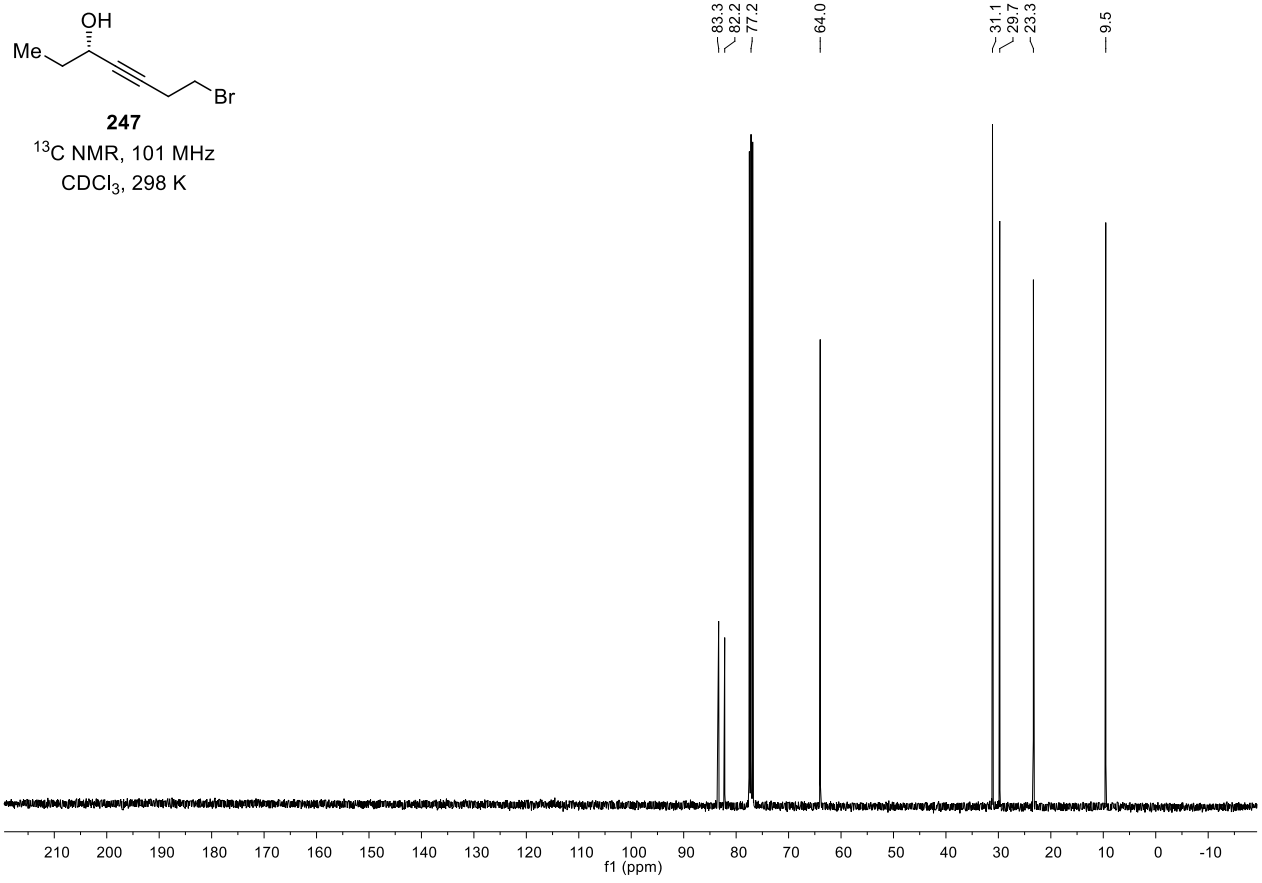
OH
Me
Br
247
13C NMR, 101 MHz
CDCl3, 298 K
83.3
82.2
77.2
64.0
31.1
29.7
23.3
9.5
f1 (ppm)

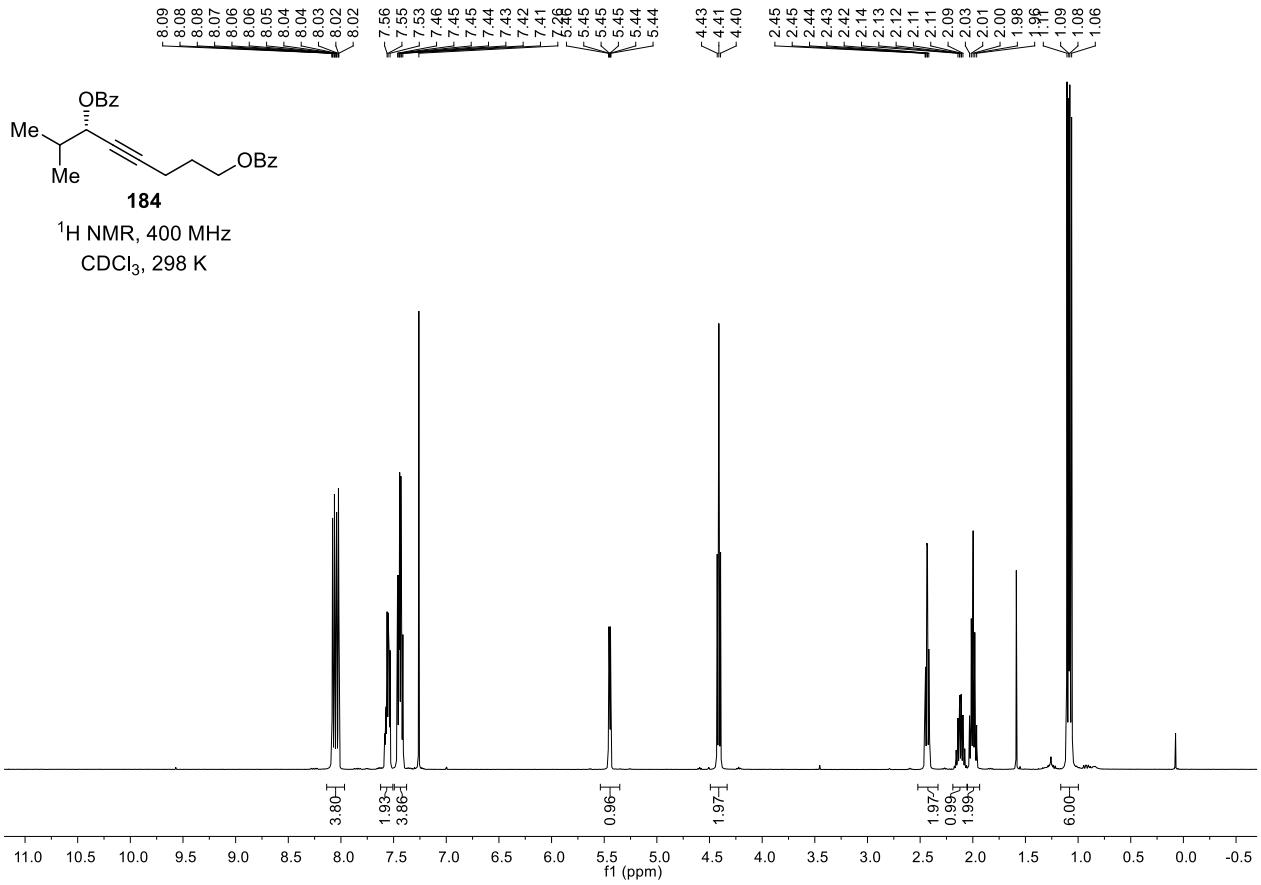
OBz
Me
Me
OBz
184
1H NMR, 400 MHz
CDCl3, 298 K
f1 (ppm)

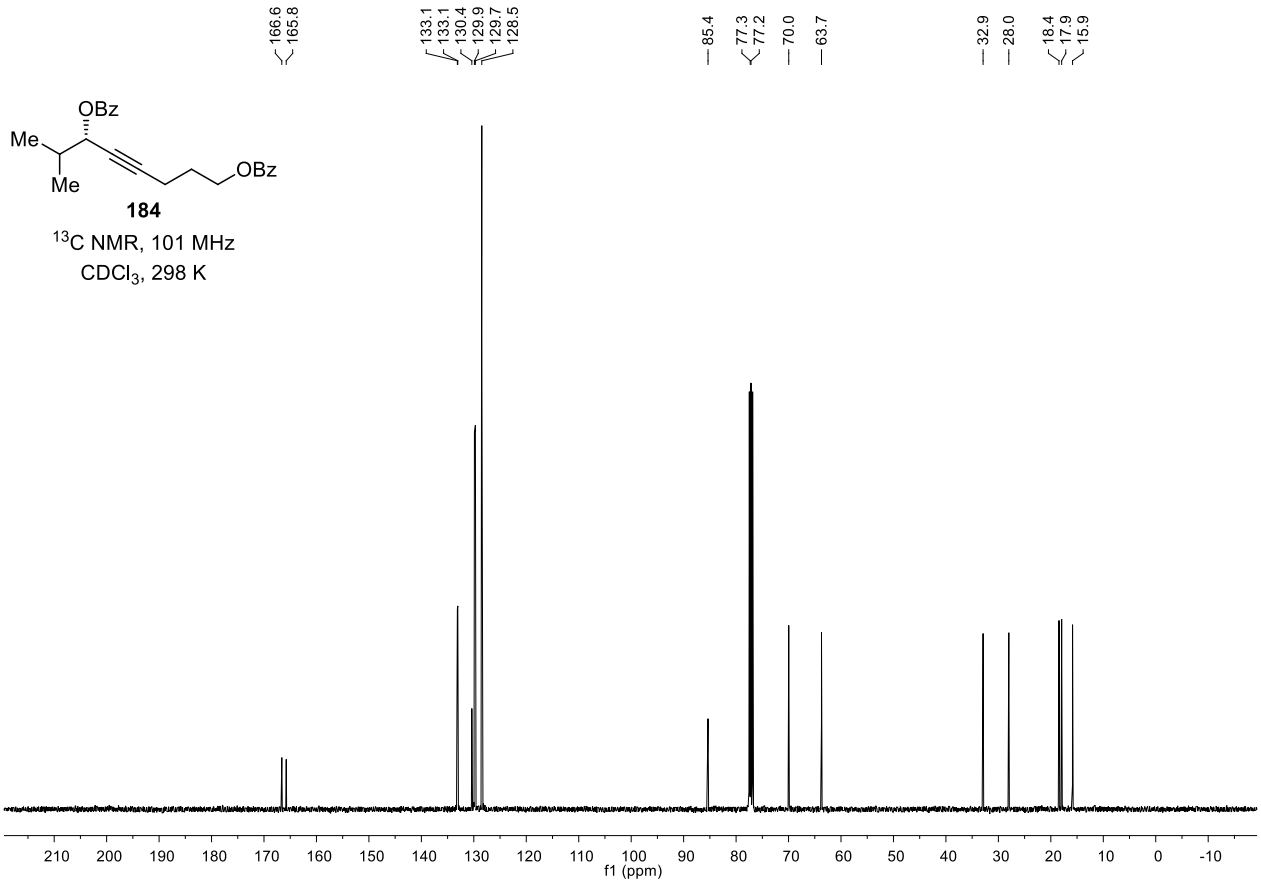
OBz
Me
Me
OBz
184
13C NMR, 101 MHz
CDCl3, 298 K
f1 (ppm)

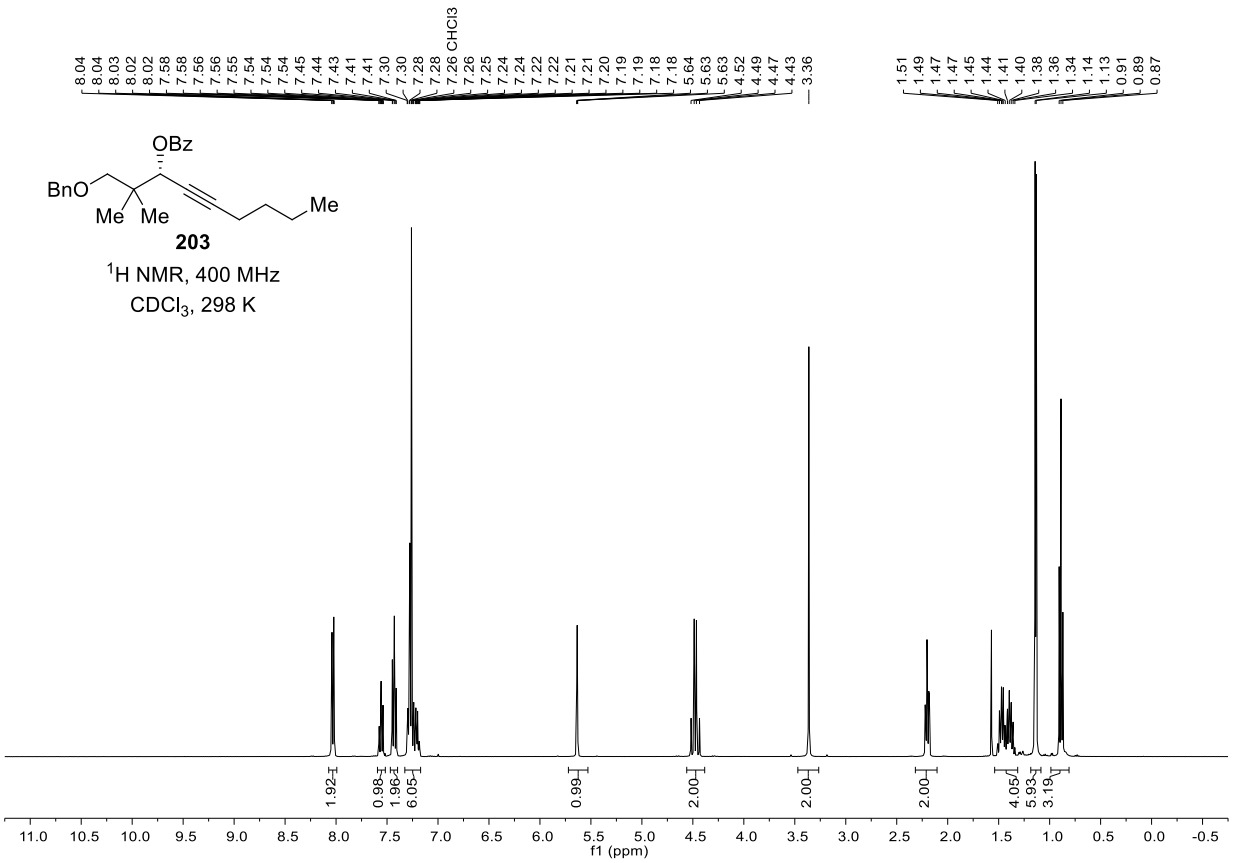
OBz
BnO
Me Me
Me
203
1H NMR, 400 MHz
CDCl3, 298 K
f1 (ppm)

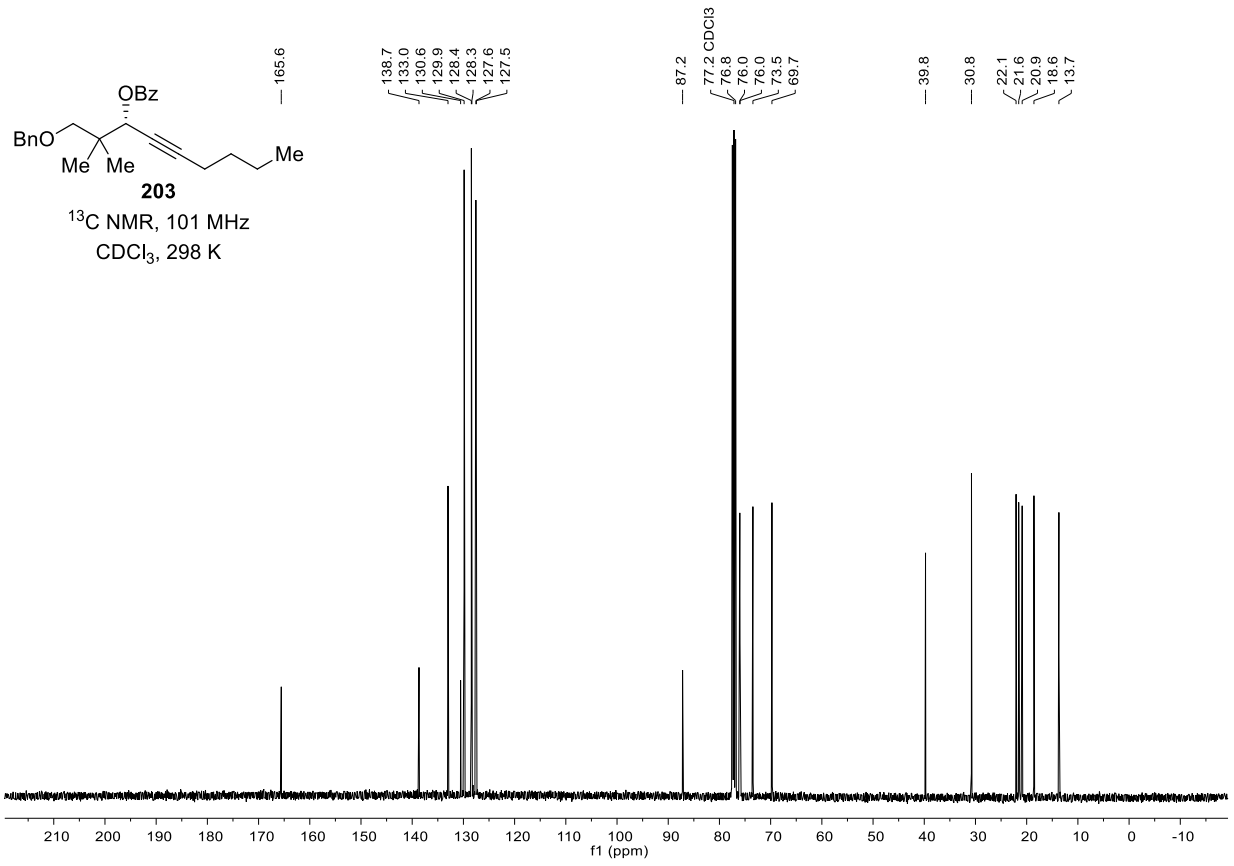
OBz
BnO
Me Me
Me
203
13C NMR, 101 MHz
CDCl3, 298 K
f1 (ppm)

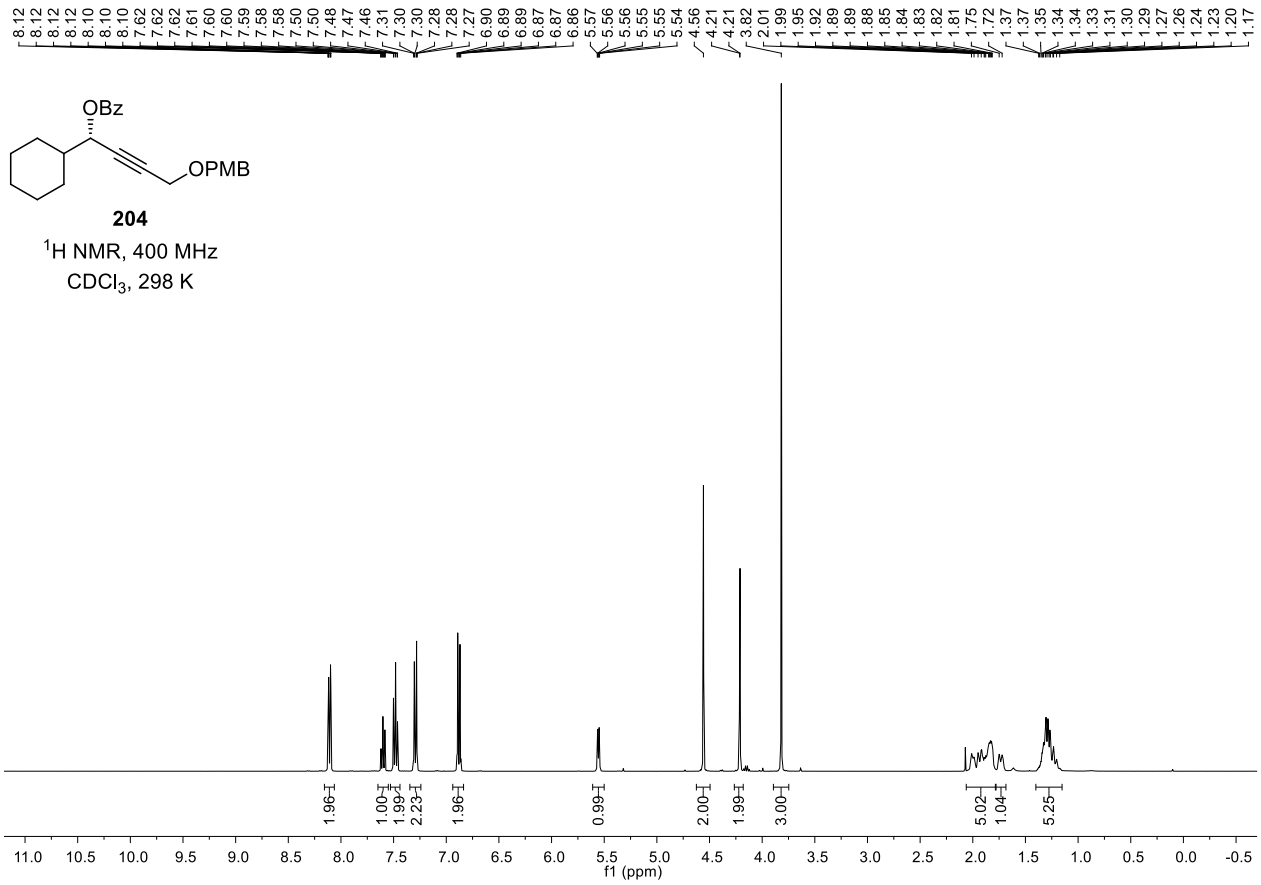
OBz
OPMB
204
1H NMR, 400 MHz
CDCl3, 298 K
f1 (ppm)

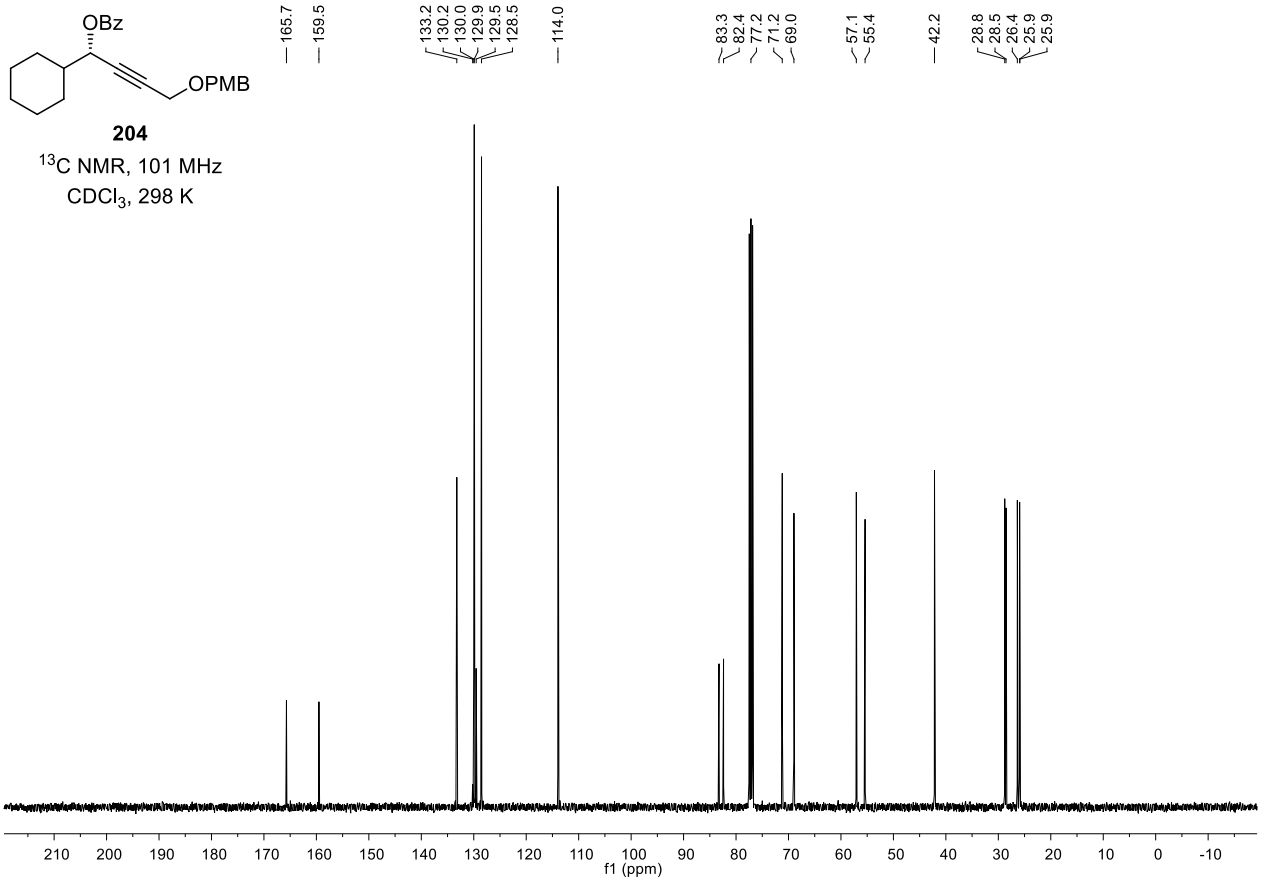
OBz
OPMB
204
13C NMR, 101 MHz
CDCl3, 298 K
f1 (ppm)

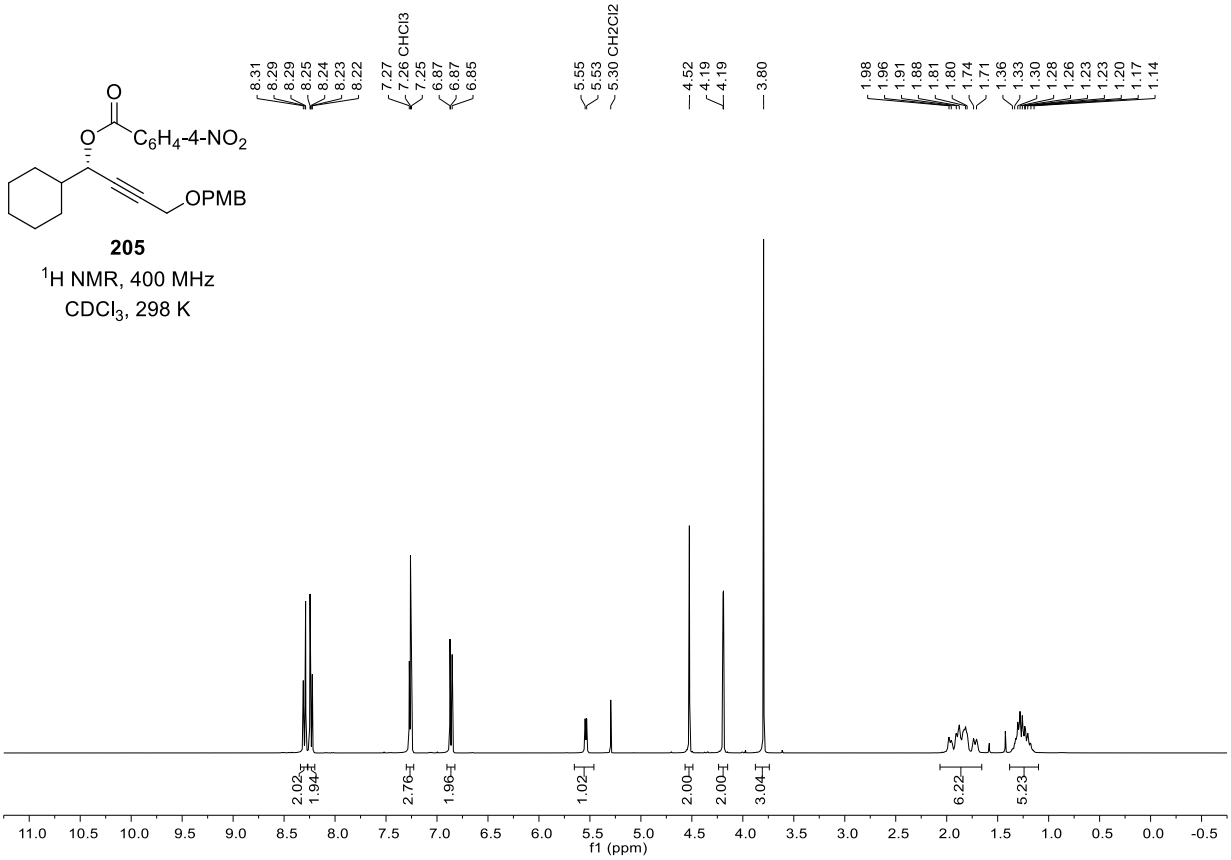

205

^{1}H NMR, 400 MHz

$CDCl_3$, 298 K

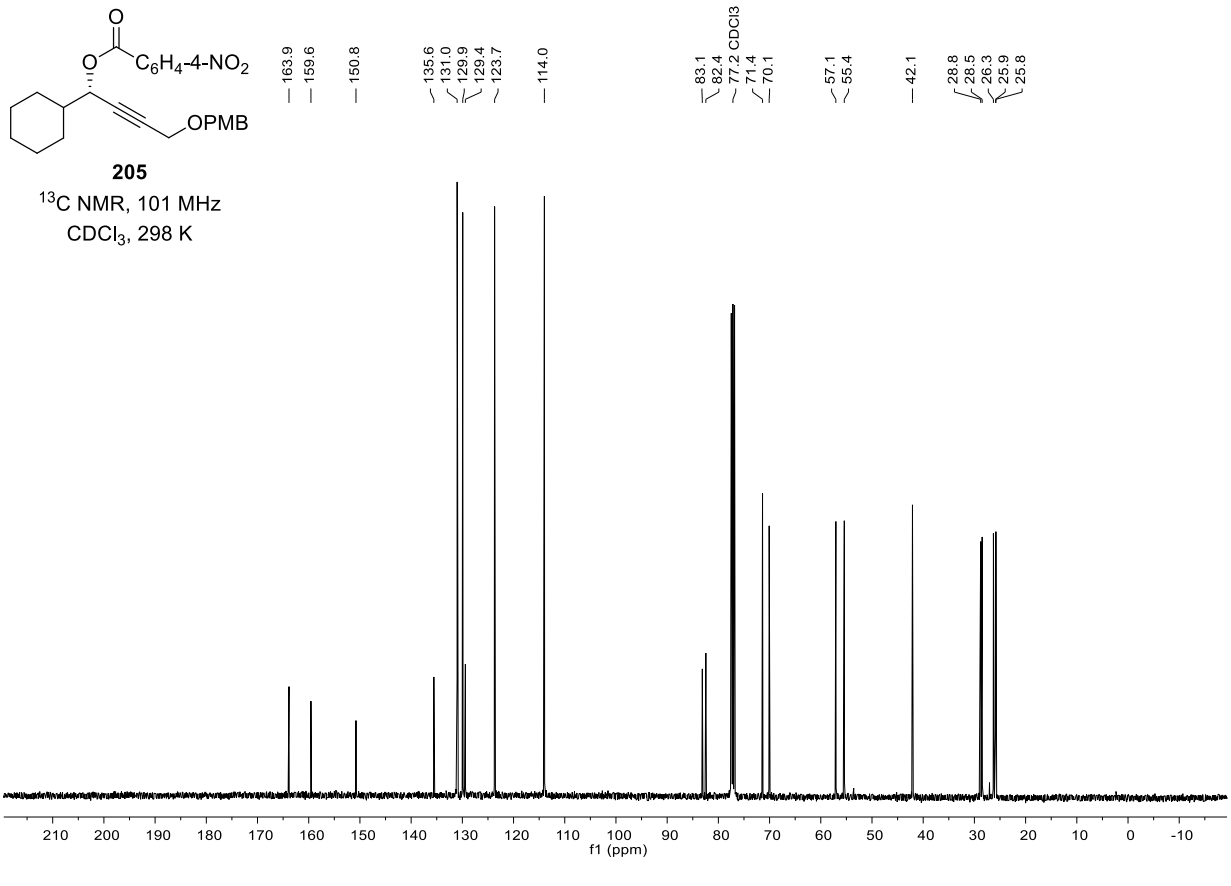

205

^{13}C NMR, 101 MHz

$CDCl_3$, 298 K

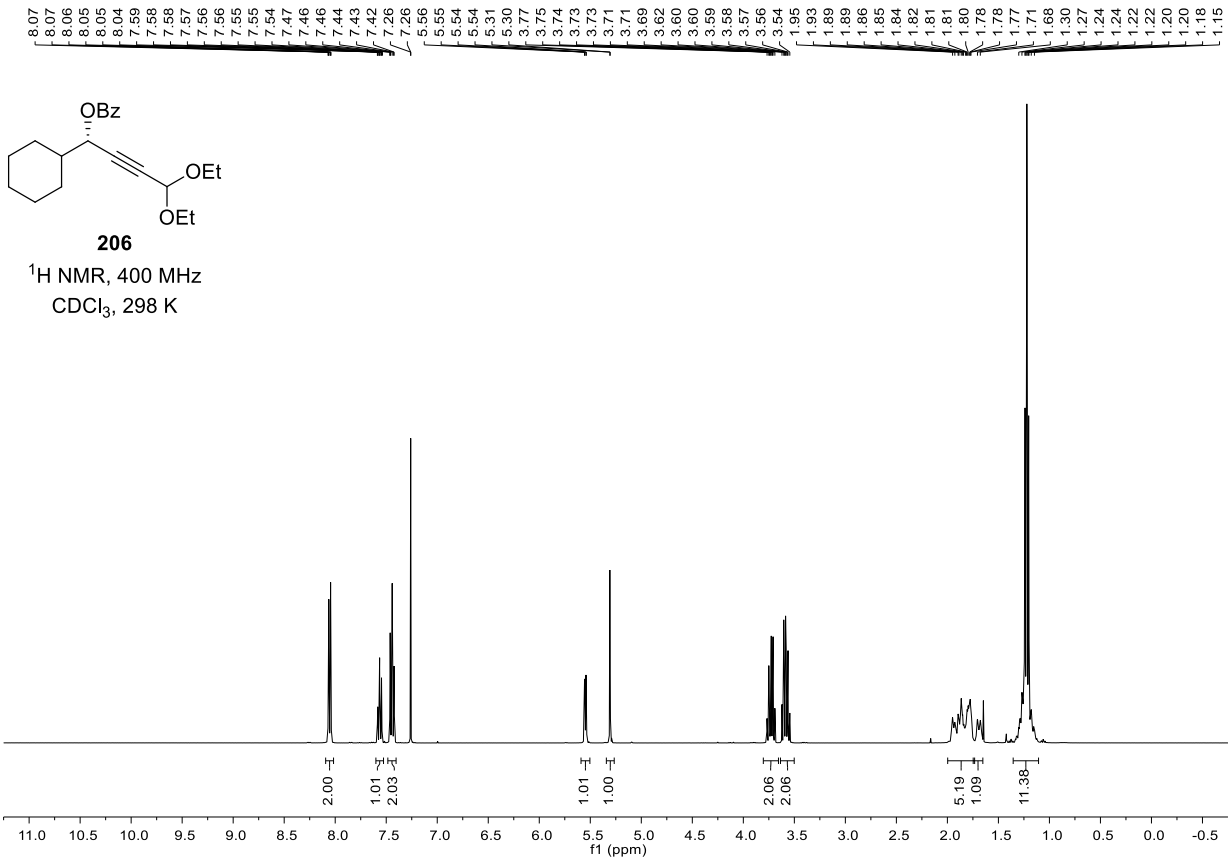
OBz
OEt
OEt
206
1H NMR, 400 MHz
CDCl3, 298 K
f1 (ppm)

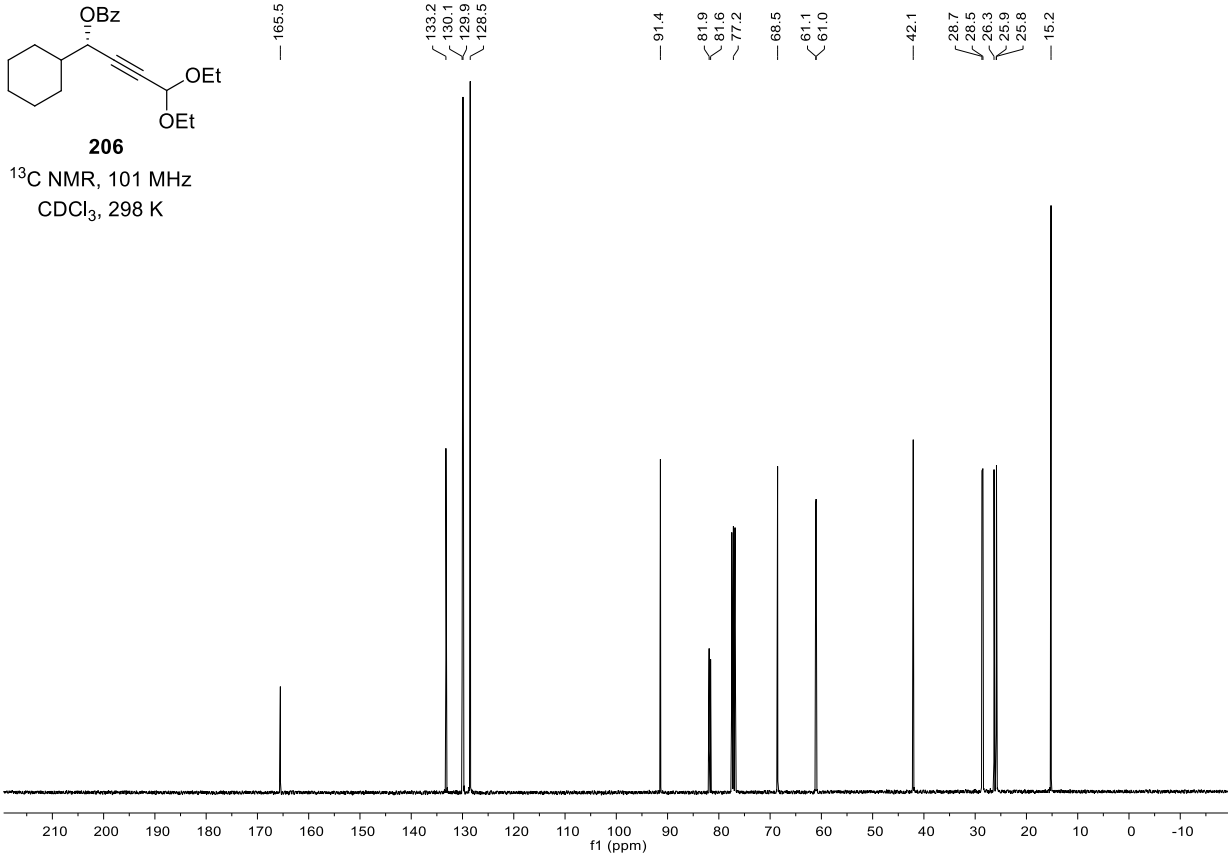
OBz
OEt
OEt
206
13C NMR, 101 MHz
CDCl3, 298 K
f1 (ppm)

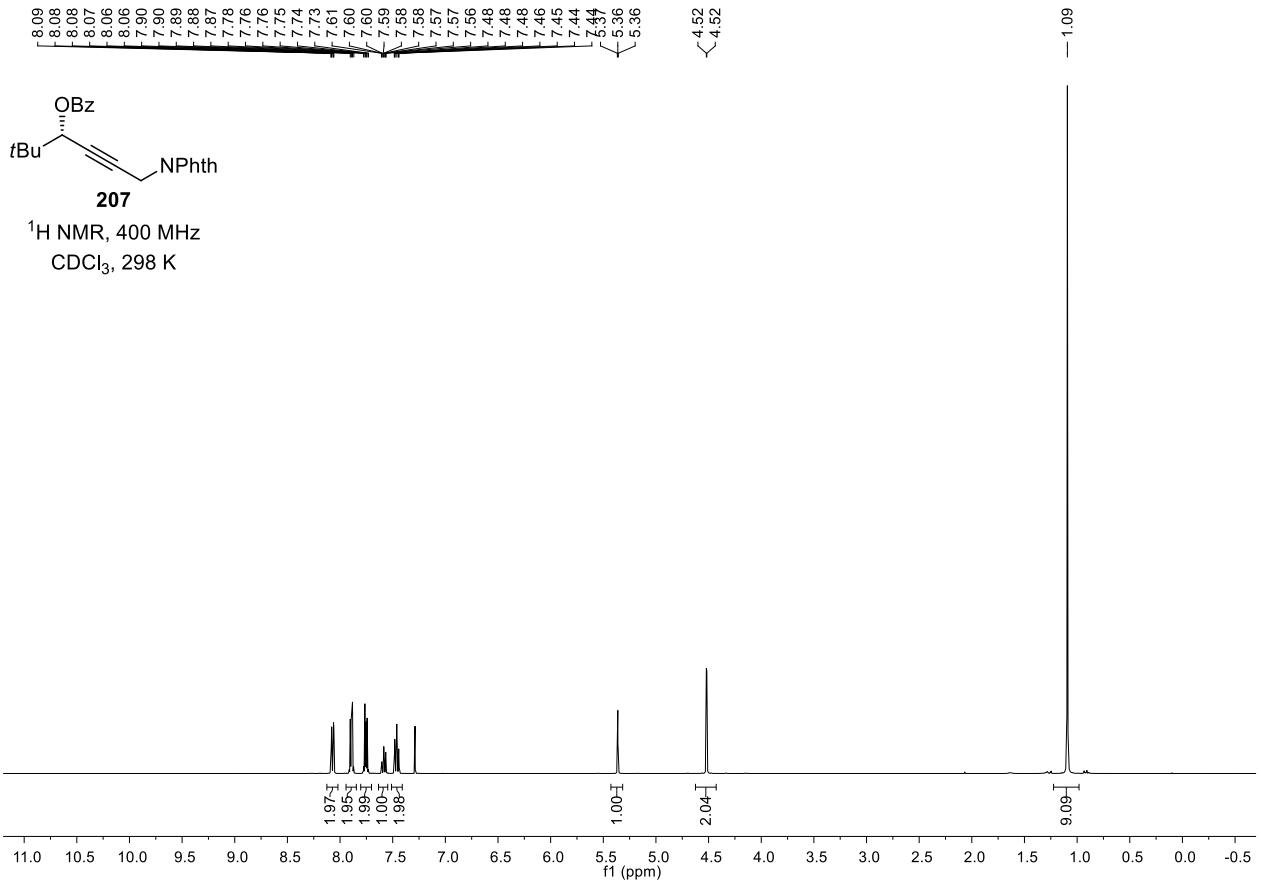
OBz
tBu
NPhth
207
1H NMR, 400 MHz
CDCl3, 298 K
f1 (ppm)

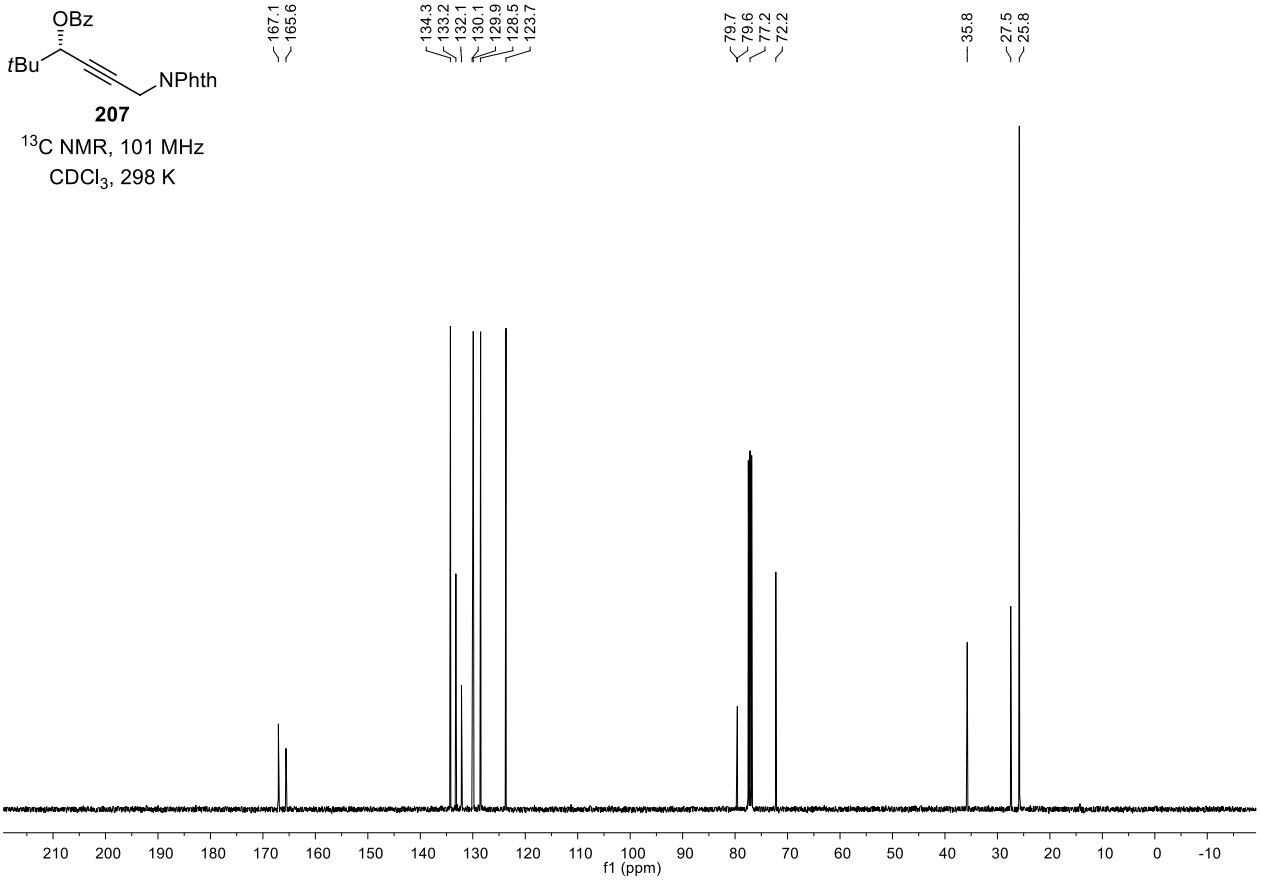
OBz
tBu
NPhth
207
13C NMR, 101 MHz
CDCl3, 298 K
f1 (ppm)

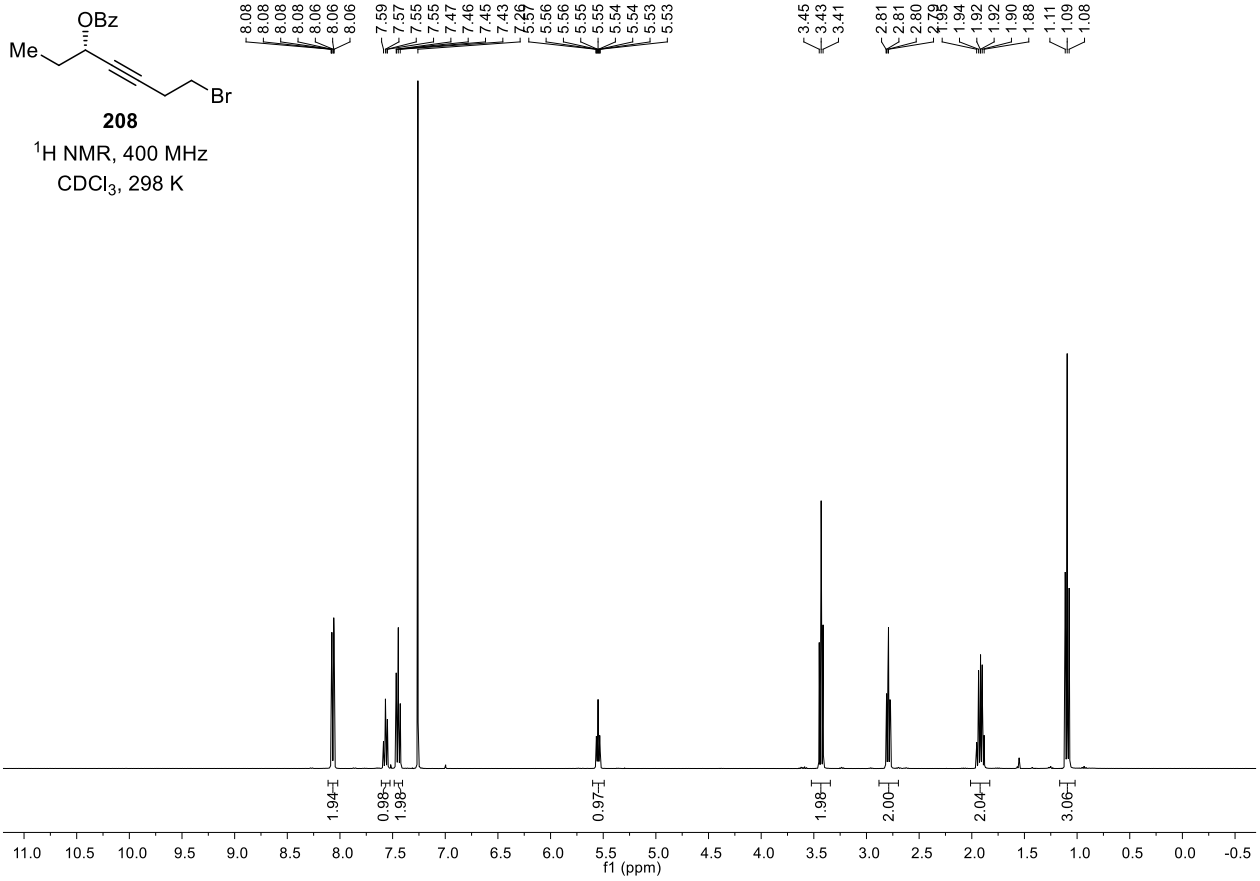
OBz
Me
Br
208
1H NMR, 400 MHz
CDCl3, 298 K
f1 (ppm)

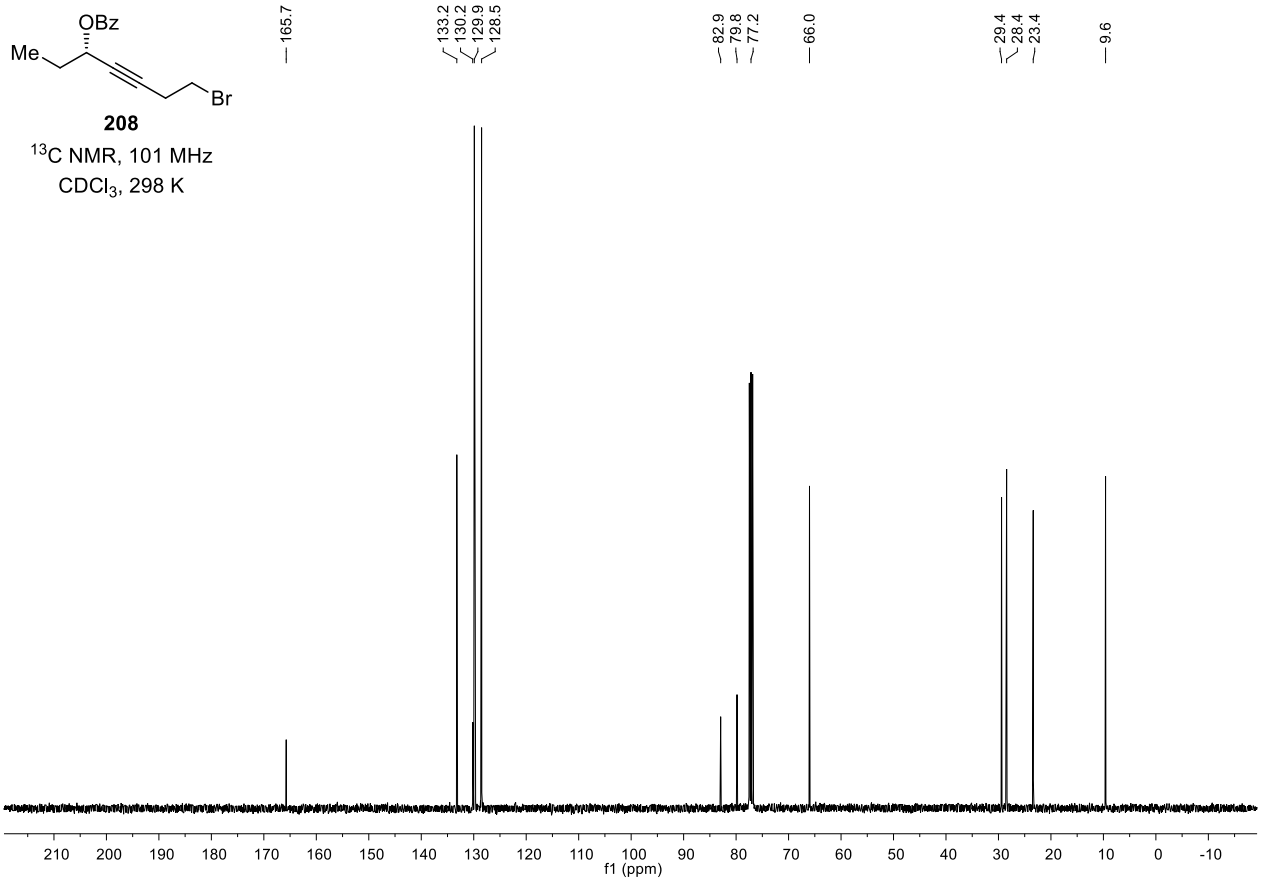
OBz
Me
Br
208
13C NMR, 101 MHz
CDCl3, 298 K
f1 (ppm)

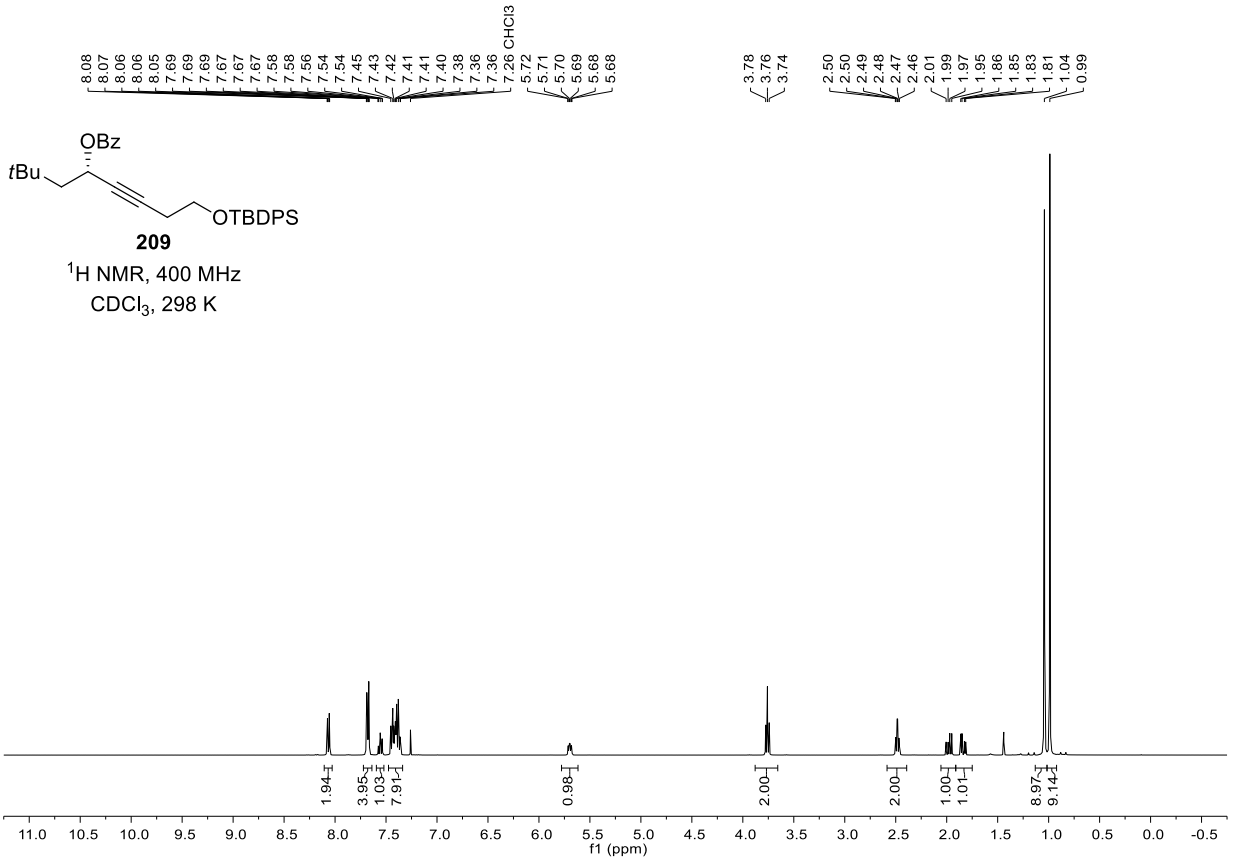
8.08 8.07 8.06 8.06 8.05 7.69 7.69 7.69 7.67 7.67 7.67 7.58 7.58 7.56 7.54 7.54 7.45 7.43 7.42 7.41 7.41 7.40 7.38 7.36 7.36 7.26 CHCl3 5.72 5.71 5.70 5.69 5.68 5.68
3.78 3.76 3.74
2.50 2.50 2.49 2.48 2.47 2.46 2.01 1.99 1.97 1.95 1.86 1.85 1.83 1.81 1.04 0.99
OBz
tBu
OTBDPS
209
1H NMR, 400 MHz
CDCl3, 298 K
1.94 3.95 1.03 7.91 0.98 2.00 2.00 1.00 1.01 8.97 9.14
11.0 10.5 10.0 9.5 9.0 8.5 8.0 7.5 7.0 6.5 6.0 5.5 5.0 4.5 4.0 3.5 3.0 2.5 2.0 1.5 1.0 0.5 0.0 -0.5
f1 (ppm)

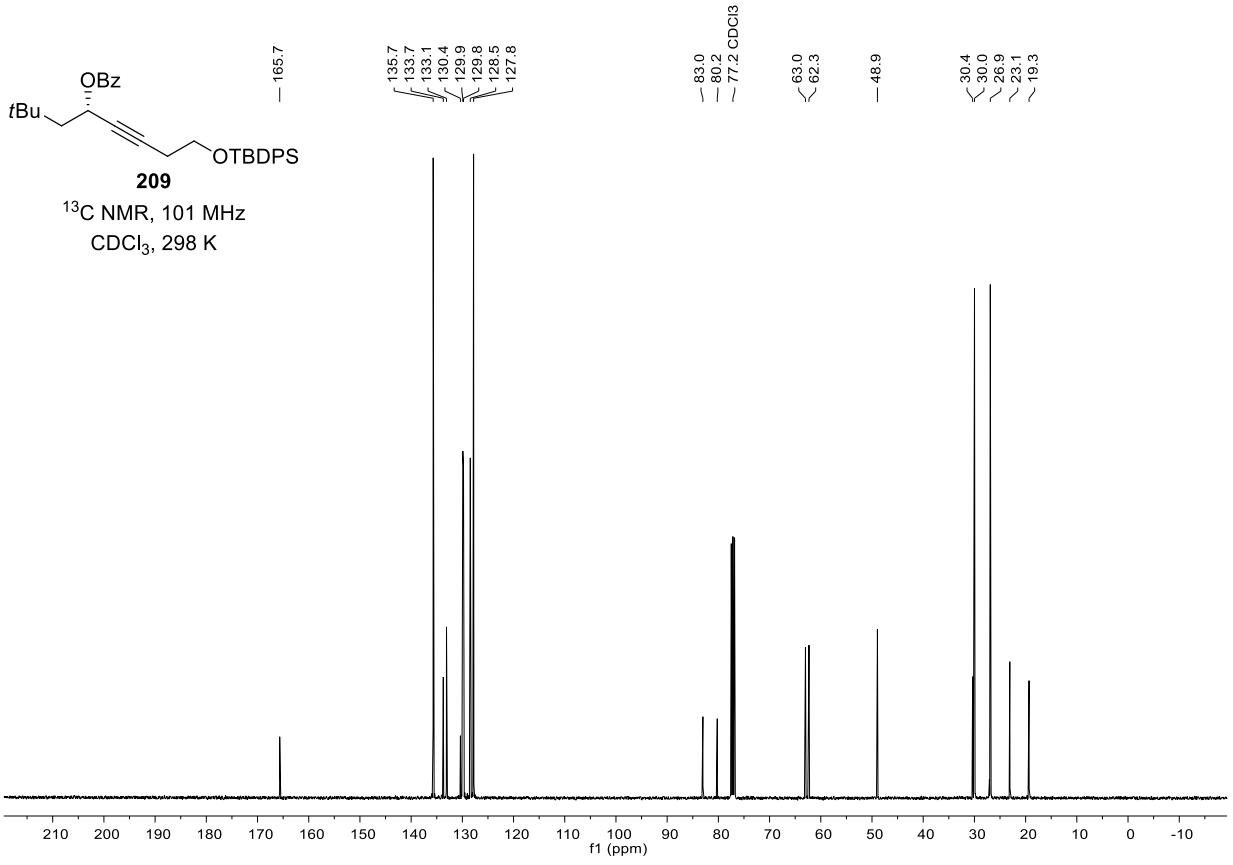
165.7
135.7 133.7 133.1 130.4 129.9 129.8 128.5 127.8
83.0 80.2 77.2 CDCl3
63.0 62.3
48.9
30.4 30.0 26.9 23.1 19.3
OBz
tBu
OTBDPS
209
13C NMR, 101 MHz
CDCl3, 298 K
210 200 190 180 170 160 150 140 130 120 110 100 90 80 70 60 50 40 30 20 10 0 -10
f1 (ppm)

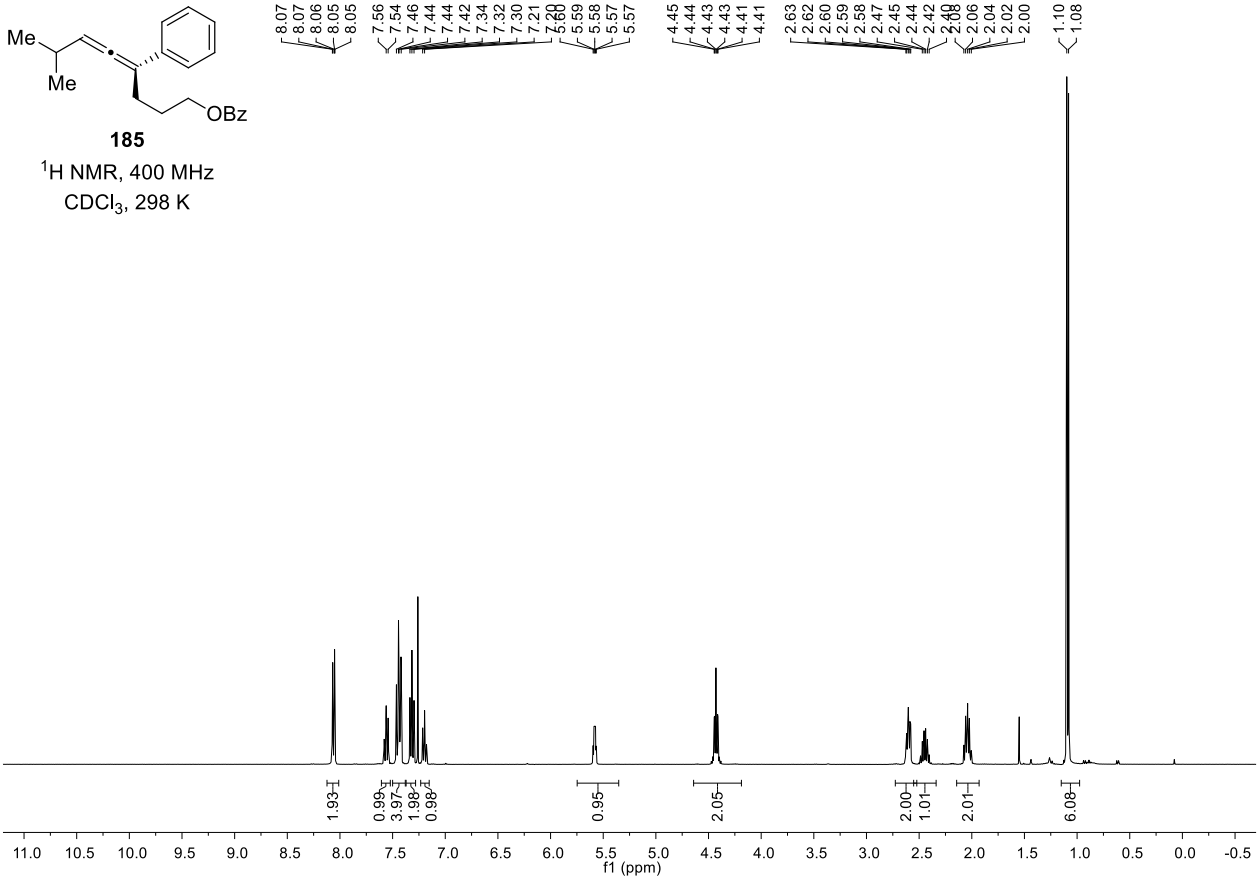
Me
Me
OBz
185
1H NMR, 400 MHz
CDCl3, 298 K
f1 (ppm)

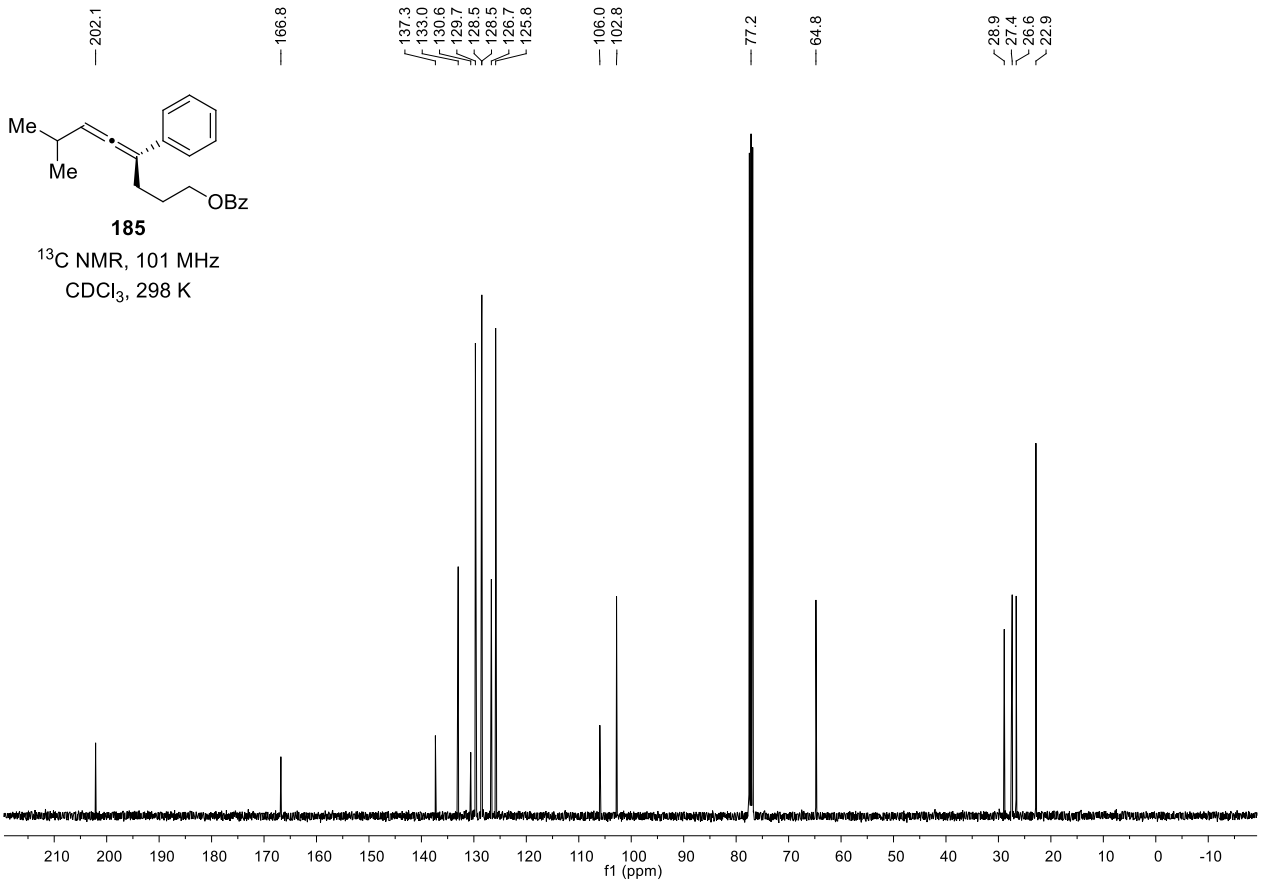
Me
Me
OBz
185
13C NMR, 101 MHz
CDCl3, 298 K
f1 (ppm)

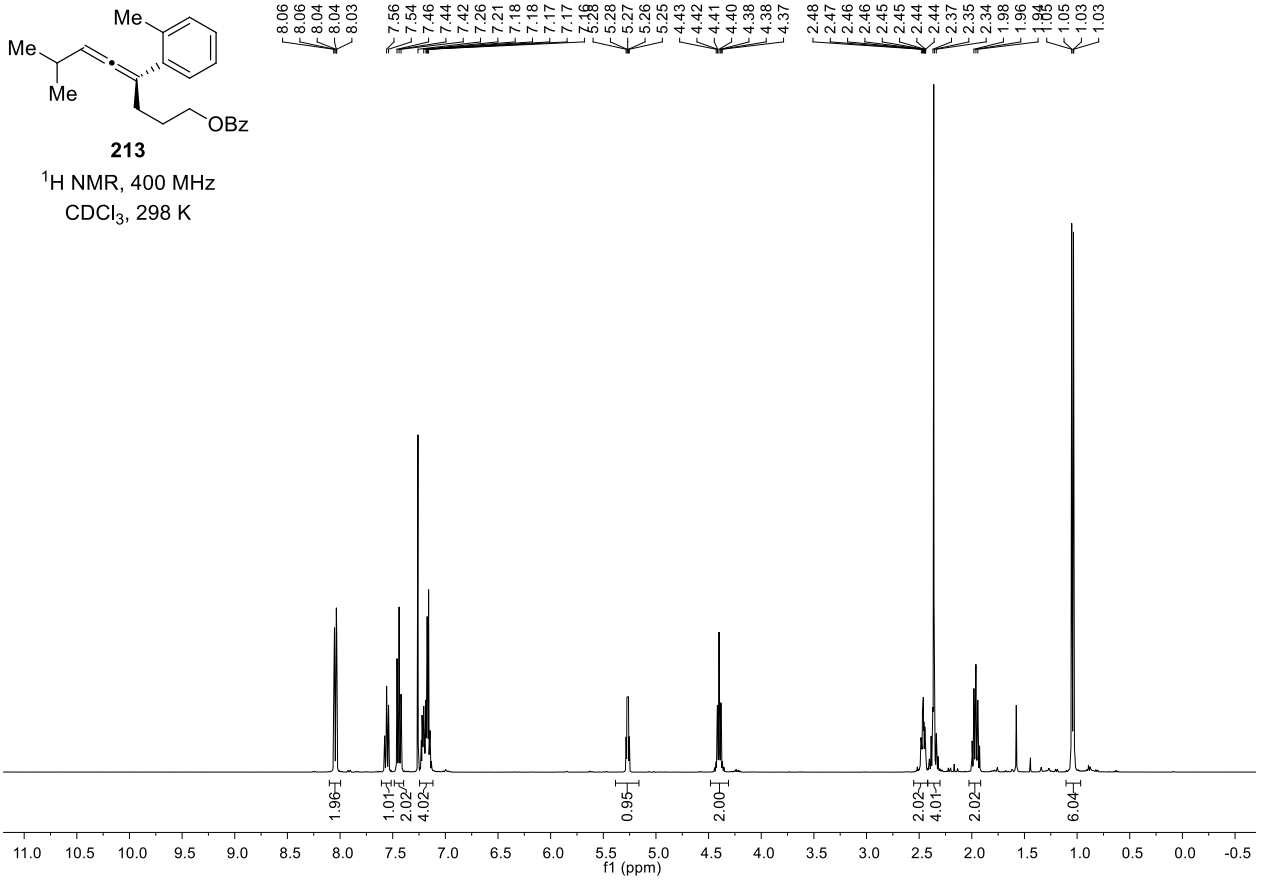
Me
Me
Me
OBz
213
1H NMR, 400 MHz
CDCl3, 298 K
f1 (ppm)

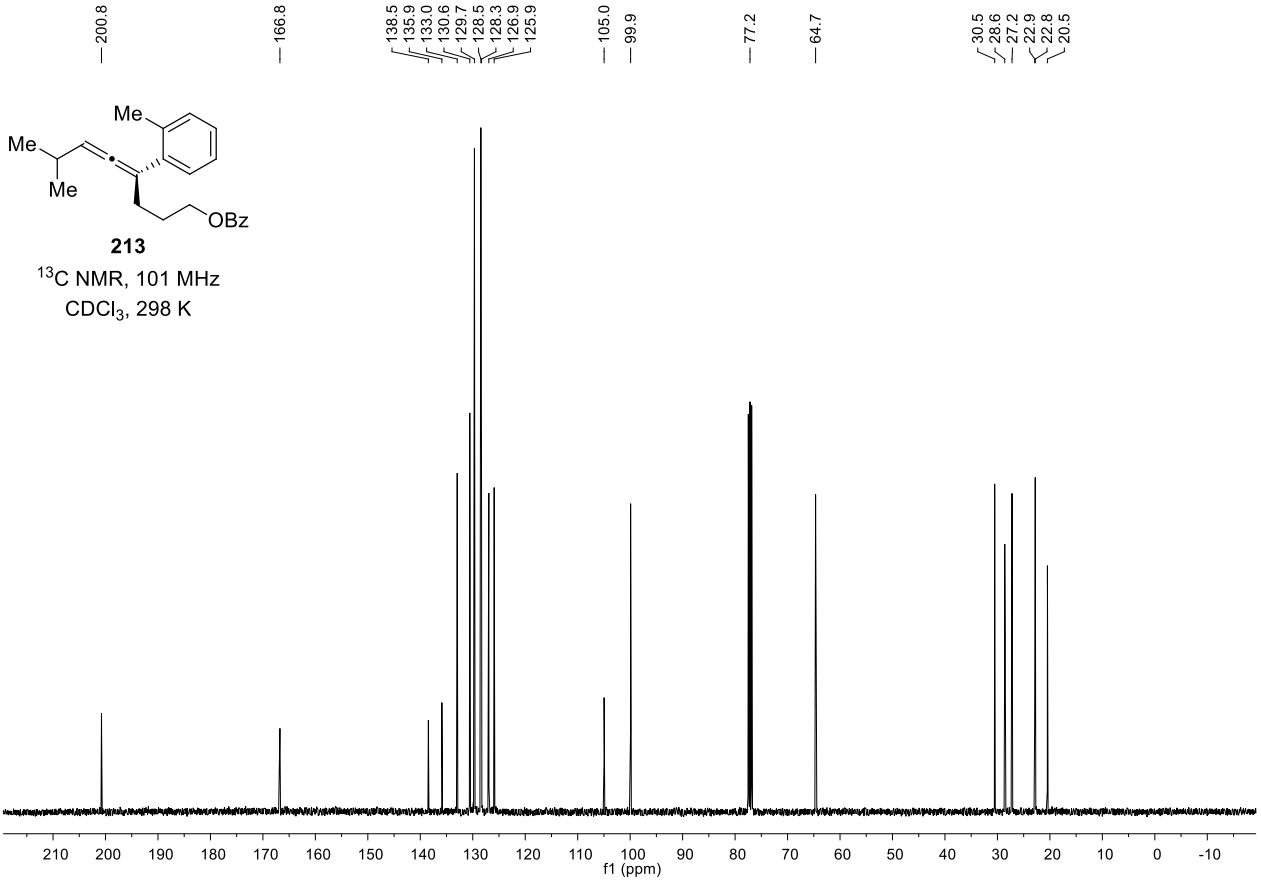
Me
Me
Me
OBz
213
13C NMR, 101 MHz
CDCl3, 298 K
f1 (ppm)

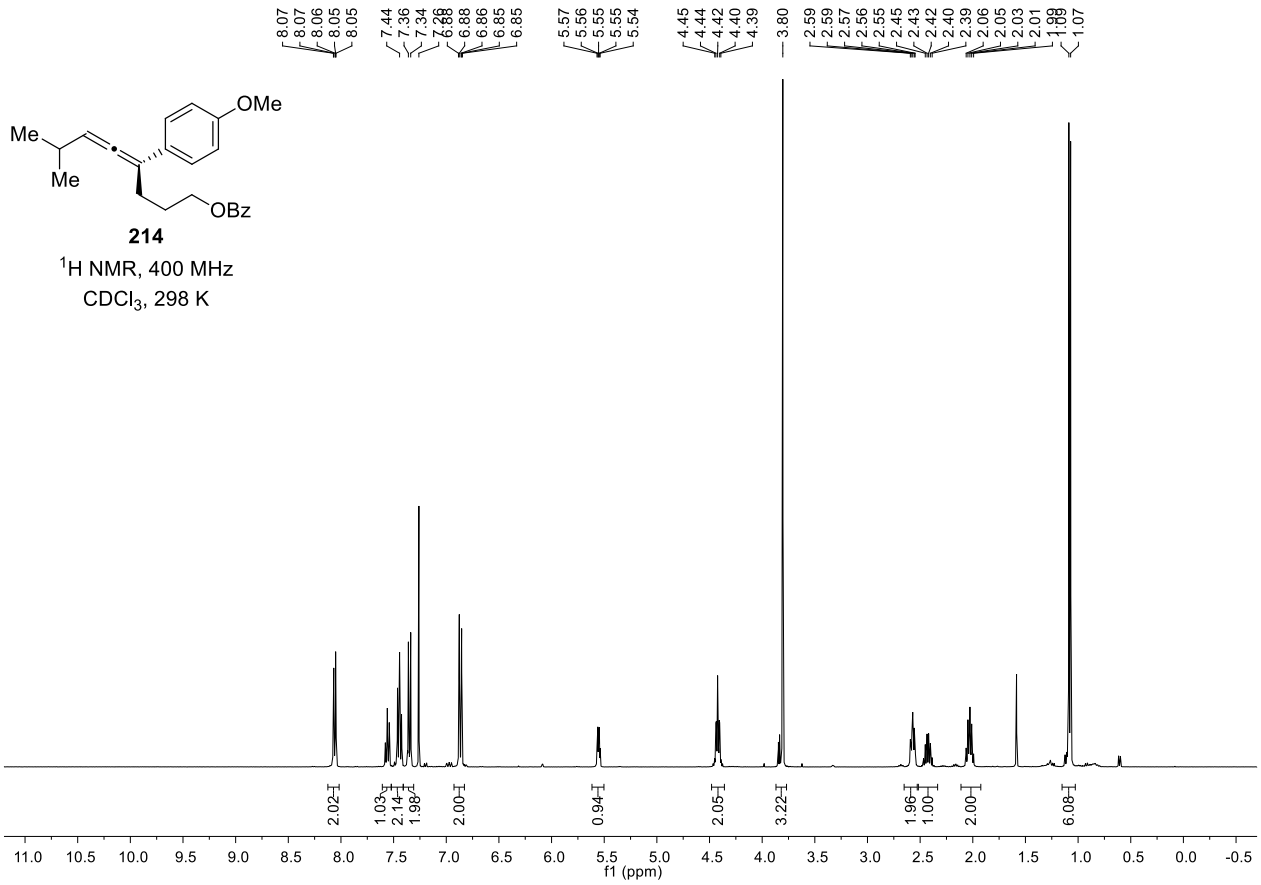
OMe
Me
Me
OBz
214
1H NMR, 400 MHz
CDCl3, 298 K
f1 (ppm)

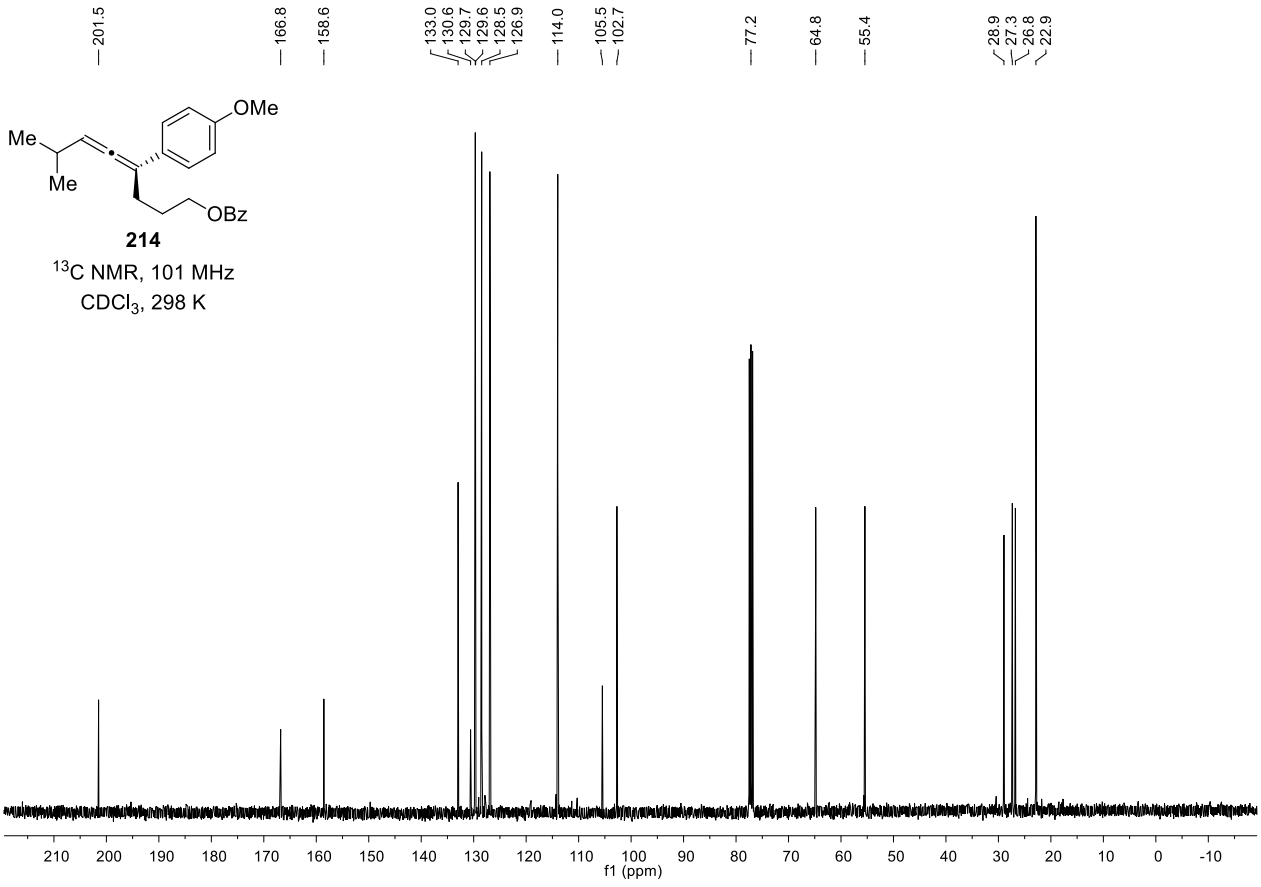
OMe
Me
Me
OBz
214
13C NMR, 101 MHz
CDCl3, 298 K
f1 (ppm)

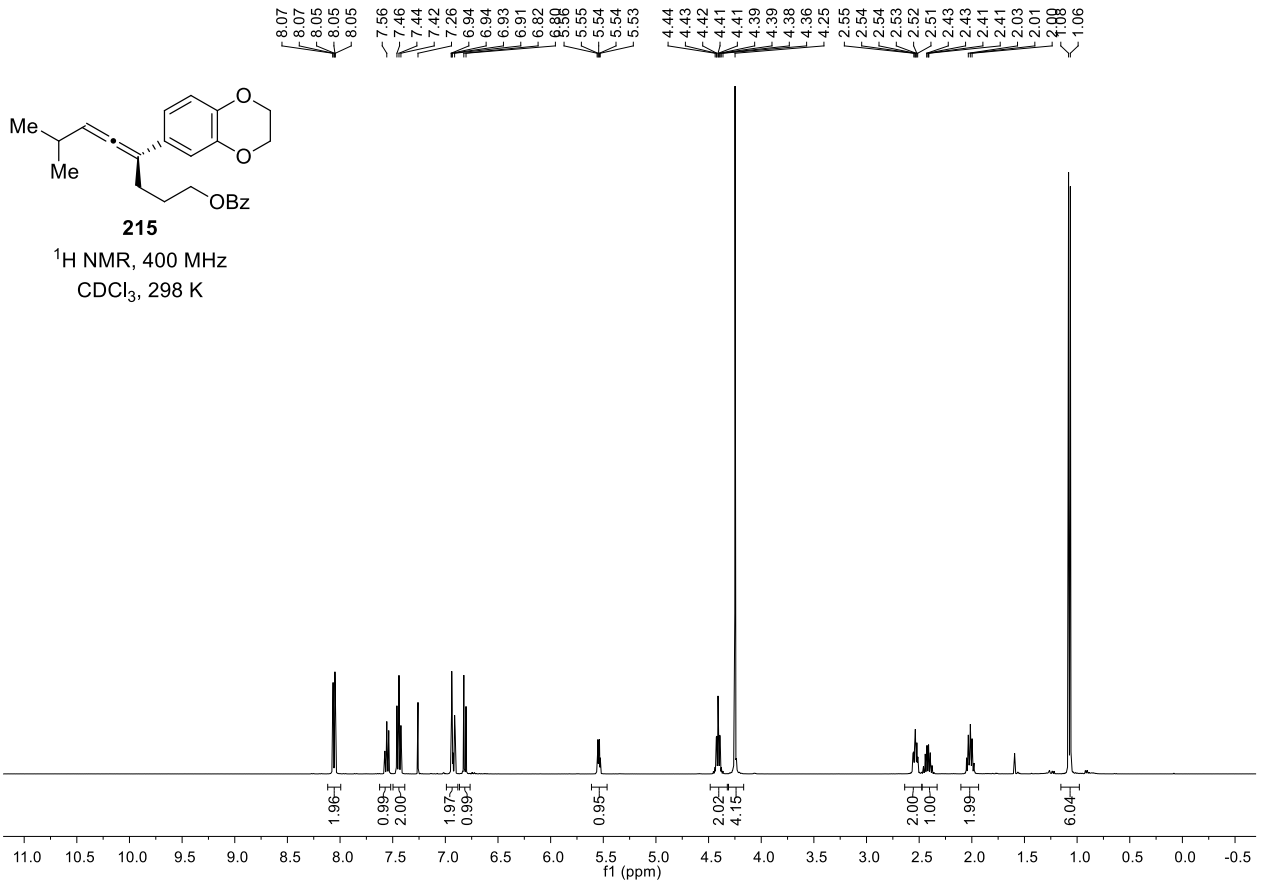
Me
Me
O
O
OBz
215
1H NMR, 400 MHz
CDCl3, 298 K
f1 (ppm)

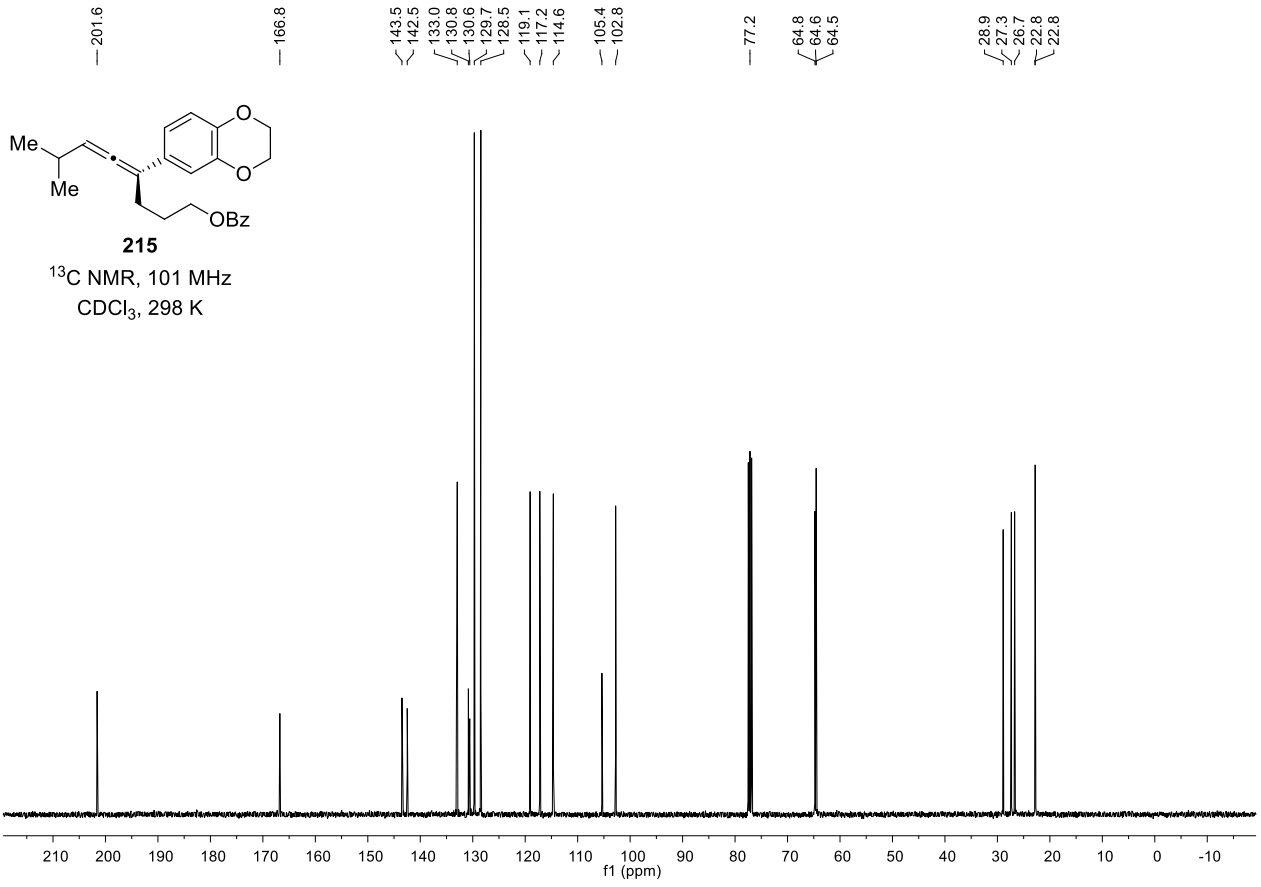
Me
Me
O
O
OBz
215
13C NMR, 101 MHz
CDCl3, 298 K
f1 (ppm)

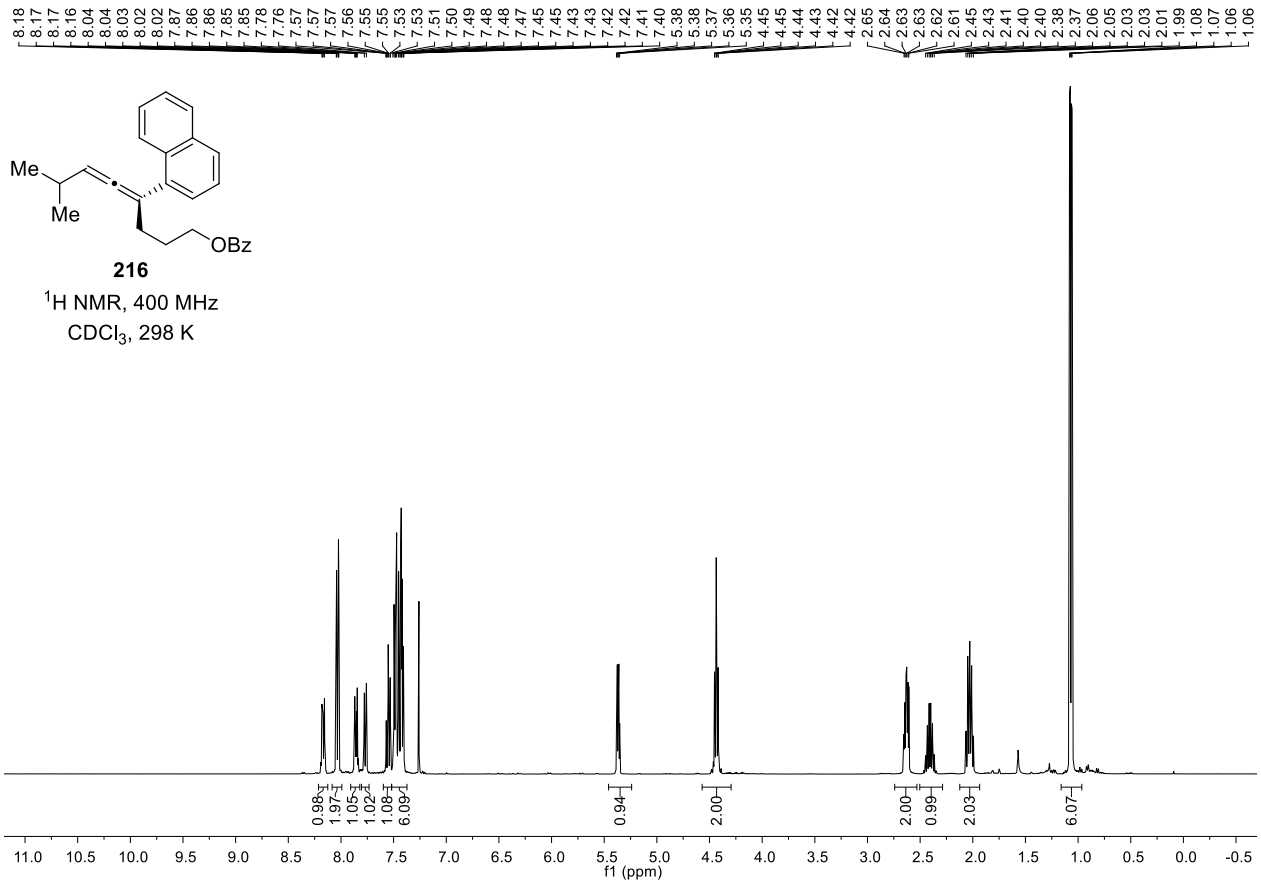
Me
Me
OBz
216
1H NMR, 400 MHz
CDCl3, 298 K
f1 (ppm)

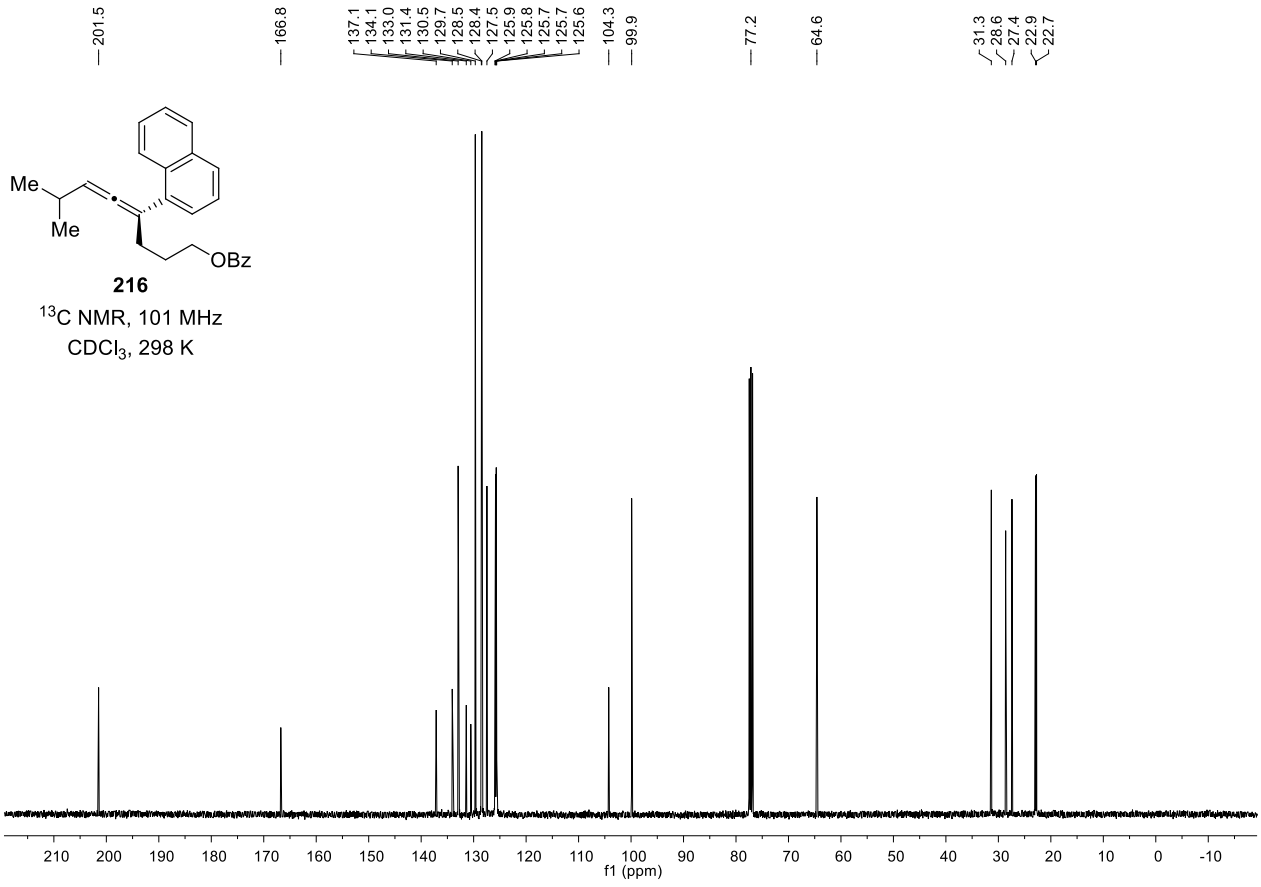
Me
Me
OBz
216
13C NMR, 101 MHz
CDCl3, 298 K
f1 (ppm)

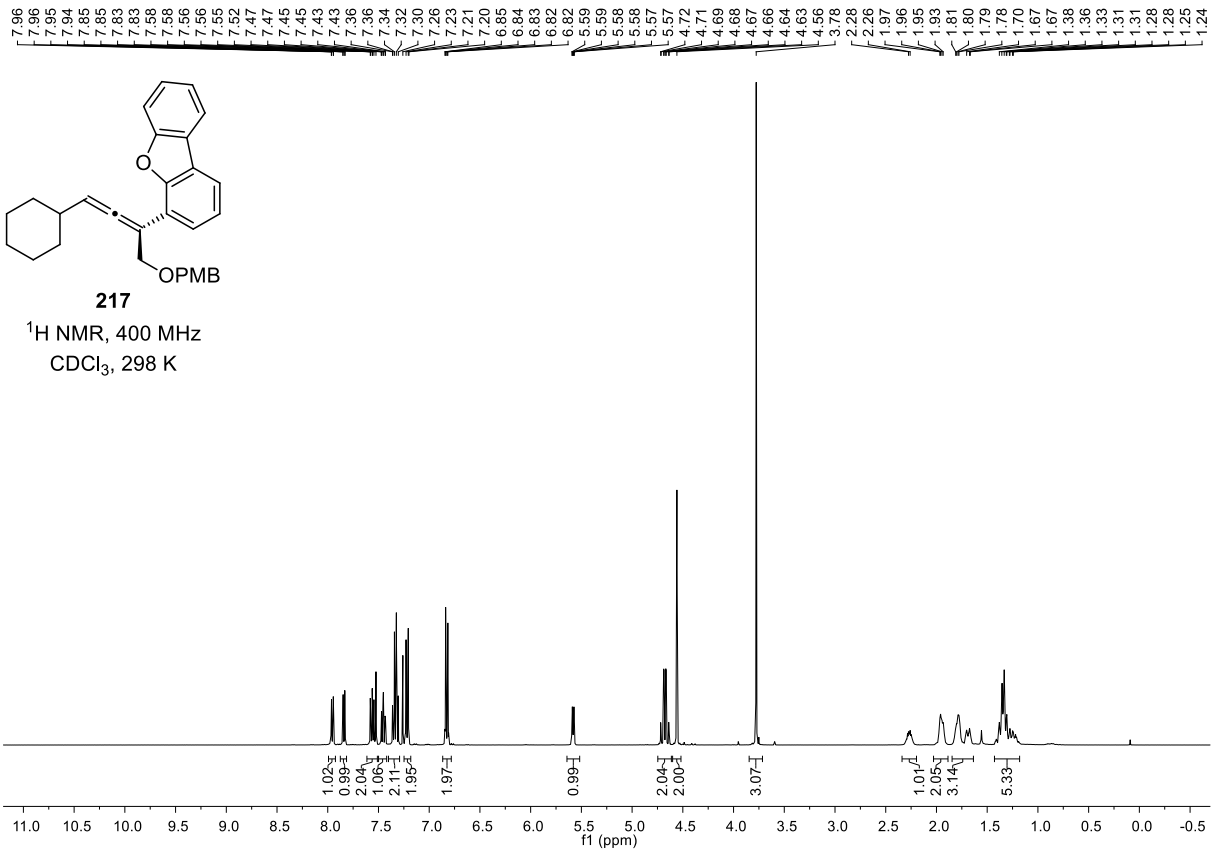
OPMB
217
1H NMR, 400 MHz
CDCl3, 298 K
f1 (ppm)

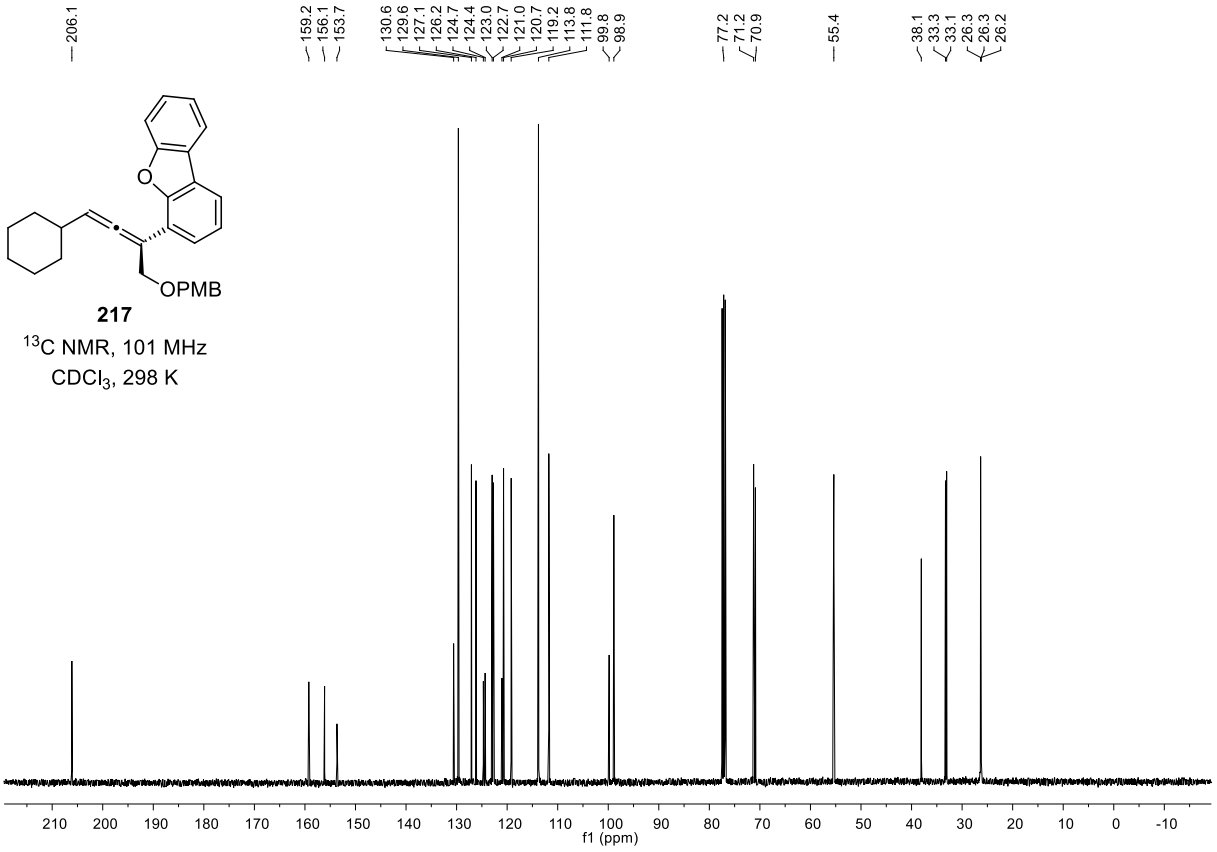
OPMB
217
13C NMR, 101 MHz
CDCl3, 298 K
f1 (ppm)

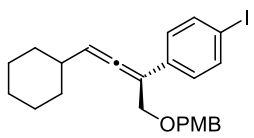

218

^{1}H NMR, 400 MHz

$CDCl_3$, 298 K

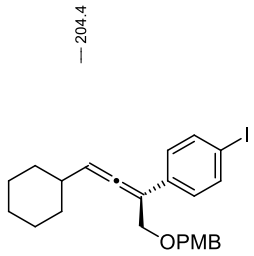

218

^{13}C NMR, 101 MHz

$CDCl_3$, 298 K

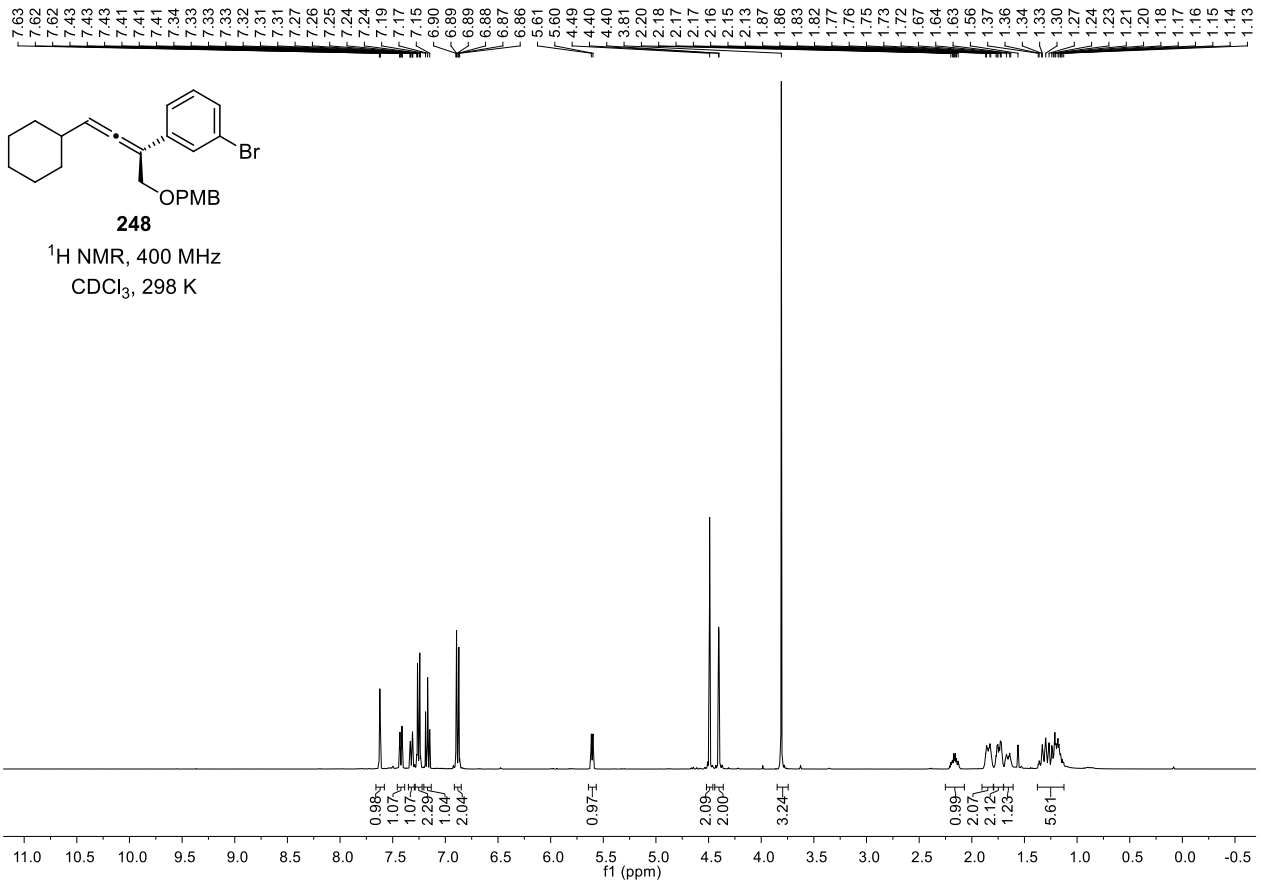
Br
OPMB
248
1H NMR, 400 MHz
CDCl3, 298 K
f1 (ppm)

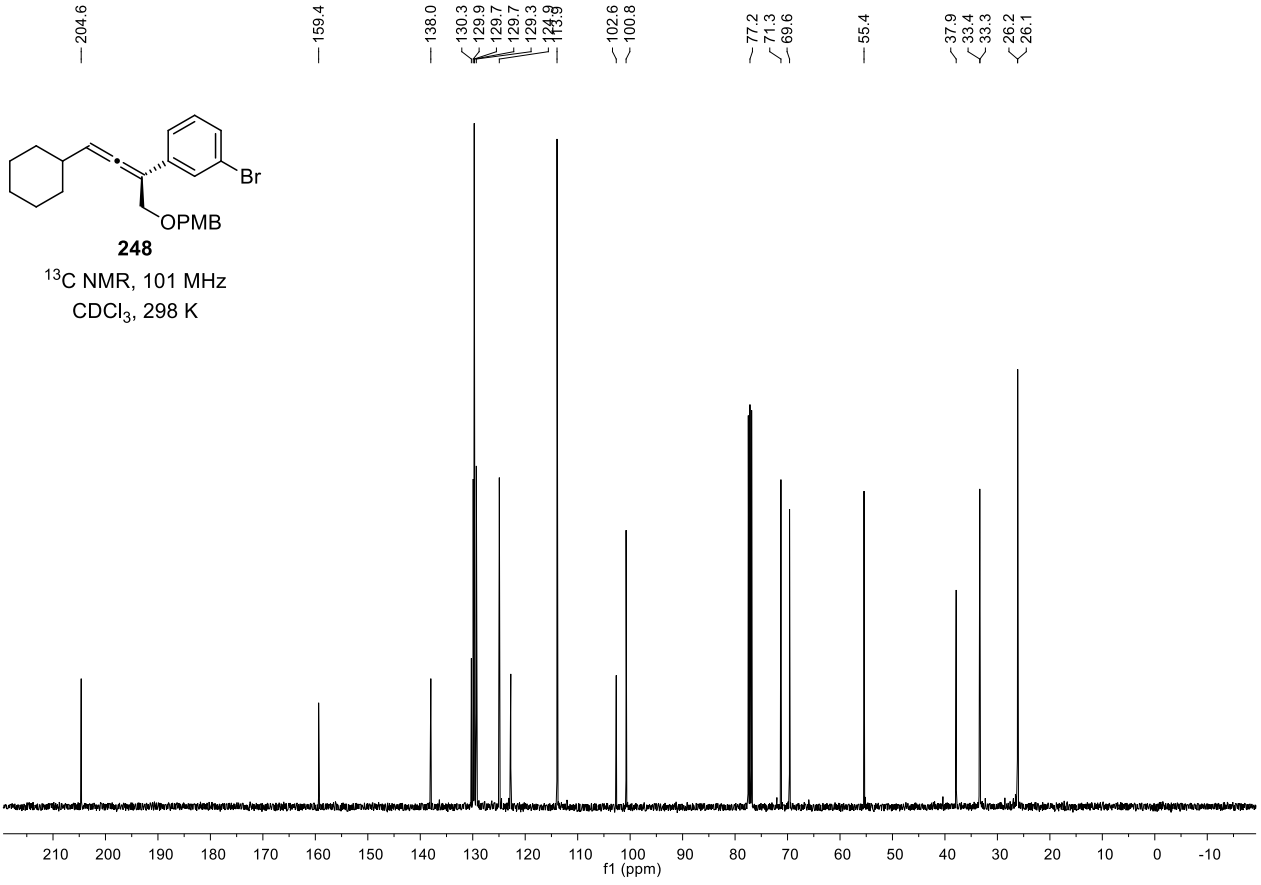
Br
OPMB
248
13C NMR, 101 MHz
CDCl3, 298 K
f1 (ppm)

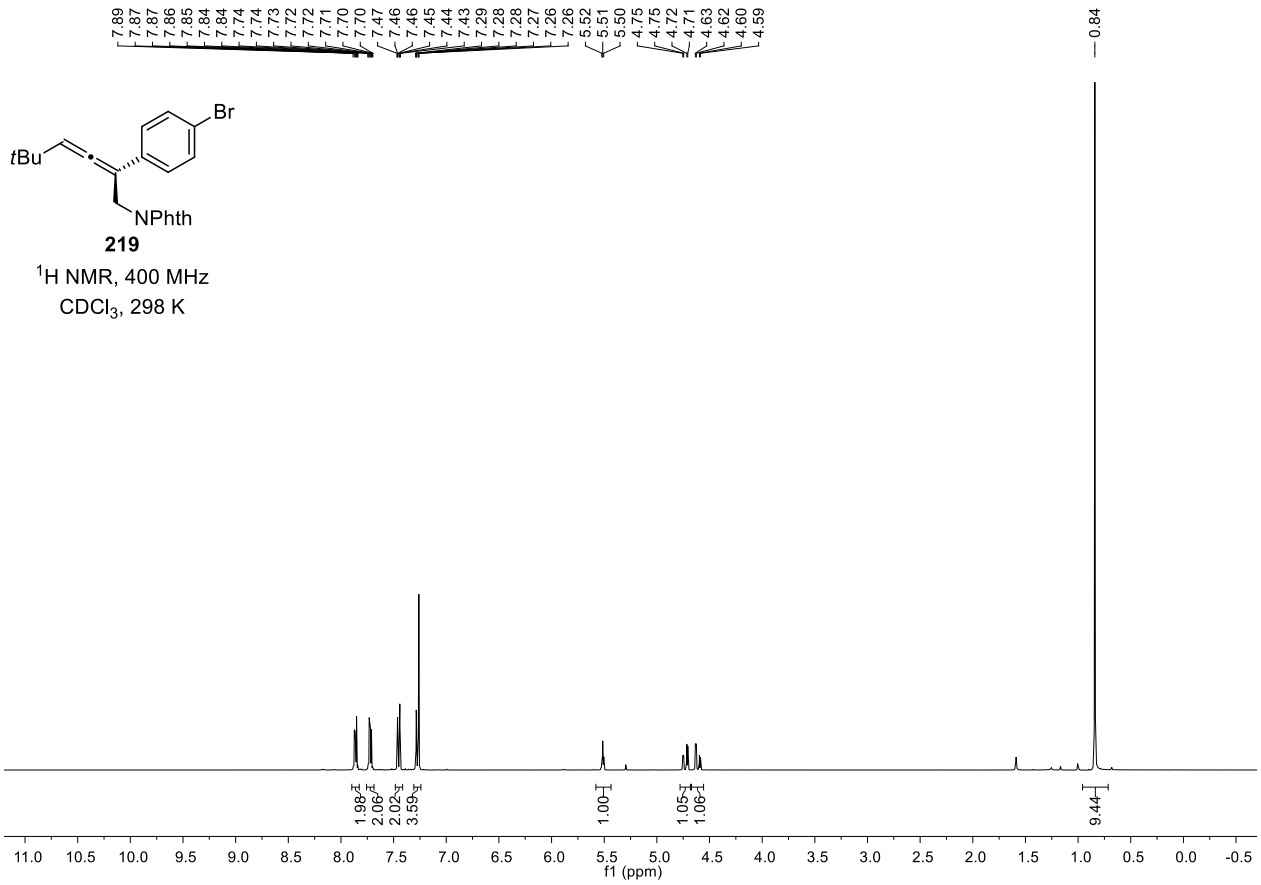

219

^{1}H NMR, 400 MHz

$CDCl_3$, 298 K

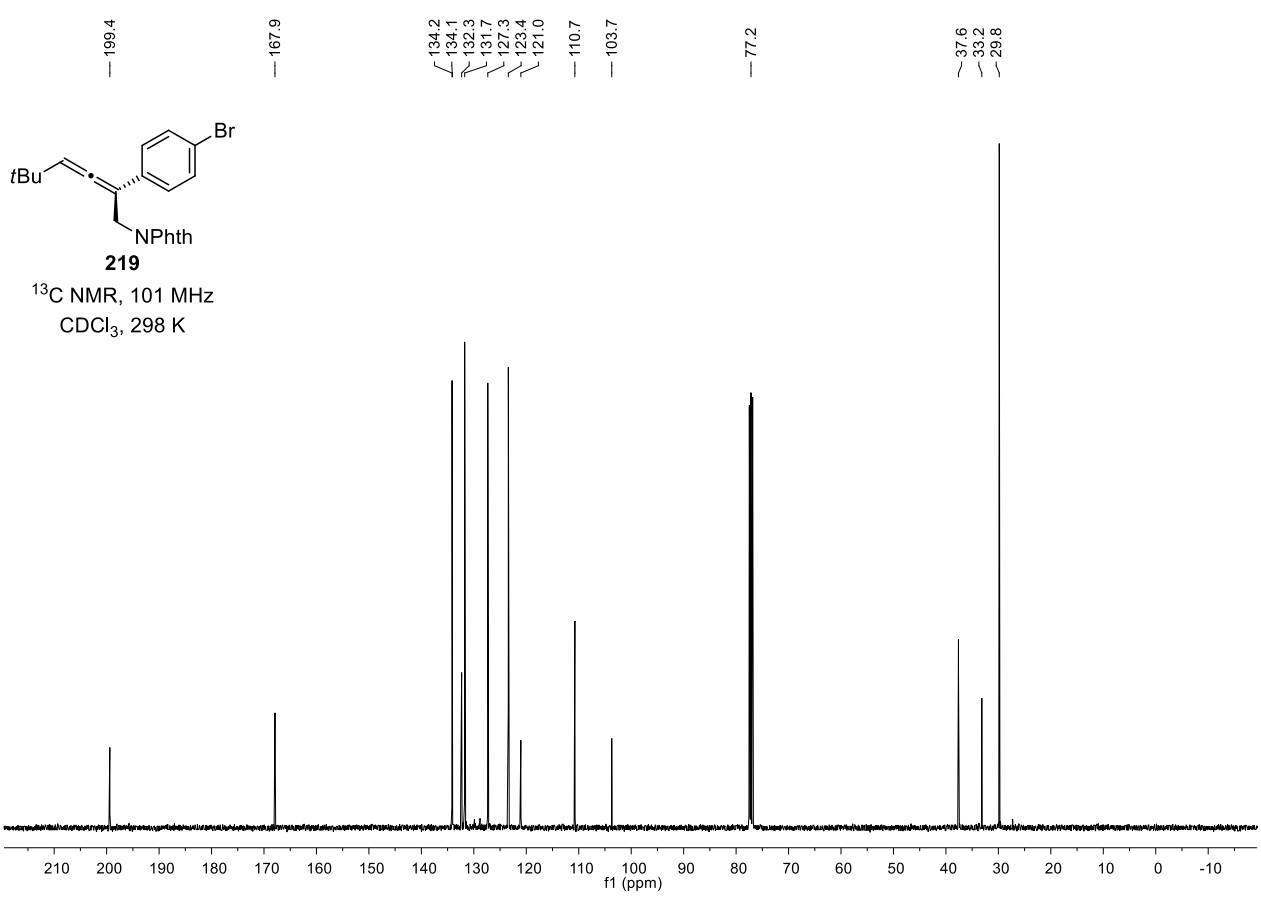

219

^{13}C NMR, 101 MHz

$CDCl_3$, 298 K

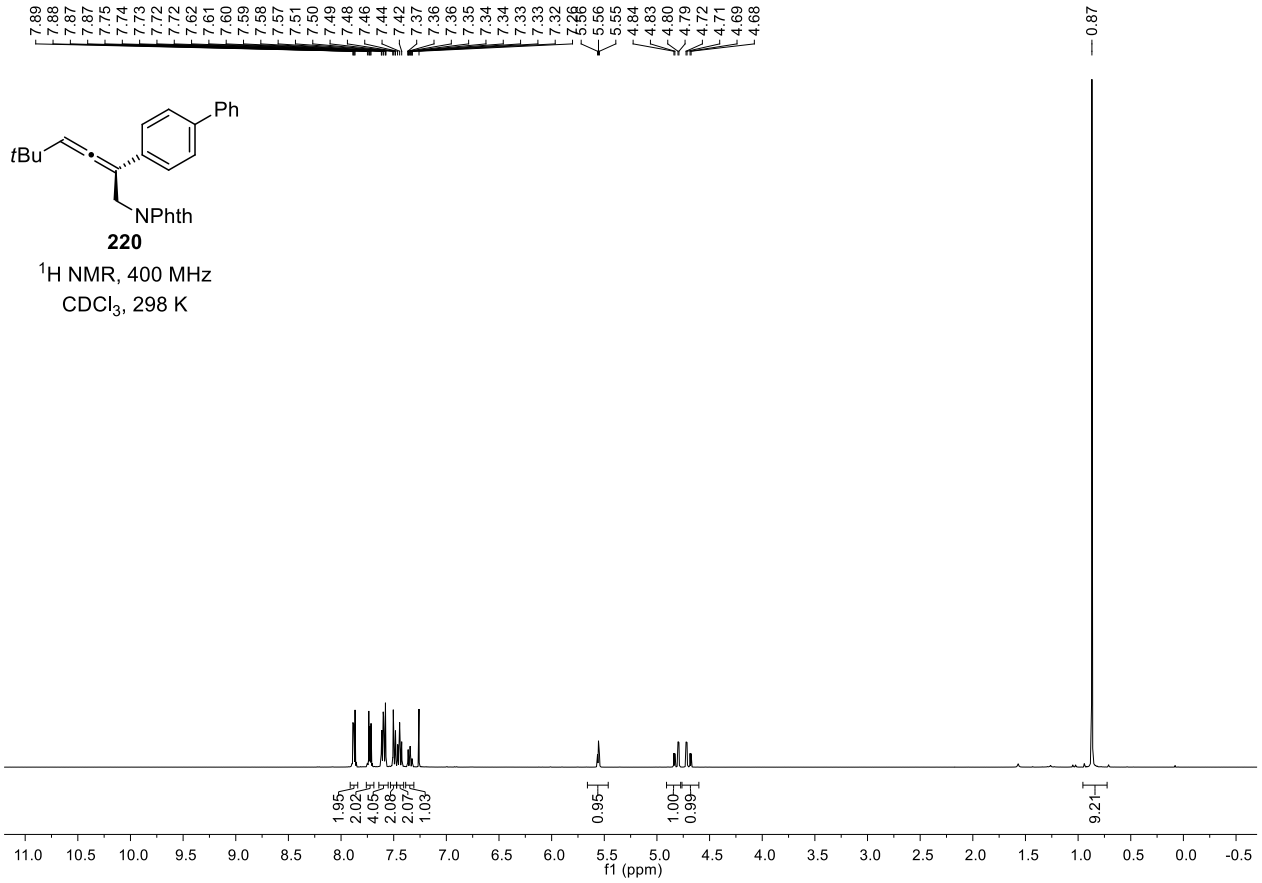
7.89
7.88
7.87
7.87
7.75
7.74
7.73
7.72
7.72
7.62
7.61
7.60
7.59
7.58
7.57
7.51
7.50
7.49
7.48
7.46
7.44
7.42
7.37
7.36
7.36
7.35
7.34
7.34
7.33
7.32
7.26
5.56
5.55
4.84
4.83
4.80
4.79
4.72
4.71
4.69
4.68
0.87
Ph
tBu
NPhth
220
1H NMR, 400 MHz
CDCl3, 298 K
1.95
2.02
4.05
2.08
2.07
1.03
0.95
1.00
0.99
9.21
f1 (ppm)

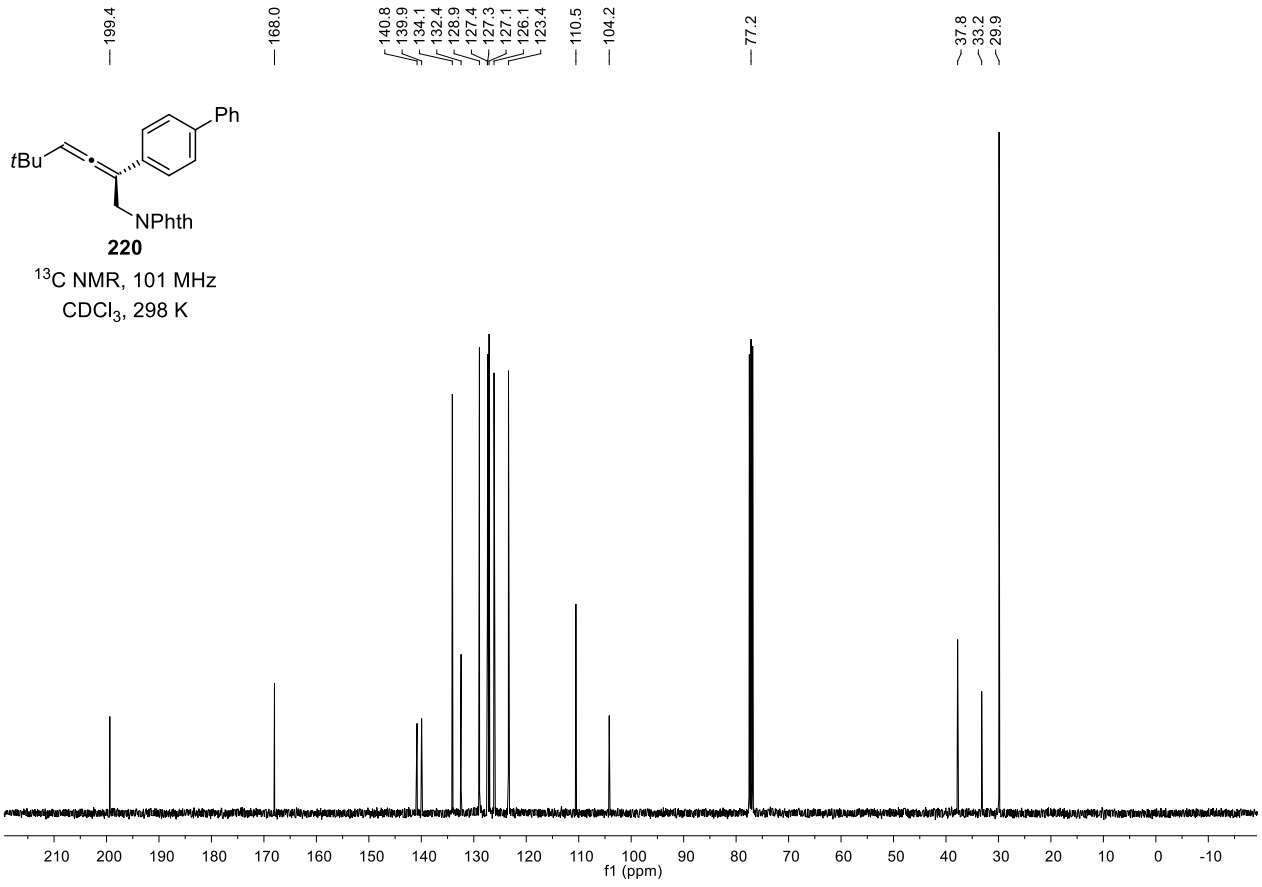
199.4
168.0
140.8
139.9
134.1
132.4
128.9
127.4
127.3
127.1
126.1
123.4
110.5
104.2
77.2
37.8
33.2
29.9
Ph
tBu
NPhth
220
13C NMR, 101 MHz
CDCl3, 298 K
f1 (ppm)

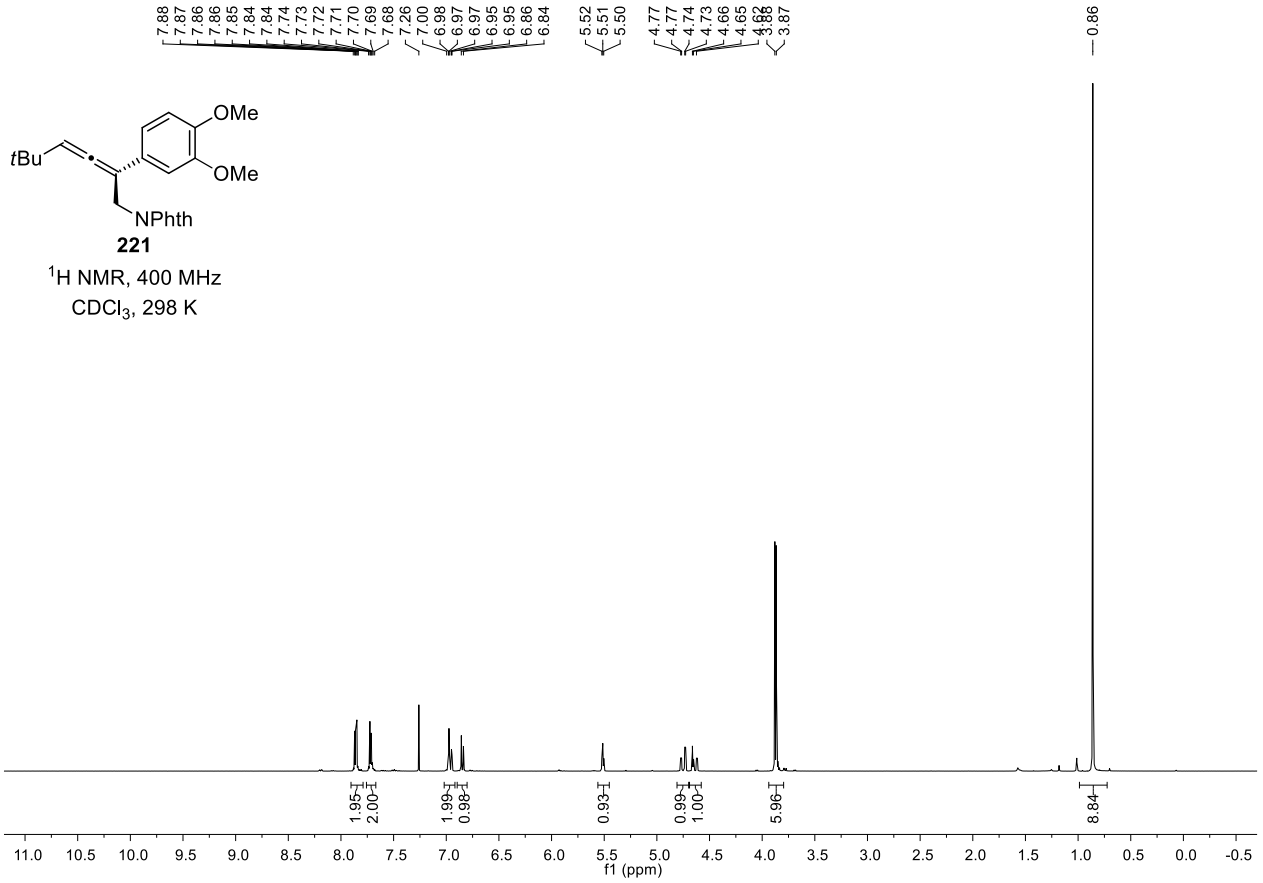
7.88
7.87
7.86
7.86
7.85
7.84
7.84
7.74
7.73
7.72
7.71
7.70
7.69
7.68
7.26
7.00
6.98
6.97
6.97
6.95
6.95
6.86
6.84
5.52
5.51
5.50
4.77
4.77
4.74
4.73
4.66
4.65
4.62
3.88
3.87
0.86
OMe
OMe
tBu
NPhth
221
1H NMR, 400 MHz
CDCl3, 298 K
1.95
2.00
1.99
0.98
0.93
0.99
1.00
5.96
8.84
f1 (ppm)

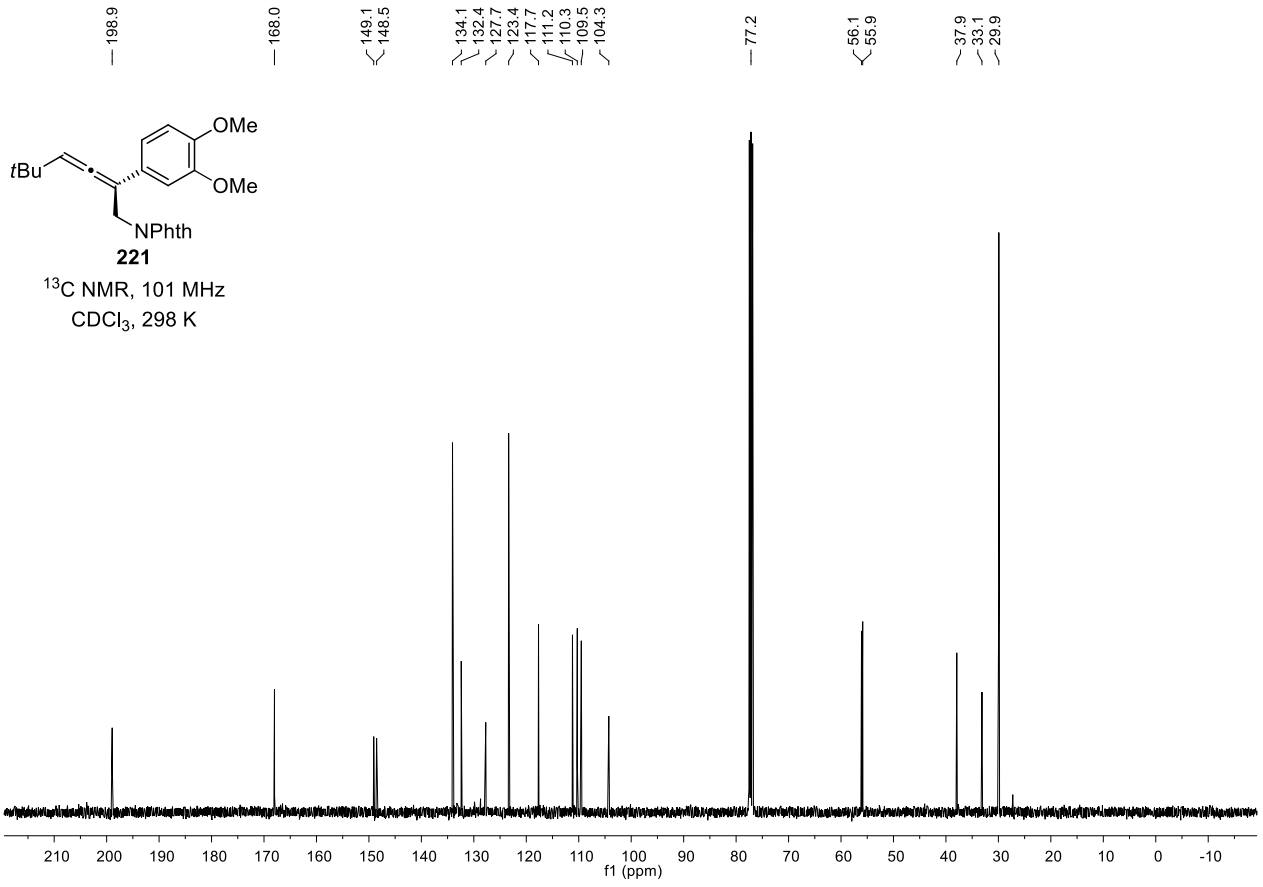
198.9
168.0
149.1
148.5
134.1
132.4
127.7
123.4
117.7
111.2
110.3
109.5
104.3
77.2
56.1
55.9
37.9
33.1
29.9
OMe
OMe
tBu
NPhth
221
13C NMR, 101 MHz
CDCl3, 298 K
f1 (ppm)

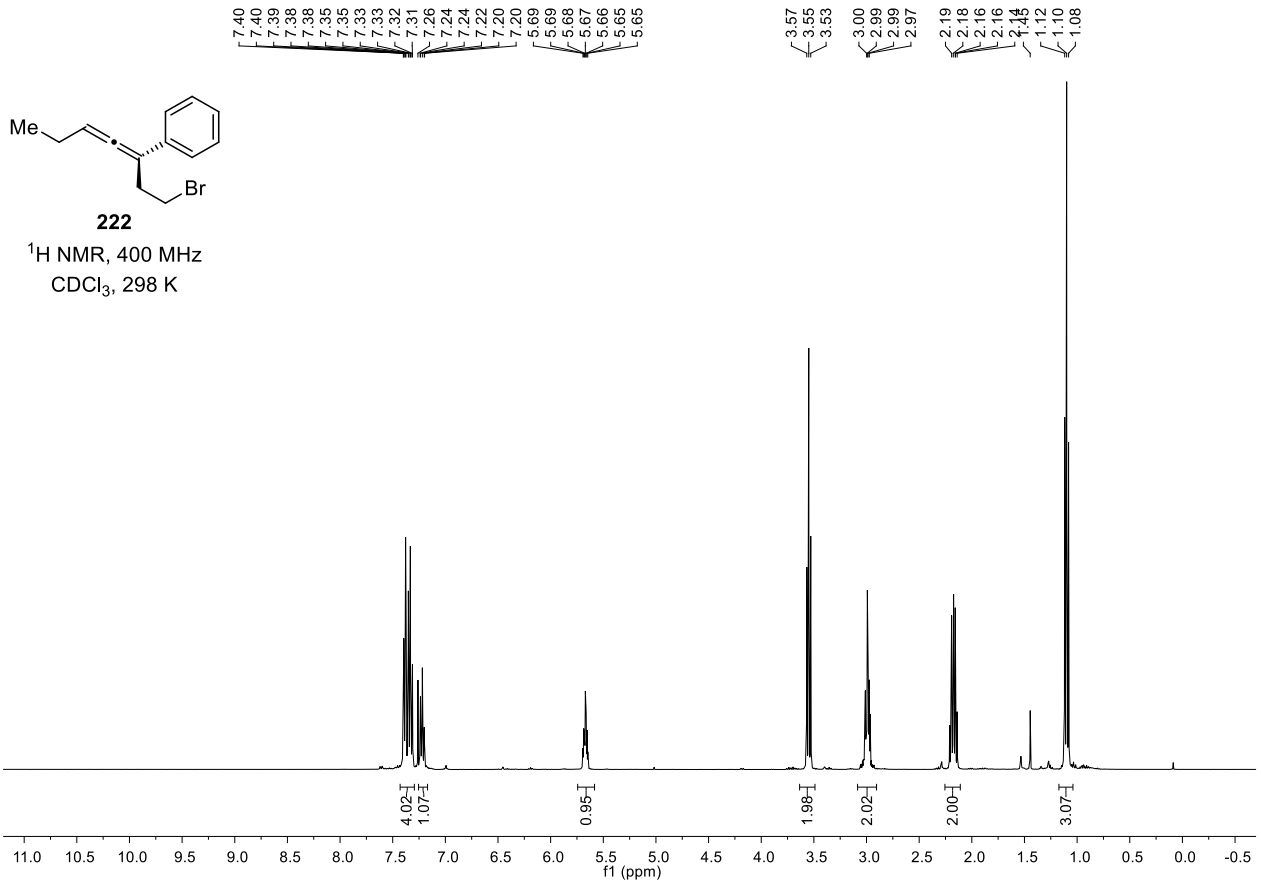

222

^{1}H NMR, 400 MHz

$CDCl_3$, 298 K

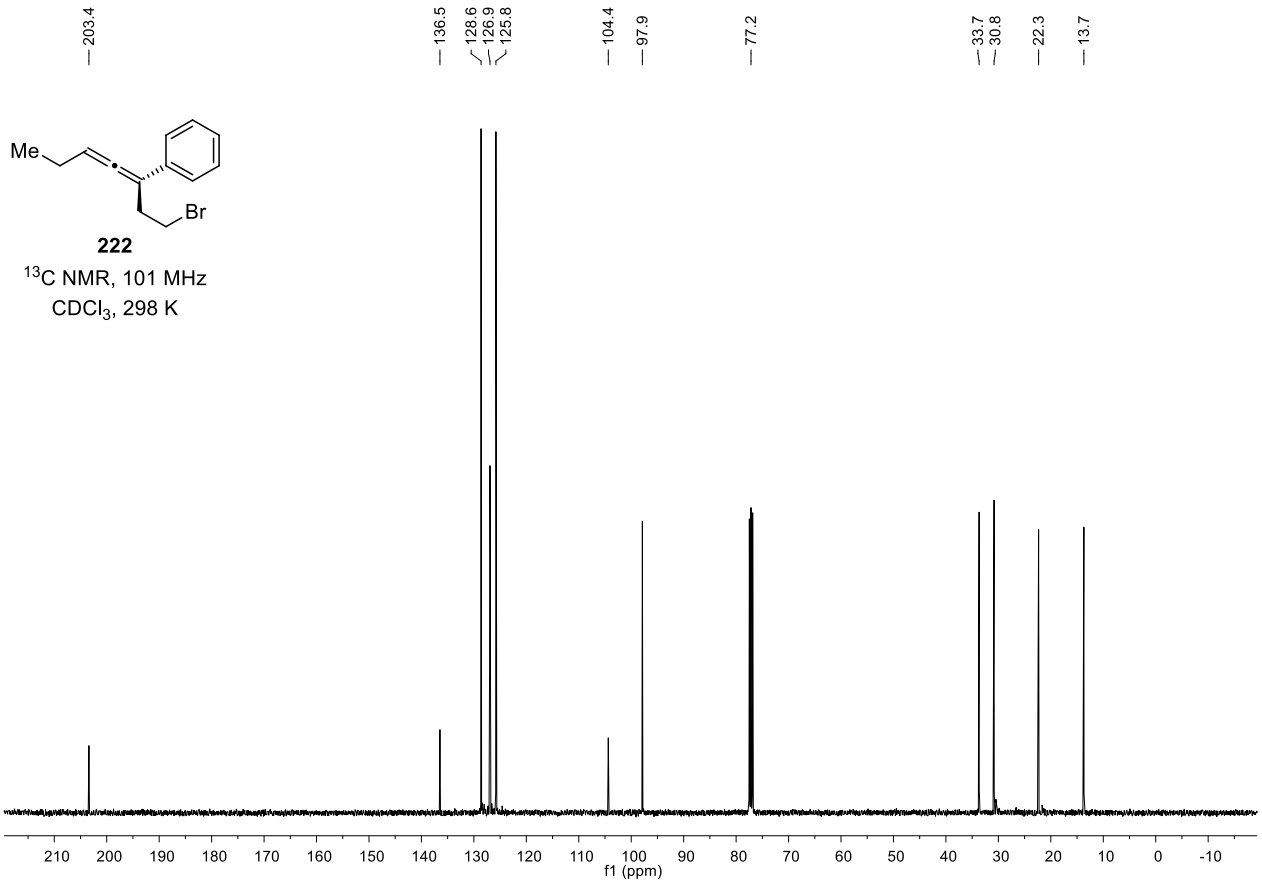

222

^{13}C NMR, 101 MHz

$CDCl_3$, 298 K